



HAL
open science

Prehistoric copper production and technological reproduction in the Khao Wong Prachan Valley of central Thailand

Thomas Pryce

► **To cite this version:**

Thomas Pryce. Prehistoric copper production and technological reproduction in the Khao Wong Prachan Valley of central Thailand. History, Philosophy and Sociology of Sciences. University College London, 2009. English. NNT: . tel-00601676

HAL Id: tel-00601676

<https://theses.hal.science/tel-00601676>

Submitted on 20 Jun 2011

HAL is a multi-disciplinary open access archive for the deposit and dissemination of scientific research documents, whether they are published or not. The documents may come from teaching and research institutions in France or abroad, or from public or private research centers.

L'archive ouverte pluridisciplinaire **HAL**, est destinée au dépôt et à la diffusion de documents scientifiques de niveau recherche, publiés ou non, émanant des établissements d'enseignement et de recherche français ou étrangers, des laboratoires publics ou privés.

Prehistoric Copper Production and
Technological Reproduction
in the Khao Wong Prachan Valley of
central Thailand

T. O. Pryce

Thesis Submitted to University College London
for the Degree of Doctor of Philosophy

UCL INSTITUTE OF ARCHAEOLOGY
UNIVERSITY COLLEGE LONDON

DECEMBER 2008

I, Thomas Oliver Pryce, confirm that the work presented in this thesis is my own. Where information has been derived from other sources, I confirm that this has been indicated in the thesis.

Abstract

Employing a technological approach derived from the ‘Anthropology of Technology’ theoretical literature, this thesis concerns the identification and explanation of change in prehistoric extractive metallurgical behaviour in the Khao Wong Prachan Valley of central Thailand. The ‘Valley’ metallurgical complex, amongst the largest in Eurasia, constitutes Southeast Asia’s only documented industrial-scale copper-smelting evidence. The two smelting sites investigated, Non Pa Wai and Nil Kham Haeng, provide an interrupted but analytically useful sequence of metallurgical consumption and production evidence spanning c. 1450 BCE to c. 300 CE. The enormous quantity of industrial waste at these sites suggests they were probably major copper supply nodes within ancient Southeast Asian metal exchange networks.

Excavated samples of mineral, technical ceramic, and slag from Non Pa Wai and Nil Kham Haeng were analysed in hand specimen, microstructurally by reflected-light microscopy and scanning electron microscopy (SEM), and chemically by polarising energy dispersive x-ray fluorescence spectrometry ([P]ED-XRF) and scanning electron microscopy with energy dispersive x-ray fluorescence spectrometry (SEM-EDS). Resulting analytical data were used to generate detailed technological reconstructions of copper smelting behaviour at the two sites, which were refined by a programme of field experimentation.

Results indicate a long-term improvement in the technical proficiency of Valley metalworkers, accompanied by an increase in the human effort of copper production. This shift in local ‘metallurgical ethos’ is interpreted as a response to rising regional demand for copper in late prehistory.

Table of Contents

Title Page - 1

Abstract - 3

Table of Contents - 4

List of Figures - 6

List of Tables - 14

Acknowledgements - 18

Chapter 1 - Introduction - 22

- 1.1 Thesis background, aims, objectives, and structure
- 1.2 Overview of the later prehistory of Thailand
- 1.3 Prehistoric Thai metallurgy

Chapter 2 - The Khao Wong Prachan Valley and its environs - 49

- 3.1 Geology of the Khao Wong Prachan Valley area
- 3.2 Archaeology of the Khao Wong Prachan Valley area
- 3.3 Previous archaeometallurgical research in the Khao Wong Prachan Valley
- 3.4 Other metallurgical sites in or near the Khao Wong Prachan Valley
- 3.5 Sampling strategy

Chapter 3 - Theoretical Approaches to Ancient Technologies - 80

- 3.1 Social constructionism and ancient technologies
- 3.2 The *chaîne opératoire technique*
- 3.3 Style and choice in metallurgical technologies
- 3.4 Organisation of production
- 3.5 The Weber fraction in archaeometallurgy
- 3.6 - Theory in experimental archaeology

Chapter 4 - Analytical Methodology - 98

- 4.1 Methods of archaeometallurgical analysis
- 4.2 Liquidus calculations in archaeometallurgy

Chapter 5 - Metallurgical Analyses and Technological Reconstruction - Non Pa Wai
Period 3 Metallurgical Phase 2 - 120

- 5.1 Minerals
- 5.2 Technical ceramic
- 5.3 Slag
- 5.4 NPW2/MeP2 technological reconstruction

Chapter 6 - Metallurgical Analyses and Technological Reconstruction - Nil Kham Haeng Period 3 Metallurgical Phase 3 - 172

- 6.1 Minerals
- 6.2 Technical ceramic
- 6.3 Slag
- 6.4 NKH3/MeP3 technological reconstructions

Chapter 7 - Experimental Archaeometallurgical Approaches to the Khao Wong Prachan Valley - 219

- 7.1 Experimental design
- 7.2 Experimental methods
- 7.3 Experimental data
- 7.4 Interpretation

Chapter 8 - The Development of Metallurgy in the Prehistoric Khao Wong Prachan Valley - 252

- 8.1 Identifying stylistic change and continuity in Valley copper smelting
- 8.2 Explaining stylistic change and continuity in Valley copper smelting
- 8.3 The origins of Khao Wong Prachan Valley metallurgy

Chapter 9 - Conclusion - 277

Appendix A: Sample catalogue - 285

Appendix B: Compositional data - 297

Appendix C: Fiafè 2007 experimental data - 310

Bibliography - 366

List of Figures

- Figure 1.1 - Regional political and relief map of Southeast Asia. Image: courtesy of the United States Central Intelligence Agency.
- Figure 1.2 - Political and relief map of Thailand with the Valley marked by a red circle. Image: courtesy of the United States Central Intelligence Agency, modified by the author.
- Figure 1.3 - Diagram outlining the prevailing chronologies for prehistoric Thailand by Charles Higham (e.g. Higham & Higham 2009) and Joyce White (e.g. 2008b), as well as the current Khao Wong Prachan Valley sequence. The capacity for significant regional variation must be emphasised and the marked boundaries are neither absolute nor certain. Image: author.
- Figure 1.4 - Proposed routes (approximately) and dates for the transmission of metallurgy into northeast Thailand, including sites mentioned in the text. Image: courtesy of Google Earth™ mapping service, modified by the author.
- Figure 2.1 - Composite satellite image of central Thailand with Lopburi Province highlighted in red. Courtesy of Google Earth™ mapping service.
- Figure 2.2 - 1:2,500,000 geological map of Thailand with the Khao Wong Prachan Valley (KWPV) and Phu Lon (PL) marked. Courtesy of the Thai Department of Mineral Resources, 1999, modified by the author.
- Figure 2.3 - 1:2,500,000 metallogenic map of Thailand with the Khao Wong Prachan Valley (KWPV) and Phu Lon (PL) marked. Courtesy of the Thai Department of Mineral Resources, 1999, modified by the author.
- Figure 2.4 - Merged 1:250,000 geological map of Ban Mi (N47-4, top) and Ayutthaya (ND47-8, bottom) districts with the Khao Wong Prachan Valley (KWPV) marked. Courtesy of the Thai Department of Mineral Resources, 1976 and 1985 respectively, modified by the author.
- Figure 2.5 - Composite satellite image of the wider Khao Wong Prachan Valley area (above) and the Valley itself (below), with sites mentioned in the text marked. Courtesy of Google Earth™ mapping service.
- Figure 2.6 - Plan of Non Pa Wai showing trenches excavated. Courtesy of TAP.
- Figure 2.7 - Schematic of Non Pa Wai and Nil Kham Haeng chronology, at the time of writing.
- Figure 2.8 - Southern section of ‘Square C’ during the 1986 season at Non Pa Wai, the current site phasing is marked. Courtesy of TAP.
- Figure 2.9 - Plan of Nil Kham Haeng showing trenches excavated. Courtesy of TAP.
- Figure 2.10 - Eastern section of ‘Operation 3’ during the 1990 season at Nil Kham Haeng, only NKH3 contexts are visible. Courtesy of TAP.
- Figure 2.11 - Crushed matrix, hotspots, and technical ceramics (red square) at Khao Sai On, image width c. 2m at base. Courtesy of LoRAP.
- Figure 3.12 - Artist’s impression of prehistoric Khao Wong Prachan Valley copper smelting, prior to the present study. Image: courtesy of Ardeth Abrams (Ban Chiang Project), modified by author.
- Figure 3.1 - A schematic of potential links between materials, knowledge, and some hypothetical characteristics of human societies. Image: author.
- Figure 4.1 – Ternary diagram for a FeO-CaO-SiO₂ slag system in equilibrium with iron metal. Image from Eisenhüttenleute 1995.
- Figure 4.2 – Ellingham Diagram from Gilchrist 1989.
- Figure 4.3 - Binary diagram showing the liquidus effect of varying ppO₂ and

- calcia content on slag system with a Fe/SiO₂ ratio of 1.1. Image from Kongoli & Yazawa 2001: Figure 8.
- Figure 4.4 - Binary diagram showing the liquidus effect of varying alumina and calcia content on slag system with a Fe/SiO₂ ratio of 1.1 and a constant ppO₂ of 1x10⁻⁸ or in equilibrium with iron metal. Image from Kongoli & Yazawa 2001: Figure 14.
 - Figure 4.5 - Binary diagram showing the liquidus effect of varying calcia content and Fe/SiO₂ ratio on slag system with a ppO₂ of 1x10⁻⁸. Image from Kongoli & Yazawa 2001: Figure 10.
 - Figure 5.1 - Scatter plot of NPW3/MeP2 mineral samples [P]ED-XRF bulk chemical data - hafnium versus tantalum, axes are in wt%. Image: author.
 - Figure 5.2: Correlation matrix of NPW3/MeP2 mineral sample [P]ED-XRF bulk chemical data - alumina, silica, calcia, and strontium. Image: author.
 - Figure 5.3 – Pit rim fragment NPWTC11. Image: author.
 - Figure 5.4 - Pit rim fragment NPWTC13 showing possible perforation evidence. Image: author.
 - Figure 5.5 - Possible smelting pit excavated in NPW3 deposit. Image: Roberto Ciarla.
 - Figure 5.6 - Crucible fragment NPWTC3. Image: author.
 - Figure 5.7 - ‘Mr Crucible’. Image: Roberto Ciarla.
 - Figure 5.8 - Crucible fragment NPWTC7 curvature. Image: author.
 - Figure 5.9 - Crucible fragment NPWTC4 cross-section. Image: author.
 - Figure 5.10 - Crucible fragment NPWTC9 slagging. Image: author.
 - Figure 5.11 - Unused and used brass casting crucibles from Ban Pa Ao. Image: author.
 - Figure 5.12 - Ternary plot of NPW3/MeP2 technical ceramic samples [P]ED-XRF bulk chemical data - major components.
 - Figure 5.13 - Correlation matrix of NPW3/MeP2 technical ceramic sample [P]ED-XRF bulk chemical data - alumina, silica, calcia, strontium, zirconium, and barium.
 - Figure 5.14 - Ternary plot of NPW3/MeP2 technical ceramic samples [P]ED-XRF bulk chemical data - selected trace elements.
 - Figure 5.15 - PPL and SEM-BSE images, both at x50, of NPWTC11 micro-features, ‘a’ micromass, ‘b’ quartz, ‘c’ iron oxide, and ‘d’ vesicles - ‘Spectrum 1’ exemplar of 1mm² EDS area scan on fabric. Images: author.
 - Figure 5.16 - PPL and SEM-BSE images, both at x50, of NPWTC3 exterior section micro-features, ‘a’ micromass, ‘b’ quartz, ‘c’ iron oxide, and ‘d’ vesicles - ‘Spectrum 1’ exemplar of 1mm² EDS area scan on fabric. Images: author.
 - Figure 5.17 - PPL and SEM-BSE images, both at x50, of NPWTC8 interior section micro-features, ‘a’ micromass, ‘b’ quartz, ‘c’ iron oxide, ‘d’ vesicles, ‘e’ copper compound penetration - ‘Spectrum 1’ exemplar of 1mm² EDS area scan on fabric. Images: author.
 - Figure 5.18 - Crucible fragment NPWTC8 mounted in 32mm polished block, widespread bloating visible throughout ceramic. Image: author.
 - Figure 5.19 - NPWTC8 crucible slag micro-features at 100x (left) and 500x (right), by plane polarised light (top) and SEM-BSE (bottom). Labels ‘a’ olivine skeletons, ‘b’ primary magnetite euhedrals, ‘c’ cryptocrystalline glass, ‘Spectrum 1’ exemplar of 0.1mm² EDS area scan on slag matrix. Images: author.
 - Figure 5.20 - NPWTC1 crucible slag micro-features at 500x under plane polarised light, ‘a’ residual magnetite, ‘b’ primary magnetite dendrites, ‘c’ copper base prills. Image: author.

- Figure 5.21 - SEM-EDS analyses of olivine phases plotted on a Flogén binary chart for slag system at a 10^{-8} ppO₂ and with 3wt% Al₂O₃. Image adapted from Kongoli & Yazawa 2001: Figure 10.
- Figure 5.22 - Flogén binary chart for slag system at a 10^{-8} ppO₂ and with 7wt% Al₂O₃. Image adapted from Kongoli & Yazawa 2001: Figure 11.
- Figure 5.23 - Crucible slag matrices plotted on a ternary diagram for a FeO-CaO-SiO₂ slag system in equilibrium with iron metal. Image adapted from Eisenhüttenleute 1995.
- Figure 5.24 - Ellingham Diagram showing redox envelope for NPW3/MeP2 crucible slags. Image adapted from Gilchrist 1989.
- Figure 5.25 - SEM-EDS analyses of slag matrices plotted on a Flogén binary chart for slag system at a 10^{-8} ppO₂ and with 3wt% Al₂O₃. Image adapted from Kongoli & Yazawa 2001: Figure 10.
- Figure 5.26 - Emilien Burger using forced blast to preheat a charcoal pit prior to a crucible-based copper smelting experiment in Fiaavè, Italy, September 2007. Image: author.
- Figure 5.27 - NPWMS6 (top) and NPWMS19 (bottom), examples of NPW3/MeP2 slag cakes. Images: author.
- Figure 5.28 - NPWMS1 (top) and NPWMS4 (bottom), examples of broken up NPW3/MeP2 slag cakes. Images: author.
- Figure 5.29 - NPWMS7 sectioned and polished to show heterogeneous texture. Image: author.
- Figure 5.30 - Scatter plot showing low correlation between copper and sulphur compounds in NPW3/MeP2 [P]ED-XRF bulk chemical slag data.
- Figure 5.31 - Scatter plot showing low correlation between copper and iron compounds in NPW3/MeP2 [P]ED-XRF bulk chemical slag data.
- Figure 5.32 - Correlation matrix of NPW3/MeP2 slag sample [P]ED-XRF bulk chemical data - silica, calcia, and iron oxide.
- Figure 5.33 - NPWMS12 (top) and NPWMS14 (bottom) slag micro-features, both at 500x, by SEM-BSE. Labels 'a¹' olivine skeletons, 'a²' olivine euhedrals, 'b¹' residual iron oxides, 'b²' primary iron oxides, 'c' slag glass, 'd' prills, 'Spectrum 1's are exemplar of 1mm² EDS area scans. Images: author.
- Figure 5.34 - NPWMS2 (top left), NPWMS3 (top right), NPWMS12 (bottom left), and NPWMS13 (bottom right) olivine skeletons and euhedrals, all at 500x, by SEM-BSE, 'Spectrum 1's and 'Spectrum 5' are exemplar of EDS point analyses. Images: author.
- Figure 5.35 - SEM-EDS analyses of olivine phases plotted on a Flogén binary chart for a slag system at a 10^{-8} ppO₂ and with 1wt% MgO. Image adapted from Kongoli & Yazawa 2001: Figure 15.
- Figure 5.36 - NPWMS8 (top) and NPWMS18 (bottom) magnetite skeletons and dendrites, both at 500x, by SEM-BSE, 'Spectrum 11' and 'Spectrum 10' are exemplar of EDS point analyses. Images: author.
- Figure 5.37 - Residual magnetite inclusions, NPWMS6 (top) under plane polarised light and NPWMS12 (bottom) by SEM-BSE, both at 50x. Images: author.
- Figure 5.38 - Sulphidic zones in residual magnetite inclusions, NPWMS6 under plane polarised light at 50x. Image: author.
- Figure 5.39 - Trigonal intergrowths of haematite in residual martitised magnetite, NPWMS7 under plane polarised light at 100x. Image: author.
- Figure 5.40 - Chalcopyrite fragment in NPWMS7 mounted in a 32mm polished block (left), under plane polarised light (top centre and top right at 100x and 500x respectively, and by SEM-BSE (bottom centre and bottom right at 100x and

- 500x respectively - 'Spectrum 1' exemplar of SEM-EDS spot analysis. Images: author.
- Figure 5.41 - Sphalerite fragment in NPWMS7, under plane polarised light (top) and by SEM-BSE (bottom, at 50x (left) and 500x (right)) - 'Spectrum 1' exemplar of SEM-EDS spot analysis. Images: author.
 - Figure 5.42 - Copper-bearing residual siliceous inclusion in NPWMS2, under plane polarised light at 50x. Image: author.
 - Figure 5.43 - NPWMS1 (top) and NPWMS14 (bottom) interstitial glass phases, both at 500x, by SEM-BSE, 'Spectrum 1' and 'Spectrum 7' are exemplar of EDS point analyses. Images: author.
 - Figure 5.44 - SEM-EDS analyses of glass phases plotted on a Flogén binary chart for a slag system at a 10^{-8} ppO₂ and with 7wt% Al₂O₃. Image adapted from Kongoli & Yazawa 2001: Figure 11.
 - Figure 5.45 - Prills of copper (top - NPWMS6), copper/matte (middle - NPWMS13), and matte (bottom - NPWMS6), all under plane polarised light at 500x. Images: author.
 - Figure 5.46 - Slag matrices plotted on a ternary diagram for a FeO-CaO-SiO₂ slag system in equilibrium with iron metal. Image adapted from Eisenhüttenleute 1995.
 - Figure 5.47 - Ellingham Diagram showing redox envelope for NPW3/MeP2 crucible slags. Image adapted from Gilchrist 1989.
 - Figure 5.48 - SEM-EDS analyses of slag matrices plotted on a Flogén binary chart for a slag system at a 10^{-8} ppO₂ and with 3wt% Al₂O₃. Image adapted from Kongoli & Yazawa 2001: Figure 10.
 - Figure 5.49 - Macro-scopically visible residual magnetite in NPWMS6, mounted in 32mm polished block. Image: author.
 - Figure 5.50 - Schematic technological reconstruction for copper smelting technique at early Iron Age Non Pa Wai. Image: author.
 - Figure 6.1 - Scatter plot of NKH3/MeP3 mineral samples [P]ED-XRF bulk chemical data - hafnium versus tantalum. Image: author.
 - Figure 6.2 - Correlation matrix of NKH3/MeP3 mineral sample [P]ED-XRF bulk chemical data - alumina, silica, calcia, strontium, and barium. Image: author.
 - Figure 6.3 - 'Slag-skin' fragments NKHTC4. Image: author.
 - Figure 6.4 - 'Slag-skin' fragments NKHTC5. Image: author.
 - Figure 6.5 - 'Furnace' fragment NKHTC1. Image: author.
 - Figure 6.6 - 'Furnace' fragment NKHTC3, with perforation highlighted. Image: author.
 - Figure 6.7 - Perforated ceramic cylinder excavated from Burial 1 Operation 4 at Nil Kham Haeng. Image: courtesy of TAP.
 - Figure 6.8 - Ternary plot of NKH3/MeP3 technical ceramic samples [P]ED-XRF bulk chemical data - selected major oxides.
 - Figure 6.9 - Ternary plot of NKH3/MeP3 technical ceramic samples [P]ED-XRF bulk chemical data - selected elements.
 - Figure 6.10 - Correlation matrix of NKH3/MeP3 technical ceramic ('furnace') sample [P]ED-XRF bulk chemical data - alumina, silica, calcia, strontium, zirconium, and barium.
 - Figure 6.11 - PPL and SEM-BSE images, both at x50, of NKHTC2 micro-features, 'a' micromass, 'b' quartz, 'c' iron oxide, and 'd' vesicles - 'Spectrum 1' exemplar of EDS area scan on fabric. Images: author.
 - Figure 6.12 - PPL and SEM-BSE images, both at x50, of NKHTC5 micro-

- features, 'a' micromass, 'b' quartz, 'c' iron oxide, and 'd' vesicles - 'Spectrum 1' exemplar of EDS area scan on fabric. Images: author.
- Figure 6.13 - PPL and SEM-BSE images, both at x50, of NKHTC6 micro-features, 'a' micromass, 'b' quartz, and 'd' vesicles - 'Spectrum 1' exemplar of EDS area scan on fabric. Images: author.
 - Figure 6.14 - Crucible fragment NKHTC5 mounted in 32mm polished block, widespread bloating visible at the ceramic/slag interface. Image: author.
 - Figure 6.15 - Ternary plot of NKH3/MeP3 technical ceramic samples: 'slag-skin' (black dot) - SEM-EDS data, 'furnace' - [P]ED-XRF data - selected major oxides.
 - Figure 6.16 - NKHTC5 'slag-skin' micro-features at 100x (left) by plane polarised light (top) and SEM-BSE (bottom), and NKHTC6 at 500x (right) by plane polarised light (top) and SEM-BSE (bottom). Labels 'a' olivine skeletons, 'b₁' primary magnetite euhedrals, 'b₂' residual magnetite inclusions, 'c' glass phase, 'Spectrum 1' exemplar of an SEM-EDS area analysis. Images: author.
 - Figure 6.17 - SEM-EDS analyses of olivine phases plotted on a Flogen binary chart for slag system at a 10⁻⁸ ppO₂ and with 7wt% Al₂O₃. Image adapted from Kongoli & Yazawa 2001: Figure 11.
 - Figure 6.18 - SEM-EDS analyses of glass phases plotted on a Flogen binary chart for slag system at a 10⁻⁸ ppO₂ and with 7wt% Al₂O₃. Image adapted from Kongoli & Yazawa 2001: Figure 11.
 - Figure 6.19 - 'Slag-skin' slag matrices plotted on a ternary diagram for a FeO-CaO-SiO₂ slag system in equilibrium with iron metal. Image adapted from Eisenhüttenleute 1995.
 - Figure 6.20 - Ellingham Diagram showing redox envelope for NKH3/MeP3 'slag-skin' slags. Image adapted from Gilchrist 1989.
 - Figure 6.21 - SEM-EDS analyses of slag matrices phases plotted on a Flogen binary chart for slag system at a 10⁻⁸ ppO₂ and with 7wt% Al₂O₃. Image adapted from Kongoli & Yazawa 2001: Figure 11.
 - Figure 6.22 - NKHMS19 (top) and inverted (bottom), examples of NKH3/MeP3 'slag casts'. Images: author.
 - Figure 6.23 - NKHMS15 (top) and NKHMS17 (bottom - inverse inset), examples of NKH3/MeP3 slag cakes. Images: author.
 - Figure 6.24 - NKHMS8 (top) and NKHMS14 (bottom), examples of crushed NKH3/MeP3 slag cakes. Images: author.
 - Figure 6.25 - Scatter plot of NKH3/MeP3 slag samples [P]ED-XRF bulk chemical data - sulphates versus copper oxide.
 - Figure 6.26 - Scatter plot of NKH3/MeP3 slag samples [P]ED-XRF bulk chemical data - iron oxide versus copper oxide.
 - Figure 6.27 - Correlation matrix of NKH3/MeP3 slag sample [P]ED-XRF bulk chemical data - silica, calcia, and iron oxide.
 - Figure 6.28 - NKHMS4 (top), NKHMS7 (centre) and NKHMS18 (bottom) slag micro-features, all at 50x, by SEM-BSE. Labels 'a₁' olivine skeletons, 'a₂' olivine euhedrals, 'b₁' residual iron oxides, 'b₂' primary iron oxides, 'c' slag glass, 'd' prills, 'Spectrum 1's are exemplar of 1mm² EDS area scans. Images: author.
 - Figure 6.29 - NKHMS5 (top) and NKHMS13 (bottom) olivine skeletons (grey), both at 500x, by SEM-BSE. 'Spectrum 1's are exemplar EDS spot analyses. Images: author.
 - Figure 6.30 - NKHMS17 olivine dendritic crystals under plane polarised light (top) at 1000x, and by SEM-BSE (bottom) at 500x. 'Spectrum 1' is an exemplar

EDS spot analysis. Images: author.

- Figure 6.31 - NKHMS17 olivine euhedral crystals (mid-grey) under plane polarised light at 1000x, width of field is 0.1mm. Image: author.
- Figure 6.32 - SEM-EDS analyses of olivine phases plotted on a Flogen binary chart for slag system at a 10^{-8} ppO₂ and with 1wt% MgO. Image adapted from Kongoli & Yazawa 2001: Figure 15.
- Figure 6.33 - Magnetite spinel euhedral crystals (bright) in NKHMS13 under plane polarised light (top left) and by SEM-BSE (bottom left) both at 500x, dendrites in NKHMS7 under plane polarised light (top right) and by SEM-BSE (bottom right) both at 1000x. Images: author.
- Figure 6.34 - Residual magnetite in NKHMS13 (top left), NKHMS7 (bottom left - a 'pseudomorph'), and NKHMS18 (top right) under plane polarised light, all at 50x, and in NKHMS18 (bottom right) by SEM-BSE at 500x. 'Spectrum 1' exemplar of an SEM-EDS spot analysis. Images: author.
- Figure 6.35 - Residual magnetite with and without intergrown covellite in NKHMS5 under plane polarised light, both at 50x. Images: author.
- Figure 6.36 - Residual quartz inclusions in NKHMS7 (top), NKHMS13 (centre), and NKHMS17 (bottom) under plane polarised light (left) and crossed polars (right), all at 50x. Images: author.
- Figure 6.37 - Cryptocrystalline glass with feathery dendrites in NKHMS17 under plane polarised light (top) and by SEM-BSE (bottom), both at 500x. Images: author.
- Figure 6.38 - SEM-EDS analyses of glass phases plotted on a Flogen binary chart for slag system at a 10^{-8} ppO₂ and with 7wt% Al₂O₃. Image adapted from Kongoli & Yazawa 2001: Figure 11.
- Figure 6.39 - Copper and matte prills in NKHMS13 (top at 500x), NKHMS17 (centre at 200x), and NKHMS18 (bottom at 500x) under plane polarised light (left), and by SEM-BSE (right), excepting the centre-right image under crossed polars. Images: author.
- Figure 6.40 - Slag matrices plotted on a ternary diagram for a FeO-CaO-SiO₂ slag system in equilibrium with iron metal. Image adapted from Eisenhüttenleute 1995.
- Figure 6.41 - Ellingham Diagram showing redox envelope for NKH3/MeP3 slags. Image adapted from Gilchrist 1989.
- Figure 6.42 - SEM-EDS analyses of slag matrices plotted on a Flogen binary chart for slag system at a 10^{-8} ppO₂ and with 7wt% Al₂O₃. Image adapted from Kongoli & Yazawa 2001: Figure 11.
- Figure 6.43 - Schematic technological reconstruction for copper smelting technique at later Iron Age Nil Kham Haeng, prior to experimental testing. Image: author.
- Figure 7.1 - Perforated ceramic cylinder configurations for NPW3/MeP2**PR** (left) and NKH3/MeP3 (right).
- Figure 7.2 - The Beaufort Scale. Image courtesy of the Mount Washington Observatory (http://www.mountwashington.org/education/center/arcade/wind/beaufort_scale_tbp.gif accessed 24th October 2008)
- Figure 7.3 - Minerals used in the Fiavè experiments, from left to right: malachite, chalcopyrite, magnetite, quartz, and lime. Image: author.
- Figure 7.4 - Vincent C. Pigott crushing malachite at the command of his PhD student, Fiavè, September 2007. Image: author.
- Figure 7.5 - The author kneading sand into clay at Fiavè, September 2007. Image: Bastian Asmus.

- Figure 7.6 - The author building perforated ceramic cylinders at Fiaavè, September 2007. Image: Bérénice Bellina.
- Figure 7.7 - The artificial wind source. Image: author.
- Figure 7.8 - Windspeed at the furnace. Image: author.
- Figure 7.9 - The anemometre. Image: author.
- Figure 7.10 - The mineral component of a smelting charge. Image: author.
- Figure 7.11 - The smelting configuration for 'Burn 5'. Image: author.
- Figure 7.12 - Graph of temperature data for Burn 1. Image: author.
- Figure 7.13 - Sections of slagged furnace chimney and unslagged crucible from Burn 1. Image: author.
- Figure 7.14 - Graph of temperature data for Burn 2. Image: author.
- Figure 7.15 - Large crack in the chimney wall during Burn 2, but the integrity of the smelt was not affected. Image: author.
- Figure 7.16 - Adhesion of chimney and crucible during Burn 2 - now known to be an archaeologically incorrect association. Image: author.
- Figure 7.17 - Graph of temperature data for Burn 3. Image: author.
- Figure 7.18 - Sectioned remains of Burn 3. Image: author.
- Figure 7.19 - Graph of temperature data for Burn 4. Image: author.
- Figure 7.20 - Graph of temperature data for Burn 5. Image: author.
- Figure 7.21 - Furnace chimney from Burn 5 being repaired for Burn 6, and placed over a clay-lined pit. Image: author.
- Figure 7.22 - Graph of temperature data for Burn 6. Image: author.
- Figure 7.23 - Burn 7 operating by night. Image: author.
- Figure 7.24 - Graph of temperature data for Burn 7. Image: author.
- Figure 7.25 - The unreacted core of Burn 7. Image: author.
- Figure 7.26 - Graph of temperature data for Burn 8. Image: author.
- Figure 7.27 - Graph of temperature data for Burn 9. Image: author.
- Figure 7.28 - Graph of temperature data for Burn 10. Image: author.
- Figure 7.29 - Mass of semi-fused charge attached to the furnace wall during Burn 10. Image: author.
- Figure 7.30 - Graph of mean temperature data for Burns 1-10. Image: author.
- Figure 7.31 - Schematic of the NPW3/MeP2 (left) and NKH3/MeP3 (right) technological reconstructions after the Fiaavè experimental campaign. Image: author.
- Figure 8.1 – Ternary plot of major oxide comparability in NPW3/MeP2 and NKH3/MeP3 technical ceramics (left) versus trace element separation. Image: author.
- Figure 8.2 - Ternary plot of the three principal slag-forming oxides in Valley slag. Image: author.
- Figure 8.3 - Scatter plot showing the lack of correlation between copper oxide and iron oxide levels in [P]ED-XRF bulk chemical analyses of Valley slag. Image: author.
- Figure 8.4 - Scatter plot showing the lack of correlation in [P]ED-XRF bulk chemical data between copper and sulphur compounds in MeP2 slags, compared with a weak relationship in MeP3 samples. Image: author.
- Figure 8.5 - Scatter plot showing the consistent absence of tin in [P]ED-XRF bulk chemical analyses of MeP2 slags, versus sporadic trace level presence in MeP3 samples. Image: author.
- Figure 8.6 - Scatter plot showing the lack of correlation in [P]ED-XRF bulk chemical data between tin compound content and MeP3 slag morphology. Image: author.

- Figure 8.7 - Scatter plot showing the positive correlation of titania and potash in [P]ED-XRF bulk chemical analyses of MeP2 and MeP3 slag samples, with increased concentrations in the latter phase. Image: author.
- Figure 8.8 - Plots showing those elements and compounds dominating variation in three principal components generated from [P]ED-XRF bulk chemical analyses of Valley slag samples. Image: author.
- Figure 8.9 - Scatter plots showing the metallurgical phase attribution of those elements and compounds dominating variation in three principal components generated from [P]ED-XRF bulk chemical analyses of Valley slag samples. Image: author.
- Figure 8.10 - Two copper-base artefacts from an Iron Age 1 burial at Ban Non Wat. Image: Charles Higham.
- Figure 9.1 - Figure 9.1 - From its supposed centre in the Altaï mountains, the proposed “Seima-Turbino transcultural phenomenon” (Chernykh 1992: 215-234 cited in White & Hamilton in press); extends c. 4000km to the northwest and the Gulf of Finland, and another c. 4000km southeast to the Mekong River. Image: courtesy of Google Earth™ mapping service, modified by the author.

List of Tables

- Table 1.1 - Summary of generalised technological characteristics distinguishing Southeast Asian and East Asian metallurgical traditions of the 2nd millennium BCE (After White 1988, 2008).
- Table 3.1 - Predominant features of prehistoric Valley technological styles.
- Table 4.1 - A classification of craft production systems based upon: the relationship between producers and consumers (Class), the location of production and the distribution of product (Supertype), and the scale of production (Type). After Clark 1995.
- Table 5.1: Macro-characteristics of NPW3/MeP2 mineral samples.
- Table 5.2: [P]ED-XRF bulk chemical analyses of NPW3/MeP2 mineral samples, selected major and minor oxides after data normalisation, analytical total presented.
- Table 5.3: [P]ED-XRF bulk chemical analyses of NPW3/MeP2 mineral samples, selected trace elements after data normalisation.
- Table 5.4 - Macro-characteristics of NPW3/MeP2 technical ceramic samples.
- Table 5.5 - [P]ED-XRF bulk chemical analyses of NPW3/MeP2 technical ceramic samples, selected major and minor oxides after data normalisation, analytical total presented.
- Table 5.6 - [P]ED-XRF bulk chemical analyses of NPW3/MeP2 technical ceramic samples, selected trace elements after data normalisation.
- Table 5.7 - Micro-characteristics of NPW3/MeP2 technical ceramic samples.
- Table 5.8 - SEM-EDS phase analyses of NPW3/MeP2 crucible slag olivine crystals, selected major and minor oxides after data normalisation, analytical total presented.
- Table 5.9 - SEM-EDS phase analyses of NPW3/MeP2 crucible slag magnetite spinel, selected major and minor oxides after data normalisation, analytical total presented.
- Table 5.10 - SEM-EDS phase analyses of NPW3/MeP2 crucible slag glass, selected major and minor oxides after data normalisation, analytical total presented.
- Table 5.11 - SEM-EDS phase analyses of NPW3/MeP2 crucible slag matrices, selected major and minor oxides after data normalisation, analytical total presented.
- Table 5.12 - Macro-characteristics of NPW3/MeP2 slag samples.
- Table 5.13 - [P]ED-XRF bulk chemical analyses of NPW3/MeP2 slag samples, selected major and minor oxides after data normalisation, analytical total presented.
- Table 5.14 - [P]ED-XRF bulk chemical analyses of NPW3/MeP2 slag samples, selected elements after data normalisation, analytical total presented.
- Table 5.15 - Micro-characteristics of NPW3/MeP2 slag samples.
- Table 5.16 - SEM-EDS phase analyses of NPW3/MeP2 slag olivines, selected major and minor oxides after data normalisation, analytical total presented.
- Table 5.17 - SEM-EDS phase analyses of NPW3/MeP2 slag magnetite spinel, selected major and minor oxides after data normalisation, analytical total presented.
- Table 5.18 - SEM-EDS phase analyses of NPW3/MeP2 slag residual magnetite inclusions, selected major and minor oxides after data normalisation, analytical total presented.
- Table 5.19 - SEM-EDS phase analyses of NPW3/MeP2 slag glass phases, selected

- major and minor oxides after data normalisation, analytical total presented.
- Table 5.20 - SEM-EDS phase analyses of NPW3/MeP2 slag prills, selected major elements after data normalisation, analytical total presented.
 - Table 5.21 - SEM-EDS phase analyses of NPW3/MeP2 slag matrices, selected major and minor oxides after data normalisation, analytical total presented.
 - Table 6.1 - Macro-characteristics of NKH3/MeP3 mineral samples.
 - Table 6.2 - [P]ED-XRF bulk chemical analyses of NKH3/MeP3 mineral samples, selected major and minor oxides after data normalisation, analytical total presented.
 - Table 6.3 - [P]ED-XRF bulk chemical analyses of NKH3/MeP3 mineral samples, selected trace elements after data normalisation.
 - Table 6.4 - Macro-characteristics of NKH3/MeP3 technical ceramic samples, NKHTC1-3 are ‘furnace’ fragments, NKHTC4-6 are ‘slag-skins’.
 - Table 6.5 - [P]ED-XRF bulk chemical analyses of NKH3/MeP3 technical ceramic (‘furnace’) samples, selected major and minor oxides after data normalisation, analytical total presented.
 - Table 6.6 - [P]ED-XRF bulk chemical analyses of NKH3/MeP3 technical ceramic (‘furnace’) samples, selected elements after data normalisation, analytical total presented.
 - Table 6.7 - Micro-characteristics of NKH3/MeP3 technical ceramic samples.
 - Table 6.8 - [P]ED-XRF bulk chemical analyses of NKH3/MeP3 ‘slag-skin’ samples, selected major and minor oxides after data normalisation, analytical total presented.
 - Table 6.9 - SEM-EDS phase analyses of NKH3/MeP3 ‘slag-skin’ olivine crystals, selected major and minor oxides after data normalisation, analytical total presented.
 - Table 6.10 - SEM-EDS phase analyses of NKH3/MeP3 ‘slag-skin’ magnetite crystals, selected major and minor oxides after data normalisation, analytical total presented.
 - Table 6.11 - SEM-EDS phase analyses of NKH3/MeP3 ‘slag-skin’ glass phases, selected major and minor oxides after data normalisation, analytical total presented.
 - Table 6.12 - SEM-EDS phase analyses of NKH3/MeP3 ‘slag-skin’ slag matrices, selected major and minor oxides after data normalisation, analytical total presented.
 - Table 6.13 - Macro-characteristics of NKH3/MeP3 slag samples
 - Table 6.14 - [P]ED-XRF bulk chemical analyses of NKH3/MeP3 slag, selected major and minor oxides after data normalisation, analytical total presented.
 - Table 6.15 - [P]ED-XRF bulk chemical analyses of NKH3/MeP3 slag, selected elements after data normalisation, analytical total presented.
 - Table 6.16 - Micro-characteristics of NKH3/MeP3 slag samples.
 - Table 6.17 - SEM-EDS phase analyses of NKH3/MeP3 olivine crystals, selected major and minor oxides after data normalisation, analytical total presented.
 - Table 6.18 - SEM-EDS phase analyses of NKH3/MeP3 magnetite spinel crystals, selected major and minor oxides after data normalisation, analytical total presented.
 - Table 6.19 - SEM-EDS phase analyses of NKH3/MeP3 residual magnetite, selected major and minor oxides after data normalisation, analytical total presented.
 - Table 6.20 - SEM-EDS phase analyses of NKH3/MeP3 slag glass, selected major and minor oxides after data normalisation, analytical total presented.
 - Table 6.21 - SEM-EDS phase analyses of NKH3/MeP3 slag prills, selected

elements after data normalisation, analytical total presented.

- Table 6.22 - SEM-EDS phase analyses of NKH3/MeP3 slag matrices, selected major and minor oxides after data normalisation, analytical total presented.
- Table 7.1 - Calculator for experiment reactants and theoretical products. ‘ELEMENTS’ contains atomic masses of constituent elements. ‘COMPOUNDS’ computes molecular masses for constituent compounds, with the olivines being calculated from SEM-EDS matrix scans under ‘KWPV SLAG’ (see Tables 5.23 & 6.23). The lower part of the table details the reactants needed for an experimental smelting charge - NPW3/MeP2^{PR} is referred to as the tests were conducted under the ‘pre-Rome’ chronology, but aside from slight differences in the slag matrix chemistry all experiments can be considered NKH3/MeP3 reconstructions.
- Table 7.2 - Major parameters of the 2007 Fiaavè experiments, thermocouple ‘depth’ refers to the protrusion of the probe from the interior chimney wall.
- Table 8.1 - Principal metallurgical style characteristics of NPW2/MeP1, NPW3/MeP2, and NKH3/MeP3.
- Table 8.2 - Means, standard deviations, and coefficients of variation for [P]ED-XRF bulk chemical analyses of slag from NPW3/MeP2 and NKH3/MeP2 contexts. Selected oxides and elements after normalisation.
- Table 8.3: Mean [P]ED-XRF bulk chemical analyses of slag from NPW3/MeP2 and NKH3/MeP2 contexts. Major oxide data (except iron oxide) associated with ash, ceramic, and gangue are re-normalised (in italics) according to the NPW3/MeP2 total.
- Table 8.4 - Summary of liquidus estimates derived from SEM-EDS matrix analyses of Valley slag samples.
- Table A.1: Contexts and macro-characteristics for KWPV mineral samples.
- Table A.2: Contexts and macro-characteristics for KWPV technical ceramic samples.
- Table A.3i: Contexts and macro-characteristics for KWPV slag samples - NPW
- Table A.3ii: Contexts and macro-characteristics for KWPV slag samples - NPW
- Table A.3iii: Contexts and macro-characteristics for KWPV slag samples - NKH
- Table A.3iv: Contexts and macro-characteristics for KWPV slag samples - NKH
- Table B.1i: KWPV Certified Reference Materials [P]ED-XRF bulk chemical analyses, all detected elements reported. Data not normalised.
- Table B.1ii: KWPV Certified Reference Materials [P]ED-XRF bulk chemical analyses, all detected elements reported. Data not normalised.
- Table B.1iii: KWPV Certified Reference Materials [P]ED-XRF bulk chemical analyses, all detected elements reported. Data not normalised.
- Table B.2: KWPV mineral sample [P]ED-XRF bulk chemical analyses, all detected elements reported. Data not normalised.
- Table B.3: KWPV technical ceramic sample [P]ED-XRF bulk chemical analyses, all detected elements reported. Data not normalised.
- Table B.4: KWPV crucible slag and slag-skin olivine crystal SEM-EDS phase analyses. Data not normalised.
- Table B.5: KWPV crucible slag and slag-skin magnetite spinel SEM-EDS phase analyses. Data not normalised.
- Table B.6: KWPV crucible slag and slag-skin glass SEM-EDS phase analyses. Data not normalised.
- Table B.7: KWPV crucible slag and slag-skin prills SEM-EDS phase analyses. Data not normalised.
- Table B.8: KWPV crucible slag and slag-skin matrices SEM-EDS phase analyses.

Data not normalised.

- Table B.9i: NPW slag samples [P]ED-XRF bulk chemical analyses, all detected elements reported. Data not normalised.
- Table B.9ii: NPW slag samples [P]ED-XRF bulk chemical analyses, all detected elements reported. Data not normalised.
- Table B.10: KWPV slag samples olivine crystal SEM-EDS phase analyses. Data not normalised.
- Table B.11: KWPV slag samples primary magnetite SEM-EDS phase analyses. Data not normalised.
- Table B.12: KWPV slag samples residual magnetite SEM-EDS phase analyses. Data not normalised.
- Table B.13: KWPV slag samples, glass phase SEM-EDS analyses. Data not normalised.
- Table B.14: KWPV slag samples, copper-base prills SEM-EDS phase analyses. Data not normalised.
- Table B.15: KWPV slag matrices SEM-EDS phase analyses. Data not normalised.

Acknowledgements

If one considers the primary influences on one's life, parental acknowledgement is as inevitable as it is gratefully given. My archaeological awakenings can probably be traced to a 1988 family holiday in Mexico, where my wonderment at humankind's achievements were stirred whilst tottering around the Temple of the Sun in Teotihuacán. This initial spark was fanned a year later during my father's posting to Egypt, where my growing rapture was fuelled by many adventures of the Nile and the desert; wearing the de rigueur dayglo Bermudas of the day. Unfortunately, this early archaeological love affair culminated in a cataclysmic temper tantrum at the Temple of Queen Hatshepsut, where I became convinced that the modern bricks being used to reinforce a column were in fact evidence the whole business was a scam. To this day I blame the hallucinogenic effects of lurid late 1980s apparel.

Leaping forward a decade, the archaeological entwinement with my parents continued as I reached the apogee of my teenage crisis, and decided I was *goin' diggin'*. Aged eighteen years and one day, I arrived at Şamuratlı Köy to participate in the excavation of Kerkenes Dag in central Anatolia - an Iron Age mountain top city of outstanding beauty. My second acknowledgment thus goes to the project director, Professor Geoffrey Summers, who took a chance on someone with only pending academic qualifications and absolutely no field experience.

My experience of the UCL Institute of Archaeology has consistently been one of encouragement and support, and this was initiated in May 1998 when Dr Daffyd Griffiths made me a 'three E' offer for my A-level entry requirement. Dr Griffiths is thus my third acknowledgment, and, in the *longue durée*, can be held responsible for cracking the door of academia to me.

However, the blame is not Dr Griffith's alone. Enthusiasm for the subject was not matched by time spent in the library, and my performance during the first two years at the IoA was not stellar. My fourth acknowledgement is therefore lodged firmly at the door of Dr Cyprian Broodbank. One fateful afternoon leaning on the boundary fence of Kythera State Airport (an unlikely tale, of which I can only point to my BSc dissertation for explanation), Dr Broodbank asked me what my intentions in archaeology were. Upon hearing it involved more than Amstel and press-ups in front of the girls, I was enlisted forthwith in the Broodbank Boot Camp, and my third year passed in a flurry of fledgling scholarship and intense weekly meetings, resulting in the occasional solid grade. However, despite the best efforts of myself and Dr Broodbank, the final degree awarded spiralled inexorably into the cavernous black hole of the Upper Second grade band.

A lesson had been learnt, and with a very low likelihood of funding, I decided to enter the 'real' world of global finance. Although draped in cobwebs both literal and metaphorical, the Dickensian drudgery of Messrs C. Hoare & Co was not a happy place for a wanderlusting archaeologist. Nevertheless, credit where it is due; in two years of quill sharpening and cap doffing, I was instilled with the essential principles of data quality, due diligence, and deadlines.

08:30 21st August 2003, notice served and share dealing security tags relinquished, I left the City with newfound skills, savings, and a determination to never again languish behind a desk with no hope of escape. I staggered blinking into the bright summer sunshine and soon found myself in Sheffield, enrolled on an MSc in Archaeomaterials. My next acknowledgement is thus to Dr Peter Day and Dr Caroline Jackson, who took a very eager, though philosophically misguided young man, and drilled me into an anthropologically-aware fledgling technologist.

My time at Sheffield University was unimaginably the richer for having met, and been taught by, Dr Mihalis Catapotis. Despite facing the rigours of his own PhD, Dr Catapotis' inspirational lectures and unbridled enthusiasm for the topic are undoubtedly what converted me to archaeometallurgy. I am forever grateful for Dr Catapotis' extreme academic generosity and willingness to share his ideas and his time. These qualities are also to be recognised in Dr Yannis Bassiakos, as my involvement in Aegean archaeology was encouraged by invitations to participate in copper smelting experiments in Athens and at the 'Aegean metallurgy in the Bronze Age' conference on Crete. Though I now work farther afield, I retain the fondest of memories of my Greek friends and their country.

My apprenticeship in Southeast Asian archaeology began in Northeast Thailand at Ban Non Wat; a much appreciated opportunity, courtesy of Professor Charles Higham, Dr Ratchanie Thosarat, and Dr Nigel Chang. My steep regional learning curve was aided by many of my fellow participants, and their company and that of the villagers made my Isaan experience an unforgettable one. My sincere thanks also go to, the then, Dr Bérénice Bellina and Ms Praon Silapanth, co-directors of the Khao Sam Kaeo archaeological mission. Not only was this my first foray into Southeast Asian protohistory, but the technological focus of the project meant I took to Peninsula metallurgy like a duck to water.

After four years of involvement in the archaeology of their country, I already owe a great debt to my Thai colleagues. I especially acknowledge the support and guidance of Ajarn Surapol Natapintu and Dr Rasmi Shoocondej, who have gone out of their way to facilitate my development as a Southeast Asian scholar. Khun Pira Venunan certainly merits a mention for his commitment and promise in regional archaeometallurgy, and also for the kindness and hospitality he has shown to me.

A cohort of regional specialists have also provided fine instruction and rousing encouragement: Dr Anna Bennett, Dr Ian Glover, Dr Elizabeth Hamilton, Professor Charles Higham, Dr Anna Källén, Dr Elizabeth Moore, and Dr William Vernon for starters, but special mention must be made of Dr Roberto Ciarla, Dr Fiorella Rispoli, and Dr Joyce White; who have all shared their homes, their food, and their wisdom with me over the last few years. Dr Elizabeth Hamilton, Professor Charles Higham, and Dr Joyce White deserve extra recognition for they generously allowing me to read and cite a number of manuscripts in press. As the reader will see, this thesis is (I hope) much the richer for having integrated the latest thinking on early Southeast Asian metal technologies.

I owe my thanks to Mr Phillip Conolly, Mr Simon Groom, and Mr Kevin Reeves for sample preparation and analysis training in the Wolfson Archaeological Laboratories, and also for monitoring my lab work during the course of my PhD. In the field of archaeological GIS and remote sensing, though I still have a great deal to learn, what knowledge I have is due to Dr Michael Abrams, Dr Andrew Bevan, and M. Georges Kozminski.

Also fundamental to the doctoral process were the shared learning experiences of my UCL archaeometallurgical contemporaries. I have benefited tremendously, both professionally and personally, from the company of Ms Lorna Anguilano, Mr Bastian Asmus, Dr Michael Charlton, Dr Claire Cohen, Ms Jane Humphris, Dr Fatma Marii, Dr Aude Mongiatti, and Dr Xander Veldhuisjen. In the wider field, I am grateful for the counsel offered by Dr Roger Doonan, Dr Emilien Burger, and Ms Eleni Silvestri.

My PhD began in late 2005, but in reality I have benefited from an outstanding level of doctoral supervision since I was accepted for the UCL programme in early 2004. Professor Vincent Pigott, Dr Marcos Martín-Torres, and Professor Thilo Rehren have individually and corporately gone far beyond the call of duty in enabling and smoothing my learning path. In the fields of analytical, regional, and theoretical archaeological wisdom, funding, and pastoral care, all expectations have been resoundingly surpassed. Indeed, Professor Pigott has cooked for me, lent me his clothes, taken me to hospital, and even introduced me to my wife! Though these scholars are, to a man, incredibly busy with administrative, research, and teaching duties, I have never once felt academically adrift, or anything other than a valued post-graduate member of the UCL archaeological community. I enjoy variety and change in my life, but the UCL Institute of Archaeology has a suite of qualities and strengths that have kept drawing me back. I can only hope that in the future, I may be as gracious a benefactor of student guidance as I have been a grateful recipient.

Talking of change. One expects a degree of personal development during the course of a PhD, but my life has turned upside down. I began my doctorate as a: selfish, long-haired, wannabe loner-biker; and I end it as a: slightly less selfish, short-haired, husband and father

living in Paris. Professor Pigott's original arrangement for me to visit Khao Sam Kaeo had unexpected consequences, and my world now revolves around Dr Bérénice Bellina-Pryce and our son Constantin - the 'Froggy-Rosbeef' clan of Southeast Asian archaeology. Though the ultrasound sessions didn't foresee it, Bérénice was surprised to find herself looking after two babies. I have been kept well-fed, clean-clothed (bathing being my own irregular duty), encouraged to play a little in the fresh air, and see my friends, but always allowed to concentrate on my work. What Bérénice has accomplished since June with Constantin, the household, and her own research, is lasting testimony to her character and natural aptitude for motherhood. I have already enjoyed six months of being a parent; now, this thesis done, I look forward to taking my share of the responsibility.

post scriptum, August 2009. Though I hope have now taken a greater share of the responsibility, I must also offer my thanks to my parents-in-law, Mme. Michèle Aschehoug, and M. Niels Aschehoug, as well as my siblings-in-law Mme. Blandine Gerenton, M. Henri Gerenton, whom have all helped take care of Constantin over the last year.

Chapter 1

Introduction

1.1 Thesis background, aims, objectives, and structure

Scientific archaeology in Southeast Asia is a maturing discipline, and although great strides have been made in the last forty years, many gaps remain in our understanding of the region's prehistory (e.g. Higham 2004). Southeast Asian archaeological research is typically split between two major geographical zones: that of mainland Southeast Asia,



Figure 1.1 - Regional political and relief map of Southeast Asia. Image: courtesy of the United States Central Intelligence Agency.

including Burma (Myanmar), Cambodia, Laos, Thailand (as far south as the northern Thai-Malay Peninsula), Vietnam, and southern PRC provinces, and those nations to the south, Malaysia, Singapore, and the rest of insular Southeast Asia (Figure 1.1). The present study concerns only the mainland zone which is usually considered part of the generic ‘Asian Old World’ (Pigott 1999b), and may have interacted with cultural transmission networks posited to have spanned Eurasia from the 4th-3rd millennium BCE onwards (e.g. Ciarla 2007a, Higham 1996, 2006, Linduff et al. 2000, Mei 2000, Pigott and Ciarla 2007a, Sherratt 2006, White 1988, 1997, White & Hamilton in press).

Due to various social and political factors (e.g. Glover 2003), the available archaeological evidence is overwhelmingly biased towards excavation and survey data from Thailand and Vietnam. The potential contribution of non-English language publications, ongoing, and forthcoming research in Burma (Myanmar), Cambodia, Laos, and the southwestern/western PRC could radically revise the prehistory of the region (e.g. Hudson 2008, Reinecke & Kuyen in press, Stark 2006, White 2008a). This geographical data bias is especially pronounced for early copper production (mining, smelting, refining, alloying, casting, and forging activities) with the evidence limited to northern Vietnam (e.g. Huyen 2004) and central and northeastern (e.g. Higham 2002) Thailand. Published evidence for extractive copper metallurgy (mining and smelting) is to date only available in Thailand: at Phu Lon on the banks of the River Mekong near Ventiane (e.g. Pigott & Weisgerber 1998) and the Khao Wong Prachan Valley [hereafter ‘the Valley’ may be used] (e.g. Pigott et al. 1997) at the southern end of the Loei-Petchabun Volcanic Belt which extends c. 400km northwards to Phu Lon (Figures 1.2, 3.2, & 3.3). Furthermore, of these two locales, only the Valley has furnished firm published evidence for prehistoric copper smelting, a vital step in the metallurgical production process¹.

This thesis comprises an archaeometallurgical investigation of prehistoric copper smelting in the Khao Wong Prachan Valley of central Thailand. The material studied came from the excavation of two sites, Non Pa Wai and Nil Kham Haeng, which are located only c. 3km apart and have an overlapping chronological sequence from c. 6/500 BCE to c. 300 CE. This period corresponds roughly to the Thai Iron Age, though there is evidence for occupation at these sites from c. 2300 BCE (Thai Neolithic at Non Pa Wai) and c. 1100 BCE (Thai Bronze Age at Non Pa Wai and Nil Kham Haeng) respectively (see Figure 1.3). As Non Pa Wai and Nil Kham Haeng currently provide the only documented evidence

1 The term ‘technology’ is employed in a holistic sense to encompass all technical and social aspects of metallurgy (see Chapter 3). ‘Copper-base metallurgy’ is a general term for the production and consumption of copper metal and its alloys (e.g. bronze, arsenical copper, leaded copper, leaded bronze).

for industrial-scale copper smelting in prehistoric Thailand and Southeast Asia, they are central to any discussion of regional copper-base metallurgy. The major research aim of the present study was to better understand the development of Valley copper smelting technologies over a period of production spanning c. 800-900 years and two neighbouring locales, within an anthropologically-informed theoretical framework.



Figure 1.2 - Political and relief map of Thailand with the Valley marked by a red circle. Image: courtesy of the United States Central Intelligence Agency, modified by the author.

The production techniques practiced by Iron Age metalworkers at Non Pa Wai and Nil Kham Haeng have left enormous quantities of metallurgical material culture - namely mineral, slag, and technical ceramic. The metallurgical assemblages and the structure of the archaeological deposits from Non Pa Wai and Nil Kham Haeng are quite dissimilar, suggesting that the copper extraction technologies employed at each site may have changed over the course of the Iron Age production period. In order to comprehend these technological changes two principal research objectives were established:

1. To generate detailed technological reconstructions of the Iron Age copper smelting activities evidenced at Non Pa Wai and Nil Kham Haeng based upon the available archaeological evidence and using an appropriate methodology incorporating laboratory analyses and experimental field-testing. Accordingly, a total of 76 excavated samples of mineral, crucible, 'furnace', 'slag-skin', and slag from Non Pa Wai and Nil Kham Haeng were analysed in hand specimen, microstructurally by reflected-light microscopy and scanning electron microscopy (SEM), and chemically by polarising energy dispersive x-ray fluorescence spectrometry (P]ED-XRF) and scanning electron microscopy with energy dispersive x-ray fluorescence spectrometry (SEM-EDS). The results of these archaeometallurgical laboratory analyses were used to produce technological reconstructions of the smelting techniques as practiced by Iron Age metalworkers from Non Pa Wai and Nil Kham Haeng. Furthermore, as the Nil Kham Haeng reconstruction was thought to incorporate a perforated 'furnace' suggestive of a wind-powered metal technology, this configuration was subjected to full-scale experimental field testing to assess its feasibility.
2. To synthesise the technological reconstructions from Non Pa Wai and Nil Kham Haeng into a diachronic account of Iron Age Khao Wong Prachan Valley copper production, structured by theoretical approaches to ancient technologies. The interpretation offered is one of a gradual improvement in copper smelting technology between 6/500 BCE and 300 CE at Non Pa Wai and Nil Kham Haeng, with increasing technical proficiency being offset by a significant increase in the labour cost of production.

Thesis Organisation

The next section of this introductory chapter provides a general overview of later prehistoric archaeology in Thailand, in particular the major sites of the Bronze and Iron Ages. Recent thinking on the nature of prehistoric Thai social complexity is presented, with a summary of White's (1995) application of the 'heterarchy' concept and White & Pigott's (1996) discussion of 'community specialisation' in craft production. The third section of the chapter concentrates on previous research on prehistoric Thai metallurgy, beginning with

a discussion of the predominant ‘origins of metallurgy’ debate, before introducing the major evidence for early copper-base metallurgical production in northeast and central Thailand. This provides the regional context for the study’s focus on the Khao Wong Prachan Valley, which is discussed in detail in Chapter 2.

Chapter 2 presents the current archaeological understanding of the prehistoric Khao Wong Prachan Valley sites of Non Pa Wai and Nil Kham Haeng, focusing on the Iron Age copper production evidence, and providing the contextual understanding for the mineral, technical ceramic, and slag samples studied. Previous archaeometallurgical research carried out in the Valley by Anna Bennett, William Rostoker, Dong Ning Wang and Michael Notis is reviewed and contrasted to the aims and objectives of the present study, and finally the present study’s sampling strategy is presented.

Chapter 3 provides a summary of the theoretical approaches which underpin the current study, derived from the ‘Anthropology of Technology’ literature. Most important are the francophone ‘*chaîne opératoire technique*’, and anglophone ‘technological choice’ and ‘technological style’ concepts. Employed together, this ‘technological approach’ structured the investigation of early Valley metallurgy and constituted the framework for data interpretation.

Chapter 4 introduces the analytical techniques (polarising energy dispersive x-ray fluorescence, optical microscopy, and scanning electron microscopy with energy dispersive x-ray fluorescence) and laboratory methodologies used to study the Valley metallurgical samples, as well as the statistical manipulations used to interpret the data.

Chapter 5 contains the results and interpretation of archaeometallurgical analyses carried out on production remains from the early Iron Age site of Non Pa Wai. The mineral, technical, ceramic, and slag samples are discussed in turn, with a case gradually being made for a variable and low technical proficiency copper smelting process being carried out within a crucible.

Chapter 6 provides the analytical data and technological reconstruction of the copper production process at the later Iron Age site of Nil Kham Haeng. As per Chapter 5, each metallurgical material is evaluated sequentially, but in this instance the evidence suggests a more standardised and skilled technology, with the smelt being performed in a chaff-

tempered clay-lined pit.

Chapter 7 details the purpose, reasoning, and outcome of an experimental archaeometallurgy campaign carried out at Fivè Palafitto (northern Italy) during September 2007 in a collaboration with archaeometallurgical research teams from France and Italy. This field testing suggests that the earlier reconstructions of a wind-powered copper smelting technology in the Iron Age Khao Wong Prachan Valley require substantial revision.

Chapter 8 employs the theoretical approaches to ancient technologies introduced earlier to synthesise to extent possible the laboratory-based copper smelting reconstructions of chapters 5 and 6 with the experimental insights of chapter 7 to produce a tentative account of technological change in the late prehistoric Khao Wong Prachan Valley. The combined results may be interpreted as a trajectory of increasing technical proficiency which, importantly, may have stemmed from a local innovation of smelting technology from existing founding experience.

Chapter 9 concludes the thesis by summarising the results of the present study, before contrasting the Khao Wong Prachan Valley data with the northeast Thai secondary production evidence, and discussing the potential significance of Valley metallurgy to the recent 'Rapid Eurasian Technological Expansion Model'. Possible avenues for future Southeast Asian archaeometallurgical research are also briefly outlined.

Appendix A contains a catalogue of the mineral, slag, and technical ceramic samples studied, comprised of photographs and tables with macroscopic observations.

Appendix B presents the complete, processed but un-normalised, compositional data from [P]ED-XRF and SEM-EDS analyses of the Khao Wong Prachan Valley samples.

Appendix C is an archive of field notes and thermocouple data from the 2007 experimental archaeology campaign in Fivè, Italy.

1.2 Overview of the later prehistory of Thailand

Although the present study concerns industrial copper production in what are currently thought to be ‘Iron Age’ (c. 6/500 BCE - c. 300 CE) Khao Wong Prachan Valley contexts, an overview of the preceding periods of Thai prehistory is necessary to understand the socio-cultural context of Valley copper smelting. To date, the predominant objectives of prehistoric Thai research have been the identification of chronological boundaries between major sociopolitical (e.g. egalitarian bands versus ranked tribes), subsistence (e.g. hunter/gathering versus farming), and technological (e.g. bronze versus iron)

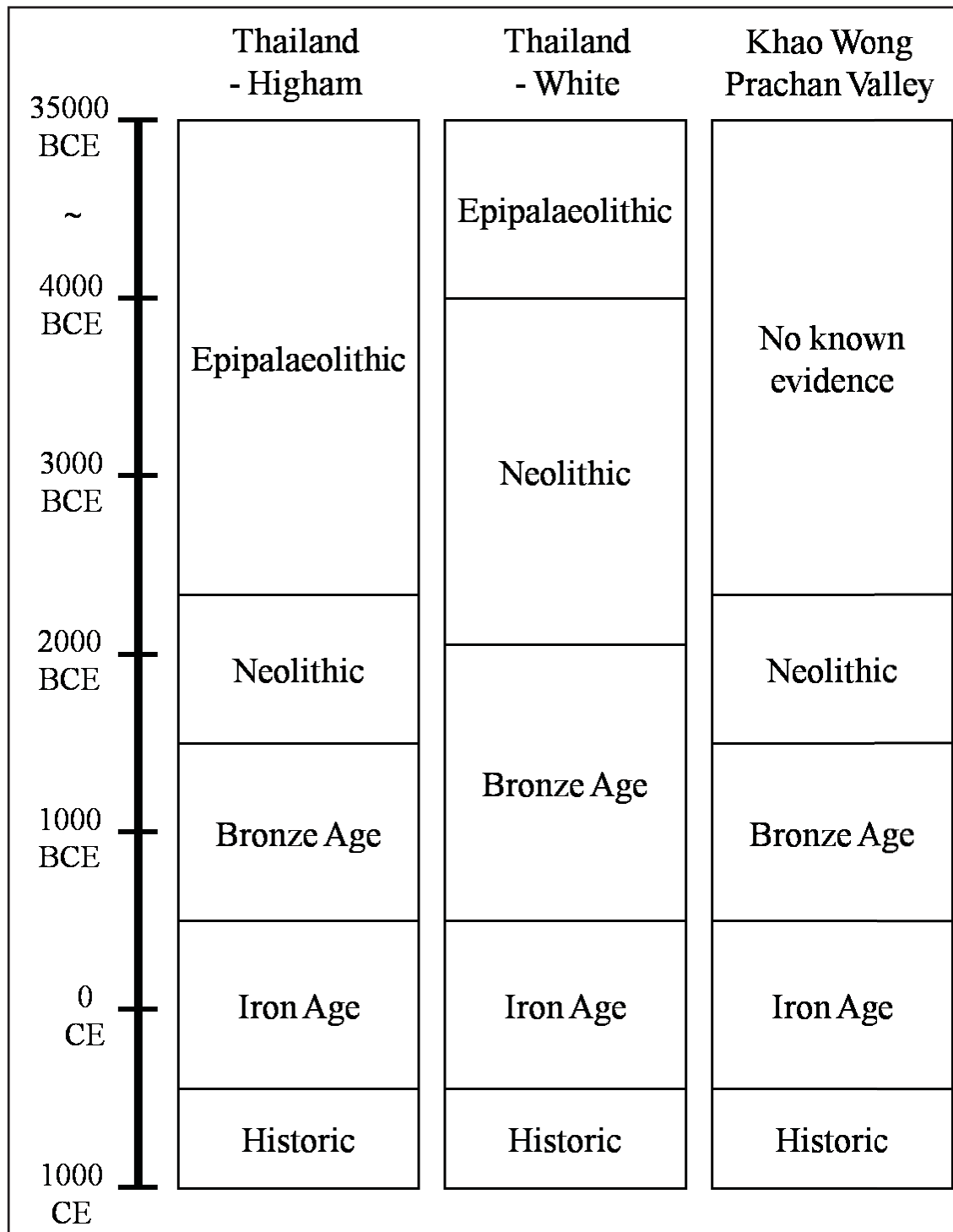


Figure 1.3 - Diagram outlining the prevailing chronologies for prehistoric Thailand by Charles Higham (e.g. Higham & Higham 2009) and Joyce White (e.g. 2008b), as well as the current Khao Wong Prachan Valley sequence. The capacity for significant regional variation must be emphasised and the marked boundaries are neither absolute nor certain. Image: author.

changes, and the assessment of whether these changes were the result of endogenous development, exogenous contact, or exogenous migration (e.g. Higham & Higham 2009, Higham in press a). Figure 1.3 depicts the major chronological periods which have been defined in Thailand generally and the Khao Wong Prachan Valley in particular. There are currently two competing Thai prehistoric chronologies, superseding the ‘General Period’ system offered by Donn Bayard in 1984, which have been labelled in Figure 1.3 for their chief proponents, Charles Higham (e.g. Higham & Higham 2009) and Joyce White (e.g. J. White 2008b). As can be seen, the discrepancy between the boundaries offered for the beginning of the Thai ‘Neolithic’ and ‘Bronze Age’ are quite significant at c. 2700 years and c. 1000 years respectively. Whilst part of this variance is almost certainly attributable to the number, provenance, and sample hygiene of radiometric determinations (see Higham & Higham 2009: 132-133), it is also extremely likely that apparent archaeological non-conformity partially reflects complex historical reality (see ‘Hierarchy versus heterarchy’ section below). As such, the labelling of periods as ‘Bronze Age’ or ‘Iron Age’ in this thesis is largely due to long-established archaeological practice (e.g. Taylor 2008a, Trigger 2006) rather than any significant proven relationship between particular technologies and cultural change (cf. White 2002, Higham & Higham 2009); the use of qualifying apostrophes will stop here unless special emphasis is intended. The critical point for the reader is that much of our understanding of Thai prehistory is in flux and that due to a relatively low and patchy coverage of archaeological data, all interpretations and hypotheses are necessarily preliminary.

1.2.1 The Thai Epipalaeolithic and Neolithic

Following colonisation by hominins at least 1 million years ago (e.g. Higham & Thosarat 1998: 23), the geographic area encompassed by present day Thailand is thought to have been inhabited by *homo sapiens* groups from around 35,000 BCE (e.g. Bellwood & Glover 2004: 13). The data for these Final Pleistocene human activities is largely limited to rock shelters in northwest Thailand (e.g. Gorman 1970, Shoocondej 2006), but they mark the earliest evidence for an Epipalaeolithic gathering and hunting lifestyle which lasted in the area for tens of thousands of years, and, in some remote areas, to the present day (Higham 1989).

Given long-standing associations between farming, economic surplus, and the ‘rise of the state’ in Southeast Asia (e.g. van Lier 1980), the appearance of rice and millet production as well as animal husbandry has been accorded great importance in accounts of Thai prehistory (e.g. Higham 2002: 83, Higham & Higham 2009). The dating of the introduction of farming, and hence a Thai ‘Neolithic’ lifestyle, remains unclear, but on competing archaeological (e.g. Higham & Higham 2009, White 1997), genetic (e.g. Fuller & Qin

2009), and linguistic (e.g. Bellwood 2005, Sanchez-Mazas *et al.* 2008) evidence varies between the 5th millennium BCE and the 2nd millennium BCE (Figure 1.2). However, post Gorman's (1969) claim for an indigenous domestication of tuber and fruit plant species at Spirit Cave, it is now widely agreed that a 'Neolithic cultural package' including agriculture, livestock management, and decorated pottery was physically introduced to Thailand by migrating social groups ultimately from the Yangtze Valley area of the present day Peoples' Republic of China (e.g. Bellwood 2005: 128-145, Higham 1996: 309, Higham & Higham 2009: 138, Sanchez-Mazas *et al.* 2008, Rispoli 2007). The general image offered is of the gradual dispersion of migrant farming communities into Thai territories via the Southeast Asia's riverine networks, "encountering and interacting" with existing gatherer/hunter groups (Higham 2006: 16-17).

The evidence for Neolithic occupation in mainland Thailand is limited to about 20 sites amongst the most well-known being in northeast Thailand: Ban Chiang, Non Nok Tha, Ban Lum Khao, Ban Non Wat; in central Thailand: Khok Charoen, Ban Tha Kae, Non Pa Wai; and in west-central Thailand: Ban Kao and Sai Yok (Higham 2002: 87). The data predominantly derive from the excavation of cemeteries, which provide evidence for long-distance exchange in exotica (e.g. marine shell) and of variable funerary practice (in terms of artefactual accoutrements). Settlement evidence is rarer, but data available from Ban Lum Khao and Ban Non Wat in the Upper Mun River Valley (northeast Thailand) indicate the presence of domesticated dogs, pigs, and water buffalo (Higham 2004: 50-51). The site of Khok Phanom Di, c. 70km ESE of Bangkok, suggests the continuation of a gathering and hunting mode of subsistence into the 2nd millennium BCE and that the population co-existed to some degree with Neolithic farming communities (Higham & Thosarat 1998: 44-63). Higham's distinction between gatherer/hunter and Neolithic groups has been disputed (e.g. White 1995: 103) as we do not at present know whether the apparent difference in subsistence practice constitutes a real cultural boundary, as Khok Phanom Di also provided substantial evidence for pottery consumption and possibly production, a 'Neolithic' cultural trait. Higham (1989: 87) also argues, based on the variable distribution of grave goods at Khok Phanom Di, that some nascent degree of differentiation in social status can be inferred within the population, at least in so much as we can glean from funerary practices (cf. Carver 2005, Olivier 1999, Parker-Pearson 1999, Ucko 1969).

1.2.2 The Thai Bronze Age

The Bronze Age is heralded by the appearance of copper-base metallurgical assemblages (metal artefacts, crucibles, moulds, and furnace features) in 2nd millennium BCE funerary and occupation contexts in central and northeast Thailand (e.g. White & Hamilton in press).

However, this juncture appears to be highly variable (Figure 1.3), with a discrepancy of up to c. 700 years between the earliest reasonably substantiated Thai evidence for copper-base metallurgy, which is dated to c. 1700 BCE at the northeastern site of Ban Chiang (e.g. J. White 2008b, though White sees c. 2000 BCE as an appropriate starting point), and that discerned c. 1000 BCE at Ban Non Wat, only c. 260km SSW (e.g. Higham in press a). It should be recalled that prehistoric Thailand, and Southeast Asia in general, was not a flat and empty landscape over which copper-base technologies could steadily encroach, sweeping away pre-existing Neolithic lifestyles. The proliferation of copper-base behaviour would have encountered resistance both geographical and cultural, and depended utterly on sustained social interaction; especially for the transmission of complex production technologies in as yet unknown learning environments (e.g. Bellina 2007, Eerkens & Lipo 2005, Gosselain 1992, Henrich 2001, Keller 2001, Keller & Keller 1996, Roux *et al.* 1995, Wenger 1998, A. White 2008, White & Hamilton in press). As per the Danube and Rhine (e.g. Davisona *et al.* 2006, Shennan 2000), it is widely acknowledged that Southeast Asia's riverine networks were likely to be "the principal arteries for communication and movement" (Higham 2006: 17), especially when compared to the considerable challenge of negotiating the region's dense forests and mountain ranges (prior to heavy agricultural clearance for the former). Though this logical observation, largely based on the experiences of 18th and 19th century European travellers (e.g. Crawford 1830, Ehlers 2002, Mouhot 2000, Pallegoix 1999) may not be historically absolute, it provides a robust, if partial, explanation for the differential appearance of copper-base technologies between the Ban Chiang Culture Area and the Upper Mun River Valley. These locales lie only a few hundred kilometres apart in a straight line, but although their current route will have altered in the intervening millennia, communication via the Huai Luang-Mekong-Mun, Songkhram-Mekong-Mun, or Chi-Mun rivers equates to around a thousand kilometres by current meanders (roughly calculated by a cumulative distance paths on Google Earth™). Thai copper-base technologies are currently agreed not to have an indigenous origin (e.g. Pigott & Ciarla 2007), but there remains considerable debate over when and how they were transmitted to prehistoric Thailand (see the 'Origins of metallurgy' section below).

Although the artefact population is rather limited and biased towards funerary assemblages, 2nd millennium BCE copper-base metal artefacts have what might be interpreted as utilitarian (e.g. axeheads, fish hooks) as well as ornamental (e.g. bangles, rings) typologies (e.g. Higham 2002), suggesting that copper alloys were used for eminently practical purposes as well as possibly display or ritual uses (e.g. White & Hamilton in press). The Bronze Age Thai sites where these artefacts are found are thought to generally have been less than 5ha, but we have little idea of their population size or habitation structures (e.g. Higham 2002: 167). Amongst the major Thai sites with Bronze Age deposits are Non

Nok Tha, Ban Chiang, and Ban Na Di, Ban Lum Khao, Ban Non Wat, Nong Nor (e.g. Higham 2002), and those in and around the Khao Wong Prachan Valley (see Chapter 2); all of which are concentrated in central and northeast Thailand, as well as in the Bangkok embayment (Nong Nor). Of these Non Nok Tha and Ban Chiang are probably the best known, due both to their early (1960s and 1970s) discovery in Southeast Asian archaeological research, but also for their now rejected 4th millennium BCE dates for Bronze Age evidence (see section 1.3.1 below). Although physically small, both sites are extremely important for our understanding of the Thai Bronze Age, with evidence for both occupation and funerary activities in 2nd and 1st millennium BCE contexts. Inhabitants of Bronze Age Non Nok Tha appear to have been familiar with using and founding copper-base artefacts due to the presence of metal artefacts, crucibles, moulds, and casting debris (e.g. Higham 2002: 128-131), as was the contemporary populace at Ban Chiang (e.g. J. White 2008b, see section 1.3.2 below for further detail on the sites and their metallurgical evidence). The occasional recovery of marine shell bracelets and beads provides limited evidence for long-distance exchange at Non Nok Tha, but paddle-and-anvil made pottery, stone adzes, and animal bone appear more frequently (e.g. Higham 2002: 128-131).

Heading south down the Khorat Plateau, Ban Na Di is another important site, where investigations in the early 1980s uncovered two areas of a Bronze Age cemetery dated c. 900 to c. 400 BCE (e.g. Higham 2002: 134-139), in addition to significant metallurgical production evidence (see section 1.3.2). Men, women, and children were buried in superimposed rows, perhaps relating to ancestral groups. Burial goods consisted of pottery with and animal bone, as well as exotic stone bangles and marine shell beads (*ibid.*). It was noted that although some typological similarities could be discerned, Bronze Age Ban Na Di pottery traditions differ significantly from those at both Non Nok Tha and Ban Chiang (*ibid.*). Although copper-base artefacts were never common, finds of bronze bracelets and anklets did seem to become increasingly frequent in Ban Na Di's upper phases. Whilst acknowledging the interpretive limitations of the site's small exposure, Higham (2002: 139) suggests that the clustering of burials with greater burial wealth at Ban Na Di is insufficiently clear to identify them as a separate social stratum.

In the midst of the Khorat Plateau, Ban Lum Khao has provided Bronze Age funerary evidence, dated c. 1400 to c. 500 BCE, subsequent to its Neolithic occupation (e.g. Higham 2002: 142-146). Excavators identified four burial phases of men, women, and children with varying orientations but generally ordered in rows. The burial assemblage was dominated by pottery but also included, shell beads and bangles, stone adzes, and ceramic spindle whorls (*ibid.*). Notably, no copper-base artefacts were recovered from the site, despite the presence of secondary metallurgical production evidence (see section

1.3.2 below). Statistical analysis of the funerary data suggested there was no significant difference in burial ritual according to sex, age, or location until the final phase 4, bordering the Iron Age (e.g. Higham 2002: 146). Conversely, Higham (2004: 55, 2009) suggests that the nearby site of Ban Non Wat does present strong evidence for social stratification c. 1000 BCE due to the presence of ‘superburials’; inhumations accompanied by enormous quantities of burial goods.

South again on the eastern margins of the Gulf of Siam, the c. 400m² exposure of Nong Nor’s Bronze Age cemetery provides a sample of 166 burials of men, women, and children in two spatially distinct groups (e.g. Higham 2002: 147-151). Burial goods included pottery, animal bone, marble bangles, shell beads, copper-base artefacts, and semi-precious stone ornaments. Whilst the excavators noted considerable variation amongst the inhumations, again there continues to be no evidence suggesting systematic differentiation in burial practice according to age or sex (*ibid.*).

As per the arrival of Neolithic farming practices, the consumption and production of copper/bronze has often been considered an important development in Thai prehistory (e.g. Higham 1996, in press a) due to the traditional association of hierarchical socio-political configurations with emerging copper-base technologies in prehistoric western Asian societies (e.g. Childe 1936: 157-201; 1942; 1951: 26-27; 1958), as epitomised in Southeast Asia by Muhly’s (1988: 16) comment that, “[i]n all other corners of the Bronze Age world ... we find the introduction of bronze technology associated with a complex of social, political and economic developments that mark the rise of the state. Only in Southeast Asia ... do these developments seem to be missing.” However, it is not clear that the evidence for incipient prehistoric Thai copper-base metallurgy is associated with any significant contemporary shift in socio-political configurations (e.g. White 1995). It has been suggested (e.g. Bacus 2006: 113) that the appearance of bronze in Thailand need not have implied its immediate and universal cultural incorporation and metal could have been selectively assimilated within existing Neolithic lifestyles and material culture, without implying any significant shift in social complexity (cf. Higham & Higham 2009: 126). This is especially likely as the archaeological record, warped though it may be by general factors like funerary assemblages and metal-specific issues like recycling, indicates that copper/bronze was probably not consumed in great quantities, nor was it uniquely associated with artefacts for social display or possible ritual use (e.g. Higham 2002: 166, White & Hamilton in press).

1.2.3 The Thai Iron Age

However, it is to some extent agreed that a discernable shift in Thai social complexity is evidenced around the mid 1st millennium BCE, the generally accepted commencement of the Iron Age (Figure 1.3). As compared with the appearance of Thai copper-base artefacts, the arrival of iron artefacts in contexts from northeast, central, west-central, and peninsular Thailand is remarkably consistent at c. 500 BCE (e.g. Higham 2004: 169). Other than iron artefacts, the Thai Iron Age transition is characterised by the development of settlement size hierarchies, defensive and/or hydraulic earthworks, and the marked differentiation of individuals and groups in burial traditions (e.g. Higham 2002). It has been argued that the increased mechanical performance of iron tools enabled agricultural intensification due to improved forest clearance, agricultural land preparation (ploughing), and water management (earthworks) (e.g. Higham 1989, 2002), an essentially Childean concept (e.g. Childe 1951: 26-27). This potential for the increased production of foodstuffs could have enabled some settlements to grow, with the burden of subsistence provision falling on a decreased proportion of the community, freeing the remainder to engage in craft activities, the redistribution of goods, and possibly political machinations (e.g. O'Reilly 2008). Thailand during the late 1st millennium BCE is thought to have been experiencing increasing contact with modern day China, India, and other parts of mainland and insular Southeast Asia, though it did not fall under the direct influence of Imperial Han China (e.g. Higham 2004: 57). Therefore, there are numerous possibilities for multi-lateral socio-economic and socio-political stimuli to have partially affected the changes seen in the Thai Iron Age (e.g. Bellina & Glover 2004, Higham 2002: 224-227, Higham 2004: 57).

The northern Khorat Plateau provides good evidence for settlement hierarchy with a cluster of sites ranging from Ban Chiang Han (38ha) and Non Chai (18ha) to what are thought to be the much smaller contemporary sites of Ban Chiang, Ban Na Di, and Don Klang (2ha) (e.g. Higham 2002: 187-192, Higham & Thosarat 1998: 169). These sites are uniformly located in areas probably suitable for wet rice agriculture in Antiquity, thus suggesting that increased food production played an important role in social change in the Thai Iron Age (e.g. O'Reilly 2008: 382, though cf. Onsuwan-Eyre 2006 who attributes some of this patterning to survey bias). Additionally, a distinct change in material culture c. 300 BCE is noted at both Ban Chiang and Ban Na Di as tools begin to be made exclusively in iron rather than bronze and pottery traditions appear to have been modified drastically (e.g. Higham 2002: 189-190). Ornaments at both sites are increasingly made of leaded bronze and high-tin bronzes appear at both sites suggesting long distance exchange with cultures to the southwest (see below for 'Ban Don Tha Phet' and 'Khao Sam Kaeo').

The Mun River Valley of the southern Khorat Plateau is another major source of evidence for socio-economic and socio-political change during the Thai Iron Age (e.g. Higham

2004: 60-64, Higham *et al.* 2007). The earliest levels at Noen U-Loke suggest the site was still quite small and that the population's burial traditions were relatively undifferentiated despite the incorporation of varied grave goods like ornaments and tools made from iron and bronze, tiger teeth, glass and hardstone beads, as well as animal remains and substantial quantities of rice (e.g. Higham 2004: 61). The fourth phase, probably dated to c. 100 to c. 300 CE, documented a big leap in the quantity and range of burial offerings, and the presence of at least one very rich individual in each cluster of inhumations. Some of the bodies had hundreds of bronze ornaments as well as precious metal jewellery, an accumulation of funerary wealth that Higham (2004: 62-3) suggests may have been due to the intensive local production of salt and iron, in addition to local bronze casting industries (see section 1.3.2 below). This seeming period of prosperity comes to an end in the fifth and final phase, with ornamental grave goods being replaced by iron tools and weapons, possibly indicating increasing agricultural intensification and violence due to growing competition with newly founded sites in the neighbourhood (*ibid.*). Geoarchaeological investigations of Noen U-Loke's earthworks have dated them to the later Iron Age, c. 100 to c. 500 CE, and attribute to them a predominantly water management function. However, changes in the routes of local sources, possibly caused by deforestation and subsequent silting, are thought to have impacted Noen U-Loke's agricultural capacity and the site was abandoned soon after (*ibid.*).

Ten kilometres southeast of Noen U-Loke, the Iron Age settlement mound of Non Muang Kao covers c. 50ha adjacent to an ancient river channel (e.g. Higham 2002: 208-210, Higham *et al.* 2007). The site appears to have been occupied from c. 50 BCE until the mid 1st millennium CE and the 11 inhumations excavated bear strong material culture similarities to those at Noen U-Loke, as does the presence of earthworks probably designed to increase water retention for agriculture (*ibid.*). Likewise, the nearby site of Ban Non Wat has a substantial Iron Age cemetery and evidence for occupation from c. 420 BCE to c. 500 CE (Higham 2008, Higham & Thosarat 2006). The site's extensive hydraulic earthworks date were first constructed at the beginning of this period and the settlement came to cover c. 7-12ha (Charles Higham & Nigel Chang pers. comm.). The high density of the burials suggests an escalation in population size at Ban Non Wat, which was now also a centre for iron forging, bronze casting, cloth weaving, and pottery manufacture (Higham & Higham 2009: 138).

During the late Thai Iron Age large quantities of glass and hardstone beads and occasional high tin bronzes throughout central and northeast Thailand are thought to represent imports or influences from the Indian subcontinent (e.g. Bellina & Glover 2004). These artefact types were especially well represented at Ban Don Tha Phet in west-central Thailand

where cemetery deposits also indicated connections to Vietnam and the Philippines with the recovery of bicephalous jade ornaments known from the contemporary maritime Southeast Asian world (e.g. Glover 1990). Similarly, recent excavations at the Upper Thai-Malay Peninsula site of Khao Sam Kaeo, dated c. 400 BCE to c. 100 CE, provide not only substantial evidence for intense cultural exchange with South Asia in the form of hard stone ornaments, rouletted pottery, and high tin bronze bowls, but there is also the suggestion of contact with Han China due to the recovery of stamped pottery, seals, and bronze mirror fragments, in addition to materials indicating exchange with the insular and littoral Southeast Asia (e.g. Bellina & Silapanth 2008). The site extends over up to 55ha and has a well-documented network of defensive and hydraulic earthworks, which would probably have involved significant coordinated labour in their construction and maintenance (*ibid.*). Though detailed burial evidence is currently lacking, Khao Sam Kaeo presents many of the hallmarks of a major Thai Iron Age site i.e. long-distance exchange, increased size, and possibly political centralisation.

1.2.4 Hierarchy versus heterarchy

The Thai Iron Age has typically been viewed as the final staging ground for the emergence of ‘Indianised’ states in the mid 1st millennium CE, as part of a developmental increase in social complexity from the Thai Neolithic and Bronze Age (e.g. Bellina & Glover 2004, Higham 2002, Higham & Thosarat 1998: 170). However, in 1995 an influential article was published, challenging not so much the evidence for that complexity, but the way in which the data may be perceived and interpreted through the lens of ‘heterarchy’ rather than the traditional ‘hierarchical’ perspective (White 1995). Regional proponents of the heterarchy concept (e.g. O’Reilly 2000, 2003, White 1995, White & Pigott 1996) emphasise a degree of exceptionalism in Southeast Asian socio-economic and socio-political relationships, such that the traditionally expected progression from band-tribe-chieftdom-state, normally equating chronologically to Neolithic-Bronze Age-Iron Age-Historic, can be argued to not fit the Thai archaeological data. Moreover, White (1995) draws upon a wide range of historical and ethnographic data to support her suggestion that a broadly ‘heterarchical Thailand’ can be discerned from prehistory to the recent past.

A major difference between a heterarchical and hierarchical approach concerns the location and transmission of power within a society (*ibid.*). White (1995: 103) suggests that hierarchical approaches assume the increasing centralisation of economic, military, and ideological power within ever more formalised socio-political structures. Conversely, heterarchy emphasises the potential for power to be diffuse, shifting, and negotiable, as well as largely attributable to the historically situated performance of individual leaders rather than uniformly inherited (*ibid.*: 104). As such it can be suggested that even

Angkor, the archetypal historical Southeast Asian state, had “strikingly chiefdom-like even big-man-like-qualities” due the frequently non-hereditary transmission of power and the importance of personal leadership qualities to attain it (*ibid.*: 103). In prehistoric Thailand, White’s (1995) heterarchical perspective stresses the sparseness and ambiguity of evidence for individuals or societies exerting authority or influence over others.

A major tenet of heterarchical thinking is “cultural pluralism” (White 1995: 105-106), which is well evidenced in the distinct localisation of material culture in Thailand between c. 2000 and c. 200 BCE. Focusing on the nearby (c. 25km) sites of Ban Chiang and Ban Na Di, White (*ibid.*) notes that pottery traditions, animal remains, ornaments, figurines, and burial rituals differed significantly between apparently contemporary deposits. Indeed this distinct regionalism is one of the reasons why there is still no broadly agreed Thai ceramic relative chronology to cross date many of the country’s sites which lack radiocarbon determinations (White & Hamilton in press). It is only at the end of the 1st millennium BCE that wider scale pottery traditions seem to appear, with, for example, ‘Phimai black’ wares recovered from late prehistoric sites across the Upper Mun River Basin area (e.g. O’Reilly 2008: 385).

Although the general recognition of uniformly small Neolithic and Bronze Age communities being superceded by an Iron Age settlement size hierarchy is accepted by White (1995), she does not accept that size variation automatically equates to smaller sites being dominated by the large. White (1995: 111) argues that there is little evidence for violent conflict in prehistoric Thailand and that the historical data show a tendency amongst the region’s numerous ethnic and cultural groups for political problems to be resolved either diplomatically or by strategic alliances rather than the unilateral aggression that might be associated with a hierarchical society. Furthermore, it could be argued that the types of weapons typically recovered from Bronze and Iron Age Thai sites, spear heads, arrow heads, and knives, are not unambiguously martial and could equally have been used for hunting activities. Indeed, even the arrowhead recovered from the spine of a male inhumation at Iron Age Noen U-Loke (e.g. Higham *et al.* 2007: 606) could arguably have been the result of a hunting accident rather than warfare.

A commonly considered aspect of hierarchical societies is the control of production and distribution of goods by elites as a means of garnering wealth and power, and it is argued (White 1995: 106-108, White & Pigott 1996) that this social strategy is unevidenced in prehistoric Thailand. Not only do individual communities often appear to have had distinct material culture traditions, suggesting that the imposition of production by external ‘others’

was weak at least, there is also the frequent duplication of relatively specialised industries like pottery making, bronze casting, iron forging, and marble and shell ornament production in neighbouring communities, all indicative of a generally decentralised economy with no apparent restriction on technical knowledge (White & Pigott 1996: 158). Even where highly specialised production occurs in the mining and smelting of copper within the Khao Wong Prachan Valley of central Thailand (see Chapter 2), there is every reason to believe that this was the independent initiative of local people, perhaps ‘subsistence trading’ metal for foodstuffs due to their agriculturally marginal environment (Mudar & Pigott 2003). The heterarchical assessment of prehistoric Valley copper production, guided by Costin’s (1991, 2001) framework for interpreting craft production systems, is that of ‘specialised craft communities’ (White 1995, White & Pigott 1996, see Chapter 3). The evidence they cite for this derives from Pigott *et al.*’s (1997, then in press) reconstruction of numerous small scale extractive metallurgical operations probably representing individuals or kin groups at most, which though their combined metal output would have been substantial, individually required little capital investment in apparatus, but a substantial commitment in labour (White & Pigott 1996: 165-167). Archaeological investigations in the Khao Wong Prachan Valley have not uncovered any evidence for a central administrative site or structure for the modest 3-5ha smelting locales, nor earthworks which might serve for defensive purposes. The presence of numerous copper artefacts in Nil Kham Haeng burials suggests that local people rather than external elites were in effective control of product distribution (*ibid.*). Furthermore, the presence of macroscopically different production technologies at the chronologically contiguous prehistoric smelting sites of Non Pa Wai and Non Pa Wai (see Chapter 2) perhaps indicates a degree of ‘cultural pluralism’ within the area, which further supports the heterarchical ‘specialised craft communities’ interpretation of production for unrestricted regional demand rather than the alternative restricted production for elite demand ‘dispersed corvée’ (Clark 1995); an aspect addressed later in this thesis.

Prior to the Thai Iron Age when funereal evidence for status differences became more apparent at some sites, White (1995) argues that variation in burial wealth within Neolithic and Bronze Age communities seems to be continuous and individualistic rather than modal and systematic. This might suggest the absence of permanent social stratification and that individuals seem to be more important than institutions in early Thai societies. As Bacus’ (2006) analysis of the available Non Nok Tha data indicates that females and older males may be tentatively discernable as separate status groups, reflecting the nuanced attribution of respect and authority within prehistoric Thai groups. The potential for grave wealth to reflect either inherited or acquired status during an individual’s lifetime was long ago recognised by Higham (1989: 153), but he does believe that White’s (1995) heterarchical approach is now undermined by the presence of c. 1000 BCE “superburials” at Bronze

Age Ban Non Wat, which he argues to represent the inhumations of “aristocrats” within a local hierarchical social system (Higham 2009). It remains to be demonstrated that feudal power structures existed in the Bronze Age Upper Mun River Valley and the heterarchical emphasis on “cultural pluralism” (White 1995: 105-106) could equally be employed to explain the apparent variability between different areas of prehistoric Thailand.

1.3 Prehistoric Thai metallurgy

The following section is intended to provide a broad contextualisation for the present study’s focus on copper smelting by discussing previous archaeometallurgical discourse in Thailand, and summarising those Thai sites with evidence for the straddling copper production activities of mining and founding; these latter sites may be considered likely consumers and redistributors of Khao Wong Prachan Valley metal.

1.3.1 The ‘origins of metallurgy debate’

For over four decades regional archaeometallurgical discussion has focused on the dating and origin of Thailand’s earliest copper-base technologies, a technological horizon which has been accorded great significance in accounts of regional prehistory, as well as being fervently disputed (Bacus 2006, Bayard 1972, 1980, 1981, Ciarla 2007a, Higham 1988a, 1989, 1996, 2002, 2004, 2006, in press a, Higham & Higham 2009, Loofs-Wissowa 1983, Muhly 1981, Pigott & Ciarla 2007, Sherratt 2006, Stech & Maddin 1988, White 1982, White 1988, J. White 2008b, White & Hamilton in press). The import attributed to Thai metallurgy is partly derived from traditionally assumed correlations between metallurgy and “major cultural changes” (e.g. Higham & Higham 2009: 126), but is also due to perceived evidence for a second, post-‘Neolithic’, wave of long-range social interactions with communities in the present-day Peoples’ Republic of China and beyond. (e.g. Ciarla 2007a, Higham in press a, Pigott & Ciarla 2007, White & Hamilton in press). This long-term concentration of scholarly resources may also be seen as an artefact of the international interest stimulated during the 1960s and 1970s by finds of copper-base artefacts in claimed 4th/3rd millennium BCE contexts at the sites of Non Nok Tha and Ban Chiang in northeastern Thailand (Figure 1.4) (e.g. Bayard 1972, 1979, 1981, Gorman and Charoenwongsa 1976, Solheim 1968). These dates for the earliest evidence of metallurgy in Southeast Asia were earlier than those in Eastern Asia, and comparable to those of Western Asia. This situation led to suggestions of an indigenous Southeast Asian invention of metallurgy (reviewed by J. White 2008b: 91), which was in itself a reaction to earlier culture-historical thinking, which attributed most developments in Southeast Asian prehistory to contact with more ‘advanced’ societies in East and South Asia (e.g. Cœdès 1969, Majumdar 1941). After the initial excitement, doubts were expressed by

the wider community (e.g. Higham 1975, Muhly 1981), and the chronologies for Non Nok Tha and Ban Chiang were subsequently found to be based on problematic and flawed interpretations of thermoluminescence and radiocarbon dates (e.g. Bronson 1972, Higham 1996-1997, Spriggs 1996-1997, White 1982, 1986). No Southeast Asian scholars now support either the very early dating, or Thailand being a centre for the independent invention of metallurgy (Higham 2006: 19, White 1988: 179). This implies that, by some means, Thai metal technologies have, to some degree, a foreign origin. The possibility of cultural interaction with South Asian metal-using societies to the west has been rejected due to the dearth of data linking the two areas prior to the 1st millennium BCE (Pigott & Ciarla 2007: 79, White & Hamilton in press). Therefore, scholarly attention has shifted north to a technology source in or via the Peoples' Republic of China, with Higham (e.g. 1996: 338) offering an early account of metallurgical knowledge transmission via Lingnan in Southeast China (Figure 1.4).

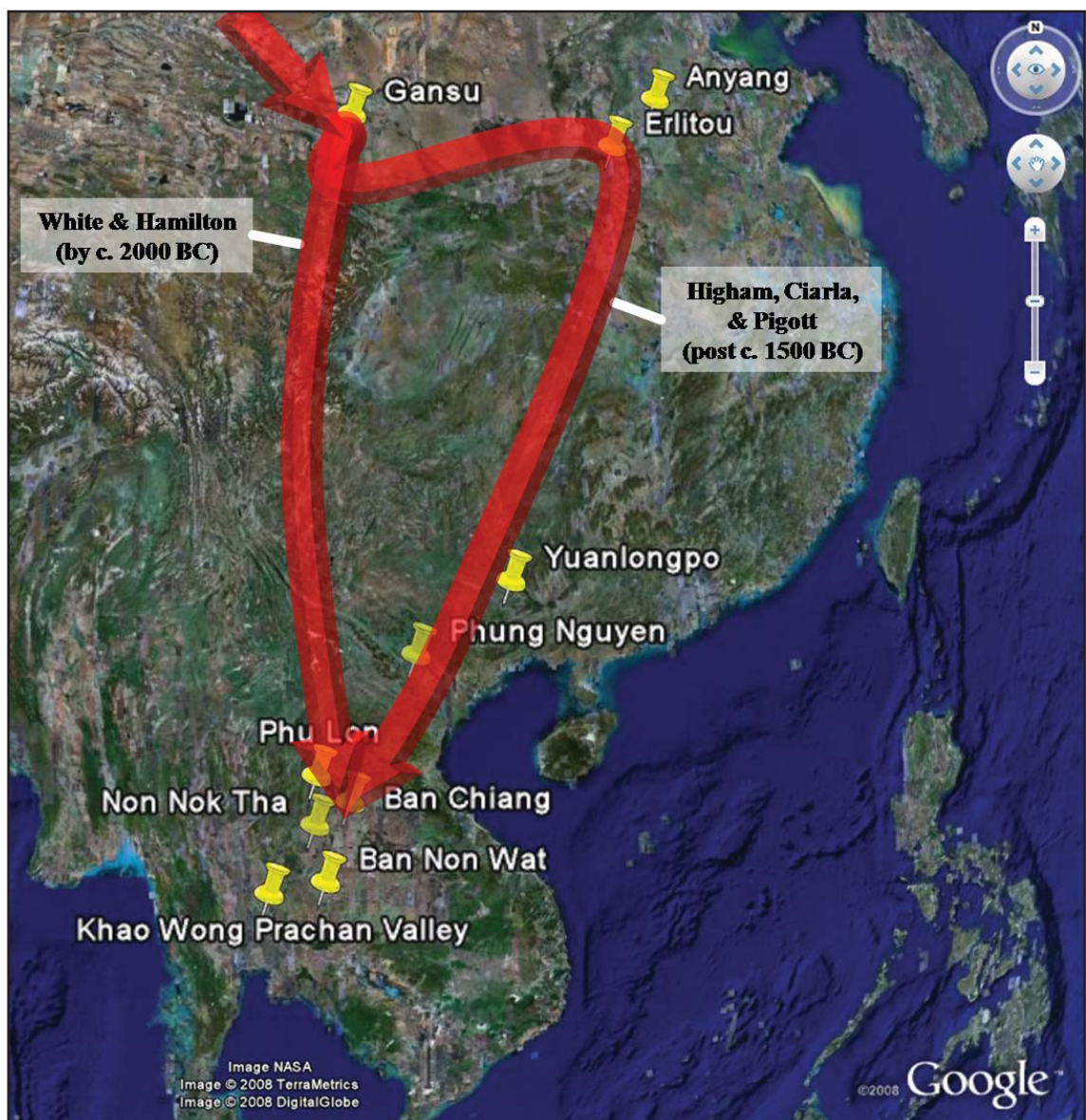


Figure 1.4 - Proposed routes (approximately) and dates for the transmission of metallurgy into northeast Thailand, including sites mentioned in the text. Image: courtesy of Google Earth™ mapping service, modified by the author.

	2nd millennium BCE Southeast Asian metallurgical tradition	2nd millennium BCE East Asian metallurgical tradition
Production context	Autonomous community centred	State centred
Assemblage type	Personal ornaments and tools	Ceremonial vessels and tools
Preferred alloy	Bronze	Leaded bronze
Crucibles	Small, internally-heated	Large, externally-heated
Moulds	Lost wax or bivalve	Piece-mould or bivalve
Smithing	Hammering and/or annealing	As cast
Hafting method	Socketed	Tanged
Founder's graves	Present	Absent

Table 1.1 - Summary of generalised technological characteristics distinguishing Southeast Asian and East Asian metallurgical traditions of the 2nd millennium BCE (after White 1988, 2008).

Constituting a major advance on the topic, White (1988) published an outline of the ‘southern metallurgical tradition’ (Table 1.1), a suite of technological characteristics distinguishing the 2nd millennium BCE metallurgical tradition of Southeast Asia, largely attested in central and northeast Thailand, from that of East Asia, evidenced primarily in the broadly contemporary Huanghe Central Plain (Figure 1.4, see ‘Erlitou’ and ‘Anyang’ for the Huanghe Central Plain). Acknowledging exceptions to the rule, White, in more recent statements has elaborated on this argument and emphasised that in terms of material culture and social context, Southeast Asian metal technologies appear to have more in common with those in wider Eurasia than the Central Plain ‘Shang’ metallurgical tradition (J. White 2008b: 100-101). Pigott and Ciarla (2007) have argued that an additional two decades of research have evidenced a second, less ‘sophisticated’ and ‘state-oriented’ East Asian metallurgical tradition. However, White & Hamilton (in press) have countered that some of the artefacts in this repertoire (e.g. non-socketed tools and ploughs) are not seen in the ‘southern metallurgical tradition’, which itself remains much closer to Eurasian technological configurations. Nevertheless, the dissimilarity of Southeast and East Asian metal technologies is, in general, currently agreed upon (e.g. Ciarla 2007a, Higham in press a, Pigott & Ciarla 2007, J. White 2008b, White & Hamilton in press). Another convergence of opinion is the possibility of a common technological ancestry for both ‘Shang’ and ‘southern’ metallurgical traditions in the ‘Qijia’ and subsequent ‘Siba’ metal-using cultures of the ‘Gansu Corridor’ in the mid-western PRC, and furthermore, that these technologies themselves may stem from interaction with other Eurasian ‘culture horizons’ like the ‘Afanasiovo’ and preceding ‘Andronovo’ (Ciarla 2007a, Chiou-Peng 1998, Higham 2002: 113-117, 2006: 18, in press a, Linduff et al. 2000, Mei 2000, 2003, 2004, Pigott & Ciarla 2007: 76, White 1997, 2008). The extant disagreement centres around the timing, routing, and cultural transmission mechanisms invoked to explain the derivation of 2nd millennium BCE Southeast Asian metallurgy from its proposed 3rd/2nd millennium BCE Eurasian antecedents. In brief, for over 25 years, White (1982, 2008) has been advocating Southeast Asian metallurgy by c. 2000 BCE, a situation which is explained (White 1986, 1997, 2008, White & Hamilton in press) by the ‘early’

transmission of metal technologies from the Gansu Corridor to northeast Thailand. The alternative 'late' model regards the 'southern metallurgical tradition' as being derived ultimately from the same mid-western PRC source, but arriving after c. 1500 BCE, via the 'Shang' Central Plain and Lingnan (Figure 1.4, see 'Yuanlongpo' for Lingnan, Ciarla 2007a, Higham 1996, in press a, Pigott & Ciarla 2007). Both of the proposed technological interactions are feasible, but which can account for the 'first' Southeast Asian metallurgy depends on the archaeological dates accepted (Higham in press a), and there is no reason to disavow the possibility of subsequent inter-regional interactions having introduced further metallurgical behavioural variability.

All current contributors to the origins of Southeast Asian metallurgy debate have consistently emphasised the preliminary nature of their hypotheses (e.g. Ciarla 2007a, Higham 1996: 338, Higham in press a, Pigott & Ciarla 2007, White 1988, White & Hamilton in press). These caveats are born of necessity as vast territories across Eurasia await archaeometallurgical investigation, and of the sites and finds already recovered, few have been subjected to detailed technological study. Typologically defined metallurgical traditions, and claims for the degree of variation between them, have yet to be quantitatively substantiated (e.g. Bettiner & Eerkens 1999, Jordan & Shennan 2003, Marwick 2008, Neiman 1995, Shennan & Wilson 2001). It cannot be stressed enough that the satisfactory demonstration of the proposed technology transmission models rests on the painstaking discovery, recovery, analysis, synthesis, and interpretation of data pertaining to all aspects of prehistoric metallurgical behaviour.

1.3.2 Principal northeast Thai sites with evidence for prehistoric copper-base production activities

Although many Bronze and Iron Age Thai sites have furnished copper alloy artefacts indicating metal consumption (see e.g. Higham 2002 for a summary), relatively few have provided evidence for metal production activities. As indicated earlier in this introduction, extractive metallurgy consists of mining and smelting, for which the prehistoric Thai evidence will be presented in detail in Chapter 2. Secondary production, or founding, relates to the refining, alloying, casting, and forging of copper-base metals. The bulk of the Thai copper-base production evidence, overviewed below, is limited to founding activities and comes from northeastern Thailand (Figure 1.2).

Upper Loei-Petchabun Volcanic Belt:

Phu Lon

The prehistoric copper mine site of Phu Lon is located around 102.0700°E, 18.1987°N, extending over two adjacent hills on the southern banks of the River Mekong, c. 250km upstream from Ban Chiang. Excavated by the Thai-American ‘Thailand Archaeometallurgy Project’ in 1984 and 1985, Phu Lon has provided substantial evidence for 1st and possibly 2nd millennium BCE mining activity, with limited occupation data suggesting non-permanent settlement on the site (e.g. Natapintu 1988, Pigott & Weisgerber 1998). Archaeological attention focused on the westernmost hill, ‘Phu Lon I’, which provided evidence for substantial mining activity, and the saddle between the two hills, the ‘Pottery Flat’, where the recovery of domestic pottery alongside crucible fragments suggests that Phu Lon was inhabited at least seasonally. Significant traces of prehistoric mining galleries remain, whose rounded walls suggest they were cut with stone rather than metal tools. This is corroborated by numerous finds of granitic hammerstones, probably made from Mekong River cobbles (Pigott 1998). Although we cannot accurately determine the entire span of mining activity at Phu Lon, at some point it appears that the deposit was so intensively undermined by tunnelling that one side of the honey-combed hill actually collapsed under the weight of the over-burden (Pigott & Weisgerber 1998).

William Vernon’s (1996-1997) technological study of Phu Lon crucible fragments have revealed a sophisticated understanding of refractory ceramics, with a siliceous lagging to the interior wall, which in addition to increasing refractoriness, could also have served to promote the slagging off of iron oxide impurities in the copper melt. The crucibles reconstructed volume was systematically less than 100ml, which would have limited the maximum content to much less than 1kg of metal, and it is thought that the crucibles had been used for melting rather than smelting copper-base metal (*ibid.*). Whilst this limitation does not rule out the production of large copper-base artefacts by the coordinated pouring of multiple crucibles, it does rather suggest that only smaller ornaments and tools were cast. White & Hamilton (in press) have termed this refractory technology “common Southeast Asian crucible production” due to the relative proliferation of comparable crucibles across northeast Thailand (Vernon 1997: 100, see below). Although it is quite likely that copper smelting did occur at Phu Lon, which Vernon’s (1996-1997) published evidence alludes to, at present the supporting arguments remain circumstantial and the Pottery Flat matrix was not noticed to have a significant component of slag (Pigott 1998). It has been noted that very high quality copper carbonates like malachite can be smelted with very little residue (e.g. Craddock 1995, Tylecote 1974), but this negative evidence argument is not very satisfying and the presence of even minor impurities would result in slag formation which we would then expect to detect archaeologically. The consistent presence of tin in the crucible scoria, an element the Phu Lon deposit does not contain in extractable quantities, suggests that prehistoric people were melting and possibly producing bronze alloys with the tin component at least from elsewhere (Pigott 1998).

Non Nok Tha

Excavated in the mid-late 1960s by a Thai-American team, the small mounded Bronze Age cemetery and settlement of Non Nok Tha is situated at 102.311640°E, 16.800908°N, c. 120km SSE of Phu Lon and c. 125km SW of Ban Chiang. The site's chronology has been heavily disputed over the years (e.g. Bayard 1981, 1996-1997, Higham 1975, 1996-1997, Spriggs 1996-1997) and the appearance of copper-base grave goods continues to be attributed as far apart as the mid 2nd millennium BCE (e.g. Higham 2002: 129) and the late 3rd millennium BCE (e.g. Bacus 2006, White & Hamilton in press). The predominant metal artefact type is a socketed axe, which are rare in the lower layers but become increasingly common. Whilst the dating remains uncertain, Non Nok Tha does provide good evidence for copper-base founding with the recovery of 4 whole and 12 fragmentary ceramic crucibles and 10 complete and 13 fragmentary sandstone moulds (Bayard 1981: 697). White & Pigott (1996: 155) have suggested that Non Nok Tha may have been a specialist producer of socketed implements due to the local availability of sandstone for bivalve moulds.

Chi River basin:

Ban Chiang

Situated at 103.301°E, 17.405°N on the northern Khorat Plateau, Ban Chiang was excavated by a Thai-American team over 1974 and 1975 (e.g. Gorman & Charoenwongsa 1976, White 1986) and has provided vital evidence for prehistoric Thai copper-base metallurgy from the period c. 2000 BCE to c. 200 CE (e.g. J. White 2008b). Concentrating on the Middle and Late Period (MP c. 900 BCE to c. 300 BCE, LP c. 300 BCE to c. 200 CE) contexts broadly contemporary with the Khao Wong Prachan Valley industrial copper production sequence (c. 6/500 BCE to c. 300 CE), the Ban Chiang metallurgical assemblage consists of 225 copper-base artefacts (MP=155, LP=70), including bangles, points, wires/rods, flat sections, and amorphous pieces that may be casting spillage, as well as 78 crucible fragments (MP=67, LP=11), 8 slag fragments (MP=2, LP=6), and 3 probable mould fragments (MP=3, LP=0), predominantly from non-funerary contexts (Ban Chiang Project n.d.). The presence of production related artefacts like crucibles, moulds, and slag probably indicate that copper-base founding was practiced on site, but there is no evidence to suggest smelting activities, which may have taken place elsewhere (J. White 2008b: 95). Of the 20 Middle and Late Period copper-base artefacts for which compositional data exists only 3 are unalloyed copper, mirroring the marked preference (40 of 44) for bronze seen in Early Period (c. 2100 BCE - c. 900 BCE) Ban Chiang artefacts (Hamilton 2001). Vernon's (1997) study of Ban Chiang crucibles suggested

they were morphometrically and technologically very similar to those from Phu Lon (see above), with the regular (55 of 76 examples) presence of a refractory quartz-rich lagging (White & Hamilton in press).

Ban Na Di

Thai-New Zealand investigations in the early 1980s at Ban Na Di, located at 103.133988°E, 17.256121°N, c. 23km southwest of Ban Chiang, revealed a mortuary and settlement site with a sequence spanning the Bronze Age (c. 900 BCE to c. 400 BCE) and Iron Age (c. 400 BCE to c. 100 BCE) (Higham 2002: 135-141). Furnace features, intact and fragmentary crucibles with adhering bronze scoria (analysed at c. 10-12wt% Sn), and sandstone axe mould fragments in Layers 8 to 6 suggest onsite secondary production activities throughout the early-mid 1st millennium BCE (Seeley & Rajpitak 1984). Evidence for Ban Na Di's founding industry continues in Iron Age Layer 5 with the discovery of in situ furnaces, rice chaff tempered crucibles, remnant of wax for 'lost-wax' casting, and clay moulds for casting bells and bracelets (e.g. Higham 1996: Figure 6.27). Notably, the Ban Na Di crucibles fit within the 'common Southeast Asian crucible production tradition' reported from Phu Lon and Ban Chiang (White & Hamilton in press). Four different associations of alloy and artefacts types were noted at Ban Na Di: most artefacts but in particular arrowheads and bracelets were low-tin bronze (c. 2–14wt% Sn), leaded copper was also used for bracelets, leaded bronze for rings and bracelets, and high-tin bronze (< c. 24wt% Sn) for wire (Seeley & Rajpitak 1984, Maddin & Weng 1984). It appears there was a shift in alloy preference to include leaded and high-tin bronzes c. 100 BCE, which is suggested to relate to the appearance of iron technologies (Higham 1988a).

Non Chai

Salvage excavated by Pisit Charoenwongsa and Don Bayard in 1978, the Upper Chi River Valley occupation site of Non Chai was located c. 4km north of Khon Kaen, where it extended over c. 18 hectares and had an Iron Age sequence from c. 400 BCE to c. 200 CE (Charoenwongsa & Bayard 1983, Higham 2002: 188). Bronze and iron artefacts were recovered in all phases, but the presence of crucible fragments and clay moulds for casting bracelets and bells in phases IV and V (c. 200 BCE to c. 200 CE), strongly suggest founding activities were practiced on site (Charoenwongsa & Bayard 1983).

Mun River basin:

Ban Lum Khao

Three of the sites investigated by the Thai-New Zealand ‘Origins of Angkor Project’ in Upper Mun River Valley between 1994 and 2007 have furnished evidence for prehistoric copper-base founding industries. The first of them, Ban Lum Kaeo, located at 102.347981°E, 15.245483°N, was excavated in 1995 and 1996, and has Neolithic (c. 1500 BCE to c. 1400 BCE) and Bronze Age (c. 1400 BCE to c. 500 BCE) funerary and occupation layers (Higham 2002: 142-146, O’Reilly 2003). The metallurgical evidence consists of fragments of crucibles and moulds for axes and projectile points and thus indicates the strong likelihood of secondary production onsite, although there is, curiously, no evidence for the consumption of bronze in funerary rituals (Higham 2002: 142).

Noen U-Loke

Noen U-Loke is a 12 hectare occupation and funerary site situated at 102.256066°E, 15.260249°N, with an Iron Age sequence from c. 300 BCE to c. 500 CE, and was excavated by the ‘Origins of Angkor’ team between 1996 and 1998 (Higham 2002: 204, Higham et al. 2007). No furnace features were recovered but finds of ceramic moulds for casting socketed axes and finger rings suggest an on-site founding industry may well have been practiced (Higham 2002: 204, Higham 2007).

Ban Non Wat

The settlement and mortuary site of Ban Non Wat is located at 102.276753°E, 15.267613°N in the Upper Mun River Valley basin on the southern Khorat Plateau (Higham 2008, 2009, Higham & Higham 2009, Higham & Thosarat 2006,). Extensive excavations by a Thai-New Zealand team since 2001 have identified a high resolution chronological sequence spanning the Neolithic through Iron Age (c. 1650 BCE to c. 500 CE) (Higham & Higham 2009). The funerary consumption of copper-base artefacts begins c. 1000 BCE, with indirect evidence for foundry activities from c. 800 BCE in the form of a ‘founders grave’ containing 26 bivalve moulds for casting bangles and socketed axes (Higham 2008b: 40). However, the discovery of several in situ clay pyrotechnological structures with numerous associated crucibles and moulds dated from c. 420 BCE provides direct support for secondary copper-base metallurgical production at Iron Age Ban Non Wat (Higham & Thosarat 2006: 103). White & Hamilton (in press) have stated that the technological configuration of late prehistoric founding activities at Ban Non Wat falls within the “common Southeast Asian crucible production” they identified at Phu Lon, Ban Chiang, and Ban Na Di hundreds of kilometres to the north. Of further interest is the excavation of two copper-base artefacts from a Ban Non Wat burial dated c. 420-200 BCE (Charles Higham pers. comm.) with very similar typologies to those known to be produced in the Iron Age Khao Wong Prachan Valley c. 170km WSW (Pigott et al. 1997,

see also Chapter 2).

Summary

In this chapter the central topic of this thesis, Iron Age copper smelting technologies in Thailand, was introduced along with the principal research aim of conducting archaeometallurgical research to better understand long-term changes in extractive metallurgical behaviour. Several paradigms of regional research were discussed, including the general paucity of archaeological evidence, regional biases in data availability, chronological uncertainties, and a still maturing research agenda that has been largely preoccupied with establishing a basic culture history for Thailand. The prehistoric cultural sequence was overviewed with brief descriptions of the major evidence for subsistence, technologies, and burial traditions in Neolithic, Bronze Age, and Iron Age Thailand, followed by a summary of the alternative frameworks for investigating Thai social complexity, namely heterarchical versus hierarchical approaches.

In the second section the chapter concentrated on prehistoric Thai metallurgy, commencing with a resumé of the ‘origins of metallurgy’ debate, before summarising the major evidence for copper/bronze production in northeast and central Thailand. Several interesting differences were shown to exist between Bronze Age and Iron Age metallurgical technologies in that there seems to be a shift away from the production of apparently utilitarian items like axes towards exclusively ornamental industries, perhaps coinciding with an increasing availability of iron tools. Furthermore, this chronological boundary also marks a partial technological transition from a widespread preference for low tin (<c. 14wt% Sn)² bronzes across northeast and central Thailand towards the increasing consumption of high tin (>c. 14wt% Sn) copper alloys with markedly different casting and working characteristics and associated with trans-Asiatic cultural exchanges with the Indian subcontinent (e.g. Bellina 2008, Bennett & Glover 1992). In the prehistoric Thai context it has been argued (e.g. White & Pigott 1996) that copper-base metallurgy was a ‘specialised community’ industry with multiple production centres, with no evidence for ‘elite’ control over what was apparently a largely utilitarian material, though this perspective is not unanimous (e.g. Higham & Higham 2009). In terms of copper-base founding technologies, the ‘common Southeast Asian crucible production’ (White & Hamilton in press), small highly-portable crucibles with a quartz-rich lagging seem to be a near universal across northeast Thailand, although differences in temper may provide a measure of regional variation as those in Phu Lon (crushed rock and rice chaff) differ markedly from those at Ban Chiang (grog then rice chaff), and Ban Na Di (rice chaff

2 See Scott (1991) for discussion of copper alloy terminology.

then sand) (Vernon 1997: 110). However, it remains to discuss in detail the prehistoric Thai archaeological evidence for industrial scale copper smelting. These data come solely from the Khao Wong Prachan Valley of central Thailand, the subject of Chapter 2.

Chapter 2:

The Khao Wong Prachan Valley and its environs

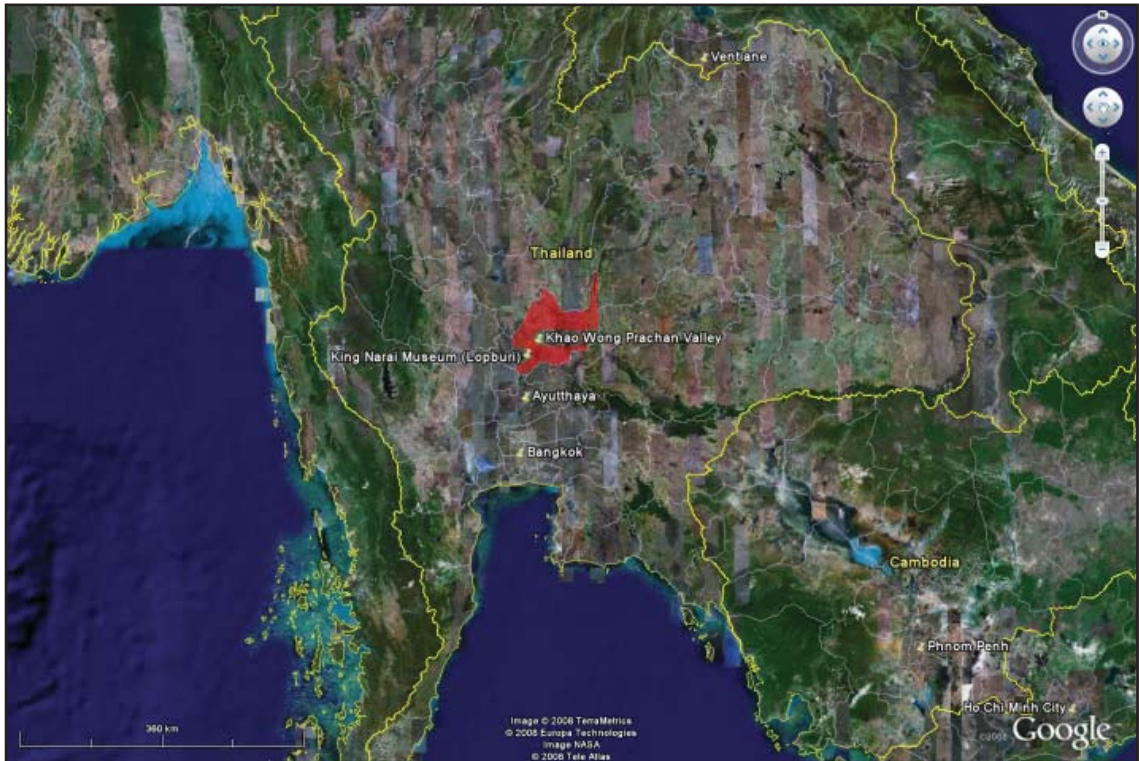


Figure 2.1 - Composite satellite image of central Thailand with Lopburi Province highlighted in red. Courtesy of Google Earth™ mapping service, modified by the author.

As introduced in Chapter 1, Lopburi Province in central Thailand (Figure 2.1) is home to the Khao Wong Prachan Valley. This chapter commences with a discussion of the geological environment that led to the formation of the metallogenically well-endowed Valley, before proceeding to document the chronology and stratigraphy of Non Pa Wai and Nil Kham Haeng, the two prehistoric Valley industrial sites focused on in this study. The archaeological contexts for Iron Age Valley smelting evidence are discussed and their limitations acknowledged. Only a pragmatic view of the difficult archaeology encountered in the Khao Wong Prachan Valley will enable a sustainable reconstruction of prehistoric extractive metallurgical activities to be developed later in this thesis. The available metallurgical evidence from the documented sites of Tha Kae, Non Mak La, and Khao Sai On is also reviewed, prior to discussion of White & Pigott's (1996) interpretation of 'community specialisation' for local copper production. The penultimate part of this chapter is dedicated to reviewing previous analytical studies of Valley copper-base metallurgy and their relation to the present study. Finally, the present study's sampling strategy is presented.

Whilst further locales doubtless remain to be discovered, the Khao Wong Prachan Valley represents a significant concentration of Thailand's prehistoric and historic extractive metallurgical industry, and although much remains to be understood, the Valley and its environs have benefited from a number of research programmes by Thai and foreign scholars over the last three decades, of which the major projects are:

- The Thai Fine Arts Department and Silpakorn University have both been active in the area for a long time, providing both a cultural heritage database on known archaeological sites (Anon. 1988), and systemically recorded excavation data (e.g. Natapintu 2007). Much of Silpakorn University's research has been led by the Central Thailand Archaeology Project, directed by Surapol Natapintu, which has conducted excavations at a number of settlement and funerary sites in the general area including Tha Kae, Phromathin Tai, and Pong Manao; the first two of which had substantial but as yet unstudied evidence for copper production (e.g. Natapintu 1979, 1980, 1984, 1985, 1988, 1991, 2005).

- The Lopburi Regional Archaeology Project (LoRAP), co-directed by Roberto Ciarla of the Istituto Italiano per l'Africa e l'Oriente (IsIAO), and Surapol Natapintu of Silpakorn University (e.g. Ciarla 1992, 2005, 2007b, Rispoli 1997, 2007) has investigated a number of occupation and funerary sites around Lopburi including Tha Kae, Khok Din, Khao Sai On, Noen Din, and Phu Noi of which the first two had evidence for copper smelting and the third for copper mining, though the metallurgical assemblages are as yet unstudied.

- The Thailand Archaeometallurgy Project (TAP), co-directed by Vincent Pigott and Surapol Natapintu (then) of the University of Pennsylvania Museum and the Thai Fine Arts Department respectively have provided the only investigation of demonstrably industrial scale copper smelting sites in Lopburi Province, Thailand, and indeed all of Southeast Asia. The two major smelting sites, Non Pa Wai and Nil Kham Haeng are the focus of the present study, but TAP also excavated a settlement at Non Mak La and recorded premodern copper mines at Khao Ph Kha (e.g. Natapintu 1988, 1991, Mudar & Pigott 2003, Pigott 1999a, Pigott & Natapintu 1986, Pigott *et al.* 1997, Pigott *et al.* 2006).

2.1 Geology of the Khao Wong Prachan Valley area

Southeast Asia lies at the junction of two continental plates, the Shan-Thai and Indochinese, and the oceanic Pacific shield (Lai *et al.* 2006). The heat generated by tectonic interaction accounts for the intense magmatic activity in the region, this being responsible for both Southeast Asia's active vulcanism and, importantly for the current study, the prevalence of zoned metallogenic deposits throughout the mainland (Gardner 1972, Sitthithaworn 1990, Takimoto & Suzuka 1968, Vernon 1988, Workman 1977).

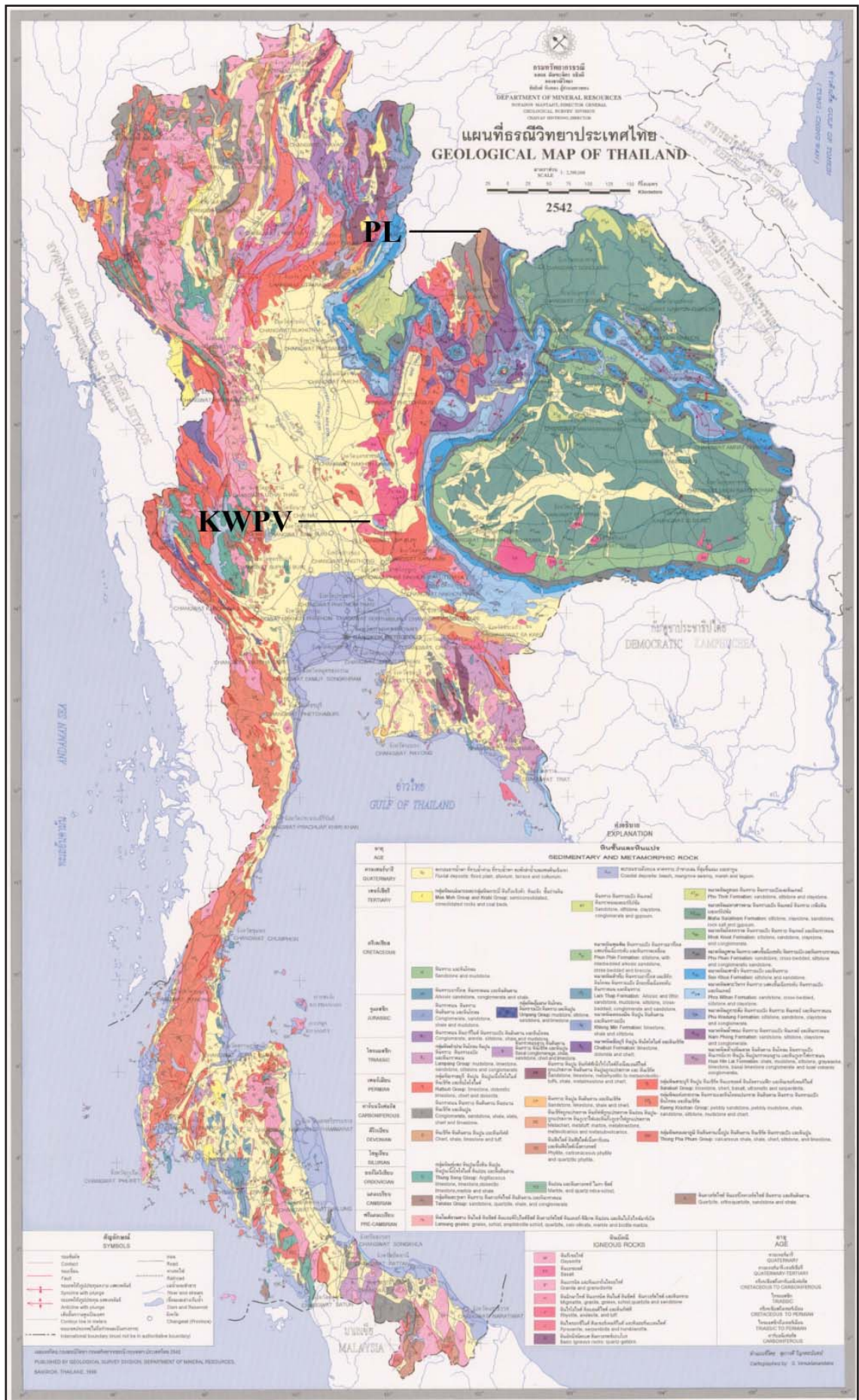


Figure 2.2 - 1:2,500,000 geological map of Thailand with the Khao Wong Prachan Valley (KWPV) and Phu Lon (PL) marked. Courtesy of the Thai Department of Mineral Resources, 1999, modified by the author.

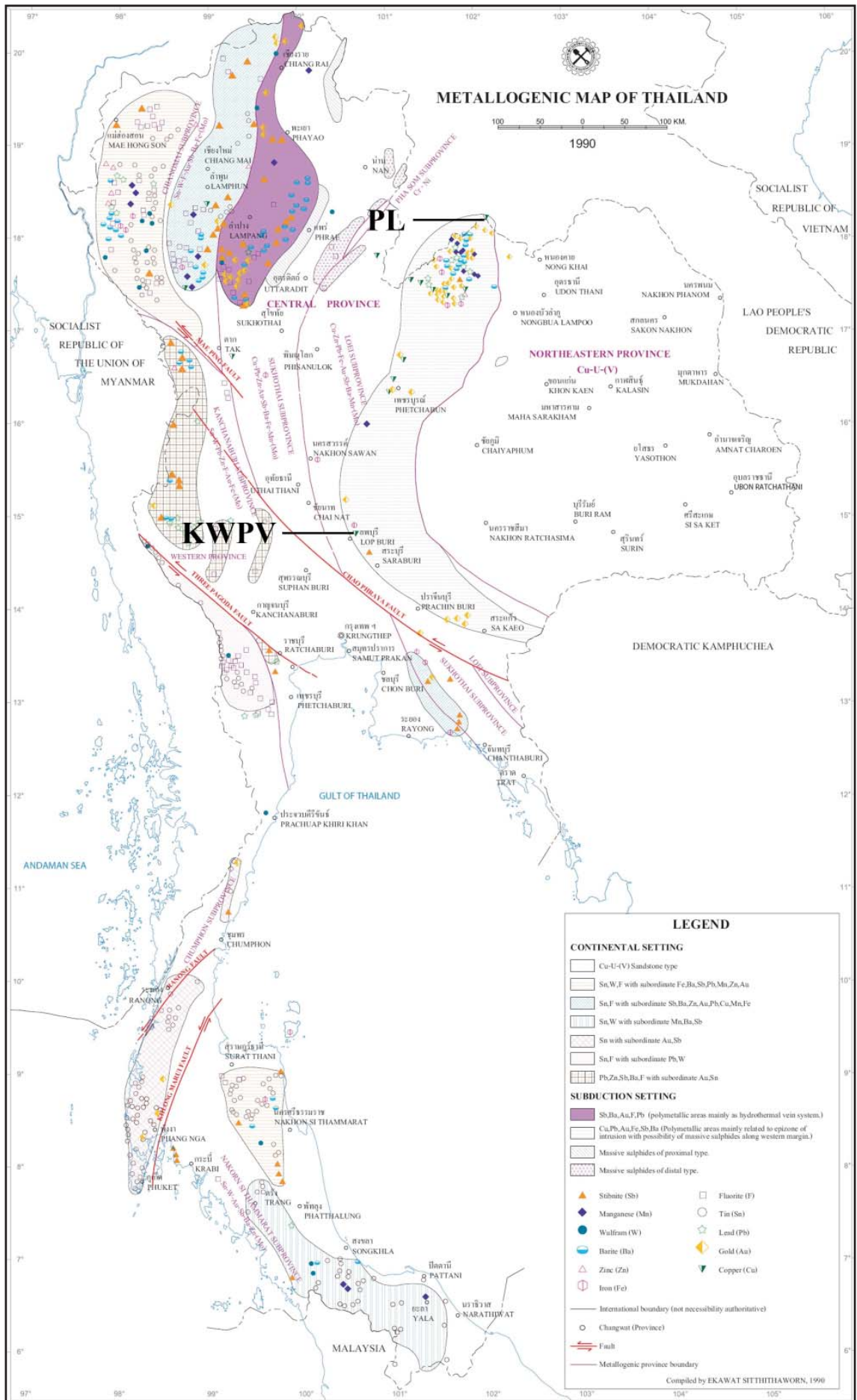


Figure 2.3 - 1:2,500,000 metallogenic map of Thailand with the Khao Wong Prachan Valley (KWPV) and Phu Lon (PL) marked. Courtesy of the Thai Department of Mineral Resources, 1999, modified by the author.

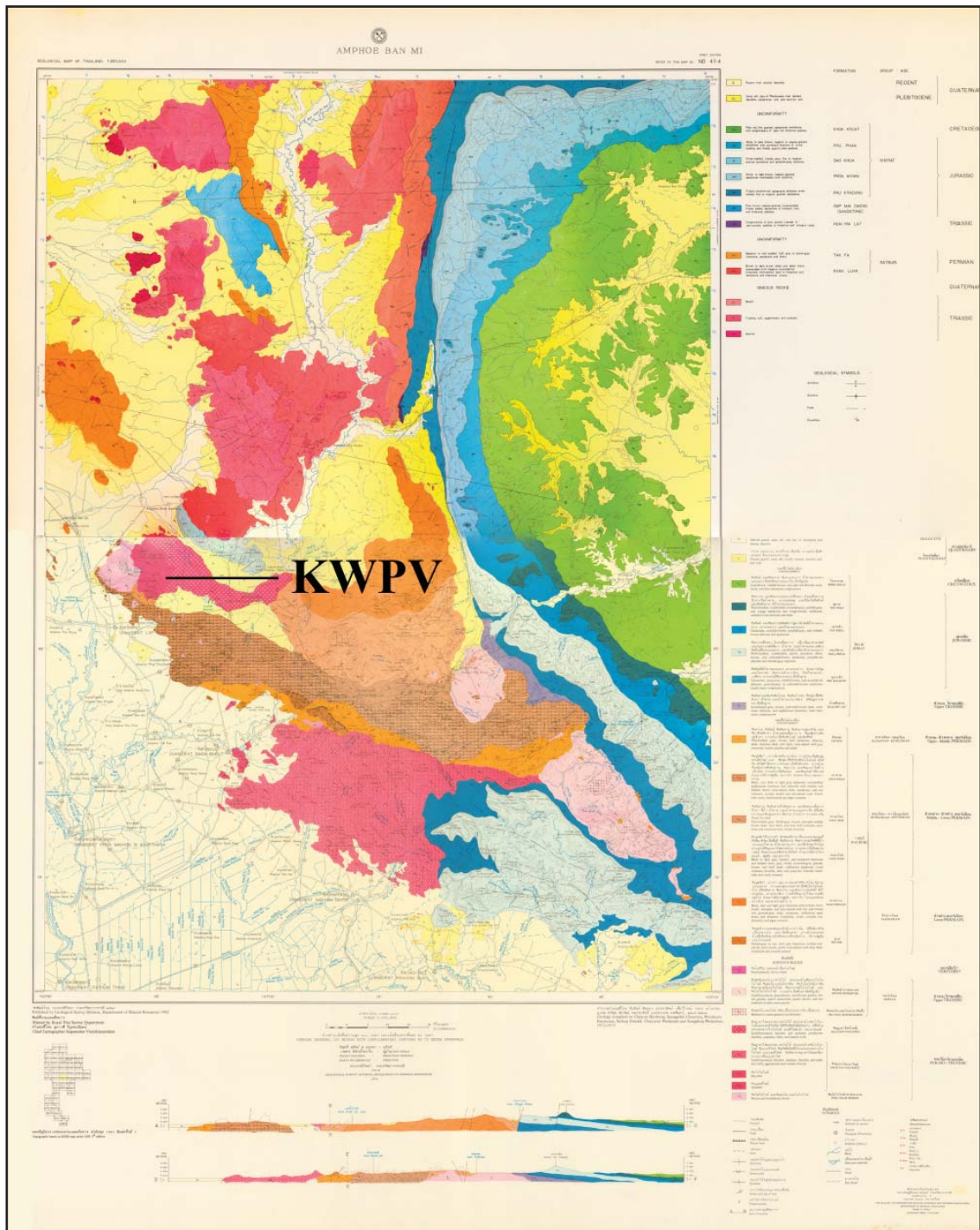


Figure 2.4 - Merged 1:250,000 geological map of Ban Mi (N47-4, top) and Ayutthaya (ND47-8, bottom) districts with the Khao Wong Prachan Valley (KWPV) marked. Courtesy of the Thai Department of Mineral Resources, 1976 and 1985 respectively, modified by the author.

Splitting Thailand asymmetrically in two, the Loei-Petchabun fault system runs approximately 400km NNE to SSW from Loei Province to Saraburi Province (Figure 2.2). The belt then turns ESE and continues for just over 200km to Buriram Province and the Cambodian border. The Loei-Petchabun system accounts for the bulk of Thailand's metallogenic geology outside the Indochina-Pacific fault, which runs up peninsular Thailand and continues along the western edge of the kingdom (Figure 2.3). The Loei-Petchabun belt is thus the closer of the two Thai metallogenic zones to what appears to be a major locus of prehistoric metal consumption, the Khorat Plateau in northeastern

Thailand. To the west of the Loei-Petchabun fault lies the central plain of Thailand, which has been identified as a large quaternary alluvial basin, some 500km long and 100km wide (Takaya 1968). The Khao Wong Prachan Valley lies on the eastern edge of this basin, after which the land climbs across the intervening range and onto the Khorat Plateau. See Eyre (2006: Chapter 4) for a fuller description of central Thailand's geological, environmental, and ecological zones.

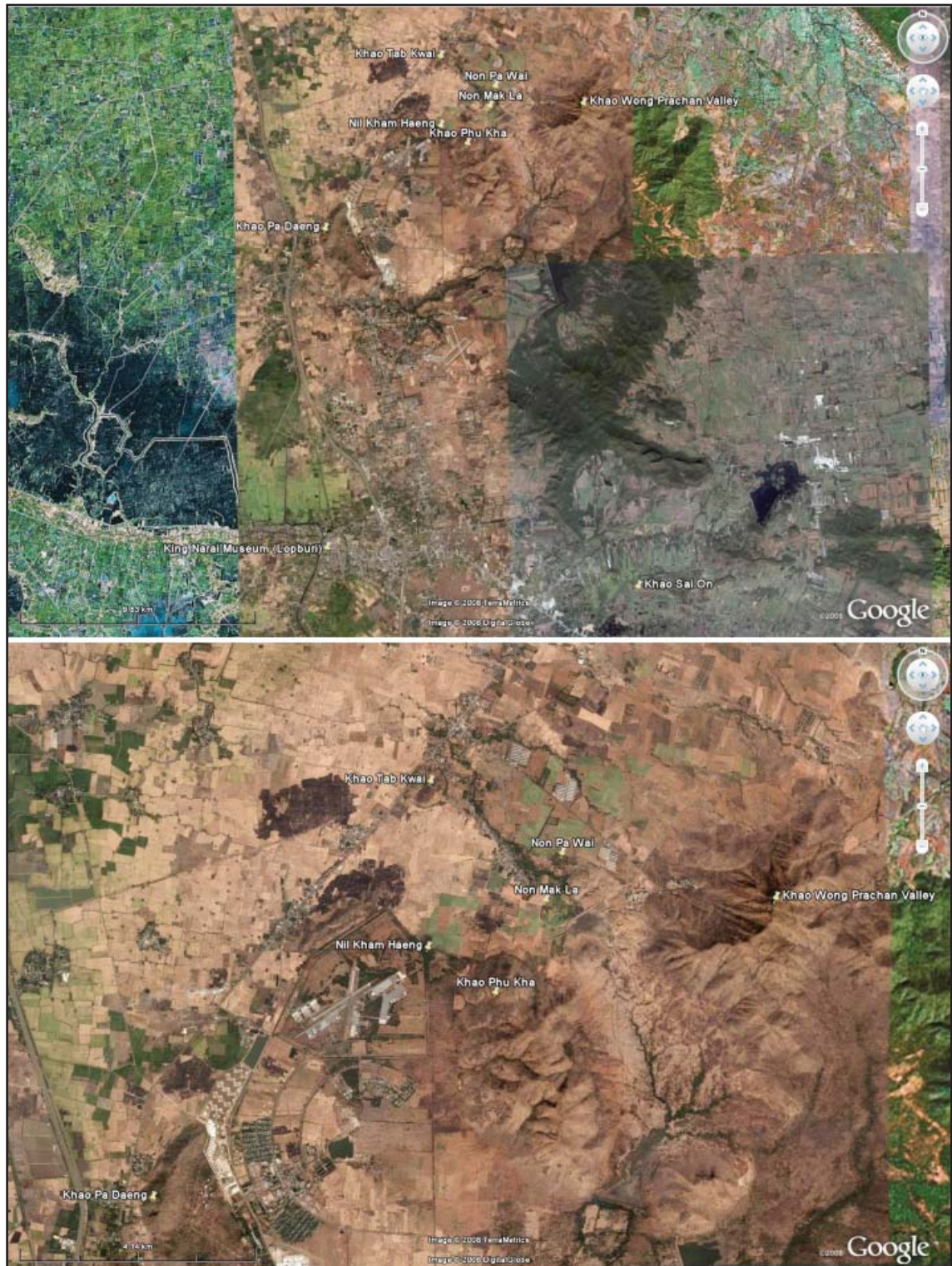


Figure 2.5 - Composite satellite image of the wider Khao Wong Prachan Valley area (above) and the Valley itself (below), with sites mentioned in the text marked. Courtesy of Google Earth™ mapping service.

The Valley geology consists of Permian calcareous and argillaceous sedimentary rocks with intrusive igneous rocks of acidic or intermediate composition, like andesite, diorite, granite, and granodiorite (Figure 2.4, e.g. Cremaschi *et al.* 1992, Nakornsri 1981, Vernon 1988). The contact zone between the igneous and sedimentary rocks is comprised of metamorphic products like marble and skarn. The Valley skarns are characterised by inclusions of garnet, vesuvianite, wollastonite, and quartz (Vernon 1988). It is also in this metamorphic contact zone that the metallogenic mineral deposits are found, consisting predominantly of haematite and chalcopyrite, and smaller quantities of magnetite and malachite, amongst others (e.g. Bennett 1988a: 128, Natapintu 1988: Table 1, Vernon 1988). The decomposition of host rocks has produced limestone-derived clay, clay-loam, or silty-clay rendzina soils, with poor water retention (e.g. Pigott & Mudar 2003, Pigott *et al.* 2006).

The TAP geological survey of the Khao Wong Prachan Valley was carried out in February 1988 by Udom Theetiparivattra, Bill Vernon, and Vincent Pigott (Vernon 1988). Their assessment of the local geology provides the basis for the current study's consideration of mineral resources relevant to prehistoric copper production, and their field notes are the sole source of small scale geological data. As well as identifying and describing the host rock geology and formation of the Khao Wong Prachan Valley (Vernon 1988), the survey team also assessed and sampled three major metallogenic mineralisations: Khao Tap Kwai, Khao Phu Kha, and Khao Pa Daeng (Figure 2.5, e.g. Natapintu 1988).

2.1.1 Khao Tab Kwai

Khao Tab Kwai is centred around 100.657°E, 14.9825°N, c. 2km from Non Pa Wai and c. 3km from Nil Kham Haeng (Figure 2.5). The mineralisation is predominantly haematite and magnetite, but also malachite and chalcopyrite, and could have potentially provided all the minerals required for prehistoric copper-smelting at Non Pa Wai and Nil Kham Haeng smelting activities. Due to its proximity to these sites, Khao Tap Kwai is a strong candidate for the source of minerals used in the Khao Wong Prachan smelting technologies. Khao Tab Kwai was exploited for its iron oxides reserves into the 1980s, and thus the mineral suite available to prehistoric metalworkers cannot be fully known.

2.1.2 Khao Phu Kha

Khao Phu Kha is situated at 100.667°E, 14.9496°N, c. 2.5km from Non Pa Wai and just over 1km from Nil Kham Haeng (Figure 2.5). However, the steep access from the valley floor to the summit and back would have necessitated huge exertions if metalworkers

sought their minerals there. The Khao Phu Kha galleries provide clear evidence of mining activity, and the suite of copper minerals (e.g. azurite, chrysocolla, chalcopyrite, and malachite) is in line with the other Valley deposits, and all are possible charge materials for local copper-smelting (Bennett 1988a, Natapintu 1988, Vernon 1988). The established TAP position is that Nil Kham Haeng is associated with Khao Phu Kha, but as the exploitation dates for the latter are unknown, it is uncertain whether the positioning of the former so close to this mine may have been for convenience, competitive control, or by coincidence.

2.1.3 Khao Pa Daeng

Khao Pha Daeng is located at 100.612°E, 14.9186°N, c. 6.5km from Nil Kham Haeng and c. 9km from Non Pa Wai (Figure 2.5). The mineralisation does have some evidence for mining, and a range of oxidic and sulphidic minerals that could have been used in copper-smelting operations at Non Pa Wai and Nil Kham Haeng (Vernon 1988). However, the increased distance of the mineralisation from the study sites to the north and north-west, suggests Khao Pa Daeng is a less likely source of material for metallurgical activities at this time, and mining operations may relate to a later period or as yet unidentified production sites.

2.2 Archeology of the Khao Wong Prachan Valley area

The Khao Wong Prachan Valley contains the largest concentration of prehistoric and historic mining and smelting sites known in Southeast Asia (Bennett 1988a, 1988b, 1989, 1990, Natapintu 1988, 1991, Pigott & Natapintu 1986, Pigott *et al.* 1997). The presence of extensive archaeometallurgical debris in the Valley was noted in the late 1970s by Thai archaeologists who conducted some important early excavations in the area (Natapintu 1979, 1980). It was however, the Thai-American TAP (e.g. Pigott & Natapintu 1986, Pigott *et al.* 1997) and Thai-Italian LoRAP (Ciarla 1992, 2005, 2007, Cremaschi *et al.* 1992) endeavours which really brought the significance of the Valley to international attention. TAP and LoRAP involve in-depth multi-site studies, concerned with understanding the entire spectrum of life in the Khao Wong Prachan Valley and the greater Lopburi region. These projects are actively pursuing research agenda to this day, LoRAP in the field and both in post-excavation study.

The current study commenced with an understanding of the Non Pa Wai and Nil Kham Haeng stratigraphy and dating that had existed largely unaltered since the period of TAP fieldwork between 1986 and 1994. In terms of Valley metallurgical activity, this

chronology recognised at Non Pa Wai an initial stage of Bronze Age copper smelting from c. 1500 BCE, followed by possible interruption (see Caliche Crust below), after which an ‘industrial’ phase of Bronze Age metal production laid the bulk of the archaeological deposit, petering out at c. 700 BCE. It was also thought that from c. 1000 BCE intensive copper smelting was being practiced at nearby Nil Kham Haeng, with production there ceasing c. 300 BCE (Natapintu 1988, Pigott *et al.* 1997).

However, as of late January 2008, the stratigraphic and chronological interpretation for the two sites was radically modified by the prodigious long term research of Fiorella Rispoli, the ceramic specialist for TAP and LoRAP (Rispoli 1997, 2007, Rispoli *et al.* forthcoming). Her regional comparative study of pottery from Valley sites has identified technological and stylistic ceramic similarities with sites in the local area, e.g. Tha Kae, Khao Sai On, and Phu Noi, and, most excitingly, with other more firmly dated sites in northeast Thailand (e.g. Ban Lum Khao), and as far as northern Vietnam. The new dating sequence has its greatest impact from the early Bronze Age to the late Iron Age, and had immediate and substantial ramifications for the current study’s interpretation of metallurgical activities in the Valley. To respond to these changes during the course of doctoral research, the author was obliged to reassess the contexts for each of the samples used in the present study¹, and in a number of cases to undertake further analyses to ensure reasonable population sizes for the revised assemblages. The new dating will be detailed in the site descriptions but awaits final publication as the Valley chronology has been subjected to further minor alterations during the course of 2008. However, the chief effect on Valley metallurgy can be summarised as undermining the established interpretation of the intensive industrial phase of copper production as a late 2nd millennium BCE (Bronze Age) phenomenon, pushing it firmly into the later 1st millennium BCE (Iron Age).

Even within a region known to suffer from poor stratigraphy due to annual monsoons and heavy bioturbation (Ciarla & Natapintu 1992 though cf. Grave & Kealhofer 1999), Non Pa Wai and Nil Kham Haeng have long been noted for their perplexing archaeological deposits (Ciarla 1993). Rispoli *et al.*’s (forthcoming) revised chronology, though of immeasurable importance, is confined to re-dating broad depositional periods (e.g. Iron Age or Bronze Age), but does not constitute a much improved intra-period resolution. This is the unfortunate consequence of the extreme taphonomic processes responsible for shaping the Valley archaeological record. The combined effects of weather, flora, fauna, and humans have conspired to dictate that the conclusions of specialist TAP studies, including the present one, must for the time being remain somewhat circumspect and adaptive.

¹ A process only made possible by the much appreciated help of Fiorella Rispoli, Roberto Ciarla, and Vincent Pigott.

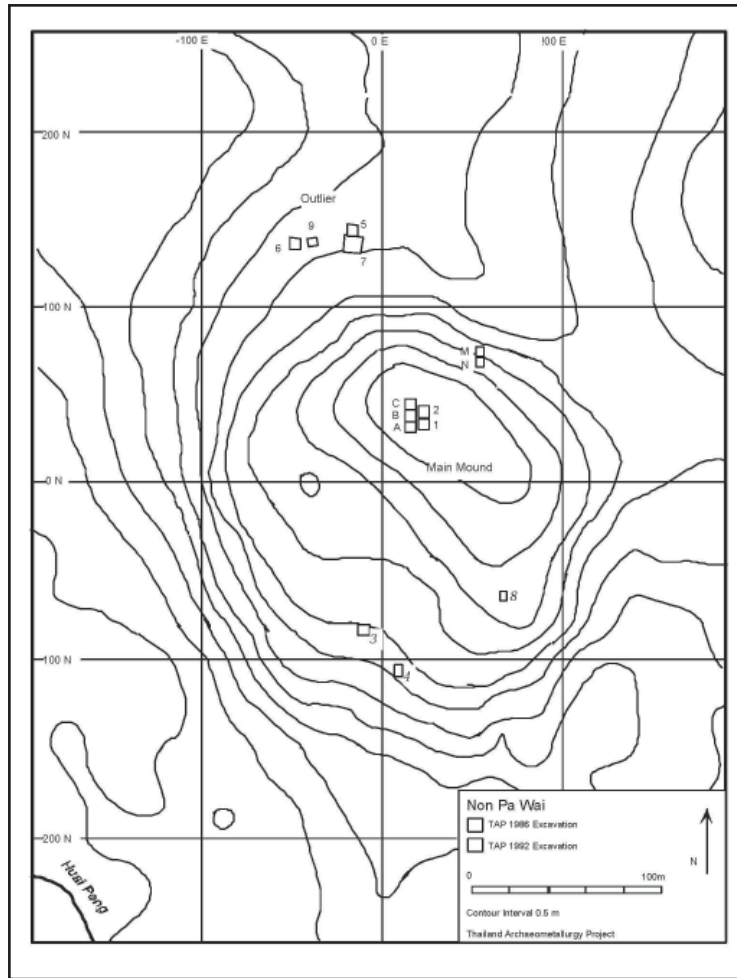


Figure 2.6 - Plan of Non Pa Wai showing trenches excavated. Courtesy of TAP.

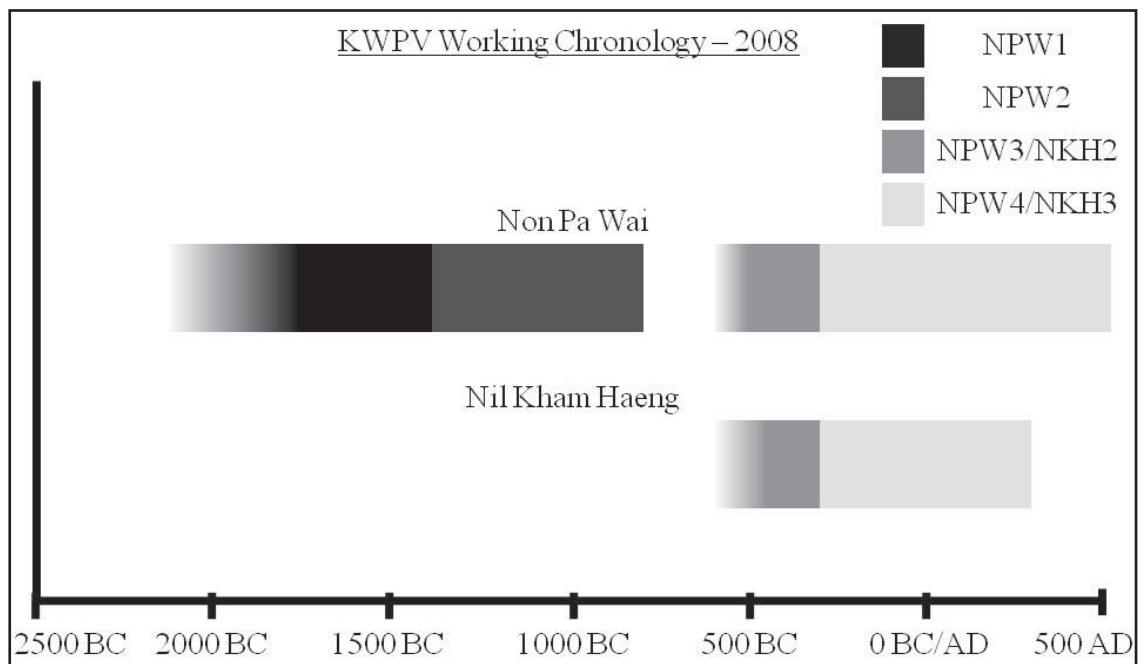


Figure 2.7 - Schematic of Non Pa Wai and Nil Kham Haeng chronology, at the time of writing.

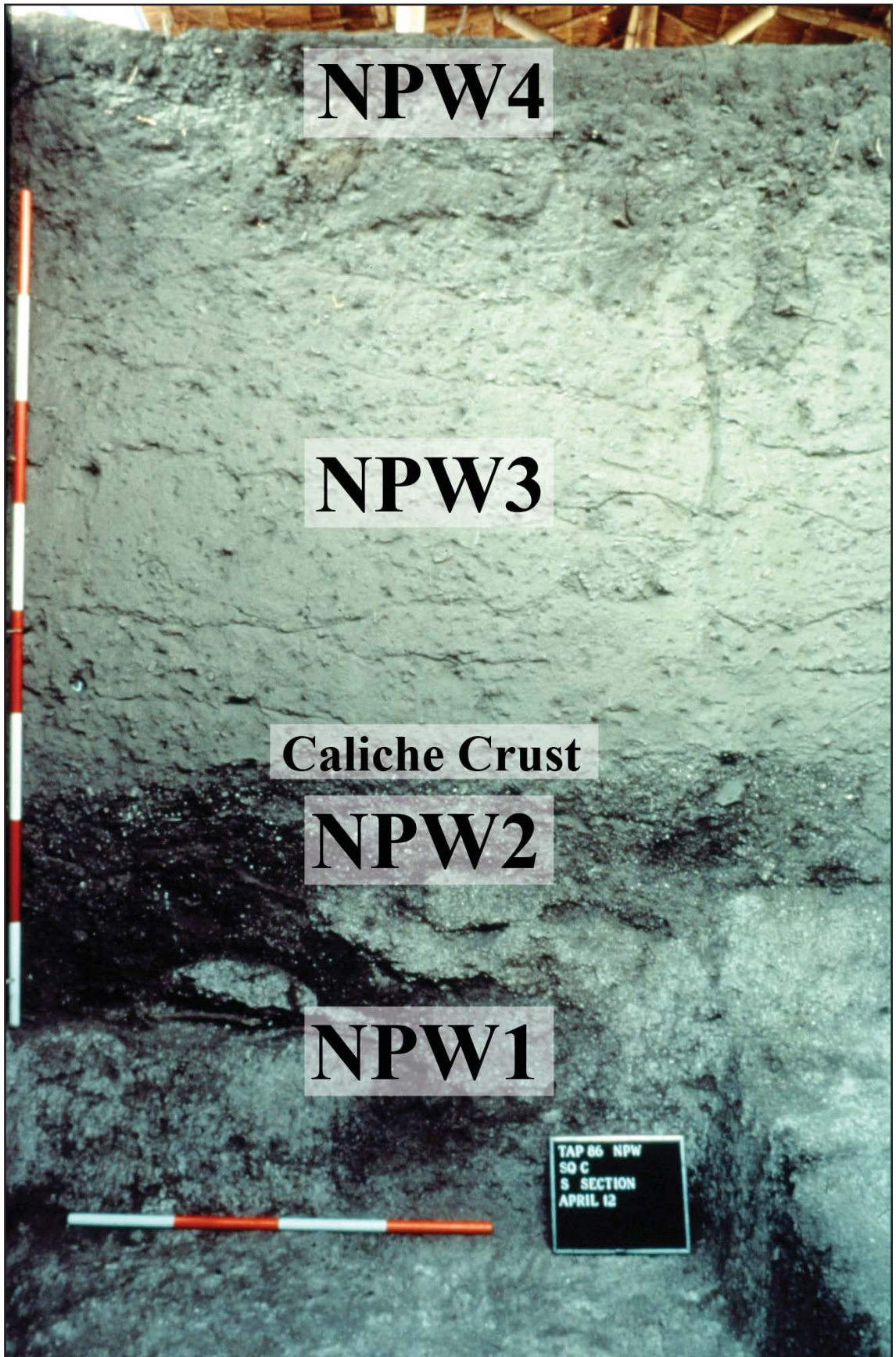


Figure 2.8 - Southern section of 'Square C' during the 1986 season at Non Pa Wai, the current site phasing is marked. Courtesy of TAP.

Taking into account the unlikelihood of Non Pa Wai or Nil Kham Haeng ever providing clear stratigraphic sequencing, the author endeavours to make the best of the evidence we have at present, and provide a range of archaeologically acceptable interpretations which can be profitably debated, rather than imposing a definitive yet shaky solution.

2.2.1 Non Pa Wai

Non Pa Wai has an archaeological sequence running from the Neolithic to the Dvararati period (c. 2200/1800 BCE to c. 600 CE), and provides some of the earliest evidence of extractive metallurgical practice in Thailand. The site is centred on 100.678°E, 14.9711°N at the northern end of the Valley and extends over approximately 50,000m² (Figure 3.5). The mound rises up to 4m above the surrounding plain, and consequently the archaeological deposits range from 0.5 to 4m in depth. Trenches with a surface area totalling 370m² were excavated in two field seasons by TAP in 1986 and 1992 (Figure 2.6). The site is uninhabited except for a lone monk who occupies a recently built temple, although the land is considered the property of the nearby village of Huai Pong. The proportion of slag in the soil would make ploughing difficult, and thus the land is uncultivated. Also, any absorbent material (e.g. bone) rapidly turns green with copper uptake, an issue which could make crops potentially dangerous for human consumption.

The site's deposits have been broken into four main periods (Figures 2.7 and 2.8, Rispoli *et al.* forthcoming), with some subdivisions:

- 'Period 1' or 'NPW1' is the Neolithic basal deposit of the mound. 'Mortuary Phase 1' (MP1) is the name attributed to the Neolithic burials excavated in 'Operations' A, B, C, 1, and 2 at the centre of the mound, and also in the peripheral 'Operations' (5, 6, 7, 9) located on the 'Outlier' (Figure 2.6). The Neolithic funerary assemblage is comparable to that from other Thai archaeological sites (see Higham 2002: Chapter 3), and consists of polished stone adzes, freshwater bivalve shells, marine *Tridacna* shell, and pottery types with red slip, 'elephant hide', and 'incised and impressed' decorations (Pigott *et al.* 1997, Rispoli 1990, Rispoli 1997, Rispoli 2007). The 'elephant hide' pottery style is characteristic of Non Pa Wai, and has rarely been encountered outside of the Valley. Its unusual surface patterning is thought to result from the pots being shaped using a basket as a mould or support, and thus leaving a woven impression on the vessel's exterior surface (Rispoli 1997: Figure 2a). The 'incised and impressed' style has comparators throughout the Neolithic Southeast Asian Mainland world and dates the Non Pa Wai deposits between c. 2200/1800 BCE and c. 1500/1400 BCE (Rispoli 2007). As yet unpublished calibrated radiocarbon dates from the Neolithic NPW1 deposit range between c. 2400 BCE and 1600 BCE, and are thus in general agreement with the ceramic typological dating. There

is no evidence of metal or metallurgy in Neolithic NPW1.

- 'Period 2' or 'NPW2' is a Bronze Age layer, and is thought to be present in all trenches excavated across the Non Pa Wai mound (Figure 2.6). The ephemeral Bronze Age deposits contain evidence for copper-base metal consumption, 'Metallurgical Phase 1' (MeP1), and a sequence of inhumation features with a material culture assemblage reported to be different to that found in NPW1 (Rispoli *et al.* forthcoming), though material culture change does not of course necessarily imply population change. On the basis of typological analogies to ceramics at sites in central Thailand and on the Khorat Plateau, Fiorella Rispoli *et al.* (forthcoming) have separated these burials into 'Mortuary Phase 2a' (MP2a) and 'Mortuary Phase 2b' (MP2b), dated from c. 1250 BCE to c. 1000 BCE, and c. 1000 BCE to c. 800 BCE, respectively. Firm evidence for Bronze Age metallurgy at Non Pa Wai exists only for the consumption of copper-base artefacts in funerary deposits. The metal burials are undated but they are intersected by later Period 2 internments, thus they are unlikely to date from the very end of the Bronze Age at Non Pa Wai. On site founding processes could be interpreted from the presence of intact pairs of bivalve moulds for large axes in two 'founder's' burials (Pigott *et al.* 1997: 122-123, Pigott & Ciarla 2007: 82), but definitive evidence of NPW2 production activity remain difficult to identify due to the shallowness of the deposit and its intercutting with Neolithic burials below and intrusive Iron Age pitting from above. However, a charcoal fragment (B-27364) from a securely provenanced copper-related context (Fissure 26) gives a *terminus ante quem* of c. 1400-1300 cal BCE for MeP1 at Non Pa Wai (Rispoli *et al.* forthcoming).

The NPW2/MeP1 metallurgical assemblage as identified from burials is comprised of two bivalve mould pairs, one socketed copper-base axe/adze, one corroded copper-base artefact, and one fish hook (Pigott *et al.* 1997: Figures 7-9).

Moulds:

The Bronze Age bivalve moulds are made in ceramic, and appear to have been used for the casting of large socketed axes. Intact examples of these moulds were found in burial 5 (Square A, see Figure 2.6), as well as in fragmentary form in disturbed contexts above and below the Caliche Crust (see below). The Non Pa Wai moulds have been compared, for example, to those reported from Tangxiahuan in Guangdong Province in China (Guangdong sheng Wenwu Kaogu Yanjiusuo 1998 in Pigott & Ciarla 2007: 84-85), Dong Den and Go Mun in northern Vietnam (Reinecke 1998: Plate 38.5 cited in Ciarla 2007a), and at Mlu Prei in Cambodia (Levy 1943). The Thai, Cambodian, Chinese, and Vietnamese contexts are consistent with large bivalve mould usage being associated with

Bronze Age metallurgical activity.

Metal:

NPW2/MeP1 burials (see above) contain a socketed copper-base axe/adze, which could have been cast in the ceramic bivalve moulds noted above. PIXE spectrometry conducted under the auspices of the Museum Applied Science Center for Archaeology at the University of Pennsylvania Museum indicated it contained c. 0.75wt% Sn (Pigott *et al.* 1997: 122 & Figure 5). TAP consensus was that this amount of tin was not indicative of intentional alloying as the tin could have been contained in the ore that was smelted (Vincent Pigott pers. comm.). The axe can be compared typologically to those found locally at Tha Kae, and much further afield from Yinxu, Anyang Province, China (Zhongguo Shihui Kexueyuan Kaogu Yanjiusuo 2006 in Pigott & Ciarla 2007: Figure 9, Ciarla 2007a).

Between them, NPW1 and NPW2 account for only 30-50cm of the c. 3m of archaeological deposits at Non Pa Wai, but provide evidence for a lengthy sequence of Neolithic and Bronze Age burial activity. The association of copper-base artefacts and ceramic moulds in some of the latter internments ('founders' burials') have been argued to represent a technological package which could indicate a socio-technical link of sorts to southern China, and perhaps to wider Eurasian traditions (Pigott & Ciarla 2007, cf. White & Hamilton in press). Above the Bronze Age deposit, a distinctive geological barrier is met - the 'Caliche Crust'.

- The Caliche Crust, a layer of calcareous concretion (called calcrete or caliche), is of some importance for our understanding of Non Pa Wai's stratigraphy. It was also enough of an obstacle that archaeologists were often forced to use pickaxes to access the layers NPW1 and NPW2 beneath². According to the TAP geomorphologist, Mauro Cremaschi (University of Milan), the crust is probably a post depositional feature caused by the differential permeability between the dense brown *rendzina* soil of the NPW2 deposit below, and the loose ashy matrix of the NPW3 deposit above. Heavy tropical rains could easily percolate through the loose upper deposit, dissolving large amounts of fuel-derived calcium carbonate, which would then crystallise at the soil interface, as the rainwater could not drain quickly (Cremaschi *et al.* 1992). At Non Pa Wai, the crust sits atop of the *rendzina* soil matrix, in which the Neolithic, Bronze Age deposits are contained, and extends as a relatively level horizon across all areas of the site excavated but varying

² As might well be expected, the Caliche Crust was at first thought to represent the sterile baserock of the site.

between 1 and 10cm thick. According to the new chronology (Rispoli *et al.* forthcoming), this would date the Caliche Crust as post NPW2 or after c. 800 BCE, but probably substantially later if the calcrete is a post-depositional feature, formed after the Iron Age NPW3 deposition had begun. The Neolithic NPW1 and Bronze Age NPW2 layers cannot be considered as uniformly culturally sealed by the crust, as the excavators believe that Iron Age NPW3 metallurgical activity (see below) had penetrated through to the *rendzina* soil on numerous occasions before the calcrete formed, pitting earlier burials as well as the basal deposit itself and depositing Iron Age archaeometallurgical materials in what were to become sub-crustal contexts (Roberto Ciarla & Fiorella Rispoli pers. comm., Rispoli *et al.* forthcoming). The archaeological meaning of the Caliche Crust remains uncertain, but as a post-depositional feature the only option is to try to understand its formation, and then to ignore it. What could prove informative in the Khao Wong Prachan Valley and surrounding area is a detailed geological reassessment of the Caliche Crust as the same calcia-rich crust was found at Non Mak La, Phu Noi, Khao Sai On, and Tha Kae (Ciarla 2005: 79, 82, 2007b).

- ‘Period 3’ or NPW3 is the Iron Age deposit which comprises the bulk of the mound, and formed directly on the basal brown soil below, the Caliche Crust being an archaeologically irrelevant feature. The stratigraphy of NPW3 is characterised by its dearth. The TAP excavators’ field notes record a lack of discernable layering in a loose-grained ashy matrix of archaeological material over 3m thick. This was termed the ‘Industrial Layer’ due to the thousands of kilogrammes of archaeometallurgical production debris recovered during excavation, which relate to Iron Age ‘Metallurgical Phase 2’ (NPW3/MeP2) in Valley copper smelting technologies. One of the fieldworkers, Roberto Ciarla (1993: 1) describes the internal uniformity of NPW3 as a “real nightmare” due to extensive disturbance by wind, rain, root growth, animal burrowing, and human pitting activity. Ciarla prefers to visualise the deposit as a spirally stratified “industrial refuse dump” (1993: 3) formed by shifting but intensive Iron Age copper smelting. The resulting heaping, flattening, and pitting resulted in a thoroughly churned and featureless mass from which the extraction of accurate provenance data has proven particularly difficult. The only subdivision the excavators are now prepared to make is between those artefacts located at the very base of the Iron Age deposit, where it intercut the Bronze Age layers, and everything else in the body of the industrial layer. On this basis samples could be divided into Metallurgical Phase 2a and Metallurgical Phase 2b, but this classification is subject to ongoing refinement by TAP archaeologists (Rispoli *et al.* forthcoming), and was not pursued in the present study.

Excavators found no features clearly evidencing NPW3 settlement, although Rispoli

has used the presence of domestic red-slipped pottery with ‘hanging triangles’ and ‘platform rims’, amongst other criteria, to date Non Pa Wai’s Iron Age deposit between c. 600/500 BCE and c. 300 BCE (Rispoli *et al.* forthcoming). It is argued that the uniform distribution of these diagnostic ceramics throughout the NPW3 matrix supports the interpretation of a highly disturbed and homogenised stratigraphy, rather than a lone unfeasibly rapid depositional event (Ciarla 1993, Rispoli *et al.* forthcoming). The c. 800 BCE end date for NPW2/MP2b mortuary practice leaves a gap of several centuries before the commencement of NPW3/MeP2 smelting activity c. 600/500 BCE. Though these chronological boundaries are necessarily hazy, a multi-generation separation of the two phases could have potentially significant ramifications for the continuity of metallurgical knowledge and traditions within the Valley (see Chapter 8).

The NPW3/MeP2 metallurgical assemblage consists of marked bivalve, cup, and conical moulds, as well as mould plugs, crucibles, furnace fragments, minerals, and slag.

Crucibles:

The crucibles which have been attributed to NPW3/MeP2 contexts are constructed of a thick organic-tempered fabric (possibly rice-chaff), usually with abundant macro-evidence for their involvement in high-temperature copper-related activities. This evidence takes the form of vitrification and bloating of the interior surface of the vessel fragments, alongside extensive green-stained slagging and scoria. Most of the crucibles excavated were too fragmentary to be reconstructed but one, ‘Mr Crucible’ (see Figure 5.7), was recovered almost complete and shows the form of the vessel to be almost hemispherical, with a diameter of c. 16cm and height of c. 8cm. However, these dimensions are approximate as the entire circumference of the rim has been broken away, in one section into a ‘pouring spout’. Although even small linear changes will have a significant volumetric effect, the original size of the vessels was probably not much larger. Unfortunately, ‘Mr Crucible’s’ context does not allow us to date it precisely within the period of Iron Age production activity. However, the likelihood, and the established assumption based on comparison with thousands of crucible fragments, is that this uniquely intact sample is representative of the fragmentary Iron Age crucibles recovered at Non Pa Wai.

Ore and gangue minerals:

The NPW3/MeP2 mineral assemblage consists of small fragments of copper carbonates sulphates, and sulphides, as well as siliceous and ferruginous hostrock. There is no clear consistency to the mineral suite, and none were recovered in contexts suggesting

individual work areas or ‘stockpiles’.

Slag:

Slag in the thousands of kilogrammes³ was recovered from NPW3 deposits across the entire site mound, with, for example, ‘Square A’, a 5x5m trench, yielding in excess of a tonne (Figure 2.5, McQuail 1986), but it is notoriously difficult to convert these waste product figures into copper metal output and labour input due to the unknown variables of ore quality, extraction efficiency, and the duration and intensity of production. For a full discussion on NPW3/MeP2 slag please see Chapter 5, but in brief the early Iron Age slag morphology appears to be based on plano-convex cakes of c. 2kg, and coarsely crushed pieces thereof (see Figure 5.27 & 5.28). The level of fragmentation is not consistent with the manual extraction of small copper prills, and stands in contrast to metallurgical behaviour at Nil Kham Haeng (see below). Both on the surface and in section, the slag has a high level of heterogeneity, representing a smelting charge that never fully reacted and liquefied. The NPW3/MeP2 slag cakes and fragments recovered below the Caliche Crust frequently have green staining on their surface, but this could well be a post-depositional effect due to differential water levels and subsequent oxidation conditions related in part to the Caliche Crust’s formation.

Pyrotechnological installations:

Whilst none of the NPW3/MeP2 deposits provided clear evidence of furnace structures, Roberto Ciarla (1993) does report shallow depressions cut into the brown soil of the Bronze Age NPW2 layers, which he thought might represent smelting installations (including the large pit where ‘Mr Crucible’ was found in 1993). These pits were noted in at least ‘Operations’ 1, 2, 3, A, and B, and were generally 30-40cm in diameter and 30-40cm deep, and perhaps included a baked clay rim (*in situ* examples F.33 and F.34) to elevate the walls of the pit. A field sketch by Ciarla (see Figure 5.5) gives a clear indication of what he meant.

The MeP2 assemblage contains what are thought to be sections of broken ceramic furnaces

3 Regarding the metallurgical assemblage metrics, “Due to the extensive ongoing process of cross-checking TAP data, it was not possible to provide estimates for the amounts of slag, technical ceramic, and minerals recovered from Non Pa Wai and Nil Kham Haeng in time for the completion of Pryce’s thesis. These data will be furnished in the future, but the fact that much of the slag is so finely crushed means, in truth, an accurate quantification of pyrotechnological waste per operation or in the site as a whole will simply not be obtainable...” (Vincent Pigott pers. comm.).

or, as they have been termed, ‘pit-rims’⁴. These fragments are made from a friable red fabric, which is clearly oxidised and not reduced. The ceramics are uniformly c. 5cm thick, but the height and circumference of their original form is unknown. There is no evidence for slagging or vitrification of the fabric, suggesting these ceramics were neither in close contact with the hot charge, nor exposed to excessive temperatures themselves. For a detailed discussion of these finds see Chapter 5.

Moulds and mould plugs:

The excavated NPW3/MeP2 moulds were noted to be dissimilar to the preceding MeP1 examples. However, due to stratigraphic disturbance, heavily eroded fragments of Bronze Age ‘big axe’ moulds were encountered, predominantly in the lower portion of the industrial deposit. There appear to be two major categories of Iron Age moulds: relatively small bivalves for the manufacture of ornaments and fishhooks, small socketed tools and weapons, as well as open conical and cup moulds, apparently for the casting of ingots (Pigott *et al.* 1997: 126, Figures 11 & 12). The mould plugs (also known as ‘suspended cores’) would have been used to create a hollow socket for hafting. Both bivalve and conical forms frequently display geometric and curvilinear designs on the outer surfaces, suggested by Pigott and Ciarla (2007: 82) to represent makers’ marks, and can be compared to the incised moulds excavated at Phu Lon (Loei Province, Thailand) and Yuanlongpo (Lingnan Province, China), both of predominantly 1st millennium BCE date (Ciarla 2007a). The Valley cup and conical moulds were not analysed by the author, but have been studied typologically by Lisa Armstrong (1994, see Pigott 1999a: Figure 11). A study of the Iron Age Non Pa Wai bivalve moulds and their markings is being carried out by Judy Voelker (University of Northern Kentucky) and they do not form part of the current study.

- ‘Period 4’ is the wind-scoured and deflated protohistoric and historic deposit making up the topmost layer of Non Pa Wai. No material was studied from this layer.

2.2.2 Nil Kham Haeng

Nil Kham Haeng has an intermittent archaeological sequence from the Neolithic to the proto-historic period, and provides continued evidence of intensive Iron Age copper smelting in the Valley. The site is located at 100.661°E, 14.9549°N at the western edge of the Valley, and was partially damaged by the construction of a reservoir by the Thai

4 The potential significance of these finds was only appreciated after the recovery of a complete perforated cylinder at Nil Kham Haeng (Vincent Pigott pers. comm.).

military (Figure 2.5). The remaining deposits extend over more than 30,000m², and lie in excess of 6m deep. A total of four trenches with a surface area totalling c. 100m² were excavated in three field seasons by TAP in 1986, 1990, and 1992 (Figure 2.9), but given the size of the site, these investigations should be considered preliminary in their scope (Pigott *et al.* 1997). The site is uninhabited due to its containment within the Sa Pra Nak Royal Thai Army airbase.

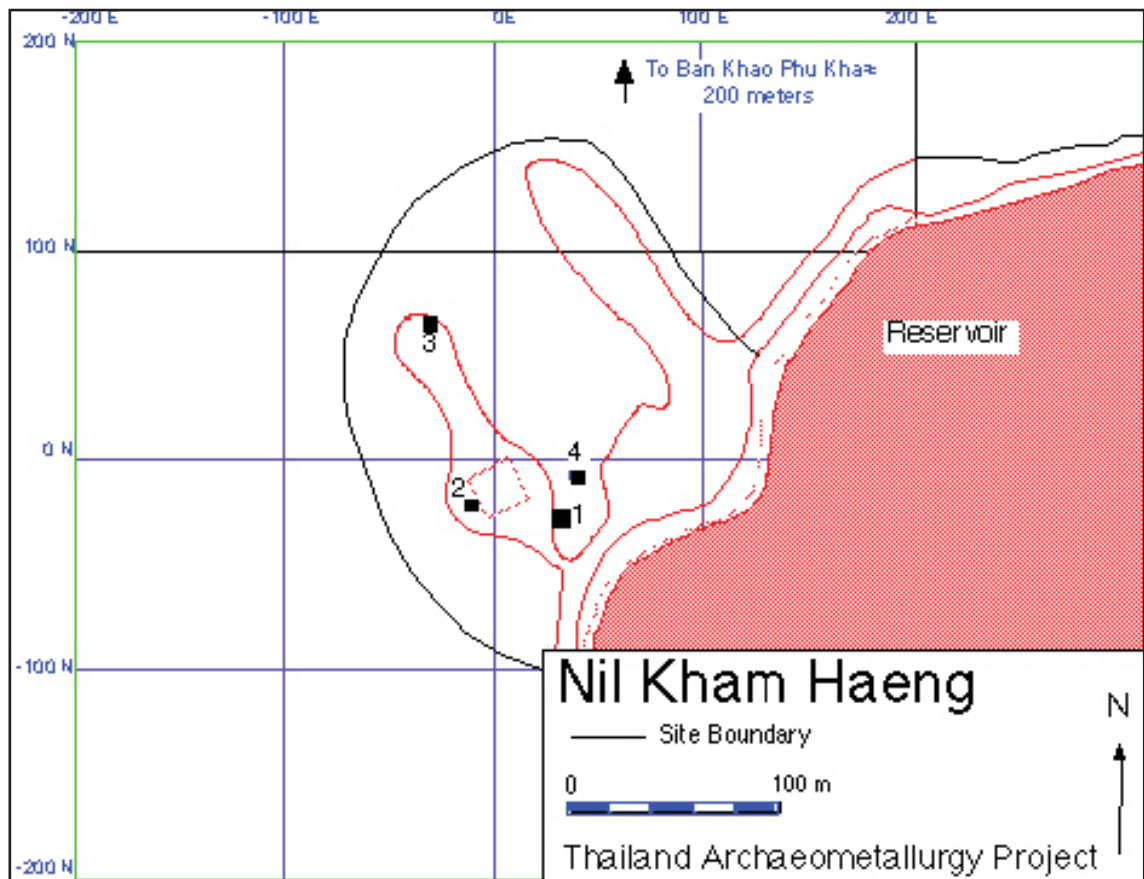


Figure 2.9 - Plan of Nil Kham Haeng showing trenches excavated. Courtesy of TAP.

The original TAP dating of Nil Kham Haeng has been substantially revised by Rispoli *et al.* (forthcoming), and is now comprised of three periods. The first of these, ‘Period 1’ or ‘NKH1’, is evidenced by only a few Neolithic sherds dating from the late 3rd to early 2nd millennium BCE, whose source at present remains uncertain.

‘Period 2’ or ‘NKH2’ is an early Iron Age deposit containing evidence for copper smelting. Due to time constraints caused by excavation at depths in excess of 6m, the exposure of this layer was limited to about 1m² at the base of Operation 1 (Weiss 1992). This small window rather limits what can be said about prehistoric activity during this period at Nil Kham Haeng, but TAP archaeologists clearly noted the distinct difference in material culture and matrix formation between NKH2 and the preceding NKH3. However, Weiss (1992: 1) specifically records that the NKH2 archaeometallurgical material was identical to that

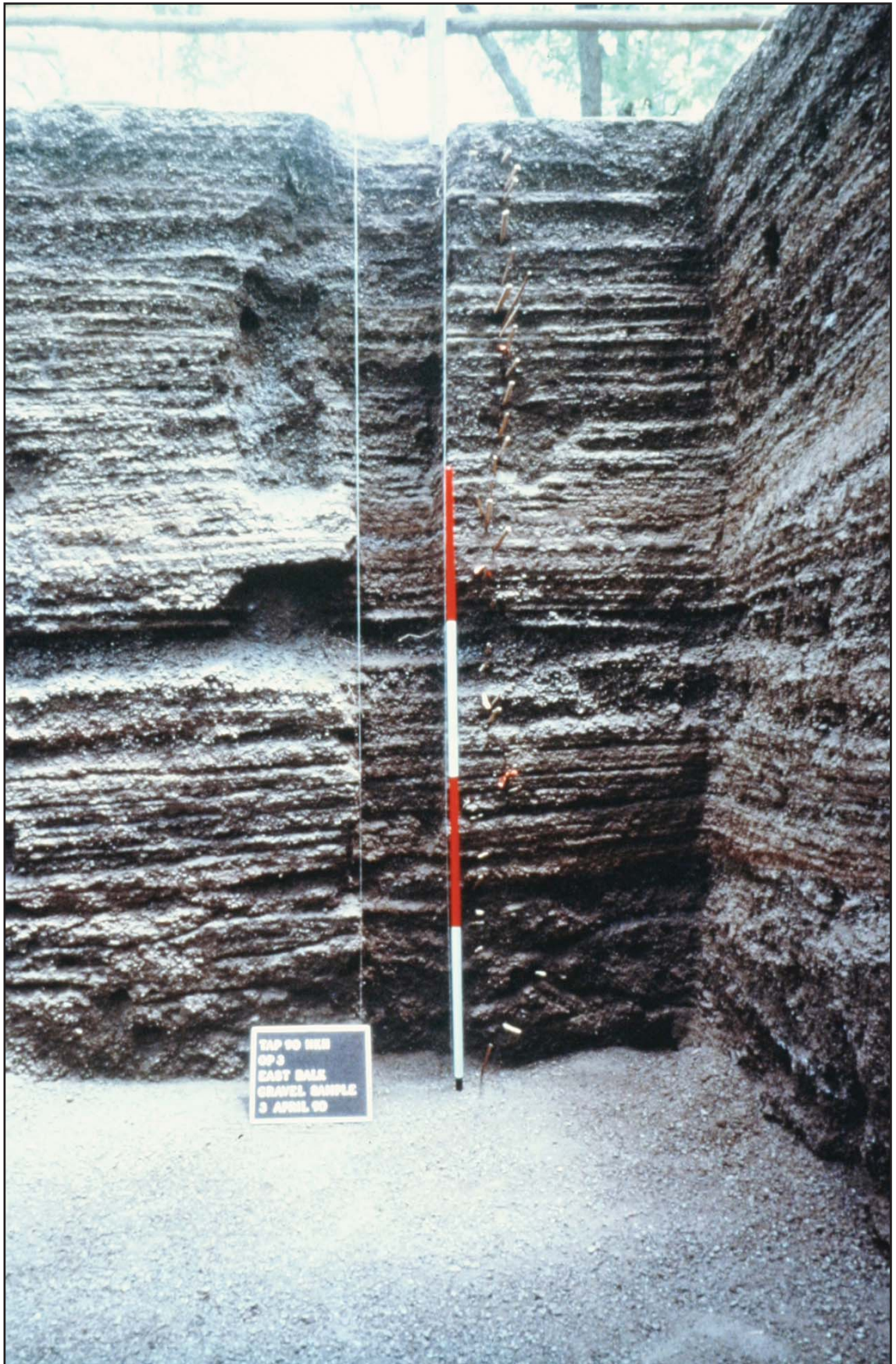


Figure 2.10 - Eastern section of 'Operation 3' during the 1990 season at Nil Kham Haeng, only NKH3 contexts are visible. Courtesy of TAP.

from Iron Age Non Pa Wai's Metallurgical Phase Two (see above). During subsequent study of the ceramic assemblage, Fiorella Rispoli (pers. comm.) found it was impossible to distinguish between NPW3 and NKH2 wares on a typological and technological basis. This would assist in dating NKH2 between c. 6/500 BCE – c. 300 BCE according to the revised Valley chronology (Rispoli *et al.* forthcoming).

Due to the very small amount of material recovered from the NKH2 exposure, no samples were analysed during the present study. Whilst this is a situation that should be remedied, the unequivocal nature of the Nil Kham Haeng excavators' NPW3 technological analogy (Weiss 1992) would incline the author to interpret Nil Kham Haeng Period Two metallurgy as being akin to Metallurgical Phase Two (NKH2/MeP2). Although preliminary, this attribution is in line with the current project's aim to examine copper smelting styles at a Valley level.

'Period 3' or 'NKH3' is also an Iron Age deposit, but with a fundamentally different character to that of NKH2. On Rispoli's current assessment, the domestic pottery dates the deposit from c. 300 BCE to c. 300 CE, and thus extends Nil Kham Haeng's chronology well into the Southeast Asian proto-historic period (Rispoli *et al.* forthcoming). The stratigraphy of NKH3 is characterised by multitudinous, thin lenses of finely crushed metallurgical materials (Figure 2.10, Pigott *et al.* 1997: Figure 14 & 15). This is in marked contrast to both the preceding Iron Age intensive copper smelting horizons in the Valley - NKH2 and NPW3 - and is in striking similarity to archaeometallurgical deposits reported from the Pottery Flat and Ban Noi loci at Phu Lon (Pigott & Weisgerber 1998), and also those recently excavated by LoRAP at contemporary Khao Sai On, 20km south-south-east of Nil Kham Haeng (Ciarla 2007b). Could this textural change in archaeometallurgical deposits be suggestive of a substantial shift in production techniques, namely the deliberate and determined comminution of enormous quantities of metallurgical materials, both before and after high-temperature processing? It has been suggested that the uniform layering of NKH3 could be interpreted as regular hydraulic redeposition of spoil heaps from beneficiation, smelting, and mechanical metal recovery processes, possibly during the monsoon period (Cremaschi *et al.* 1992).

Perhaps due to this regular natural modification of cultural deposits, occupation evidence in the form of domestic ceramics, faunal assemblages, and inhumations were interspersed with the copper processing remains that comprise the bulk of the NKH3 matrix (Pigott *et al.* 1997). What appeared to be living surfaces were discerned by TAP archaeologists, interleaved within the many layers of crushed copper production debris. One particular

inhumation was contained within a log coffin, and may be comparable to examples from Dong Son and Ongbah (Ha Van Tan 1994, Weiss 1992: 2). Of interest, the ‘founders’ burials of Non Pa Wai Mortuary Phases 2a and 2b seems to continue or revive in NKH3. At least seven NKH3 graves contained metal artefacts, including cordiform socketed implements, bracelets, rings, and a spearpoint. Two burials were interred with copper minerals and one had a complete perforated ceramic cyclinder, initially interpreted as a furnace chimney by Pigott *et al.* (1997: 130, Figure 10).

Metallurgical areas were detectable only as vague scorched ‘hotspots’ and slag concentrations (Weiss 1992), but the enormous quantities of related materials recovered are indicative of a similar scale of production intensity to Non Pa Wai’s Period 3. The NKH3/MeP3 metallurgical assemblage includes metal, crushed ore, gangue, and slag, along with perforated ‘furnace’ fragments, smelting pit linings (‘slag-skins’), with some bivalve, cup and conical moulds, and crucible sherds.

Ore and gangue minerals:

As mentioned above, crushed mineral accounts for the vast bulk of the NKH3 matrix, tens of thousands of tonnes distributed over c. 3ha and more than 6m deep in places. The amount of labour this represents is hard to over-estimate, and certainly evidences a rigorous and long-term commitment to extract the maximum available metal from the best possible smelting charge by Nil Kham Haeng metal workers in the later Iron Age. The mineral assemblage has a distinctly sulphidic nature compared to that recovered from Non Pa Wai.

Slag:

As per the minerals above, slag is also a major constituent of the NKH3 matrix and metallurgical assemblage. Thousands of kilogrammes of slag are recorded as having been found in TAP excavations, a number which can be multiplied manyfold across the entire site. The fragmentary nature of the slag means the original morphology is usually unclear, but some can be described as ‘slag cakes’ or ‘slag casts’. There is a visibly greater homogeneity and glassiness when compared to Non Pa Wai material. For a full analysis of NKH3/MeP3 slag please see Chapter 6.

Crucibles:

Crucibles are thought to have been rare in the MeP3 deposit, due perhaps to their being used repeatedly, or perhaps having a different purpose in later Iron Age copper production, but they appear not to have played a fundamental role in the smelting of copper – the author’s focus. The NKH3/MeP3 crucible sherds have yet to be studied in any detail by TAP archaeologists and the lack of any intact or near complete vessels means their typology is at present imprecisely known.

‘Slag skins’:

The considerably reduced quantities of crucibles is currently best explained by the presence of enormous quantities of fragments of rice chaff-tempered baked clay with an adhering layer of slag, suggesting the NKH3/MeP3 copper smelting reaction was not contained within crucibles as in NPW3/MeP2 production, but in shallow pits lined with clay to isolate the hot smelting system from the ground (Pigott *et al.* 1997, Weiss 1992).

Perforated ceramics:

Perforated ceramic cylinder sections were recovered from NKH3 industrial deposits, and were recognised as being fragments of the near complete artefacts found in, for example, graves 1 and 5 in ‘Operation 4’ and ‘Operation 1’ respectively (Pigott *et al.* 1997: Figures 18 & 19, White & Pigott 1996: Figure 13.9). These cylinders, with perhaps four to six perforations c. 3cm in diameter (e.g. Figure 6.7), were made from a friable rice chaff-tempered clay which fired bright red, although a thin white layer is often present on the interior wall. The complete examples have a wall thickness of c. 5cm, stand c. 20cm tall, and are c. 20cm in diameter. Interestingly, the ceramics are neither slagged nor vitrified but TAP archaeologists have initially interpreted them as being furnace chimneys for copper smelting operations (*ibid.*: 130, see also Ciarla 2007b). For further discussion please see Chapters 6, 7, and 8.

Metal:

TAP excavators recovered a number of copper-base artefacts from NKH3 burials, substantially in excess of the few copper-base artefacts excavated from NPW2 and NPW3 contexts (Pigott *et al.* 1997: Figure 17, Wang *et al.* 1998). The majority of the NKH3 metal was unalloyed copper in the form of thin ‘cordiform’ implements, which occurred, for example, in a burial in a group of 60 or more, but they were corroded into one somewhat amorphous mass making exact counts impossible. Only through extensive conservation will the final count be ascertained exactly. The casting of these artefacts in unalloyed copper means they would have had limited mechanical utility, especially when they were

so thin and frequently miscast. Though previous scholars have interpreted them as ‘copper socketed points’ (Pigott *et al.* 1997: 131) or ‘arrowheads’ (Bennett 1989: 337), the author prefers Pigott *et al.*’s (1997: 131) alternative suggestion of the cordiform implements as a distinctive ingot type, perhaps identifying NKH3’s standardised copper output. The author suggests the pseudo-functional form of these ‘ingots’ might then represent what the metal could become when alloyed, cast, and worked into a final artefact, a form of prehistoric branding (cf. Wengrow 2008)? Examples of similar artefacts have been reported from Nong Nor and Ban Chaimongkol in central Thailand (Higham *et al.* 1997: 177, Figure 5, Onsuwan-Eyre 2006), Ban Non Wat in northeastern Thailand (Charles Higham pers. comm.). There are even reports of similar ‘ingots’ from Bali (Peter Bellwood pers. comm., Soejono 1972), an island with no known copper sources but contained within extensive prehistoric maritime exchange networks (e.g. Bellina 2007). Ciarla (2007a: 321, Figure 17) has also noted typological resemblance between the Nil Kham Haeng ‘ingots’ and the ‘axes’ from broadly contemporary 4th c. BCE Warring States site of Hejiashan in Yunnan. The recovery of a NKH3 mould for the cordiform artefacts suggests they are part of the on site production sequence (Pigott 1999a: Figure 17). Whether comparable artefacts found outside the Valley can be analytically attributed to its metalworkers or other regional producers is obviously one of great significance for evidencing long distance social interaction throughout Iron Age Southeast Asia (see Chapter 9).

2.3 Other metallurgical sites in or near the Khao Wong Prachan Valley

2.3.1 Non Mak La

Non Mak La is dispersed around 100.675°E, 14.9639°N, less than 1km from Non Pa Wai, and was excavated by TAP in 1994 (Pigott *et al.* 1997). The limits of the site are uncertain, due in part to extensive ploughing, but the core surface-realised distribution is approximately 40,000m², and up to 2m deep. The sequence ranges from Neolithic, Bronze Age, and Iron Age phases, as well as historical material. Previously, scholars had maintained that Non Mak La’s chronology overlaps that of Non Pa Wai on the basis of shared material culture (Pigott & Natapintu 1996-1997). However, Fiorella Rispoli (pers. comm., and following on from Rispoli 1997) identifies an at best weak connection between domestic pottery traditions at the two sites, a situation which need not rule out contemporaneity.

The larger number of primary burials (56), and the presence of domestic ceramics, faunal remains, and other craft activities suggest Non Mak La was a multi-activity site, but probably included settlement. Whilst there is at least one copper-related metallurgical slag concentration at Non Mak La, it remains imprecisely dated, and by no means compare in

volume to those at Non Pa Wai and Nil Kham Haeng (Bennett 1988a, Natapintu 1988), thus materials from this site were not analysed during the current study.

2.3.2 Tha Kae

Tha Kae is located c. 15km northeast of the Khao Wong Prachan Valley. The site, covering c. 120,000m², was investigated by the Fine Arts Department in the late 1970s (Natapintu 1979, 1980, 1984), and subsequently by LoRAP in the late 1980s (Ciarla 1992, 2005, Rispoli 1992). Looting and construction activity had seriously affected Tha Kae's archaeological deposits since the 1970s, and excavators were forced to focus on a small undisturbed section named 'The Central Island'.⁵ The result was an archaeological sequence spanning the Bronze and Iron Ages, with concentrations of slag being reported in the latter (Ciarla 2005: 82). Of further interest, a horizon of calcrete comparable to Non Pa Wai's Caliche Crust separated the two layers, and suggests that the conditions which led to its development maybe a regional phenomenon.



Figure 2.11 - Crushed matrix, hotspots, and technical ceramics (red square) at Khao Sai On, image width c. 2m at base. Courtesy of LoRAP.

2.3.3 Khao Sai On

5 Tha Kae is now completely destroyed.

Khao Sai On refers to a cluster of sites centred around 100.73°E, 14.7845°N, approximately 20km southeast from the Khao Wong Prachan Valley (Figure 3.5). The locale is currently under investigation by LoRAP, who report a complete metallurgical production sequence of mining and smelting evidence, contemporary with Nil Kham Haeng Period 3 (Ciarla 2007b). Of the greatest interest, the investigators report that the matrix of the smelting area is almost identical to that of NKH3, and is composed of crushed ore, gangue, slag, and perforated ceramic fragments, and incorporating ‘hotspots’ with closely associated pit features (Figure 2.11). To further cement the technological connection, a burial (Ciarla 2007b: 400-401) contained a complete perforated ceramic cylinder, and fragments of others, entirely comparable to that reported from Nil Kham Haeng (see above). On the basis of current LoRAP evidence, the author would tentatively assign Khao Sai On’s metallurgical assemblage⁶ to the later Iron Age MeP3 tradition, and would regard the site as providing support for a regional sequence in copper-smelting behavioural development.

2.4 Previous archaeometallurgical research in the Khao Wong Prachan Valley

In part due to the outstanding, and to date unique, confluence of high-volume, high-intensity archaeological evidence for prehistoric copper production, the Khao Wong Prachan Valley became a foci for archaeometallurgical studies in Southeast Asia in the 1980s and 1990s, with original laboratory-based contributions from Anna Bennett, William Rostoker, and Dong Ning Wang. However, their analytical insights were also to a large extent enabled by the laudable supply-side TAP research objectives of Surapol Natapintu and Vincent Pigott, and the sustained metallurgical focus of the entire TAP team.

Bennett 1988b:

In a pioneering doctoral study, Anna Bennett’s analyses of metal, slag, and technical ceramic samples from the 1986 TAP season, surface survey, and private collections, identified many of the metal-related activities taking place at sites in and around the Khao Wong Prachan Valley, in what may be considered the first technological study of copper-base extractive metallurgy in Southeast Asia (Bennett 1988b). Using data and material available in the mid 1980s, Bennett’s analytical programme included the sites of Non Mak La (*ibid.*: 143-216), Non Pa Wai (*ibid.*: 217-259), Nil Kham Haeng (*ibid.*: 260-283), Wat Tung Singto (*ibid.*: 284-291), Tha Kae (*ibid.*: 292-297), Khao Sam Yoi (*ibid.*: 298-320), and the mineralisations Khao Phra Bat Noi, Khao Phu Kha, and Khao Tab Kwai (*ibid.*: 231-325), ranging from the regional Metal Age right up to the Dvararati and Sukhothai periods (*ibid.*: 338)⁷. As such, Bennett’s doctorate had a wide remit to study and

6 Samples of which were not available for study.

7 Bennett’s thesis was submitted in November 1988, and thus she did not have

interpret all the metal-related remains emerging from an exciting period of archaeological investigation in the Khao Wong Prachan Valley area. In summary, Bennett's reconstructed metallurgical practice in the prehistoric Valley and its environs as the smelting of local copper minerals in an efficient crucible-based reaction fluxed with local iron minerals, producing copper with significant but varying levels of arsenic and sulphur (Bennett 1989: 347). The Valley sulphidic arsenical copper alloy product was seen as the likely source for copper-base artefacts of similar composition then (mid/late 1980s) reported around central Thailand (*ibid.*), although this has never substantiated with a systematic large-scale programme of lead isotope and/or trace element analyses (see Chapter 9).

Although material from some of the same sites have been analysed in both Bennett's doctorate and the current study, the research objectives are quite dissimilar. Whilst Bennett aimed to provide a preliminary overview of pre-modern metallurgical activities in the Lopburi area whilst TAP excavations were ongoing, the current author was tasked with deriving higher resolution technological reconstructions to begin to address long-term change in prehistoric smelting behaviour at just two sites, Non Pa Wai and Nil Kham Haeng, with the benefit of many years of post-excavation study and interpretation by the TAP team. In addition to providing a diachronic perspective, the present study also differs from Bennett's in that the author believes the Non Pa Wai production technique was anything but 'efficient' (see Chapter 5) and that the presence of residual iron minerals in Valley slags is probably not indicative of 'fluxing' (see Chapter 8). Nevertheless, the broad scope and analytical competence of Bennett's research in central Thailand (Bennett 1988a, 1988b, 1989, 1990) ensures it remains a cornerstone of archaeometallurgical knowledge in Southeast Asia and, combined with her work in west-central Thailand (Bennett 1982, 1992) and ongoing efforts on regional metal technologies (e.g. Bennett 2008), cements a scholarly contribution which continues to this day.

Rostoker *et al.* 1989 and Wang & Notis n.d.:

At the same time as Bennett was finishing her PhD in London, William Rostoker, at the invitation of Vincent Pigott, was working on a copper smelting reconstruction based on the exothermic co-smelting reaction between oxidic (malachite) and sulphidic (chalcopyrite) copper minerals known to be available within the Valley (Rostoker & Dvorak 1991, Rostoker *et al.* 1989, Vernon 1988). Co-smelting, or the production of metal from mixed ore sources, has long been known to industrial metallurgists (e.g. Hofman 1914: 66-99), but the Khao Wong Prachan Valley was the first proposed employment in an archaeological context (see Lechtman 1991, 1996, Lechtman & Klein 1999 for

access to any TAP material from Nil Kham Haeng, or later seasons at Non Pa Wai.

other examples). A subsequent study by Dong Ning Wang and Michael Notis at Lehigh University argued in support of Valley co-smelting on the basis of comparable sulphur-rich inclusions within archaeological and experimental copper microstructures, but this has never been fully published (Wang *et al.* n.d.).

Whilst thermodynamically correct and practically plausible, Rostoker *et al.*'s (1989, 1991) reconstruction was largely theoretical and based on experiments conducted under laboratory conditions, which tend to be much more consistent and manageable than those in field simulations (see Chapter 7). Without a detailed consideration given to how co-smelting might have been conceived and practiced in a prehistoric setting, the author prefers to see the theory as a technical likelihood at the chemical level, but probably not a deliberate and intentional strategy by Valley metalworkers as we remain unaware of the exact composition of the smelting charge and the ratio of oxidic to sulphidic minerals. Though significant advances in the technical understanding of pre-modern co-smelting processes have been made (e.g. Artioli *et al.* 2007, Burger *et al.* 2007), it is not the subject of detailed investigation in the present study, which instead focuses follows a more

Characteristic	MeP1	MeP2	MeP3
Founders' graves	X	-	X
Artefact moulds	X	X	X
Ingot moulds	-	X	X
Pit features	-	?	X
Smelting crucibles	-	X	-
'Slag-skins'	-	-	X
Installation superstructure	-	X	X (perforated)
Slag homogeneity	-	Low	Medium
Site matrix	-	Ashy	Crushed

Table 2.1 - Predominant features of prehistoric Valley technological styles.

'human-level' approach via the reconstruction of prehistoric Valley *chaînes opératoires* (see Chapter 3).

The technical efforts of the scholars above have definitely furthered our understanding of prehistoric copper smelting in the Valley, and have enabled over twenty years of profitable discussion on Thai extractive metallurgy. Likewise, the established TAP interpretation (Figure 2.12) of prehistoric Khao Wong Prachan Valley copper industry has received wide acceptance and been extremely influential upon those synthesising Southeast Asian metallurgical evidence (e.g. Higham 1996: 269-274; 2002: 118-122; White & Hamilton in press). However, reassessing the evidence from first principles, including the excavator's original observations and over two decades of regional archaeological advances, suggests

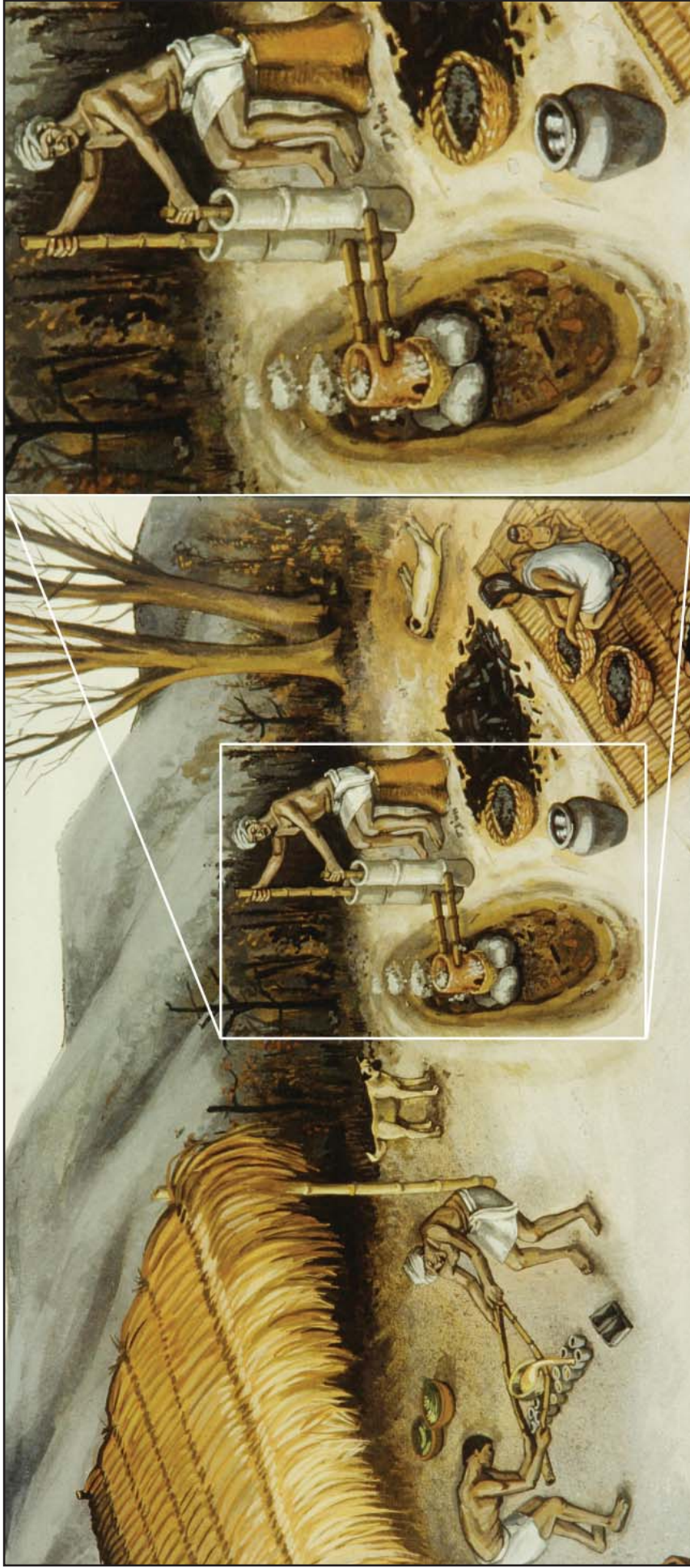


Figure 2.12 - Artist's impression of prehistoric Khao Wong Prachan Valley copper smelting, prior to the present study. Image: courtesy of Ardeth Abrams (Ban Chiang Project), modified by author.

the established technological reconstructions are in need of modification. As remarked repeatedly throughout this chapter, the re-dating of the Khao Wong Prachan Valley sites, along with an improved appreciation of their formation, appears to separate the metallurgical evidence into a sequence of three phases spanning the Bronze and Iron Age periods, of which the diagnostic features can be seen in Table 2.1. Metallurgical phases 1 refers to consumption and founding, phases 2 and 3 refer to extraction, founding, and consumption. Phases 1 and 2 seem to be present at Non Pa Wai, and phases 2 and 3 at Nil Kham Haeng, as well as phase 3 also being likely at Khao Sai On. Thus, before a single laboratory analysis is considered, our knowledge of local metallurgical development is already hugely refined.

2.5. Sampling strategy

The TAP excavations in the Khao Wong Prachan Valley recovered many tonnes of mineral, slag, and technical ceramic. The bulk of this archaeometallurgical material is stored in the King Narai Palace Museum in Lopburi, Thailand, but a substantial sub-sample was exported to the US and is held at the University of Pennsylvania Museum in Philadelphia. It is increasingly recognised that sample populations for archaeometallurgical study are often far from statistically significant (e.g. Humphris *et al.* 2009), but this is an unfortunate reality given the size and nature of industrial deposits, as well as the time and financial cost of analysis. Given these practical limitations, studying material from every context at every TAP site was simply not feasible. The current research project was concerned with discerning technological choices and styles (see Chapter 3) in prehistoric Valley copper smelting behaviour and thus focused on the two major production sites of Non Pa Wai and Nil Kham Haeng. The lack of stratigraphic resolution, given the highly disturbed deposits at the former and probable hydrodynamic layering at the latter, means it was only possible to generate general *chaînes opératoires* (or technological reconstructions, see Chapter 3) for copper smelting activities at each site and mitigated against any investigation of intra-site technological change. Nevertheless, the chronological and spatial contiguity between Non Pa Wai and Nil Kham Haeng provided an excellent opportunity for inter-site comparison and the discussion of long-term technological change between the two.

Samples for analysis were selected during two visits to the TAP archives in Philadelphia during December 2005 and October 2006. The material from Non Pa Wai and Nil Kham Haeng was held in an organised system separating the material into boxes by site and artefact type, but the Khao Wong Prachan Valley collection in the United States alone is

massive. Attempting to derive a sub-sample that was to some degree representative of the original industrial deposits, the author employed a ‘stratified sampling frame’ to select boxes representing contexts extending horizontally and vertically across each site (Orton 2000)⁸. From these boxes a ‘random sampling strategy’ was used to select samples (*ibid.*), on the proviso that a bag contained sufficient material to produce [P]ED-XRF pellets and RLM/SEM-EDS polished blocks (see Chapter 4). In total a selection of 18:20 slag samples, 13:6 mineral samples, and 13:3 technical ceramic samples, were taken from Non Pa Wai and Nil Kham Haeng respectively. Bulk compositional analysis (see Chapter 4) of these samples (excepting ‘slag-skins’) guided sub-sampling of the population for microanalysis by identifying chemical variability and those samples from the two sites or overlapping and outlying values. In summary, the sampling strategy was intended to provide a selection of all available materials (mineral, technical ceramic, and slag) probably involved in Valley copper smelting, in sufficient quantities to produce higher resolution (though still preliminary) *chaînes opératoires* for both sites so as to potentially identify past technological choices and styles, as well as enabling the discussion of technological change in the Valley over the course of the attested Iron Age production period, as per the research aim. However, it is conceded that the statistical significance of current study’s sample cannot be assessed and thus the data are open to alternative interpretations.

Summary

This chapter has provided the geological background and detailed information on the major mineralogical and archaeological deposits in the prehistoric Khao Wong Prachan Valley, as well as discussions of neighbouring sites and prior archaeometallurgical in the area. Building upon the previous interpretations of TAP and related project members, the Valley data have been drawn together to give an initial reconstruction of small scale but intensive crucible and bowl furnace copper smelting operations. It is thought that industrial activities were organised at a household level though evidence for individual work and/or habitations areas is absent in the remarkably uniform distribution of metallurgical artefacts in the matrices of both smelting sites. Now, having discussed the contexts, assemblages, and sampling of Non Pa Wai and Nil Kham Haeng, Chapter 3 introduces the theoretical framework with which the current study’s archaeometallurgical analysis of prehistoric extractive Valley metallurgy was underpinned.

⁸ In the sample catalogue, the ‘Op.’ or ‘operation’ indicates the excavation square or the horizontal variant (see Figures 2.6 and 2.9), and the ‘Level’ represents the vertical component; a higher number indicating greater depth.

Chapter 3

Theoretical approaches to ancient technologies

The primary purpose of this thesis is to use archaeometallurgical evidence to investigate diachronic technological behaviour in the prehistoric Khao Wong Prachan Valley, but to achieve this it is necessary to establish a sound theoretical framework. Thankfully, this need can be adequately provisioned from a rich theoretical literature developed by scholars for whom technology has long been a core concern. Due to the close association of material culture studies and archaeology, the conceptual frameworks for addressing patterning and variation in ancient technologies have waxed and waned largely in line with theoretical trends within the wider discipline and the social sciences generally (e.g. Bintliff 2008, Costin 2001, Henry 2002, Trigger 2006). For many years ancient technology researchers have combined social and physical science techniques but have been argued to have failed in uniting their philosophies (cf. Jones 2004, Killick 2005). The present study is hoped to move beyond this paradigm by employing a technological approach to material culture whose investigative and interpretive framework is derived from the ‘Anthropology of Technology’ theoretical literature (see e.g. Miller 2007 for overview), ultimately sourced from a range of fields in the social sciences.

The purpose of this chapter is to justify the technological approach and show how this perspective is central to the investigation of Khao Wong Prachan Valley metallurgy. The first section will discuss what contemporary archaeologists mean by ‘technology’ and how this can differ from the wider public perception. The second section introduces the francophone concept of the *chaîne opératoire*, whilst the third deals with the concepts of ‘technological style’ and ‘technological choice’; all of which are essential for the generation of technological reconstructions for Iron Age metallurgical behaviour at Non Pa Wai and Nil Kham Haeng (detailed in Chapters 5 and 6 and synthesised into a long-term account of Valley metallurgy in Chapter 8). The fourth section broaches the ‘organisation of production’, a topic dominated by Cathy Lynne Costin’s framework which attempts to intertwine technological issues with those of economy and social complexity. The fifth section concerns the application of the Weber fraction to archaeometallurgical assemblages, and the sixth and final section will discuss the theoretical background for the present study’s experimental archaeological programme, the results and findings of which can be seen in Chapter 7.

3.1 Social constructionism and ancient technologies

As noted by Killick (2004a: 571), social constructionism does not refer to a well-defined cohesive intellectual school, but is a collective term for approaches to archaeological material culture including: technological style (e.g. Lechtman 1977, White 1988, Veldhuijzen & Rehren 2007), technological choice (e.g. Lemonnier 1993, Sillar & Tite 2000), and advocates of practice, agency, and materiality in archaeological theory (e.g. Dobres & Hoffman 1994, Gardner 2008, Jones 2002, Martín-Torres *et al.* 2007, Martín-Torres & Rehren 2008, Taylor 2008). Though varied, these inter-related bodies of thought offer perspectives on material culture arguably conceived in response to the generalising and mechanistic tendencies of processual archaeology in the 1960s and 1970s (Shanks 2008), and certainly influenced by concurrent developments in the social sciences (e.g. Appadurai 1986, Geschiere 2005, Gosden & Marshall 1999, Knappett 2005, Miller 2005, Pfaffenberger 1992).

The references cited represent a significant scholarly diversity, but much of the variation is expressed in nuance and emphasis. What social constructionists can be argued to share is a rejection of the general Western public perception of material culture, described by Bryan Pfaffenberger (1992) as the ‘Standard View of Technology’. In this paradigm, artefacts, and the technologies which produced them, are divorced from culture and society at large and are predominantly measured in degrees of optimised functional efficiency. The prejudiced selection of the most efficacious technical solution would tend to assume a unilinear trajectory of technological development, typically synonymous with increasing social complexity and progress (*ibid.*). Social constructionists would generally argue the ‘Standard View’ is highly unacceptable for the study of technologies across vast stretches of space and time, due not only to the potential for extreme divergence in the value systems and motivations for endeavour in pre-modern and non-Western societies, but also because technologies must be seen as integral and not peripheral to societies (e.g. Killick 2004a). Social constructionists would also make the case for the existence of multiple technological solutions for most tasks, and thus the preferences expressed by people through technological choices can reflect to a high degree their particular historical context. Therefore, changes in archaeological material culture derive from technological choices that were, in part, socially constructed.

A common conviction of social constructionists is that technologies and the material culture they create are socially contextualised, and that this embedded social meaning is created through networks of reciprocal relationships between objects and people (e.g. Appadurai 1986, Appadurai 1998, Binsbergen 2005, Brück 2005, Costin 2001, David & Kramer 2001, Demarrais *et al.* 1996, Gabora 2008, Gardner 2008, Gosden & Marshall 1999, Hays-Gilpin 2008, Jones 2002, Jones 2008, Knappett 2005, Kopytoff 1986, Lahiri

1995, Lemonnier 1989, 1992, 1993, Pfaffenberger 1988, 1992, Taylor 2008). Defining ‘technology’ as ‘technical plus social’ will not normally satisfy a social constructionist, as innumerable ethnological and ethnoarchaeological studies (reviewed in e.g. David & Kramer 2001) have repeatedly demonstrated that in many societies, perceptions of material culture do not divide neatly into the objective and subjective, active and passive, functional and stylistic. ‘Physical’ objects and ‘social’ humans interact, exchange, and modify each others’ corporeality and identity in dynamic socio-technological systems where the boundaries between the two are both blurred and permeable (Pfaffenberger 1992). For social constructionists, ‘technology’ is a concept that can encapsulate the entire sphere of human experience pertaining to material culture. Though we can never hope to unravel the full complexity of past societies, a contextualised high resolution understanding of ancient technologies does have the potential to give us some insight into the people that produced and consumed artefacts (Taylor 2008: 297). Social constructionists believe understanding technological behaviour is important in its own right as a significant element of human lives (e.g. Killick 2004a, Knapp *et al.* 1998, White 1988).

The use of social constructionist perspectives in archaeology has often been led by those researching lithic materials (e.g. Bellina 2007, Roux *et al.* 1995, Sinclair 2000) and ceramic technologies (e.g. Bacus 2004, Bouvet 2008, Courty & Roux 1995, Rispoli 2007), but perhaps in part due to the physical sciences background of many practitioners, anthropological approaches to archaeometallurgy are not as prevalent as they should be (though cf. Childs 1991, Killick 2004b, Lechtman 1984, 1988, 1991, 1993, 1996, 1999, Lechtman & Klein 1999, Martín-Torres *et al.* 2007 amongst other notable exceptions), although significant efforts continue to be made to address this issue (i.e. Rehren *et al.* 2007 and the Minds Behind the Metal session at the 2008 meeting of the Society of American Archaeologists in Vancouver). In Southeast Asian archaeology, social constructionist approaches have already made significant strides towards identifying the ‘invention’, ‘diffusion’, or ‘innovation’ of regional technologies (e.g. Adams 1977, Bellina 2001, 2003, 2007, Bellina 2008, Ciarla 2007a, Pigott & Ciarla 2007, Rispoli 2007, White 1988, White & Hamilton in press), though there remains an enormous potential for technological research within the region to inform more broadly on social behaviour.

3.2 The *chaîne opératoire* technique

Often, the first step in studies of ancient technologies is to use all the available evidence (archaeological, archaeometric, ethnographic, experimental, textual etc.) to reconstruct the network of human behaviours and physical acts involved in the production, exchange, and consumption of archaeological material culture. This approach is known as the *chaîne opératoire technique* (loosely rendered in English as ‘technological reconstruction’), due

to its Francophone theoretical origins (e.g. Leroi-Gourhan in Audouze 2002 and Ingold 1999), though others (e.g. Killick 2004a: 573) make the case for an independent, though later, invention in North America. The *chaîne opératoire technique*, whether employed explicitly or implicitly, can be argued to constitute the foundations of most contemporary technological studies. The current approach to a large extent derives from the work of anthropologist André Leroi-Gourhan (e.g. Audouze 2002, Ingold 1999) and his focus on ‘gesture’ in ethnographic production techniques; literally the physical movements of the human body that control the application of ‘energy’ to ‘matter’ via the medium of ‘objects’ (tools) and guided by ‘knowledge’ (or the more practical ‘knowhow’). Leroi-Gourhan, and subsequently Pierre Lemonnier (e.g. 1988, 1992), regard individual technological systems as being the particular configurations of these five major components, and that by reconstructing technological *chaînes opératoires* one can approach, at least indirectly, multilateral relationships within the societies that produced them. The approach requires the conceptualisation, description, and organisation of all possible factors and actors involved in the process of creating, using, curating, and disposing of an object, and should certainly be regarded as a relational web rather than a linear chain of connection (cf. Schiffer 1972, 2004).

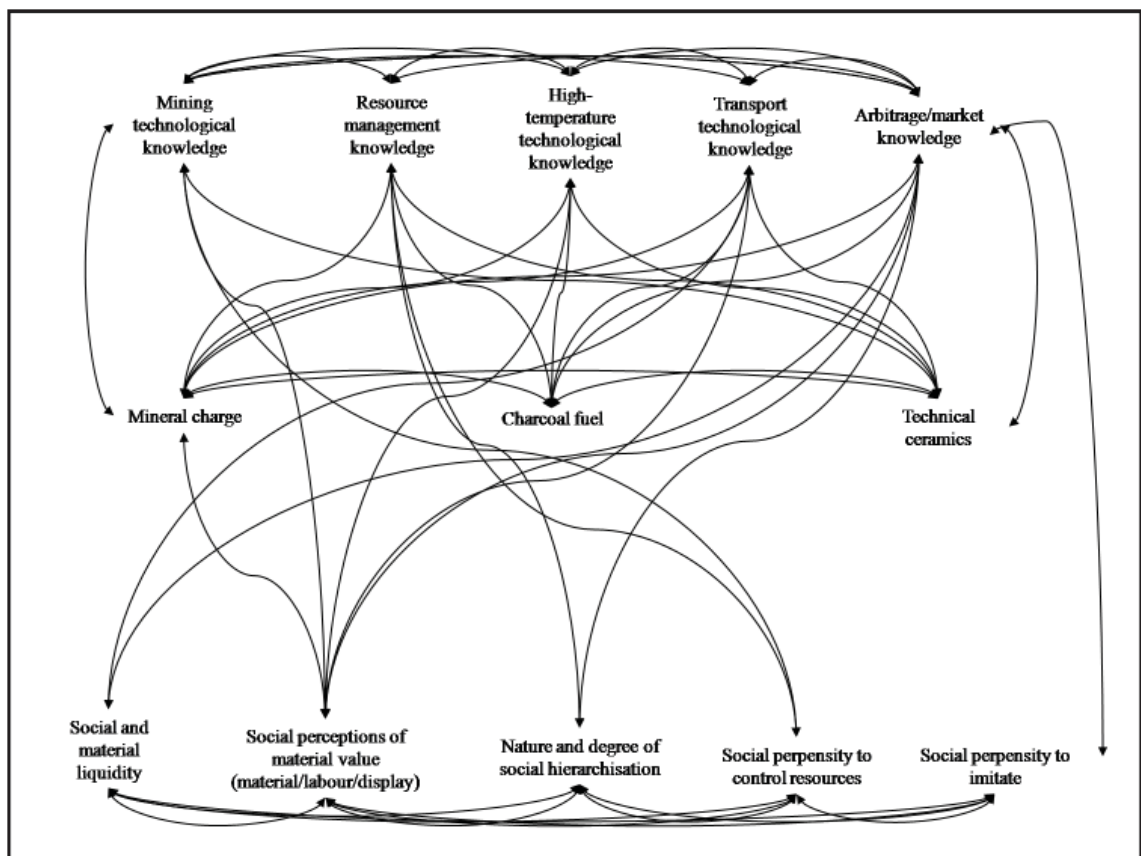


Figure 3.1 - A schematic of potential links between materials, knowledge, and some hypothetical characteristics of human societies. Image: author.

Technological networks have an almost fractal degree of complexity, with the choices of

each actor cascading to other agents and structures via a potential multitude of interaction paths (cf. Bentley 2008). An attempt to display this complexity can be seen in Figure 2.1, which depicts a highly simplified network of the possible agents and structures involved in a hypothetical copper smelting operation imperfectly and artificially divided into materials, knowledge, and societal characteristics. Figure 2.1 indisputably bears a degree of resemblance to processual systems diagrams of the 1960s and 1970s (e.g. Flannery 1968, Renfrew 1972), but how one perceives such a schematic is largely determined by one's theoretical background and analytical objectives. A proponent of systems theory might try to use the network as a scaffold from which to build up generalising laws for human behaviour. However, the social constructionist would probably regard the network as a socially-glutinous web of interaction, from which the agency of different actors and structures can be extracted and related. In either configuration there is no denying the intricacy of even a rudimentarily represented network, the chaotic lattice of interconnections merely demonstrative of the deep contextual entanglement of technologies within intra and inter-societal relationships and multi-directional cultural transmissions.

Of course, when it comes to the archaeological record many of these interactions are obscured or missing, and thus reconstructing past *chaînes opératoires* and technological networks tends to be problematic in practice. Nevertheless, Shennan's (1999) study of extractive copper production in the Bronze Age Austrian Alps is an excellent case study of how ancient technologies can be approached analytically and argued to be intimately bound with socio-political and economic issues. Using an ethnographic economic model based on the relative labour costs of exchanged commodities like palm oil and iron in Cameroon (*ibid.*: 353), Shennan examined the choices made by inhabitants of the Mitterberg mining region from the beginning of the 2nd millennium BCE. Despite the wide availability of copper ores in the area, primary copper production seems to have been practiced only by small autonomous communities living high up in the valley, in an environment with few subsistence alternatives. Compared to the communities nearer the valley bottoms, fewer exotic goods were excavated from the metalworking sites, suggesting the inhabitants had poorer access to, and/or economic power within, regional exchange systems. Due to the fairly rudimentary smelting technique employed by the metalworkers, Shennan suggested that extractive metallurgical knowledge was not a 'secret' in the area, and that whilst demand for copper was fairly universal, communities with superior agricultural and/or pastoral land preferred to acquire metal via exchange. Crucially, Shennan interpreted that due to the lack of economic options for the miners and smelters, and the low productivity of their labour, they were forced to accept a poor rate of exchange for their copper, producing and reinforcing local social inequalities (*ibid.*: 360).

Although the Bronze Age Mitterberg is but one metallurgical example, it remains a truism that each utilised resource will be owned, controlled, or husbanded, each material will have a dynamic socially-prescribed value within a non-linear spectrum between pragmatic and symbolic, each technology involves skills and knowledge that must be learnt, maintained, and taught, and each community will have its own interplay of social and ideational structures that will determine how people invent, adopt, and adapt technologies within geographical, geological, historical, and thermodynamic constraints (e.g. Arnold 1985, Blackman *et al.* 1993, Budd & Taylor 1995, Childs 1991, Costin 2001, Courty & Roux 1995, Dods 2004, Lahiri 1995, Nakou 1995, Roux *et al.* 1995, Tabor *et al.* 2005). Thinking about technologies is more than considering the production sequence of an artefact, and as such, utilisation of the *chaîne opératoire technique* implies at least a consideration of the innumerable connections between ideas, objects, people, and society, and the realisation that one's own study should strive to extract as much as is possible of this social information from archaeological material culture.

3.3 Style and choice in metallurgical technologies

Within the *chaîne opératoire technique* the concepts of technological choice and technological style are the tools with which variation in archaeometallurgical assemblages can be separated into that representing 'forced moves' i.e. geological or thermodynamic constraints, and that which may to some degree represent the technology's original social context and thus identify a cultural tradition. The archaeological use of the term 'style' has been much debated since the 1970s (e.g. Dunnell 1978, Hegmon 1992, 1998, 2003, Sackett 1977, 1985, 1990, Wiessman 1983, 1985), and as a result is often tightly defined before its use in scholarly enquiry (e.g. Bacus 2004, David & Kramer 2001: 168-224, Hegmon 2003). This thesis relies predominantly on Lechtman's (1977: 6) concept of 'technological style' or, "the many elements that make up technological activities - for example, by technical modes of operation, attitudes towards materials, some specific organisation of labor, ritual observances - elements which are unified nonrandomly in a complex of formal relationships" (Lechtman 1977: 6). Nevertheless, it is necessary to consider some of the alternative definitions and their appropriateness for the present study.

'Style', it is generally agreed, represents that portion of formal variability that can represent the particular way something was done in a certain place at a certain time, and has long been used archaeologically as a marker of temporal-spatial relations in assemblages (e.g. David & Kramer 2001, Hegmon 1992, Sackett 1977, Wiessner 1983, Wobst 1977). The role of material culture style in facilitating the exchange, whether deliberate or otherwise, of information about social identities is also frequently emphasised (e.g. Hegmon 1992,

2003, Wiessner 1983, Wobst 1977). An artefact's style is represented by its configuration of formal characteristics, which were imbued by cultural choices during its manufacture and/or life history. Thus, at some level, style can be said to represent social boundaries, though these identity markers may be deliberately manipulated for socio-economic or socio-political reasons (e.g. David & Kramer 2001: 219-221, Hegmon 1992, 1998). Therefore, a spatially and/or diachronically consistent configuration of archaeometallurgical styles may be used to characterise the way metallurgy was done, used, or conceived in a certain context - an archaeometallurgical style (e.g. Lechtman 1984, 1996, White 1988, White & Hamilton in press). A sensitive appreciation of style, especially in technology studies, suggests that far from being in opposition to function, an understanding of archaeological styles can perform an analytical function in identifying interactions between material and social worlds (Hegmon 1998: 529).

In 1983, Polly Wiessner differentiated between 'emblemic' and 'assertive' types of style. Emblemic style "transmits a clear message to a defined target population...about a conscious affiliation" (Wiessner 1983: 257), whereas assertive style "carries information supporting individual identity" (*ibid.*: 258). For the purposes of this thesis, where variation in a waste product assemblage is the source of information, the author considers it unlikely that much deliberate and especially 'clear' information was even intended to be sent at either a group or individual level. However, this does not disregard the possibility that prehistoric Valley metallurgical behaviour did not exhibit stylistic signalling of some form. Had we the opportunity to interview a prehistoric Valley metalworker about the particular idiosyncrasies of their smelting technique, we might expect to be told that, "this is how it is done", a commonly reported ethnographic response (e.g. David & Kramer 2001). However, within the environs of small specialised craft community (White & Pigott 1996) it is perhaps unlikely that individuals would want to vary significantly from the established smelting technique, either to avoid the risk of experimentation, or to avoid this being a socially isolating move as style has also been argued to constitute "identification via comparison" (Wiessner 1984). With regard to production activities like copper smelting, Sackett's (1990: 36-37) differentiation between 'active' and 'passive' style is of relevance. Active style constitutes "ethnic 'messaging' generated by what is essentially self-conscious, deliberate, and premeditated behaviour on the part of the artisans". Whilst this sort of style may well have been employed by Valley metalworkers in their products, especially the potentially branded (*sensu* Wengrow 2008) MeP3 'ingots', it is extremely unlikely that they wished to intentionally convey social information in their waste products – the materials normally available for the study of metal production. The typical archaeometallurgical assemblage may thus exhibit passive style, the "latent, inherent" execution of choices (Sackett 1990: 36-37). Whilst passive style implies cultural choices it does not suggest those choices were intentionally imbued with social meaning,

and were activities become habitual or performed without conscious input, the resulting style may be described as ‘vernacular’ (*ibid.*).

The reconstruction of ancient *chaînes opératoires* implies that the researcher must strive to comprehend the past craftspersons’ many alternative choices to achieve desired technical solutions, although these options are not infinite, as “technological practices are obviously constrained by the laws of physics and chemistry and by their geological, ecological and historical setting” (Killick 2004a: 572). Sackett’s (1982: 73) introduction of the “isochrestic” style perspective, meaning ‘equivalent in use’, may be seen as closely aligned to Lemonnier’s (e.g. 1993, see also Sillar & Tite 2000) ‘technological choice’ concept. That one or more methods and techniques were repeatedly practiced in the past may carry significant social information for questions of the expression of inclusion or individuality through technological choices (e.g. Martineau *et al.* 2007, Petrequin 1993, Shennan & Wilkinson 2001, Sillar & Tite 2000). The interpretation of what could have been done (the potential technological alternatives) minus what we understand was done (the actual technological choices made, as inferred from the reconstructed *chaîne opératoire*) allows us to identify the defining characteristics of a technology - or a ‘technological style’ (e.g. Appadurai 1998, Hegmon 1992, 1998, Lechtman 1977, Steinberg 1977). To the author’s mind, ‘technological style’ encompasses the materialisation of a technology’s ethos, or those elements or essences that differentiate it from other similar technologies. The analytical utility of the technological style concept lies in its capacity to detect and differentiate multiple, subtle dimensions and choices in the production and consumption of material culture. Utilising this array of comparative factors, technological arguments for ancient social interaction have the potential to be more robustly substantiated than typological studies alone.

The capacity for stylistic variation in metal-related behaviour is enormous, and best attested by ethnoarchaeometallurgical research on African iron production (e.g. Childs & Herbert 2005, Chirikure 2007, Chirikure & Rehren 2004, Haaland 2004, Killick 2004b, Miller 2002, Miller *et al.* 2001, Rehren *et al.* 2007), though there are some Southeast Asian sources (summarised in Bronson & Charoenwongsa 1994). Therefore, the archaeometallurgist must consider that for populations which practiced metallurgy many aspects of their technology may represent choices (e.g. Lechtman 1984, 1988, 1996, Lechtman & Klein 1999). The identification of archaeometallurgical choices is by no means a simple process, nor one that is always fully accomplished. The macro and microanalysis (see Chapter 4) of an archaeometallurgical assemblage is used by the researcher to produce a technological reconstruction of what metallurgical processes and activities were being performed, within a particular social context. The archaeometallurgist can then compare this reconstruction

with other solutions that past metalworkers could have chosen, considering the affordances of their material and social landscape. The hypothetical (and highly interpreted) equation 'potential technologies minus actual technologies' can give added credence to our understanding of why particular archaeometallurgical choices were made. For example, a smelting population may be equidistant between two ore sources, but the reconstruction indicates that only one source was used at a particular time. The archaeometallurgist can then combine their interpretation with those of the other archaeological evidence to produce possible explanations for this decision, i.e. was the other source likely to have been known by the metalworkers, was access prevented by a competing social group, or perhaps the source was located in a taboo area? Thus, the concept and interpretation of archaeometallurgical choices can be correlated closely to other technical and non-technical factors contributing to a particular archaeometallurgical style. Whilst many metallurgical processes are constrained by the availability of materials and governed by the laws of thermodynamics (Killick 2004a), human beings always retain a degree of will or choice in their actions (Rehren *et al.* 2007). A metal producing and/or consuming population may have had many options with regard to raw materials, techniques, and products, or they may have had very few alternatives, but there was always the possibility of doing nothing at all. At its extreme, this approach could be applied to a population with no ore minerals, clays, or fuel, for whom smelting would not be a logically practicable activity, however that population has made the technological choice not to practice smelting via the long range acquisition of materials and metallurgical knowledge. As per any archaeological analogy, archaeometallurgical styles cannot be blindly contrasted over millennia or continents without risking the drawing of humanly irrelevant correlations, although juxtaposing technologies from a purely technical ahistorical vantage point can provide interesting perspectives (e.g. Craddock 1995, Tylecote 1992).

Many scholars regard the study of technical ceramics as an especially useful means of defining archaeometallurgical styles (Bayley & Rehren 2007, Martín-Torres & Rehren 2009, Veldhuijzen 2005, White & Hamilton in press). Whether a metallurgical process yields slag or not, and the mineralogy of that slag (e.g. Bourgarit 2007: Table 1) are factors affected by human choices, but these traits are also heavily influenced by geological factors and universal physico-chemical laws. However, the incorporation and design of furnaces, crucibles, tuyères, and moulds is arguably an arena for substantial variation in archaeometallurgical style, due to the literal and metaphorical plasticity of clay affording a wide range of potential archaeometallurgical choices. Analysis of technical ceramics does not deflect from the importance of other forms of evidence, recent studies of slag composition (e.g. Humphris *et al.* 2009) or metallurgical microstructures (e.g. Artioli 2007) have demonstrated that with ingenuity, perseverance, and a holistic approach to archaeometallurgical assemblages, technological style evidence can be successfully

identified and employed in aiding archaeological interpretation.

Technological notions of skill are derived from ethnological and cognitive psychological analyses of apprenticeship learning environments (e.g. Epstein 1998, Keller & Keller 1996, Roux *et al.* 1995). As metals are unevenly distributed resources, it follows that metallurgical production behaviours are not universal phenomena and that the transfer of specialist knowledge and skilled practices are often implicit in the consideration of metallurgical technologies (e.g. Pigott & Ciarla 2007, White & Hamilton *in press*). Although the question of skill may have been involved in defining archaeometallurgical styles, it is inevitably the focus of their comparison - contrasting two distinct metal technologies will be difficult if much of the difference between them is attributable to factors with little human influence (like geology). The transmission of archaeometallurgical knowledge becomes especially interesting when certain behaviours that make up a style require a great deal of learning and practice before they can be conducted effectively. Therefore, there is some justification for stating that similar skilful traits between technological styles, not too far apart spatially nor chronology, may be at least partially the result of technological transfer (see Bleed 2008 for lithics). This evidence, or counter evidence, for sociocultural interaction is arguably one of the most significant contributions archaeometallurgy can make to the wider discipline.

3.4 Organisation of production

The most complete treatise on the organisation of production can be attributed to Cathy Lynne Costin (e.g. 1991, 2001, see also Clark 1995). Costin's approach is primarily concerned with the socio-economic aspects of organisation and offers a clear terminology for the definition of different modes of craft production, focusing predominantly on aspects such as specialisation, technological variation, and social complexity. Costin's 'craft production system' (1991, 2001) is largely comparable to Pfaffenberger's (1992) 'sociotechnical system', and constitutes a holistic consideration of all the agents and structures impacted by technologies, including: producers, consumers, intermediaries, artefacts, the means and organisation of their production, and the nature of their distribution and consumption (Costin 1991, 2001). Taphonomic factors dictate that the evidence for identifying archaeological craft production systems may be fragmentary, misleading, or plain missing, and that alternative interpretations are often possible (Costin 2001, 278). Nevertheless, the framework provided by Costin's craft production concepts can permit archaeological data pertaining to technologies to be approached systematically and thoroughly, as per White & Pigott's (1996, see also Chapter 1) analysis of the Khao Wong Prachan Valley data (see Chapter 2).

A specialist producer may be defined broadly as one who produces more of a type of object or foodstuff than is required for personal consumption, which may include that of their family too (e.g. Costin 2001). The nature of the specialisation can vary according to: whether elite consumption (attached specialisation) or for general consumption (individual specialisation), the distribution network for the product (local versus regional), the location of producers relative to consumers (communities versus administered settings), the scale of the production unit (individuals to households to workshops), and the intensity of production (part-time versus full-time (Costin 1991, 2001). Many of these factors can overlap, e.g. prehistoric Valley copper smelting is thought to have taken place in small, possibly family, units, but overall production seems to have been industrial in scale (White & Pigott 1996, Pigott *et al.* 1997), but by following the criteria for different modes of production a reasoned interpretation of the organisation may be reached (Table 3.1). Another critical aspect of specialisation is often agreed to be that of ‘skill’, such that more complex technologies require more skill and are therefore more specialised (e.g. Costin 2001). The author would argue that all metal production is to some degree skilful due to the relative complexity of most metallurgical technologies, but that consideration of skill in metal production can be extremely important for interpreting the nature of the industry (see Chapters 5, 6, and 8). As a specialist producer is at least partially occupied with their particular activity in lieu of a purely subsistence lifestyle, it is commonly thought that they must in some way be compensated or supplied with those materials that they are not producing themselves (e.g. Costin 2001). It is this notion that leads Pigott & Mudar (2003) to suggest that Valley metalworkers may have exchanged copper for foodstuffs

Level 1 (Class)	Level 2 (Supertype)	Level 3 (Type)	Type Name
Unrestricted Consumption (General Demand). Individual Specialisation	Local Consumption	Autonomous Individuals or Households	Individual Specialisation
		Larger Workshop	Dispersed Workshop
	Regional Consumption	Autonomous Individual or Household-Based Unit Aggregated within a Single Community	Community Specialisation
		Larger Workshop Aggregated Within a Single Community	Nucleated Workshop
Restricted Consumption for Elite or Government Institutions (Elite Demand). Attached Specialisation	Household or Local Community Setting	Part-time Labour	Dispersed Corvée
	Administered Setting such as Palace or Special Purpose Facility	Individual Artisans, usually Full-time	Individual Retainer
		Part-time Labour Recruited by Government Institution	Nucleated Corvée
		Large-scale with Full-time Artisans	Retainer Workshop

Table 3.1 - A classification of craft production systems based upon: the relationship between producers and consumers (Class), the location of production and the distribution of product (Supertype), and the scale of production (Type). After Clark 1995.

due to a poor agricultural environment. Furthermore, it is sometimes presumed that wet weather absolutely precludes metallurgical activities, and thus White & Pigott (1996) suggest that Valley production was probably part-time due to the pronounced wet season in the area (see Chapter 8 for further thoughts on this issue).

Costin (1991, 2001) considers that reconstruction of a technology's *chaîne opératoire* is required to properly characterise archaeological production systems. By generating a *chaîne opératoire* it may be possible to consider five factors linking technology to the organisation of production, and their interpretative affordances and limitations are discussed below:

- 'Technological complexity' is sometimes thought to be synonymous with organisational complexity, but this ignores the potential for complex configurations of both technical and ritual skill and knowledge being involved in technological activities that might appear 'basic', e.g. many of the ethnoarchaeologically attested African iron smelting operations are superficially straightforward and/or rudimentary, but the attendant cosmological knowledge required is extremely complex (e.g. Schmidt 1997, see also Hegmon 1998: 279).

- 'Efficiency' can be defined as the relationship between the raw materials, time, and energy input for each unit of output, but this could be said to be a modern Western market-driven perspective which undermines alternative views of what is acceptable or desirable in a craft practice (e.g. Costin 2001). Archaeometallurgical studies frequently refer to the 'efficiency' of a technology (e.g. Bamberger & Wincierz 1990, Bennett 1989, Thomas & Young 1999), but both the conceptualisation and the tools (see section on liquidus calculation in Chapter 4) have been largely derived from modern industry and thus do not necessarily reflect the social context of past production systems, which may emphasise social considerations over technical ones (e.g. Lechtman 1977, 1996).

- 'Output' typically refers to the quantity of product, both at an absolute scale and per unit time. A high degree of specialisation might be associated with an elevated output, but highly skilled artisans may also produce small amounts of products which required a high labour input (e.g. Costin 2001). Furthermore, in archaeometallurgical studies the output of a particular industry is notoriously difficult to calculate due to typical lack of metal recovered at production sites and the many technical factors affecting the calculation of output from the waste products, this coupled with the challenges of providing accurate chronologies for large and complex deposits of mineral, slag, and technical ceramic (e.g. Bachmann 1982).

- 'Control' of specialised production, and in particular metallurgy (e.g. Childe 1936, 1942), has traditionally been regarded as evidence for greater social complexity via the

marshalling of raw materials, skilled artisans, and products to concentrate wealth and influence for the benefits of political elites (e.g. Costin 2001). However, the archaeological record is frequently reticent to provide data strongly indicating elite control over the organisation of production, except in obvious ‘palatial’ contexts (e.g. Rehren & Pusch 1997). More often than not production sites produce little evidence to support detailed analysis of this aspect of craft production systems, as seems to currently be the case in the Khao Wong Prachan Valley (White & Pigott 1996).

- ‘Standardisation’ of *chaînes opératoires* and their products has frequently been seen as indicating specialised production and possibly elite control of that production (reviewed in e.g. Costin 2001). This can be a dangerous leap on two major counts. Firstly, we often do not know how ‘standardised’ different industries, their products and waste products, may look archaeologically, as suggested by the study of single iron smelting (e.g. Humphris *et al.* 2009) and pottery firing (e.g. Blackman *et al.* 1993) episodes, as well as the frequent absence of systematic ethnoarchaeological analogy (e.g. Roux 2007). Likewise, whilst the association of elite consumption and highly skilled technologies can sometimes be made (e.g. Bellina 2007), it is wrong to assume that ‘mass produced’ goods, though perhaps the result of skilled processes like wheel throwing pottery (e.g. Roux 2003), are necessarily destined for, or controlled by, elites, who indeed may prefer more exclusive individualised goods, though still the result of skilled artisans. Thus, whilst it appears that the copper ‘ingots’ from Nil Kham Haeng (Pigott *et al.* 1997) may be standardised, at least typologically, there is no reason to suggest that this automatically implies social stratification in the later Iron Age Khao Wong Prachan Valley (White & Pigott 1996), and, as suggested in Chapter 2, the ‘ingots’ could represent some sort of community-level product branding (*sensu* Wengrow 2008) for recognition by regional consumers.

Costin (2001) explicitly concedes that in practice archaeological evidence for each of the preceding aspects may be difficult to detect or ambiguous to interpret. However, her careful dissection and discussion of craft production systems means that we do have a common language with which to describe and discuss the organisation of production. Via the careful reconstruction of *chaînes opératoires* and the application of Costin’s (1991, 2001) framework we can seek to identify multiple lines of evidence for better understanding ancient technologies, or at least highlighting the weaknesses in our data to produce balanced interpretations.

3.5 The Weber fraction in archaeometallurgy

An important issue to the present study is that of making interpretive headway with the variation in compositional data, especially for that of the slag samples. Akin to ‘mutation’

in biological models, 'random variation' or 'copying error' can introduce new behavioural and/or artefactual variation due to the inability of humans to exactly replicate. Its archaeological application largely developed by scholars working with an evolutionary theoretical perspective, a quantitative measure of 'copying error', the 'Weber fraction', has been derived from cognitive psychological studies of human sensory perception and motor skills in a wide range of skilled and unskilled social learning environments, from various cultural backgrounds (Eerkens 2000; Eerkens & Bettinger 2001; Eerkens & Lipo 2005; Eerkens & Lipo 2007). The Weber fraction dictates that without aids (i.e. a ruler or mould) people will on average introduce a replication error of up to 5% for each successive generation; presupposing they only have reference to the immediate generation before.

Ignoring any other cultural mechanism which may be operating on variation, the cumulative effect of an up to 5% 'copying error' per generation can rapidly produce substantial behavioural and/or artefactual divergence. If the 'coefficient of variation' (CV) per generation within an assemblage is up to 5% then the null hypothesis is that all material culture change can be accounted for by 'copying error' and there is no need to invoke more complex transmissions of cultural information (Bentley *et al.* 2004: 1449). If the observed CV is significantly less than 5%, then some sort of biased transmission may be responsible for constraining people's choices. If the observed CV is significantly in excess of 5%, then we may be seeing the introduction of new behavioural variants through experimentation and innovation. A number of studies on modern and ancient data have demonstrated that much of the material culture variation can be explained simply by cumulative copying error (e.g. Eerkens & Lipo 2005). However, of consequence for the present study, the 5% CV figure relates to the variability of final artefacts; the entities upon which people can presumably exercise their full sensory judgement of replication fidelity. We do not currently have quantitative data for the expected variability of the other materials resulting from production processes (cf. Humphris *et al.* 2009). This is something of an issue for a study based on metallurgical waste products.

Unfortunately, this approach cannot be applied directly to compositional data. The Weber fraction was derived from studies of artefact production in numerous social contexts, where the human subjects had only their natural sensory skills (e.g. hearing, sight, smell, taste, and touch) to control product variation (Eerkens 2000; Eerkens & Bettinger 2001; Eerkens & Lipo 2005). As identified by Humphris *et al.* (2009), this implies two major problems in the application of the Weber fraction to slag-based traits:

- Firstly, slag is a by-product not a product, and whilst metalworkers may have sought to constrain or exaggerate variation in their products, we do not know what quantitative effect this would have on by-product variability.

- Secondly, ancient metalworkers would not be able to control variation in slag chemistry to the same degree as artefact variability ($\pm 5\%$) by human senses alone.

However, the effects of slag variation would have been detectable in terms of the performance and efficacy of the smelt, slag formation and behaviour during the smelt, and its physical characteristics when cooled. Therefore, it is not unreasonable to expect metalworkers to have correlated, to some degree, the quality of their product and by-product with the composition of their smelting charge. As suggested by Marcos Martín-Torres (pers. comm.), the only realistic means with which these issues could be overcome, is an extensive programme of experimental testing involving skilled and unskilled smelters to attempt to reliably correlate variation in product (metal) to variation in by-product (slag). Though an expensive proposition, this approach would provide the objective reference data on slag composition needed to assess the degree of variation in archaeological samples. In lieu of this, the Weber fraction in particular, and CV in general, remain qualitative though useful means of interpreting slag variability for the present study (Chapters 5, 6, and 8).

3.6 - Theory in experimental archaeology

Archaeological experimentation has almost as long a history as its parent subject, and has evolved into a valuable avenue of research. However, the conceptual approaches to, and expectations of, experimental archaeology have been significantly modified over the years, largely in line with theoretical changes in the wider discipline. An early interest with ancient materials and technologies (e.g. Cushing 1894) led to a desire for more rigorous procedures (e.g. Ascher 1961), and an increasing realisation of the importance of experimentation for archaeological interpretation and public dissemination (e.g. Coles 1979, Mathieu 2002, Stone & Planel 1999). A number of scholars have also come to argue that the act of experimenting can provide archaeological inferences of equal interest to the material results (e.g. Townend 2002).

Cushing's (1894) paper is particularly pertinent here, relating as it does to copper, for demonstrating early uses of archaeological experimentation. Cushing's advocacy of the skill and ingenuity of indigenous North American metal workers is exemplar of how a practical understanding of a technology can enlighten archaeological interpretation. Against a backdrop of contemporary racial prejudice, Cushing's insistence upon the potential for simple metallurgical techniques and tools to produce complex artefacts must be lauded as an especially sympathetic treatment of material culture and its social significance. The development of archaeology in the mid 19th century as a reputable academic pursuit (e.g. Trigger 2006), coincided with a general global decline in traditional

craft skills and knowledge. Thus, the initial use of archaeological experimentation was to acquaint Western scholars of the Industrial Age with the practicalities and potential of previous modes of settlement, subsistence, and production. This stage of experimental archaeology can be regarded as an important awakening, but by the New Archaeology of the 1960s, it began to face criticism for a lack of scientific rigour. Ascher (1961: 793) characterised 'imitative experiments' as a unique means with which to translate hypotheses or beliefs into substantiated archaeological inferences. This notion of experimentation as serving to legitimise interpretation was shared by Coles (1979: 243), and was likewise in accordance with the scientific aspirations of contemporary archaeological thought (e.g. Trigger 2006). However, it was also noted that archaeological experiments seek to imitate past cultural patterning, whereas the Baconian experimental model was designed for modelling natural phenomena, and the two are thus, at some level, fundamentally different (e.g. Ascher 1961: 807, Coles 1979: 246, Henry 2002). Coles (1979: 243) also pragmatically acknowledged the inability of an archaeological experimental approach to provide absolute proof in relating reproduced materials to archaeological examples.

To date, experimental reconstruction based on laboratory evidence has proven to be extremely useful for the interpretation of archaeometallurgical evidence, and has opened previously inconceived windows of understanding (e.g. Burger *et al.* 2007, Crew & Crew 1997, Doonan 1996, Merkel 1990, Rothenberg *et al.* 1978, Timberlake 2007, Tylecote & Merkel 1985). Physical testing of an ancient metallurgical technology can be used to establish whether theoretical reconstructions actually work in laboratory or field conditions, and enable the experimenter to practice, and, if necessary, adjust reconstructions until they can reliably produce metal and associated debris (slag and technical ceramic) of a form and composition that is to some degree comparable to that of the archaeological material.

The influence of postprocessualism, ethnoarchaeology, and other alternative philosophies is evident in more recent thinking on archaeological experimentation (e.g. Andrews & Doonan 2003, David & Kramer 2001, Killick 2001, Mathieu 2002, Townend 2002, Trigger 2006). Although our ethnoarchaeometallurgical insights are based largely on recent historical iron production in Africa (e.g. Killick 2004b, Schmidt 1997), the wealth of data revealed by participant-observation and reconstruction experiments suggests that attempts to clinically reproduce ancient technologies were producing useful technical information, but failing to appreciate the socially embedded nature of these behaviours. One of the most sophisticated reappraisals is Townend's (2002) summary of his doctoral research on Heideggerian approaches to experimental archaeology. A central tenet of this paper is that it is not the physical products but the interactions and encounters between

people and things which provide the greatest archaeological insight. Although the Heideggerian terminology requires a degree of commitment, Townend's argument follows that archaeological reconstructions can be used to study how participants of different skill levels negotiate the tasks facing them, and that the social mechanics of problem solving, or encountering no problems at all, could affect material patterning in the archaeological record (Townend 2002: 89).

Thus it may be argued that an important value of experimentation is for the researcher to personally acclimatise and interact with the ancient technologies themselves. In line with a technological approach, the performance of experimental archaeology is more than 'doing science', and the experimenter's own relationship and learning experience with the technology may provide otherwise unknown insights into ancient metallurgical behaviour (e.g. Brück 2005, Doonan & Andrews in press, Killick 2004a, Townend 2002). To that end, the recording and presentation of the tests (Chapter 7 and Appendix C) is as full and frank as possible, in the belief that 'warts and all' documentation will permit readers to more critically assess the work and, if necessary, reinterpret the results.

Summary

This chapter began by discussing the contemporary anthropological perspective that technologies are socially-contextual rather than existing in isolation to culture. Therefore, it can be argued that by investigating ancient technologies, for which we often have reasonable archaeological evidence, we are in fact studying the societies and the people that constructed those technologies. Central to this endeavour is the francophone *chaîne opératoire technique*, which is the approach taken to reconstruct all the technical stages and associated social factors in the production of artefacts. Within the *chaîne opératoire* it may be possible to identify the past 'technological choices' that people made in the sequence of producing and consuming those artefacts, and taken together those choices may be seen to represent a 'technological style'. The section on the 'organisation of production' discussed some of the socio-economic factors which embed technologies within societal considerations, and how these may be detected in the archaeological record. The final section concerned the theoretical perspectives behind the experimental archaeological methodology employed in Chapter 7.

It is hoped that by drawing on the intellectual traditions of the 'Anthropology of Technology', the technological reconstruction of copper smelting in the Iron Age Khao Wong Prachan Valley are adequately justified (Chapters 5, 6, and 8), but first it is necessary to discuss how *chaînes opératoires* may be generated, technological choices identified,

and technological styles defined through archaeometallurgical analytical methodologies (Chapter 4).

Chapter 4

Analytical Methodology

Having covered the regional and local archaeological background, as well as the theoretical framework of a ‘technological approach’ in Chapters 1, 2, and 3, this chapter introduces the archaeometallurgical analytical methodology employed in the present study. The mineral, slag, and technical ceramic samples from early Iron Age Non Pa Wai and later Iron Age Nil Kham Haeng were evaluated by macro-analysis, bulk chemical analysis (polarising energy dispersive x-ray spectrometry), micro-structural analysis (reflected light microscopy and electron microscopy), compositional phase analysis (electron microscopy with energy dispersive x-ray spectrometry), and the statistical analysis of resulting chemical data. Each analytical technique employed has a sequential discussion of its purpose, method, preparation, and equipment. The multiple technique analytical methodology was intended to provide a range of data types of use for unravelling prehistoric Valley copper smelting *chaînes opératoires* and identifying technological choices and styles. A critique of the archaeometallurgical calculation of slag melting (or liquidus) temperatures forms the second part to this chapter, as this element of the Valley technological reconstructions is of some importance for the discussion of technological change in Chapter 8. Jones (2002) has observed that as a scholar applies increasingly sophisticated techniques to produce ever more detailed data, their interpretations often become more hazy and circumspect. This inverse relationship between analytical resolution and interpretive resolution is perhaps due to cumulative error margins eroding confidence. The author recognises that escalating analytical complexity demands increased determination to ensure these data are of archaeological use, and has endeavoured to err towards interpretive conservatism throughout the present study.

4.1 Methods of archaeometallurgical analysis

4.1.1 Investigations at the artefact scale: macro-analysis

Although the earliest metallurgical processes are in part characterised by a lack of residual waste (e.g. Bourgarit 2007, Tylecote 1974), many production technologies produce large quantities of slag, technical ceramic, host rock, and ore mineral (e.g. Rostoker & Dvorak 1991, Rostoker *et al.* 1989). To the trained practitioner they are an abundant source of information on past metallurgical practice and socioeconomic activity, and should thus receive an anthropologically-enlightened treatment as artefacts, as outlined in Chapter 2 (e.g. Jones 2004, Miller 2007, Taylor 2008). The first task of archaeometallurgical macro-analysis is to determine whether the artefacts found actually relate to metal production

or were one of the many materials that can be mistaken as such: rocks, ceramic wasters, vitrified earth etc¹. The second purpose of macro-analysis is to attempt a classification of the finds into groups with similar characteristics, and to form initial interpretations for their technical origins. Although these initial characterisations, classifications and interpretations can be modified by later laboratory analyses, they are a vital step in archaeometallurgical research and constitute a familiarisation with the material and provide the holistic understanding of the assemblage necessary for an integrated and well-reasoned final interpretation.

In 1982, Hans-Gert Bachmann published what remains to this day a seminal guide to field archaeometallurgy and macro-analytical study. Bachmann's geological and mineralogical background dictates an approach to archaeometallurgical materials based on field characterisation of physical attributes perceptible to humans like: colour, crystallinity, density, homogeneity, inclusions, magnetism, morphology, porosity, even smell. The essential toolkit is comprised of eyes and knowledge, but can be supplemented by an eyeglass, prospector's magnet, scratch plate, and a phial of hydrochloric acid - or mineral blowpipe apparatus for the ambitious. The macro-analysis can be qualitative such that the described materials can be grouped into classes with probable archaeological meaning - i.e. a group of slags with a consistently higher than average magnetic susceptibility and porosity combined with a plano-convex morphology may represent evidence for iron smithing, a distinct human activity with social and economic meaning. These field techniques can also be quantitative given that estimations of a slag heap's volume and density can give a rough indication of the intensity or longevity of production (e.g. Bachmann 1982: 5, Juleff & Bray 2007, Meyer *et al.* 2007).

The author has employed a modified Bachmann system of description, identification, classification, and interpretation on a number of Thai archaeometallurgical assemblages (Ban Kao Din Tai, Ban Non Wat, Khao Sam Kaeo, Nil Kham Haeng, and Non Pa Wai), and has found it a consistent investigative and explanatory framework for archaeometallurgical deposits. Although Bachmann himself is undoubtedly a master of his craft, the rigorous application of his macro-analytical protocol by any archaeometallurgist can produce convincing interpretations of metallurgical behaviour at a site, without any recourse to the laboratory (e.g. Pigott *et al.* 1997).

1 This should be done especially carefully if non-metallurgical materials were found in secure metal-related contexts, and may then have meaningful technological associations

Method:

Archaeometallurgical materials (minerals, technical ceramic, slag) were recorded as per any artefact: for context, metric data (mass, linear dimensions), and photographed for archiving and pertinent features. Recording of characteristics particular to archaeometallurgy (e.g. crystallinity, magnetism, streak colour, calcification, hardness, morphology etc) was based on the Bachmann (1982) system. The density and colour of powdered samples (from a scratch on a streak plate) are commonly the most diagnostic criteria for identifying archaeometallurgical materials, whereas metric data can be more useful for quantifying production (mass), technology (crushing, tapping), and general archival requirements.

Preparation:

Excess soil was removed by hand, and if necessary the artefact was washed under a tap. The generation of a freshly fractured surface was often found to aid characterisation and identification.

Equipment:

- Digital calipers.
- Digital camera.
- Diluted $\text{HCl}_{(aq)}$.
- Electronic balance.
- Geological hand lens.
- Naked eye.
- Porcelain streak plate.
- Prospector's magnet.
- Steel dental pick.

4.1.2 Entering the phasescape: bulk chemical analysis by Polarising Energy Dispersive X-Ray Fluorescence

Phasescape refers to investigation at the abstracted sub-artefact level, deriving increased archaeometallurgical interpretative power from chemical and microstructural evidence.

The laboratory-based analytical encounter moves beyond the realm of the human sensory array, examining material properties of which past metalworkers can only have had empirical knowledge. Therein lies a value of microscopic or compositional analysis: the potential to investigate habitual or unpremeditated metallurgical behaviour through attributes which cannot have been deliberately created. That is, if we wish to understand past technological knowledge or skill we can examine microstructural and/or physico-chemical aspects of metallurgical processes, that were of course affected by past human technological choices, but cannot realistically have been scientifically informed. We can therefore compare what was achieved technically with what we might interpret was intended to be achieved, enabling us to discuss the proficiency and potential motivations of past craftpersons.

It is at the phasescape that archaeometallurgy implicitly enters the laboratory, and probably accords most accurately with some archaeologists' conception of the subdiscipline as a purely scientific pursuit. This section will outline a number of instances where the physical structure and chemical composition of artefacts can provide technological detail of past metallurgical activities, unachievable without specialised analytical techniques and the archaeometallurgical knowledge to apply them. However, the author hopes to have been consistently clear that a great deal of archaeometallurgy can be effectively undertaken in the field and office, and that laboratory investigation often confirms or only slightly modifies the original interpretation (Veldhuijzen & Rehren 2007).

Bulk chemical analyses are typically the first laboratory analyses conducted on archaeometallurgical materials, the question being "what is it?"². The bulk chemistry of a sample refers to its mean composition, assuming homogeneity and ignoring differential phases. If a sample is heterogeneous, and many in archaeometallurgy are, then it is normally crushed to standardise the matrix analysed (see 4.3.2 below). However, it must be recalled that crushing will evenly distribute the chemistry of individual phases and may substantially skew the bulk compositional data if the sample is not representative of the whole (e.g. Humphris *et al.* 2009), though the NPW3/MeP2 and NKH3/MeP3 slag cakes are relatively small and thus the samples taken are likely to be representative. The potential problems caused by unreacted minerals in slag liquidus calculations (e.g. Bachmann 1982) was avoided in the present study by combining both bulk and micro compositional studies.

2 This information can be used to further screen out non-archaeometallurgical materials.

Beyond “what is it?”, the aim of bulk chemical analysis is to further refine the macro-analytical interpretation of past metallurgical behaviour. A common approach to the technological reconstruction of metallurgical processes is ‘mass balancing’, whereby the chemistry of materials inputted (ore, gangue, flux, fuel, clay) must be accounted for in the composition of the output materials (slag, ceramic, metal). This method can be extremely useful for assessing the coherence of an archaeometallurgical assemblage, or ascertaining whether materials pertaining to certain aspects of the production process are missing, i.e. ore minerals or metal artefacts. As long as there are not too many gaps in the assemblage, it may be possible to infer what the missing materials were likely to have been and how they may have played a part in the metallurgical process.

As well as mass balancing, bulk chemical data should be examined critically for patterns and relationships of interest between the materials involved, and checked for anomalous results indicating unusual materials, or potential analytical problems. Once subjected to this stage of interpretation, compositional data can be processed statistically to determine whether any archaeologically significant chemical correlations may exist. It may be preliminarily assumed that compositional clustering within samples of an artefact class (e.g. slag or furnace wall) perhaps relates to different technologies or technological styles being practiced - these to be tested in subsequent analytical steps. For the current study’s application of these analytical procedures to the Khao Wong Prachan Valley bulk analytical dataset please refer to Chapters 5, 6, and 8.

Method:

X-ray fluorescence spectrometry is based on the principle that materials emit energy characteristic of their chemical composition when excited by high-energy radiation. In this case the excitation is provided by a beam of X-ray (Röntgen) radiation of about 1^{-10} m wavelength. The energy (E) of an electromagnetic wave is defined as its frequency (ν , the inverse of the wavelength: $1/\lambda$) multiplied by Planck’s constant (h), thus, $E = h\nu$. The energy provided by the X-ray excitation beam is sufficient to overcome the electrons’ bonds to the atomic nuclei of the component elements of the sample, and therefore an electron is displaced from the electron cloud, and an electrical imbalance created. (Atkins & Paula 2002, Bertin 1975, Jenkins 1974, 1999). These positively charged atoms (ions) are electrically unstable and will almost immediately attract another free electron to regain a neutral electrical charge. As energy in the form of an X-ray beam was required to dislodge an electron from a stable particle, it follows that replacing an electron will release energy - a secondary X-ray. This energy emission is not random but corresponds to the movement of electrons between orbitals and sub-orbitals, and these movements having characteristic energy emissions for each atom. Therefore, measuring the energy

released after a sample's excitation by X-ray can identify which electron displacements and replacements have occurred, and thus which elements are present. The rate at which the energy is received by the detector quantifies the amount of that element. The basic XRF system then involves: an X-ray source, a sample, and a detector unit, prior to computing and data output. There were two methods of detection in analytical X-ray fluorescence spectrometry: Energy Dispersive (EDS) and Wavelength Dispersive (WDS), both of which are discussed below.

Energy Dispersive units rely on highly sensitive crystalline detectors measuring the energy and intensity of secondary X-rays emitted from the excited sample. In an ED system the detector measures the X-rays released by all constituent elements of the sample simultaneously. This does reduce the resolution of each element's reading, but means the analysis is rapid. An issue in EDS analysis is that the energy levels corresponding to movements of electrons between orbitals can be similar between certain elements, giving rise to the problem of peak overlap in the resultant spectra of a sample. It must be stressed that XRF analyses rely heavily on interpretation, from the sample preparation through to spectra interpretation, and with a large part played by computer software in resolving the many complex algorithms that provide us with our chemical data (Veldhuijzen 2003). Therefore, deciding whether an energy peak on a sample spectra corresponds to one element's sub-orbital or another's is all part of the analytical process.

Given that $E = hv$ and $v = c/\lambda$, where c is the constant speed of light in a vacuum, it is also possible to determine the energy of electromagnetic radiation, like that emitted by excited samples, by measuring the wavelength of the X-rays released after they have been diffracted through sensitive optics. This is the principle of Wavelength Dispersive Spectrometry, which has the advantage of measuring emission intensity at each wavelength, resulting in typically higher resolution than an EDS system, but has the disadvantage that the detector must physically move across the range of X-ray diffraction angles for each element of interest and thus it takes a lot longer than EDS analyses.

For bulk chemical analysis in the Wolfson laboratories of the UCL Institute of Archaeology, a polarising Energy Dispersive - [P]ED-XRF - unit was used since it has significantly better resolution than SEM-EDS (see below). One of the chief limitations on EDS resolution is the obscuring of less intense energy peaks by the 'background noise' seen on the spectra. In a polarising system the incident X-ray beam is first directed at one of a series of 'targets', which have the effect of setting the radiation in one plane and concentrating primary X-rays to excite particular ranges of the electromagnetic spectrum.

The plane-polarised beam then strikes the sample and causes the generation of secondary X-rays by the excitation of constituent elements, which were then measured by the EDS detection system. Thus, [P]ED-XRF can resolve down to parts per million (ppm) for most elements, and maintains the speed advantage over the WDS alternative (Veldhuijzen 2003: 104).

Reference materials, certified (CRMs) or otherwise (RMs), were included in all analyses to monitor the accuracy and precision of the [P]ED-XRF system. CRMs are pressed pellets of a standardised chemical composition, independently agreed by a number of laboratories, and are used as an analytical control. The selection of a CRM for inclusion within a particular XRF run was based on the expected composition of the sample being reasonably close to that of the control, and thus the inter-element effects experienced by their respective matrices when exposed to X-ray radiation would be comparable. The purpose of CRMs is to provide confidence that the XRF instrument was both 'accurate', determining compositions comparable to those published for the reference materials, and 'precise', not suffering from analytical drift between operations. The accuracy and precision of the present study's analyses can be assessed in Appendix B (Table B.1).

Preparation:

For the current project, the first stage of bulk XRF preparation was to cut a sample from the archaeometallurgical material in question, mechanically removing all weathered or previously exposed surfaces. The sample was then washed, first under a running tap to remove heavy dirt, and then in an ultra-sonic bath for a thorough cleaning before drying with a fan heater. All surfaces and materials were kept meticulously clean with industrial methylated spirits (IMS), ethylenediaminetetraacetic acid (EDTA), and sand abrasion as there was a high risk of contamination from this stage of preparation (Van Grieken & Markowicz 2002: 933-944). The sample was then crushed in a steel punch to a grain size of 5-10mm. For [P]ED-XRF analysis of pressed pellets it is necessary to have a maximum grain size of 50 μ m to minimise the effects of X-ray diffraction and refraction by the crystalline matrix of the material in question (Veldhuijzen 2003). The sample powders were pulverised to 50 μ m in a planetary mill with two contra-rotating canisters containing ball bearings, all made from tungsten carbide. The mill was run with alternating loads of sample and sand in each of the canisters, the sand scours out contamination whilst alternation prevents similar samples from being confused. The analytical powders were decanted into glass phials and placed in an oven to eliminate any moisture that would prevent the pellets from forming correctly. The dried sample was weighed in a fine balance and combined with an industrial binding wax at a ratio of 1:0.1125, to give a total of 6-8g of thoroughly mixed powder. This mixture was placed into an aluminium cup before

forming into a pellet using a press applying 15 tonnes of pressure for 3 minutes. Pellets were labelled, and stored in a low-moisture environment to prevent rehydration until they were used.

Equipment:

- Fritsch Pulverisette 7 planetary mill.
- Oertling LA164 electronic balance.
- Plasplugs commercial tile cutter.
- SPECAC 25 tonne press.
- Spectro X-Lab Pro 2000 Polarising Energy Dispersive X-Ray Spectrometer with version 2.3 analytical software package.
- Ultra-sonic bath.

The samples run in archaeometallurgical analyses often have a high iron component, one that is not compatible with the geology-based algorithms provided with the [PJED-XRF hardware, as the iron readings can overwhelm the response of lighter elements. A specific algorithm, 'Slag_Fun', written by Veldhuijzen (2003), was used for slag material, and the standard algorithm, 'Turboquant', for ceramics and minerals. Quantitative analyses in the Wolfson laboratories were run overnight in batches of 15-17 samples (dependent on the number of CRMs, see above), and were repeated three times to ensure data quality and monitor precision, trace element data are not provided for the CRFs. All analyses were generally accurate and are acceptable given the resolution required for sound technological interpretation. Differences from the certified values range from several hundreds or tenths of a weight percent for the minor oxides, to a few weight percent for the major oxides - one seeming exception was the detection of iron oxide in 'Swedish Slag W25:R', but the consistent variance corresponds to the stoichiometric difference between Fe_2O_3 (reported) and FeO (the valency expected in slag). Precision was lower in those oxides in lower concentrations. There does appear to have been some analytical drift between analyses refereed by BHV0-2 in December 2006 and those in January 2007, but these are not problematic as all the technical ceramic samples were rerun in the 2007 batches. See Appendix B for all [PJED-XRF analytical data, as well as selected data in Chapters 5, 6, and 8. Trace elements below 10ppm are reported as '<10' and not used for interpretation.

4.1.3 Phase analysis: Reflected Light Microscopy

Having assessed the bulk chemistry of an assemblage, and derived a preliminary interpretation of the metallurgical process, the next stage of archaeometallurgical analysis involves another, more literal, phasescape. Optical microscopy is used in archaeometallurgy to describe and identify phases of interest in explaining the formation and composition of the sample (Bachmann 1982, Scott 1991). As mentioned above, bulk compositional data assumes homogeneity, and as this is rarely the case, microstructural study is used to explain chemical groupings in terms of phases present: e.g. slags commonly contain a large amount of iron oxide, but bulk analyses were unable to tell us whether this iron was chemically bonded to silica in the slag (e.g. Fe_2SiO_4), or was present in its original (residual) mineral form, or has precipitated from the slag as primary (anthropogenic) iron oxides, or even as secondary (post-depositional) oxidation, although this should have been cut away during preparation. Phase analysis can also provide information on the physico-chemical (e.g. furnace temperature and redox atmosphere) conditions that were present when the material was formed, and thus aid the technological reconstruction of the process. However, attempting to identify and explain *all* the phases seen in, typically, heterogeneous samples will not necessarily help an archaeological interpretation of the material and technology, macroanalytical work should be largely focused on addressing questions generated by the bulk chemical data, whilst remaining vigilant for phases of interest.

Method:

Samples were examined at magnifications between 50 and 1000 times in plane-polarised (PPL) and cross-polarised light (XPL), as well as slightly-crossed-polars (sXPL). Phase identifications were achieved with standard mineralogy textbooks but with an understanding of the anthropogenic phases produced rapidly at high temperatures during metallurgical processes (Ineson 1989, Nesse 2003). Ceramic fabrics were recorded using a simplified version of Whitbread's (1989, 1996) paste recording system, with some consideration given to forming technique (e.g. Courty & Roux 1995, Courty & Roux 1998, Rye 1981), the onus being on establishing the role of technical ceramics in copper smelting procedures. Photomicrographs were taken systematically throughout the analysis and hand-drawn sketches served the function of 'mapping' the sample prior to examination under the scanning electron microscope.

Preparation:

Samples were cut to a size that would fit comfortably in the 32mm diameter resin moulds. Where a sample was cut was very much an interpretive process, as it determines what

phases will be visible in a heterogeneous material. Where possible, samples were taken from areas adjacent to those sampled for bulk chemical analysis, so phase analysis of that sample would correspond as closely as possible to the bulk chemistry of its neighbour³.

Cold-curing resin was prepared by carefully mixing epoxy and hardener in a ratio of 4:1, with approximately 7.5g of resin allowed per sample, although this depends on the volume and porosity of the material being mounted. Once poured into the moulds, the resin cured at room temperature under a fume extraction hood for 24 hours. The samples were then cut to a standard thickness of 10mm, to reduce the adjustment of focal length between samples, using a specially designed jig. The analytical surface was then cleansed of any excess resin by hand grinding on low grade grits (320-600) on an electric wheel. This was done carefully as aggressive abrasion can easily remove too much material and set the sample face at an angle, leading to focusing problems during analysis. The mounted sample was then ground on progressively finer grades of abrasive paper from 1200–4000, rotating the analytical surface through 90° at each stage to remove the striations left by the previous grade. The samples were rinsed under a tap after each grind to prevent the cross-contamination of grits. After the 4000 grade paper, the sample was cleaned in an ultrasonic bath before progressing to polishing on textile discs embedded with industrial diamond paste and lubricant. The finishing was done on an automated polisher with 1µm and 1/4µm grade pastes. The samples were cleaned ultrasonically again, dried with a fan heater, and then kept in a low-moisture environment to avoid oxidation.

Equipment:

- Eposet cold-curing resin and hardener.
- Leica DM LM metallurgical microscope with a Nikon Coolpix 9100 digital camera.
- Metaserv Universal Polisher with grits from 320 to 4000.
- Plasplugs commercial tile cutter.
- Struers LaboPol-5 automated polished with 1 and 1/4 micron diamond pastes.
- Ultra-sonic bath.

³ The two batches of samples, pelleted and mounted, were cut and prepared simultaneously.

4.1.4 Phase analysis: Scanning Electron Microscope with Energy Dispersive X-Ray Fluorescence

Optical mineralogy is an accurate technique, but one designed for minerals forming under natural conditions over geological time scales. Although the same physical laws apply to anthropogenic materials, the rates, temperatures and redox atmospheres at which they were produced can result in configurations of matter not normally found in nature. Understanding how these anthropogenic materials and structures relate to past technological choices necessitates micro-structural and chemical analyses of small phases, a task well suited to a SEM-EDS (Scanning Electron Microscope with Energy Dispersive Spectrometry) or similar systems (e.g. Brandon & Kaplan 1999, Chescoe & Goodhew 1990, Goldstein *et al.* 2003, Olsen 1988, Reed 1996, Watt 1997). The compositionally-reinforced identification of phases, and the interpretation of their formation conditions, allows the confirmation and/or modification of the reconstructed *chaîne opératoire* generated by macro, bulk, and microscopic analyses.

Method:

Optical microscopy using visible light reaches a magnification limit when the wavelength of the electromagnetic radiation (approx. 400-700nm) begins to approach the size of objects under examination, e.g. very small slag crystals. At this point the light radiation is increasingly diffracted through the sample's crystalline matrix, thus limiting the ability of an optical microscope to provide a clear image of very small areas. The principle of a Scanning Electron Microscope (SEM) is to use a much smaller wavelength of radiation to resolve at a higher resolution. The SEM works by directing a high-energy beam of electrons at a sample in a vacuum. These electrons induce three principal emissions in the sample: secondary electrons (SE), Back-Scattered Electrons (BSE), and secondary X-rays. The SE emission is related to the reflection of incident electrons by the topography of the sample, and is electronically converted to a visible image for assessing a material's surface (Chescoe & Goodhew 1990, Goldstein *et al.* 2003). The BSE emission is also reflected from the surface, but its dispersion is related to the atomic mass density of the sample, providing a visual impression of the material's composition. The secondary X-ray is caused by the incident electron beam displacing electrons from the orbitals of atoms within the sample, this excitation principle is exactly as described for XRF bulk chemical analyses (see above). The energy of X-rays emitted is detected by an Energy Dispersive X-Ray unit (EDS) and used to provide quantitative readings for sample composition, and can be directed for spot, line, and area scans to aid identification of phases within the material (Chescoe & Goodhew 1990, Goldstein *et al.* 2003).

Phase analysis in archaeometallurgy is usually performed on polished (flat) samples, with little requirement for the topographic (SE) imaging of a SEM, but BSE imaging is widely used to identify areas of interest for examination with the EDS unit (Olsen 1988). The JEOL JXA8600 unit used was actually a microprobe, with excellent vacuum and current, stability, and thus analytical reliability. The probe was fitted with an Oxford Instruments INCA X-sight Energy Dispersive Spectrometer system, controlled by INCA software via a PC. The proprietary software also processed, displayed, and stored the images and spectra acquired by the analyser. A cobalt standard was used to calibrate the EDS analyser, and was scanned every session to guard against analytical drift - almost nil on the JEOL JXA8600 unit. The Khao Wong Prachan Valley samples were analysed using an accelerating voltage of 15kV, and a current of 1.5×10^{-8} A. NaO₂ is not reported due to volatilisation-based inaccuracy. The instrument has as an accurate detection limit of around 0.3wt%, lower values are reported as indicative of presence/absence only. This level of accuracy was sufficient for the technological reconstructions and the interpretive objectives of the present study. Oxygen was added by stoichiometry where appropriate, taking into account the likely predominant iron valency in slag (Fe²⁺) and ceramics/minerals (Fe³⁺). Data presented in the thesis have been normalised, those in Appendix B have not.

Preparation:

SEM-EDS analysis was performed on the same samples as were studied by reflected light microscopy. The only difference was the addition of a layer of carbon, applied by a sputter coater. This carbon layer touches the metal skeleton of the SEM and allows the analytical surface to conduct electrons whilst being analysed, and grounds the sample so it does not become charged.

Equipment:

- Edwards Auto306 carbon sputter coater.
- JEOL JXA8600 microprobe with Oxford Instruments INCA X-sight Energy Dispersive Spectrometer (EDS) and INCA analytical software package.

4.1.5 Statistical analysis of compositional data

Although not a laboratory analysis in itself, comprehending, treating and manipulating the data resulting from macro and microanalyses is another abstracted perspective on archaeometallurgical material, and the human technologies that produced them - and as

such is a form of phasescape. An ongoing process of archaeometallurgical analysis is trying to combine different forms of analytical data in an attempt to discern patterns that may have archaeological meaning (Fletcher & Lock 2005, Shennan 1997). As these data are a primary means of generating technological reconstructions, and thus of identifying technological choices and styles (see section 4.2.2 below), we should be very interested in any grouping that appears *and* is possibly related to unintentional, uncontrolled, or deliberate human metallurgical behaviour. Within a large archaeometallurgical dataset we may assume that a consistent compositional and micro-structural signature for an artefact class corresponds to a particular technological process or style of process, but we must always remain wary of imposing the patterning we are predisposed to seek.

Many archaeometallurgical data are chemical in scalar form and can be processed using simple bivariate plots to assess relationships between materials. After compositional analyses (bulk or micro), each sample may have many chemical variables, making it difficult to determine archaeologically-significant grouping without statistical processing. Correlations identified by basic means can provide very useful information regarding technological reconstruction, and can screen out those data which do not correlate to anything and merely produce background noise. At this juncture, more sophisticated statistical processing like Principal Components Analysis (PCA) can be used to reduce the number of variables by generating ‘factors’ to explain multi-variate trends between samples (Jolliffe 2002). This is very much an interpretive process as the researcher must decide which variables to factorise, PCA may show groups that have no bearing on ancient technological choices. For statistical protocol please see 4.3.5 below.

Preparation:

The output of chemical data from the analytical equipment is not ‘raw’, and has been heavily processed by the systems’ software from the original energy spectra to produce quantitative results. However, it is not in a form suitable for uploading to the SPSS™ statistical software package, and must first be scrutinised, cleaned, and organised. Any data looking ‘odd’ were checked, and, if necessary, repeated.

Scrutinisation: The standard CRM measurements are particularly useful for assessing any problematic analyses as their readings should be very uniform, and for ‘making sense’ within an empirical understanding of the sample being analysed.

Cleaning: Each sample is analysed three times in the XRF system and these readings must

be averaged for each element. Elements that are not detected in samples, 'nd', need to be converted to '0' or they will not be recognised by the statistical software. Major elements are usually reported as stoichiometric oxides and trace elements in elemental form, but this needs to be checked - data for 'Fe₂O₃' were converted to 'FeO' for slag analyses.

Organisation: The compositional data needs to be arranged into groups of similar material. There is no point using PCA to separate the artefacts into slag, ceramic, and mineral when we already know this.

Equipment:

Microsoft Office 2004 (Mac) and 2007 (PC).

SPSS v14.0 (Mac).

Procedure:

Bulk chemical data were uploaded to SPSS from Excel and saved as a '.sav' file. These figures were then processed as a 'data reduction' by 'factor', with a set of 10 to 15 oxides and elements selected as variables on the basis of technological relevance and trial and error. Processing and output options selected included: 'univariate descriptives', 'coefficients', 'scree plots', loading plots', and 'save as variables - regression', with the method as 'principal components' and extracted according to the number of variables selected. This procedure was repeated with many permutations of variables until more than 70% of compositional variation could be accounted for by the first three factors, *and* the resulting groups made technological sense. For a full description of PCA procedure please refer to Charlton 2007: 118-121.

4.1.6 Experimental archaeometallurgy

Another archaeometallurgical methodology critical to the present study is that of field experimentation. This topic is dealt with in detail in Chapter 7 and there is no need for repetition here.

4.2 Liquidus calculations in archaeometallurgy

Historiographically, a common element of archaeometallurgical reports has been the

reconstruction of the operating temperatures and atmospheres of ancient pyrotechnological processes (e.g. Bachmann 1982: 13, Morton & Wingrove 1969, 1972, Tylecote 1962: 193, 1987: 295). These calculations are based on industrially-derived thermodynamic models (e.g. Davenport *et al.* 2002: 62, 207) applied to archaeometallurgical materials, predominantly slag and alloy systems, and can potentially add valuable detail to our understanding of past metallurgical practice. For archaeologists not trained in metallurgy, the ability to generate temperature and gaseous environment estimates from slag samples was doubtless impressive and reinvigorated scholarly interest in the interpretive potential of ancient pyrotechnologies from many periods and contexts. Nevertheless, the author has some reservations about these techniques, especially when applied in non-ferrous archaeometallurgy. This concern is methodological in basis, but the potential problems are exposed predominantly in the uniformity of temperature and redox estimates, and the apparent inability to derive anthropologically significant interpretations from these figures. Whilst there is no doubting technologies can develop and operate via innumerable paths and contexts, there are some guiding physico-chemical criteria which must be fulfilled for certain events to occur. In copper smelting, copper always melts at the same temperature and has the same minimum partial pressure requirement wherever and whenever extraction processes take place (Ellingham 1944). Worldwide, related geological processes produce analogous metallogenic formations with comparable mineral suites, and, excepting very pure copper ores, similar gangue components to be slagged off. Thus we are familiar with operating parameters for ancient copper smelting activities of 1150-1250°C and partial pressures of oxygen (ppO_2) between 1×10^{-5} and 1×10^{-9} . With most determinations falling within this range, it could be argued that liquidus and redox calculations do not provide a sufficiently distinctive characterisation of ancient technologies for the purpose of comparing past *chaînes opératoires*.

In an experimental copper smelting furnace, one might directly measure process parameters with thermocouple arrays and efflux gas analysers (e.g. Burger *et al.* 2007, Merkel 1990), but in archaeology we must work with the assemblage at hand, and although there are means of assessing the thermal regime to which technical ceramics have been exposed (e.g. Hein *et al.* 2007), archaeometallurgists typically rely heavily on slag sample *liquidus* determinations⁴. The method most commonly used to calculate liquidus is the plotting of slag samples' three principal bulk chemical components (although like compounds can be grouped) on to a normative ternary phase diagram (e.g. Figure 4.1 but see Eisenhüttenleute 1995 and, Nürnberg 1981 for exhaustive permutations). This figure is then transposed

4 Alternative direct techniques for measuring the same parameters include reheating archaeological slags until their liquidus is reached, and determining the relative valencies of iron within the sample by wet chemistry or Mössbauer analysis (e.g. Adetuji *et al.* 1995)

to an Ellingham (1944) diagram where the intersection of the liquidus line with phase boundaries relevant to the slag can be used to estimate ancient redox conditions (Figure 4.2). This reasoning sequence indicates that the accuracy of a redox determination is contingent on the accuracy of the liquidus.

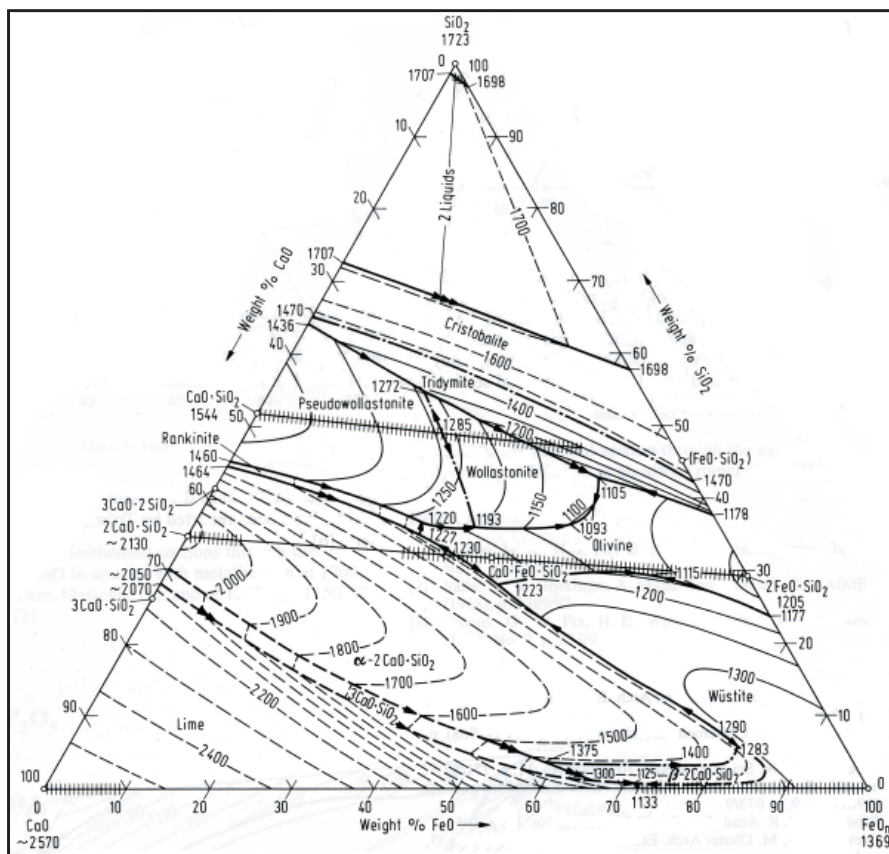


Figure 4.1 - Ternary diagram for a FeO-CaO-SiO₂ slag system in equilibrium with iron metal. Image from Eisenhüttenleute 1995.

Every archaeometallurgist who produces liquidus figures does so in the knowledge that they are indirect imperfect estimations based on a large number of assumptions and simplifications. However, some of these calculatory concessions are so great as to render the entire exercise problematic - especially in non-ferrous archaeometallurgy:

- The Oxford English Dictionary definition of ‘liquidus’ is, “...a temperature..., above which a mixture is entirely liquid and below which it consists of liquid and solid in equilibrium...” (www.oed.com, accessed 17th June 2008). Thus, slag liquidus represents only a *minimum* temperature for the smelting process, which has been experimentally demonstrated to potentially run several hundred degrees centigrade hotter (e.g. Merkel 1990, Bassiakos *et al.* 2008).
- An archaeological operating temperature derived from a slag liquidus determination relates only to that zone of the reaction where slag was formed, normally towards the base of the crucible/structure.
- Liquidus calculations assume the slag is fully fused and homogeneous when ancient processes produced slags that are regularly heterogeneous and often

partially fused (Artioli *et al.* 2007, Bachmann 1982, Bourgarit 2007, Burger *et al.* 2007).

- Ternary phase diagrams are modelled from experimental data in controlled laboratory conditions, typically used for understanding and improving industrial materials and production methods, and not for archaeological application. Our use of this technique necessitates selecting a diagram with the closest compositional fit to the slag data, which are then reduced to three major constituents (or groups of constituents) and normalised, thus ignoring the possible thermodynamic effects of minor and/or trace components on non-equilibrium and non-optimised ancient smelting systems (Bachmann 1982: 11, Kongoli & Yazawa 2001: 583).
- Bulk chemical analyses report iron as a common constituent of ancient slags, but cannot independently distinguish between Fe, as in iron or ferrite, Fe²⁺, as in fayalite or wüstite, Fe³⁺, as in haematite and limonite, or Fe^{2+/3+}, as in magnetite. Slags, especially from non-ferrous production, frequently contain multiple iron valencies, but this variability cannot usually be accounted for by existing ternary phase diagrams without excluding other major components.
- Not only do ternary phase diagrams assume thermodynamically stable fully molten systems, they are usually calculated for oxygen partial pressures in equilibrium with air or metallic iron (Kongoli & Yazawa 2001: 583). Whilst the latter is acceptable for ancient iron smelting process, it is arguably inappropriate for non-ferrous archaeometallurgy where reactions probably took place at intermediate, though variable, partial pressures (Bassiakos *et al.* 2008).
- As noted above, the calculation of ancient redox conditions by Ellingham diagram is contingent upon the liquidus determination, but recent slag research shows that liquidus is significantly influenced by the partial pressure of oxygen to which the system is exposed (e.g. Kongoli & Yazawa 2001). Thus our process parameter reconstructions have a potentially wide error margin due to the cumulative application of circular arguments - our liquidus figure is influenced by redox but is then used to calculate redox.

In combination, these factors contrive to make traditional liquidus calculations for non-ferrous production processes either analytically inaccurate or of limited descriptive and interpretative power. Of course, it is easy to criticise and harder to construct, but in theory, if it is possible to improve the accuracy and validity of liquidus calculations, the subsequent parameter reconstructions for ancient non-ferrous processes could prove valuable discriminatory criteria in defining metallurgical styles.

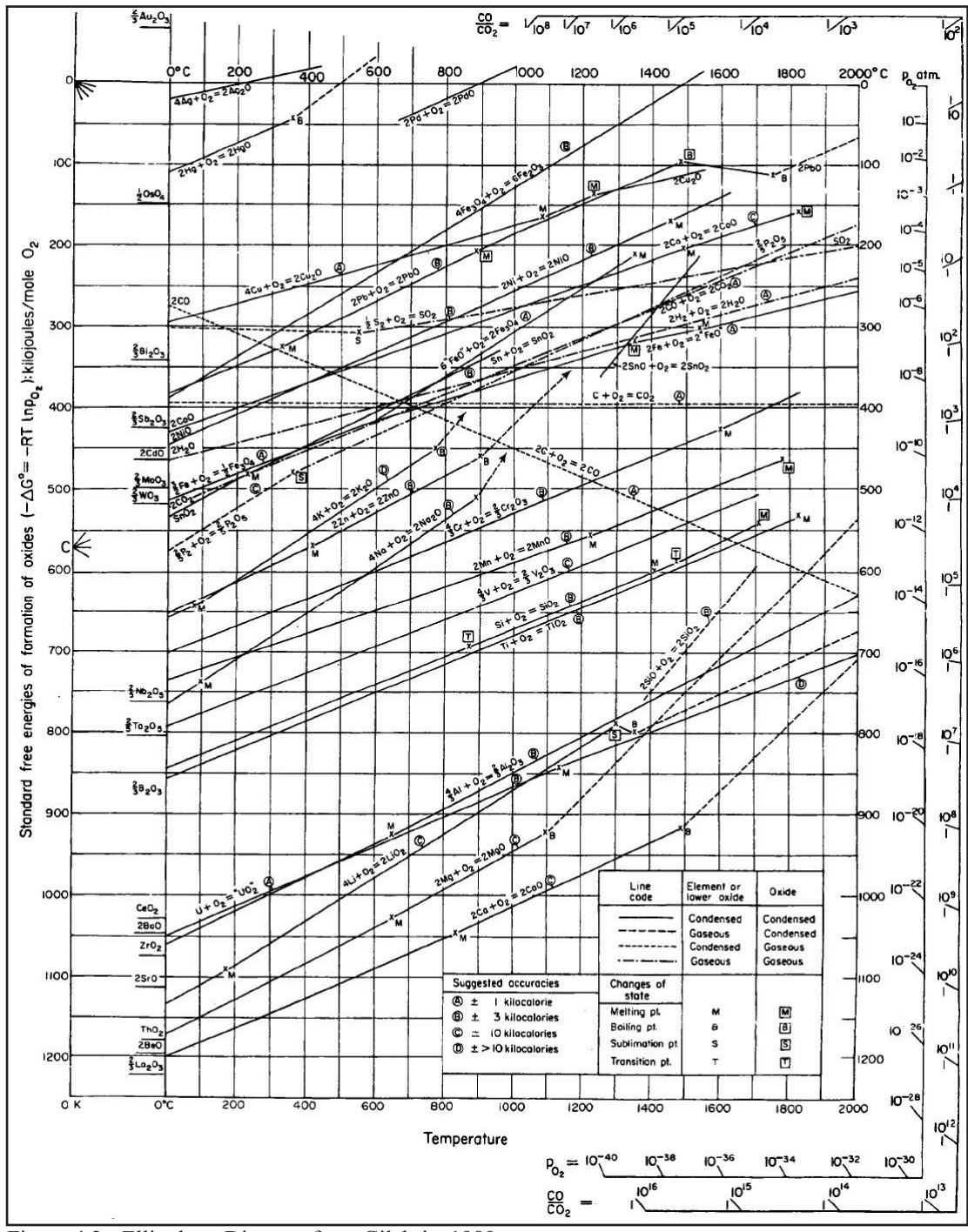


Figure 4.2 - Ellingham Diagram from Gilchrist 1989.

The following literature was introduced to the author by Mihalis Catapotis⁵, and although these techniques are presented as an improvement to the existing methodology, they too are built on multiple assumptions derived from modern industrial research, the foremost issue for archaeometallurgists is that reactions proceed to equilibrium. Over the last decade a core of researchers [henceforth 'Flogen group'] have been developing and testing improved thermodynamic models for extractive metallurgy, but specifically for slag systems formed in intermediate oxygen partial pressures, and taking further into account the effect of minor additives to the melt (e.g. Kongoli & Felton 1998, Kongoli *et al.* 1999, Kongoli & Yazawa 2001, 2003, Kongoli *et al.* 2003).

5 Whilst Catapotis was lecturing at the University of Sheffield in 2003/2004.

The predominance of ternary phase diagrams in equilibrium with metallic iron is not only problematic in archaeometallurgy. Industrial metallurgists have also reported unpredicted and hitherto inexplicable issues in large-scale copper production, typically the unforeseen precipitation of magnetite, raising slag viscosity, and subsequently increasing copper loss (Davenport *et al.* 2002: 173). The Flogen group demonstrate that the traditional definition of slag components as acidic, basic, or neutral is not universally valid due to variable and often inverted melt behaviour at intermediate oxygen partial pressures (cf. Davenport *et al.* 2002: 59). In particular, common minor oxides like calcia and magnesia, normally considered to be fluxes, can in fact increase liquidus and viscosity at intermediate partial pressures (e.g. Figure 4.3, Kongoli & Yazawa 2001: 585). Likewise, small amounts of alumina, normally thought to be a refractory network-former, can actually reduce liquidus and improve slag liquidity (Figure 4.4, Kongoli & Yazawa 2001: 587). The copper oxide content (frequently high in ancient slags) can also play a significant role in slag formation (Kongoli & Yazawa 2001: 590). Clearly, the situation is far from straightforward, as the behaviour of each slag component is intricately context specific, and dependent on its relative abundance within the melt, as well as the energetic, thermal, and gaseous environment. However, it is beyond the scope of this thesis to provide a detailed explanation of the technical complexities of slag systems with multiply shifting and mutually influencing variables.

In practice, the use of Kongoli *et al.*'s (e.g. 2001) Flogen diagrams requires a significantly greater interpretative input than traditional liquidus calculation, which is no bad thing considering that archaeometallurgy is a human-oriented discipline at heart. All phase diagrams should be chosen carefully for their relevance to the archaeological data, but Flogen diagrams must also be selected for appropriate redox conditions and the contribution of minor oxides. Considering that traditional archaeometallurgical redox estimates using an Ellingham Diagram are systematically imprecise, being built upon potentially inaccurate liquidus calculations, and indicating a wide range of possible gaseous environments, it is perhaps safer to bypass the vague and circularly contingent determination of redox via liquidus, and instead make an educated estimate of likely prevailing gaseous atmospheres. For copper, this appraisal would, inevitable variability accepted, lie between a p_{O_2} of 1×10^{-6} and 1×10^{-8} (Figure 4.2), and an appropriate diagram may thus be chosen.

In order to take into account minor oxides within a phase diagram of limited dimensions, it is necessary to rationalise the iron content of slags, which would otherwise have to be

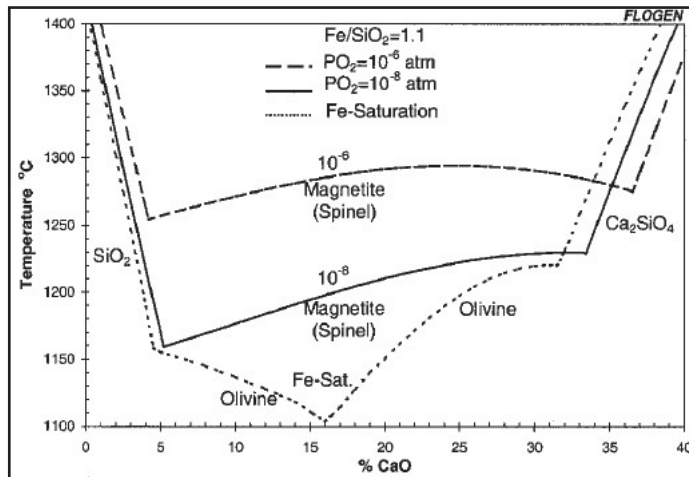


Figure 4.3 - Binary diagram showing the liquidus effect of varying ppO_2 and calcia content on slag system with a Fe/SiO_2 ratio of 1.1. Image from Kongoli & Yazawa 2001: Figure 8.

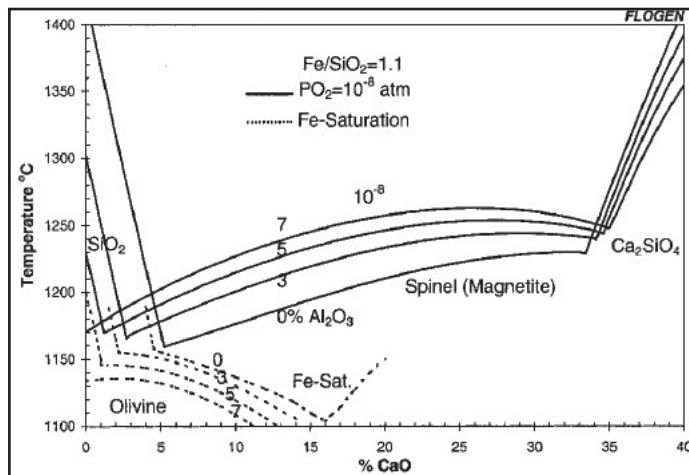


Figure 4.4 - Binary diagram showing the liquidus effect of varying alumina and calcia content on slag system with a Fe/SiO_2 ratio of 1.1 and a constant ppO_2 of 1×10^{-8} or in equilibrium with iron metal. Image from Kongoli & Yazawa 2001: Figure 14.

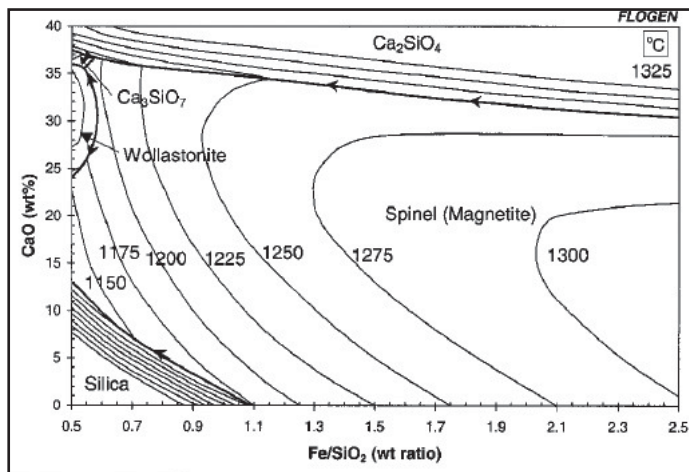


Figure 4.5 - Binary diagram showing the liquidus effect of varying calcia content and Fe/SiO_2 ratio on slag system with a ppO_2 of 1×10^{-8} . Image from Kongoli & Yazawa 2001: Figure 10.

represented with variables for 'Fe', 'FeO', 'Fe₃O₄', and 'Fe₂O₃'. Whether compositional data is calculated for elements or oxides (stoichiometrically) is a matter of interpretation, as most analytical techniques cannot determine valency state⁶. Likewise, estimating iron ion ratios by the relative abundance of wüstite and magnetite precipitations is problematic, as Fe²⁺ ions will be underrepresented due to their bonding with silica within the slag matrix. Therefore, it is perhaps safest to convert all iron oxide data to metallic iron, and calculate the ratio 'Fe/SiO₂' as a meaningful indicator of a slag's core composition.

The Fe/SiO₂ ratio is normally the x-axis of Flogen diagrams, with calcia content typically forming the y-axis. The effect of quaternary components is modelled by plotting isotherms for constant levels of minor oxide (e.g. Figure 4.5). The result is a series of simple two-dimensional diagrams, far more suitable for non-ferrous archaeometallurgical data than ternary phase plots calculated in equilibrium with air or metallic iron, though they still assume the reaction has proceeded to a stable state. The use of Flogen diagrams implies a degree of choice over appropriate redox conditions, but informed subjectivity and critical data examination are perhaps preferable to the nebulous liquidus and redox output of the traditional technique. Indeed, the Ellingham diagram is still of use, as the Flogen-calculated liquidus can be plotted against the known redox conditions (i.e. ppO₂ of 1x10⁻⁸), and used to crosscheck that all the phases identified microscopically within the slag are thermodynamically possible given the liquidus determination. A further advantage of the revised methodology is that the diagrams are binary rather than ternary, allowing archaeologists not trained in metallurgy better access to archaeometallurgical knowledge. The present study will employ ternary plots as they remain an excellent means of illustrating compositional groupings, but they will be used to calculate liquidus only for comparative purposes with the Flogen models.

Summary

Archaeometallurgical study is thus an iterative sequential process for interpreting physical characteristics like the chemical composition and microstructure of samples in terms of raw materials and process parameters and translating them into an understanding of past *chaînes opératoires* and the technological choices that constituted them and the technological styles that define them. Every cycle of the archaeometallurgical hermeneutic is layered with archaeological and scientific theory, interpretation and subjectivity, which should be as explicit as possible. In particular, the use of complex analytical instruments does not imply 'correct' results but builds in many more factors of potential error. However, without these specially developed techniques and approaches, archaeology would be largely devoid

6 See footnote 4.

of detailed insights into ancient metallurgical behaviour. These interpretive opportunities and limitations were borne in mind as the analytical methodologies described above were applied to metallurgical samples from early Iron Age Non Pa Wai (Chapter 5) and later Iron Age Nil Kham Haeng (Chapter 6), an identical approach ensuring subsequent data comparability (Chapter 8).

Chapter 5

Metallurgical Analyses and Technological Reconstruction - Non Pa Wai Metallurgical Phase

Two

An accurate and detailed reconstruction of *chaînes opératoires* lie at the core of any discussion of metal in a social context. Previous chapters have laid the theoretical (Chapter 3) and methodological (Chapter 4) foundations for this, tempered by the realities of the archaeological data (Chapter 2). This chapter presents the analyses, reconstruction, and interpretation of copper smelting activities at early Iron Age Non Pa Wai Period 3 Metallurgical Phase 2. The samples of NPW3/MeP2 mineral, technical ceramic, and slag were prepared for macroscopic, bulk compositional, microscopic, and phase compositional analysis according to the methodology detailed in Chapter 4. A sample catalogue and complete analytical data are presented in Appendices A and B.

5.1 Minerals

Mineral finds were classified according to whether they clearly did not originate from the immediate geology of the site, and subsequently must have been moved by people. The present study examined only minerals from secure NPW3/MeP2 contexts.

5.1.1 - Macro analysis

Of the thirteen samples assessed, nine (NPWM1, NPWM4, NPWM5, NPWM6, NPWM8, NPWM9, NPWM11, NPWM12, NPWM13) have visible signs of copper compound presence. These signs consisted usually of staining, but in two instances veining, with malachite and azurite - as identified macroscopically. None of the samples had visibly discernable copper sulphide compounds, although one (NPWM13) did contain pyrite. The key characteristics of the samples are summarised in Table 5.1, and detailed in Appendix A.

In terms of the gangue, seven (NPWM1, NPWM2, NPWM3, NPWM4, NPWM5, NPWM7, NPWM8) samples appear to be largely silica-based, whereas three (NPWM6, NPWM10, NPWM12) samples seem to be predominantly iron oxide-based. Two samples

(NPWM11, NPWM9) have gangue comprised of both silica and iron oxide, and one sample (NPWM13) is almost exclusively iron sulphide. The issue of whether minerals have been ‘roasted’ prior to smelting is an interesting technological consideration (e.g. Craddock 1995), but within the NPW3/MeP2 mineral assemblage there is no indication of any of the samples having been heat treated to increase their mechanical or chemical suitability for smelting.

Overall, the visual impression is of an oxide-biased mineral assemblage of siliceous and ferruginous rocks containing various degrees of copper compound staining and/or veining. Only NPWM13 stands out significantly with its obviously sulphidic matrix.

Sample	Siliceous	Ferruginous	Pyritic	Copper Carbonates	Copper Sulphides
NPWM1	X			X	
NPWM2	X				
NPWM3	X				
NPWM4	X			X	
NPWM5	X			X	
NPWM6		X		X	
NPWM7	X				
NPWM8	X			X	
NPWM9	X	X		X	
NPWM10		X			
NPWM11	X	X			
NPWM12		X		X	
NPWM13	X	X	X	X	

Table 5.1: Macro-characteristics of NPW3/MeP2 mineral samples.

5.1.2 Bulk Chemistry

NPW3/MeP2 mineral samples were prepared for [P]ED-XRF bulk analysis and the resulting data processed as per the procedures detailed in Chapter 4. Complete chemical data may be seen in Appendix B (Table B.1).

At the major element level, the chemical data (Table 5.2) for the Iron Age Non Pa Wai samples are consistent with the macro-analytical identifications above, that is a suite of siliceous rocks containing varying amounts of lime, alumina, and oxidic copper minerals. The clear exceptions to this, again noted in hand specimen are: NPWM6, NPWM10, and NPWM12 whose very high iron oxide concentrations confirm their identification as predominantly iron oxide minerals, and NPWM13, whose composition is pyritic. The Non Pa Wai samples contain c. 5wt% copper oxide on average, but of those only the

10g NPWM11 is definitely ore quality with c. 27wt% copper. The slightly low analytical totals may be due to the presence of carbonate compounds.

	MgO	Al ₂ O ₃	SiO ₂	SO ₃	CaO	Fe ₂ O ₃	CuO	Total
	wt%	wt%	wt%	wt%	wt%	wt%	wt%	wt%
NPWM1	0.1	8.5	69.7	0.0	10.3	8.7	1.6	95.3
NPWM2	0.1	6.1	71.7	0.0	5.8	7.4	7.9	95.2
NPWM3	0.1	2.5	84.6	0.0	0.3	8.2	3.0	90.4
NPWM4	0.3	4.2	71.4	0.0	7.4	13.2	2.1	93.9
NPWM5	1.4	15.7	67.2	0.0	1.8	4.3	2.3	92.6
NPWM6	2.7	3.5	7.8	0.0	2.8	77.6	4.3	96.5
NPWM7	0.1	8.3	60.6	0.0	8.3	13.6	8.1	90.8
NPWM8	0.1	0.8	85.3	0.1	0.7	3.8	7.2	90.3
NPWM9	1.7	14.8	37.0	0.0	21.0	21.0	2.5	87.3
NPWM10	0.2	0.7	1.2	0.3	0.1	96.8	0.1	99.5
NPWM11	9.7	11.6	20.4	0.1	0.2	28.9	27.5	78.2
NPWM12	0.4	1.1	4.2	0.1	0.1	91.9	1.3	91.9
NPWM13	0.1	0.0	22.0	23.3	4.6	45.6	1.3	83.2
mean	1.3	6.0	46.4	1.8	4.9	32.4	5.3	
std dev	2.7	5.4	31.7	6.4	6.0	34.3	7.2	
CV	205%	90%	68%	350%	122%	106%	134%	

Table 5.2: [P]ED-XRF bulk chemical analyses of NPW3/MeP2 mineral samples, selected major and minor oxides.

	Ni	Zn	Sr	Hf	Ta
	ppm	ppm	ppm	ppm	ppm
NPWM1	10	61	1118	73	82
NPWM2	122	851	709	175	196
NPWM3	19	122	23	102	152
NPWM4	53	283	391	87	98
NPWM5	180	1027	757	79	88
NPWM6	31	1156	47	<10	2
NPWM7	62	270	821	213	220
NPWM8	102	230	29	155	174
NPWM9	12	154	376	110	126
NPWM10	19	218	12	70	78
NPWM11	448	4157	11	<10	<10
NPWM12	33	1032	<10	192	218
NPWM13	1557	82	42	132	298
mean	204	742	333	107	133
std dev	424	1103	393	66	88
CV	208%	149%	118%	62%	66%

Table 5.3: [P]ED-XRF bulk chemical analyses of NPW3/MeP2 mineral samples, selected trace elements.

At the trace level, zinc, strontium, nickel, tantalum, and hafnium are the predominant elements, though they are irregularly distributed with a mean CV of 120% (Table 5.3). Scatter plots suggest there is a strong positive relationship ($R^2 = 0.761$) between hafnium and tantalum (Figure 5.1), although it has not been possible to ascertain with which major element these traces are associated. The concentration of strontium is largely correlated with the level of alumina and silica within the sample, although calcia is perhaps somewhat related (Figure 5.2).

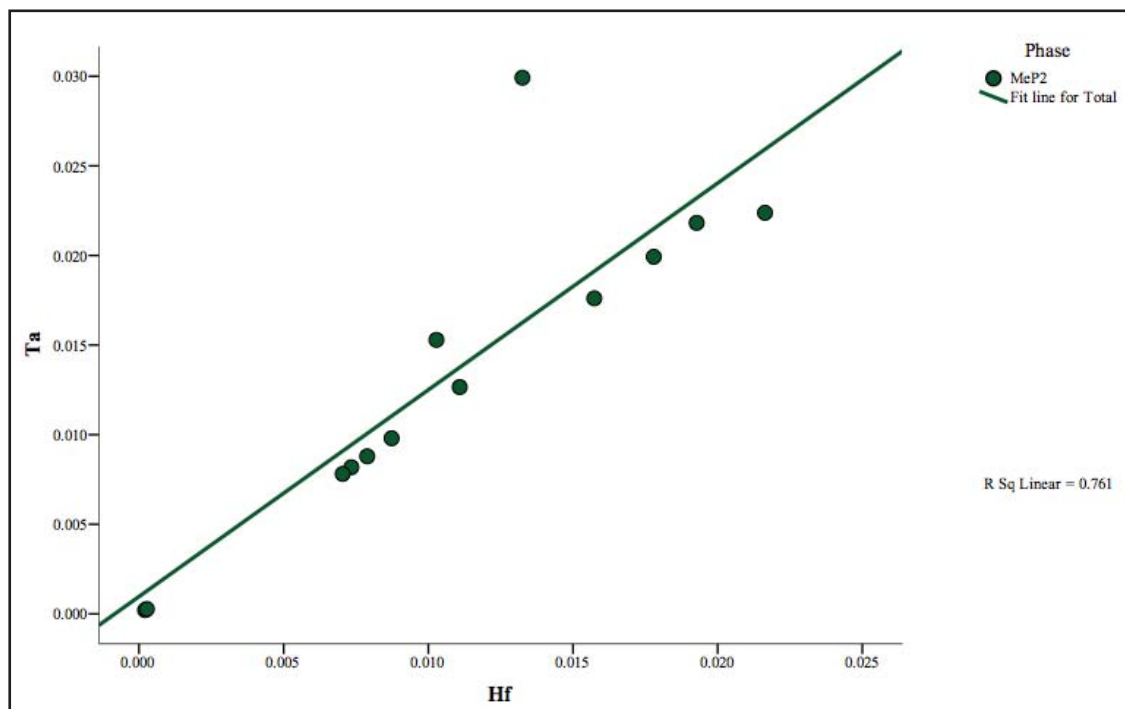


Figure 5.1: Scatter plot of NPW3/MeP2 mineral samples [P]ED-XRF bulk chemical data - hafnium versus tantalum, axes are in wt%. Image: author.

		Al ₂ O ₃	SiO ₂	CaO	Sr
Correlation	Al ₂ O ₃	1.000	.184	.503	.555
	SiO ₂	.184	1.000	.145	.508
	CaO	.503	.145	1.000	.488
	Sr	.555	.508	.488	1.000

Figure 5.2: Correlation matrix of NPW3/MeP2 mineral sample [P]ED-XRF bulk chemical data - alumina, silica, calcia, and strontium. Image: author.

5.1.3 Discussion

The problems with excavated mineral assemblages are recognised (e.g. Craddock 1995), and in the churned NPW3/MeP2 deposit we cannot be certain whether the relatively dispersed and low density mineral finds were due to ore-sorting choices or accidental losses by the metalworkers. Despite the best endeavours of the excavators there remains the possibility of sample recovery variation in the field, with fieldworkers perhaps primed for blue/green copper carbonates, but less familiar with sulphides and gangue minerals. The mineral assemblage is, on the whole, arguably associated with Non Pa Wai's copper smelting activities, and is commensurate with the Valley geology.

5.2 Technical ceramic

Technical ceramics were defined as non-domestic ceramics associated with industrial activities, and included: moulds, crucibles, and possible ‘furnace’ fragments; the moulds are undergoing study by Judy Voelker. The present study examined only crucible and ‘furnace’ fragments from secure NPW3/MeP2 contexts, and was principally intended to evaluate their potential role within the copper smelting *chaîne opératoire*.

5.2.1 Macro Analysis

Of the thirteen samples assessed, ten (NPWTC1 through NPWTC10) were crucible fragments, and three (NPWTC11, NPWTC12, NPWTC13) were ‘furnace’ fragments, as classified by the TAP excavators. The key visual characteristics of the samples are summarised in Table 5.4, and detailed in Appendix A.

Sample	Hi-fired	Lo-fired	Bloated/ Vitrified	Slagged	Copper sign	Perforated
NPWTC1	X		X	X	X	
NPWTC2	X		X	X		
NPWTC3	X		X	X	X	
NPWTC4	X		X	X	X	
NPWTC5	X		X	X	X	
NPWTC6	X		X	X	X	
NPWTC7	X		X	X	X	
NPWTC8	X		X	X	X	
NPWTC9	X		X	X	X	
NPWTC10	X		X	X	X	
NPWTC11		X				
NPWTC12		X				
NPWTC13		X			X	?

Table 5.4 - Macro-characteristics of NPW3/MeP2 technical ceramic samples.

‘Pit-rim’ fragments:

The supposed ‘furnace’ or ‘pit-rim’ samples were made from a friable low-fired oxidised red coarse organic-tempered fabric. The fragments are consistently around 40mm thick, and range from 50mm to 100mm in diameter. The samples have a rectilinear appearance with apparently flattened rims and bases but little curvature (Figure 5.3). One of the samples has a possible perforation in what appears to be the base, but the evidence is ephemeral at best (Figure 5.4). There is no clear evidence of manufacturing technique, but coiling, moulding, or slabbing are probable, throwing would be highly unlikely. Although the furnace fragments are low-fired, two of the three samples (NPWTC11 and NPWTC12)

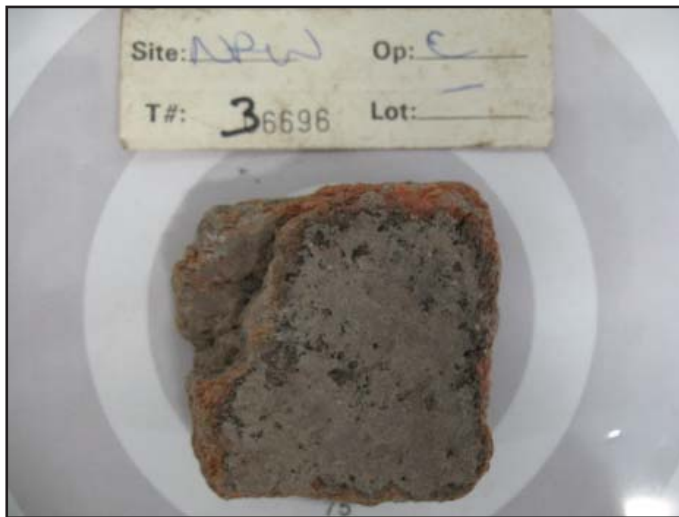


Figure 5.3 - Pit rim fragment NPWTC11. Image: author.

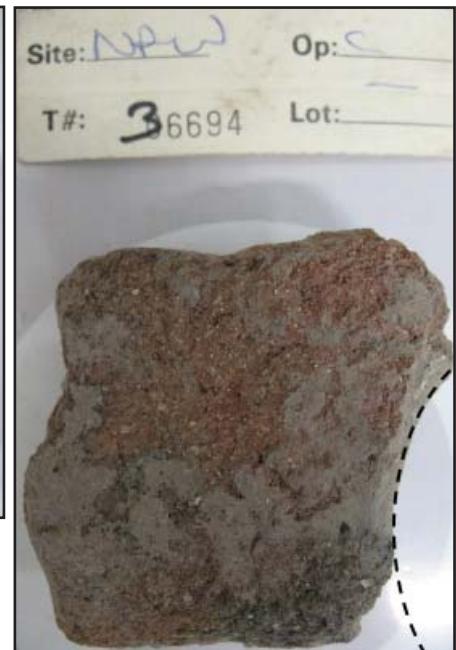


Figure 5.4 - Pit rim fragment NPWTC13 showing possible perforation evidence. Image: author.

do have a slight thermal/redox gradient in their profile, with a slightly higher-fired grey layer adhering to what appears to be the interior surface (Figure 5.3). There is no sign of any bloating, slagging or vitrification, although NPWTC13 does have some sign of corroded copper.

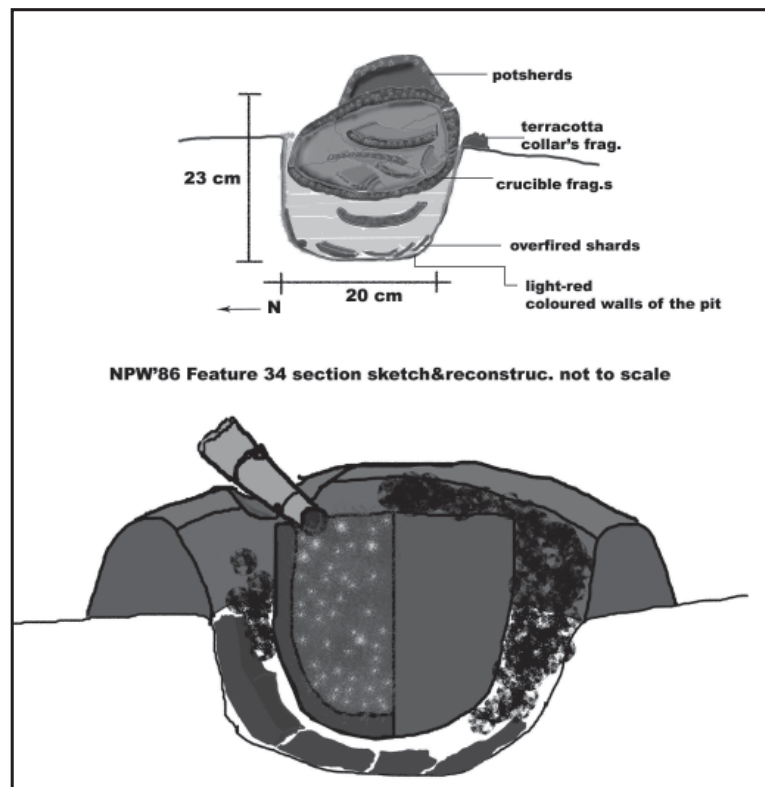


Figure 5.5 - Possible smelting pit excavated in NPW3 deposit. Image: Roberto Ciarla.

With no complete examples for comparison it is hard to reconstruct the stand and form of the ‘furnaces’, and the best impression we have is a sketch by Roberto Ciarla in his 1986 field notebook for the Non Pa Wai excavation (Figure 5.5), which illustrates a low ceramic rim around a shallow pit. This ‘pit-rim’ could have conceivably served to contain charcoal within the pit (cf. Los Millares smelting pit Craddock 1999: Figure 1), though a similar effect could have been achieved by using a slightly deeper pit. The low-fired condition of the fragments would be consistent with the high-temperature reaction being contained within the crucibles.



Figure 5.6 - Crucible fragment NPWTC3. Image: author.



Figure 5.7 - ‘Mr Crucible’. Image: Roberto Ciarla.



Figure 5.8 - Crucible fragment NPWTC7 curvature. Image: author.



Figure 5.9 - Crucible fragment NPWTC4 cross-section. Image: author.



Figure 5.10 - Crucible fragment NPWTC9 slagging. Image: author.



Figure 5.11 - Unused and used brass casting crucibles from Ban Pa Ao. Image: author.

Crucibles:

The crucibles were constructed from a tough well-fired reduced black coarse organic-tempered fabric (Figure 5.6). The fragments exist as rim, body, and base sherds ranging from 10mm to 60mm in thickness, and 50mm to 150mm in diameter. The samples generally exhibit clear curvature, and can be reasonably correlated to the sole complete example (known as ‘Mr Crucible’, Figure 5.7), which was recovered from a NPW3/MeP2 context. The generic reconstructed form of the crucibles is a bowl approximately 200mm in diameter, with an almost hemispherical base up to 60mm thick, and walls that progressively thin to around 10mm with a rounded rim (Figure 5.8).

All of the crucible fragments have a strong thermal/redox profile (Figure 5.9), with varying degrees of bloating, vitrification, and slagging on their concave surfaces (Figure 5.10). This combined evidence strongly suggests high temperature processes took place entirely within the crucibles, internal rather than external heating. This interpretation would be commensurate with the insulating qualities of the organic-tempered fabric: were the crucibles externally heated, the energy would have to be conducted through the vessel wall, leaving greater heat damage on the exterior (Bayley & Rehren 2007).

The substantial quantity of slag adhering to all of the samples is consistent with the crucibles having been used as smelting reaction vessels (Figure 5.10), as is further evidenced by microanalysis. The melting of even a relatively dirty metal would normally result in a lesser degree of scoria - compare an ethnographic example of a brass casting crucible from Ban Pa Ao, near Ubon Ratchatani in northeast Thailand (Figure 5.11). The fact that nine of the ten samples (only NPWTC2 excepted) have visible copper staining suggests the adhering slag was from a relatively low efficiency smelting process, although it is possible the crucibles were used for both smelting and melting purposes.

5.2.2 Bulk Chemistry

The technical ceramic samples from Non Pa Wai were prepared for [P]ED-XRF bulk analysis and the resulting data processed as per the methodology detailed in Chapter 4. Complete chemical data may be seen in Appendix B (Table B.2).

	Al ₂ O ₃	SiO ₂	CaO	Fe ₂ O ₃	CuO	Total
	wt%	wt%	wt%	wt%	wt%	wt%
NPWTC1 crucible	16.1	68.3	4.5	7.1	0.2	92.5
NPWTC2 crucible	19.5	60.7	5.6	9.6	0.1	88.3
NPWTC3 crucible	20.1	60.1	5.2	9.6	0.1	89.1
NPWTC4 crucible	18.1	62.3	5.2	8.6	0.5	87.9
NPWTC5 crucible	20.9	59.8	4.6	9.3	0.2	91.9
NPWTC6 crucible	17.5	64.3	5.2	8.0	0.4	94.1
NPWTC7 crucible	17.5	64.9	5.4	8.0	0.1	92.1
NPWTC8 crucible	19.6	59.4	5.4	9.7	1.2	93.7
NPWTC9 crucible	19.1	58.5	4.9	9.2	3.3	93.7
NPWTC10 crucible	17.5	63.6	5.3	8.3	0.2	93.4
NPWTC11 pit-rim	18.4	60.8	6.5	8.8	0.2	89.6
NPWTC12 pit-rim	18.4	62.2	5.5	8.7	0.3	88.0
NPWTC13 pit-rim	18.6	61.7	5.5	9.1	0.3	89.4
mean	18.6	62.0	5.3	8.8	0.5	
std dev	1.3	2.7	0.5	0.8	0.9	
CV	7%	4%	9%	9%	161%	

Table 5.5 - [P]ED-XRF bulk chemical analyses of NPW3/MeP2 technical ceramic samples, selected major and minor oxides after data normalisation, analytical total presented.

The NPW3/MeP2 crucibles and furnace fabrics share a similar major oxide chemistry, and have a mean composition of 62.0wt% silica, 18.6wt% alumina, 8.8wt% iron oxide, and 5.3wt% calcia (Table 5.5). Iron oxide and calcia have the highest CVs at 9%, but the mean coefficient for the above oxides is fairly low at around 7%, probably indicating a standard clay source for the technical ceramics, chemically commensurate with the local geology¹. The copper oxide content of the samples ranges between 0.1wt% to 3.3wt%, but averages 0.6wt% in the crucibles and 0.3wt% in the pit-rims, most likely reflecting slag contamination in the former. None of the other major oxides show any significant differentiation between the two artefact classes, again suggesting the use-lives of the ceramics did not substantially disrupt the paste uniformity (Figure 5.12). The refractoriness of the ceramics would be relatively low, but was doubtless sufficient for the probably limited duration of the technical tasks in hand (e.g. Childs 1990, Freestone 1989, Rehren & Bayley 2007, Tite *et al.* 1985, Tite *et al.* 1990). Again, low analytical totals suggest

¹ The current inhabitants of the Khao Wong Prachan Valley do not produce pottery, and local clay sources have been neither located nor sampled.

carbonates may be present.

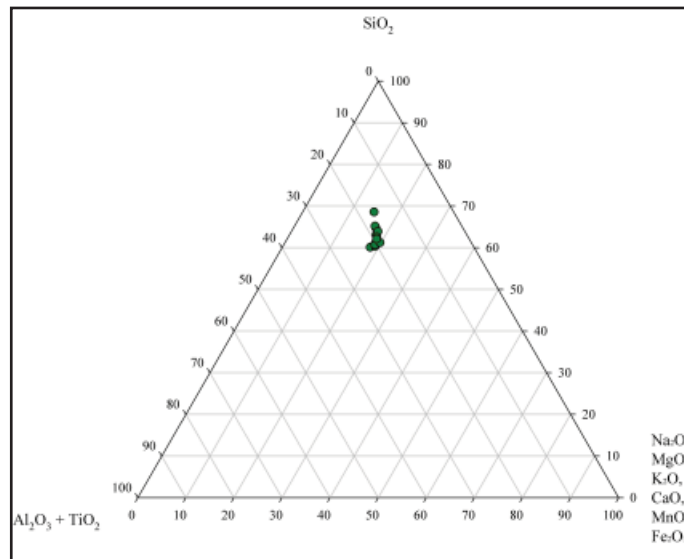


Figure 5.12 - Ternary plot of NPW3/MeP2 technical ceramic samples [P]ED-XRF bulk chemical data - selected major oxides.

	Zn	Sr	Zr	Ba
	ppm	ppm	ppm	ppm
NPWTC1 crucible	59	458	111	219
NPWTC2 crucible	111	706	70	252
NPWTC3 crucible	74	591	84	202
NPWTC4 crucible	131	711	65	533
NPWTC5 crucible	94	544	68	179
NPWTC6 crucible	61	580	67	194
NPWTC7 crucible	97	572	97	164
NPWTC8 crucible	88	699	73	211
NPWTC9 crucible	94	564	60	184
NPWTC10 crucible	83	591	71	249
NPWTC11 pit-rim	83	689	65	333
NPWTC12 pit-rim	107	645	65	389
NPWTC13 pit-rim	95	688	72	341
mean	91	618	74	265
std dev	20	78	15	107
CV	22%	13%	20%	40%

Table 5.6 - [P]ED-XRF bulk chemical analyses of NPW3/MeP2 technical ceramic samples, selected trace elements after data normalisation.

Strontium appears to dominate the trace element chemistry of both crucibles and furnaces, with a mean of 618ppm and a CV of only 13%. Other leading traces include barium (mean 265ppm), zinc (mean 91ppm), and zirconium (mean 74ppm), all of which have CVs of 40% or less (Table 5.6). The strontium within the samples appear to be positively correlated with calcia and alumina and negatively to silica, whereas zirconium has a strong

positive correlation to silica and a negative correlation to alumina and calcia (Figure 5.13). A ternary plot of the samples' content of strontium, zinc, and zirconium shows a tight cluster for the NPW3/MeP2 ceramics (Figure 5.14). There does not appear to be any significant trace element variation between crucible and furnace samples, suggesting the relatively uniform trace element chemistry is a function of a single clay source being used for NPW3/MeP2 technical ceramics.

	Al ₂ O ₃	SiO ₂	CaO	Sr	Zr	Ba
Correlation Al ₂ O ₃	1.000	-.883	.018	.321	-.494	-.145
SiO ₂	-.883	1.000	-.254	-.500	.723	-.002
CaO	.018	-.254	1.000	.732	-.359	.361
Sr	.321	-.500	.732	1.000	-.592	.608
Zr	-.494	.723	-.359	-.592	1.000	-.364
Ba	-.145	-.002	.361	.608	-.364	1.000

Figure 5.13 - Correlation matrix of NPW3/MeP2 technical ceramic sample [P]ED-XRF bulk chemical data - alumina, silica, calcia, strontium, zirconium, and barium.

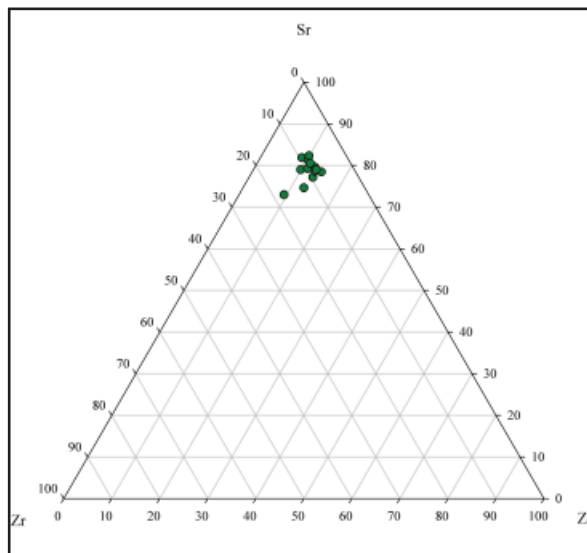


Figure 5.14 - Ternary plot of NPW3/MeP2 technical ceramic samples [P]ED-XRF bulk chemical data - selected trace elements.

Sample	Thermal degradation gradient	Elongate vesicles	Modified inclusions	Olivine skeletons	Crypto 'glass'	Iron oxide (primary)	Iron oxide (residual)	Prills
NPWTC1	X	X	X	X	X	X	X	X
NPWTC3	X	X	X	X	?	X	X	X
NPWTC8	X	X	X	X	X	X	X	X
NPWTC11	-	X	-					
NPWTC12	-	X	-					
NPWTC13	-	X	-					

Table 5.7 - Micro-characteristics of NPW3/MeP2 technical ceramic samples.

5.2.3 Micro analysis

The macro and bulk analysis technical ceramic population was sub-sampled for further study by OM and SEM-EDS. The Non Pa Wai crucibles were selected for microanalysis according to which of them appeared most likely to provide a section including slag and vitrified ceramic as well as the more intact fabric: NPWTC1, NPWTC3, and NPWTC8. Due to the low population, all of the ‘pit-rim’ fragments were analysed. The key micro-characteristics of the samples are summarised in Table 5.7.

A problem for the present study, both in optical and scanning electron microscopy, was the occasionally poor quality of polish on the analytical surface. Despite careful preparation of the mounted samples, the friable nature of the furnace fragments, and the bloated vesicles of the crucible fabric suffered constantly from plucking and gouging. Excessive topography could also render EDS compositional study problematic due to the diffraction of incident X-rays, but chemical microanalysis was focused on the crucible slag layers, which were acceptably polished. Whilst the following paste descriptions and interpretations would certainly be improved by petrographic thin section analysis, important information was extracted from the NPW3/MeP2 technical ceramic assemblage.

Pit-rim fragments:

The pit-rim fragments have a relatively uniform microstructure across the section due to the lack of a thermal profile. The paste is composed of an optically-active red micromass, with frequent sub-angular to sub-rounded fragments of quartz and iron oxide ranging from c. 0.01mm to c. 0.5mm, and few sub-rounded fragments of iron oxide ranging from c. 0.01mm to c. 0.2mm (Figure 5.15). The inclusions are relatively well sorted, with no clear evidence of preferred orientation, and their size distribution seems to be polymodal. Especially interesting is the frequent presence of elongate curvilinear vesicles c. 0.1mm to c. 0.2mm wide and up to c. 1mm in length, and also without preferred orientation (Figure 5.15).

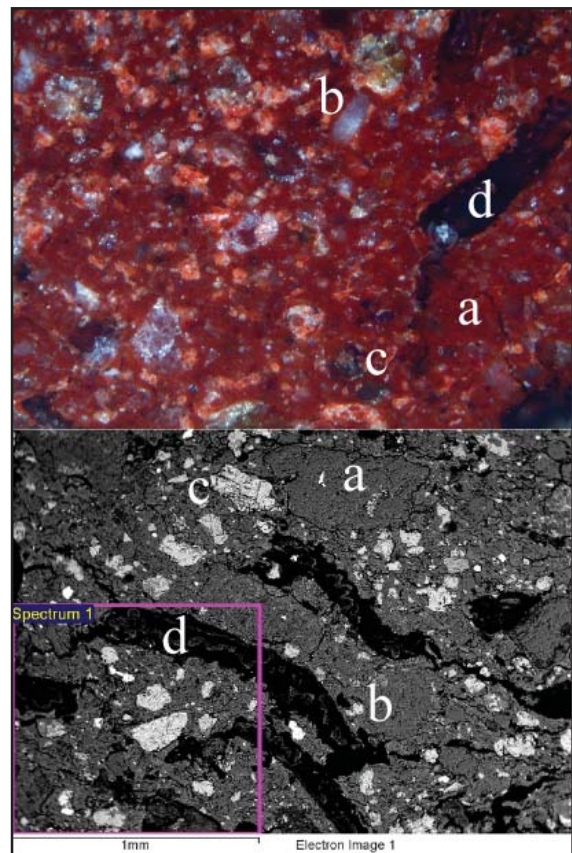


Figure 5.15 - Optical (ppl) and SEM-BSE images, both at x50, of NPWTC11 micro-features, ‘a’ micromass, ‘b’ quartz, ‘c’ iron oxide, and ‘d’ vesicles - ‘Spectrum 1’ exemplar of 1mm² EDS area scan on fabric. Images: author.

These characteristics would suggest the furnaces were produced from a sedimentary (non-pure) clay due to the presence of multiple mineral inclusions. The weathered (not freshly fractured) appearance of these particles, and the apparent absence of a modal distribution suggests they are either natural contaminants or evidence for non-systematic inorganic tempering. However, the paste was likely modified by substantial quantities of plant matter, which, after having burnt out during firing, could explain the extended airspaces in the furnace fabric. The lack of preferred orientation in the microstructure further reinforces the suggestion that the ancient metalworkers most likely used hand-building techniques to produce their ‘furnace’ structures.

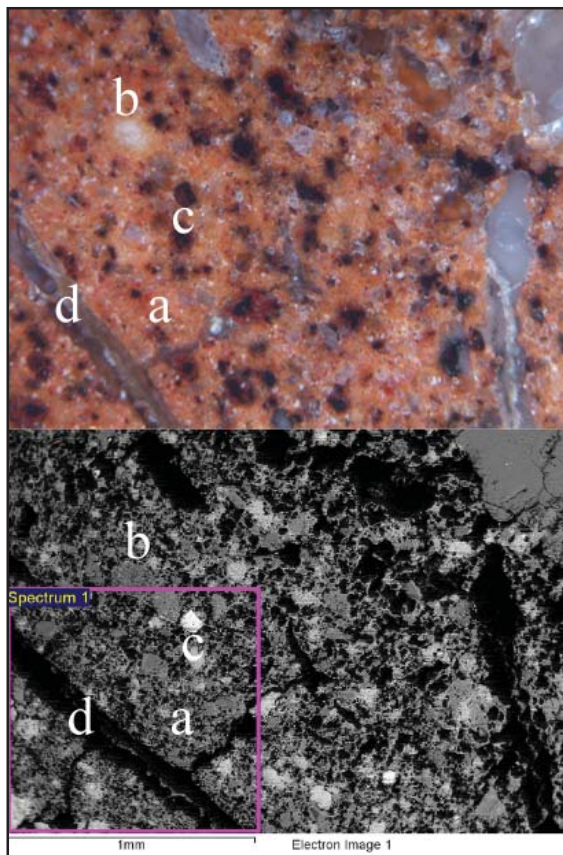


Figure 5.16 - Optical (ppl) and SEM-BSE images, both at x50, of NPWTC3 exterior section micro-features, ‘a’ micromass, ‘b’ quartz, ‘c’ iron oxide, and ‘d’ vesicles - ‘Spectrum 1’ exemplar of 1mm² EDS area scan on fabric. Images: author.

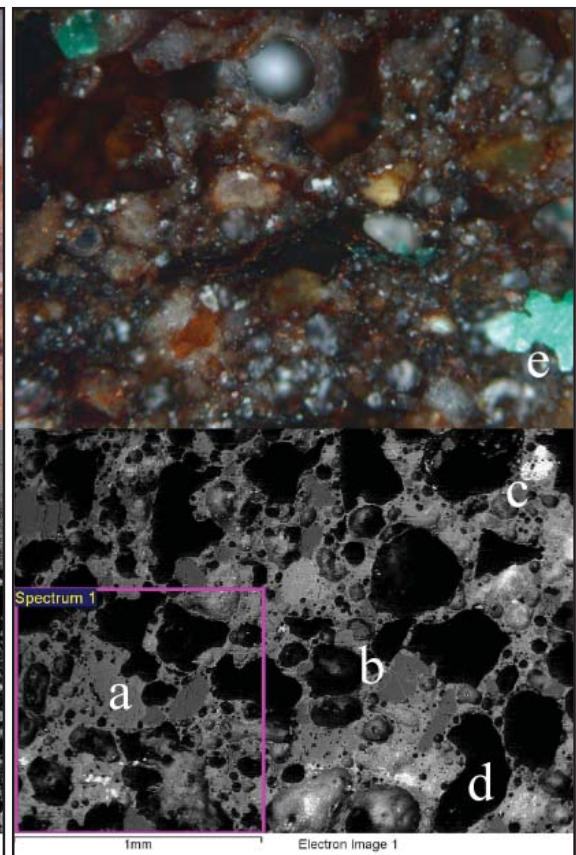


Figure 5.17 - Optical (ppl) and SEM-BSE images, both at x50, of NPWTC8 interior section micro-features, ‘a’ micromass, ‘b’ quartz, ‘c’ iron oxide, ‘d’ vesicles, ‘e’ copper compound penetration - ‘Spectrum 1’ exemplar of 1mm² EDS area scan on fabric. Images: author.

Crucible fragments - paste:

The crucible fragments have a distinct microstructural gradient across the section due to the thermal profile. Towards the exterior, less heat-damaged, surface the paste is composed of an optically slightly active red micromass, with regular sub-rounded fragments of semi-fused quartz ranging from c. 0.05mm to c. 0.2mm, and sub-rounded fragments of iron oxide ranging from c. 0.05mm to c. 0.15mm, all of which seem to have a fairly

tight size distribution (Figure 5.16). The inclusions are relatively well sorted and have no clear evidence of preferred orientation, perhaps due to their blurred partially-melted boundaries. Elongate curvilinear vesicles c. 0.1mm to 0.2mm wide and up to c. 1mm in length, are frequent and without preferred orientation (Figure 5.16).

The interior crucible surface is highly vitrified and bloated to the point of substantially obscuring the microstructure (Figure 5.17). The micromass, where it can be seen, is optically inactive, with regular fused grains of quartz c. 0.1mm to c. 0.3mm in diameter, and occasional iron oxide fragments c. 0.2mm in diameter, it was not possible to identify further mineral species within the heat-damaged matrix. Large sub-spherical vesicles, c. 0.1mm to c. 0.5mm in diameter, are widely distributed up to c. 10mm from the ceramic/slag interface (Figure 5.18), a degree of high-temperature modification also attested by the penetration of copper compounds into the section (Figure 5.17). As would be expected, the sorting of inclusions appears to be similar to that seen in the exterior fabric, and evidence for preferred orientation is even more indistinct.

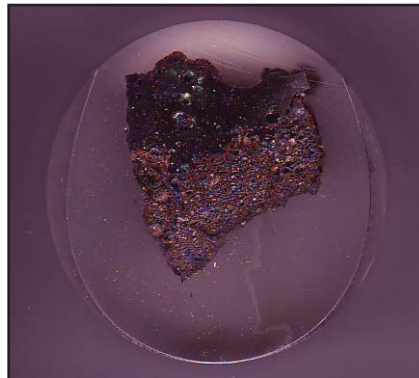


Figure 5.18 - Crucible fragment NPWTC8 mounted in 32mm polished block, widespread bloating visible throughout ceramic. Image: author.

These characteristics would suggest the crucibles were also produced from a sedimentary clay tempered with organic material, and possibly modified (levigation?) to reduce the quantity of very large (c. 0.5mm) quartz grains seen in the 'pit-rim' ceramic paste. The microstructural evidence for a thermal gradient corroborates the macro evidence, and indicates the crucibles were subjected to strong internal heating. The exterior crucible fabric is under going vitrification, its high temperature exposure appears to have been enough for sintering to begin diffusing grain boundaries and reducing optical activity. However, the interior fabric is heavily degraded, with extensive bloating (perhaps developed from the original elongate vesicles), and some penetration of copper-rich slag products.

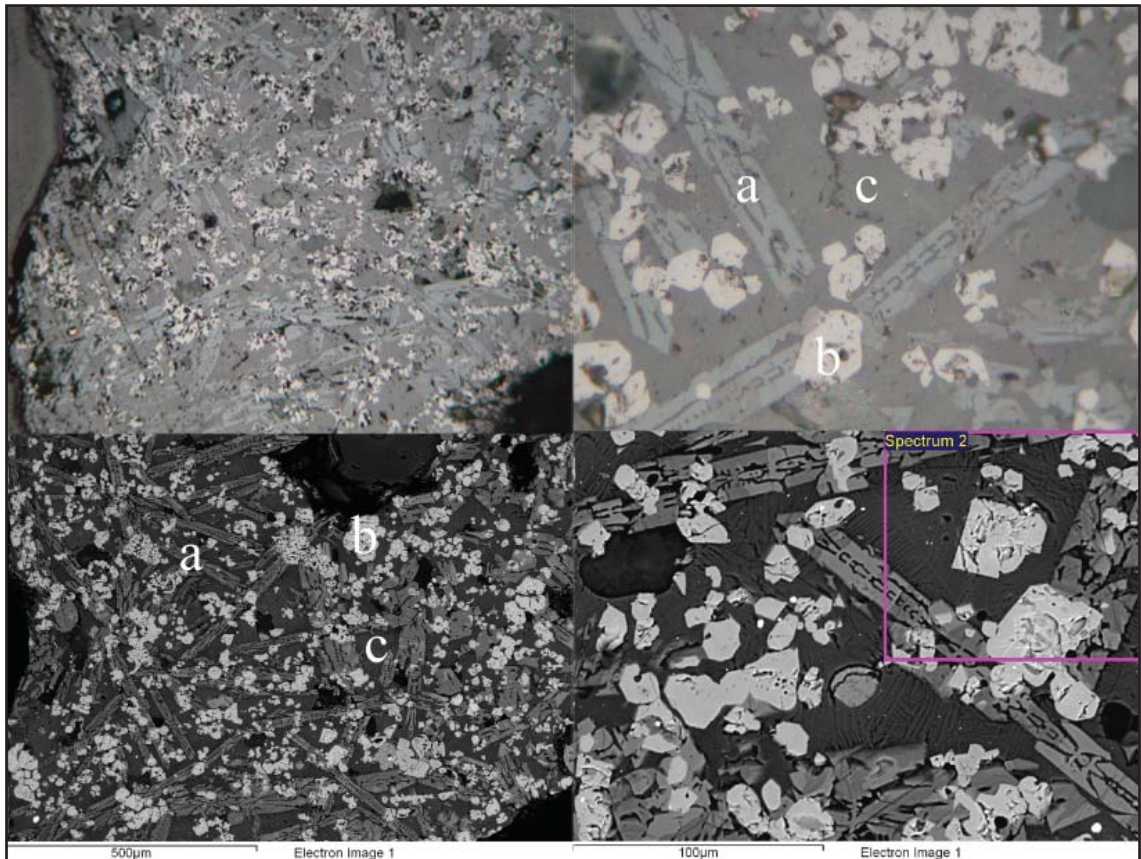


Figure 5.19 - NPWTC8 crucible slag micro-features at 100x (left) and 500x (right), by plane polarised light (top) and SEM-BSE (bottom). Labels 'a' olivine skeletons, 'b' primary magnetite euhedrals, 'c' cryptocrystalline glass, 'Spectrum 1' exemplar of 0.1mm² EDS area scan on slag matrix. Images: author.

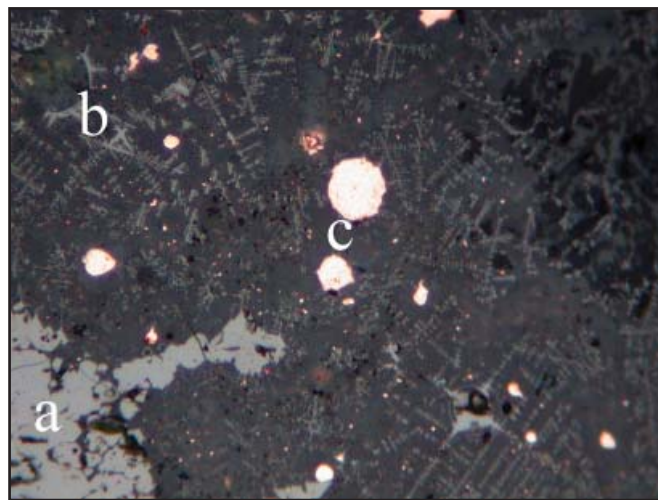


Figure 5.20 - NPWTC1 crucible slag micro-features at 500x under plane polarised light, 'a' residual magnetite, 'b' primary magnetite dendrites, 'c' copper base prills. Image: author.

Crucible fragments - slag:

The microstructure of slag adhering to the three crucible samples assessed is composed of three major components: interstitial glass, spinel and iron oxide crystals (Figure 5.19), as well as copper prills and residual iron oxide minerals (Figure 5.20).

	MgO	Al ₂ O ₃	SiO ₂	CaO	FeO	CuO	Total	Fe/SiO ₂
	wt%	wt%	wt%	wt%	wt%	wt%	wt%	wt ratio
NPWTC1	0.5	2.1	18.3	2.6	74.8	0.6	88.5	3.2
NPWTC3	0.9	1.5	33.5	10.4	50.7	0.3	85.8	1.2
NPWTC8	0.7	1.1	30.5	4.1	61.8	0.7	86.1	1.6
mean	0.7	1.6	27.4	5.7	62.4	0.5		
std dev	0.2	0.5	8.0	4.2	12.1	0.2		
CV	31%	30%	29%	73%	19%	43%		

Table 5.8 - SEM-EDS phase analyses of NPW3/MeP2 crucible slag olivine crystals, selected major and minor oxides after data normalisation, analytical total presented.

Olivine skeletons - Elongate olivine crystal skeletons are a frequent feature of the NPW3/MeP2 crucible slags, and range in width from c. 0.02mm to c. 0.04mm, and in length from c. 0.1mm to c. 0.5mm (Figure 5.19a). Olivines should not be able to form under intermediate partial pressures (Kongoli & Yazawa 2001: 585), that they have is indicative of variable redox conditions during the crucible reaction. The presence of olivine skeletons rather than fully developed euhedral crystals suggests the crucibles and the slag they contained may have cooled relatively rapidly, though not quenched (Donaldson 1976).

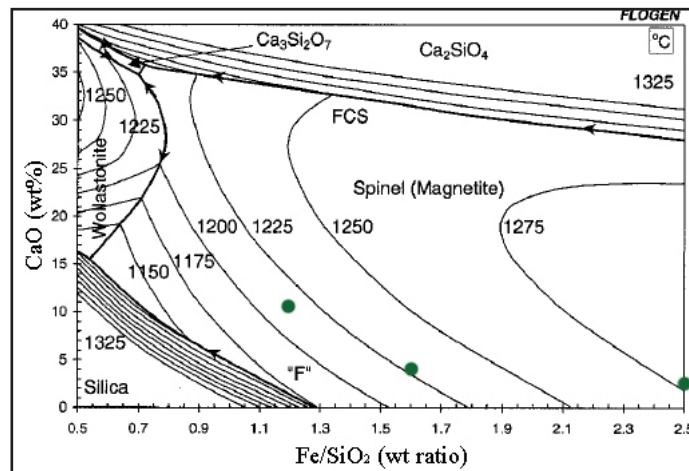


Figure 5.21 - SEM-EDS analyses of olivine phases plotted on a Floggen binary chart for slag system at a 10^{-8} ppO₂ and with 3wt% Al₂O₃. Image adapted from Kongoli & Yazawa 2001: Figure 10.

By SEM-EDS spot analyses, the major chemical components of the skeletons are FeO (mean 62.4wt%), SiO₂ (mean 27.4wt%), CaO (mean 5.7wt%), Al₂O₃ (mean 1.6wt%) and MgO (mean 0.7wt%) (Table 5.8). Their respective CVs (19%, 29%, 73%, 30% and 31%) suggest olivine composition between crucible samples is relatively variable (especially CaO in NPWTC3), possibly indicating erratic formation conditions and a non-standardised mineral/fuel charge. Plotting the Fe/SiO₂ ratio against CaO on a binary Floggen diagram, calculated for 3wt% Al₂O₃ (Kongoli & Yazawa 2001: Figure 10), indicates that the olivine phases began to crystallise between c. 1215°C and c. 1280°C, with a mean precipitation

temperature of c. 1240°C (Figure 5.21).

Magnetite spinel - Rhombic, skeletal, and dendritic crystals are also common within NPW3/MeP2 crucible slags, with dimensions for the former two habits prevalent in NPWTC8 ranging from c. 0.01mm to c. 0.05mm (Figure 5.19b), and the dendrites heavily represented in NPWTC1 ranging from c. 0.001mm to c. 0.05mm (Figure 5.20b)². All three phases are identified as the iron oxide ‘magnetite’ due to their optical behaviour and angularity (Ineson 1989), but the existence of different habits between samples is further evidence of variability in crucible slag formation. Also present are occasional angular fragments of iron oxide up to c. 1mm in size (Figure 5.20a). This phase is also identified as magnetite, but the fragments’ irregular boundaries, which appear to be dissolving into the melt rather than forming from it, indicate these are residual (unreacted natural) minerals. The presence of residual magnetite is further suggestive of chemically imbalanced reaction charges (discussed at length later in the chapter) but would certainly mean the crucible slag was saturated with iron oxide.

	MgO	Al ₂ O ₃	SiO ₂	CaO	TiO ₂	FeO	CuO	Total	Fe/SiO ₂
	wt%	wt%	wt%	wt%	wt%	wt%	wt%	wt%	wt ratio
NPWTC1 primary	0.3	0.6	0.9	0.4	0.0	96.7	0.6	91.6	87.3
NPWTC3 primary	0.1	0.8	0.1	0.1	0.0	96.8	1.9	90.9	627.6
mean	0.2	0.7	0.5	0.3	n.a	96.7	1.2		
std dev	0.2	0.2	0.5	0.2	n.a	0.1	0.9		
CV	75%	25%	107%	74%	n.a	0%	75%		

Table 5.9 - SEM-EDS phase analyses of NPW3/MeP2 crucible slag magnetite spinel, selected major and minor oxides after data normalisation, analytical total presented.

SEM-EDS spot analyses indicate the principal chemical components of the magnetite spinel are FeO³ (mean 96.7wt%), CuO (mean 1.2wt%), Al₂O₃ (mean 0.7wt%), SiO₂ (mean 0.5wt%), CaO (mean 0.3wt%) and MgO (mean 0.2wt%), the latter two being below confident accuracy levels, and TiO₂ (often associated with magnetite) not detected by the analytical equipment (Table 5.9). Binary Floggen diagrams are not available for such high Fe/SiO₂ ratios, but a ternary plot calculated for intermediate oxygen partial pressures indicates these phases would begin to precipitate at around 1300°C (Kongoli & Yazawa 2001: Figure 6). This would suggest the primary (not residual mineral) magnetite spinel crystallised before the olivine, which could account for the relatively uniform and pure composition.

2 NPWTC3 images were too poor for phases to be confidently identified.
 3 An approximation as magnetite has the formula Fe₃O₄.

Slag glass - Binding the crucible slag crystals of spinel and magnetite is an interstitial glass (Figure 5.19c). Although labelled a glass, it is noted that at 500 times magnification the phase is actually cryptocrystalline rather than glassy. These crystals range in width between c. 0.001mm to c. 0.005mm, and in length between c. 0.01mm to c. 0.02mm, and have a feathery dendritic habit whose dimensions appear to be delimited by the surrounding olivine and magnetite spinel microstructure.

SEM-EDS spot analyses indicate the major chemical components of this phase are SiO₂ (mean 43.6wt%), FeO (mean 33.1wt%), CaO (mean 16.4wt%), Al₂O₃ (mean 3.7wt%), MgO (mean 1.3wt%), and CuO (mean 0.4wt%) (Table 5.10). The respective CVs (8%, 18%, 14%, 40% and 73%) suggests the interstitial glass was fairly variable in its major oxides, especially FeO, and quite erratic in minor oxide concentrations. Plotting the data on the same Flogen diagram is problematic as one sample falls near the silica saturation zone, nevertheless the crucible slag glass would have begun to solidify between c. 1125°C and c. 1150°C, with a mean precipitation temperature of c. 1140°C (Figure 5.22). The precipitation temperatures are below those for the olivine and the magnetite spinel,

	MgO wt%	Al ₂ O ₃ wt%	SiO ₂ wt%	CaO wt%	FeO wt%	CuO wt%	Total wt%	Fe/SiO ₂ wt ratio
NPWTC1	1.7	5.3	47.6	16.2	27.0	0.8	81.1	0.4
NPWTC3	2.0	2.6	41.3	18.9	33.6	0.1	82.8	0.6
NPWTC8	0.2	3.1	42.0	14.2	38.7	0.2	83.4	0.7
mean	1.3	3.7	43.6	16.4	33.1	0.4		
std dev	1.0	1.5	3.5	2.4	5.9	0.4		
CV	73%	40%	8%	14%	18%	92%		

Table 5.10 - SEM-EDS phase analyses of NPW3/MeP2 crucible slag glass, selected major and minor oxides after data normalisation, analytical total presented.

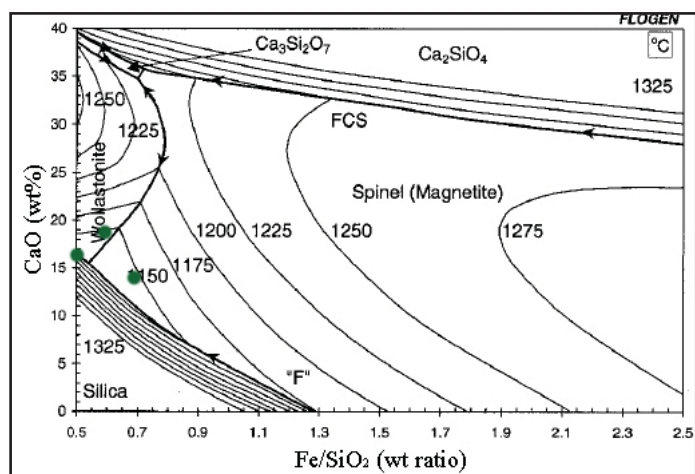


Figure 5.22 - SEM-EDS analyses of glass phases plotted on a Flogen binary chart for slag system at a 10⁻⁸ ppO₂ and with 7wt% Al₂O₃. Image adapted from Kongoli & Yazawa 2001: Figure 11.

suggesting the cryptocrystalline ‘glass’ was the last major phase to form as the slag solidified. The composition of this phase, as well as the dimensions, would have been determined by the prior formation of olivine and magnetite spinel, and the ‘glass’ is thus enriched in calcia and incorporated the remaining melt reactants.

Slag prills - Highly reflective metallic prills are abundant in the NPWTC1 slag layer (Figure 5.20) but are almost absent from that of NPWTC3 and NPWTC8, a situation confirmed by slag area analyses (see below). In NPWTC1, the prills range in diameter between c. 0.001mm and c. 0.03mm, although there is some bimodality to the distribution, with a constellation of tiny specks and a few much larger droplets. The SEM-EDS analyses performed indicate the prills are almost entirely copper (96.7wt%), with a little iron (3.3wt%), but no sulphur or tin. There is almost no bronze (and thus tin) in the entire Non Pa Wai assemblage, so the use of the crucibles for melting and casting bronze has never been proposed. However, the absence of sulphur from the prills could suggest the crucibles were used to smelt predominantly oxidic copper minerals.

Slag matrix - Aside from the residual magnetite, the individual crucible slag matrices are relatively homogeneous, with low porosity and well formed crystals, suggesting the slag had been almost fully liquid when hot. The olivine morphology indicates the slag formed over a relatively short period, suggesting the crucibles may have been cooled quite rapidly. The presence of areas where the slag had been fully molten means the general matrices are suitable for targeted bulk analysis, which, due to tight dimensions, were scanned in 0.1mm² sections (Figure 5.19, Table 5.11). This limited area conceivably reduces the representivity of the resulting data, but presentation of three area scans per sample matrix should serve to ameliorate any such issues. These ‘bulk’ data are not comparable to the [P]ED-XRF analysis of pelletised slag (see below) as they omit unreacted inclusions.

However, comparing the mean readings of SEM-EDS area scans from different crucible slags can be used to assess *inter* sample chemistry, whereas contrasting each scan represents *intra* sample variability. This approach is of use for interpreting whether the charge and operating conditions varied between or within crucible reactions, the former a proxy for standardisation, the latter for reaction equilibrium (cf. Humphris *et al.* 2009).

Comparing across the crucible samples, the major chemical components of the slag microstructure are FeO (mean 45.6wt%), SiO₂ (mean 35.8wt%), and CaO (mean 10.5wt%), and their respective CVs (35%, 25%, 54%) suggests there was little standardisation of

charge and/or technique in the crucible reactions. The elevated levels of TiO₂ in NPWTC1 and MnO in NPWTC3 supports the interpretation of non-standardised charges being largely responsible for inter sample variation. The mean Cu reading of 2.9wt% for the slag matrix is not excessive, but a CV of 80% suggests high variability in process efficiency, as seen in the abundance of prills in NPWTC1, but there seems to be no correspondence between high iron oxide values causing increased copper losses due to viscosity (Davenport *et al.* 2002: 273, Gilchrist 1989). Sulphur compounds were not detected in any of the crucible slag matrices.

	MgO wt%	Al ₂ O ₃ wt%	SiO ₂ wt%	SO ₃ wt%	CaO wt%	TiO ₂ wt%	MnO wt%	FeO wt%	CuO wt%	Total wt%	Fe/SiO ₂ ratio
NPWTC1 spectrum 1	1.2	4.7	43.0	0.0	10.2	1.1	0.0	34.5	4.7	86.2	0.6
NPWTC1 spectrum 2	1.0	4.1	40.8	0.0	9.3	1.0	0.0	36.7	6.8	86.8	0.7
NPWTC1 spectrum 3	1.4	5.0	43.7	0.0	10.4	1.5	0.0	32.9	4.8	85.5	0.6
<i>NPWTC1 mean</i>	<i>1.2</i>	<i>4.6</i>	<i>42.5</i>	<i>n.a.</i>	<i>10.0</i>	<i>1.2</i>	<i>n.a.</i>	<i>34.7</i>	<i>5.5</i>	<i>86.1</i>	<i>0.6</i>
<i>NPWTC1 std dev</i>	<i>0.2</i>	<i>0.4</i>	<i>1.5</i>	<i>n.a.</i>	<i>0.6</i>	<i>0.3</i>	<i>n.a.</i>	<i>1.9</i>	<i>1.2</i>		
<i>NPWTC1 CV</i>	<i>19%</i>	<i>9%</i>	<i>4%</i>	<i>n.a.</i>	<i>6%</i>	<i>22%</i>	<i>n.a.</i>	<i>5%</i>	<i>22%</i>		
NPWTC3 spectrum 1	1.4	2.2	39.6	0.0	17.0	0.0	1.5	37.0	1.0	82.9	0.7
NPWTC3 spectrum 2	1.1	2.6	37.4	0.0	15.3	0.0	1.6	39.9	1.7	84.0	0.8
NPWTC3 spectrum 3	1.3	1.7	40.3	0.0	17.1	0.0	1.4	37.1	0.7	82.7	0.7
<i>NPWTC3 mean</i>	<i>1.3</i>	<i>2.2</i>	<i>39.1</i>	<i>n.a.</i>	<i>16.5</i>	<i>n.a.</i>	<i>1.5</i>	<i>38.0</i>	<i>1.1</i>	<i>84.7</i>	<i>0.8</i>
<i>NPWTC3 std dev</i>	<i>0.1</i>	<i>0.4</i>	<i>1.5</i>	<i>n.a.</i>	<i>1.0</i>	<i>n.a.</i>	<i>0.1</i>	<i>1.6</i>	<i>0.5</i>		
<i>NPWTC3 CV</i>	<i>11%</i>	<i>20%</i>	<i>4%</i>	<i>n.a.</i>	<i>6%</i>	<i>n.a.</i>	<i>6%</i>	<i>4%</i>	<i>47%</i>		
NPWTC8 spectrum 1	0.0	1.8	21.9	0.0	4.0	0.0	0.5	70.3	1.3	88.2	2.5
NPWTC8 spectrum 2	0.0	2.1	26.1	0.0	5.6	0.0	0.5	63.4	1.5	87.7	1.9
NPWTC8 spectrum 3	0.0	2.1	29.3	0.0	6.0	0.0	0.4	58.6	3.2	85.8	1.6
<i>NPWTC8 mean</i>	<i>n.a.</i>	<i>2.0</i>	<i>25.8</i>	<i>n.a.</i>	<i>5.2</i>	<i>n.a.</i>	<i>0.5</i>	<i>64.1</i>	<i>2.0</i>	<i>87.3</i>	<i>1.9</i>
<i>NPWTC8 std dev</i>	<i>n.a.</i>	<i>0.2</i>	<i>3.7</i>	<i>n.a.</i>	<i>1.1</i>	<i>n.a.</i>	<i>n.a.</i>	<i>5.9</i>	<i>1.0</i>		
<i>NPWTC8 CV</i>	<i>n.a.</i>	<i>10%</i>	<i>14%</i>	<i>n.a.</i>	<i>21%</i>	<i>n.a.</i>	<i>n.a.</i>	<i>9%</i>	<i>52%</i>		
NPWTC mean	1.2	2.9	35.8	n.a.	10.5	1.2	n.a.	45.6	2.9	87.5	1.0
NPWTC std dev	0.0	1.5	8.9	n.a.	5.7	n.a.	n.a.	16.1	2.3		
Inter NPWTC CV	2%	50%	25%	n.a.	54%	n.a.	n.a.	35%	80%		
Mean intra NPWTC CV	15%	13%	7%	n.a.	11%	22%	n.a.	6%	40%		

Table 5.11 - SEM-EDS phase analyses of NPW3/MeP2 crucible slag matrices, selected major and minor oxides after data normalisation, analytical total presented.

Looking within individual samples, the CVs for FeO (5%, 4%, 9%), SiO₂ (4%, 4%, 14%), and CaO (6%, 6%, 21%) would corroborate the notion of crucible slags being generally well reacted, with the exception of NPWTC8 which has greater chemical variability. As would be expected, the minor oxides show higher, though still reasonable,

levels of variation, and copper oxide CVs (22%, 47%, 52%) suggest prill distribution is far from uniform. Nevertheless, there is arguably a great deal less variation within each crucible reaction than there is between them. Though all the processes could be described as relatively inefficient, the slag matrix data could be interpreted as showing that crucible reactions proceeded to completion, but NPW3/MeP2 metalworkers did not share a standardised charge recipe or operating procedures. Given the three samples may represent up to 400 years of industrial activity, it is highly plausible this is evidence for diachronic technological variation.

Using the traditional archaeometallurgical technique for calculating operating temperatures from slag liquidus, the primary chemical components (iron^(II) oxide, silica, and calcia) would indicate the slag adhering to the crucibles was exposed to minimum temperatures of between c. 1140°C and c. 1300°C (Figure 5.23). Transposing the mean liquidus of c. 1200°C onto an Ellingham Diagram, and extending two lines to the intersections of the liquidus with the ‘ $4\text{Cu} + \text{O}_2 = 2\text{Cu}_2\text{O}$ ’ and ‘ $6\text{FeO} + \text{O}_2 = 2\text{Fe}_3\text{O}_4$ ’ boundaries (representing the likely redox envelope for a process reducing copper to metallic form, and containing divalent as well as trivalent iron), indicates a ppO_2 between c. 1×10^{-5} and c. 1×10^{-9} (Figure 5.24), a typically broad range of operating parameters for a copper smelting reconstruction.

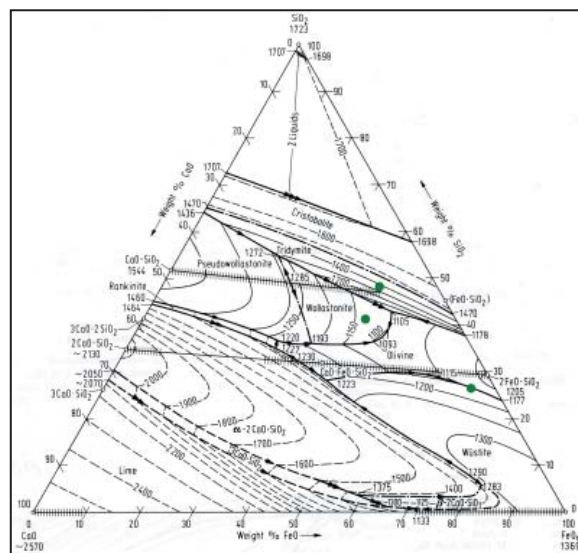


Figure 5.23 - Crucible slag matrices plotted on a ternary diagram for a FeO-CaO-SiO₂ slag system in equilibrium with iron metal. Image adapted from Eisenhüttenleute 1995.

The most appropriate Floggen diagram for the NPW3/MeP2 crucible slag layer describes a system with 3wt% alumina in a ppO_2 of 1×10^{-8} , with Fe/SiO₂ ratio and calcia as variables (Kongoli & Yazawa 2001: Figure 10). Plotting the data from Table 5.12 onto Figure 5.25

gives a liquidus reading of between c. 1175°C and c. 1300°C, giving a mean minimum slag temperature of c. 1245°C. The traditional figure of 1200°C may be only c. 50°C adrift from the Flogen reading, but the latter was calculated from experimentally tested thermodynamic models arguably more suitable for extractive copper metallurgy. Nevertheless, given the slag contains near pure magnetite precipitations in probable intermediate oxygen partial pressures, it is likely the crucibles were exposed to temperatures in excess of 1300°C, even if these levels were not constant.

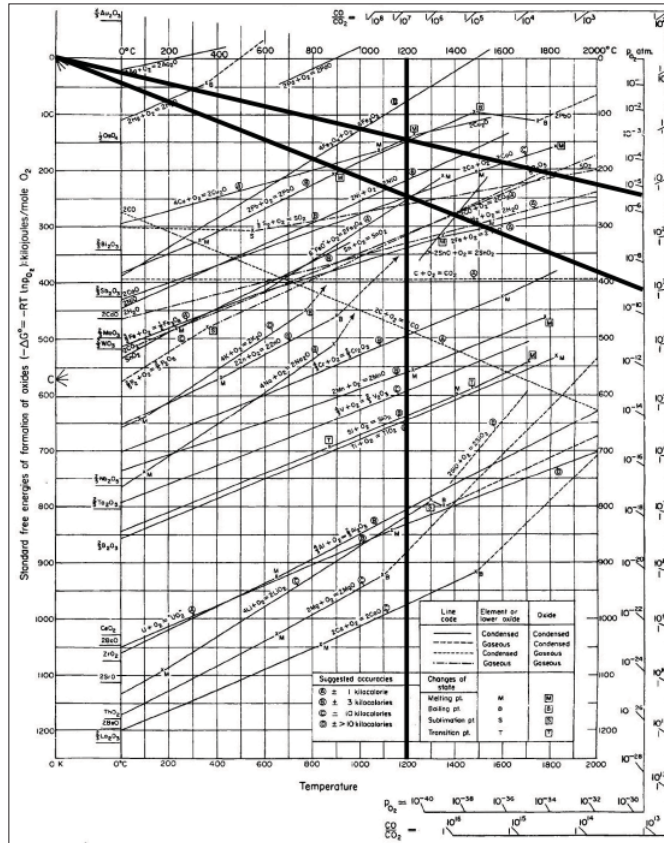


Figure 5.24 - Ellingham Diagram showing redox envelope for NPW3/MeP2 crucible slags. Image adapted from Gilchrist 1989.

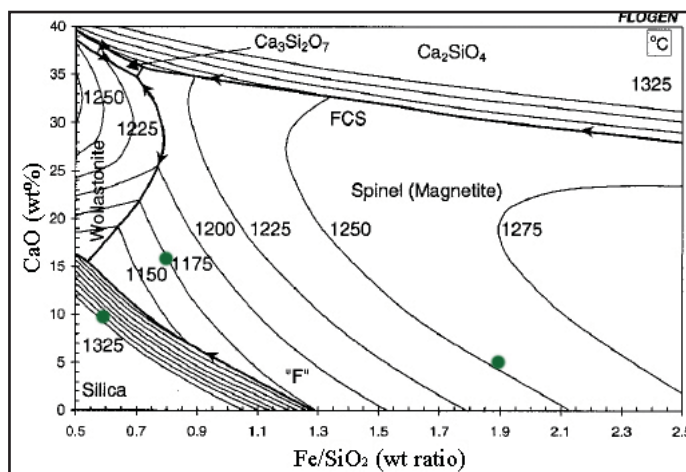


Figure 5.25 - SEM-EDS analyses of slag matrices plotted on a Flogen binary chart for slag system at a 10^{-8} pp O_2 and with 3wt% Al_2O_3 . Image adapted from Kongoli & Yazawa 2001: Figure 10.

5.2.4 Discussion

The analysis of NPW3/MeP2 crucible and ‘pit-rim’ fragments, whilst not exhaustive, has revealed substantial evidence to support the interpretation of their involvement in the copper smelting *chaîne opératoire*. All the technical ceramics appear to have been made from a mineralogically and chemically homogeneous secondary clay, perhaps from the Huay Pong stream or a tributary. Whilst both sets of artefacts have been organically tempered, it is possible the crucible paste was also modified to remove some of the more sizeable inclusions found in the ‘pit-rim’ fabric. If correct, this technological choice would theoretically reduce the risk of large quartz grains undergoing volumetric phase inversions at high temperatures, potentially undermining the tensile strength of the crucibles and propagating cracks which could be attacked by the molten slag.

Given Roberto Ciarla’s sketch (Figure 5.5) and the copper content (Table 5.5) there is little doubt the ‘pit-rim’ fragments were used in metallurgical processes, although admittedly this evidence could conceivably relate to copper refining or melting as well as smelting. The relative lack of heat damage to the fragments indicates that the structure was at some distance or was somewhat insulated from the high temperature core of the process. This would be the case if the reaction were contained within a crucible, and aerated from above. The author has observed charcoal surrounding a crucible smelting operation burning at a low heat in the absence of natural or artificial air sources to maintain elevated temperatures (Figure 5.26).



Figure 5.26 - Emilien Burger using forced blast to preheat a charcoal pit prior to a crucible-based copper smelting experiment in Fiaavè, Italy, September 2007. Photo: author.

The NPW3/MeP2 crucibles are consistent with a contained smelting reaction due to the clear evidence of internal heating in the samples studied. Extensive interior fabric degradation and heavy slagging are testimony to past high temperature activities, and the degree of copper staining indicates this was certainly the metal being processed within the vessels. Analysis of the adhering slag layer has identified a range of microstructures and phase compositions suggesting operating conditions well in excess of 1000°C, and in intermediate oxygen partial pressures appropriate for the reduction of copper metal from oxidic ores. The significant degree of compositional variation between crucible slags is suggestive of non-standardised procedures and/or mineral/fuel charges, but each individual smelting episode appears to have been carried out to near completion, and thus intra sample chemical variation is low. It does appear the vessels were cooled quite quickly, which could be explained by them being lifted to pour out the slag, though there is no microstructural evidence for the crucibles having been quenched. The combined evidence demonstrates the crucibles could conceivably have been used for the smelting of copper from a mineral charge rich in magnetite and silica, and with varying levels of calcia (though this could also be affected by fuel ash). The technical ceramic evidence is thus consistent with the excavated mineral assemblage, and the copper smelting interpretation is reinforced in the next section.

5.3 Slag

Slag is an extremely complex material and its composition and microstructure could be examined *ad infinitum*. The following discussion focuses on identifying the likely process reactants and operating conditions evidenced by the slag, and explaining what these mean in terms of the copper smelting *chaîne opératoire*. The effects of post-depositional alteration on the NPW3/MeP2 slag were hard to assess due to the samples' considerable anthropogenic heterogeneity, but to remain prudent all external surfaces were liberally cut off and only the remaining core analysed. It goes without saying more analytical data would be preferable, and there remains a great deal of intra-assemblage variability to be explored - perhaps via material from LoRAP's planned re-excavation of Non Pa Wai (Roberto Ciarla pers. comm.). However, the macro, micro, and compositional analyses of NPW3/MeP2 slag employed resulted in a reasonably cohesive understanding of the past technological choices that produced them.

5.3.1 Macro Analysis

Of the nineteen samples assessed, three (NPWMS6, NPWMS7, NPWMS19) were complete slag cakes, nine (NPWMS1, NPWMS2, NPWMS3, NPWMS4, NPWMS9, NPWMS11, NPWMS16, NPWMS20, NPWMS21) were probable fragments of slag cakes,

and two (NPWMS17, NPWMS18) were of an indeterminate morphology. The original form of samples NPWMS5, NPWMS8, NPWMS12, NPWMS13, and NPWMS14 is also unknown due to their having been uniformly crushed by Anna Bennett in the 1980s for her doctoral study. The key characteristics of the samples are summarised in Table 5.12, and detailed in Appendix A⁴. The subjective descriptions of Table 5.12 are relative to the assemblage and not to copper smelting slags generally, in no instance is there anything like a ‘glassy’ NPW3/MeP2 slag.

Sample	Mass (g)	Size (mm)	Morphology	Homogeneity	Porosity	Magnetism	Fe stain	Cu stain	Viscosity
NPWMS1	1640	<100	Broken slag cake	Medium	Medium	Weak	Strong	Weak	Medium
NPWMS2	240	<80	Broken slag cake	Low-Medium	Medium	Strong	None	None	Medium
NPWMS3	140	<80	Broken slag cake	Medium-High	Medium	Strong	None	None	Medium
NPWMS4	160	<60	Broken slag cake	Low-Medium	Medium	Strong	Weak	Strong	High
NPWMS5	150	<30	AB crushed	Low-Medium	Medium	Strong	None	Strong	Medium
NPWMS6	1325	<140	Slag cake	Medium-High	Medium	Strong	None	Weak	Medium
NPWMS7	NA	<150	Slag cake	Low	High	Strong	Weak	Strong	High
NPWMS8	300	<50	AB crushed	Low-Medium	Medium	Strong	Weak	Strong	High
NPWMS9	90	<70	Broken slag cake	Medium	High	Weak	None	Weak	High
NPWMS11	160	<70	Broken slag cake	Medium	Medium	Strong	Weak	Weak	Medium
NPWMS12	170	<60	AB crushed	Medium	Medium	Strong	Weak	Strong	Medium
NPWMS13	110	<40	AB crushed	Medium	Medium	Strong	Weak	Strong	Medium
NPWMS14	670	<40	AB crushed	Medium-High	Medium	Strong	Weak	Strong	Medium
NPWMS16	45	<50	Broken slag cake	Medium-High	Medium	Strong	None	Strong	Medium
NPWMS17	110	<70	Indeterminate	Medium-High	Medium	Strong	None	None	Medium
NPWMS18	25	<50	Indeterminate	Medium-High	Medium	Weak	None	Weak	Medium
NPWMS19	780	<140	Slag cake	Medium	Medium	Weak	Weak	Weak	Medium
NPWMS20	110	<80	Broken slag cake	Low-Medium	Medium	Strong	Weak	Strong	High
NPWMS21	930	<100	Broken slag cake	Low-Medium	Medium	Strong	Weak	Weak	High

Table 5.12 - Macro-characteristics of NPW3/MeP2 slag samples.

⁴ NPWMS10 was excluded due to it having been previously mislabelled as slag when it was iron oxide mineral, NPWMS15 was excluded due to severe analytical problems caused by a poorly pressed pellet, and there being insufficient material to make a second.



Figure 5.27 - NPWMS6 (top) and NPWMS19 (bottom), examples of NPW3/MeP2 slag cakes. Images: author.



Figure 5.28 - NPWMS1 (top) and NPWMS4 (bottom), examples of broken up NPW3/MeP2 slag cakes. Images: author.

The complete slag cakes have a diameter of c. 15cm, a depth of between c. 5cm to c. 10cm, and a mass of up to 1.5kg. The cakes have a plano-convex form and volume comparable to the NPW3/MeP2 crucibles (Figure 5.7), and thus commensurate with the reaction having taken place within these vessels. However, it seems likely that the slag was poured into a depression in the ground whilst still semi-molten, as evidenced by the ‘stiff’ folds and ridges of the cakes’ upper surfaces (Figure 5.27), and the presence of ceramic sherds and stones on the lower surfaces. There is also no sign of an ‘ingot meniscus’ which would have suggested the slag was floating on freshly smelted copper. Fragments of charcoal fuel are occasionally visible (4 of 19) embedded within the slags, but have not yet been identified to species. Most of the other slag samples have a similarly viscous appearance and appear to be broken up fragments of these cakes, ranging from c. 5cm to c. 10cm in diameter, and several tens to several hundreds of grammes (Figure 5.28). The samples are deliberately described as ‘broken up’ rather than ‘crushed’ in the usual archaeometallurgical terminology (Bachmann 1982), as the level of fragmentation does not correspond with the expected meticulous crushing by metalworkers diligently recovering copper prills or preparing to resmelt slag. It is at present unknown why some of the slag cakes are complete and why some are fragmentary, but it does appear that early Iron Age Non Pa Wai metalworkers regarded the slag output of their production process as waste not worthy of further processing.



Figure 5.29 - NPWMS7 sectioned and polished to show heterogeneous texture. Image: author.

In terms of optimisation, those metalworkers were over-zealous in jettisoning their slag cakes, as in section they are highly heterogeneous, porous and semi-fused (Figure 5.29). Partially reacted slags are indicative of smelting operations which were of an insufficient temperature and/or duration, and could have been either caused or exacerbated by a chemically unbalanced charge. NPWMS7's profile clearly reveals the presence of siliceous minerals in the process of dissolving into the melt, but, perhaps more interestingly, there are also large silvery fragments of seemingly unreacted mineral iron oxide. The typical interpretation stemming from the identification of iron oxide addition might be that of fluxing of a silica-saturated slag, but in this instance it doesn't appear to have worked - the reaction has not proceeded to equilibrium and there are extant pieces of both silica and iron oxide. Nevertheless, the macroscopic presence of residual iron oxide in the smelting slags is a very interesting potential link to similar phases noted in the crucible slags (see above).

Given that NPW3/MeP2 is an early Iron Age phase, and there are local deposits of high quality iron oxide at Khao Tab Kwai, it is conceivable iron smelting was also taking place at the Non Pa Wai. Indeed, a degree of rusty staining (10 of 19) and magnetism (15 of 19) is common within the sampled slag assemblage, representing the presence of iron compounds, and in particular $Fe^{2+/3+}$ ions. However, iron compounds are a normal component of copper smelting slags, and the recurrent green staining (16 of 19) of the samples indicates copper was certainly the desired metal product. The presence of macroscopically visible metal prills suggests slag crushing would have recovered more copper had it been performed (Figure 5.29).

The three complete slag cakes (Figure 5.27) appear to represent the primary slag morphology of the NPW3/MeP2 process, and were described as “exemplar” by TAP co-director Vincent Pigott (pers. comm.). However, it is hard to apply the term ‘exemplar’

to an assemblage whose macroscopic characteristics indicate wide variation between samples and significant heterogeneity within samples. In almost every measure, the slags give the resounding impression of a metallurgical process not yet perfected, though there is the ever-present threat of process conflation when dealing with distorted high temperature materials. There is no pejorative sense to describing the NPWM/MeP2 process as rudimentary or unsophisticated, the metalworkers of early Iron Age Non Pa Wai employed a technology suited to their needs and environment, and probably had no need to avoid wastefulness. However, from macroscopic inspection alone, there is some discrepancy between the author's findings and Bennett's (1989: 348) description of "copper production operating efficiently" in the Iron Age Khao Wong Prachan Valley.

5.3.2 Bulk Chemistry

The slag samples from Non Pa Wai were prepared for [P]ED-XRF bulk chemical analysis and the resulting data processed as per the methodology detailed in Chapter 3. Complete chemical data may be seen in Appendix B (Table B.8). These data cannot be used to assess intra-sample variability as only one bulk analysis was performed per sample, see 'micro-analysis' below. However, the slag bulk chemistry is of use for evaluating variation between slag samples and tentatively inferring what this might mean in terms of collective technological choices in NPW3/MeP2 copper production.

The slags have a mean major oxide composition of 52.1wt% iron oxide, 27.1wt% silica, 8.7wt% calcia, 3.2wt% alumina (Table 5.13). Iron oxide has the lowest CV at the relatively high level of 20%, and an average CV of 35% for the major slag-forming components suggests a significant degree of chemical variability between slag samples. The normalised mean minor oxides, soda (0.5wt%), magnesia (0.5wt%), manganese oxide (0.3wt%), phosphorous pentoxide (0.2wt%), potash (0.1wt%), and titania (0.1wt%), have a similarly elevated mean CV of 69% further indicating substantial compositional irregularity in the slag cake assemblage. The slags also contain on average 4.2wt% of copper and 2.5wt% sulphates⁵, unevenly distributed amongst the samples with CVs of 93% and 116% respectively. There exist no 'absolutes' for waste-product variation (though cf. Humphris *et al.* 2009 for a thorough multi-site and multi-sample analysis of slag variability) which can be caused by geological as well as behavioural factors, but the above bulk chemical data are indicative of high variation in copper smelting materials and/or procedures, and suggest non-standardised technological choices at early Iron Age Non Pa Wai, though we cannot discern whether this is a diachronic trend.

5 Reported copper and sulphur are likely to be present as both oxide and element.

	Na ₂ O	MgO	Al ₂ O ₃	SiO ₂	P ₂ O ₅	SO ₃	K ₂ O	CaO	TiO ₂	MnO	FeO	CuO	Total
	wt%	wt%	wt%	wt%	wt%	wt%	wt%	wt%	wt%	wt%	wt%	wt%	wt%
NPWMS1	0.7	0.3	1.4	24.0	0.0	2.6	0.0	10.5	0.1	0.1	54.0	6.1	92.8
NPWMS2	0.5	0.3	3.2	34.7	0.0	0.9	0.1	11.3	0.1	0.2	46.6	2.0	91.1
NPWMS3	0.5	0.5	3.8	24.9	0.4	1.5	0.2	4.8	0.1	0.3	62.0	0.9	94.4
NPWMS4	0.5	0.7	2.7	20.6	0.0	6.0	0.1	8.4	0.1	0.2	58.0	2.6	99.8
NPWMS5	0.3	0.5	4.8	36.7	0.1	0.7	0.2	9.0	0.1	0.4	45.3	1.6	94.0
NPWMS6	0.4	0.2	1.9	13.9	0.0	3.0	0.1	4.8	0.0	0.1	71.0	4.4	97.1
NPWMS7	0.2	0.0	3.8	31.1	0.1	12.4	0.1	10.1	0.1	0.5	32.2	3.5	96.3
NPWMS8	0.6	0.1	1.7	20.7	0.0	0.9	0.0	5.0	0.0	0.1	66.0	4.6	87.8
NPWMS9	0.4	1.1	4.5	30.3	0.2	1.6	0.2	9.8	0.1	0.2	50.6	0.7	93.9
NPWMS11	0.5	1.2	6.4	25.9	0.6	0.8	0.3	13.3	0.1	0.6	48.1	2.0	97.0
NPWMS12	0.9	0.4	4.8	25.9	0.1	0.9	0.1	6.0	0.1	0.4	53.3	7.0	92.0
NPWMS13	0.8	0.2	1.3	19.4	0.1	0.4	0.1	6.4	0.0	0.6	59.4	11.1	96.7
NPWMS14	0.4	0.1	3.4	35.1	0.0	1.3	0.1	13.9	0.1	0.3	44.2	0.9	93.6
NPWMS16	0.6	0.4	2.8	22.8	0.1	3.0	0.1	6.4	0.1	0.3	59.1	4.3	96.5
NPWMS17	0.4	0.2	2.2	26.7	0.7	2.0	0.1	4.9	0.1	0.2	61.3	1.2	95.5
NPWMS18	0.7	0.3	2.2	25.6	0.2	5.8	0.1	4.8	0.0	0.2	44.2	15.7	113.2
NPWMS19	0.4	1.4	3.0	40.7	0.3	0.7	0.1	18.0	0.0	0.6	32.8	1.9	90.0
NPWMS20	0.8	0.1	1.7	24.2	0.1	1.3	0.2	3.1	0.0	0.1	59.9	8.2	92.1
NPWMS21	0.5	0.9	5.3	32.1	0.0	1.4	0.3	15.6	0.1	0.3	41.8	1.5	94.5
mean	0.5	0.5	3.2	27.1	0.2	2.5	0.1	8.7	0.1	0.3	52.1	4.2	
std dev	0.2	0.4	1.4	6.7	0.2	2.9	0.1	4.2	0.0	0.2	10.6	4.0	
CV	33%	88%	45%	25%	121%	116%	65%	48%	51%	58%	20%	93%	

Table 5.13 - [P]ED-XRF bulk chemical analyses of NPW3/MeP2 slag samples, selected major and minor oxides after data normalisation, analytical total presented.

The mean trace element data for the NPW3/MeP2 slags is dominated by zinc (3849ppm), though the CV (341%) reflects the large concentration in NPWMS7 (Table 5.14). Other significant traces include strontium (165ppm) and barium (53ppm), though the presence of the former is more consistent (CV 68%) than the latter (CV 128%). Arsenic is almost absent and tin below confident detection limits, in accordance with these elements' low abundance in the local geology (William Vernon pers. comm.), and consistent with the production of an unalloyed copper from the minerals immediately available.

Copper losses of up to 15.7% (NPWMS18) suggest an inefficient smelting technique, comparable to other developing Eurasian processes, though these are often much earlier in date (Bourgarit 2007: Table 1). The extant copper could be present in unreacted ore minerals, chemically bonded with sulphur in matte compounds (Bachmann 1982: 16-17, Craddock 1995: 149-153, Yazawa 1980), or trapped mechanically in the slag (Davenport *et al.* 2002: 177, Gilchrist 1989). However, the lack of correlation ($R^2 = 0.025$) between sulphur and copper (Figure 5.30) suggests the copper content of Non Pa Wai slags probably cannot be explained by the presence of matte phases, as confirmed by micro-analysis.

	Zn	As	Sr	Sn	Ba
	ppm	ppm	ppm	ppm	ppm
NPWMS1	318	13	22	<10	34
NPWMS2	951	15	195	<10	127
NPWMS3	1022	12	182	<10	7
NPWMS4	449	13	45	<10	7
NPWMS5	666	7	293	<10	7
NPWMS6	588	20	23	<10	8
NPWMS7	57946	13	336	<10	7
NPWMS8	936	14	31	<10	41
NPWMS9	385	8	183	<10	124
NPWMS11	649	9	200	<10	29
NPWMS12	1195	11	183	<10	255
NPWMS13	1452	16	137	<10	8
NPWMS14	1480	13	217	<10	90
NPWMS16	822	13	124	<10	36
NPWMS17	1905	12	96	<10	7
NPWMS18	832	13	269	<10	67
NPWMS19	495	5	98	<10	144
NPWMS20	685	67	70	<10	36
NPWMS21	351	9	430	<10	27
mean	3849	13	165	n.a	53
std dev	13107	15	112	n.a	68
CV	341%	113%	68%	n.a	128%

Table 5.14 - [P]ED-XRF bulk chemical analyses of NPW3/MeP2 slag samples, selected elements after data normalisation

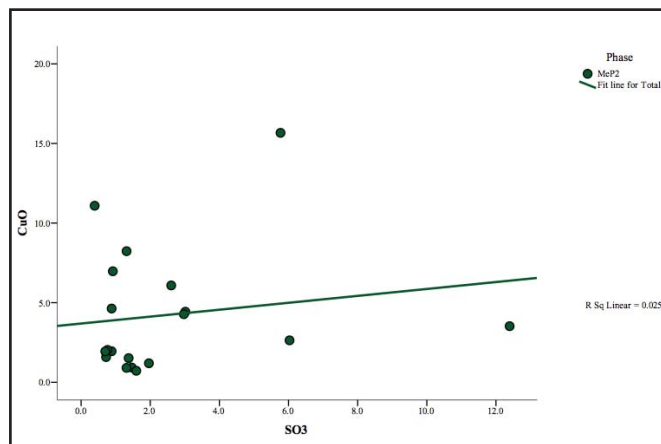


Figure 5.30 - Scatter plot showing low correlation between copper and sulphur compounds in NPW3/MeP2 [P]ED-XRF bulk chemical slag data.

Likewise, plotting iron oxide against copper (Figure 5.31) provides a weak association ($R^2 = 0.016$) not indicative of viscous magnetite formation within the slag preventing the separation of metal and slag by density (Davenport *et al.* 2002: 177). Therefore, the highly variable and apparently weakly correlated levels of iron, sulphur and copper are most likely to represent the presence of unreacted minerals trapped within the slag, although it

is uncertain from the bulk chemistry whether these elements entered the smelting system as ore, gangue, flux, or for non-technical requirements (to be discussed in the following section).

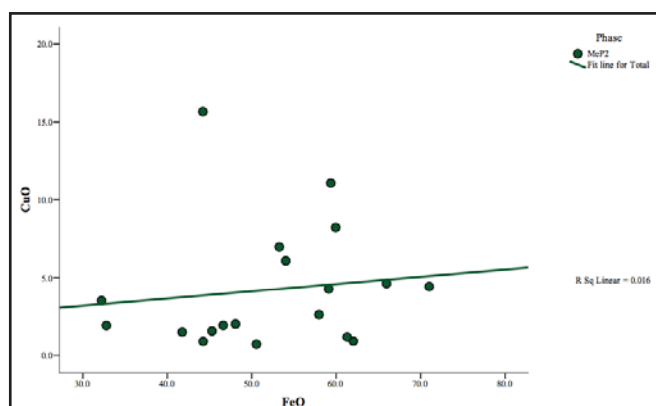


Figure 5.31 - Scatter plot showing low correlation between copper and iron compounds in NPW3/MeP2 [P]ED-XRF bulk chemical slag data.

The calcia content of NPW3/MeP2 technical ceramics (c. 5wt%, Table 5.5) suggests thermal degradation during smelting is unable to fully explain the calcia levels seen in the slags (c. 9wt%, Table 5.13). Though fuel ashes have a variable composition (Jackson *et al.* 2005), they tend to be rich in alkali oxides, particularly calcia, and are known to contribute significantly towards slag formation (e.g. Humphris *et al.* 2009, Merkel 1990: 110, Rehren *et al.* 2007). The remaining major source of calcia is the gangue content of the smelting charge, and it can be seen that calcia concentrations in the slag are positively correlated to those of silica (Figure 5.32), as well as being commensurate with the excavated mineral assemblage (Table 5.2). Figure 5.32 also shows silica and calcia are negatively correlated to iron oxide, suggesting both ferruginous and siliceous/calcareous copper ores may have been inconsistently used by early Iron Age metalworkers at Non Pa Wai. An alternative is that one of these mineral species was not gangue but flux. Macro examination (Figure 5.29) would suggest iron oxide was the flux, but the bulk chemistry is not so clear, iron oxide has the lowest major oxide CV (20%), whereas those for silica and calcia are higher (25% and 48% respectively) indicating iron oxide was the more constant component of the smelting charge. This important issue is pursued further below.

		SiO2	CaO	FeO
Correlation	SiO2	1.000	.711	-.832
	CaO	.711	1.000	-.746
	FeO	-.832	-.746	1.000

Figure 5.32 - Correlation matrix of NPW3/MeP2 slag sample [P]ED-XRF bulk chemical data - silica, calcia, and iron oxide.

Due to their massive textural heterogeneity and unreacted phases, the NPW3/MeP2 slag bulk chemical data are not suitable for the temperature and redox conditions of the early Iron Age smelting operation, however, these estimates are provided below in the micro-analytical section.

5.3.3 Micro analysis

The macro and bulk analysis slag population was sub-sampled for further study by OM and SEM-EDS. These samples were originally selected by grouping the PCA distribution of [P]ED-XRF bulk compositional data of slags from both NPW3/MeP2 and NKH3/MeP3 contexts into clusters representing 'extreme', 'normal', and 'overlapping' examples of each sites' slag chemistry (Pryce & Pigott 2008: Figure 13). From Non Pa Wai these were NPWMS1, NPWMS2, NPWMS3, NPWMS6, NPWMS7, and NPWMS13. However, after the Rispoli *et al* chronology shift (Chapter 4), it was decided to check for potential variation between MeP2a and MeP2b slags, and thus samples NPWMS5, NPWMS8, NPWMS12, NPWMS14, NPWMS18, and NPWMS19 were also analysed. It later transpired that at this stage it is not possible to securely differentiate the MeP2 samples stratigraphically, and thus all are regarded as MeP2 for the time being.

The microstructures of the NPW3/MeP2 slags assessed are composed of six major components: olivine skeletons (a1), euhedral olivine crystals (a2), residual iron oxide (b1), primary iron oxide (b2), interstitial glass (c), and metallic prills (d) (Figure 5.33, Table 5.15).

Olivine crystals - The NPW3/MeP2 slags contain both skeletal (NPWMS1, NPWMS2, NPWMS6, NPWMS8, NPWMS12, NPWMS13, NPWMS18) and euhedral (NPWMS3, NPWMS5, NPWMS7, NPWMS14, NPWMS19) crystalline habits. The elongate skeletons range in width from c. 0.005mm to c. 0.3mm, and in length from c. 0.05mm to c. 0.5mm, and the euhedral crystals range in diameter between c. 0.05mm and c. 0.1mm (Figure 5.34). There is no apparent correspondence between slag macro-morphology and microstructure - both 'broken up' and 'cake' slags exhibit both skeletons and euhedral crystals. Thus, the presence of two crystal habits is most likely related to differing formation conditions and cooling rates between the samples (Donaldson 1976), and is further suggestive of variable smelting practices at early Iron Age Non Pa Wai.

Sample	Olivine skeletons	Olivine euhedrals	Iron oxide skeletons	Iron oxide euhedrals	Iron oxide (residual)	Sphalerite (residual)	Siliceous gangue	Slag glass	Prills
NPWMS1	X		X		X			X	X
NPWMS2	X		X		X		X	X	X
NPWMS3		X	X		X			X	X
NPWMS5		X	X		X			X	X
NPWMS6	X		X		X			X	X
NPWMS7		X	X		X	X		X	X
NPWMS8	X		X		X			X	X
NPWMS12	X		X		X			X	X
NPWMS13	X		X		X			X	X
NPWMS14		X	X		X			X	X
NPWMS18	X		X	X	X			X	X
NPWMS19		X	X		X			X	X

Table 5.15 - Micro-characteristics of NPW3/MeP2 slag samples.

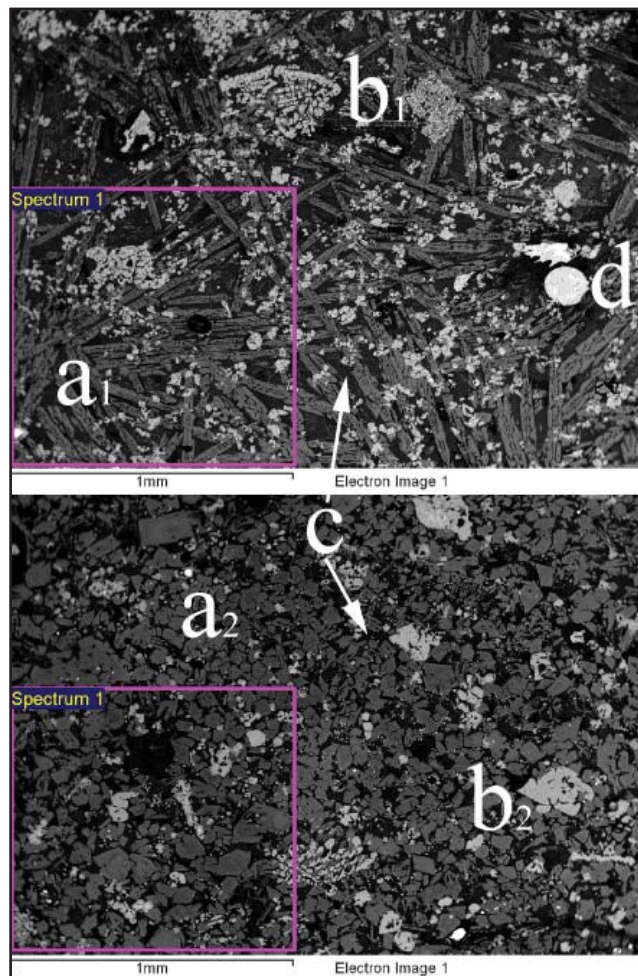


Figure 5.33 - NPWMS12 (top) and NPWMS14 (bottom) slag micro-features, both at 500x, by SEM-BSE. Labels 'a¹' olivine skeletons, 'a²' olivine euhedrals, 'b¹' residual iron oxides, 'b²' primary iron oxides, 'c' slag glass, 'd' prills, 'Spectrum 1's are exemplar of 1mm² EDS area scans. Images: author.

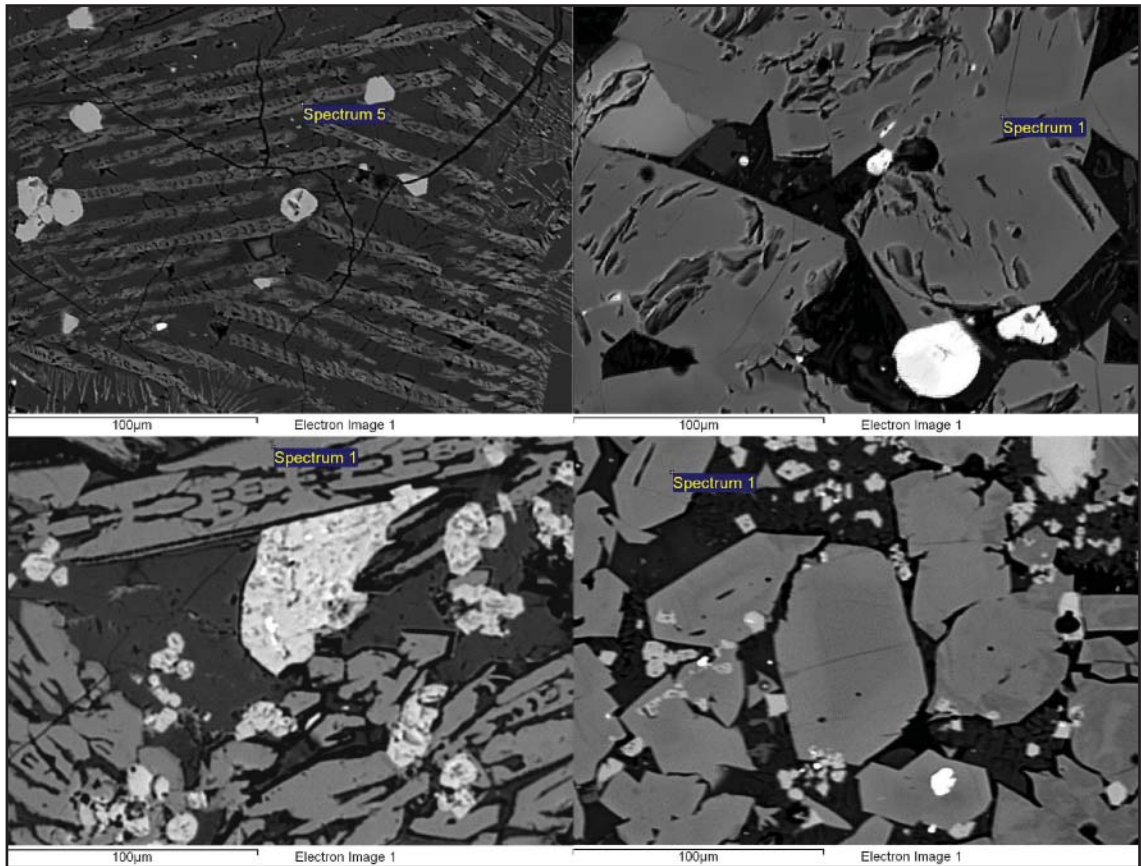


Figure 5.34 - NPWMS2 (top left), NPWMS3 (top right), NPWMS12 (bottom left), and NPWMS13 (bottom right) olivine skeletons and euhedrals, all at 500x, by SEM-BSE, ‘Spectrum 1’s and ‘Spectrum 5’ are exemplar of EDS point analyses. Images: author.

	MgO	Al ₂ O ₃	SiO ₂	CaO	MnO	FeO	Total	Fe/SiO ₂
	wt%	wt%	wt%	wt%	wt%	wt%	wt%	wt ratio
NPWMS1	1.3	0.0	27.6	6.8	0.0	64.3	96.0	1.8
NPWMS2	0.6	0.7	31.2	5.5	0.0	61.9	92.0	1.5
NPWMS3	1.0	0.0	24.9	1.1	0.3	72.8	90.9	2.3
NPWMS5	1.0	0.0	20.5	4.8	0.7	73.1	80.0	2.8
NPWMS6	0.7	0.4	28.7	13.0	0.1	56.9	94.2	1.5
NPWMS7	4.8	0.0	26.8	1.8	1.3	59.4	88.1	1.7
NPWMS8	0.8	0.0	27.8	12.6	0.0	58.8	95.0	1.6
NPWMS12	0.8	0.0	20.9	6.5	1.5	70.3	79.7	2.6
NPWMS13	1.4	0.0	26.0	4.8	2.6	64.9	90.7	1.9
NPWMS14	3.6	0.0	30.6	1.1	0.4	64.3	103.5	1.6
NPWMS18	0.0	4.8	36.7	15.9	0.2	41.9	68.6	0.9
NPWMS19	0.4	0.0	21.9	13.8	1.6	62.3	76.6	2.2
mean	1.4	0.5	26.9	7.3	0.7	62.6		
std dev	1.4	1.4	4.7	5.2	0.8	8.4		
CV	102%	277%	17%	72%	114%	13%		

Table 5.16 - SEM-EDS phase analyses of NPW3/MeP2 slag olivines, selected major and minor oxides after data normalisation, analytical total presented.

As per the NPW3/MeP2 crucibles (above), the probable formation of the slags under intermediate oxygen partial pressures, with a consequent dearth of Fe^{2+} ions, should mean olivines and fayalites were unable to form (Kongoli & Yazawa 2001: 585). However, the morphology and chemistry of the crystals identifies them as olivines, and this probably indicates non-equilibrium redox conditions during the smelt. By SEM-EDS spot analyses, the major chemical components of the olivines are FeO (mean 62.6wt%), SiO_2 (mean 26.9wt%), CaO (mean 7.3wt%), MgO (mean 1.4wt%), MnO (mean 0.7wt%), and AlO_3 (mean 0.5wt%) (Table 5.16). Their respective CVs (13%, 17%, 72%, 102%, 114%, and 277%) suggest olivine crystal composition between slag samples is highly variable outside of the predominant oxides, probably indicating erratic formation conditions and a non-standardised mineral/fuel charge. It is possible there may be lower levels of calcia in the euhedral crystals, but generally there are insufficient data to identify significant chemical difference between the olivine habits.

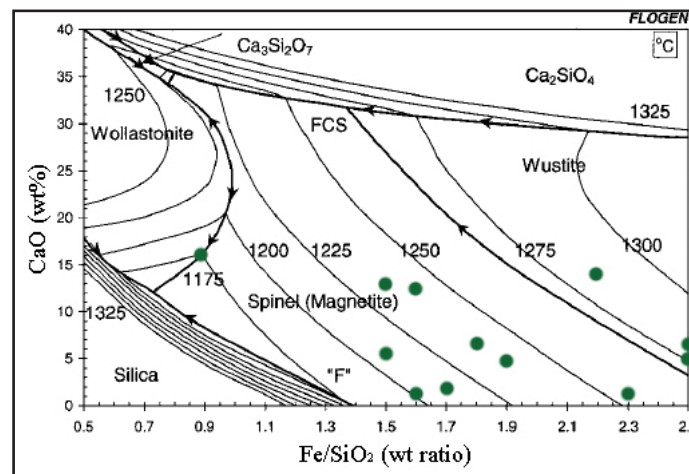


Figure 5.35 - SEM-EDS analyses of olivine phases plotted on a Flogen binary chart for a slag system at a 10^{-8} ppO₂ and with 1wt% MgO. Image adapted from Kongoli & Yazawa 2001: Figure 15.

In this instance, the predominant quaternary oxide is magnesia, and thus the Fe/SiO_2 ratio is plotted against CaO on a binary Flogen diagram, calculated for 1wt% MgO (Kongoli & Yazawa 2001: Figure 15), indicates the olivine began to crystallise between c. 1175°C and c. 1285°C (the latter figure assumed for NPWMS12 which plots off the chart), with a mean precipitation temperature of c. 1240°C (Figure 5.35).

Magnetite spinel - Euhedral iron oxide crystals are a universal feature of the NPW3/MeP2 slags assessed, and iron oxide skeletons occasionally discernable (NPWMS18, but there may be other samples with smaller as yet undetected crystals) The dimensions for the euhedral habit range from c. 0.05mm to c. 0.1mm, and the skeletons seen in NPWMS18 range from c. 0.001mm to c. 0.01mm (Figure 5.35). Both phases are identified as the iron

oxide magnetite due to their optical behaviour and angularity (Ineson 1989).

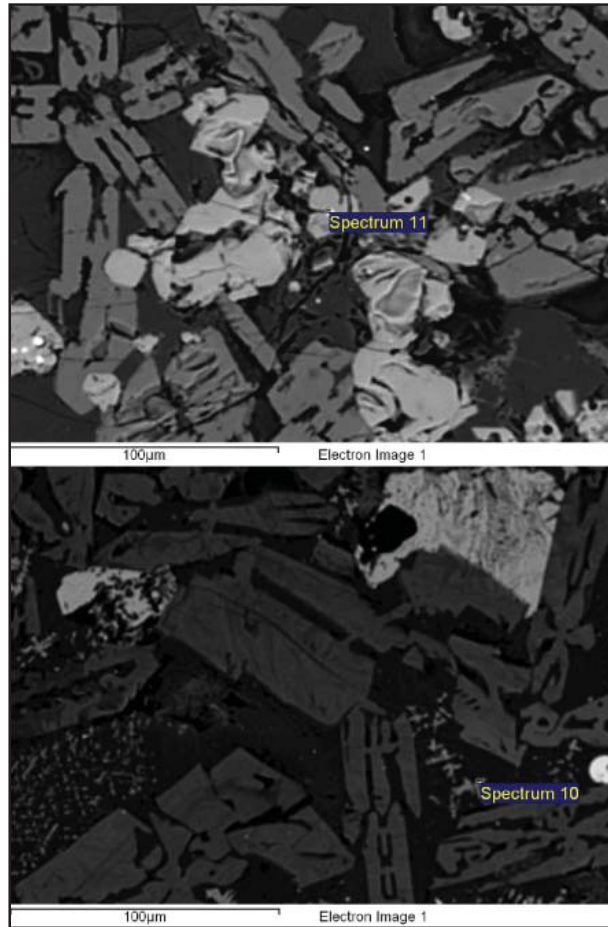


Figure 5.36 - NPWMS8 (top) and NPWMS18 (bottom) magnetite euhedrals and skeletons, both at 500x, by SEM-BSE, 'Spectrum 11' and 'Spectrum 10' are exemplar of EDS point analyses. Images: author.

	Al ₂ O ₃	SiO ₂	CaO	TiO ₂	FeO	Total	Fe/SiO ₂
	wt%	wt%	wt%	wt%	wt%	wt%	wt ratio
NPWMS1	2.8	1.0	0.4	1.8	94.1	93.5	72.3
NPWMS2	1.8	0.8	0.2	0.4	96.8	93.0	100.1
NPWMS5	1.6	0.3	0.2	0.4	97.6	85.7	290.9
NPWMS6	2.7	0.0	0.0	0.0	97.3	93.2	n.a.
NPWMS7	0.2	0.0	0.0	0.0	99.8	91.3	n.a.
NPWMS8	0.3	0.0	0.2	0.0	99.6	86.8	n.a.
NPWMS12	0.8	0.2	0.3	0.0	98.6	85.8	470.2
NPWMS13	0.2	0.0	0.2	0.0	99.4	90.4	n.a.
NPWMS14	6.4	6.0	1.8	0.6	82.9	96.6	10.7
NPWMS18	1.7	8.6	1.8	0.3	87.6	84.8	7.9
mean	1.8	1.7	0.5	0.3	95.4		
std dev	1.9	3.1	0.7	0.5	5.7		
CV	102%	182%	137%	159%	6%		

Table 5.17 - SEM-EDS phase analyses of NPW3/MeP2 slag magnetite spinel, selected major and minor oxides after data normalisation, analytical total presented.

SEM-EDS spot analyses indicate the principal chemical components of the primary magnetite phases are FeO^6 (mean 95.4wt%), Al_2O_3 (mean 1.8wt%), SiO_2 (mean 1.7wt%), CaO (mean 0.5wt%), and TiO_2 (mean 0.3wt%) (Table 5.17). Binary Floggen diagrams are not available for very high Fe/ SiO_2 ratios, but a ternary plot calculated for intermediate oxygen partial pressures indicates the magnetite phases would begin to precipitate at around 1300°C (Kongoli & Yazawa 2001: Figure 6). This would suggest the primary (not residual mineral) magnetite crystallised before the olivine, which could account for the relatively uniform and pure composition. The low CV for iron oxide (6%) suggests the formation of this phase was a consistent feature of NPW3/MeP2 smelting.

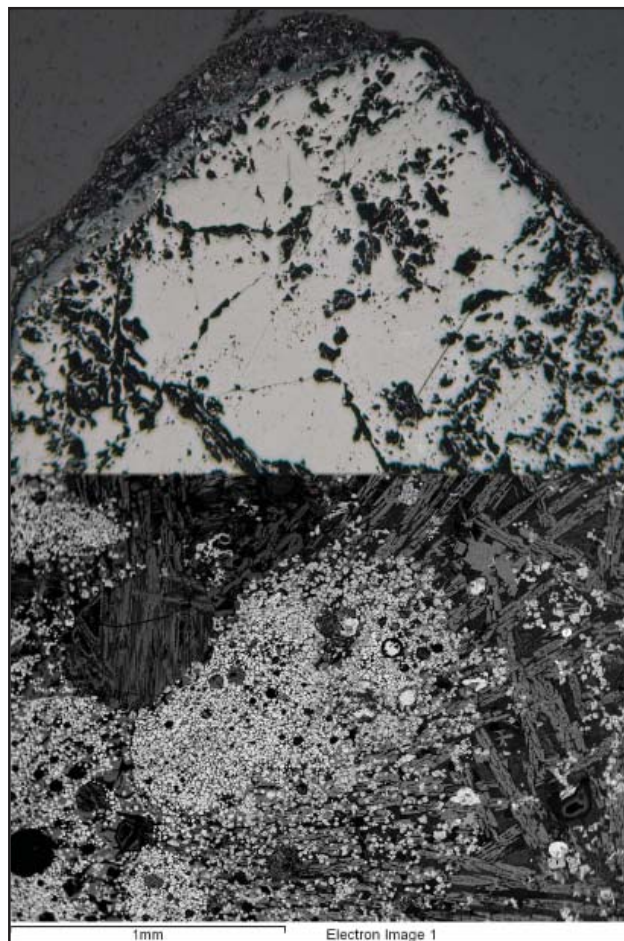


Figure 5.37 - Residual magnetite inclusions, NPWMS6 (top) under plane polarised light and NPWMS12 (bottom) by SEM-BSE, both at 50x. Images: author.

Residual minerals - In striking correlation with the NPW3/MeP2 crucibles, the microscopically examined slags universally contained inclusions of angular to sub-rounded porous residual magnetite. These fragments vary between entirely unreacted and partially dissolved, and have dimensions ranging from fractions of a millimetre to tens of millimetres (Figure 5.37). SEM-EDS spot analyses indicate the main chemical component

of the residual magnetite phases is FeO⁷ (mean 99.2wt%), Al₂O₃ (mean 0.4wt%), SiO₂ (mean 0.3wt%), and CuO (mean 0.2wt%) - SO₃ was undetected (Table 5.18).

	Al ₂ O ₃	SiO ₂	SO ₃	FeO	CuO	Total	Fe/SiO ₂
	wt%	wt%	wt%	wt%	wt%	wt%	wt ratio
NPWMS1	0.0	0.0	0.0	100.0	0.0	95.2	n.a.
NPWMS6	0.3	0.5	0.0	98.6	0.5	89.8	140.7
NPWMS7	0.4	0.3	0.0	99.2	0.1	91.9	250.9
NPWMS13	0.7	0.5	0.0	98.8	0.0	91.5	170.2
mean	0.4	0.3	n.a.	99.2	0.2		
std dev	0.3	0.2	n.a.	0.6	n.a.		
CV	78%	73%	n.a.	1%	n.a.		

Table 5.18 - SEM-EDS phase analyses of NPW3/MeP2 slag residual magnetite inclusions, selected major and minor oxides after data normalisation, analytical total presented.

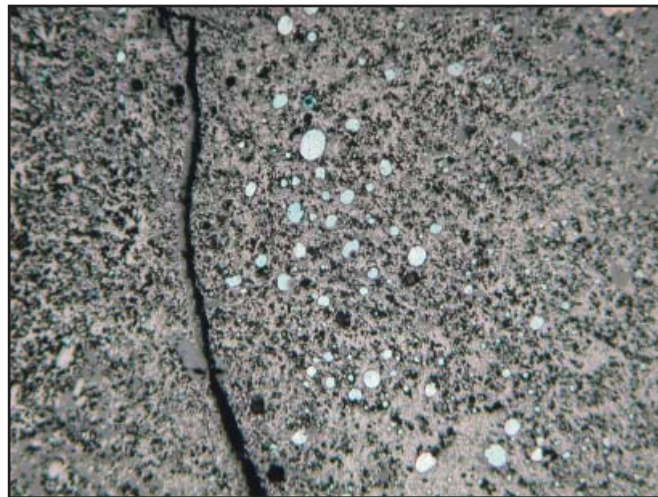


Figure 5.38 - Sulphidic zones in residual magnetite inclusions, NPWMS6 under plane polarised light at 50x. Image: author.

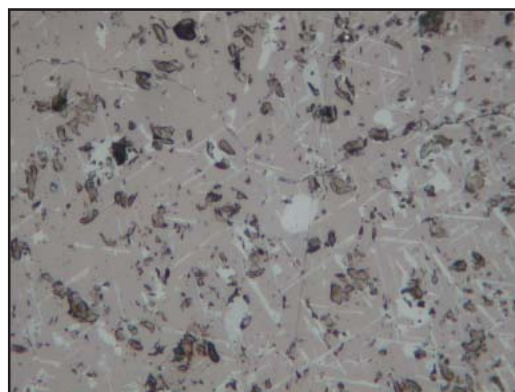


Figure 5.39 - Trigonal intergrowths of haematite in residual martitised magnetite, NPWMS7 under plane polarised light at 100x. Image: author.

NPWMS6's 'extreme' composition according to [P]ED-XRF bulk chemical analysis can be attributed to its especially high content of residual magnetite. NPWMS6 also provides the clearest evidence (Figure 5.38) for sulphidic copper phases embedded within the residual magnetite, suggesting some association between iron and copper at the mineral source. Perhaps more interesting is the identification of martitised magnetite in NPWMS7, a relatively rare form of magnetite with trigonal intergrowths of haematite (Figure 5.39). Magnetite from nearby Khao Tab Kwai has not yet been studied microscopically, but bulk analysis of one sample indicated very low levels of titania (c. 0.1wt%), compatible with the residual magnetite seen in the NPW3/MeP2 slags. Were martitised magnetite confirmed at Khao Tab Kwai, in known association with sulphidic and oxidic copper minerals, we may be in a substantially stronger position to analytically substantiate the metallogenic outcrop's likely position as an early Iron Age mineral source in the Valley.

NPWMS7 was the most heterogeneous of all the slag samples (again resulting in 'extreme' composition status from [P]ED-XRF bulk chemical data), and contained fragments of chalcopyrite (Figure 5.40), a mineral known to be available at Khao Tab Kwai. NPWMS7 also contained a large lustrous inclusion (Figure 5.41), and SEM-EDS spot analyses indicate its composition to be Zn (69.2wt%), S (28.8wt%), and Fe (2.0wt%), which would identify it as residual sphalerite.

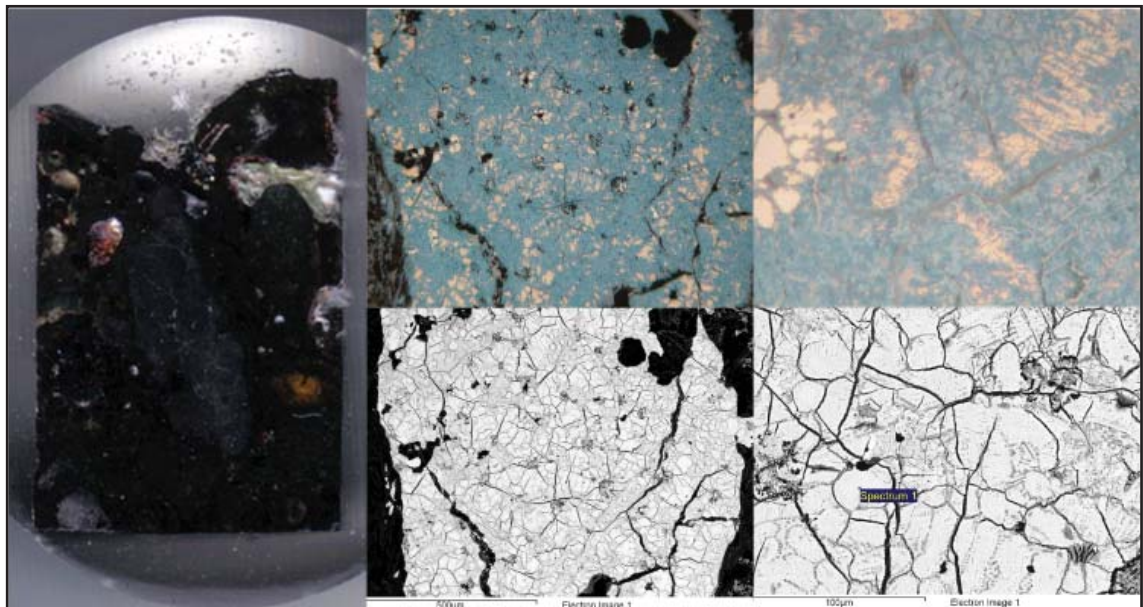


Figure 5.40 - Chalcopyrite fragment in NPWMS7 mounted in a 32mm polished block (left), under plane polarised light (top centre and top right at 100x and 500x respectively, and by SEM-BSE (bottom centre and bottom right at 100x and 500x respectively) - 'Spectrum 1' exemplar of SEM-EDS spot analysis. Images: author.

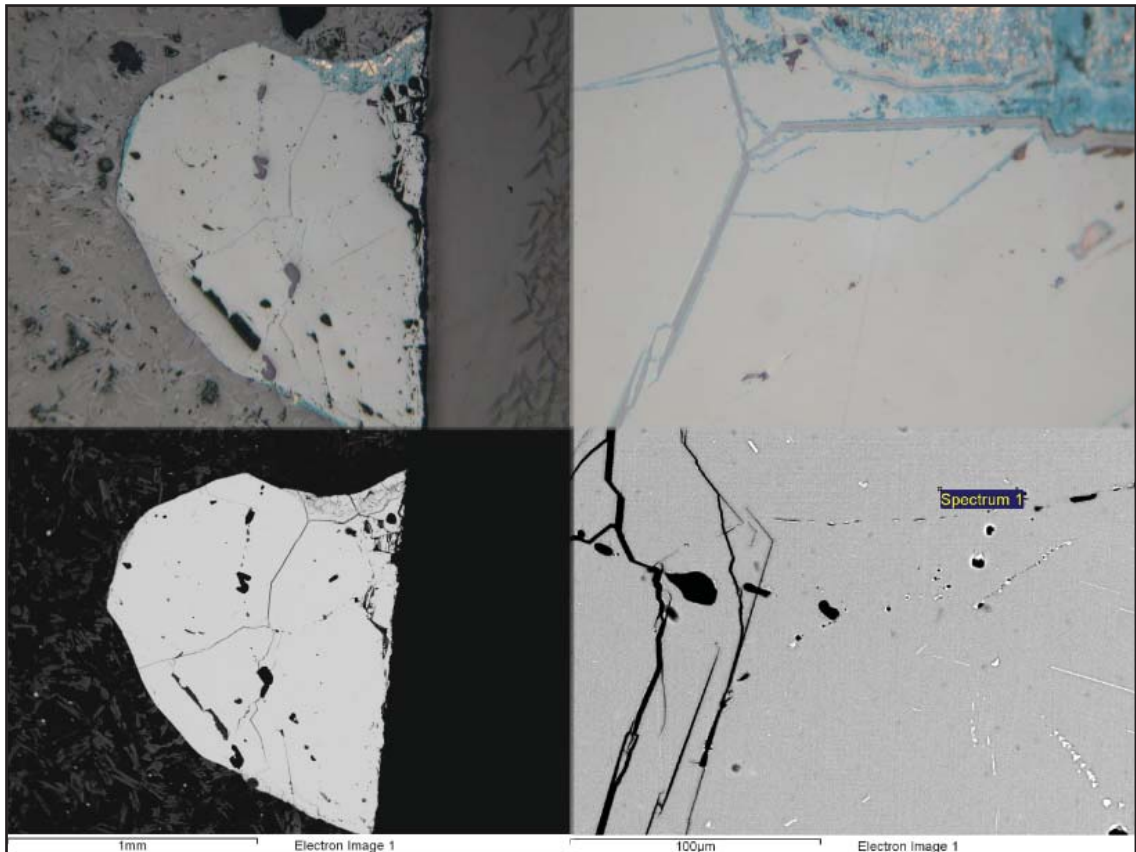


Figure 5.41 - Sphaerite fragment in NPWMS7, under plane polarised light (top) and by SEM-BSE (bottom, at 50x (left) and 500x (right) - 'Spectrum 1' exemplar of SEM-EDS spot analysis. Images: author.

NPWMS2 contained a fragment of siliceous gangue, approximately 1mm in diameter (Figure 5.42). Notably, the inclusion also shows sign of copper carbonates, perhaps suggesting either separate ferruginous and siliceous copper ore sources, or one source containing both. Regardless, the presence of such large and abundant residual mineral fragments within the NPW3/Me2 slags is strongly indicative of insufficient process parameters like temperature, atmosphere, or duration, and may also be evidence of chemically unbalanced smelting charges.

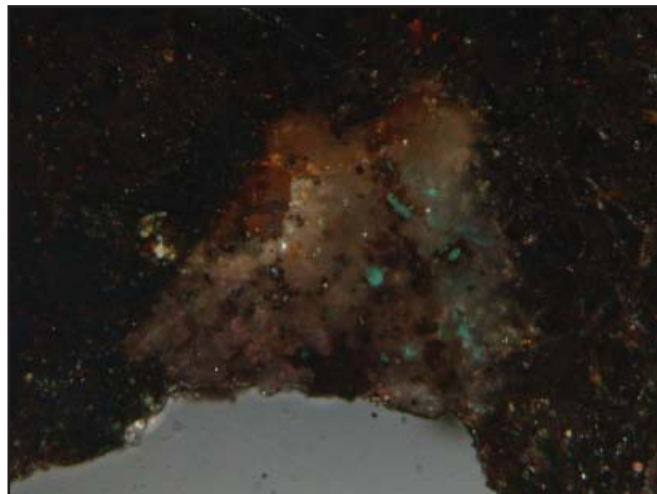


Figure 5.42 - Copper-bearing residual siliceous inclusion in NPWMS2, under plane polarised light at 50x. Image: author.

Slag glass - Binding the heterogeneous NPW3/MeP2 slags is an interstitial glass, with no cryptocrystallinity detected (Figure 5.43). SEM-EDS spot analyses indicate the major chemical components of this phase are SiO_2 (mean 38.1wt%), FeO (mean 35.0wt%), CaO (mean 20.0wt%), and Al_2O_3 (mean 5.4wt%), and MgO (mean 0.5wt%), with SO_3 below accurate detection levels (Table 5.19). The respective CVs (8%, 15%, 14%, 59%, 210%) suggests the interstitial glass phase was quite variable between slag samples. Plotting the data on a Flogen diagram calculated for 7wt% alumina (Kongoli & Yazawa 2001: Figure 11) indicates the slag glass would have begun to solidify between c. 1125°C and c. 1225°C, with a mean precipitation temperature of c. 1180°C (Figure 5.44). The precipitation temperatures are below those for the olivine and magnetite spinel, suggesting the glass was the last major phase to form as the slag cooled. The composition of this phase would have been determined by the prior formation of olivine and magnetite spinel, and the glass is enriched in calcia and other minor oxides.

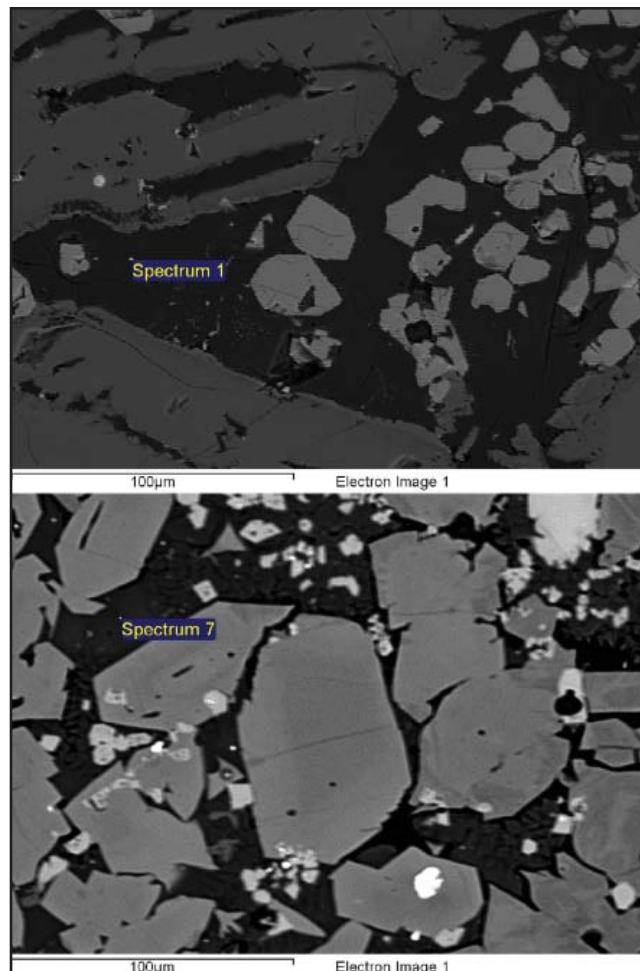


Figure 5.43 - NPWMS1 (top) and NPWMS14 (bottom) interstitial glass phases, both at 500x, by SEM-BSE, 'Spectrum 1' and 'Spectrum 7' are exemplar of EDS point analyses. Images: author.

	MgO	Al ₂ O ₃	SiO ₂	SO ₃	CaO	FeO	Total Fe/SiO ₂	
	wt%	wt%	wt%	wt%	wt%	wt%	wt%	wt ratio
NPWMS1	0.0	3.7	37.9	0.0	20.0	38.2	93.8	0.8
NPWMS2	0.0	3.8	41.0	0.0	20.5	34.7	91.4	0.7
NPWMS3	0.0	11.6	39.1	1.2	14.4	30.1	72.9	0.6
NPWMS5	0.0	7.5	32.9	0.0	21.2	36.4	66.6	0.9
NPWMS6	0.0	6.7	38.7	0.0	22.3	32.3	90.1	0.6
NPWMS7	3.3	3.1	42.6	0.0	22.2	25.9	81.7	0.5
NPWMS8	0.0	3.8	34.9	0.0	20.5	40.7	69.8	0.9
NPWMS12	0.1	3.5	33.6	0.0	20.9	41.8	69.6	1.0
NPWMS13	0.5	2.2	40.2	0.0	22.0	35.1	84.4	0.7
NPWMS14	0.0	10.8	42.4	0.0	16.8	29.1	102.2	0.5
NPWMS18	0.0	4.8	36.7	0.0	16.0	42.0	68.5	0.9
NPWMS19	2.4	2.6	37.7	0.0	22.7	34.1	67.2	0.7
mean	0.5	5.4	38.1	0.1	20.0	35.0	99.1	0.7
std dev	1.1	3.2	3.2	n.a.	2.7	5.1		
CV	210%	59%	8%	n.a.	14%	15%		

Table 5.19 - SEM-EDS phase analyses of NPW3/MeP2 slag glass phases, selected major and minor oxides.

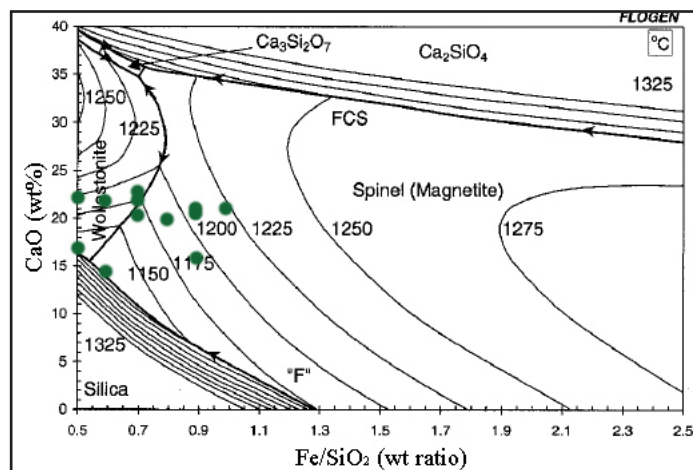


Figure 5.44 - SEM-EDS analyses of glass phases plotted on a Floggen binary chart for a slag system at a 10⁻⁸ ppO₂ and with 7wt% Al₂O₃. Image adapted from Kongoli & Yazawa 2001: Figure 11.

Slag prills - Highly reflective metallic prills are common in the NPW3/MeP2 slags, and range in diameter between c. 0.001mm and c. 0.1mm, though there is some bimodality to their distribution, with a larger number of tiny specks and a few much larger prills (Figure 5.45). Optically the prills are divisible into copper and matte, with some containing both phases. SEM-EDS analyses (Table 5.20) indicate most of the prills contain substantial levels of sulphur (excepting NPWMS13) and fluctuating quantities of iron (CV 85%). The presence of matte prills is to be expected when any sulphidic minerals are included within a smelting charge (Stos-Gale 1989), and the association of oxidic and sulphidic minerals at Khao Tab Kwai renders this quite plausible. The generally wide range of prill compositions between, and occasionally within, the NPW3/MeP2 slags is suggestive of

a non-standardised charge and/or non-equilibrium conditions for the processing of those minerals. The brassy prill in NPWMS7 is probably due to the large sphalerite inclusion reported above.

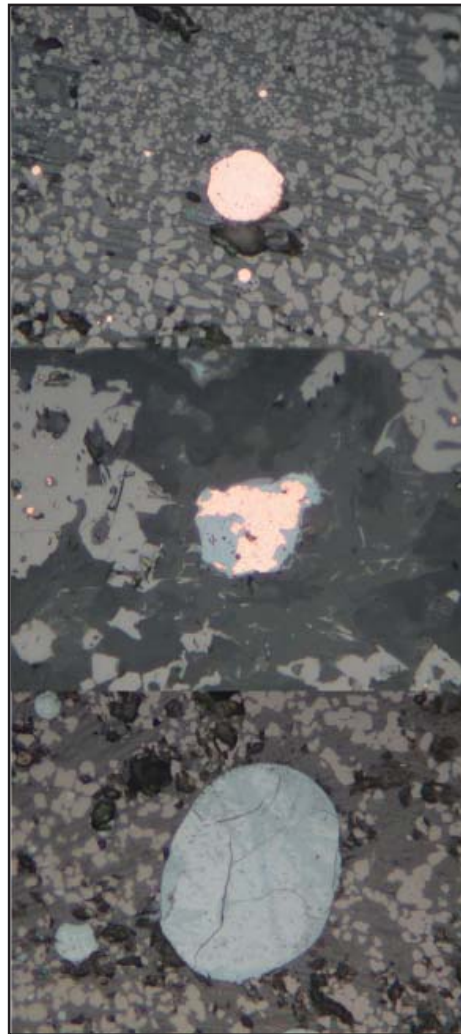


Figure 5.45 - Prills of copper (top - NPWMS6), copper/matte (middle - NPWMS13), and matte (bottom - NPWMS6), all under plane polarised light at 500x. Images: author.

	S	Fe	Cu	Zn	Total
	wt%	wt%	wt%	wt%	wt%
NPWMS1	26.8	42.1	30.7	0.5	96.1
NPWMS3	28.3	26.2	45.4	0.0	92.1
NPWMS6	20.5	5.8	73.7	0.0	100.2
NPWMS7	28.9	10.4	32.1	28.6	95.2
NPWMS13i	0.0	32.0	68.0	0.0	75.5
NPWMS13ii	1.1	8.4	90.5	0.0	63.0
mean	17.6	20.8	56.7	4.8	
std dev	13.5	14.8	24.3	11.6	
CV	77%	71%	43%	240%	

Table 5.20 - SEM-EDS phase analyses of NPW3/MeP2 slag prills, selected major elements.

Slag matrix - The common presence of residual minerals means the NPW3/MeP2 slags can be considered significantly unreacted and internally heterogeneous, with frequent porosity representing the ongoing release of gases by reacting minerals at the time of solidification. The slags would have been far from fully liquid during the smelt, although they could have been poured from the crucible, a thick minestrone soup perhaps being an appropriate culinary analogy. Nevertheless, the charge was in the process of forming a slag, and there were substantial areas of matrix suitable for targeted area scans of 1mm² (Figure 5.33, Table 5.21). These data are not directly comparable to the [P]ED-XRF results which incorporate the residual inclusions. However, contrasting the average readings of SEM-EDS area scans from different slags can be used to assess variation in reactants and/or techniques between samples, whereas comparing each scan provides a measure of process heterogeneity within a sample (see Humphris *et al.* 2009).

Across the samples, the major chemical components of the slag matrices are FeO (mean 54.5wt%), SiO₂ (mean 27.9wt%), CaO (mean 10.8wt%), and Al₂O₃ (mean 2.9wt%). Their respective CVs (33%, 34%, 48%, and 46%) indicate significant differences in NPW3/MeP2 charge compositions and/or processing techniques. The inconsistent presence of SO₃ (NPWMS1, NPWMS3, NPWMS6, NPWMS7), MnO (NPWMS7, NPWMS12, NPWMS13), and ZnO (NPWMS7) suggests that a non-standardised mineral charge is probably the major cause of inter sample chemical variation. The mean copper oxide reading of 1.8wt% for the slag matrix is not high, though a CV of 93% suggests substantial inconsistency, the copper content of unreacted minerals was the most likely cause.

Within slag samples, the CVs for FeO (mean intra CV 2%), SiO₂ (mean intra CV 3%) would suggest some major oxide stability within matrices, but compositional variability increases rapidly in the minor oxides, and the CVs for copper oxide (mean intra CV 39%) suggest prill distribution is not uniform. There is certainly less variation within slags than there is between them, but it is clear that individual NPW3/MeP2 reactions were not reaching equilibrium, and there is no evidence for the standardisation of smelting charges and techniques. However, given the lack of chronological control we could be seeing intra MeP2 variability over time rather than contemporary variability in the technological choices made by metalworkers.

Using the traditional archaeometallurgical technique for calculating operating temperatures from slag liquidus, the primary chemical components (iron^(II) oxide, silica, and calcia) would indicate the slag was exposed to minimum temperatures of between c. 1093°C and c. 1260°C (Figure 5.46). Transposing the mean liquidus of c. 1170°C onto an Ellingham

	MgO	Al ₂ O ₃	SiO ₂	SO ₃	CaO	MnO	FeO	CuO	ZnO	Total	Fe/SiO ₂
	wt%	wt%	wt%	wt%	wt%	wt%	wt%	wt%	wt%	wt%	wt ratio
NPWMS1 spectrum 1	0.6	2.4	30.0	2.0	12.2	0.0	53.0	0.0	0.0	95.2	1.4
NPWMS1 spectrum 2	0.0	2.2	28.9	1.8	11.2	0.0	55.2	0.7	0.0	92.0	1.5
NPWMS1 spectrum 3	0.7	2.3	28.6	1.7	11.0	0.0	55.2	0.6	0.0	95.3	1.5
<i>NPWMS1 mean</i>	<i>0.4</i>	<i>2.3</i>	<i>29.2</i>	<i>1.8</i>	<i>11.4</i>	<i>0.0</i>	<i>54.5</i>	<i>0.4</i>	<i>0.0</i>		
<i>NPWMS1 std dev</i>	<i>0.4</i>	<i>0.1</i>	<i>0.7</i>	<i>0.1</i>	<i>0.6</i>	<i>0.0</i>	<i>1.3</i>	<i>0.4</i>	<i>0.0</i>		
<i>NPWMS1 CV</i>	<i>88%</i>	<i>4%</i>	<i>2%</i>	<i>8%</i>	<i>6%</i>	<i>n.a</i>	<i>2%</i>	<i>87%</i>	<i>n.a</i>		
NPWMS2 spectrum 1	0.0	3.1	36.8	0.0	13.9	0.0	45.4	0.8	0.0	91.0	1.0
NPWMS2 spectrum 2	0.6	3.2	35.6	0.0	14.4	0.0	46.2	0.0	0.0	91.6	1.0
NPWMS2 spectrum 3	0.5	3.2	35.7	0.0	14.3	0.0	45.3	1.1	0.0	91.4	1.0
<i>NPWMS2 mean</i>	<i>0.3</i>	<i>3.2</i>	<i>36.0</i>	<i>0.0</i>	<i>14.2</i>	<i>0.0</i>	<i>45.6</i>	<i>0.6</i>	<i>0.0</i>		
<i>NPWMS2 std dev</i>	<i>0.3</i>	<i>0.1</i>	<i>0.7</i>	<i>0.0</i>	<i>0.3</i>	<i>0.0</i>	<i>0.5</i>	<i>0.6</i>	<i>0.0</i>		
<i>NPWMS2 CV</i>	<i>88%</i>	<i>2%</i>	<i>2%</i>	<i>n.a</i>	<i>2%</i>	<i>n.a</i>	<i>1%</i>	<i>88%</i>	<i>n.a</i>		
NPWMS3 spectrum 1	0.4	2.8	21.5	1.0	15.5	0.3	56.9	1.1	0.0	90.5	2.1
NPWMS3 spectrum 2	0.4	3.2	22.9	1.1	12.8	0.0	57.6	1.3	0.0	100.1	2.0
NPWMS3 spectrum 3	0.5	3.2	21.8	0.8	15.1	0.0	57.1	0.7	0.0	93.7	2.0
<i>NPWMS3 mean</i>	<i>0.4</i>	<i>3.1</i>	<i>22.1</i>	<i>0.9</i>	<i>14.5</i>	<i>0.1</i>	<i>57.2</i>	<i>1.1</i>	<i>0.0</i>		
<i>NPWMS3 std dev</i>	<i>0.0</i>	<i>0.3</i>	<i>0.7</i>	<i>0.1</i>	<i>1.5</i>	<i>0.2</i>	<i>0.4</i>	<i>0.3</i>	<i>0.0</i>		
<i>NPWMS3 CV</i>	<i>11%</i>	<i>9%</i>	<i>3%</i>	<i>13%</i>	<i>10%</i>	<i>173%</i>	<i>1%</i>	<i>29%</i>	<i>n.a</i>		
NPWMS5 spectrum 1	0.5	2.3	18.4	0.0	8.7	0.4	67.7	1.6	0.0	73.2	2.9
NPWMS5 spectrum 2	0.4	2.6	21.2	0.3	8.4	0.0	64.1	2.4	0.0	73.9	2.4
NPWMS5 spectrum 3	0.4	2.6	19.9	0.0	8.0	0.4	65.8	2.4	0.0	74.3	2.6
<i>NPWMS5 mean</i>	<i>0.4</i>	<i>2.5</i>	<i>19.8</i>	<i>0.1</i>	<i>8.4</i>	<i>0.2</i>	<i>65.9</i>	<i>2.1</i>	<i>0.0</i>		
<i>NPWMS5 std dev</i>	<i>0.0</i>	<i>0.2</i>	<i>1.4</i>	<i>0.2</i>	<i>0.3</i>	<i>0.2</i>	<i>1.8</i>	<i>0.5</i>	<i>0.0</i>		
<i>NPWMS5 CV</i>	<i>6%</i>	<i>7%</i>	<i>7%</i>	<i>173%</i>	<i>4%</i>	<i>87%</i>	<i>3%</i>	<i>22%</i>	<i>n.a</i>		
NPWMS6 spectrum 1	0.0	3.4	27.9	1.6	13.1	0.0	52.4	1.6	0.0	92.9	1.5
NPWMS6 spectrum 2	0.0	3.2	26.7	1.3	10.9	0.0	54.6	3.3	0.0	90.5	1.6
NPWMS6 spectrum 3	0.4	3.1	27.6	1.6	13.6	0.0	51.7	2.0	0.0	95.1	1.5
<i>NPWMS6 mean</i>	<i>0.1</i>	<i>3.2</i>	<i>27.4</i>	<i>1.5</i>	<i>12.5</i>	<i>0.0</i>	<i>52.9</i>	<i>2.3</i>	<i>0.0</i>		
<i>NPWMS6 std dev</i>	<i>0.3</i>	<i>0.1</i>	<i>0.6</i>	<i>0.2</i>	<i>1.4</i>	<i>0.0</i>	<i>1.5</i>	<i>0.9</i>	<i>0.0</i>		
<i>NPWMS6 CV</i>	<i>173%</i>	<i>4%</i>	<i>2%</i>	<i>13%</i>	<i>11%</i>	<i>n.a</i>	<i>3%</i>	<i>38%</i>	<i>n.a</i>		
NPWMS7 spectrum 1	1.1	5.4	34.1	1.1	13.4	0.6	36.9	0.0	7.4	85.3	0.8
NPWMS7 spectrum 2	1.0	4.9	32.8	1.8	12.8	0.7	37.8	0.0	7.9	83.7	0.9
NPWMS7 spectrum 3	1.1	5.0	34.0	1.3	13.0	0.7	36.3	0.0	8.3	87.0	0.8
<i>NPWMS7 mean</i>	<i>1.1</i>	<i>5.1</i>	<i>33.7</i>	<i>1.4</i>	<i>13.1</i>	<i>0.7</i>	<i>37.0</i>	<i>0.0</i>	<i>7.9</i>		
<i>NPWMS7 std dev</i>	<i>0.0</i>	<i>0.3</i>	<i>0.7</i>	<i>0.4</i>	<i>0.3</i>	<i>0.0</i>	<i>0.8</i>	<i>0.0</i>	<i>0.5</i>		
<i>NPWMS7 CV</i>	<i>1%</i>	<i>5%</i>	<i>2%</i>	<i>28%</i>	<i>2%</i>	<i>7%</i>	<i>2%</i>	<i>n.a</i>	<i>6%</i>		
NPWMS8 spectrum 1	0.3	1.7	21.9	0.0	6.8	0.4	67.8	1.0	0.0	68.9	2.4
NPWMS8 spectrum 2	0.3	2.0	23.8	0.0	7.3	0.0	65.9	0.7	0.0	72.9	2.2

NPWMS8 spectrum 3	0.4	1.8	22.1	0.0	7.5	0.0	67.4	0.9	0.0	74.1	2.4
<i>NPWMS8 mean</i>	<i>0.3</i>	<i>1.8</i>	<i>22.6</i>	<i>0.0</i>	<i>7.2</i>	<i>0.1</i>	<i>67.0</i>	<i>0.9</i>	<i>0.0</i>		
<i>NPWMS8 std dev</i>	<i>0.0</i>	<i>0.1</i>	<i>1.0</i>	<i>0.0</i>	<i>0.4</i>	<i>0.2</i>	<i>1.0</i>	<i>0.2</i>	<i>0.0</i>		
<i>NPWMS8 CV</i>	<i>8%</i>	<i>8%</i>	<i>5%</i>	<i>n.a</i>	<i>5%</i>	<i>173%</i>	<i>1%</i>	<i>19%</i>	<i>n.a</i>		
NPWMS12 spectrum 1	0.4	1.8	23.0	0.0	10.1	0.9	62.5	1.2	0.0	70.9	2.1
NPWMS12 spectrum 2	0.3	2.0	23.1	0.0	9.3	0.7	60.9	3.6	0.0	73.0	2.0
NPWMS12 spectrum 3	0.3	1.9	24.2	0.0	9.0	0.8	60.6	3.2	0.0	74.4	1.9
<i>NPWMS12 mean</i>	<i>0.3</i>	<i>1.9</i>	<i>23.4</i>	<i>0.0</i>	<i>9.5</i>	<i>0.8</i>	<i>61.3</i>	<i>2.7</i>	<i>0.0</i>		
<i>NPWMS12 std dev</i>	<i>0.0</i>	<i>0.1</i>	<i>0.6</i>	<i>0.0</i>	<i>0.6</i>	<i>0.1</i>	<i>1.0</i>	<i>1.3</i>	<i>0.0</i>		
<i>NPWMS12 CV</i>	<i>11%</i>	<i>5%</i>	<i>3%</i>	<i>n.a</i>	<i>6%</i>	<i>10%</i>	<i>2%</i>	<i>48%</i>	<i>n.a</i>		
NPWMS13 spectrum 1	0.0	1.9	24.3	0.0	8.8	1.2	56.2	7.6	0.0	88.6	1.8
NPWMS13 spectrum 2	0.0	1.5	25.5	0.0	6.3	0.8	59.2	6.7	0.0	90.8	1.8
NPWMS13 spectrum 3	0.5	1.8	24.9	0.0	9.5	1.1	58.2	4.1	0.0	88.2	1.8
<i>NPWMS13 mean</i>	<i>0.2</i>	<i>1.7</i>	<i>24.9</i>	<i>0.0</i>	<i>8.2</i>	<i>1.0</i>	<i>57.9</i>	<i>6.1</i>	<i>0.0</i>		
<i>NPWMS13 std dev</i>	<i>0.3</i>	<i>0.2</i>	<i>0.6</i>	<i>0.0</i>	<i>1.7</i>	<i>0.2</i>	<i>1.6</i>	<i>1.8</i>	<i>0.0</i>		
<i>NPWMS13 CV</i>	<i>173%</i>	<i>12%</i>	<i>2%</i>	<i>n.a</i>	<i>20%</i>	<i>22%</i>	<i>3%</i>	<i>30%</i>	<i>n.a</i>		
NPWMS14 spectrum 1	1.1	4.8	34.3	0.0	3.8	0.0	52.2	3.3	0.0	94.4	1.2
NPWMS14 spectrum 2	1.1	4.7	33.7	0.0	4.4	0.3	53.3	2.6	0.0	99.5	1.2
NPWMS14 spectrum 3	1.2	4.6	34.0	0.0	4.3	0.0	53.5	2.3	0.0	98.8	1.2
<i>NPWMS14 mean</i>	<i>1.1</i>	<i>4.7</i>	<i>34.0</i>	<i>0.0</i>	<i>4.2</i>	<i>0.1</i>	<i>53.0</i>	<i>2.7</i>	<i>0.0</i>		
<i>NPWMS14 std dev</i>	<i>0.1</i>	<i>0.1</i>	<i>0.3</i>	<i>0.0</i>	<i>0.3</i>	<i>0.2</i>	<i>0.7</i>	<i>0.5</i>	<i>0.0</i>		
<i>NPWMS14 CV</i>	<i>8%</i>	<i>2%</i>	<i>1%</i>	<i>n.a</i>	<i>7%</i>	<i>173%</i>	<i>1%</i>	<i>18%</i>	<i>n.a</i>		
NPWMS18 spectrum 1	0.3	2.7	30.7	0.2	7.0	0.0	57.9	1.1	0.0	67.2	1.5
NPWMS18 spectrum 2	0.4	2.8	29.8	0.1	7.4	0.0	58.0	1.4	0.0	72.0	1.5
NPWMS18 spectrum 3	0.4	2.8	29.5	0.3	7.7	0.0	57.3	2.1	0.0	74.4	1.5
<i>NPWMS18 mean</i>	<i>0.4</i>	<i>2.8</i>	<i>30.0</i>	<i>0.2</i>	<i>7.4</i>	<i>0.0</i>	<i>57.7</i>	<i>1.6</i>	<i>0.0</i>		
<i>NPWMS18 std dev</i>	<i>0.1</i>	<i>0.0</i>	<i>0.6</i>	<i>0.1</i>	<i>0.3</i>	<i>0.0</i>	<i>0.4</i>	<i>0.5</i>	<i>0.0</i>		
<i>NPWMS18 CV</i>	<i>16%</i>	<i>2%</i>	<i>2%</i>	<i>54%</i>	<i>4%</i>	<i>n.a</i>	<i>1%</i>	<i>31%</i>	<i>n.a</i>		
NPWMS19 spectrum 1	1.2	2.5	31.6	0.0	19.2	0.8	44.3	0.5	0.0	65.9	1.1
NPWMS19 spectrum 2	1.2	2.6	31.7	0.0	19.0	1.0	44.2	0.4	0.0	68.9	1.1
NPWMS19 spectrum 3	1.3	2.5	32.4	0.0	19.4	0.8	42.7	0.6	0.0	71.7	1.0
<i>NPWMS19 mean</i>	<i>1.2</i>	<i>2.5</i>	<i>31.9</i>	<i>0.0</i>	<i>19.2</i>	<i>0.9</i>	<i>43.7</i>	<i>0.5</i>	<i>0.0</i>		
<i>NPWMS19 std dev</i>	<i>0.1</i>	<i>0.1</i>	<i>0.4</i>	<i>0.0</i>	<i>0.2</i>	<i>0.1</i>	<i>0.9</i>	<i>0.1</i>	<i>0.0</i>		
<i>NPWMS19 CV</i>	<i>7%</i>	<i>3%</i>	<i>1%</i>	<i>n.a</i>	<i>1%</i>	<i>15%</i>	<i>2%</i>	<i>18%</i>	<i>n.a</i>		
NPWMS mean	0.5	2.9	27.9	0.5	10.8	0.3	54.5	1.8	0.7		
NPWMS std dev	0.4	1.3	9.6	0.6	5.1	0.4	18.1	1.6	2.3		
Inter NPWMS CV	74%	46%	34%	116%	48%	120%	33%	93%	n.a		
Mean intra NPWMS CV	49%	5%	3%	24%	7%	55%	2%	39%	n.a		

Table 5.21 - SEM-EDS phase analyses of NPW3/MeP2 slag matrices, selected major and minor oxides after data normalisation, analytical total presented.

Diagram, and extending two lines to the intersections of the liquidus with the '4Cu+O₂ = 2Cu₂O' and '6FeO+O₂ = 2Fe₃O₄' boundaries (representing the likely redox envelope for a process reducing copper to metallic form, and containing divalent as well as trivalent iron), indicates a ppO₂ between c. 1x10⁻⁶ and c. 1x10⁻¹⁰ (Figure 5.47).

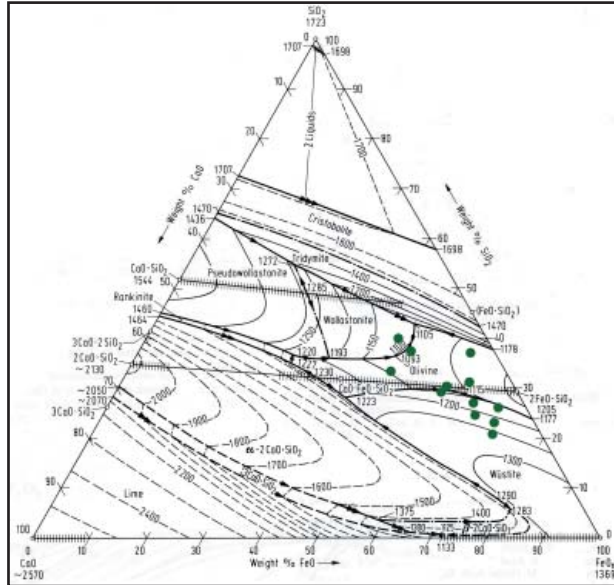


Figure 5.46 - Slag matrices plotted on a ternary diagram for a FeO-CaO-SiO₂ slag system in equilibrium with iron metal. Image adapted from Eisenhüttenleute 1995.

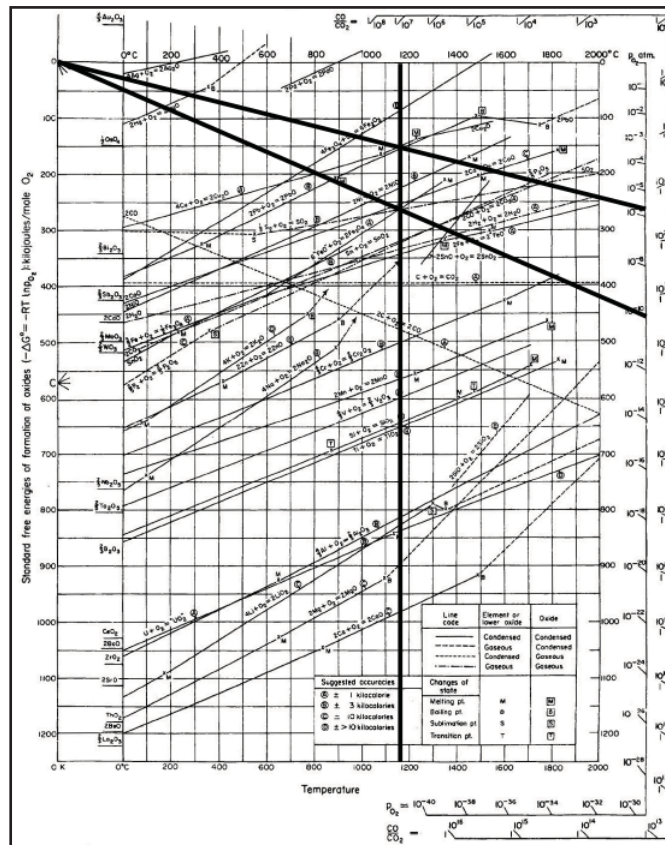


Figure 5.47 - Ellingham Diagram showing redox envelope for NPW3/MeP2 crucible slags. Image adapted from Gilchrist 1989.

The most appropriate Flogen diagram for the NPW3/MeP2 slags describes a system with 3wt% alumina in a p_{O_2} of 1×10^{-8} , with Fe/SiO₂ ratio and calcia as variables (Kongoli & Yazawa 2001: Figure 10). Plotting data from Table 5.21 onto Figure 5.48 gives a liquidus reading of between c. 1180°C and c. 1290°C (extrapolating NPWMS5's high Fe/SiO₂ ratio), giving a mean minimum slag temperature of c. 1240°C. Considering the NPW3/MeP2 slags have magnetite precipitations in probable intermediate oxygen partial pressures, it is likely the slags were exposed to temperatures in excess of 1300°C, even if these conditions were not prolonged enough to result in a complete liquefaction of the charge.

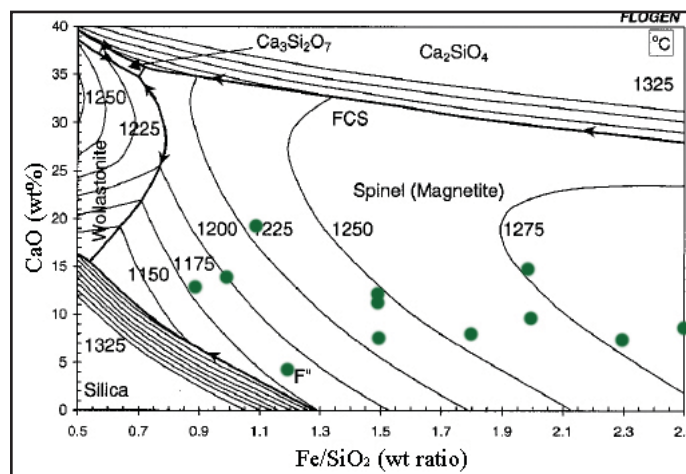


Figure 5.48 - SEM-EDS analyses of slag matrices plotted on a Flogen binary chart for a slag system at a 10^{-8} p_{O_2} and with 3wt% Al₂O₃. Image adapted from Kongoli & Yazawa 2001: Figure 10.

5.3.4 - Discussion

The NPW3/MeP2 slag evidence is entirely consistent with the expected waste product of a copper smelting operation. There are strong indications that the ancient metalworkers were not proficient smelters, though as previously mentioned, we are not here to pass judgement on past technological choices as adapted to peoples' needs. The principal signs of the early Iron Age *chaîne opératoire* as a developing technology is the extreme heterogeneity of the slag between and within samples, as evidenced by macro, bulk, and micro analysis (e.g. Eerkens & Lipo 2005, Eerkens & Lipo 2007 note that high CVs represent periods of experimentation and/or innovation, as opposed to behavioural convergence [standardisation] producing low CVs). These characteristics could result from insufficient smelting temperatures, insufficient smelting duration, or insufficiently balanced smelting charges, but on the basis that there is microanalytical evidence for the formation of primary crystalline and glassy phases from c. 1100°C to c. 1300°C, the author is inclined to discount the first contention - that of inadequate temperature. Therefore, the unreacted nature of the slag is almost certainly a combination of an

unduly brief smelt and/or a poorly prepared smelting charge. The interpretation can be pressed further by highlighting the short processing time (a few hours) required for the relatively low quantities of material involved in the process. It is unlikely that the early Iron Age smelters at Non Pa Wai never chose to continue their smelt a little longer to ensure a more complete reaction. It is more probable they stopped due to inadequate heat distribution through a block of partially fused minerals, and thus continued high temperature processing with the technology available could not significantly improve the result. This would leave the composition of the mineral/fuel charge as the primary culprit for process inefficiency. The crucible technology could certainly produce the necessary heat (at least whilst the temperature could be evenly distributed), and the charge contained copper ores and slag forming minerals, but the proportions of the latter conspired against the substantial liquefaction of gangue. The slag that was produced formed at near eutectic compositions from the minerals in contact (as per glass in Rehren 2000), but the viscosity of the slag and embedded residual minerals may still have prevented even temperature distribution and caused the smelt to stall. However, unlike Rehren's proposed glass production technique, the NPW3/MeP2 slags do not appear to have been crushed and sorted for the re-smelting of residual minerals⁸. The author does not consider the provision of an adequate gaseous atmosphere to have been an issue restricting the NPW3/MeP2 smelt. The evidence for a relatively 'open' crucible reaction (not a tightly enclosed structure which might promote highly reducing conditions), combined with the efficacy of the CO gas producing Boudouard reaction, would conspire towards intermediate redox conditions suitable for the reduction of copper (Gilchrist 1989, Bassiakos *et al.* 2008).



Figure 5.49 - Macro-scopically visible residual magnetite in NPWMS6, mounted in 32mm polished block. Image: author.

The composition of the smelting charge is of great interest, as it would seem to give a reasonably direct insight into the technological choices of the ancient smelters. The author does not consider that fragments of chalcopyrite, sphalerite, and especially magnetite up

⁸ There is of course a difference between glass production where glass is the product, and metal production where slag is the waste product, but good slag formation remains a reliable proxy for good metal production.

to tens of millimetres in length to be accidental additions to the smelting charge (Figure 5.49). In which case they were intentionally included within the charge, even though their presence was most likely a hindrance to the copper extraction process. There is no clear relationship between copper and sulphur in the slag, suggesting that although sulphidic minerals were present, any interpretation of matte smelting or deliberate co-smelting would be somewhat far-fetched (cf. Rostoker & Dvorak 1991, Rostoker *et al.* 1989). Likewise, interpreting the magnetite fragments as evidence of deliberate fluxing of the charge is implausible given their utter failure in this respect (cf. Bennett 1989). Perhaps the solution to the NPW3/MeP2 charge requires us to disregard some of our modern knowledge. Magnetite, chalcopyrite, and sphalerite are all dense, dark coloured, somewhat iridescent, and can be found adjacent to oxidic copper minerals; indeed they are at Khao Tab Kwai. It is then not unreasonable to suggest that in addition to the brightly coloured copper carbonates selected for the smelting charge, early Iron Age Non Pa Wai metal workers also indiscriminantly included copper sulphide and iron oxide minerals due to their close association to known copper-bearing materials available locally, this resulting in the enormous variability seen in the slag evidence.

5.4 The Non Pa Wai copper smelting *chaîne opératoire*

The combined weight of the macro-analytical, bulk chemical, and microanalytical study of minerals, technical ceramics, and slags from early Iron Age Non Pa Wai provides reasonable evidence to support the interpretation of the predominant on-site metallurgical activity as the crucible smelting of copper.

All of the minerals recovered from NPW3/MeP2 contexts would have been locally available from mineralisations in and around the Valley. Most of the samples are consistent with the ores and host rock species one might expect in a copper smelting process, including both oxidic minerals like malachite, as well as sulphidic minerals like chalcopyrite. The lack of consistency to the assemblage suggests the mineral charge was to some extent mixed, though it is unknown whether the excavated minerals were lost accidentally, or intentionally screened out during beneficiation and charge preparation. Though there is no evidence of their having been roasted, it could be considered unlikely considering the seeming absence of other systematic mineral processing.

The technical ceramic evidence suggests the probable use of local clays for the production of simple yet effective forms for metal production activities. The nature and degree of heat damage and slagging to the vessels is fully consistent with the interpretation of a crucible-based smelting process, although the exact purpose of the ‘pit-rims’ is more

ephemeral. The assemblage requires further investigation to be properly understood at a technological level, but the possible difference in clay modification between crucibles and ‘pit-rims’ will be extremely interesting to follow up. Comparing and contrasting the domestic and technical ceramics would doubtless be a fruitful exercise.

The heterogeneous appearance and bulk chemistry of the NPW3/MeP2 slags can be interpreted as evidence for the practice of sub-ideal smelting techniques, and behaviourally as the metalworkers being inexpert at identifying, sorting, and combining the required minerals for copper production. Given the highly variable levels of sulphur in the slags it could be suggested that sulphidic copper minerals were not a constant constituent of the smelting charge, and thus that oxidic minerals predominated - as might be expected by metalworkers exploiting the oxidised secondary mineralisation near the surface of a metallogenic deposit. Inconsistent technological choices in these parameters could well account for the incomplete slag formation and high copper losses witnessed at Non Pa Wai.

The NPW3/MeP2 reconstruction is heavily influenced by the notes and comments of the original TAP excavators at Non Pa Wai. In particular, Roberto Ciarla’s sketch (Figure 5.5) of a shallow depression in association with a low ceramic rim is key to arriving at the current reconstruction for the major on-site industrial activity (Figure 5.50). Although the smelt would be open to the atmosphere above, the crucible walls and exterior furnace rim would certainly prevent any natural drafts from aspirating the reaction. Therefore, in the absence of any tuyères, the smelt would have presumably been powered by blowpipes, perhaps of bamboo. The limited air delivery capacity of blowpipes would have imposed quite a limit on the scale of an individual smelting operation (Rehder 1994), and may also have been partly responsible for the uneven and incomplete reaction of the charge.

Although our stratigraphic and chronological understanding of Valley archaeology remains imperfect, the industrial evidence from NPW3/MeP2 contexts is testimony to the production of substantial quantities of metal between c. 5/600 BCE and c. 300 BCE. This technology would have been theoretically totally sustainable with minerals, fuels, and clays available in the Khao Wong Prachan Valley, and there is no implicit requirement for external materials, especially given the lack of tin/bronze.

Although far apart in terms of period and context, the NPW3/MeP2 smelting *chaîne opératoire* is comparable to what are termed ‘chalcolithic’ smelting technologies in

western Eurasia (Bourgarit 2007: 5). The use of a crucible to contain the smelt can be compared to the early metallurgical complexes of Al Claus and St. Veran in the Franco-Italian Alps (e.g. Artioli *et al.* 2007, Burger *et al.* 2007) and Los Millares and Valencina de la Concepción in Southern Iberia (e.g. Craddock 1999: see Figure 1 for a smelting pit and ceramic rim comparator, Nocete *et al.* 2008, Ruiz 1993).

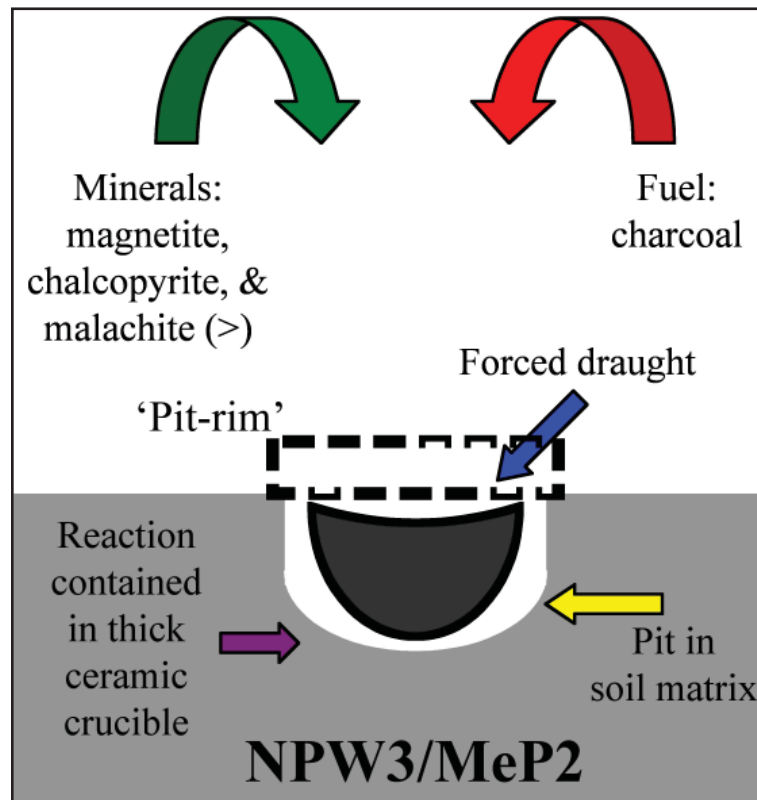


Figure 5.50 - Schematic technological reconstruction for copper smelting technique at early Iron Age Non Pa Wai. Image: author.

Chapter 6

Metallurgical Analyses and Technological Reconstruction - Nil Kham Haeng Metallurgical Phase Three

Following on from the NPW3/MeP2 reconstruction, this chapter lays out an interpretation of the copper smelting *chaîne opératoire* at later Iron Age Nil Kham Haeng Period 3 Metallurgical Phase 3. The samples of NKH3/MeP3 mineral, technical ceramic, and slag were prepared for macroscopic, bulk compositional, microscopic, and phase compositional analysis according to the methodology detailed in Chapter 4. A sample catalogue and complete analytical data may be consulted in Appendices A and B.

6.1 Minerals

Mineral finds were defined as natural materials not derived from the immediate geology of the site, and thus representing anthropogenic deposits. The present study examined only minerals from secure NKH3/MeP3 contexts.

6.1.1 Macro-analysis

Of the six samples assessed, four (NKHM1, NKHM2, NKHM5, NKHM6) have visible evidence of copper compounds (Table 6.1). Of these, three (NKHM1, NKHM2, NKHM5) have copper carbonate staining indicative of malachite or azurite presence, and two (NKHM5, NKHM6) contain copper sulphides, probably chalcopyrite. In terms of gangue content, all of the samples appear to be both siliceous and ferruginous, but NKHM5 and NKHM6 are also pyritic. The minerals do not exhibit any evidence of having been roasted to modify their physical structure or copper content, though this could conceivably been part of the MeP3 production process (e.g. Craddock 1995). The key macro-characteristics of the samples are summarised in Table 6.1.

Overall, the visual impression of the NKH3/MeP3 mineral samples is an assemblage of rocks with siliceous, ferruginous, and pyritic components, and with varying degrees of copper compound staining.

Sample	Siliceous	Ferruginous	Pyritic	Copper Carbonates	Copper Sulphides
NKHM1	X	X		X	
NKHM2	X	X		X	
NKHM3	X	X			
NKHM4	X	X			
NKHM5	X	X	X	X	
NKHM6	X	X	X		X

Table 6.1 - Macro-characteristics of NKH3/MeP3 mineral samples.

6.1.2 Bulk Chemistry

At the major oxide level, the chemical data (Table 6.2) are compatible with the macro-analytical identifications for the Nil Kham Haeng samples, and are predominantly siliceous/ferruginous rocks. However, there is also a fairly consistent presence of sulphur compounds, which suggests that the copper concentrations seen represent both primary (sulphidic) and secondary (oxidic) copper minerals. The Nil Kham Haeng samples contain c. 9wt% copper on average, but of those only two might reasonably be called an ore; these are the chalcopyritic NKHM5 and NKHM6 with 16-17wt% each. The lower analytical totals of some samples may relate to the presence of carbonates.

	MgO	Al ₂ O ₃	SiO ₂	SO ₃	CaO	Fe ₂ O ₃	CuO	Total
	wt%	wt%	wt%	wt%	wt%	wt%	wt%	wt%
NKHM1	4.0	10.8	35.9	5.0	21.3	18.0	3.5	89.3
NKHM2	0.6	8.6	64.2	0.0	8.0	10.6	6.1	92.7
NKHM3	0.7	2.1	78.0	4.8	3.1	6.8	3.4	100.4
NKHM4	0.4	5.8	71.9	1.5	6.2	8.4	5.2	100.8
NKHM5	0.4	4.6	43.3	8.4	6.3	20.3	15.5	101.3
NKHM6	0.4	1.0	43.4	13.8	4.0	18.4	17.5	92.2
mean	1.1	5.5	56.1	5.6	8.2	13.8	8.5	
std dev	1.4	3.8	17.5	5.0	6.7	5.8	6.3	
CV	134%	69%	31%	89%	82%	42%	74%	

Table 6.2 - [P]ED-XRF bulk chemical analyses of NKH3/MeP3 mineral samples, selected major and minor oxides after data normalisation, analytical total presented.

At the trace element level, zinc (mean 1073ppm) and strontium (mean 625ppm) are again the predominant elements, but barium (mean 184ppm) joins tantalum (mean 97ppm), hafnium (mean 88ppm), and nickel (mean 85ppm) as significant traces, albeit with a high degree of variation, as indicated by a mean CV of 112% (Table 6.3). The relatively large amount of zinc in NKHM3, in association with elevated sulphur levels, may indicate the presence of sphalerite within the sample. The mean value for arsenic is also distorted by a high concentration in NKHM6, presumably corresponding to the presence of arsenopyrite. As per Non Pa Wai, hafnium and tantalum have a highly positive ($R^2 =$

1) though apparently isolated correlation (Figure 6.1), but strontium and barium in the Nil Kham Haeng samples appear to be related only to alumina and calcia, with silica seemingly disassociated (Figure 6.2).

	Ni	Zn	As	Sr	Zr	Ba	Hf	Ta
	ppm	ppm	ppm	ppm	ppm	ppm	ppm	ppm
NKHM1	102	263	<10	1303	83	654	134	149
NKHM2	69	266	66	1031	102	33	158	173
NKHM3	82	3752	17	287	<10	23	100	110
NKHM4	73	112	<10	627	56	63	136	149
NKHM5	168	414	12	358	<10	126	<10	<10
NKHM6	14	1629	1330	142	<10	206	<10	<10
mean	85	1073	238	625	40	184	88	97
std dev	50	1425	536	457	46	240	71	78
CV	59%	133%	226%	73%	115%	130%	80%	80%

Table 6.3 - [P]ED-XRF bulk chemical analyses of NKH3/MeP3 mineral samples, selected trace elements after data normalisation.

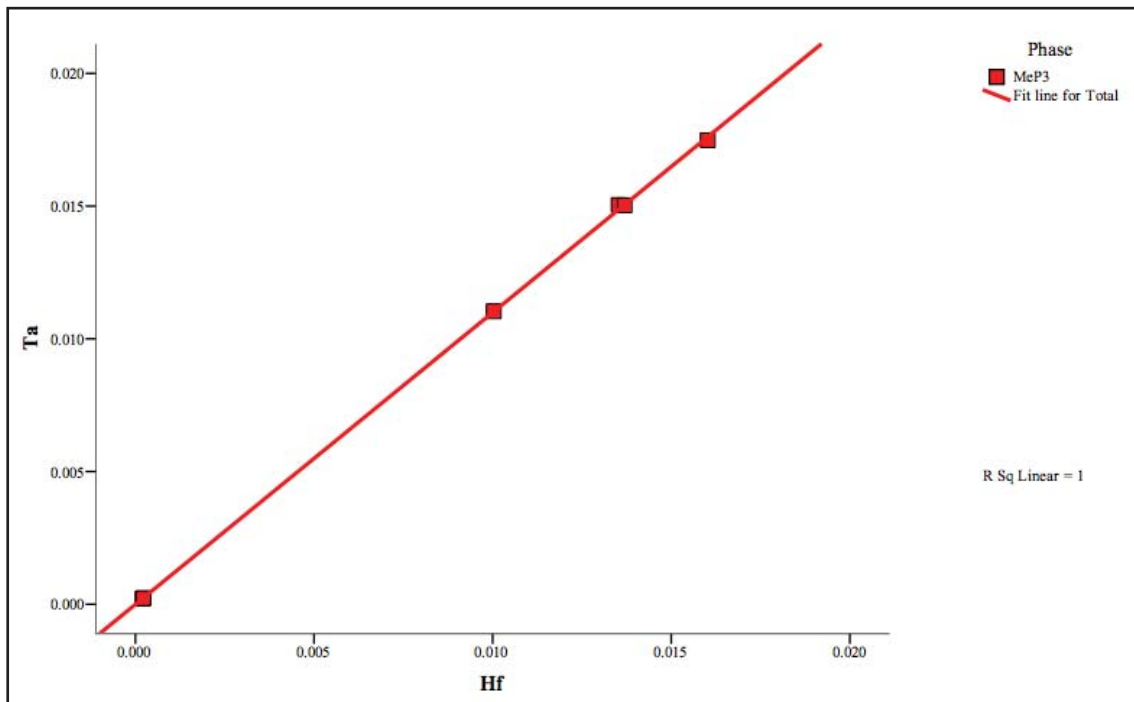


Figure 6.1 - Scatter plot of NKH3/MeP3 mineral samples [P]ED-XRF bulk chemical data - hafnium versus tantalum.

Correlation Matrix

		Al2O3	SiO2	CaO	Sr	Ba
Correlation	Al2O3	1.000	-.250	.847	.982	.552
	SiO2	-.250	1.000	-.568	-.206	-.748
	CaO	.847	-.568	1.000	.857	.907
	Sr	.982	-.206	.857	1.000	.578
	Ba	.552	-.748	.907	.578	1.000

Figure 6.2 - Correlation matrix of NKH3/MeP3 mineral sample [P]ED-XRF bulk chemical data - alumina, silica, calcia, strontium, and barium.

6.1.3 Discussion

As stated before (Chapter 5), the difficulties of interpreting excavated mineral assemblages are well known (e.g; Craddock 1995). However, the industrial deposit at Nil Kham Haeng is largely the result of intensive ore and slag crushing activity, and thus the uniformity of the assemblage perhaps indicates that mineral samples are representative of those chosen by ancient metalworkers. Whether the samples recovered represent minerals awaiting processing, minerals awaiting smelting, or minerals for some reason rejected remains uncertain. The NKH3/MeP3 sample population is small, with only six mineral fragments, but commensurate with a copper smelting locale.

6.2 Technical ceramic

Technical ceramics were defined as non-domestic ceramics associated with industrial activities, and included: ‘slag-skin’, ‘furnace’, mould, and crucible fragments. As previously explained (Chapter 2), NKH3/MeP3 crucibles are very scarce, and moulds are less relevant to the present study’s focus on extractive metallurgy. Therefore, only ‘slag-skin’ and ‘furnace’ fragments from secure NKH3/MeP3 contexts were analysed.

6.2.1 Macro-analysis

Of the six samples assessed, three (NKHTC1, NKHTC2 NKHTC3) were ‘furnace’ fragments, and three (NKHTC4, NKHTC5, NKHTC6) were ‘slag-skin’ fragments (thought to be the remnants of clay lining from smelting pits). The key visual macro-characteristics of the samples are summarised in Table 6.4.

Sample	Hi-fired	Lo-fired	Bloated/Vitrified	Slagged	Copper sign	Perforated
NKHTC1		X				
NKHTC2		X				
NKHTC3		X				X
NKHTC4	X		X	X	X	
NKHTC5	X		X	X	X	
NKHTC6	X		X	X	X	

Table 6.4 - Macro-characteristics of NKH3/MeP3 technical ceramic samples, NKHTC1-3 are ‘furnace’ fragments, NKHTC4-6 are ‘slag-skins’.

The three ‘slag-skin’ samples assessed consist of an unevenly consolidated but well-fired coarse organic-tempered paste, embedded with fragments of ceramic and small stones on the exterior, and coated with slag on the interior (Figure 6.3). The samples range from c. 10mm to c. 15mm in thickness, and c. 30mm to c. 50mm in diameter, with weak curvature, and no clear evidence for rims or bases. All of the fragments have a strong

thermal and redox gradient, whereby the slagged surface is bloated and reduced black, and the other is less heat-damaged and oxidised red, one of the samples (NKHTC5) has a whitish layer underneath the slag (Figure 6.4). The slag coating itself is patchy, porous and heterogeneous, with clear copper staining present in all cases.

The slagging and heat damage would suggest the ceramic was in direct contact with a high-temperature process, and the irregular surfaces and frequent inclusions of small stones are consistent with the 'slag-skins' being interpreted as clay linings moulded into a pit, rather than fragments of a free-standing vessel. The general amorphousness of the samples renders a reconstruction problematic, but if the 'slag-skins' are associated with the furnaces, then we might expect a lined pit c. 200mm in diameter.



Figure 6.3 - 'Slag-skin' fragments NKHTC4. Image: author.



Figure 6.4 - 'Slag-skin' fragments NKHTC5. Image: author.



Figure 6.5 - 'Furnace' fragment NKHTC1. Image: author.



Figure 6.6 - 'Furnace' fragment NKHTC3, with perforation highlighted. Image: author.



Figure 6.7 - Perforated ceramic cylinder excavated from Burial 1 Operation 4 at Nil Kham Haeng. Image: courtesy of TAP.

The ‘furnace’ fragments were made from a friable low-fired oxidised red coarse organic-tempered fabric, (Figure 6.5). The fragments are c. 40mm to c. 50mm thick, and range from c. 50mm to c. 130mm in diameter. The samples have regular flattened bases, sub-rounded rims, and a reasonable indication of curvature. Two of the samples (NKHTC2 and NKHTC3) have evidence of wall perforation, especially clear in the latter (Figure 6.6). Although the ‘furnace’ fragments are low-fired, two of the three samples (NKHTC2 and NKHTC3) do have evidence for localised heat damage, with a slightly higher-fired grey layer adhering to the interior wall and perforated surfaces (Figure 6.6). There is no sign of any bloating, vitrification, slagging, or copper staining on any of the studied samples, though the latter is visible on the extant whole example (Figure 6.7).

The fabric and formal characteristics of the ‘furnace’ fragments makes for a strong correlation with the complete perforated ceramic cylinder recovered from a secure NKH3/MeP3 burial context (Figure 6.7), which would reconstruct them as c. 200mm tall and c. 200mm in diameter. These structures have previously been interpreted as smelting furnaces (Pigott *et al.* 1997), and the technological choice of perforation suggests the reaction may have been wind-powered - as per perforated furnaces from the Bronze Age Near East and Aegean, medieval Sri Lanka, and the recent historical Southern Andes (Bunk *et al.* 2004, Catapotis *et al.* 2008, Tabor *et al.* 2005, Van Buren & Mills 2005).

6.2.2 Bulk Chemistry

The technical ceramic samples from Nil Kham Haeng were prepared for [P]ED-XRF bulk chemical analysis and the resulting data processed as per the methodology detailed in Chapter 4. Complete chemical data may be seen in Appendix B (Table B3). Due to the close mechanical and interstitial chemical association between ceramic and slag in the ‘slag-skin’ fragments¹ (NKHTC4, NKHTC5, NKHTC6) bulk chemical analysis was deemed an unsuitable technique - it would be impossible to reliably separate the two components in sample preparation, and thus the results would be mutually obscured by their independent chemistries. Please see 6.2.3 below for results of the micro-analytical study of Nil Kham Haeng ‘slag-skins’.

The major oxide chemistry of the three Nil Kham Haeng ‘furnace’ fragments is uniform, with a mean composition of 59.1wt% silica, 21.2wt% alumina, 10.9wt% iron oxide, and

1 The NPW3/MeP2 crucible fragments were predominantly ceramic, with a little bit of slag, whereas the proportion was approximately 50:50 for the NKH3/MeP3 ‘slag-skins’.

5.0wt% calcia (Table 6.5, Figure 6.8). Calcia has the highest CV at 16%, but the mean CV for the above oxides is fairly low at around 8%, although the very low sample population will have a disproportionate effect on mean figures. The technical ceramic major oxide chemistry is similar to that of Non Pa Wai (Figure 5.12), and commensurate with a clay source in the local geological area. The copper oxide content of the samples averages 0.2wt%, indicating either the ‘furnace’ fragments had a degree of contact with copper production activities, or a copper-rich burial environment. Carbonate compounds may again be responsible for low analytical totals.

	Al ₂ O ₃	SiO ₂	CaO	Fe ₂ O ₃	CuO	Total
	wt%	wt%	wt%	wt%	wt%	wt%
NKHTC1 furnace	21.4	59.1	4.5	11.1	0.2	87.7
NKHTC2 furnace	20.1	61.3	4.6	10.0	0.3	89.9
NKHTC3 furnace	22.0	57.1	5.9	11.7	0.2	91.2
mean	21.2	59.1	5.0	10.9	0.2	
std dev	1.0	2.1	0.8	0.9	0.0	
CV	5%	4%	16%	8%	13%	

Table 6.5 - [P]ED-XRF bulk chemical analyses of NKH3/MeP3 technical ceramic (‘furnace’) samples, selected major and minor oxides after data normalisation, analytical total presented.

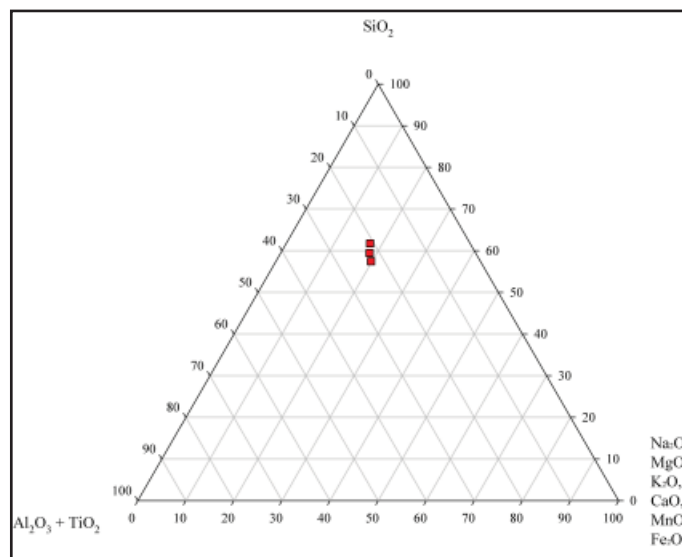


Figure 6.8 - Ternary plot of NKH3/MeP3 technical ceramic samples [P]ED-XRF bulk chemical data - selected major oxides.

Barium is the predominant trace element, with a mean of 344ppm and a relatively high CV of 49%. Other leading traces include strontium (mean 207ppm), zinc (mean 204ppm), and zirconium (mean 116ppm), all of which have CVs less than 21% (Figure 6.9, Table 6.6). At Nil Kham Haeng the levels of barium and strontium are positively correlated

to silica, and negatively to alumina, whereas zirconium has the opposite relationship to both major oxides (Figure 6.10). Only barium has a reasonable correlation to calcia. Care must be taken due to the limited number of Nil Kham Haeng samples, but the internal uniformity of the trace element chemistry would suggest a single clay source being used for NKH3/MeP3; the patterning is almost the opposite to that seen in the Non Pa Wai samples (Figure 5.13).

	Zn	Sr	Zr	Ba
	ppm	ppm	ppm	ppm
NKHTC1 furnace	214	176	117	281
NKHTC2 furnace	211	257	114	533
NKHTC3 furnace	187	189	116	218
mean	204	207	116	344
std dev	15	43	2	167
CV	7%	21%	1%	49%

Table 6.6 - [P]ED-XRF bulk chemical analyses of NKH3/MeP3 technical ceramic ('furnace') samples, selected elements after data normalisation.

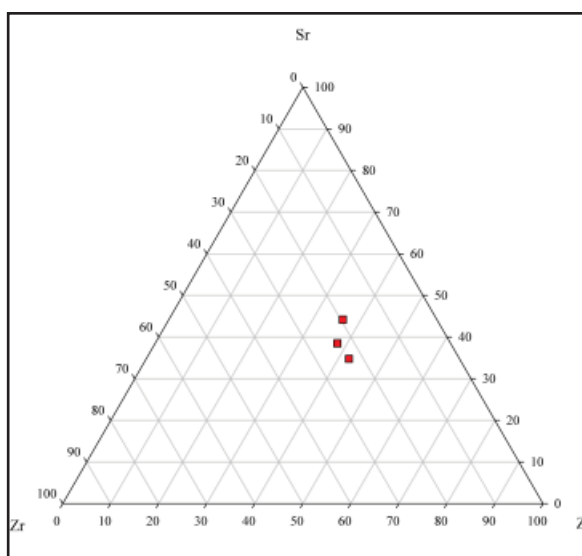


Figure 6.9 - Ternary plot of NKH3/MeP3 technical ceramic samples [P]ED-XRF bulk chemical data - selected elements.

Correlation Matrix

		Al2O3	SiO2	CaO	Sr	Zr	Ba
Correlation	Al2O3	1.000	-.986	.708	-.883	.886	-.990
	SiO2	-.986	1.000	-.816	.793	-.797	.952
	CaO	.708	-.816	1.000	-.294	.300	-.599
	Sr	-.883	.793	-.294	1.000	-1.000	.942
	Zr	.886	-.797	.300	-1.000	1.000	-.944
	Ba	-.990	.952	-.599	.942	-.944	1.000

Figure 6.10 - Correlation matrix of NKH3/MeP3 technical ceramic ('furnace') sample [P]ED-XRF bulk chemical data - alumina, silica, calcia, strontium, zirconium, and barium.

6.2.3 Micro-analysis

The technical ceramic population was sub-sampled for further study by OM and SEM-EDS. Due to the low population, the microanalytical sub-sample included the entire technical ceramic assemblage including the “slag-skins” not assessed by bulk chemical analysis. The key micro-characteristics of the samples are summarised in Table 6.7.

Sample	Thermal degradation gradient	Elongate vesicles	Modified inclusions	Olivine skeletons	Crypto ‘glass’	Magnetite (primary)	Magnetite (residual)	Prills
NKHTC1	-	X	-					
NKHTC2	-	X	-					
NKHTC3	-	X	-					
NKHTC4	X	X	-	X	?	X	X	X
NKHTC5	X	X	-	X	?	X	X	X
NKHTC6	X	X	-	X	?	X	X	X

Table 6.7 - Micro-characteristics of NKH3/MeP3 technical ceramic samples, NKHTC1-3 are ‘furnace’ fragments, NKHTC4-6 are ‘slag-skins’.

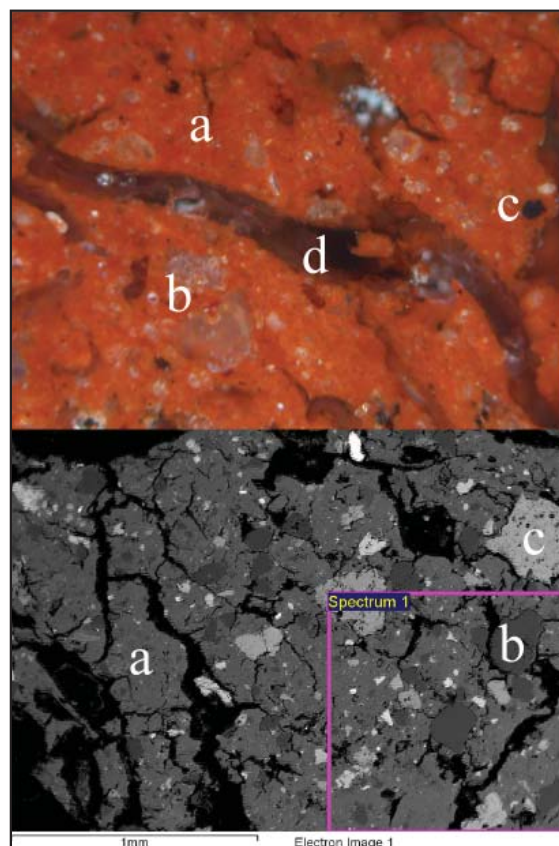


Figure 6.11 - PPL and SEM-BSE images, both at x50, of NKHTC2 micro-features, ‘a’ micromass, ‘b’ quartz, ‘c’ iron oxide, and ‘d’ vesicles - ‘Spectrum 1’ exemplar of EDS area scan on fabric. Images: author.

‘Furnace’ fragments:

Due to the lack of a thermal profile, the furnace fragments have a relatively uniform microstructure across the section. The paste is composed of an optically-active red micromass, with frequent sub-angular to sub-rounded fragments of quartz ranging from c. 0.01mm to c. 0.4mm, and iron oxide ranging from c. 0.01mm to c. 0.4mm (Figure 6.11). The inclusions are reasonably well sorted, with no distinct evidence of preferred orientation, and their size distribution appears to be polymodal. As per the Non Pa Wai samples are the frequent presence of elongate curvilinear vesicles c. 0.1mm to c. 0.2mm wide and up to c. 2mm in length, and also without preferred orientation (Figure 6.11).

The presence of multiple mineral species would indicate the furnaces were made from a sedimentary clay. The weathered appearance of these particles, and the apparent absence of a modal distribution suggests they are either natural contaminants or evidence for non-systematic inorganic tempering. The extended airspaces in the furnace fabric are probably explained by modification of the paste with large quantities of plant matter, which would have subsequently burnt out. The lack of preferred orientation in the microstructure suggests the furnaces were coiled or slabbed, and almost certainly not thrown (Courty & Roux 1995, Rye 1981, Whitbread 1989).

‘Slag-skin’ fragments - paste:

The continuous heat damage across the ‘slag-skins’ profile results in a less pronounced microstructural gradient than that seen in the NPW3/MeP2 crucibles, perhaps indicating a longer or hotter exposure for a similar thickness of material. Towards the exterior, less heat-damaged, surface the paste is composed of a red-brown micromass with some optical activity, regular sub-rounded fragments of slightly fused quartz ranging from c. 0.05mm to c. 0.5mm, and sub-rounded fragments of semi-fused iron oxide ranging from c. 0.05mm to c. 0.1mm (Figure 6.12). The quartz inclusions appear to have a wide size distribution, comparable to the ‘furnace’ fragments, but the iron oxide particle boundaries are now more diffused, probably due to their fluxing the micromass at high temperatures. There is no evidence of preferred orientation, possibly due to the heat-distorted grain boundaries. As per the ‘furnace’ fragments, elongate curvilinear vesicles c. 0.1mm to 0.2mm wide and c. 1mm in length, are frequent and without preferred orientation (Figure 6.12).

The ‘slag-skin’ fabric adjacent to the slag layer is extremely bloated, with very little microstructural detail (Figure 6.13). The visible micromass is optically inactive, with regular fused grains of quartz c. 0.05mm to c. 0.2mm in diameter, no other mineral

species were discernable within the heat-damaged matrix. Large sub-spherical to sub-elongate vesicles, c. 0.2mm to c. 1mm in size, are widely distributed up to c. 10mm from the ceramic slag interface (Figure 6.14). The sorting of inclusions appears to be similar to that seen in the exterior fabric, though evidence for preferred orientation is even less distinct.

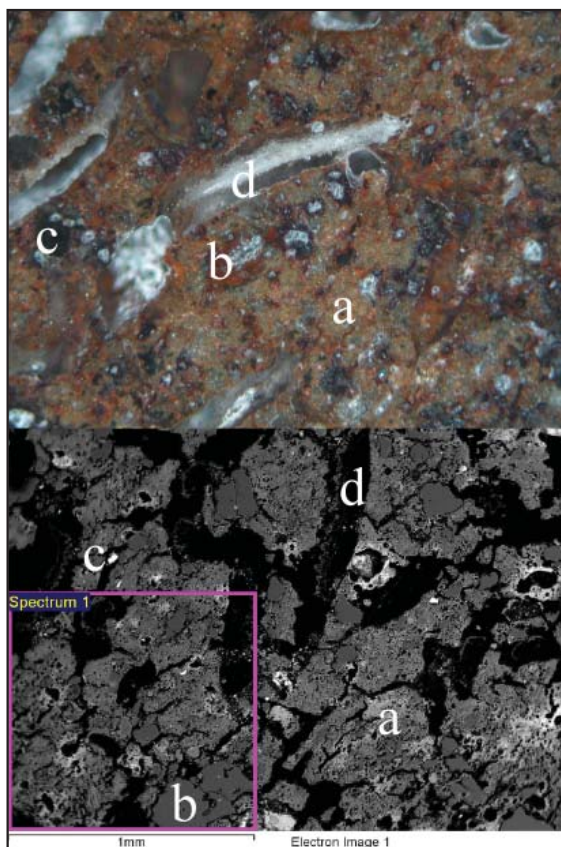


Figure 6.12 - PPL and SEM-BSE images, both at x50, of NKHTC5 micro-features, 'a' micromass, 'b' quartz, 'c' iron oxide, and 'd' vesicles - 'Spectrum 1' exemplar of EDS area scan on fabric. Images: author.

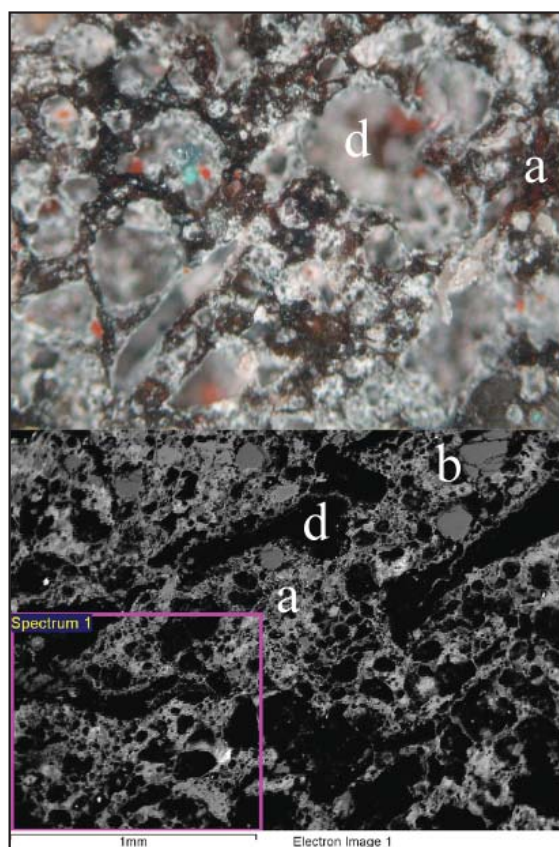


Figure 6.13 - PPL and SEM-BSE images, both at x50, of NKHTC6 micro-features, 'a' micromass, 'b' quartz, and 'd' vesicles - 'Spectrum 1' exemplar of EDS area scan on fabric. Images: author.

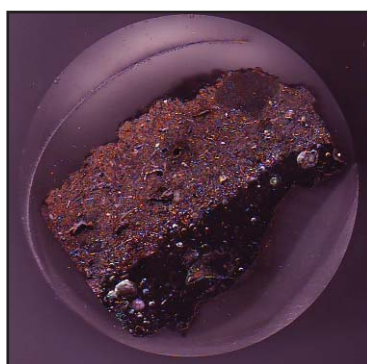


Figure 6.14 - Crucible fragment NKHTC5 mounted in 32mm polished block, widespread bloating visible at the ceramic/slag interface. Image: author.

These characteristics would suggest the ‘slag-skins’ were produced from a sedimentary clay tempered with organic material. The non-vitrified ‘slag-skin’ fabric is entirely comparable to that of the ‘furnace’ fragments, and does not seem to have been modified as per the NPW3/MeP2 crucible paste. The microstructural evidence for a thermal gradient corroborates the macro evidence, and indicates the ‘slag-skins’ were subjected to intense internal heating. Although the exterior ‘slag-skin’ fabric is less heat damaged than the interior, its high temperature exposure reduced optical activity and blurred grain boundaries. The interior fabric is heavily degraded, with the elongate vesicles seeming to have expanded into extensive bloating.

	Al ₂ O ₃	SiO ₂	K ₂ O	CaO	TiO ₂	Fe ₂ O ₃	Total
	wt%	wt%	wt%	wt%	wt%	wt%	wt%
NKHTC4	10.1	72.7	1.1	5.1	0.8	10.2	42.0
NKHTC5	18.3	56.3	1.1	6.4	1.2	16.8	45.9
NKHTC6	17.2	52.7	2.4	5.8	1.1	20.8	31.6
mean	15.2	60.6	1.5	5.8	1.0	15.9	
std dev	4.4	10.7	0.8	0.6	0.2	5.4	
CV	29%	18%	51%	0%	21%	34%	

Table 6.8 - SEM-EDS area scans of NKH3/MeP3 ‘slag-skin’ samples, selected major and minor oxides after data normalisation, analytical total presented.

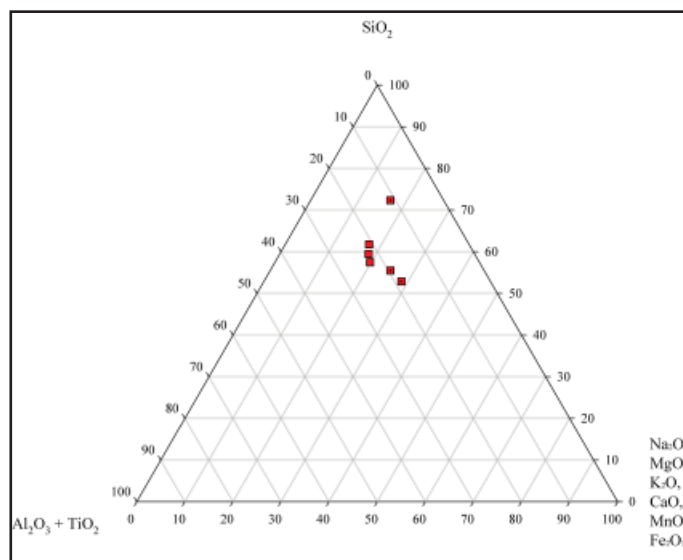


Figure 6.15 - Ternary plot of NKH3/MeP3 technical ceramic samples: ‘slag-skin’ (black dot) - SEM-EDS data, ‘furnace’ - [P]ED-XRF data - selected major oxides.

As mentioned earlier in the chapter, bulk chemical analysis of the technical ceramic paste was not possible due to the intimate association between fabric and slag. However, this problem can be partially overcome with SEM-EDS area scans of the paste on less heat damaged portions of the profile (Table 6.8). It should be noted that the high degree of

porosity in even the unbloated ‘slag-skin’ results in very low analytical totals, which must be interpreted with caution. These caveats in hand, the SEM-EDS ‘slag-skin’ data is comparable to the [P]ED-XRF ‘furnace’ data (Table 6.5), indicating fabrics with similar refractory qualities (Figure 6.15).

‘Slag-skin’ fragments - slag:

The microstructure of slag adhering to the three ‘slag-skin’ samples assessed is composed of three major components: interstitial glass, olivine and iron oxide crystals, as well as copper prills and residual iron oxide minerals (Figure 6.16).

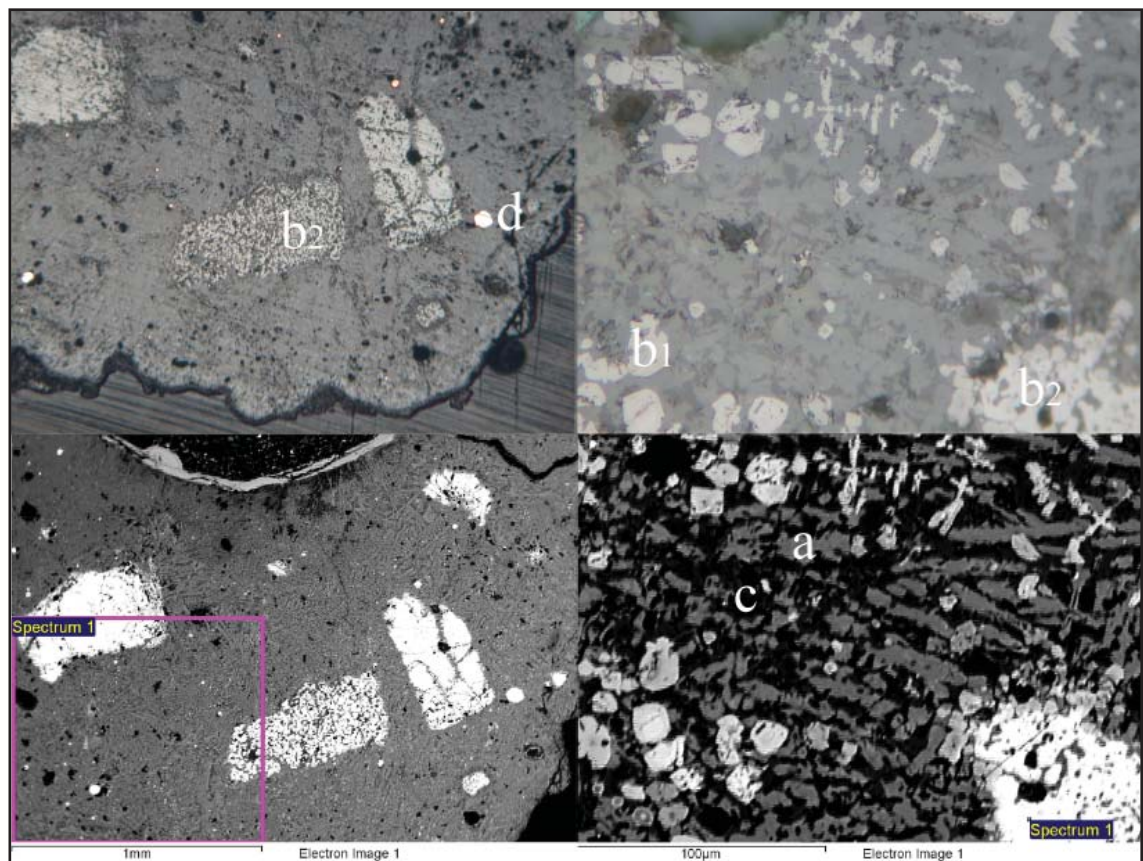


Figure 6.16 - NKHTC5 ‘slag-skin’ micro-features at 100x (left) by plane polarised light (top) and SEM-BSE (bottom), and NKHTC6 at 500x (right) by plane polarised light (top) and SEM-BSE (bottom). Labels ‘a’ olivine skeletons, ‘b₁’ primary magnetite euhedrals, ‘b₂’ residual magnetite inclusions, ‘c’ glass phase, ‘d’ prill, ‘Spectrum 1’ exemplar of an SEM-EDS area analysis. Images: author.

Olivine crystals - Elongate olivine skeletons are a frequent feature of the NKH3/MeP3 ‘slagskins’, and range in width from c. 0.01mm to c. 0.02mm, and in length from c. 0.05mm to c. 0.3mm (Figure 6.16). As discussed in Chapter 5, olivine should not be able to form under intermediate partial pressures (Kongoli & Yazawa 2001: 585), and thus its presence once again in the slag microstructure indicates redox conditions were variable. The skeletal crystalline habit suggests the ‘slag-skins’ were subject to relatively

fast cooling, which is interesting as one might expect a ceramic-lined pit to have retained heat for some time.

	MgO	Al ₂ O ₃	SiO ₂	CaO	FeO	CuO	Total	Fe/SiO ₂
	wt%	wt%	wt%	wt%	wt%	wt%	wt%	wt ratio
NKHTC4	0.4	6.4	34.1	10.2	44.4	0.1	83.4	1.0
NKHTC5	2.7	2.8	28.8	19.6	44.2	0.3	83.2	1.2
NKHTC6	0.5	7.5	34.4	19.0	36.2	1.2	83.1	0.8
mean	1.2	5.6	32.4	16.3	41.6	0.5		
std dev	1.3	2.5	3.1	5.2	4.7	0.6		
CV	110%	44%	10%	32%	11%	104%		

Table 6.9 - SEM-EDS phase analyses of NKH3/MeP3 'slag-skin' olivine crystals, selected major and minor oxides after data normalisation, analytical total presented.

By SEM-EDS spot analyses, the major chemical components of the skeletons are FeO (mean 41.6wt%), SiO₂ (mean 32.4wt%), CaO (mean 16.3wt%), Al₂O₃ (mean 5.6wt%) and MgO (mean 1.2wt%) (Table 6.9). The CVs for iron oxide, silica, and calcia (11%, 10%, 32% - the latter elevated result due to NKHTC4's divergent reading) are substantially lower than those for NPW3/MeP2 crucible slag olivines (Table 5.8), potentially indicating more regular formation conditions and an increasingly standardised mineral/fuel charge in the later Iron Age process. Plotting the Fe/SiO₂ ratio against CaO on a binary Flogen diagram, calculated for 7wt% Al₂O₃ (Kongoli & Yazawa 2001: Figure 11), indicates the olivine phases began to crystallise between c. 1210°C and c. 1265°C, with a mean precipitation temperature of c. 1230°C (Figure 6.17).

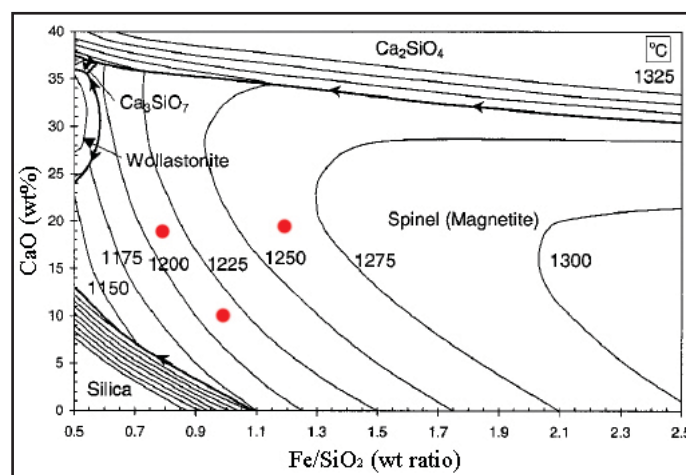


Figure 6.17 - SEM-EDS analyses of olivine phases plotted on a Flogen binary chart for slag system at a 10⁻⁸ ppO₂ and with 7wt% Al₂O₃. Image adapted from Kongoli & Yazawa 2001: Figure 11.

Magnetite spinel - Euhedral and dendritic crystals are also common within NKH3/MeP3 ‘slag-skins’, with dimensions ranging from c. 0.005mm to c. 0.03mm (Figure 6.16). The euhedral phases are identified as the iron oxide magnetite due to their optical behaviour and angularity (Ineson 1989), but some of the dendrites have a degree of roundedness which suggests they are wüstite. The ‘slag-skins’ also contain occasional angular to sub-angular fragments of iron oxide up to c. 1mm in size (Figure 6.16). These are also identified as magnetite, but are in this instance almost certainly residual minerals, which appear to be dissolving into the melt rather than precipitating from it. The presence of residual magnetite represents a strong technological choice analogy to NPW3/MeP2 (to be discussed in Chapter 8), and ensures the slag system was buffered with iron oxide.

SEM-EDS spot analyses indicate the principal chemical components of the iron oxide phases are FeO² (mean 93.4wt%), Al₂O₃ (mean 2.7wt%), SiO₂ (mean 1.0wt%), MgO (mean 0.6wt%), CaO (mean 0.6wt%), and TiO₂ (mean 0.4wt%), with CuO present but below confident accuracy levels (Table 6.10). Binary Flogen diagrams are not available for such high Fe/SiO₂ ratios, but a ternary plot calculated for intermediate oxygen partial pressures indicates these phases would begin to precipitate at around 1300°C (Kongoli & Yazawa 2001: Figure 6). This would suggest the primary (not residual mineral) magnetite spinel crystallised before the olivine, which might account for the relatively uniform and pure composition.

	MgO	Al ₂ O ₃	SiO ₂	CaO	TiO ₂	FeO	CuO	Total	Fe/SiO ₂
	wt%	wt%	wt%	wt%	wt%	wt%	wt%	wt%	wt ratio
NKHTC5 residual	1.2	1.4	0.4	0.2	0.5	93.3	0.1	96.9	204.8
NKHTC6 residual	0.2	0.3	0.5	0.3	0.1	98.3	0.1	95.0	165.4
NKHTC6 primary	0.4	6.3	2.3	1.3	0.7	88.5	0.3	86.6	30.4
mean	0.6	2.7	1.0	0.6	0.4	93.4	0.2		
std dev	0.5	3.2	1.1	0.6	0.3	4.9	0.2		
CV	87%	119%	104%	99%	75%	5%	92%		

Table 6.10 - SEM-EDS phase analyses of NKH3/MeP3 ‘slag-skin’ magnetite crystals, selected major and minor oxides after data normalisation, analytical total presented.

Slag glass - Binding the closely packed ‘slag-skin’ crystals of olivine and magnetite spinel is an interstitial glass (Figure 6.16). Unlike NPW3/MeP2 crucible slags, there is no discernable crypto-crystallinity to this phase, which, composition notwithstanding, may suggest a faster cooling rate for the NKH3/MeP3 ‘slag-skins’.

2 An approximation as magnetite has the formula Fe₃O₄.

SEM-EDS spot analyses report that the major chemical components of this glass are SiO₂ (mean 34.8wt%), FeO (mean 34.5wt%), CaO (mean 20.3wt%), Al₂O₃ (mean 7.1wt%), MgO (mean 2.0wt%), and some CuO below accurate detection levels (Table 6.11). The respective CVs (20%, 21%, 15%, 35% and 38%) suggest the interstitial glass composition was quite variable between samples, indeed consistently more so than the NPW3/MeP2 equivalent phase. Plotting the data on the same Flogen diagram as the olivine indicates the ‘slag-skin’ glass would have begun to solidify between c. 1175°C and 1260°C, with a mean precipitation temperature of c. 1215°C. These precipitation temperatures are below that for the olivine and magnetite, suggesting the glass phase was the last to form as the slag cooled. The dense packing of the olivine crystals, and their very similar precipitation temperature, could suggest the mineral/fuel charge composition was chemically well balanced, with only calcia and minor oxides left to be incorporated into the relatively sparse and compositionally variable glass phase.

	MgO	Al ₂ O ₃	SiO ₂	CaO	FeO	CuO	Total	Fe/SiO ₂
	wt%	wt%	wt%	wt%	wt%	wt%	wt%	wt ratio
NKHTC4	2.9	5.8	39.8	21.4	29.1	0.0	80.1	0.6
NKHTC5	1.9	10.0	26.9	16.8	42.5	0.1	80.3	1.2
NKHTC6	1.3	5.6	37.6	22.7	32.0	0.1	80.7	0.7
mean	2.0	7.1	34.8	20.3	34.5	0.1	98.8	0.8
std dev	0.8	2.5	6.9	3.1	7.1	0.1		
CV	38%	35%	20%	15%	21%	83%		

Table 6.11 - SEM-EDS phase analyses of NKH3/MeP3 ‘slag-skin’ glass phases, selected major and minor oxides after data normalisation, analytical total presented.

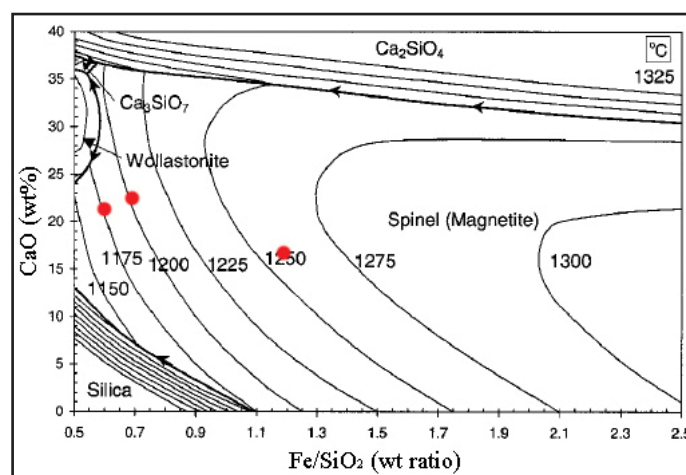


Figure 6.18 - SEM-EDS analyses of glass phases plotted on a Flogen binary chart for slag system at a 10⁻⁸ ppO₂ and with 7wt% Al₂O₃. Image adapted from Kongoli & Yazawa 2001: Figure 11.

Slag prills - Although the slag area analyses (see below) would suggest otherwise, metallic prills are rare in NKHTC4 and NKHTC6, but more frequent in the NKHTC5 slag, where they range in diameter between c. 0.01mm and c. 0.1mm (Figure 6.16 - top and bottom left). The SEM-EDS spot analyses performed show substantial variation in the levels of sulphur, iron, and copper (S not detected - 22.2wt%, Fe 1.4 - 73.5wt%, and Cu 4.3 - 98.6wt%). The presence of sulphur in the slag system is not conclusive evidence of a sulphidic smelting operation, but it would suggest the 'slag-skins' were involved earlier (smelting) rather than later (casting) in the copper production sequence.

Slag matrix - Residual iron oxide aside, the 'slag-skin' matrices are relatively homogeneous, with low porosity and well formed crystals, suggesting the slag had been almost fully liquid when hot. The skeletal olivine morphology and lack of any crytocrystallinity to the glassy phase indicates the 'slag-skins' may have cooled quite quickly, though there is no evidence for quenching. The general slag homogeneity means the matrices are suitable for targeted bulk chemical analysis, which were scanned in 1mm² sections³ (Figure 6.16, Table 6.12). These 'bulk' data are not comparable to the [P]ED-XRF analysis of pelletised slag (see below) as they omit unreacted inclusions as much as possible, but, as per Chapter 5, they permit the interpretation of inter and intra sample chemical variability, which relate to process standardisation and equilibrium respectively (cf. Humphris *et al.* 2009).

Comparing across the 'slag-skin' samples, the major chemical components of the slag microstructure are FeO (mean 44.2wt%), SiO₂ (mean 29.7wt%), and CaO (mean 13.2wt%). Despite potential analytical issues (see Footnote 3) the respective CVs for these oxides (16%, 22%, 7%) are uniformly lower than the NPW3/MeP2 crucible slag matrices' (Table 5.11), indicating the MeP3 process had a more stable charge composition and/or operating parameters. The mean CuO reading of 2.0wt% is quite low, but a CV of 84% on this measure suggests inter smelt variability in process efficiency is rather high, and in the samples studied seems to be caused by the unexplained copper losses in the NKHTC6 slag layer. There appears to be no correlation between iron oxide content and increased copper losses due to viscosity (Davenport *et al.* 2002: 273, Gilchrist 1989). Sulphur compounds were detected in the NKHTC4 matrix alone.

Looking within individual samples, the CVs for FeO (4%, 6%, 13%), SiO₂ (2%, 7%, 11%), CaO (5%, 9%, 2%), CuO (35%, 24%, 37%) suggest, unsurprisingly, the slag was

3 It was not possible to completely avoid residual inclusions given the limited dimensions, and thus iron oxide levels may be some what elevated in the 'slag-skin' matrix analyses.

less variable within than between processes, but certainly not fully reacted, and unusually these CVs are moderately higher than their NPW3/MeP2 equivalents (Table 5.11). Though individual ‘slag-skin’ slags seem not to have fully reacted, the matrix data show a greater degree of inter-sample compositional agreement. This might be interpreted as showing NKH3/MeP3 metalworkers chose more standardised mineral charges or process parameters, but, from the technical ceramic evidence at least, the performance of each smelt was not similarly ameliorated.

	MgO wt%	Al ₂ O ₃ wt%	SiO ₂ wt%	SO ₃ wt%	K ₂ O wt%	CaO wt%	MnO wt%	FeO wt%	CuO wt%	Total wt%	Fe/SiO ₂ wt ratio
NHKTC4 spectrum 1	1.9	8.0	36.6	0.7	0.8	14.9	0.7	35.2	0.7	75.9	0.7
NKHTC4 spectrum 2	1.4	7.7	35.2	1.0	0.9	13.6	0.6	38.1	1.0	79.8	0.8
NKHTC4 spectrum 3	1.3	8.7	35.0	0.8	0.9	13.7	0.7	38.1	0.5	69.1	0.8
<i>NKHTC4 mean</i>	<i>1.5</i>	<i>8.1</i>	<i>35.6</i>	<i>0.9</i>	<i>0.9</i>	<i>14.1</i>	<i>0.6</i>	<i>37.1</i>	<i>0.7</i>	<i>74.6</i>	<i>0.8</i>
<i>NKHTC4 std dev</i>	<i>0.4</i>	<i>0.5</i>	<i>0.8</i>	<i>0.1</i>	<i>0.1</i>	<i>0.7</i>	<i>0.1</i>	<i>1.6</i>	<i>0.3</i>		
<i>NPWTC8 CV</i>	<i>23%</i>	<i>7%</i>	<i>2%</i>	<i>16%</i>	<i>7%</i>	<i>5%</i>	<i>12%</i>	<i>4%</i>	<i>35%</i>		
NHKTC5 spectrum 1	2.1	7.4	23.9	n.d	0.7	14.2	0.4	49.6	1.2	83.7	1.6
NKHTC5 spectrum 2	2.2	6.6	21.1	n.d	0.5	11.9	0.5	55.2	1.7	85.1	2.0
NKHTC5 spectrum 3	2.0	7.7	23.7	n.d	0.7	13.6	0.6	50.3	1.2	83.0	1.6
<i>NKHTC5 mean</i>	<i>2.1</i>	<i>7.2</i>	<i>22.9</i>	<i>n.a</i>	<i>0.6</i>	<i>13.2</i>	<i>0.5</i>	<i>51.7</i>	<i>1.4</i>	<i>83.9</i>	<i>1.8</i>
<i>NKHTC5 std dev</i>	<i>0.1</i>	<i>0.6</i>	<i>1.6</i>	<i>n.a</i>	<i>0.1</i>	<i>1.2</i>	<i>n.a</i>	<i>3.0</i>	<i>0.3</i>		
<i>NPWTC5 CV</i>	<i>5%</i>	<i>8%</i>	<i>7%</i>	<i>n.a</i>	<i>21%</i>	<i>9%</i>	<i>n.a</i>	<i>6%</i>	<i>24%</i>		
NHKTC6 spectrum 1	0.8	6.2	31.0	n.d	0.8	12.2	0.6	44.3	3.6	77.1	1.1
NKHTC6 spectrum 2	0.8	6.8	27.0	n.d	0.4	12.2	0.5	49.1	2.6	80.4	1.4
NKHTC6 spectrum 3	0.9	7.7	33.8	n.d	0.6	12.6	0.6	38.1	5.5	71.6	0.9
<i>NKHTC6 mean</i>	<i>0.8</i>	<i>6.9</i>	<i>30.6</i>	<i>n.a</i>	<i>0.6</i>	<i>12.3</i>	<i>n.a</i>	<i>43.8</i>	<i>3.9</i>	<i>76.4</i>	<i>1.1</i>
<i>NKHTC6 std dev</i>	<i>0.0</i>	<i>0.7</i>	<i>3.4</i>	<i>n.a</i>	<i>n.a</i>	<i>0.2</i>	<i>n.a</i>	<i>5.5</i>	<i>1.4</i>		
<i>NPWTC6 CV</i>	<i>4%</i>	<i>11%</i>	<i>11%</i>	<i>n.a</i>	<i>n.a</i>	<i>2%</i>	<i>n.a</i>	<i>13%</i>	<i>37%</i>		
NKHTC mean	1.5	7.4	29.7	n.a	n.a	13.2	n.a	44.2	2.0	78.6	1.2
NKHTC std dev	0.6	0.6	6.4	n.a	n.a	0.9	n.a	7.3	1.7		
Inter NKHTC CV	42%	9%	22%	n.a	n.a	7%	n.a	16%	84%		
<i>Mean intra NKHTC CV</i>	<i>11%</i>	<i>8%</i>	<i>7%</i>	<i>n.a</i>	<i>n.a</i>	<i>5%</i>	<i>n.a</i>	<i>8%</i>	<i>32%</i>		

Table 6.12 - SEM-EDS phase analyses of NKH3/MeP3 ‘slag-skin’ slag matrices, selected major and minor oxides after data normalisation, analytical total presented.

Using the traditional archaeometallurgical technique for calculating operating temperatures from slag liquidus, the primary chemical components (iron^(II) oxide, silica, and calcia) would indicate the slag adhering to the crucibles was exposed to minimum temperatures of between c. 1125°C and c. 1225°C (Figure 6.19). Transposing the mean liquidus of c.

1160°C onto an Ellingham Diagram, and extending two lines to the intersections of the liquidus with the ‘ $4\text{Cu} + \text{O}_2 = 2\text{Cu}_2\text{O}$ ’ and ‘ $6\text{FeO} + \text{O}_2 = 2\text{Fe}_3\text{O}_4$ ’ boundaries (representing the likely redox envelope for a process reducing copper to metallic form, and containing divalent as well as trivalent iron), indicates a p_{O_2} between c. 1×10^{-6} and c. 1×10^{-10} (Figure 6.20).

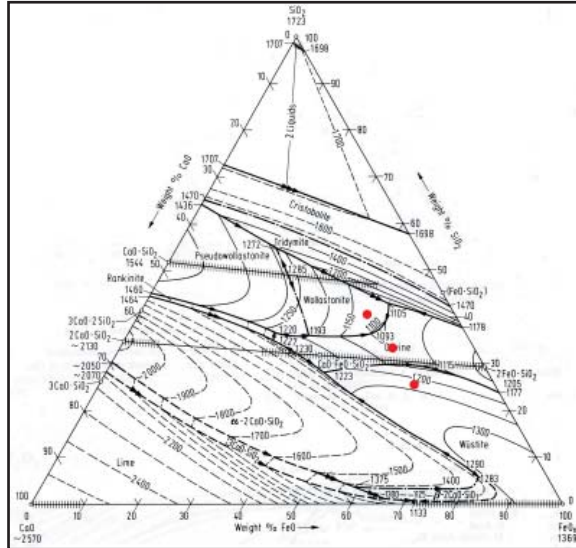


Figure 6.19 - ‘Slag-skin’ slag matrices plotted on a ternary diagram for a FeO-CaO-SiO₂ slag system in equilibrium with iron metal. Image adapted from Eisenhüttenleute 1995.

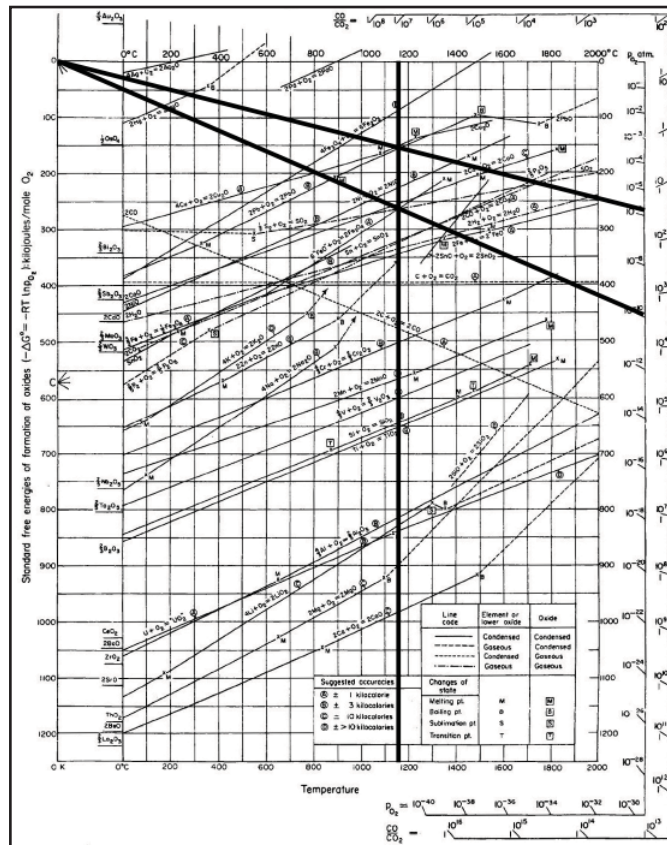


Figure 6.20 - Ellingham Diagram showing redox envelope for NKH3/MeP3 ‘slag-skin’ slags. Image adapted from Gilchrist 1989.

The most appropriate Flogen diagram for the NKH3/MeP3 ‘slag-skin’ slag layer describes a system with 7wt% alumina in a ppO_2 of 1×10^{-8} , with Fe/SiO₂ ratio and calcia as variables (Kongoli & Yazawa 2001: Figure 11). Plotting the data from Table 6.13 onto Figure 6.21 gives a liquidus reading of between c. 1200°C and c. 1285°C, giving a mean minimum slag temperature of c. 1240°C. The traditionally derived figure of 1160°C is only 80°C adrift from the Flogen reading, but in the opposite direction from that normally expected. This is another example of how using thermodynamic models at intermediate oxygen partial pressures can produce higher than expected liquidus readings when the slag contains ‘fluxing’ minor oxides like alumina and calcia. It is likely the true operating temperature for the ‘slag-skins’ was closer to 1300°C, given the precipitation of near pure magnetite in the slag.

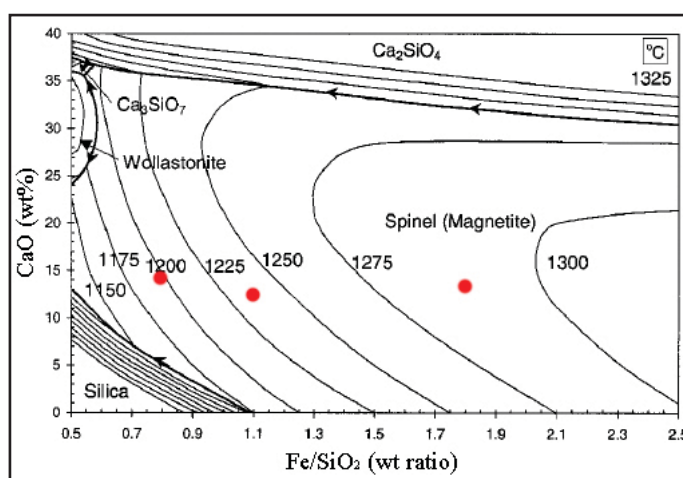


Figure 6.21 - SEM-EDS analyses of slag matrices phases plotted on a Flogen binary chart for slag system at a 10^{-8} ppO_2 and with 7wt% Al_2O_3 . Image adapted from Kongoli & Yazawa 2001: Figure 11.

6.2.4 Discussion

The present study’s analysis of NKH3/MeP3 ‘slag-skin’ fragments has produced sufficient evidence to reasonably establish their involvement within the on-site copper smelting *chaîne opératoire*. Though the ‘furnaces’ remain to be firmly attributed to a particular production activity. All the technical ceramics appear to have been made from a mineralogically and chemically homogeneous secondary clay, perhaps from one of the local water courses flowing from Khao Phu Kha. Both sets of artefacts have been tempered with organic material, but there is no evidence for further clay modification, the ‘slag-skin’ and ‘furnace’ paste would probably have been identical prior to use.

The existence of complete perforated ceramic cylinders from burials at Nil Kham Haeng (Figure 6.7), and Khao Sai On leaves little doubt the fragments analysed in the present study, containing trace levels of copper (Table 6.5), were associated with copper production

processes at these sites. The established TAP reconstruction (Figure 1.4) would have these cylinders as integral to the NKH3/MeP3 smelting process. However, the relative lack of heat damage suggests these perforated structures were at some distance or somewhat insulated from very high temperatures, considering the very extensive heat exposure of the ‘slag-skins’. Given the lack of a better suggestion (refining, and/or casting) the perforated ‘furnace’ configuration was retained for further testing (Chapter 7)

The NKH3/MeP3 ‘slag-skin’ evidence is consistent with the ceramic fragments having been used to line a shallow pit. The samples appear to have been in direct contact with a high temperature activity, resulting in a heavily slagged and bloated interior surface. Macroscopic copper staining and microscopic copper prills identify the metal being processed, and the analysis of slag phases indicates operating conditions substantially above 1000°C, and in redox conditions suitable for reducing copper ores. The olivine morphology is not consistent with a smelting furnace left to cool slowly, nor a reaction quenched, but perhaps the precipitate digging up of the smelting pit to extract the slag cake is a reasonable explanation and would account for the fragmentary technical ceramics. There is no doubt the ‘furnace’ and ‘slag-skin’ fragments would benefit from further study, the current emphasis having been to establish a solid link between the technical ceramics and the heavily attested copper production activities at Nil Kham Haeng.

6.3 Slag

As per the Non Pa Wai material, the current analytical focus is on understanding past technological choices and identifying styles, though there is always space for more detail given the complexities of slag systems. Although the NKH3/MeP3 slag was morphologically and compositionally more regular than NPW3/MeP2 samples, all external surfaces were cut away and only the remaining core analysed. The present study examined only slag samples from secure NKH3/MeP3 contexts, and resulted in a reasonably cohesive understanding of the *chaîne opératoire* that produced them. Needless to say, more analytical data would be preferable, and it would be very interesting to compare the later Iron Age Nil Kham Haeng material to that from the LoRAP excavation of the nearby and apparently contemporary site of Khao Sai On (Ciarla 2007b).

6.3.1 Macro-analysis

Of the nineteen samples assessed, two (NKHMS11, NKHMS19) were complete ‘slag casts’ (as termed by TAP) and two (NKHMS5, NKHMS18) were fragments thereof. All the other samples are probable fragments of slag cakes, though seven (NKHMS2,

NKHMS10, NKHMS13, NKHMS15, NKHMS17, NKHMS20, NKHMS21) were substantially larger and had a more discernable morphology than the remaining eight (NKHMS3, NKHMS4, NKHMS6, NKHMS7, NKHMS8, NKHMS9, NKHMS12, NKHMS14). The key characteristics of the samples are summarised in Table 6.14, and detailed in Appendix A⁴. The subjective descriptions of Table 6.13 are relative to the KWPV assemblage and not to copper smelting slags generally, in no instance is there a perfectly uniform NKH3/MeP3 slag.

Sample	Mass (g)	Size (mm)	Morphology	Homogeneity	Porosity	Magnetism	Fe stain	Cu stain	Fuel	Viscosity
NKHMS2	265	<140	Crushed slag cake	Low-Medium	Medium	Strong	Strong	Strong	Yes	Medium
NKHMS3	45	<40	Crushed slag cake	Medium-High	Low-Medium	Strong	None	Weak	No	Low-Medium
NKHMS4	45	<50	Crushed slag cake	Medium-High	Low-Medium	Weak	None	Weak	No	Low-Medium
NKHMS5	30	<30	Slag cast fragment	Low-Medium	Medium	Strong	Weak	Strong	No	Medium
NKHMS6	30	<40	Crushed slag cake	Low	High	Strong	None	Strong	No	Medium-High
NKHMS7	30	<50	Crushed slag cake	Medium-High	Low-Medium	Weak	Weak	None	No	Medium
NKHMS8	65	<60	Crushed slag cake	Medium-High	Low-Medium	Strong	Weak	Weak	No	Low-Medium
NKHMS9	150	<70	Crushed slag cake	Medium	Medium	Strong	None	Strong	No	Medium-High
NKHMS10	95	<70	Crushed slag cake	Medium	Low-Medium	Strong	Strong	Strong	No	Medium
NKHMS11	100	<60	Slag cast	Medium-High	Low-Medium	Strong	Weak	Strong	No	Low-Medium
NKHMS12	70	<80	Crushed slag cake	Medium-High	Low-Medium	Strong	None	None	No	Medium
NKHMS13	175	<100	Crushed slag cake	Medium	Medium	Weak	Weak	Weak	Yes	Low-Medium
NKHMS14	125	<60	Crushed slag cake	Medium	Medium	Strong	Weak	Strong	No	Medium
NKHMS15	200	<120	Crushed slag cake	Medium	Medium	Strong	Weak	Weak	Yes	Medium
NKHMS17	110	<80	Crushed slag cake	Medium	Low-Medium	Weak	Weak	Strong	No	Low-Medium
NKHMS18	100	<70	Slag cast fragment	Medium	Low-Medium	Strong	None	Weak	No	Medium
NKHMS19	195	<60	Slag cast	Medium	Medium	Strong	Strong	Strong	Yes	Low-Medium
NKHMS20	150	<70	Crushed slag cake	Medium	Low-Medium	Strong	None	Strong	No	Medium
NKHMS21	140	<90	Crushed slag cake	Medium	Medium	Strong	Weak	Strong	Yes	Medium

Table 6.13 - Macro-characteristics of NKH3/MeP3 slag samples.

⁴ NKHMS1 was subsequently renamed NPWMS21 due to a labelling error. NKHMS16 was excluded due to severe analytical problems caused by a poorly pressed pellet, and there being insufficient material to make a second.

There are two distinct primary slag morphologies in the assemblage: cakes and casts. The ‘slag casts’ were so named because their consistent dimensions and cylindrical shape strongly suggests they formed in a mould of some sort (Figure 6.22). The complete examples range from c. 5cm to c. 6cm in diameter and from c. 50g to c. 100g in mass. The slag-cast fragments appear to be broken rather than crushed, and range in diameter between c. 3cm and c. 4cm, and in mass from c. 20g to c. 30g. How slag was potentially transferred into a mould is unclear given the scarcity of NKH3/MeP3 crucibles.



Figure 6.22 - NKHMS19 (top) and inverted (bottom), examples of NKH3/MeP3 ‘slag casts’. Images: author.

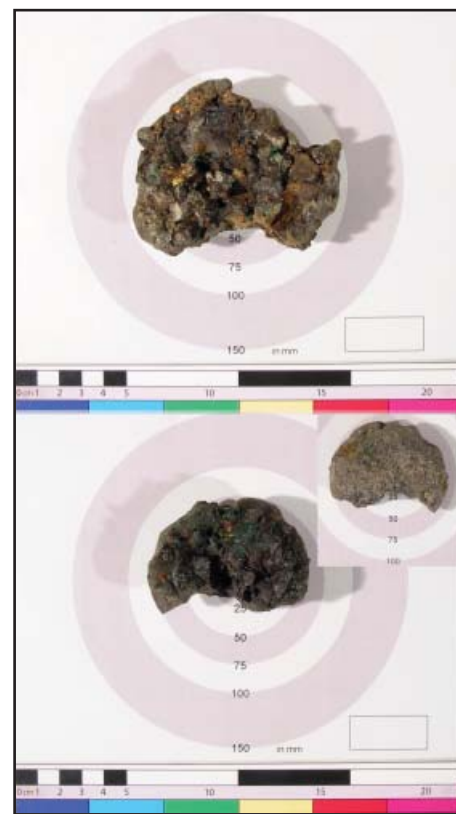


Figure 6.23 - NKHMS15 (top) and NKHMS17 (bottom - inverse inset), examples of NKH3/MeP3 slag cakes. Images: author.

The dimensions of the most complete slag cakes would reconstruct a complete example of c. 7cm to c. 10cm in diameter and up to 0.5kg in mass (Figure 6.23). The cakes are roughly plano-convex, but the uniform underside of NKHMS17 (Figure 6.23 inset) would suggest they solidified on a prepared surface, perhaps correlating to the ‘slag-skin’ ceramic pit linings (see above). The slag cake fragments range in diameter from c. 2cm to c. 5cm and have a mass of several tens of grammes (Figure 6.24). Especially with respect to the NKH3/MeP3 matrix’s uniformity, the relatively standardised size distribution of the slag cake fragments may be regarded as evidence of deliberate crushing at later Iron Age Nil Kham Haeng. This was presumably done to mechanically extract copper prills, but may also be indicative of preparing the slags for re-smelting.

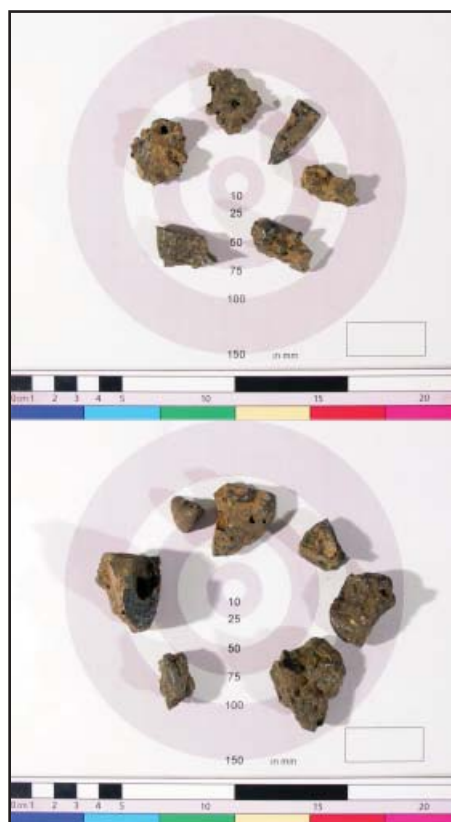


Figure 6.24 - NKHMS8 (top) and NKHMS14 (bottom), examples of crushed NKH3/MeP3 slag cakes. Images: author.

In section, both the slag-cakes and the slag casts are relatively homogeneous, with most of the unreacted mineral, ceramic, and charcoal inclusions confined to the surfaces, though, notwithstanding the limited sample population, the slag cakes seem slightly less homogeneous overall. The slag textures are generally crystalline, although there are instances of glassiness, particularly on the slag-casts (Figure 6.22).

Considering the local deposits of high quality iron oxide at Khao Tab Kwai, it is possible iron smelting residues are intermixed in the NKH3/MeP3 deposit. A measure of rusty staining (12 of 19) and magnetism (19 of 19) is common within the sampled slag assemblage, representing the presence of iron compounds, and especially $\text{Fe}^{2+/3+}$ ions. However, iron compounds are a normal component of copper smelting slags, and the recurrent green staining (17 of 19) of the samples indicates copper was without doubt the desired metal product.

As the original TAP excavators testify (Roberto Ciarla and Vincent Pigott pers. comm.), it is not easy to explain the presence of two separate, though probably related slag morphologies in NKH3/MeP3 contexts. There is therefore the strong possibility of

interpretive blurring across the assemblage, which was monitored throughout the present study. However, there is at present no more convincing explanation for the presence of both cake and cast morphologies than the re-smelting of slags. Considering the slightly more homogeneous texture of the slag-casts, it may be that these were the reprocessed slags, and the cakes were either awaiting crushing or rejected from reprocessing. This macroscopic interpretation is acknowledged to be extremely tentative, and there are no signs of a ‘meniscus’ separation of metal and slag. Though the later Iron Age Nil Kham Haeng copper smelting *chaîne opératoire* appears to be more intensive and proficient than that at early Iron Age Non Pa Wai, there is no suggestion of any inevitability in this development, which largely reflects the varying social context of metal production in the Khao Wong Prachan Valley, though the long-term exploitation of local deposits may have altered the mineral suite available to later Iron Age metalworkers.

6.3.2 Bulk Chemistry

The slag samples from Non Pa Wai were prepared for [P]ED-XRF bulk chemical analysis and the resulting data processed as per the methodology detailed in Chapter 4. Complete chemical data may be seen in Appendix B (Table B.8). These data cannot be used to assess intra-sample variability as only one bulk analysis was performed per sample. However, the slag bulk chemistry is of use for evaluating variation between slags and preliminarily interpreting what the patterning may mean in terms of collective technological choices in NKH3/MeP3 smelting.

The NKH3/MeP3 slags have a mean major oxide composition of 45.1wt% iron oxide, 31.3wt% silica, 11.8wt% calcia, 5.5wt% alumina (Table 6.14). Iron oxide has the lowest CV at 14%, and an average coefficient of 23% for the major slag-forming components suggests a reduced degree of chemical variability in the slag assemblage when compared with Non Pa Wai (Table 5.13). The mean minor oxides - magnesia (1.1wt%), soda (0.5wt%), manganese oxide (0.4wt%), potash (0.3wt%), phosphorous pentoxide (0.2wt%), and titania (0.2wt%) - have a mean CV of 41%, further indicating increased assemblage compositional uniformity compared with Non Pa Wai. The NKH3/MeP3 slags also contain on average 1.8wt% sulphates⁵ and 1.7wt% of copper oxide, and these constituents also have a more even distribution amongst the samples with CVs of 72% and 42% respectively. All of the above data are suggestive of increasingly standardised smelting practices, relating to lower variation in copper smelting materials and/or improved techniques at later Iron Age Nil Kham Haeng when compared to early Iron Age Non Pa Wai (Chapter 5).

5 Reported copper and sulphur is likely to be present as both oxide and element.

	Na ₂ O	MgO	Al ₂ O ₃	SiO ₂	P ₂ O ₅	SO ₃	K ₂ O	CaO	TiO ₂	MnO	FeO	CuO	Total
	wt%	wt%	wt%	wt%	wt%	wt%	wt%	wt%	wt%	wt%	wt%	wt%	wt%
NKHMS2	0.7	0.6	4.3	30.4	0.4	4.5	0.3	8.8	0.2	0.3	46.7	2.8	94.6
NKHMS3	0.5	2.3	7.7	27.5	0.2	0.8	0.4	13.5	0.3	0.4	45.3	1.0	94.8
NKHMS4	0.5	0.7	6.1	29.8	0.4	3.2	0.3	8.2	0.2	0.4	47.8	2.3	97.9
NKHMS5	0.4	0.8	3.5	24.3	0.1	1.2	0.2	8.9	0.1	0.3	58.5	1.4	93.7
NKHMS6	0.5	1.0	3.4	31.8	0.1	1.3	0.3	16.8	0.1	0.2	42.7	1.7	96.1
NKHMS7	0.4	0.9	3.0	32.4	0.0	0.9	0.0	4.9	0.0	0.2	55.2	1.8	94.5
NKHMS8	0.2	1.6	4.6	39.9	0.3	1.0	0.2	12.1	0.1	0.6	38.5	0.8	96.0
NKHMS9	0.5	0.8	5.3	38.5	0.4	1.7	0.4	9.5	0.1	0.3	41.5	1.0	97.4
NKHMS10	0.5	0.9	7.1	26.8	0.1	1.9	0.3	12.1	0.2	0.4	47.4	2.0	93.0
NKHMS11	0.5	1.1	5.5	37.1	0.0	0.7	0.1	15.6	0.1	0.6	37.5	1.0	93.4
NKHMS12	0.5	1.3	7.1	31.5	0.3	0.4	0.5	12.1	0.2	0.5	44.3	1.3	94.0
NKHMS13	0.6	0.8	7.5	32.1	0.2	4.5	0.5	6.6	0.3	0.3	43.8	2.6	94.8
NKHMS14	0.4	1.7	6.7	28.3	0.1	0.9	0.3	20.3	0.2	0.4	39.3	1.2	93.8
NKHMS15	0.5	0.8	5.5	33.0	0.2	3.7	0.5	5.9	0.2	0.3	47.8	1.6	96.3
NKHMS17	0.5	1.5	6.8	35.3	0.4	1.3	0.6	12.9	0.2	0.4	38.9	1.0	90.9
NKHMS18	0.7	1.1	6.4	34.6	0.1	1.2	0.6	16.6	0.2	0.2	34.7	2.9	92.1
NKHMS19	0.5	0.7	3.3	23.9	0.1	3.3	0.2	12.5	0.1	0.2	52.3	2.7	96.7
NKHMS20	0.4	0.6	5.5	27.1	0.3	1.0	0.3	9.3	0.2	0.3	52.3	2.6	92.3
NKHMS21	0.3	0.9	4.7	30.4	0.1	1.0	0.4	18.0	0.1	0.3	42.5	1.2	91.5
mean	0.5	1.1	5.5	31.3	0.2	1.8	0.3	11.8	0.2	0.4	45.1	1.7	
std dev	0.1	0.4	1.5	4.5	0.1	1.3	0.1	4.3	0.1	0.1	6.3	0.7	
CV	25%	42%	28%	14%	63%	72%	43%	36%	39%	32%	14%	42%	

Table 6.14 - [P]ED-XRF bulk chemical analyses of NKH3/MeP3 slag, selected major and minor oxides after data normalisation, analytical total presented.

The mean trace element data for the NKH3/MeP3 slags indicates zinc is the preminent (909ppm), though somewhat irregular (CoV 86%) element (Table 6.15). Other significant traces include strontium (322ppm, CoV 106%) and barium (97ppm, CoV 87%), whose levels are approximately double that of the Non Pa Wai slags, possibly indicating an increased ceramic contribution in the NKH3/MeP3 technology (see below). Arsenic continues to be almost absent (<10ppm, CoV 127%) but tin levels of up to 94ppm (mean 27ppm, CoV 102%) are significantly higher than those at Non Pa Wai. Given the local geology remains the same, it is possible the slags' tin content can be explained by the introduction of foreign (extra-Khao Wong Prachan Valley) minerals or metals into the later Iron Age Nil Kham Haeng copper production system.

Although the copper levels are relatively low, the lack of correlation with iron oxide ($R^2 = 0.089$, Figure 6.25) suggests metal losses in the slag are probably related to unreacted minerals rather than magnetite formation (Davenport *et al.* 2002), though to a lesser extent than NPW3/MeP2 slag. Sulphur shows a weak positive relationship with copper ($R^2 = 0.359$, Figure 6.26), suggesting matte phases may be present in NKH3/MeP3 slags.

	Zn	As	Sr	Sn	Ba
	ppm	ppm	ppm	ppm	ppm
NKHMS2	817	<10	273	94	89
NKHMS3	452	<10	178	<10	54
NKHMS4	804	28	262	74	129
NKHMS5	980	12	171	22	33
NKHMS6	746	<10	193	52	48
NKHMS7	903	10	133	<10	8
NKHMS8	830	22	377	50	204
NKHMS9	691	10	417	60	181
NKHMS10	2502	20	377	13	7
NKHMS11	881	<10	455	23	9
NKHMS12	422	<10	348	<10	91
NKHMS13	654	10	161	43	86
NKHMS14	376	<10	210	<10	71
NKHMS15	484	<10	186	31	108
NKHMS17	580	<10	394	13	159
NKHMS18	3542	<10	1649	20	335
NKHMS19	620	10	110	10	14
NKHMS20	615	10	87	<10	166
NKHMS21	375	<10	137	12	81
mean	909	7	322	27	97
std dev	786	9	341	28	85
CV	86%	127%	106%	102%	87%

Table 6.15 - [P]ED-XRF bulk chemical analyses of NKH3/MeP3 slag, selected elements after data normalisation.

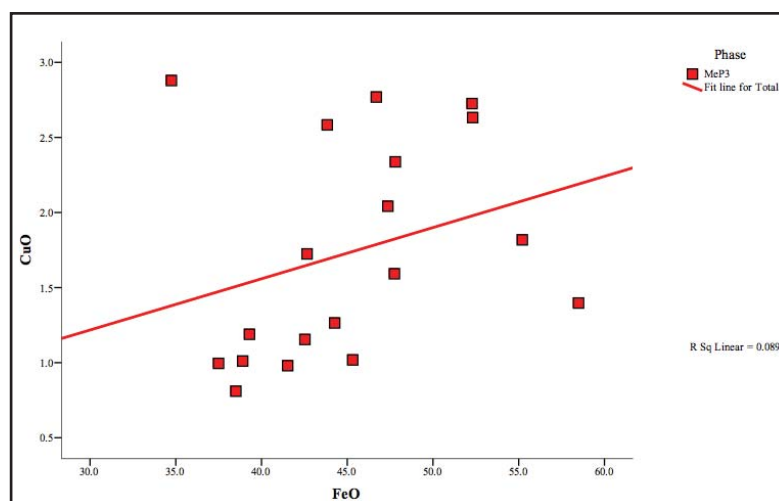


Figure 6.25 - Scatter plot of NKH3/MeP3 slag samples [P]ED-XRF bulk chemical data - sulphates versus copper oxide.

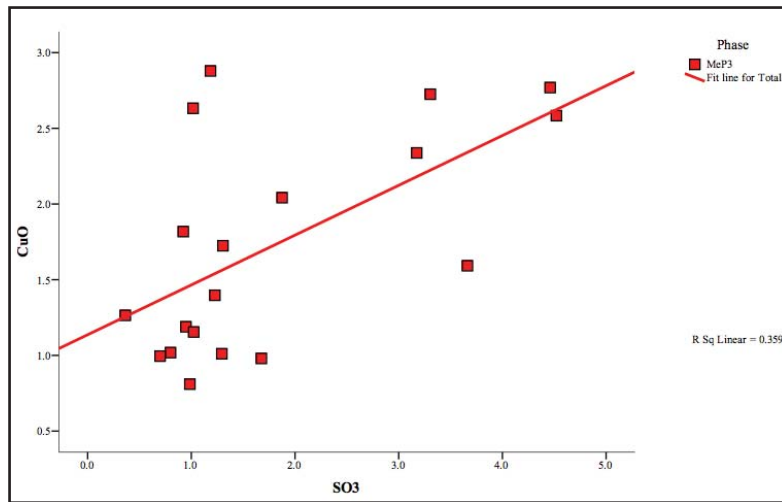


Figure 6.26 - Scatter plot of NKH3/MeP3 slag samples [P]ED-XRF bulk chemical data - iron oxide versus copper oxide.

Correlation Matrix

		SiO2	CaO	FeO
Correlation	SiO2	1.000	.009	-.681
	CaO	.009	1.000	-.619
	FeO	-.681	-.619	1.000

Figure 6.27 - Correlation matrix of NKH3/MeP3 slag sample [P]ED-XRF bulk chemical data - silica, calcia, and iron oxide.

The correlation matrix for the three major slag forming oxides (Figure 6.27) shows that, as per the NPW3/MeP2 process, the concentrations of silica and calcia are negatively correlated to the amount of iron oxide, suggesting ferruginous matter entered the smelting system independent of the former. However, in striking contrast to the NPW3/MeP2 process, calcia and silica do not seem to be correlated at all. This result possibly indicates two separate gangue additions, but also the probably significant contribution of fuel ash, especially considering the elevated levels of magnesia and potash in the samples (Table 6.15 and cf. Jackson *et al.* 2005, Merkel 1990, Rehren *et al.* 2007). This situation could result from a higher fuel to mineral ratio in the smelting charge, and/or that the smelt was hotter, and/or was of a longer duration.

Due to their significant textural heterogeneity and occasional unreacted phases, the NKH3/MeP3 slag bulk chemical data are not suitable for the temperature and redox conditions of the later Iron Age smelting operation, however, these estimates are provided below in the micro-analytical section.

6.3.3 Micro-analysis

The macro and bulk analysis slag population was sub-sampled for further study by OM and SEM-EDS. These samples were originally selected by grouping the PCA distribution of bulk compositional data of slags from both NPW3/MeP2 and NKH3/MeP3 contexts into clusters representing extreme, normal, and overlapping examples of each sites' slag composition (Pryce & Pigott 2008: Figure 13). From Nil Kham Haeng these were NKHMS4, NKHMS5, NKHMS7, NKHMS13, NKHMS17, and NKHMS18.

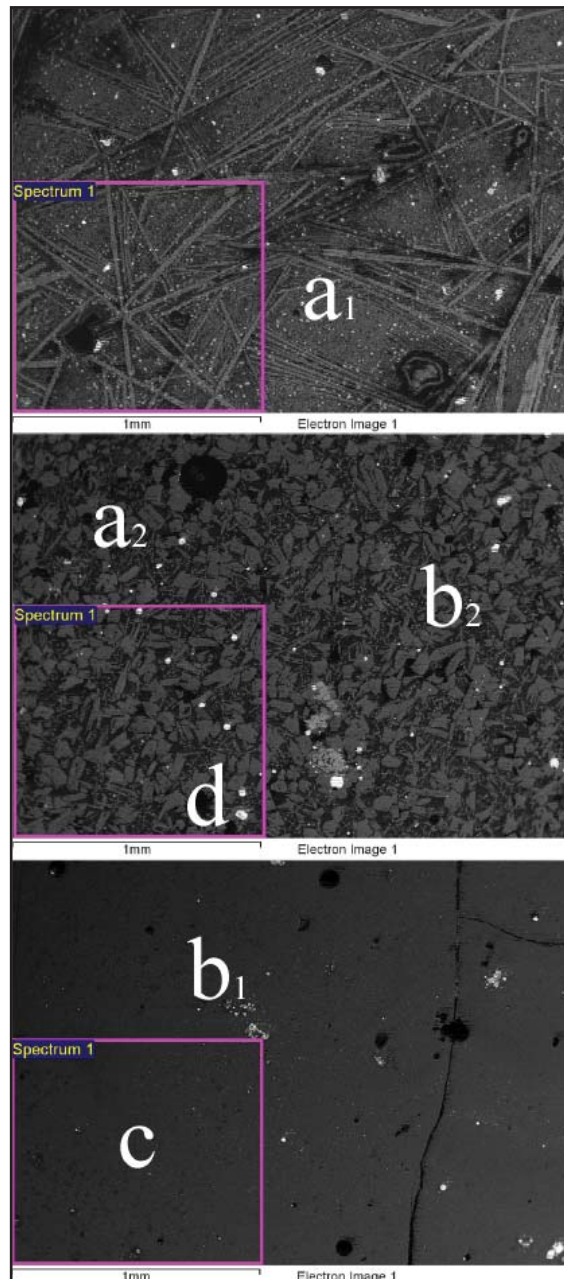


Figure 6.28 - NKHMS4 (top), NKHMS7 (centre) and NKHMS18 (bottom) slag micro-features, all at 50x, by SEM-BSE. Labels 'a₁' olivine skeletons, 'a₂' olivine euhedrals, 'b₁' residual iron oxides, 'b₂' primary iron oxides, 'c' slag glass, 'd' prills, 'Spectrum 1's are exemplar of 1mm² EDS area scans. Images: author.

Sample	Olivine skeletons	Olivine euhedrals	Olivine dendrites	Iron oxide euhedrals	Iron oxide dendrites	Iron oxide (residual)	Siliceous gangue	Slag glass	Prills
NKHMS4	X			X		X	X	X	X
NKHMS5	X			X		X	X	X	X
NKHMS7		X			X	X	X	X	X
NKHMS13	X			X		X	X	X	X
NKHMS17			X		X	X	X	X	X
NKHMS18						X	X	X	X

Table 6.16 - Micro-characteristics of NKH3/MeP3 slag samples.

The microstructures of the NKH3/MeP3 slags assessed are composed of six major components: skeletal (a1) and euhedral (a2) olivine crystals, residual iron oxide (b1), primary iron oxide crystals (b2), glass (c), and metallic prills (d) (Table 6.17, Figure 6.28). NKHMS17 and NKHMS18 are notable for having a cryptocrystalline matrix though they have different macro-morphologies.

Slag crystals - The NKH3/MeP3 slags contain skeletal (NKHMS4, NKHMS5, NKHMS13), and euhedral (NKHMS7, NKHMS17) crystalline habits. The elongate skeletons range in width from c. 0.005mm to c. 0.3mm, and in length from c. 0.05mm to c. 1mm (Figure 6.28 & Figure 6.29). The euhedral crystals range in diameter between c. 0.02mm and c. 0.2mm in NKHMS7 (Figure 6.30), and from c. 0.01mm to c. 0.05mm in NKHMS17 (Figure 6.31). There is no discernable correlation between slag macro-morphology and microstructure - both 'cast' and 'cake' slags exhibit both skeletons and euhedral crystals. Therefore, the presence of multiple crystal morphologies is most likely related to differing formation conditions and/or cooling rates between the samples, but all share olivine morphological and compositional characteristics (Donaldson 1976), again indicating variable redox conditions within the smelt (Kongoli & Yazawa 2001: 585).

By SEM-EDS spot analyses, the major chemical components of the olivines are FeO (mean 63.4wt%), SiO₂ (mean 27.5wt%), CaO (mean 5.0wt%), MgO (mean 1.8wt%), Al₂O₃ (mean 1.6wt%), and MnO (mean 0.5wt%) (Table 6.17). The CVs for iron oxide and silica (15%, 4%) are lower than the NPW3/MeP2 equivalents (Table 5.16) and suggest comparative uniformity in olivine composition between NKH3/MeP3 samples. The minor oxides show high variability (CVs: 100%, 19%, 206%, and 61%) but much of this stems from NKHMS17, where the electron beam may have caused excitation in the glassy phase around and below the tiny crystals. The data do not indicate a significant chemical difference between the skeletal and euhedral habits.

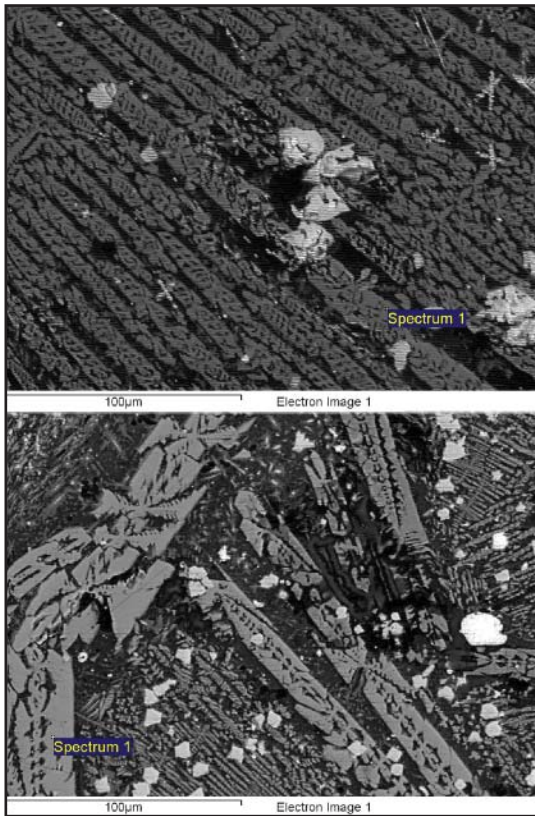


Figure 6.29 - NKHMS5 (top) and NKHMS13 (bottom) olivine skeletons (grey), both at 500x, by SEM-BSE. 'Spectrum 1's are exemplar EDS spot analyses. Images: author.

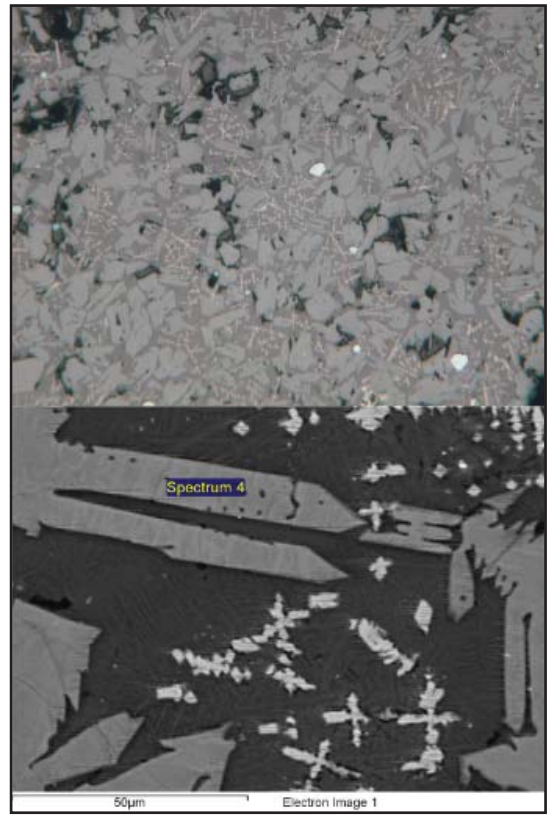


Figure 6.30 - NKHMS7 olivine euhedral crystals under plane polarised light at 50x (top) and by SEM-BSE at 1000x (bottom). 'Spectrum 1' is an exemplar EDS spot analysis. Images: author.

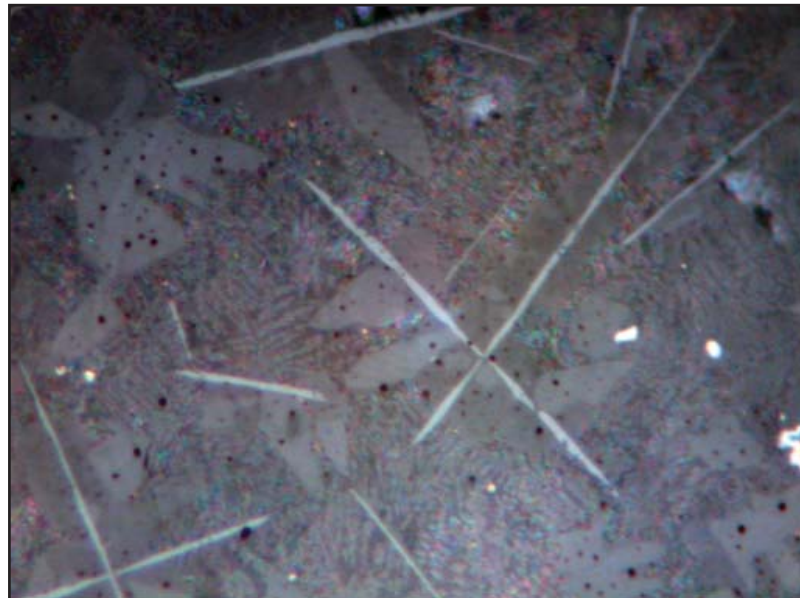


Figure 6.31 - NKHMS17 olivine euhedrals and denrities (mid-grey) with acicular magnetite under plane polarised light at 1000x, width of field is 0.1mm. Image: author.

	MgO	Al ₂ O ₃	SiO ₂	CaO	MnO	FeO	Total	Fe/SiO ₂
	wt%	wt%	wt%	wt%	wt%	wt%	wt%	wt ratio
NKHMS4	2.2	0.0	27.6	3.4	0.8	66.1	95.4	1.9
NKHMS5	1.9	0.0	27.5	5.7	0.7	64.1	94.5	1.8
NKHMS7	1.4	0.0	27.7	0.7	0.0	70.2	87.9	2.0
NKHMS13	2.1	0.5	25.7	1.9	0.6	69.2	89.9	2.1
NKHMS17	1.6	7.6	28.8	13.2	0.5	47.4	93.0	1.3
mean	1.8	1.6	27.5	5.0	0.5	63.4		
std dev	0.3	3.4	1.1	5.0	0.3	9.3		
CV	19%	206%	4%	100%	61%	15%		

Table 6.17 - SEM-EDS phase analyses of NKH3/MeP3 olivine crystals, selected major and minor oxides after data normalisation, analytical total presented.

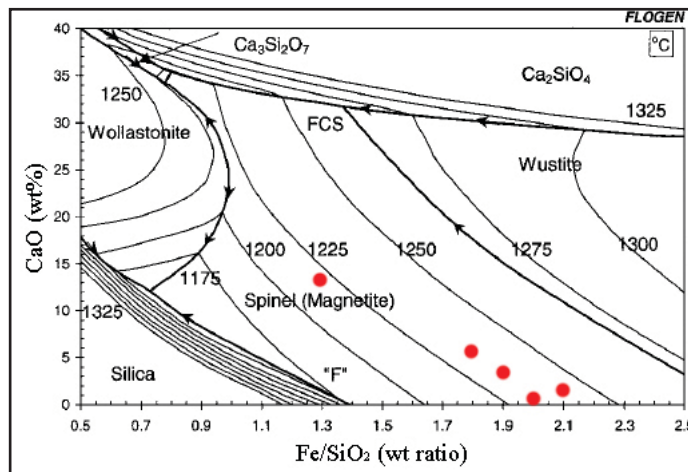


Figure 6.32 - SEM-EDS analyses of olivine phases plotted on a Floggen binary chart for slag system at a 10^{-8} ppO₂ and with 1wt% MgO. Image adapted from Kongoli & Yazawa 2001: Figure 15.

In this instance, the consistently predominant quaternary oxide is magnesia, and thus the Fe/SiO₂ ratio is plotted against CaO on a binary Floggen diagram, calculated for 1wt% MgO (Kongoli & Yazawa 2001: Figure 15), indicating the spinel phases began to crystallise between c. 1220°C and c. 1245°C, with a mean precipitation temperature of c. 1235°C (Figure 6.32).

Magnetite - Euhedral and dendritic iron oxide crystals are common within the NKH3/MeP3 slags assessed, the former in NKHMS4, NKHMS5, and NKHMS13, and the latter in NKHMS7 and NKHMS17 (and possibly more given their small size) (Figure 6.33). The dimensions for the euhedral habit range from c. 0.05mm to c. 0.2mm, and the dendrites range from c. 0.005mm to c. 0.05mm. Both phases are identified as magnetite spinel due to their optical behaviour and angularity (Ineson 1989).

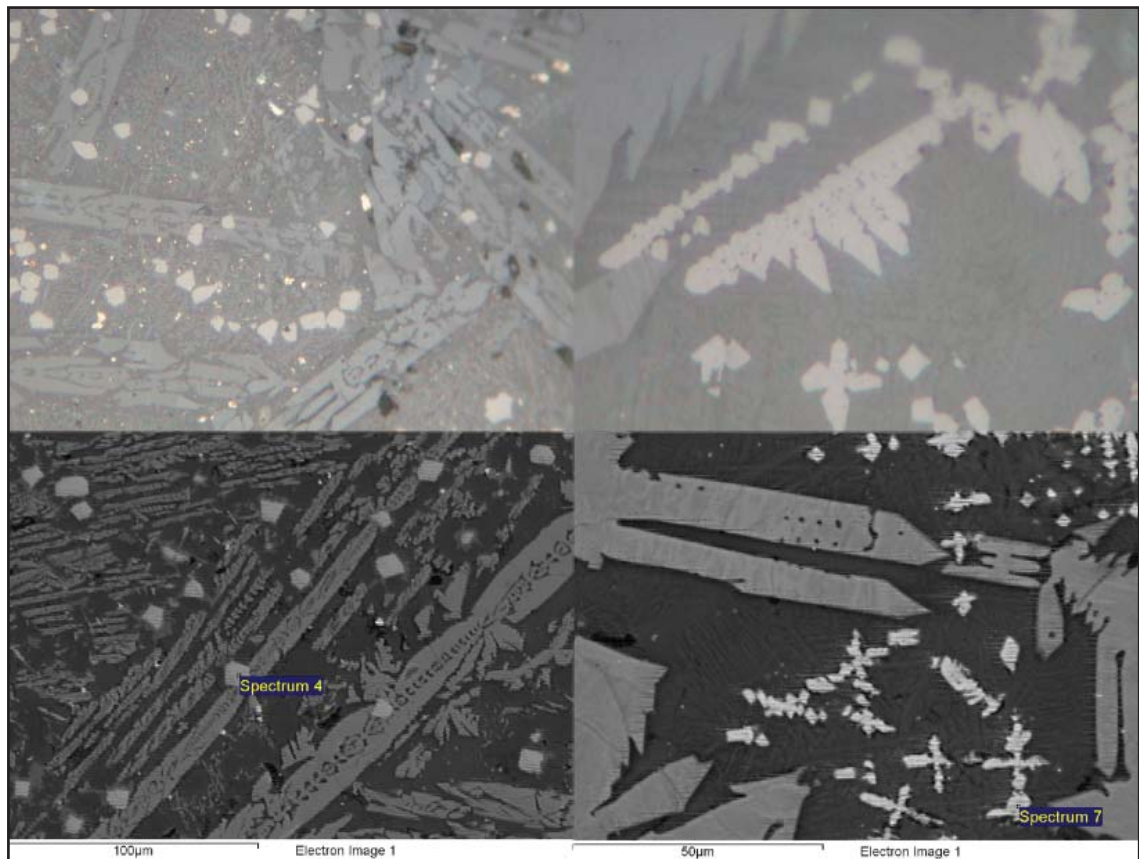


Figure 6.33 - Magnetite spinel euhedral crystals (bright) in NKHMS13 under plane polarised light (top left) and by SEM-BSE (bottom left) both at 500x, dendrites in NKHMS7 under plane polarised light (top right) and by SEM-BSE (bottom right) both at 1000x. Images: author.

	Al ₂ O ₃	SiO ₂	CaO	TiO ₂	FeO	Total	Fe/SiO ₂
	wt%	wt%	wt%	wt%	wt%	wt%	wt ratio
NKHMS4	4.9	2.6	0.9	1.5	90.1	92.1	27.1
NKHMS5	3.6	2.8	1.5	0.5	91.6	92.3	25.2
NKHMS7	1.9	9.3	1.8	0.0	87.1	91.3	7.3
NKHMS13	6.9	2.0	0.5	2.3	88.3	88.6	34.8
mean	4.3	4.2	1.2	1.1	89.2		
std dev	2.1	3.4	0.6	1.0	2.0		
CV	49%	82%	49%	95%	2%		

Table 6.18 - SEM-EDS phase analyses of NKH3/MeP3 magnetite spinel crystals, selected major and minor oxides after data normalisation, analytical total presented.

SEM-EDS spot analyses indicate the principal chemical components of the primary magnetite phases are FeO⁶ (mean 89.2wt%), Al₂O₃ (mean 4.3wt%), SiO₂ (mean 4.2wt%), and CaO (mean 1.2wt%), and TiO₂ (mean 1.1wt%) (Table 6.18). Binary Floggen diagrams are not available for very high Fe/SiO₂ ratios, but a ternary plot calculated for intermediate

6 The quantity of FeO is correct for wüstite precipitations, but slightly inaccurate for magnetite (Fe₃O₄).

oxygen partial pressures indicates the magnetite phases would begin to precipitate at around 1300°C (Kongoli & Yazawa 2001: Figure 6). This would suggest the primary (not residual mineral) magnetite crystallised before the olivine, which could, with the exception of NKHMS17, account for the relatively uniform and pure composition, with a low CV for iron oxide (2%) and only minor contaminants.

Residual minerals - In parallel with the NKH3/MeP3 ‘slag-skins’, the microscopically examined slags contained inclusions of angular to sub-rounded porous residual magnetite, even in the glassy matrices of NKHMS17 and NKHMS18 (Figure 6.34). These fragments vary from entirely unreacted to partially dissolved and re-crystallised ‘pseudomorphs’, and have dimensions ranging from fractions of a millimetre to millimetres. SEM-EDS spot analyses indicate the main chemical components of the residual magnetite phases are FeO⁷ (mean 93.4wt%), SiO₂ (mean 3.4wt%), Al₂O₃ (mean 1.5wt%), CuO (mean 0.9wt%), and SO₃ (mean 0.8wt%) (Table 6.19).

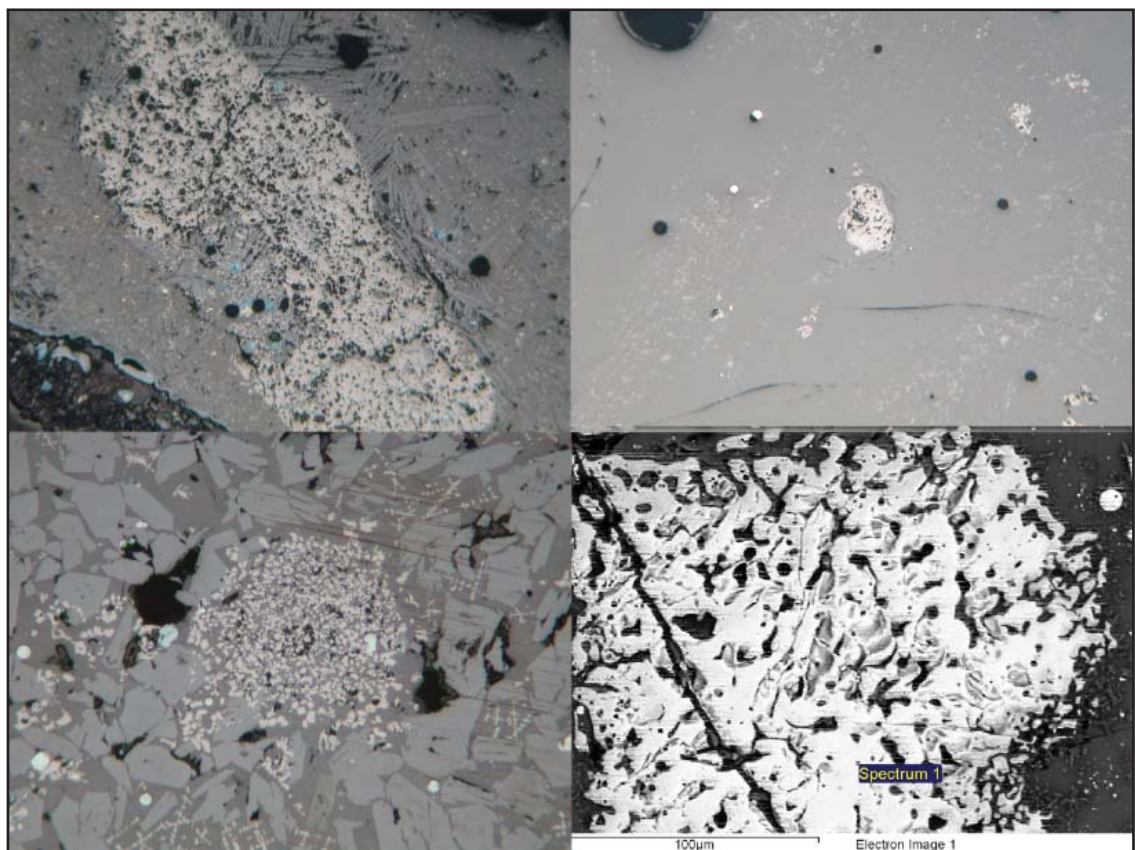


Figure 6.34 - Residual magnetite in NKHMS13 (top left), NKHMS7 (bottom left - a ‘pseudomorph’), and NKHMS18 (top right) under plane polarised light, all at 50x, and in NKHMS18 (bottom right) by SEM-BSE at 500x. ‘Spectrum 1’ exemplar of an SEM-EDS spot analysis. Images: author.

7 See footnote 6.

	Al ₂ O ₃	SiO ₂	SO ₃	FeO	CuO	Total Fe	Fe/SiO ₂
	wt%	wt%	wt%	wt%	wt%	wt%	wt ratio
NKHMS4	1.5	0.8	0.0	97.2	0.5	93.8	91.4
NKHMS5	0.7	10.9	3.1	82.5	2.9	77.2	5.9
NKHMS13	3.6	0.5	0.0	95.7	0.2	90.8	147.8
NKHMS18	0.5	1.2	0.0	98.3	0.0	90.1	63.0
mean	1.5	3.4	0.8	93.4	0.9		
std dev	1.4	5.0	n.a	7.4	1.3		
CV	92%	150%	n.a	8%	146%		

Table 6.19 - SEM-EDS phase analyses of NKH3/MeP3 residual magnetite, selected major and minor oxides after data normalisation, analytical total presented.

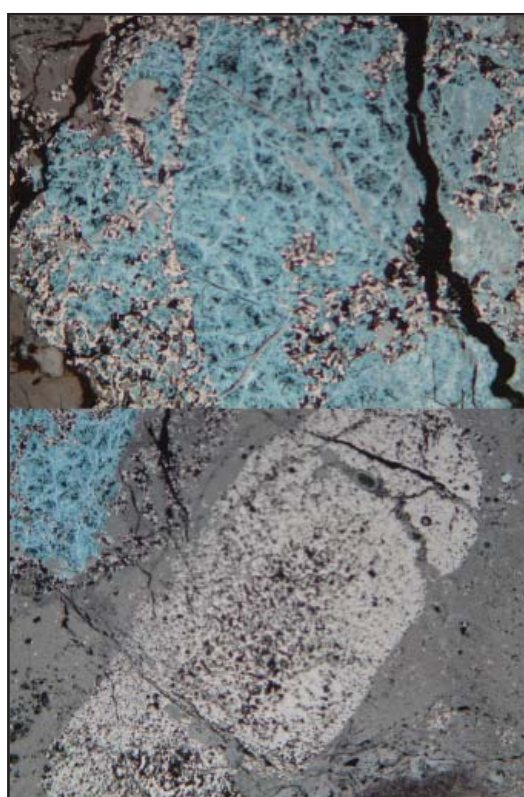


Figure 6.35 - Residual magnetite with and without intergrown covellite in NKHMS5 under plane polarised light, both at 50x. Images: author.

There is a strong correspondence between magnetite and sulphidic copper, as frequently evidenced by metallic phases embedded within the residual mineral (Figure 6.34). However, magnetite inclusions within NKHMS5 appear to be intermittently intergrown with covellite, and immediately adjacent to magnetite with no evidence of sulphur (Figure 6.35). The covellite is unlikely to be residual but probably represents chalcopyrite altered by the smelting process and/or burial conditions. Nevertheless, the intimate association between copper, iron, and sulphur suggests this relationship extends back to the original mineralisation, a very common occurrence, such as at nearby Khao Tab Kwai where plentiful magnetite can be found in immediate proximity to sulphidic and oxidic copper

minerals (Vernon 1988). Magnetite from Khao Tab Kwai has not yet been studied microscopically, but bulk analysis of one sample indicated very low levels of titania (c. 0.1wt%), not incompatible with magnetite seen in the NPW3/MeP3 slags, and further increasing the likelihood of the metallogenic outcrop being a later Iron Age mineral source in the Valley. No sign of martitisation was noted in any of the magnetite inclusions (cf. Chapter 5), though this is normally hard to detect.

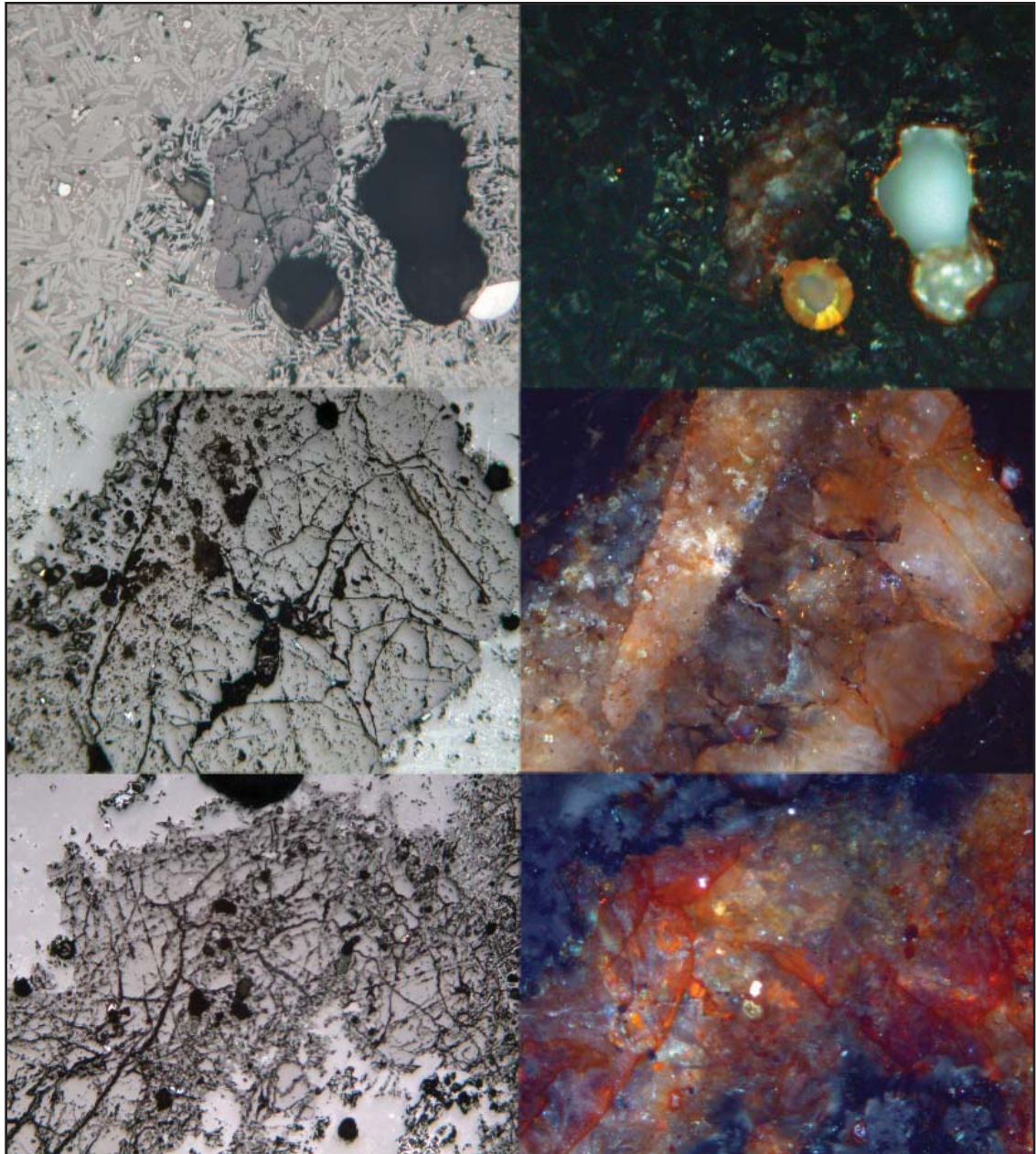


Figure 6.36 - Residual quartz inclusions in NKHMS7 (top), NKHMS13 (centre), and NKHMS17 (bottom) under plane polarised light (left) and crossed polars (right), all at 50x. Images: author.

Occasional large fragments of residual mineral quartz are seen in the slag samples, with dimensions up to c. 2mm (Figure 6.36). The quartz does not seem to be pure, and is regularly contaminated with iron and some copper. The presence of both oxidic and sulphidic copper minerals with siliceous and ferruginous gangue suggests either the

exploitation of multiple mineralisations, or a single one hosting all species, as seen at Khao Tab Kwai. It should be stressed that although the NKH3/MeP3 slags contain some large residual mineral fragments, they are the exception within an otherwise well-reacted melt, as contrasted with NPW3/MeP2 slags where the opposite situation presides. It should be noted, despite the small sample population, the absence of residual calcareous inclusions suggests that the relatively high CaO derives from another source such as fuel ash and/or ceramic degradation.

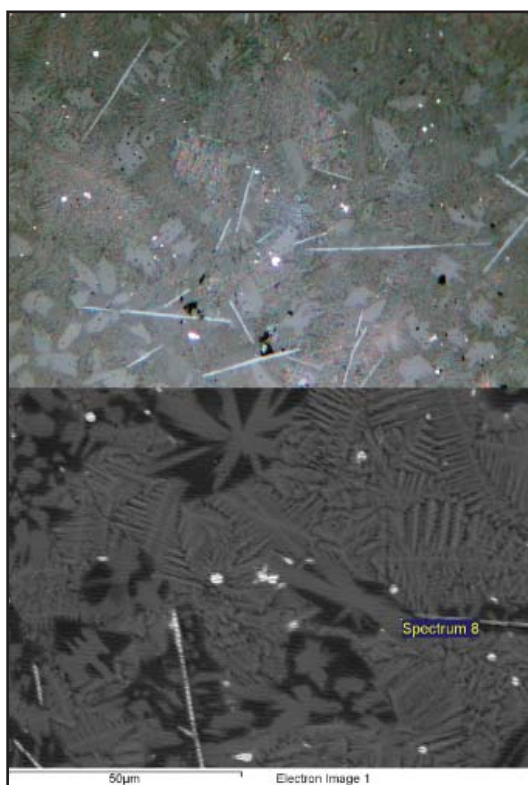


Figure 6.37 - Cryptocrystalline glass with feathery dendrites in NKHMS17 under plane polarised light (top) and by SEM-BSE (bottom), both at 500x. Images: author.

Slag glass - Binding the NKH3/MeP3 slags is an interstitial glass, displaying cryptocrystallinity in the form of feathery dendrites at high magnifications (Figure 6.37). SEM-EDS spot analyses indicate the major chemical components of this phase are SiO_2 (mean 39.8wt%), FeO (mean 33.1wt%), CaO (mean 18.2wt%), Al_2O_3 (mean 6.8wt%), MgO (mean 0.7wt%), and SO_3 (mean 0.6wt%) (Table 6.21). The respective CVs (11%, 3%, 16%, 22%, 150% and 153%) suggests the interstitial glass was relatively uniform between samples in its major and minor oxides, with the extensive variation being limited to magnesia and sulphates. Plotting the data on a Flogen diagram calculated for 7wt% alumina (Kongoli & Yazawa 2001: Figure 11) indicates the slag glass would have begun to solidify between c. 1130°C and c. 1195°C, with a mean precipitation temperature of c. 1175°C (Figure 6.38). The precipitation temperatures are below those for the olivine and the magnetite spinel, suggesting the glass was the last major phase to form as the

slag cooled. The composition of this phase would have been determined by the prior formation of olivine and magnetite spinel, and the glass is enriched in calcia and other minor oxides.

	MgO	Al ₂ O ₃	SiO ₂	SO ₃	CaO	FeO	Total	Fe/SiO ₂
	wt%	wt%	wt%	wt%	wt%	wt%	wt%	wt ratio
NKHMS4	0.8	6.0	39.1	0.0	21.8	32.1	90.7	0.6
NKHMS5	0.2	6.6	37.0	1.0	20.0	34.4	91.1	0.7
NKHMS7	0.0	5.8	47.5	0.0	14.6	32.1	82.9	0.5
NKHMS13	0.0	9.4	37.1	2.2	15.9	33.6	81.9	0.7
NKHMS17	2.4	6.1	38.4	0.0	18.8	33.3	91.4	0.7
mean	0.7	6.8	39.8	0.6	18.2	33.1		
std dev	1.0	1.5	4.4	1.0	2.9	1.0		
CV	150%	22%	11%	153%	16%	3%		

Table 6.20 - SEM-EDS phase analyses of NKH3/MeP3 slag glass, selected major and minor oxides after data normalisation, analytical total presented.

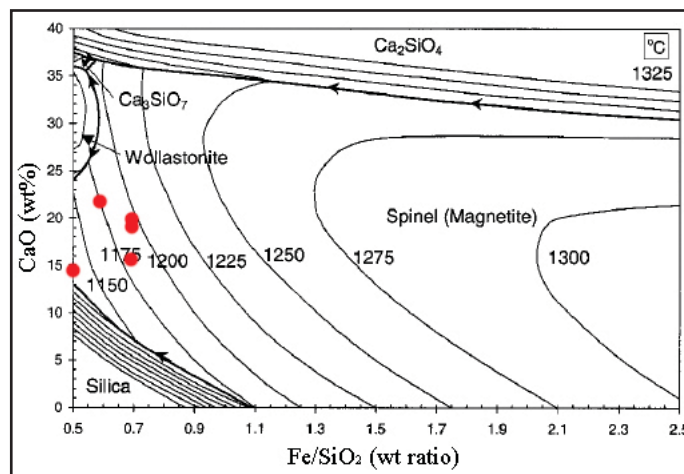


Figure 6.38 - SEM-EDS analyses of glass phases plotted on a Flögen binary chart for slag system at a 10^{-8} ppO₂ and with 7wt% Al₂O₃. Image adapted from Kongoli & Yazawa 2001: Figure 11.

Slag prills - Highly reflective metallic prills are common in the NKH3/MeP3 slags, and range in diameter between c. 0.001mm and c. 1mm, though there is some bimodality to their distribution, with a larger number of tiny specks and a few much larger prills (Figure 6.39). Optically, copper, matte, and intermediary phases are present, which is confirmed by SEM-EDS analyses indicating a mean composition of copper (68.1wt%), sulphur (19.0wt%), and iron (12.7wt%). Only one prill in NKHMS18 contains detectable levels of nickel (Table 6.21). The CVs (29%, 48%, 119% respectively for the major elements) suggest prills of copper sulphide are more common than those of iron-copper-sulphide.

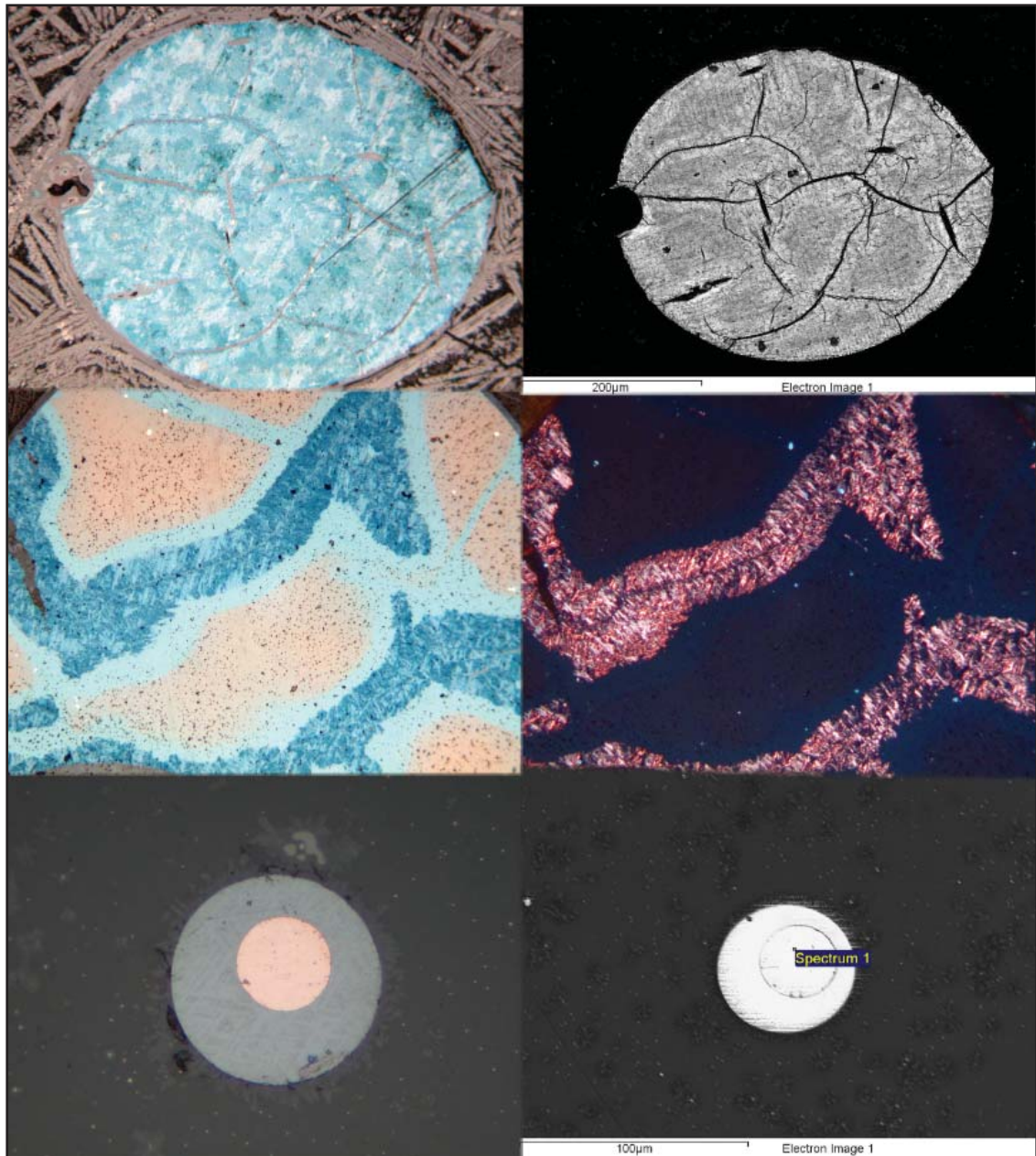


Figure 6.39 - Copper and matte prills in NKHMS13 (top at 500x), NKHMS17 (centre at 200x), and NKHMS18 (bottom at 500x) under plane polarised light (left), and by SEM-BSE (right), excepting the centre-right image under crossed polars. Images: author.

	S	Fe	Ni	Cu	Total
	wt%	wt%	wt%	wt%	wt%
NKHMS4	23.1	10.8	0.0	66.1	99.8
NKHMS5	29.4	6.9	0.0	63.7	93.4
NKHMS7i	19.0	3.4	0.0	77.6	94.6
NKHMS7ii	18.9	4.1	0.0	77.0	97.6
NKHMS13i	16.2	37.4	0.0	46.4	83.5
NKHMS13ii	28.5	35.7	0.0	35.8	88.0
NKHMS18i	0.0	1.0	1.2	97.8	101.1
NKHMS18ii	17.2	2.1	0.0	80.8	96.1
mean	19.0	12.7	0.2	68.1	
std dev	9.2	15.1	n.a.	19.8	
CV	48%	119%	n.a.	29%	

Table 6.21 - SEM-EDS phase analyses of NKH3/MeP3 slag prills, selected elements after data normalisation, analytical total presented.

	MgO	Al ₂ O ₃	SiO ₂	P ₂ O ₅	SO ₃	K ₂ O	CaO	MnO	FeO	CuO	Total	Fe/SiO ₂
	wt%	wt%	wt%	wt%	wt%	wt%	wt%	wt%	wt%	wt%	wt%	wt ratio
NKHMS4 spectrum 1	0.9	4.9	32.8	0.7	1.0	0.5	11.2	0.0	47.2	0.7	92.2	1.1
NKHMS4 spectrum 2	0.7	5.4	34.0	0.6	0.9	0.4	10.7	0.4	46.9	0.0	90.2	1.1
NKHMS4 spectrum 3	0.5	5.3	34.0	0.0	1.0	0.5	12.0	0.5	45.3	0.7	92.7	1.0
<i>NKHMS4 mean</i>	<i>0.7</i>	<i>5.2</i>	<i>33.6</i>	<i>0.5</i>	<i>1.0</i>	<i>0.5</i>	<i>11.3</i>	<i>0.3</i>	<i>46.5</i>	<i>0.5</i>	<i>91.7</i>	<i>1.1</i>
<i>NKHMS4 std dev</i>	<i>0.2</i>	<i>0.2</i>	<i>0.7</i>	<i>0.4</i>	<i>0.1</i>	<i>0.1</i>	<i>0.7</i>	<i>0.3</i>	<i>1.0</i>	<i>0.4</i>		
<i>NPWMS8 CV</i>	<i>27%</i>	<i>4%</i>	<i>2%</i>	<i>87%</i>	<i>5%</i>	<i>12%</i>	<i>6%</i>	<i>89%</i>	<i>2%</i>	<i>87%</i>		
NKHMS5 spectrum 1	0.8	3.4	30.4	0.0	0.8	0.3	11.2	0.0	52.0	1.0	91.0	1.3
NKHMS5 spectrum 2	0.9	3.8	29.8	0.0	0.6	0.4	11.4	0.5	51.7	0.9	94.6	1.3
NKHMS5 spectrum 3	1.0	3.7	30.9	0.0	0.8	0.0	10.8	0.0	51.5	1.3	91.3	1.3
<i>NKHMS5 mean</i>	<i>0.9</i>	<i>3.6</i>	<i>30.4</i>	<i>0.0</i>	<i>0.7</i>	<i>0.2</i>	<i>11.1</i>	<i>0.2</i>	<i>51.7</i>	<i>1.1</i>	<i>92.3</i>	<i>1.3</i>
<i>NKHMS5 std dev</i>	<i>0.1</i>	<i>0.2</i>	<i>0.6</i>	<i>0.0</i>	<i>0.1</i>	<i>0.2</i>	<i>0.3</i>	<i>0.3</i>	<i>0.3</i>	<i>0.2</i>		
<i>NPWMS5 CV</i>	<i>10%</i>	<i>5%</i>	<i>2%</i>	<i>n.a</i>	<i>12%</i>	<i>93%</i>	<i>3%</i>	<i>173%</i>	<i>1%</i>	<i>21%</i>		
NKHMS7 spectrum 1	0.6	2.6	34.8	0.0	0.0	0.0	6.1	0.0	54.5	1.3	86.2	1.2
NKHMS7 spectrum 2	0.8	2.9	35.0	0.0	0.0	0.0	6.4	0.0	53.8	1.1	87.7	1.2
NKHMS7 spectrum 3	0.5	2.8	35.3	0.0	0.5	0.0	6.1	0.0	53.9	0.9	85.1	1.2
<i>NKHMS7 mean</i>	<i>0.7</i>	<i>2.8</i>	<i>35.0</i>	<i>0.0</i>	<i>0.2</i>	<i>0.0</i>	<i>6.2</i>	<i>0.0</i>	<i>54.1</i>	<i>1.1</i>	<i>86.3</i>	<i>1.2</i>
<i>NKHMS7 std dev</i>	<i>0.1</i>	<i>0.1</i>	<i>0.2</i>	<i>0.0</i>	<i>0.3</i>	<i>0.0</i>	<i>0.2</i>	<i>0.0</i>	<i>0.4</i>	<i>0.2</i>		
<i>NPWMS6 CV</i>	<i>17%</i>	<i>5%</i>	<i>1%</i>	<i>n.a</i>	<i>173%</i>	<i>n.a</i>	<i>3%</i>	<i>n.a</i>	<i>1%</i>	<i>19%</i>		
NKHMS13 spectrum 1	0.6	5.7	31.2	0.0	1.3	0.5	8.2	0.0	51.7	0.7	85.3	1.3
NKHMS13 spectrum 2	0.7	5.8	31.1	0.0	1.7	0.6	8.6	0.0	51.5	0.0	85.6	1.3
NKHMS13 spectrum 3	0.6	5.8	30.8	0.0	1.6	0.4	7.8	0.4	51.9	0.8	84.0	1.3
<i>NKHMS13 mean</i>	<i>0.6</i>	<i>5.8</i>	<i>31.0</i>	<i>0.0</i>	<i>1.5</i>	<i>0.5</i>	<i>8.2</i>	<i>0.1</i>	<i>51.7</i>	<i>0.5</i>	<i>85.0</i>	<i>1.3</i>
<i>NKHMS13 std dev</i>	<i>0.1</i>	<i>0.0</i>	<i>0.2</i>	<i>0.0</i>	<i>0.2</i>	<i>0.1</i>	<i>0.4</i>	<i>0.2</i>	<i>0.2</i>	<i>0.4</i>		
<i>NPWMS6 CV</i>	<i>12%</i>	<i>1%</i>	<i>1%</i>	<i>n.a</i>	<i>15%</i>	<i>16%</i>	<i>5%</i>	<i>173%</i>	<i>0%</i>	<i>87%</i>		
NKHMS17 spectrum 1	1.4	6.1	33.9	0.0	0.0	0.8	14.7	0.0	43.2	0.0	90.1	1.0
NKHMS17 spectrum 2	1.2	6.2	33.9	0.0	0.6	0.6	14.6	0.0	43.0	0.0	92.4	1.0
NKHMS17 spectrum 3	1.2	6.1	33.4	0.8	0.6	0.7	14.2	0.6	42.4	0.0	93.0	1.0
<i>NKHMS17 mean</i>	<i>1.3</i>	<i>6.1</i>	<i>33.7</i>	<i>0.3</i>	<i>0.4</i>	<i>0.7</i>	<i>14.5</i>	<i>0.2</i>	<i>42.9</i>	<i>0.0</i>	<i>91.8</i>	<i>1.0</i>
<i>NKHMS17 std dev</i>	<i>0.1</i>	<i>0.0</i>	<i>0.3</i>	<i>0.5</i>	<i>0.3</i>	<i>0.1</i>	<i>0.2</i>	<i>0.3</i>	<i>0.4</i>	<i>0.0</i>		
<i>NPWMS6 CV</i>	<i>9%</i>	<i>0%</i>	<i>1%</i>	<i>173%</i>	<i>87%</i>	<i>14%</i>	<i>2%</i>	<i>173%</i>	<i>1%</i>	<i>n.a</i>		
NKHMS18 spectrum 1	1.6	5.4	32.3	0.0	0.0	0.7	19.5	0.0	40.6	0.0	82.1	1.0
NKHMS18 spectrum 2	1.4	5.5	32.1	0.0	0.0	0.7	19.2	0.0	39.2	0.9	83.9	0.9
NKHMS18 spectrum 3	1.5	5.7	31.7	0.0	0.0	0.7	19.5	0.0	40.3	0.7	83.9	1.0
<i>NKHMS18 mean</i>	<i>1.5</i>	<i>5.5</i>	<i>32.0</i>	<i>0.0</i>	<i>0.0</i>	<i>0.7</i>	<i>19.4</i>	<i>0.0</i>	<i>40.0</i>	<i>0.5</i>	<i>83.3</i>	<i>1.0</i>
<i>NKHMS18 std dev</i>	<i>0.1</i>	<i>0.1</i>	<i>0.3</i>	<i>0.0</i>	<i>0.0</i>	<i>0.0</i>	<i>0.2</i>	<i>0.0</i>	<i>0.8</i>	<i>0.5</i>		
<i>NPWMS6 CV</i>	<i>6%</i>	<i>3%</i>	<i>1%</i>	<i>n.a</i>	<i>n.a</i>	<i>7%</i>	<i>1%</i>	<i>n.a</i>	<i>2%</i>	<i>88%</i>		
NKHMS mean	1.0	4.8	32.6	0.1	0.6	0.4	11.8	0.1	47.8	0.6		
NKHMS std dev	0.4	1.3	1.8	0.2	0.6	0.3	4.7	0.1	5.6	0.4		
Inter NKHMS CV	38%	28%	5%	162%	89%	64%	40%	88%	12%	69%		
Mean intra NKHMS CV	14%	3%	1%	43%	49%	24%	3%	101%	1%	50%		

Table 6.22 - SEM-EDS phase analyses of NKH3/MeP3 slag matrices, selected major and minor oxides after data normalisation, analytical total presented.

Slag matrix - The only occasional presence of residual minerals means the NKH3/MeP3 slags can be considered relatively homogeneous. Though the melt was not completely reacted it would have been fairly liquid, and there are substantial areas of matrix suitable for targeted bulk analysis, avoiding any inclusions with scans of 1mm² (Figure 6.28, Table 6.22). As per previous sections of this and the preceding chapter, these data are not directly comparable to the [P]ED-XRF results which do incorporate residual inclusions, but contrasting the mean readings of SEM-EDS area scans between slags can be used to assess variation in reactants and/or techniques between samples, whereas comparing individual scans indicates intra-sample homogeneity and the completeness of a reaction (cf. Humphris *et al.* 2009).

Across the samples, the major chemical components of the slag microstructure are FeO (mean 47.8wt%), SiO₂ (mean 32.6wt%), CaO (mean 11.8wt%), Al₂O₃ (mean 4.8wt%), MgO (mean 1.0wt%). Their respective CVs (12%, 5%, 40%, 28%, and 38%) suggest a greater consistency in NKH3/MeP3 charge compositions and/or processing techniques when compared to NPW3/MeP2 (Table 5.21). Sulphur compound concentrations are low and variable (CV 89%), but are a regular component of the slags, and thus presumably of the smelting charge. The mean copper oxide reading of 0.6wt% and a CV of 69% for the slag matrix suggests an efficient and relatively standardised process, as measured by waste products at least. The reduced level of residual mineral inclusions and a reasonable positive correlation between copper oxide and iron oxide concentrations suggests copper losses can be largely attributed to poor separation (Davenport *et al.* 2002: 273, Gilchrist 1989).

Within slag samples, the very low CVs for FeO (mean intra CV 1%), SiO₂ (mean intra CV 1%), CaO (mean intra CV 3%), and Al₂O₃ (mean intra CV 3%) indicates the NKH3/MeP3 slags had largely reached equilibrium⁸, and copper oxide (mean intra CV 50%) was relatively uniformly distributed. Though variation between slags is greater than that within them, the overall picture is of far greater standardisation in smelting charge and operating parameters than the NPW3/MeP2 slags (Table 5.21).

Using the traditional archaeometallurgical technique for calculating operating temperatures from slag liquidus, the primary chemical components (iron^(II) oxide, silica, and calcia)

8 This is of course contrary to the 'slag-skin' slag matrices, but the NKHMS samples are probably the ones to trust as their larger volumes would have been less susceptible to post-depositional modification, and there is less chance of uneven ceramic contamination.

would indicate the slag was exposed to minimum temperatures of between c. 1093°C and c. 1160°C (Figure 6.40). Transposing the mean liquidus of c. 1130°C onto an Ellingham Diagram, and extending two lines to the intersections of the liquidus with the '4Cu+O₂ = 2Cu₂O' and '6FeO+O₂ = 2Fe₃O₄' boundaries (representing the likely redox envelope for a process reducing copper to metallic form, and containing divalent as well as trivalent iron), indicates a ppO₂ between c. 1x10⁻⁶ and c. 1x10^{-10.5} (Figure 6.41).

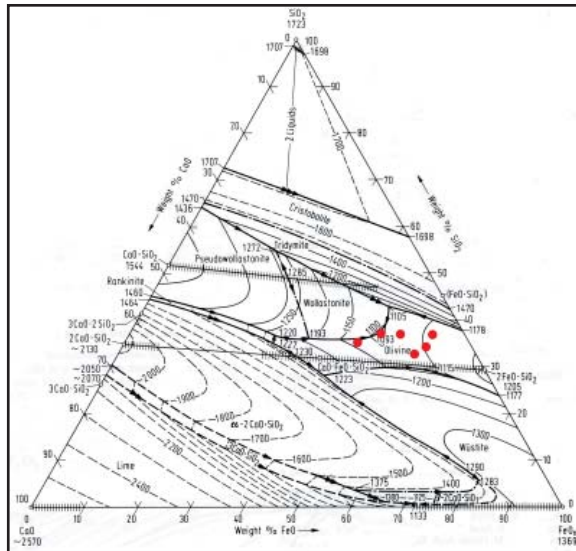


Figure 6.40 - Slag matrices plotted on a ternary diagram for a FeO-CaO-Si₂ slag system in equilibrium with iron metal. Image adapted from Eisenhüttenleute 1995.

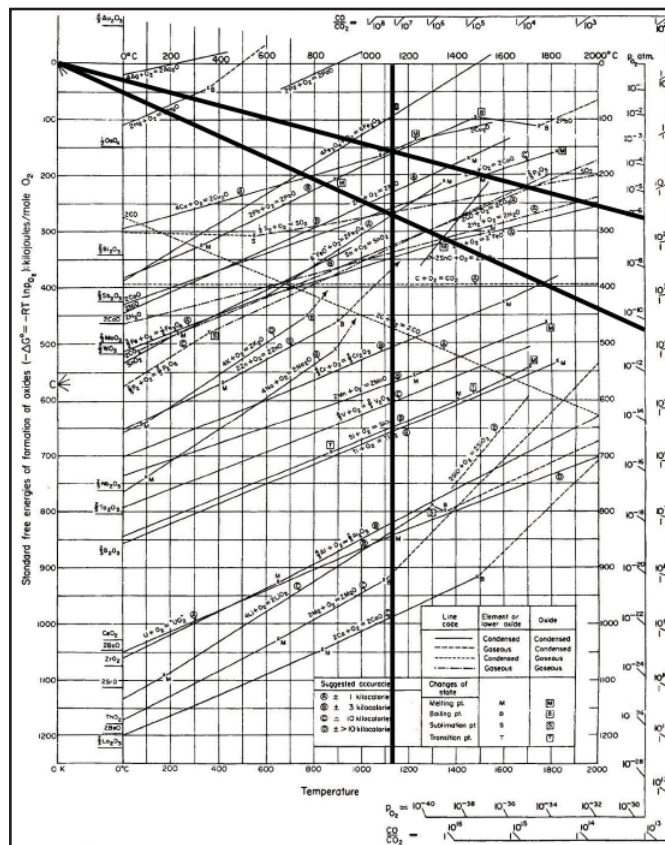


Figure 6.41 - Ellingham Diagram showing redox envelope for NKH3/MeP3 slags. Image adapted from Gilchrist 1989.

The most appropriate Flogén diagram for the NKH3/MeP3 slags describes a system with 7wt% alumina in a $p\text{pO}_2$ of 1×10^{-8} , with Fe/SiO₂ ratio and calcia as variables (Kongoli & Yazawa 2001: Figure 11). Plotting the data from Table 6.22 onto Figure 6.42 gives a liquidus reading of between c. 1225°C and c. 1255°C, and a mean minimum slag temperature of c. 1240°C. In this instance, the traditional liquidus figure of c. 1130°C is c. 110°C cooler than the Flogén reading.

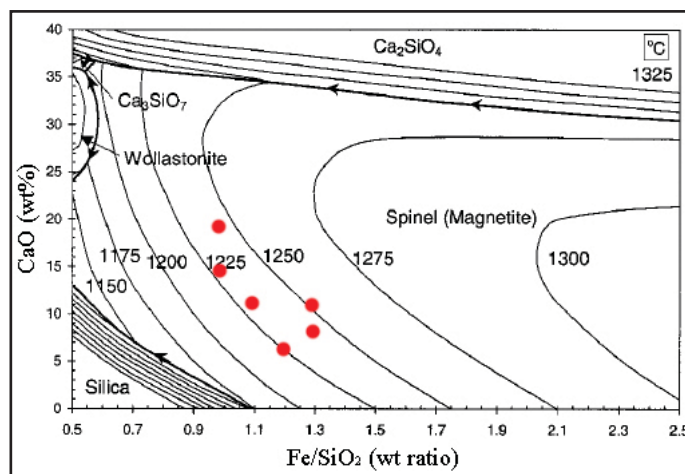


Figure 6.42 - SEM-EDS analyses of slag matrices plotted on a Flogén binary chart for slag system at a 10^{-8} $p\text{pO}_2$ and with 7wt% Al₂O₃. Image adapted from Kongoli & Yazawa 2001: Figure 11.

6.3.4 Discussion

The NKH3/MeP3 slag evidence is entirely consistent with the expected waste product of an ancient copper smelting *chaîne opératoire* utilising oxidic and sulphidic copper minerals in calcareous, ferruginous, and siliceous host rocks, though the calcia contribution is probably substantially derived from fuel ash and/or technical ceramic. The slag characteristics consistently indicate the later Iron Age metalworkers were more skilled smelters than their early Iron Age antecedents at Non Pa Wai. The principal sign of this technological change is the increased homogeneity of the slag, as evidenced by macro, bulk, and micro-analysis. This technical improvement could result from higher smelting temperatures, longer smelting duration, or better balanced smelting charges. The modified Flogén liquidus figures for crystalline and glassy phases in the NKH3/MeP3 slags range from c. 1100°C to c. 1300°C. These temperatures are not significantly different than those calculated for NPW3/MeP2 slags (Chapter 5), due to the inverted fluxing behaviour at certain concentrations of calcia, alumina, and magnesia at intermediate oxygen partial pressures. It is therefore unlikely the improved slag homogeneity was largely due to the generation of higher smelting temperatures.

This would leave smelting duration and smelting charge as possible factors, but the author is again inclined to discount the former as a major influence given the limited time needed to produce both NKH3/MeP3 or NPW3/MeP2 slag cakes (in the order of a few hours). Thus the significant improvement in slag homogeneity, and subsequently metal recovery, probably reflects a amelioration of the technological choices made by NKH3/MeP3 metalworkers in their smelting charge composition. The uniform and well-balanced later Iron Age mineral charges were able to form a relatively standardised slag without requiring the input of excessive heat energy, and thus promoting copper recovery by liquidity separation. Likewise, an improved control over granulometry, as evidenced by the intensively crushed NKH3/MeP3 matrix as well as relative dearth of unreacted minerals, would have permitted a more even consumption of charge reactants. Although there are no consistent microstructural or compositional difference between NKH3/MeP3 slag cakes and slag casts, it is possible the latter represent the reprocessing of the former, perhaps in a manner akin to that proposed by Rehren (2000) for incompletely reacted glass. The author does not consider the provision of an adequate gaseous atmosphere to have been an issue restricting the 'slag-skin' contained NKH3/MeP3 smelt. The production of CO gas from partial fuel combustion, and the reaction of that gas with unburnt charcoal (Boudouard), would probably be sufficient to generate a suitable redox atmosphere for copper smelting (Gilchrist 1989, Bassiakos *et al.* 2008).

Further contrasting the early and later Iron Age smelting charges is of great interest for our understanding of the development of technological choices in the Khao Wong Prachan Valley. In NPW3/MeP2 slags, the overwhelming presence of residual magnetite fragments could be excused as inexperience. However, for the same behaviour to be occurring in NKH3/MeP3 slags is very curious, considering the enormous improvement in smelting technique evidenced. Were the inclusions of haematite or another iron oxide it would be possible they served as a reservoir of gaseous oxygen to promote sulphur removal at the heart of the smelt (Artioli *et al.* 2007, Burger *et al.* 2007), but magnetite does not release significant quantities of gas when heated (Kaiura & Tohuri 1979: 605). Therefore, the author is disposed to regard the addition of excess magnetite fragments as a particularly notable element of the overall metallurgical style of Iron Age copper production in the Khao Wong Prachan Valley. Although not comparable in proficiency and sophistication to some ancient processes (e.g. Bassiakos & Catapotis 2007, Bourgarit 2007), the NKH3/MeP3 slags are indicative of smelting processes operating at appropriate temperatures and durations, using a reasonably well-balanced mineral/fuel charge.

6.4 The Nil Kham Haeng copper smelting *chaînes opératoires*

From every level of archaeometallurgical analysis it is clear the later Iron Age Nil Kham

Haeng metalworkers were more proficient smelters when compared with those at early Iron Age Non Pa Wai, though this development is not presented as inevitable or desirable.

MeP2:

Due to no samples having been taken from the very small exposure of basal Nil Kham Haeng in Operation 1, it is for the time being necessary to accept the excavator's observation that metallurgical remains from these strata were identical to MeP2 material from Non Pa Wai (Weiss 1992). Therefore, it is assumed that the extractive metal technology employed at early Iron Age Nil Kham Haeng was comparable to that of early Iron Age Non Pa Wai (see Chapter 5).

MeP3:

Due to their spatial proximity and overlapping chronological sequences, there exist obvious similarities between the *chaînes opératoires* generated for Nil Kham Haeng and its neighbour. Copper smelting by later Iron Age Nil Kham Haeng metalworkers is entirely consistent with the range of materials to be found within a few kilometres radius. A limited range of minerals was excavated at the site, with a generally more sulphidic character than Non Pa Wai, suggesting that chalcopyrite may have played a more important role relative to malachite than at the earlier site, although there is no evidence for the samples having been roasted prior to smelting. It is again unknown how these samples entered the archaeological record.

The ceramic fabrics used at Nil Kham Haeng have a composition conforming to that of the local geological environment, making it likely that metalworkers did not travel far from Nil Kham Haeng, although they do appear to have been choosing a different source to that used at Non Pa Wai. The fabric also appears to have been tempered with plant material, which may have reduced shrinkage problems in production, and increased insulation properties during use - though this would be of limited importance if the perforated ceramics were interpreted as wind-powered furnaces (cf. Catapotis *et al.* 2008, Tabor *et al.* 2005, Van Buren & Mills 2005). The excavators at Nil Kham Haeng envisioned the furnace chimneys sitting above a clay-lined pit in the ground (Figure 1.4), and this interpretation is shared by Roberto Ciarla (2007b) following the excavation of similar artefacts from nearby Khao Sai On.

The comparatively homogeneous appearance and chemistry of the Nil Kham Haeng slags

can be interpreted as evidence for more standardised smelting techniques relative to Non Pa Wai. In view of the low sulphur content in MeP3 slag and the presumed presence of sulphidic minerals in the charge, roasting and/or an optimised charge composition are entirely plausible. A more consistent processing and selection of minerals by Nil Kham Haeng metalworkers would have produced more consistent results, reflected archaeologically in the greater uniformity of the waste material. This increased charge formation competence, possibly combined with an elevated fuel to mineral ratio may be responsible for reduced copper losses evidenced at Nil Kham Haeng. Although far apart in terms of period and context, the NPW3/MeP2 smelting technology is comparable to those reported in the Bronze Age Aegean (Catapotis & Bassiakos 2007, Catapotis *et al.* 2008) and in the Bronze Age Levant (Bunk *et al.* 2004). The post-laboratory reconstruction for the NKH3/MeP3 smelting technique, for the mean time including the established (Pigott *et al.* 1997) placement of the perforated ceramic cylinder, is schematised in Figure 6.43, prior to testing in the field (Chapter 7).

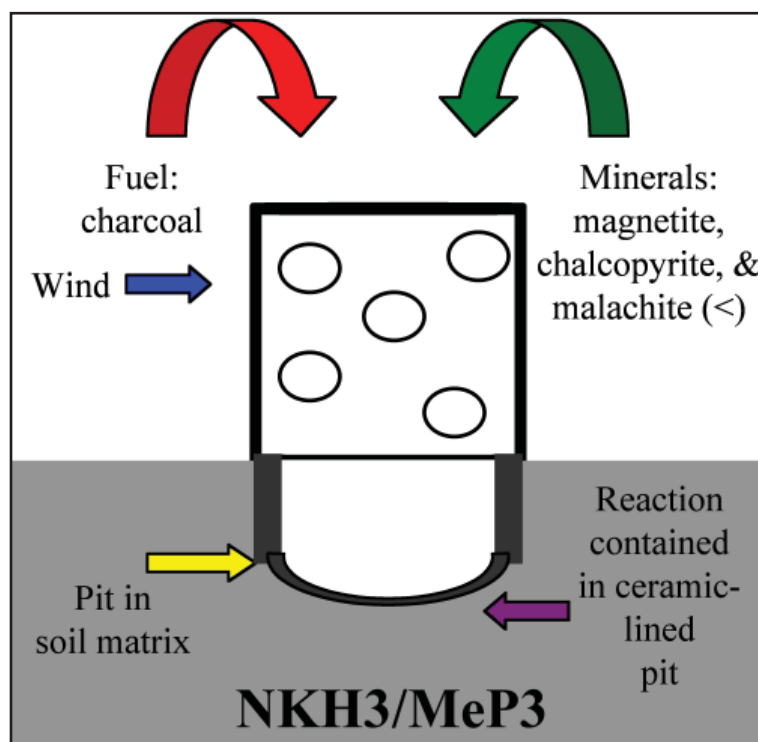


Figure 6.43 - Schematic technological reconstruction for copper smelting technique at later Iron Age Nil Kham Haeng, prior to experimental testing. Image: author.

Chapter 7

Experimental Archaeometallurgical Approaches to the Khao Wong Prachan Valley

“Clearly an important further step in the investigations of copper smelting in this area, would be to build such a crucible [for the Non Pa Wai reconstruction] and operate it under simulations of conceivable field methods.” (Bennett 1988b: 334).

The current project incorporated a very informative experimental programme, which is thought to be the first ever carried out for prehistoric Southeast Asian metal technologies. The campaign was conducted during September 2007 at the archaeological site of Fiaavè Palafitto, in the Provincia Autonoma di Trento, Italia, and in collaboration with research teams from the Soprintendenza per i Beni Archeologici, and the Centre de Recherche et de Restauration des Musées de France. Permission to do the experiments at the site of Non Pa Wai in central Thailand was sought, and granted, in early 2007, but it was decided, for the sake of cost and time, that a European collaborative venture would be more expedient.

The original purpose of the experimentation was to assess and improve the reconstructed *chaînes opératoires* derived from archaeometrical analyses of the Khao Wong Prachan Valley evidence, described in Chapters 5 and 6 for Non Pa Wai and Nil Kham Haeng, respectively. Whilst the general aim of the tests was to assess how well the analytical data meshed with field-scale reality, the specific objective was to attempt to replicate prehistoric slag morphology, within the constraints of the Valley archaeological evidence¹.

1 The Fiaavè experiments were carried out prior to the Valley chronological revision in January 2008. On that basis, 7 of the 10 experiments (Table 7.2) are now intrinsically incorrect as a perforated cylinder was placed over a crucible (cf. Figure 5.50). However, the experimental data as a whole are highly recoverable. Aside from some minor differences in the slag compositions driving charge calculations (Table 7.1), the technical performance of a buried crucible and a clay-lined pit is the same during the smelt, even though there are behavioural ramifications in how the slag and metal are subsequently processed (see Chapter 8). Therefore, in essence, all the Fiaavè tests can be considered as NKH3/MeP3 reconstructions. From this point the following nomenclature will be used to distinguish between the NPW3/MeP2 smelting reconstruction before and after January 2008, the ‘pre-Rome’ instances will be marked ‘NPW3/MeP2**PR**’, whereas the ‘post-Rome’ understanding of the Valley archaeology will continue to be denoted by the familiar ‘NPW3/MeP2’ nomenclature.

In line with the earlier TAP interpretations of perforated ceramic fragments and the lack of evidence for a forced draught (e.g. Pigott *et al.* 1997), the experiments were designed to test the hypothesis of wind-powered smelting technologies in the later Iron Age Valley. The primary conclusion of the 2007 field testing programme was that wind, even when delivered in consistent experimental conditions, cannot produce smelting debris (slag and technical ceramic) consistent with the archaeological evidence. Not only does this suggest archaeologically-invisible forced draught provision is a technological necessity in the Valley, it also imposes a major rethink of the NKH3/MeP3 smelting reconstruction (see Chapter 8).

7.1 - Experimental design

Attempting to reproduce ancient technologies of any kind can easily introduce more variables than can be adequately controlled, recorded, and analysed. Therefore, it is necessary to accurately define what the experiment aims to achieve, and to plan the research in a way that limits unwanted variability, ensures the controlled recording of data, but leaves room for experimental procedure to be modified in light of ongoing experience.

Archaeometallurgical experiments are in themselves notorious for involving an enormous number of independent and conjoined parameters. It was intended that the current experimentation be a field-scale assessment of the Valley technological reconstructions which, although totally guided and constrained by the archaeological evidence, would not constitute attempts to re-enact the ancient techniques. It is sufficiently understood that metallurgical technologies are often too complex or the archaeological data insufficiently complete to wholly replicate, thus efforts to do so merely undermine the potential insights of a more pragmatic approach.

Therefore, the first task faced when planning the present experiments was to lay out a series of foundation assumptions, around which the experimental design could be built. The most important of these assumptions relate to the smelting charge, technical ceramics, and wind speed. These are detailed below, and the charge calculations can be followed numerically in Table 7.1.

Assumption 1: NPW3/MeP2**PR** whole slag cakes have a mass of c. 2kg (Figure

5.27), and are thought to represent a single smelt, whereas the relationship is less clear for NKH3/MeP3 slag due to the lower incidence of complete cakes. However, the use of common use [sic] of furnace chimney suggests that the total amount of slag produced by each smelt may have been similar. Therefore it was decided that each test should attempt to produce 2kg of a heterogeneous but pourable slag.

Assumption 2: However, as typical Valley slag contains unreacted material, it would be incorrect to calculate the experimental charge based on 2kg of pure slag². Stating 50wt% as a reasonable estimation (Fig 5.29) of the proportion of fully formed slag versus residual minerals, allows us to base reactant calculations on the production of 1kg of an olivine slag. The composition of the experimental olivine differs from NPW3/MeP2**PR** to NKH3/MeP3, based on mean readings of SEM-EDS area scans of previously molten phases in the archaeological samples (see Chapters 5 & 6, Table 7.1).

Assumption 3: The production of an olivine slag requires the provision of iron in the reactants. Based on the archaeometric evidence presented in Chapters 5 and 6, chalcopyrite and magnetite are both iron-bearing minerals present in slags from NPW3/MeP2**PR** and NKH3/MeP3. For the purpose of calculating the experimental charge, 50% of the iron in the olivine system is assumed to have come from the chalcopyrite, and the other 50% from the magnetite. This statement drives the quantities of these two minerals required to make up the smelting charge (Table 7.1). However, seeing as there is commonly an extreme excess of residual magnetite in the Valley slags, an extra 50% by mass of magnetite was included.

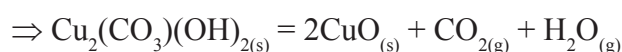
Assumption 4: The present study's consideration of Rostoker *et al.*'s (1989) co-smelting hypothesis in the Valley technological reconstructions has been heavily influenced by the work of Emilien Burger *et al.* (2007). In particular, Burger's laboratory and small-scale field experiments have demonstrated the envelope in which a varying ratio of oxidic (malachite) to sulphidic (chalcopyrite) copper mineral reactants can produce archaeologically attested material outcomes, and at temperatures and partial pressures appropriate to ancient pyrotechnical installations. Burger's co-smelting parameters also state that all the oxygen required to remove sulphur from the chalcopyrite is provided by the malachite

2 This represents an experimentally-informed modification of the original plan which *was* calculating for 2kg of pure slag. The first experiment, Burn 1, was sufficient to demonstrate that 11kg of mineral reactants were never going to fit in a Valley furnace.

(Burger *et al.* 2007).

It was decided to assign either extreme of the possible ratio values to each of the two sites, O:S = 2.5 for NPW3/MeP2**PR**, and O:S = 1 for NKH3/MeP3. It was not possible to determine quantitative values for the relative amounts of residual malachite and chalcopyrite in the Valley slags by analytical means. Thus, these ratio assignments are based on the logic that metalworkers from Non Pa Wai, as the earlier site, may have had a greater access to oxidic minerals located closer to the surface of the Valley copper-bearing mineralisations. Their smelting charges might then have a higher proportion of malachite than metalworkers at Nil Kham Haeng, who being later in time, may have been mining deeper in the mineral deposit. Of course, all evidence of this at Khao Tab Kwai has been obliterated by recent iron oxide mining.

Assumption 5: Considering the moderate conditions required to convert malachite (copper carbonate) to cuprite (copper oxide), it was assumed that by the time the mixed oxidic/sulphidic charge had begun to react in the high temperature zone of the furnace, all the $\text{CO}_{2(g)}$ and $\text{H}_2\text{O}_{(g)}$ would have been driven off the copper carbonate³. Therefore, given that there are two atoms of copper in malachite ($\text{Cu}_2(\text{CO}_3)(\text{OH})_{2(s)}$), a conversion to cuprite ($\text{CuO}_{(s)}$) will bring two moles of oxygen for every mole of malachite.



The quantity of malachite in the charge was calculated by the desired ratio to chalcopyrite (see Assumption 4 and Table 7.1).

Assumption 6: Calculating the silica ($\text{SiO}_{2(s)}$) contribution of the technical ceramic to the production of an experimental olivine slag is impractical given the number of unknowns and variables. Therefore, the silica part of the mineral charge was calculated to be solely fulfilled by the addition of builders' sand⁴, and relative to the olivine chemistry of the NPW3/MeP2**PR** and NKH3/MeP3 slags (Table 7.1).

3 This was empirically shown to be true by the immediate blackening of malachite fragments as they were charged to the furnace, cuprite being a much darker mineral.

4 Whilst mineral granulometry was one of the two chief variables, the silica component was only available in quartz sand form, and thus its grain size could not be varied with the other charge minerals.

Assumption 7: As with the silica, the calcia ($\text{CaO}_{(s)}$) contribution of fuel ash and technical ceramic to slag production was hard to model with any accuracy. Thus, the calcia content of the charge was calculated directly from the olivine composition required for the reconstructions, but the quantities were modified to reflect the input material being slaked lime⁵ ($\text{Ca(OH)}_{2(s)}$).

It should be noted in Table 7.1, that the mineral charge quantities required to produce 1kg of olivine slag can seem quite high, c. 6kg for NPW3/MeP2**PR**, and c. 4kg for NKH3/MeP3. The mineral is of course not the only charge component that the furnace must cope with, both reconstructions include the use of charcoal as a fuel. Whilst the Valley charcoal was most likely produced from local oak-dipterocarp species (Vincent Pigott pers. comm.), the material used for the tests was commercially available high-quality hardwood fuel. Therefore:

Assumption 8: Although the co-smelting reaction is exothermic, and may produce reducing $\text{SO}_{2(g)}$, the quantities are unknown at the field-scale (cf. Burger *et al.* 2007, Rostoker & Dvorak 1991). Thus, the partial combustion of charcoal fuel was assumed to provide the heat and reducing gases ($\text{CO}_{(g)}$) required to power the Fiavè tests. The quantities of fuel used for the Valley reconstructions were based on the findings of previous scholars working with comparable copper smelting technologies (e.g. Merkel 1990), whilst also noting the likely difference in fuel:mineral ratios between NPW3/MeP2**PR** and NKH3/MeP3. Ratios of 1:1 and 2:1 were tested for both reconstructions.

The technological reconstructions generated for Iron Age Non Pa Wai and Nil Kham Haeng account for the enormous quantities of technical ceramic recovered from the two sites. Therefore:

Assumption 9: Replica crucibles for the NPW3/MeP2**PR** reconstruction (see below for dimensions) were placed in a pit just large enough to accommodate them. The same pit was lined with tempered clay for the NKH3/MeP3 model. For both reconstructions, a replica chimney was placed on top of the pit - its base flush with the land surface (Figure 7.1).

5 The calcia posed a similar problem to silica, as the slaked lime used was in a powdered form.

ELEMENTS		COMPOUNDS		MASS FRACTIONS		TOTAL	KWPV SLAG		CaO	SiO ₂	FeO
COPPER	63.5	MAGNETITE	Fe ₃ O ₄	168	64	232.0	<u>NPW3/MeP2PR</u>	12%	30%	58%	
IRON	56	CHALCOPYRITE	CuFeS ₂	63.5	56	183.5					Mean
SULPHUR	32	MALACHITE	Cu ₂ (CO ₃)(OH) ₂	127	60	221.0					<u>NKH3/MeP3</u>
SILICON	28	CUPRITE	Cu ₂ O	63.5	16	79.5	Mean	13%	35%	52%	
CALCIUM	20	SILICA	SiO ₂	28	32	60.0	Normalised 1mm ² slag scans				
OXYGEN	16	LIME	Ca(OH) ₂	20	32	54.0					
CARBON	12	NPW OLIVINE	CaO.SiO ₂ .FeO	36.0	60.0	64.2					
HYDROGEN	1	NKH OLIVINE	CaO.SiO ₂ .FeO	36.0	60.0	63.2					
		SULPHUR DIOXIDE	SO ₂	32	32	64.0					
				50.0%	50.0%						
NPW/MeP2PR O/S RATIO:		2.5		NKH3/MeP3 O/S RATIO:		1					
REACTANTS	MASS (kg)	PRODUCTS	MASS (kg)	REACTANTS	MASS (kg)	PRODUCTS	MASS (kg)				
MAGNETITE	0.81	OLIVINE	1.00	MAGNETITE	0.72	OLIVINE	1.00				
CHALCOPYRITE	0.96	COPPER	1.99	CHALCOPYRITE	0.85	COPPER	0.88				
MALACHITE	2.88			MALACHITE	1.02						
LIME	0.31			LIME	0.35						
SILICA	0.64			SILICA	0.76						
	5.60				3.69						

Table 7.1 - Calculator for experiment reactants and theoretical products. 'ELEMENTS' contains atomic masses of constituent elements. 'COMPOUNDS' computes molecular masses for constituent compounds, with the olivines being calculated from SEM-EDS matrix scans under 'KWPV SLAG' (see Tables 5.2.1 & 6.2.2). The lower part of the table details the reactants needed for an experimental smelting charge - NPW3/MeP2PR is referred to as the tests were conducted under the 'pre-Rome' chronology, but aside from slight differences in the slag matrix chemistry all experiments can be considered NKH3/MeP3 reconstructions.

The theoretical mineral charges, fuel, and technical ceramics for the Non Pa Wai and Nil Kham Haeng reconstructions accounted for, the experimental design must also account for air supply or wind power:



Figure 7.1 - Perforated ceramic cylinder configurations for NPW3/MeP2PR (left) and NKH3/MeP3 (right). Images: author.

Assumption 10: Southeast Asia's climate is highly influenced by the South Asian monsoon and the western Pacific El Niño Southern Oscillation (Chen & Yoon 2000, Slingo & Annamalai 2000). The interaction between these two complex weather systems is largely responsible for Thailand's seasonality and in all likelihood⁶, the marked windiness of the cool-dry season in the Valley between November and February. Given the lack of evidence for forced draught (tuyères, bellows etc.) but having perforated technical ceramics, the location of Non Pa Wai and Nil Kham Haeng in an area with a distinct windy season, could indicate a wind-driven smelting technology (cf. Bassiakos *et al.* 2008, Bunk *et al.* 2004, Tabor *et al.* 2005, Van Buren & Mills 2005). A Thai archaeologist, Pira Venunan, was kind enough to research wind speed data pertinent to the Valley by contacting the Thai Meteorological Department and the local military airbase at Sa Pran Nak. Unfortunately, these data consisted of annual and monthly averages, and thus could not identify the highly specific local meteorological peculiarities that the excavators of Non Pa Wai and Nil Kham Haeng had noted. Therefore, the TAP co-directors were questioned using the Beaufort scale (Huler 2004, Vincent Pigott & Surapol Natapintu pers. comm.), and their recollections of the perceptible effects of the wind (dust flying, branches swaying etc.) were used to generate an experimental wind speed of mid-Force 4, or c. 7 ms^{-1} (Figure 7.2).

⁶ There are no known meteorological publications in any language for the Valley locality.

Beaufort Scale














Beaufort number	Wind Speed (mph)	Seaman's term		Effects on Land
0	Under 1	Calm		Calm; smoke rises vertically.
1	1-3	Light Air		Smoke drift indicates wind direction; vanes do not move.
2	4-7	Light Breeze		Wind felt on face; leaves rustle; vanes begin to move.
3	8-12	Gentle Breeze		Leaves, small twigs in constant motion; light flags extended.
4	13-18	Moderate Breeze		Dust, leaves and loose paper raised up; small branches move.
5	19-24	Fresh Breeze		Small trees begin to sway.
6	25-31	Strong Breeze		Large branches of trees in motion; whistling heard in wires.
7	32-38	Moderate Gale		Whole trees in motion; resistance felt in walking against the wind.
8	39-46	Fresh Gale		Twigs and small branches broken off trees.
9	47-54	Strong Gale		Slight structural damage occurs; slate blown from roofs.
10	55-63	Whole Gale		Seldom experienced on land; trees broken; structural damage occurs.
11	64-72	Storm		Very rarely experienced on land; usually with widespread damage.
12	73 or higher	Hurricane Force		Violence and destruction.

Figure 7.2 - The Beaufort Scale. Image courtesy of the Mount Washington Observatory (http://www.mountwashington.org/education/center/arcade/wind/beaufort_scale_tbp.gif accessed 24th October 2008).

7.2 - Experimental methods

Consumables

The minerals required for the Fiavè experiments were: malachite, chalcopyrite, magnetite, quartz, and lime. The latter two of this list were acquired from Italian building merchants as coarse grains and powder respectively. The copper and iron minerals were sourced from a supplier in Yorkshire (UK) and shipped overland to the experimental site in July 2007. The amounts ordered were: 100kg malachite, 75kg chalcopyrite, 30kg magnetite, 50kg quartz (including clay temper), and 25kg of slaked lime.

The quantities of reactants were determined by the calculations shown in Table 7.1, and on estimations of performing two smelts per day over ten days. The intent was to conduct smelts that would test the laboratory reconstructions, and hopefully reproduce

the prehistoric Valley slag and technical ceramic evidence. It was never intended that the experiments would exactly replicate the ancient techniques, as this would require not only unattainably perfect technological reconstructions, but also access to all the local minerals, clays, and fuels, an approach which would be unaffordable in every sense - and this considers only the physical requirements of exact replication.

Instead, it was decided to use as high quality an assemblage of materials as could be reasonably afforded and sourced. Grade II minerals were ordered to provide a low degree of gangue content, and subsequently a high degree of certainty over compositional standardisation (Figure 7.3)⁷. The purity level of the minerals was intended to reduce unwanted constituents upsetting the calculated slag chemistry, but also to render more useful future analytical work on the reactants and products of the reconstructed smelting processes. Other than the quartz and lime, the grain size of the minerals was modified using a stone anvil and a 1kg steel hammer (Figure 7.4), mechanical impurities, gangue, were removed by hand at this stage. Mineral granulometry was measured using sieves of 2mm, 5mm, 10mm, and 20mm mesh sizes.

150kg hardwood charcoal fuel was sourced locally in the Trentino area, and was similarly crushed and sorted to a size appropriate for the Valley furnaces (20-50mm).



Figure 7.3 - Minerals used in the Fiavè experiments, from left to right: malachite, chalcopyrite, magnetite, quartz, and lime. Image: author.

Likewise, the clay used for constructing the crucibles, perforated chimneys, and furnace linings was obtained in the Trentino area. In recognition of the relatively low refractory qualities of the Valley ceramics, 100kg of a standard potting clay were ordered. The clay was modified by the addition of quartz temper in the form of builders' sand in a 1:1 ratio by mass. For the sake of simplicity, it was decided not to organically temper the experimental ceramics, as per the Valley originals. The paste was homogenised by hand kneading and

⁷ Grade I minerals are collectors' specimens and priced as such.



Figure 7.4 - Vincent Pigott crushing malachite, Fiavè, September 2007. Image: author.

foot treading (Figure 7.5). The crucibles were constructed as large ‘thumb pots’, whereas the chimneys were fashioned using a combination of slab and coiling techniques (Figure 7.6, Rye 1981). The furnaces were built as uniformly as possible to a 20cm internal diameter, 20cm tall, and with 2cm thick walls, as per the only whole example from NKH3/MeP3 (Figure 6.7). The crucibles were based on the only complete example from NPW3/MeP2^{PR} (Figure 5.7) 20cm internal diameter with 1cm thick walls at the rim, increasing to a 5cm thick base, and their height being 10cm. Due to the ceramics being

handmade there was some variation in dimensions, sometimes exacerbated by slumping and/or shrinkage. It was always intended to air dry clay components prior to use, but the tight schedule often dictated their being fired damp if not wet, at the subsequent, though not critical, cost of cracking.



Figure 7.5 - The author kneading sand into clay at Fiaavè, September 2007. Image: Bastian Asmus.



Figure 7.6 - The author building perforated ceramic cylinders at Fiaavè, September 2007. Image: Bérénice Bellina.

Equipment

The most critical element of the Valley field reconstructions was the provision of air, in the form of artificial wind. An economical, though deafening, solution for artificial wind was found in an electric fan from a Trento hardware store (Figure 7.7). The 1800W unit provided a stable blast of 6.5 to 7.5 ms⁻¹ at the furnace when positioned 1.5 m away (Figure 7.8).



Figure 7.7 - The artificial wind source. Image: author.



Figure 7.8 - Windspeed at the furnace. Image: author.



Figure 7.9 - The anemometre. Image: author.

Local wind conditions were monitored using a Vortex™ anemometer via a Sony VAIO™ laptop with Windware™ software (Figure 7.9), but local wind speeds were much less than expected, and probably had negligible effect on the experiments. Also connected to the laptop was a Picotech™ datalogger with, at the outset, 8 type N 30cm Pyrosil™ thermocouple probes rated for continuous use at 1250°C. Significant durability problems were encountered and by the end of the campaign only two of the probes were still functional. It is thought that the presence of sulphur in the smelting charge played a large role in the rapid degradation of the array, a reminder of the toxicity and danger that ancient metalworkers were also exposed to. The inconsistent recording of temperatures for the Fiaavè tests has obvious implications for data quality, but it was necessary to accept these limitations under field conditions.

For documentation purposes, both video and still images were recorded using a Sony™ PC150 and a Canon™ A630 respectively. All aspects and sequences of the experimentation were visually documented for archival and presentation purposes. A 20cm scale bar was used where temperatures permitted.

In addition to the data recording equipment:

- Electrical power was supplied by a 4kW petrol generator.
- Point wind speeds were measured with a Kestrel 1000 hand-held anemometer.
- Masses were measured using an electronic balance with a 5kg limit, and a +/-2g tolerance.
- All other data were recorded on pre-printed paper forms (see Appendix C).

Procedures

At Fiaavè the first concern was safety. The smelting areas were cleared of combustible material and a safe perimeter established for curious observers. Due consideration was given to the downwind effects of hot sparks and carbon monoxide gas. A 25 litre jerry can of water and a bucket of sand were available to subdue any overly boisterous reactions.

Given the amount of time available for the campaign, the manufacture of the necessary technical ceramics was identified as the major bottleneck of the experimental process. The time required to mix clay to the correct composition and consistency, the construction of

the required chimneys and crucibles, and their extended drying time, dictated the technical ceramics should be prepared well in advance. The crushing of minerals to the desired size was a laborious close second to the ceramics, and brought a very real understanding to the significance of the enormous deposits of mechanically processed minerals and slag later Iron Age Nil Kham Haeng (see Chapter 8).

The charge for each smelt was calculated using Table 7.1, and the required reactants measured using the electronic balance, and mixed in large bucket (Figure 7.10). The charcoal was emptied from its bags and sorted for size, prior to crushing, sieving, and weighing for inclusion in the smelting charge - or by itself for the preheat.



Figure 7.10 - The mineral component of a smelting charge. Image: author.

For each test, the smelting area was thoroughly cleared of the debris from previous experiments, and the prefabricated chimneys either arranged over a crucible buried in a pit (NPW3/MeP2**PR** reconstruction), or over the same pit lined with tempered clay (NKH3/MeP3 reconstruction). Once the smelting installation was constructed, the thermocouples were positioned in the wall of the chimney. As mentioned above, the campaign started with 8 probes and finished with two, and thus the location of the thermocouple array was not standard. However, the available probes were always arranged so as to be equally spaced around the furnace at comparable elevations. The probe tips were either protruding 10mm into the furnace, or were flush with the interior chimney wall. The temperature data are

only indicative of the heat exposure of the chimney and do not represent the ‘core’ of the smelt; they cannot thus be directly compared to the laboratory reconstruction liquidi which are slag-based minima. The thermocouple cables were protected from excess heat by stones and heaped earth (Figure 7.11).



Figure 7.11 - The smelting configuration for ‘Burn 5’. Image: author.

With the furnace, mineral and fuel charge, and recording equipment all ready, the fan/piston bellows, temperature and wind speed datalogging were started simultaneously. Each smelt then followed three main stages: preheat, smelt, and sampling. All additions to the furnace were recorded and timed (see Appendix C).

Preheat - The preheat was required to bring the entire furnace system up to a working temperature well in excess of 1000°C. The time this took was largely determined by the moisture content of the technical ceramic and the surrounding soil matrix. As occurred on a number of occasions, smelting commenced with damp ceramics, and in these instances the preheat was undertaken with restraint. Excess heat could cause the build up of steam within the paste, resulting in damaged ceramics and potentially human injury. Assuming a relatively dry furnace system, the preheat would take somewhat less than one hour, and consume 3-4kg of charcoal.

Smelting - The charging cycle commenced as soon as the furnace was hot and dry, and consisted of keeping the chimney full to the stokeline with fuel and mineral, whilst recording the timing and nature of charge consumption. The ratio of fuel to mineral was one of the controlled variables of the Fiavè tests, but the method of charging was common to all. The fuel and mineral were weighed separately in 1kg batches, and then mixed thoroughly in a bucket, thus making 2kg or 3kg of charge, depending on the fuel ratio. It is acknowledged that the Khao Wong Prachan smelters may have calculated smelting charges based on the volume of reactants rather than their mass. However, given the significant difference in density between minerals and charcoal, it was more practical to produce mass-based charges.

The charge was fed gradually and evenly to the furnace, as and when there was room. For a NPW3/MeP2**PR** furnace the total charge (fuel + mineral) after preheating was 12kg and 8kg for the NKH3/MeP3 reconstruction (or 18kg and 12kg respectively with a 2:1 fuel to mineral ratio). This quantity of material did not feed at an even rate for either of the models. The initially voracious consumption soon began to decline as the furnaces choked with slag and unreacted charge, until an end point was reached and the chimneys could take no more. The specific reasons for this are discussed below in the results section.

Sampling - The furnaces were sampled as soon as they were cool enough to do so. The pressing objective in doing this was to clear the smelting area for the next test to begin, and also to look for immediate evidence that would modify the proceeding experiment's parameters e.g. did the previous test's fuel to mineral ratio produce an acceptable slag cake? Time concerns aside, the purpose of the sampling was to recover as much as possible of the slag, metal, ceramic, and unreacted mineral from each smelt. Given small grain sizes for the quartz (and the entire mineral charge in Burns 7 and 8), it was not possible to find all the smaller and lighter material in the mass of charcoal, ash, and vitrified ceramic each test produced. The sampling was undertaken with the objective

of providing material for analytical work to better understand the complex interactions taking place in the furnace⁸.

The above section constitutes the standard procedure for the Fiavè campaigns. Details specific to each test are provided in the results section below.

7.3 - Experimental data

The temperature data and field notes produced during the Fiavè experiments are documented in Appendix C. A summary of these results can be seen in Table 7.2, and an expanded description of each of them is given below.

Burn	Date	Reconstruction	Fuel/ Grain		Thermocouples	Duration	Charge	Products+	
			Mineral	size				Charcoal	Byproducts
				(mm)	number + depth	(hr)	(kg)	(kg)	(kg) _(recovered)
1	4-Sep-07	NPW3/MeP2PR	1:1	20-30	8 @ 10mm	3:23	0.95	5.0	0.7
2	5-Sep-07	NPW3/MeP2PR	1:1	<10	4 @ 10mm	2:44	3.00	7.0	1.5
3	5-Sep-07	NPW3/MeP2PR	1:1	<10	4 @ 10mm	3:45	4.00	7.0	1.4
4	6-Sep-07	NPW3/MeP2PR	2:1	<10	4 @ 10mm	3:20	2.90	7.8	0.8
5	7-Sep-07	NPW3/MeP2PR	1:1	<10	4 @ 0mm	3:32	5.71	9.7	2.6
6	7-Sep-07	NKH3/MeP3	1:1	<10	4 @ 0mm	1:32	3.74	5.7	3.0
7	9-Sep-07	NPW3/MeP2PR	1:1	<2	3 @ 0mm	3:02	5.71	10.7	2.6
8	10-Sep-07	NKH3/MeP3	1:1	<2	3 @ 0mm	3:13	3.74	8.7	0.2
9	11-Sep-07	NPW3/MeP2PR	2:1	<10	2 @ 0mm	3:18	5.71	17.9	3.0
10	11-Sep-07	NKH3/MeP3	2:1	<10	2 @ 0mm	2:52	3.74	12.5	2.0

Table 7.2 - Major parameters of the 2007 Fiavè experiments, thermocouple 'depth' refers to the protrusion of the probe from the interior chimney wall.

Burn 1 - 4th September 2007

The first NPW3/MeP2PR reconstruction was ignited at 09:57 with the thermocouple probes at 10mm, and measurements were recorded for 190 minutes. The steep experimental archaeology learning curve was fully evidenced during Burn 1, it soon became apparent that the initial assumption of producing a 2kg cake of pure slag (and thus charging the furnace with c. 12kg of mineral) was too much material for the small furnace to handle. Reflecting the maximum residual mineral dimensions in the archaeological slags, Burn

⁸ Once the impact of the revised chronology was realised, it was clear that extensive laboratory analyses on the experimental assemblage would not be worthwhile. However, macroscopic assessment was sufficient to assess the MeP3 reconstruction given the obvious differences between the archaeological and experimental products.

1 was conducted with a charge granulometry (ex quartz and lime) of 20mm. As can be seen in Figure 7.12, about 80 minutes after ignition, 7 of the 8 probes indicate a steady loss of temperature, suggesting that a furnace of this size could not cope with such large fragments, only 1.95kg of mineral was charged during the first experiment. As a smelt, Burn 1 was undoubtedly a failure, but as an archaeometallurgical experiment its value was immeasurable - in less than 60 minutes of firing it had been ascertained that one of the core assumptions (quantity of slag production) required modifying, and that the charge grain size variable had an upper limit. Due to the consistent loss of temperature, and obviously unsuitable burden dynamics, Burn 1 was abandoned at 13:20.

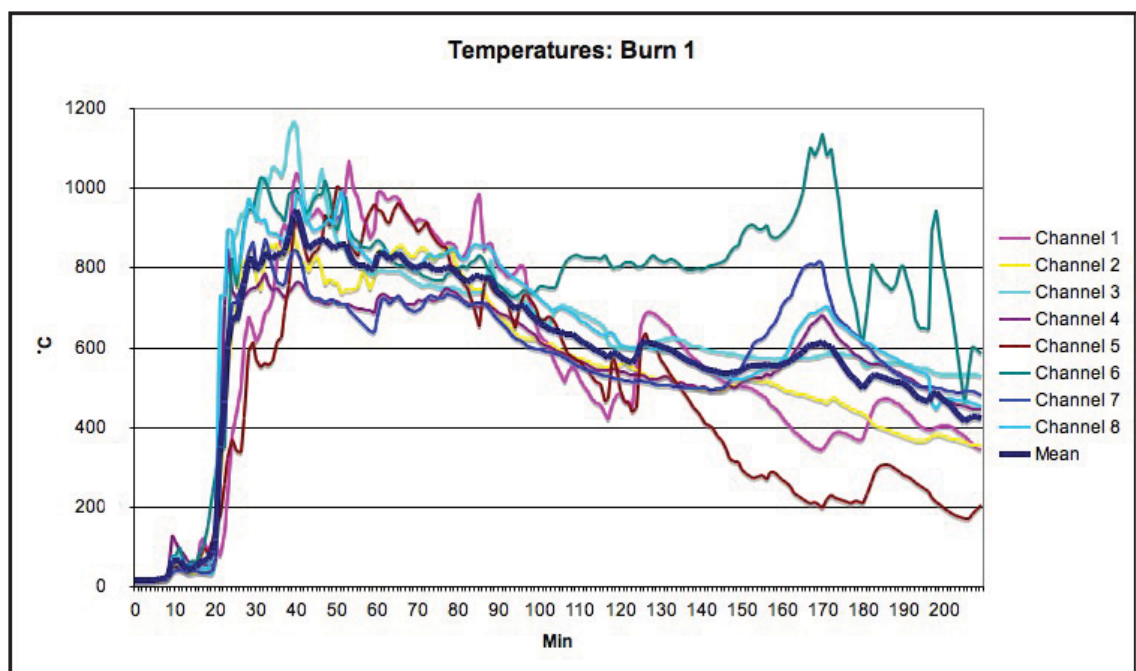


Figure 7.12 - Graph of temperature data for Burn 1. Image: author.

Upon sampling the furnace, the observation of inappropriate grain size was confirmed by the relatively small amount of sintered slag (c. 0.5kg) and the quantity of unreacted charge (c. 0.2kg) - the remaining mass having burnt off as gas or lost in the general debris. A very small amount of copper was seen to have formed as prills and filaments in the slag, but in no way commensurate with the copper metal potential of the minerals that had been charged. In Burn 1, and in subsequent tests, it was not possible to give estimates for the amount of metal produced due to its being dispersed throughout the slag. To quantify it would require crushing all of the experimental slags, and that could not be done in the field for practical as well as procedural reasons i.e. if the experimental material was to be studied in the future, it would be better not to have destroyed all the macro-morphological evidence.

It was noted that the slag produced had adhered to the interior chimney wall, just above

the perforation facing the air stream (Figure 7.13). As might have been expected, this was the hottest part of the furnace, and thus where the minerals were able to fuse, but critically, the archaeological perforated ceramic fragments provided no evidence of having been slagged (Chapter 4). Why this should be the case was a question that persisted during the 2007 Fiavè campaign.



Figure 7.13 - Sections of slagged furnace chimney and unslagged crucible from Burn 1. Image: author.

Burn 2 - 5th September 2007

From the outset it was intended that the first few experiments would be similar, to allow the basic performance of the reconstruction arrangement to become apparent. Thus, the second test was a NPW3/MeP2PR construction, but experience with the mineral grain size was taken into account, and modified to 10mm. Burn 2 was ignited at 11:41, with the temperature monitored by 4 equally spaced thermocouples at 10mm probe depth

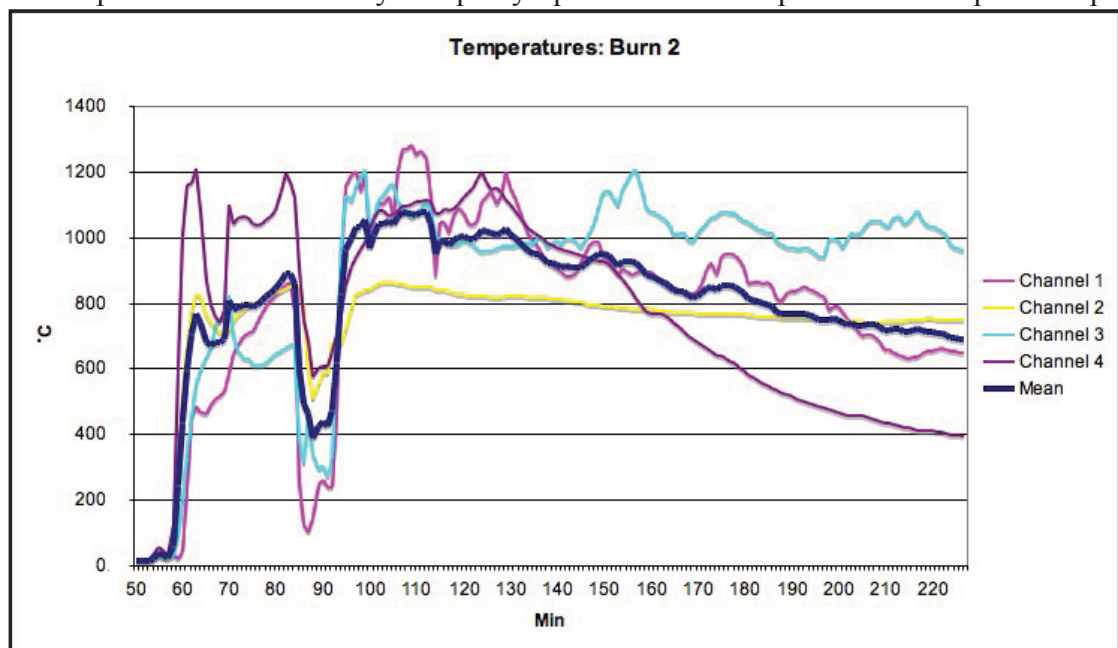


Figure 7.14 - Graph of temperature data for Burn 2. Image: author.

(Figure 7.14). The test lasted 164 minutes until 14:25, and demonstrated that with a more appropriate granulometry, the furnace was able to perform much better. However, the furnace was still only able to consume half of the full c. 6kg of minerals calculated for the test. Burn 2 was started with a damp furnace, which soon resulted in a large fissure developing on the side of the chimney facing the air stream (Figure 7.15). This was of neither surprise nor concern, it being appreciated the primary purpose of a copper smelting furnace is to give the charge shape, and not to exclude oxygen.



Figure 7.15 - Large crack in the chimney wall during Burn 2, but the integrity of the smelt was not affected. Image: author.



Figure 7.16 - Adhesion of chimney and crucible during Burn 2 - now known to be an archaeologically incorrect association. Image: author.

During sampling, the improved performance of the reconstruction was immediately apparent in the greater proportion of slag and sinter recovered from the smelting debris (Table 7.2). Although a slag cake comparable to the archaeological examples had not formed, sufficient liquid slag had been produced to bond the chimney to the crucible below (Figure 7.16).

Burn 3 - 6th September 2007

Burn 3, ignited at 10:36, with the same NPW3/MeP2PR operational parameters as Burn 2, and constituted the last of the ‘acclimatisation’ smelts (Figure 7.17). The experiment was also conducted in the presence of Vincent Pigott, and as one of the principal investigators of the Valley excavations, his comments at this juncture were given credence. Pigott’s opinion at the end of the test (14:21) was that the crucibles and chimneys were under-sized compared to the majority of those he excavated. The suggested revision of the internal diameter of the experimental ceramics, and the height of the chimney, from 180mm to 200mm was not large linearly (~10%), but the ramifications for the volume of the furnace would be significant - an increase of ~40%, from approximately ~18l to ~25l. This problem was largely caused by dimension changes as the clay was first dried, then fired, and merely necessitated an adjustment of the production procedure to account for shrinkage.

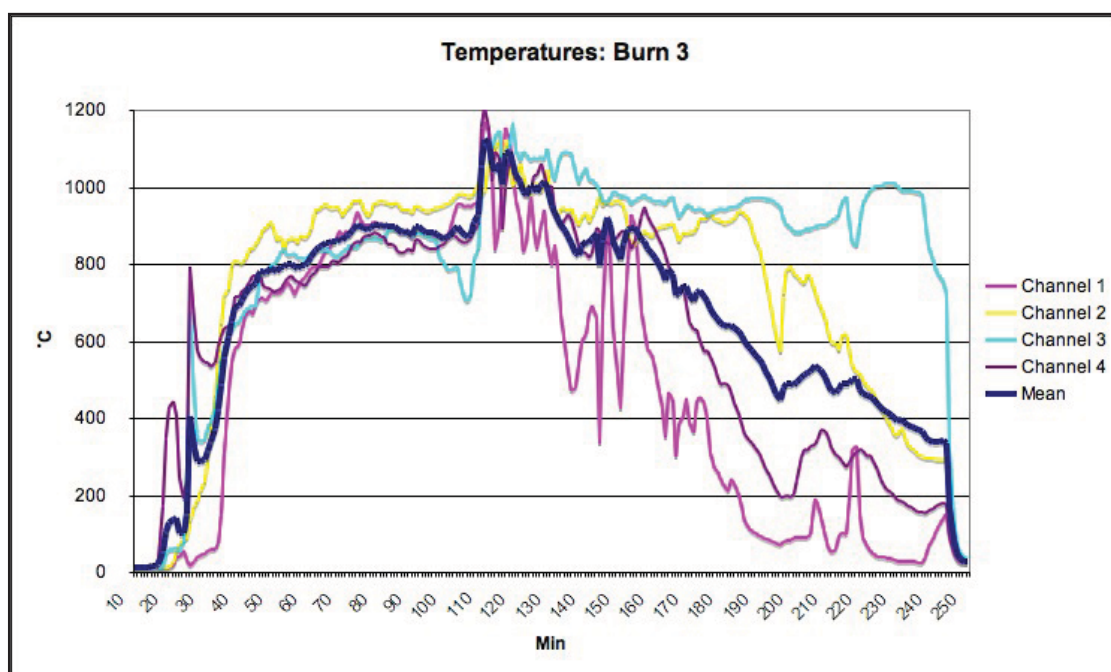


Figure 7.17 - Graph of temperature data for Burn 3. Image: author.

Burn 3 was able to take only 4kg of the calculated charge but was found to have produced a reasonable amount of slag and sinter (Table 7.2). This material had bonded the chimney to the crucible, but had not formed the desired slag cake. Examination of the conglomerate, starting from its base, revealed a clear and consistent patterning of well-formed slag,

through bonded sinter, scorched, and finally unreacted mineral charge (Figure 7.18). The aim of the Fiaivè tests was to produce an archaeologically comparable heterogeneous slag cake, but already by the end of Burn 3 it was apparent that something was amiss with the wind-powered technological reconstruction.



Figure 7.18 - Sectioned remains of Burn 3. Image: author.

Burn 4 - 6th September 2007

The fourth experiment was a further NPW3/MeP2PR reconstruction using the unmodified ceramic dimensions, and conducted with an increased fuel to mineral ratio of 2:1, in an attempt to produce a more liquid and fully reacted slag than the previous three smelts. However, despite the extra fuel, there was very little difference in the resulting debris, if anything, there was less slag produced from the 2.9kg of minerals charged (Table 7.2). The furnace was lit at 14:55 and abandoned after 200 minutes at 18:15 (Figure 7.19).

Although ceramic dimensions were not intended to be an experimental variable, it was noted that the chimney for Burn 4 (reused from Burn 1) was slightly smaller than that for Burn 3. Given the extra fuel charged during Burn 4, it was appreciated that getting the furnace proportions correct was of the utmost importance for the Khao Wong Prachan reconstructions. Vincent Pigott's comments regarding the ceramics on 5th September were heeded, and during the 6th September a new batch of crucibles and chimneys were constructed.

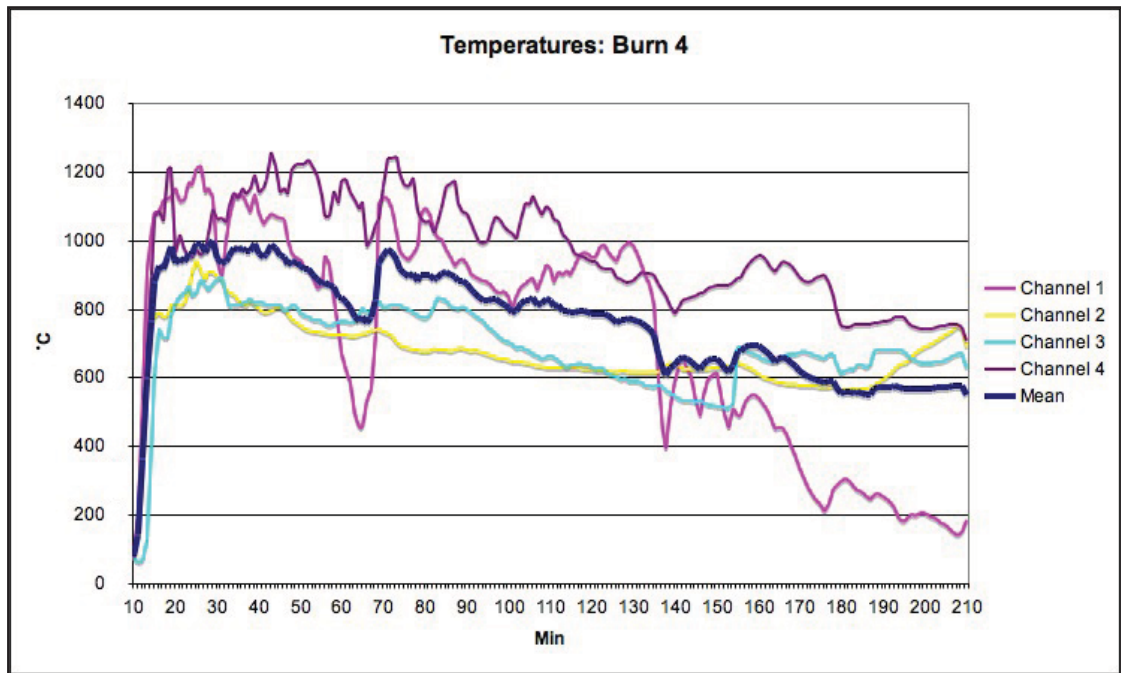


Figure 7.19 - Graph of temperature data for Burn 4. Image: author.

Burn 5 - 7th September 2007

The fifth experiment was essentially a repetition of the NPW3/MeP2PR reconstructions in Burns 2 and 3, but with the resized crucible and chimney. Using a mineral grain size of 10mm (ex quartz and lime) and a fuel to mineral ratio of 2:1, the new furnace was found to perform extremely well. After a 11:00 ignition, the increased volume of the smelting system seemed to have the effect of smoothing the charging cycle and accelerating charge consumption through to the 14:32 termination of the test (Figure 7.20).

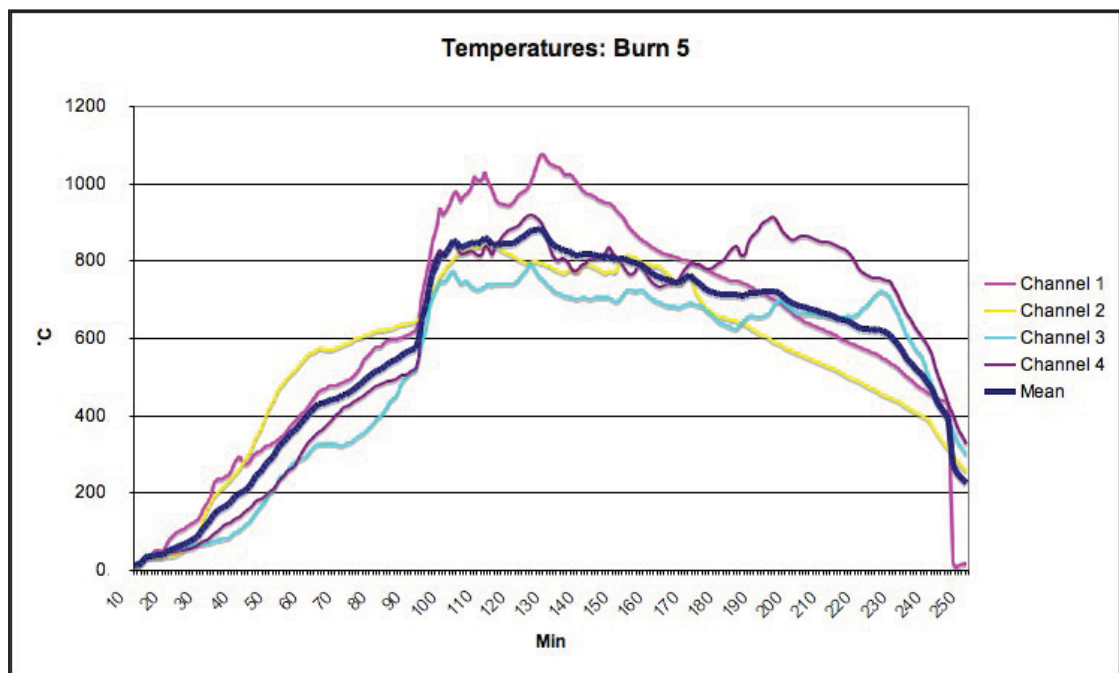


Figure 7.20 - Graph of temperature data for Burn 5. Image: author.

When sampled, the crucible was once again found to be bonded to the chimney. However, despite the apparently augmented operation of the furnace, there was still no slag cake approximating the archaeological examples, but for the first time the entire 5.71kg of minerals had been consumed. Though more evenly formed, the majority of the slag (c. 2.6kg) was once again found adhering to the interior of the chimney wall facing the air stream.

Burn 6 - 7th September 2007

Burn 6 was the first NKH3/MeP3 reconstruction, it employed the same variables as Burn 5, but used the appropriate charge composition and a 1:1 oxygen to sulphur ratio - i.e. much less malachite. The chimney stack from the previous test was repaired and reused, and the pit lined with clay (Figure 7.21). The experiment commenced at 15:28 and proceeded smoothly and swiftly - unsurprising given the total charge was nearly half the volume of a NPW3/MeP2PR one - until completion at 17:00 (Figure 7.22, Table 7.2).



Figure 7.21 - Furnace chimney from Burn 5 being repaired for Burn 6, and placed over a clay-lined pit. Image: author.

When sampled, the furnace was fused as normal, and contained a large mass (c. 3kg) of fused slag and ceramic (Table 7.2). However, the slag had again failed to form a cake, despite the enlarged furnace design and reduced charge quantity of the NKH3/MeP3 reconstruction.

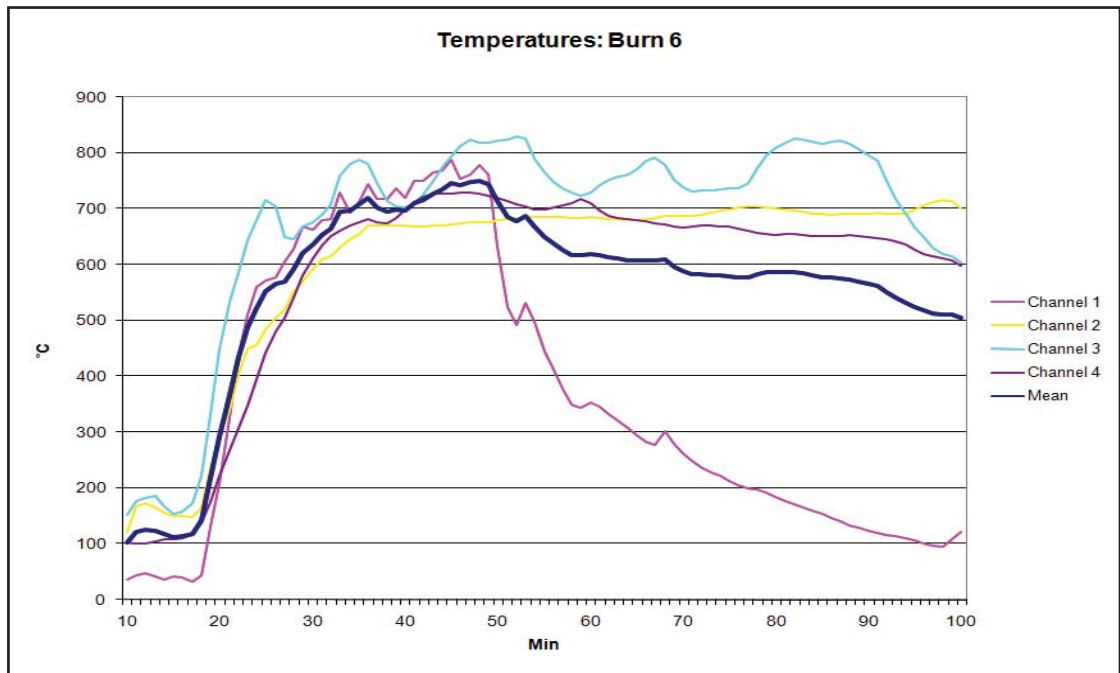


Figure 7.22 - Graph of temperature data for Burn 6. Image: author.

Burn 7 - 9th September 2007

The seventh experiment was another NPW3/MeP2PR reconstruction, used to test the effect of reducing the mineral grain size down to c. 2mm. Not only would this replicate the lower size range of residual minerals noted in the archaeological slags (Chapter 5 and 6, Burn 1 representing an attempt with the largest dimensions at 20mm), but it would also mean the metal-bearing minerals would for the first time be of a similar size to the quartz and lime - their previously different sorting characteristics perhaps having caused problems with slag formation in earlier tests. Burn 7 was ignited at dusk (18:20) (Figure 7.23) and continued into the night (21:22) (Figure 7.24). Whilst the lack of external light enhanced the visibility of the internal dynamics of the furnace, and the combustion of $\text{CO}_{(g)}$, it made the recording of external features harder.



Figure 7.23 - Burn 7 operating by night. Image: author.

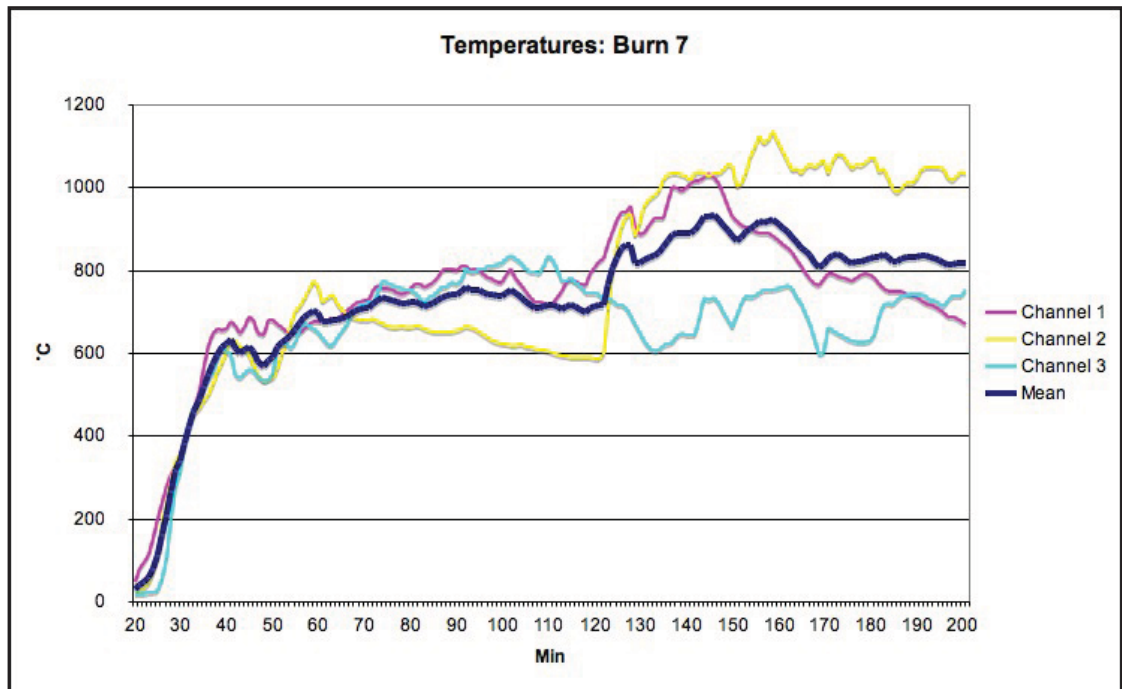


Figure 7.24 - Graph of temperature data for Burn 7. Image: author.

Sampling the furnace on the morning of the 10th, it was clear that charging powdered minerals into a Valley furnace was unlikely to produce a suitable outcome. Although a reasonable amount of slag (c. 2.55kg) had formed on the interior furnace wall, the crucible was completely empty, and a large dark core to the debris consisted solely of unconsumed powdered charge (Figure 7.25).



Figure 7.25 - The unreacted core of Burn 7. Image: author.

Burn 8 - 10th September 2007

Despite the conclusively negative result of the previous test, for the sake of consistency it was decided to pursue the 2mm mineral grain size for a NKH3/MeP3 reconstruction. After a 10:45 ignition, the problem noted in Burn 7 was seen to be recurring: the powdered charge was smothering the furnace to a very deleterious extent (Figure 7.26). Despite the small quantity of the charge, c. 4kg, the smelt took 193 minutes, and hopes were not high for the result.

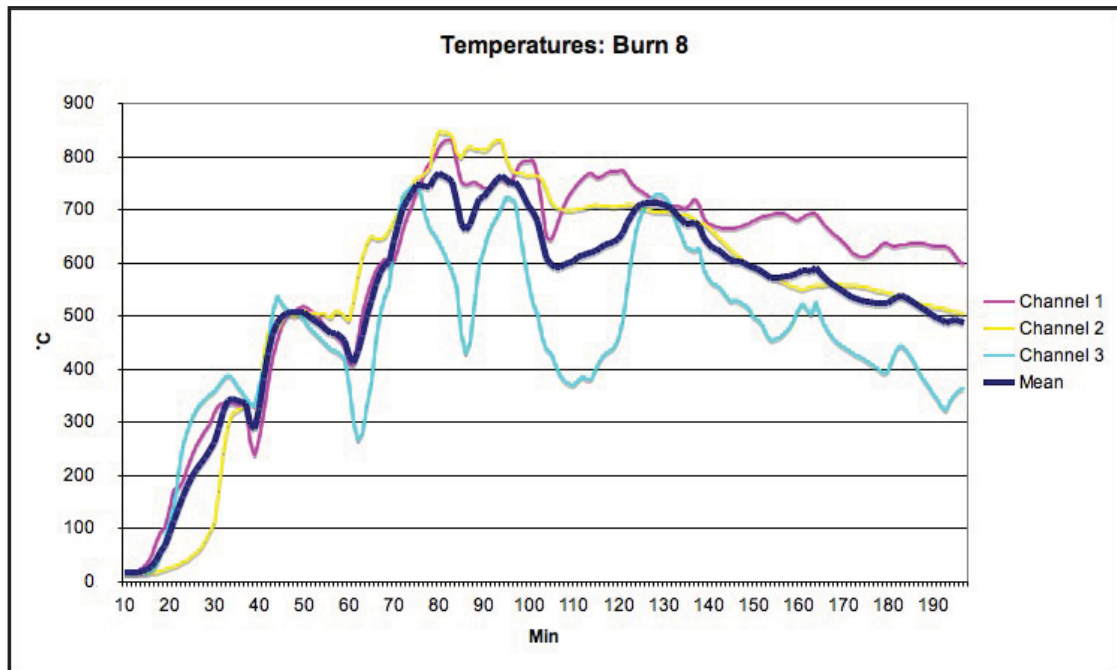


Figure 7.26 - Graph of temperature data for Burn 8. Image: author.

When sampled, the furnace, as expected, was found to be choked with unreacted mineral. Not only was a lot of charge wasted, and unrecoverable due to its grain size, the amount of slag produced was the least since Burn 1 - a mere 200g (Table 7.2). A low mineral grain size was definitively removed from the list of variables, and all subsequent tests returned to what seemed to be a reasonable optimum of 10mm (ex quartz and lime).

Burn 9 - 11th September 2007

In the limited time remaining, the last variable to be assessed with the resized ceramics was the fuel to mineral ratio. Therefore, Burn 9 was conducted as a NPW3/MeP2 PR reconstruction, as per Burn 5, but with a charge ratio of 2:1. The crucible from Burn 7 was reused, and the last three thermocouples arranged at 120° to each other and flush to the furnace wall. Burn 9 was initiated at 10:02 and lasted 198 uneventful minutes (Figure 7.27, Table 7.2). The result was, once again, a chimney firmly slagged to an empty crucible.

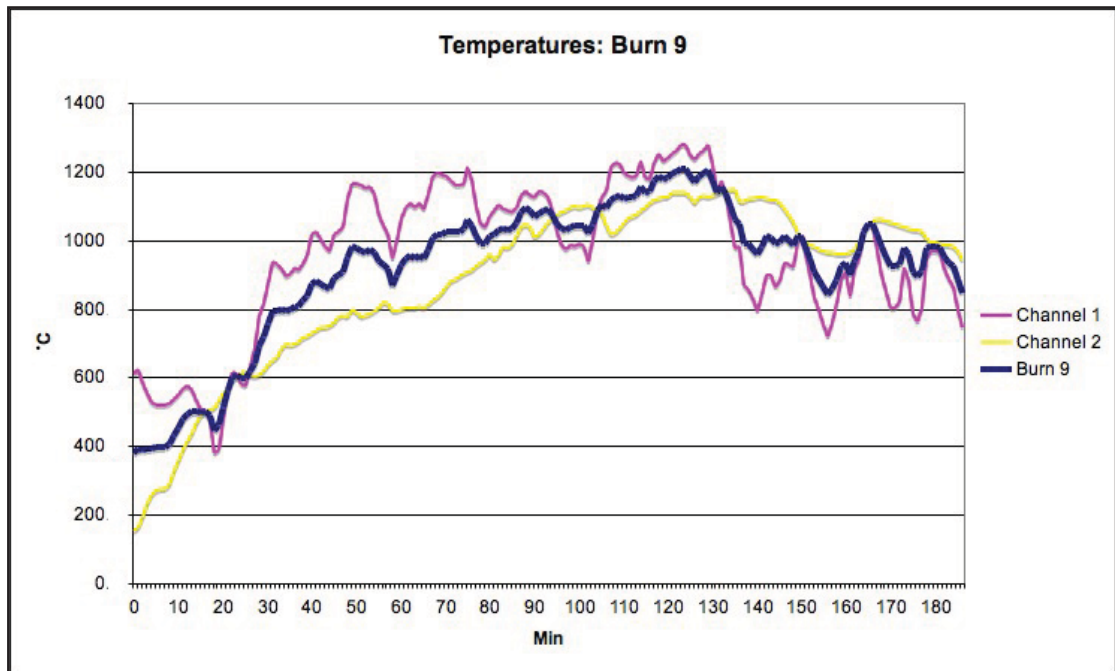


Figure 7.27 - Graph of temperature data for Burn 9. Image: author.

Burn 10 - 11th September 2007

The final experiment of Fiaivè 2007 was a NKH3/MeP3 reconstruction run to the same parameters as Burn 6, excepting the fuel to mineral ratio of 2:1. The furnace was seen to burn extremely hot, with the foremost of the two extant thermocouples registering up to 1200°C when flush with the furnace wall (Figure 7.28). Again, the small amount of mineral, c. 4kg, was rapidly consumed with the rest of the fuel, c. 8kg, and the smelt proceeded for 192 minutes without interruption after ignition at 14:50.

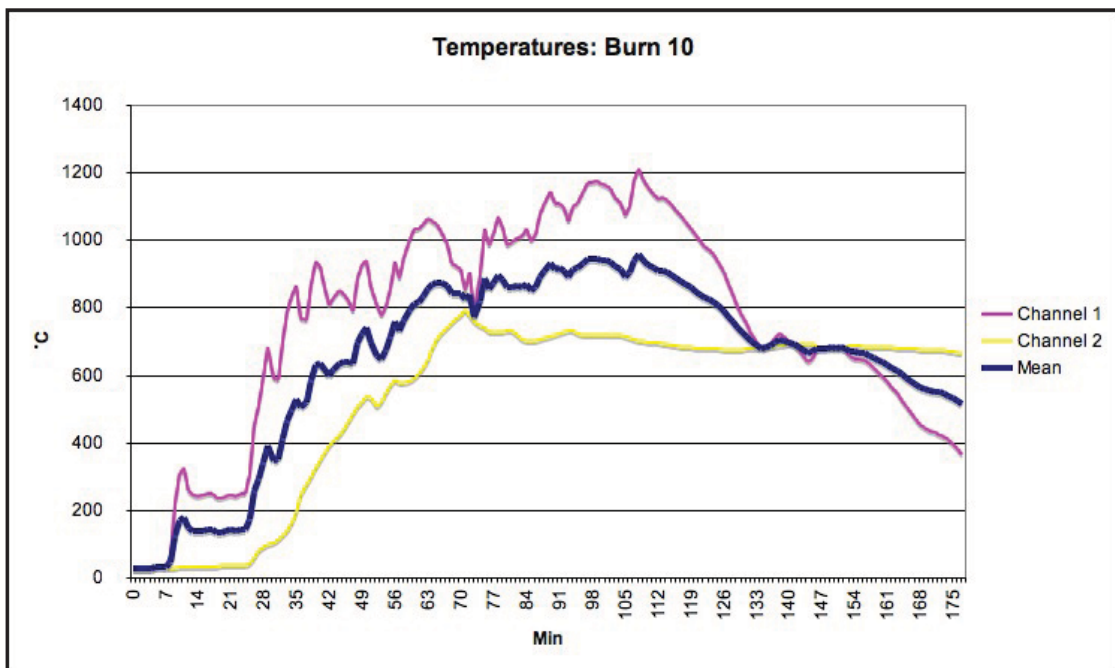


Figure 7.28 - Graph of temperature data for Burn 10. Image: author.

The furnace was sampled and seen to have produced a large amount of slag (Table 7.2), but again, the mass was attached to the chimney wall, and had not formed a cake in the base of the furnace (Figure 7.29).



Figure 7.29 - Mass of semi-fused charge attached to the furnace wall during Burn 10. Image: author.

7.4 - Interpretation

Given the many layers of archaeological and archaeometrical interpretation required just to plan a reconstructed smelt, it follows inferences deriving from experiments are necessarily cautious. However, the Fiaavè campaign provides strong indications the established TAP reconstruction of copper smelting at later Iron Age Nil Kham Haeng may be in need of substantial modification.

The long-held interpretation of the NKH3/MeP3 technology as wind-powered is derived largely from the recovery of perforated ceramic fragments in the industrial matrix, their complete cylindrical comparators from burial contexts, the seasonal presence of strong winds, and the existence of wind-powered furnaces elsewhere in the world (e.g. Bunk *et al.* 2004, Catapotis *et al.* 2008, Tabor *et al.* 2005, van Buren & Mills 2005), and this is the logical technological paradigm within which the author approached the evidence. However, whilst most of the Fiaavè copper smelts were ‘successful’ in that they produced copper metal, they also highlighted the consistent failure of the wind-powered perforated

cylinder ‘furnace’ reconstruction to produce archaeologically-comparable slag and technical ceramic debris. As seen in other experiments with wind-powered furnaces (e.g. Catapotis *et al.* 2008), the smelts were seen to have a strong thermal gradient perpendicular to the blast, with several hundred °C difference from front to back, easily seen in the thermocouple data from Burns 9 and 10 as the two remaining probes were positioned at the front and back of the chimney (Figures 7.27 and 7.28). This uneven heat distribution caused the preferential formation of slag on the interior wall of the chimney facing the fan (Figures 7.13, 7.16, 7.18, and 7.29). This conglomeration of reacted, partially reacted, and unreacted charge would eventually block the perforations, causing temperatures to drop as gas circulation reduced, and thus ended each smelt before the charge was fully consumed or an acceptable slag cake formed.

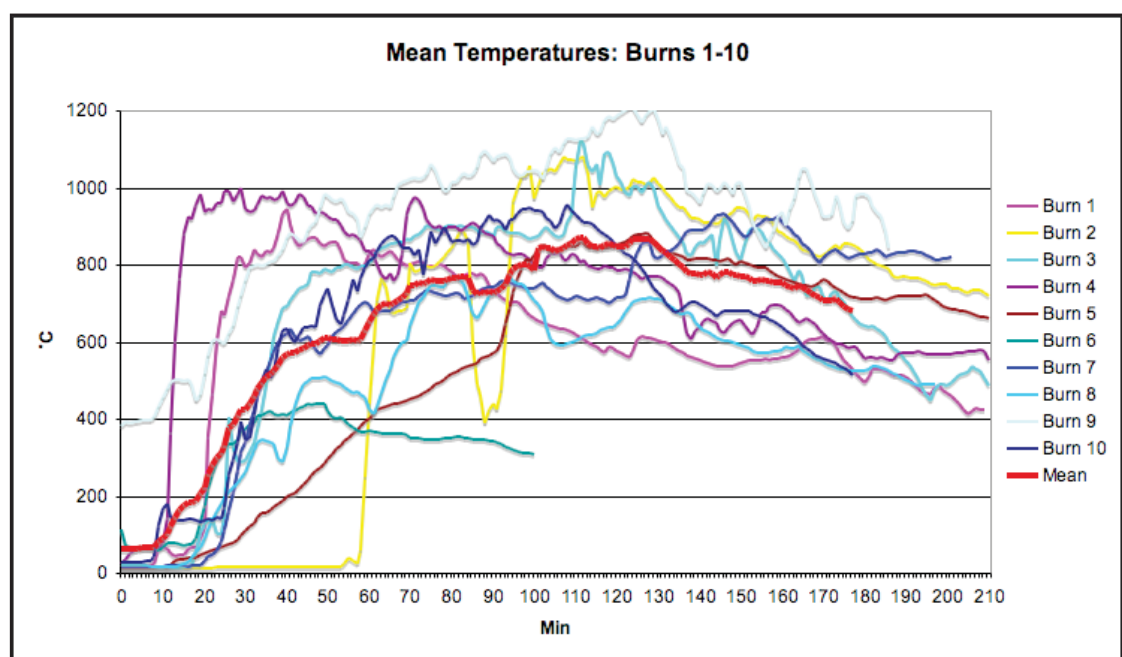


Figure 7.30 - Graph of mean temperature data for Burns 1-10. Image: author.

These results could be partially attributed to the author’s relative lack of smelting expertise, but the consistent recurrence of these issues with varying fuel:mineral ratio and granulometric parameters, and in spite of the uniform fan-generated airflow, suggests the Fivè campaign highlight real problems with the NKH3/MeP3 reconstruction. In essence, the subterranean part of the furnace is a dead spot as far as smelting goes, due to the lack of air blast and thus heat reaching this area. Though the perforated furnaces could produce high temperatures (Figure 7.30), the heat energy required to drive the smelt was concentrated high up, and to the front of, the structure. Thus, all charge reaction seems to have taken place there, with no slag ever forming in the space below. Significantly, this correspondence of high temperature and reaction activity meant the degree of slagging and vitrification on the experimental chimneys was vastly in excess to that seen on the archaeological examples. Though no analytical characterisation of the experimental slag

was carried out, but it's obvious macroscopically that they were less reacted and more wasteful than the archaeological ones, regardless of charge composition and granulometry. Therefore, the following experimental inferences may be drawn:

1. The NKH3/MeP3 smelting process was unlikely to be wind-powered due to the inability of the perforated 'furnace' to provide a sufficient, sustainable, and uniformly high temperature for the charge to react and a slag cake to form.

2. The implausibility of wind-power implies the NKH3/MeP3 smelting process required the provision of a forced blast, which, in keeping with the archaeological evidence, must be organic. The MeP2 crucible and the MeP3 ceramic-lined pit would necessitate the heating of substantial volumes of volume of smelting charge, but this could have been reasonably achieved with the use of multiple air sources, as has been widely documented ethnographically in Africa (e.g. David & Kramer 2001, Rehder 1994, Schmidt 1997). Within Southeast Asia, the ethnographic precedent of bamboo and teak piston bellows (e.g. Anon. 1886, Bronson & Charoenwongsa 1994, Wake 1882) provides a plausible regional analogy, but skin bellows or blowpipes could also account for the lack of extant remains. Whilst the MeP2 and MeP3 reconstructions are still relatively small scale, it is not unreasonable to envisage two or three bellows being operated, or a group of people using blowpipes, though the technological choice of using a forced blast represents a significant expenditure of effort in comparison to wind-powered operations. In any event, the technological reconstructions do not require the provision of perfect air delivery as the archaeological slag evidence suggests the heating was substantially uneven, and the numbers of people potentially involved in each smelting operation is still commensurate with White & Pigott's (1996) interpretation of a 'community specialisation' organisation of production.

3. Despite the clear archaeological association between smelting debris and perforated ceramic fragments at later Iron Age Nil Kham Haeng (and contemporary Khao Sai On), it may be necessary to drastically reinterpret the function of the perforated ceramic cylinders. Laboratory analyses (Chapter 6) indicate the NKH3/MeP3 'slag-skin' and 'furnace' fabrics are chemically and microstructurally very similar, if not identical, and thus their refractory performance should be comparable, all else being equal. How then can we correlate the extensive vitrification and bloating evidenced in the 'slag-skins' with the optically active micromass and only slight heat damage of the archaeological 'furnace' samples, as well as the heavy slagging seen on the experimental chimneys? It seems very likely that the thermal and/or chemical exposure of these two artefact classes

was rather different. It is this corroboration of macroscopic, chemical, microscopic, and experimental evidence which leads the author to propose that the perforated ceramic cylinders probably weren't involved in copper smelting processes, as close contact between the ceramics with fluxes in the mineral charge (i.e. iron oxide) and fuel ash (i.e. calcia) would typically produce extensive slagging at high temperature. Though we lack NKH3/MeP3 crucible evidence, it is conceivable however that the cylinders functioned as *casting* furnaces. With the alloy melt contained, the perforated cylinder would only be exposed to the fluxing effects of the fuel, perhaps explaining the lower degree of heat damage as well as the copper 'splash' seen in Figure 6.7. This is a significant modification of the established TAP *chaîne opératoire* (Figure 1.4, Ciarla 2007b, Pigott *et al.* 1997), and the implications of this tentative reinterpretation will be discussed in Chapter 8.

4. With the NKH3/MeP3 reconstruction potentially 'superstructureless', there would remain very little difference between its configuration and that of the NPW3/MeP2 smelting process (Figure 7.31). Both are essentially 'bowl' furnaces, but whereas the early Iron Age Non Pa Wai 'bowl' is a crucible in a pit, the later Iron Age Nil Kham Haeng 'bowl' is a clay-lined pit, but both would need a forced air blast to generate temperatures suitable for copper smelting. It should be noted that if the uncoupling of perforated ceramic cylinders from smelting activities is accepted, then the diameter of the clay-lined smelting pit can no longer be based on that of the 'furnace chimney' as it was in Chapter 6 - nevertheless, the pits' dimensions are likely to have been modest in light of the mean slag cake mass of c. 500g. Given the typical dearth of evidence for pyrotechnological installations and highly fragmentary nature of the archaeometallurgical assemblage from both Valley smelting sites, the proposed reconstructions are considered to be conservative offerings, though the potential for them to be modified is explicitly acknowledged.

Summary

The experimentally-inspired interpretations above represent a significant departure from previous TAP reconstructions and, perhaps importantly, highlight just how similar, and possibly related, the two prehistoric Valley copper smelting processes may have been. In addition to refining the laboratory-based *chaînes opératoires* (Chapters 5 and 6), the Fiavè experimental campaign, and hopefully others to follow, have reiterated the need to carefully unravel ancient metallurgical behaviours from the archaeological evidence, in order to identify the significant changes in Valley copper production during the Iron Age.

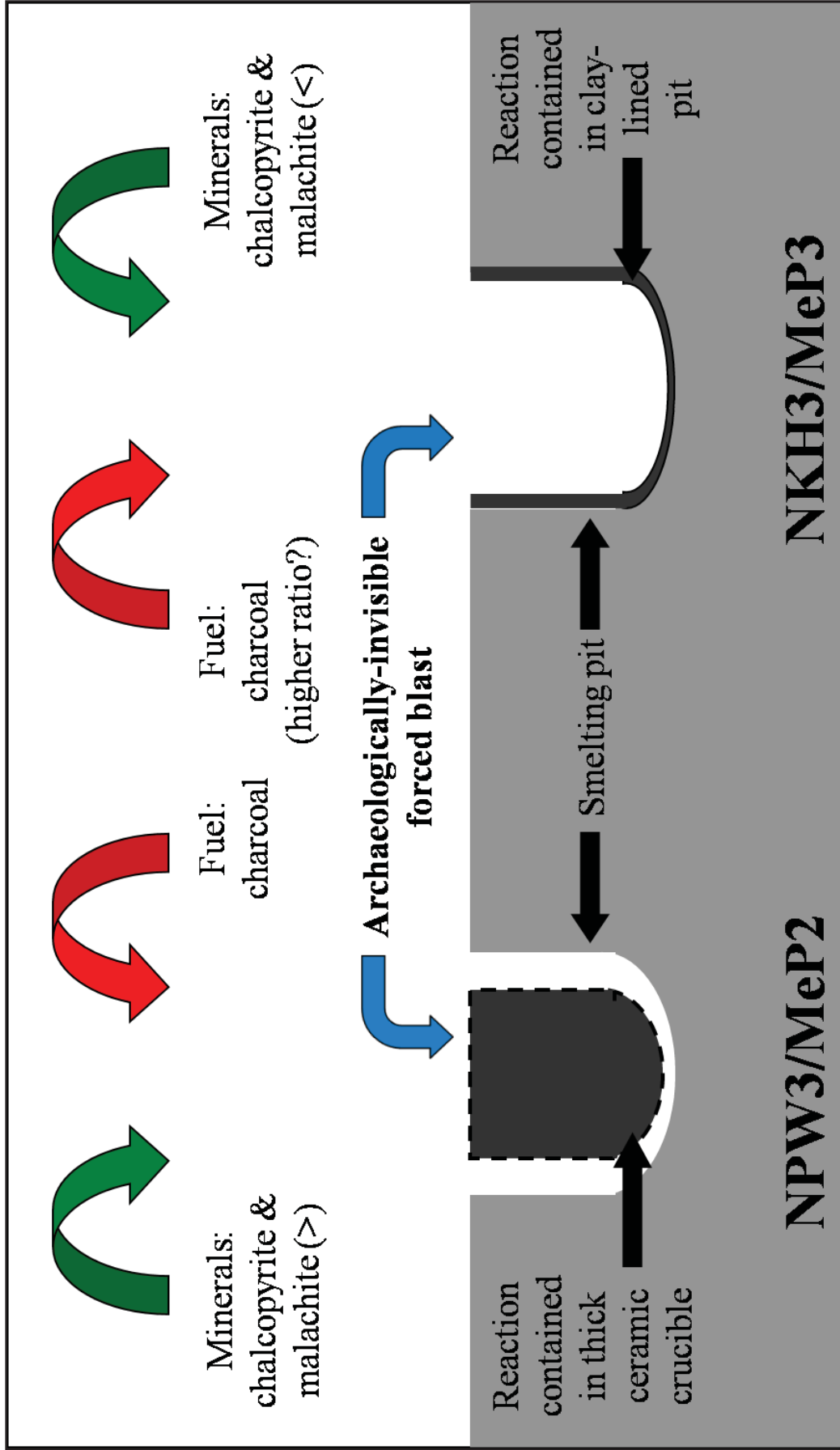


Figure 7.31 - Schematic of the NPW3/MeP2 (left) and NKH3/MeP3 (right) technological reconstructions after the Fiavé experimental campaign. Image: author.

Chapter 8

The Development of Metallurgy in the Prehistoric Khao Wong Prachan Valley

The extensive efforts of the TAP team, combined with, and refined by, the present study, permit a tentative account of the long-term interaction between metal, metallurgy and people in the Khao Wong Prachan Valley during the period c. 6/500 BCE to c. 300 CE. Subject to the vagaries of taphonomic chance, any such history is necessarily far from definitive, and as has been stated several times, a finer chronological and contextual resolution for the archaeological evidence would doubtless reveal a wealth of important detail. Nevertheless, juxtaposing the technological reconstructions from early Iron Age Non Pa Wai (Chapter 5) and later Iron Age Nil Kham Haeng (Chapters 6 and 7), exposes significant changes in local extractive metallurgical traditions. The mid/late 1st millennium BCE and early 1st millennium CE chronological window of the Non Pa Wai and Nil Kham Haeng evidence corresponds to a period of probable increasing social complexity in Iron Age Thai societies, marked by the appearance of site size hierarchies, earthworks for defensive and/or hydraulic purposes, and the marked ranking of individuals and groups in burial traditions (overviewed in Chapter 1, see also e.g. Higham 2004, O'Reilly 2003, White 1995). This transition is metallurgically-marked by an increasing deposition of metal, especially bangles, in predominantly funerary contexts (e.g. Higham 2002), and is presumed to represent a notable escalation in general consumption. This chapter discusses how this potentially elevated regional demand for metal may have been reflected in supply behaviour in the Iron Age Khao Wong Prachan Valley. The first section concentrates on the identification of metallurgical behavioural change within Valley copper production *chaînes opératoires* using the archaeometallurgical evidence described in Chapter 2, 5, 6, and 7. The second section attempts to provide some explanation for these changes with relation to stimuli from the wider region, and the third and final section offers some commentary on the 'origins' of copper-base metallurgy in the Khao Wong Prachan Valley.

To reiterate the reconstructed *chaînes opératoires* for early Iron Age Non Pa Wai and later Iron Age Nil Kham Haeng provided at the end of Chapters 5 and 6 (the latter modified in light of the field experimentation detailed in Chapter 7):

- The NPW3/MeP2 process has been interpreted as a crucible-based copper smelting operation, taking place within a roughly hemispherical crucible of c. 20cm diameter, constructed in a coarse organic-tempered fabric that frequent slagging and heat damage.

The limited archaeological evidence suggests these crucibles were positioned within in a small pit, which was itself surrounding by a low ceramic rim, made from a fabric similar to that of the crucibles. The mineral charge is uncertain but included both oxidic (e.g. malachite) and sulphidic (e.g. chalcopyrite) copper minerals, as well as iron oxide minerals (predominantly magnetite). The composition and structure of the slags indicates that the smelting operation was often incomplete and that there was considerable variation in the smelting charge. The absence of any evidence for tuyères suggests that the smelt must have been driven by an organic mechanism (like piston bellows) or simply by blowpipes (reconstruction summarised in Figure 5.50).

- The NKH3/MeP3 process has been interpreted as a bowl furnace-based copper smelting operation, taking place within a clay-lined pit of unknown but certainly limited dimensions. These pit-linings or ‘slag-skins’ were made in a coarse organic-tempered fabric and were heavily slagged and heat damaged. The smelting charge is also uncertain, but appears to have been more consistently sulphidic than that seen in the MeP2. The MeP3 slag chemistry has a much decreased variability and an increased concentration of minor oxides indicative of ceramic and fuel ash contributions to the melt. Together these data suggest that the MeP3 smelting charge was more standardised than that of MeP2 and that the process may have been longer and/or hotter. In light of the experimental data the perforated ceramic cylinders are not now thought to be part of the copper smelting *chaîne opératoire*, which means the process must have been driven by an archaeologically-invisible air delivery system (reconstruction summarised in Figure 5.43).

The following section will discuss how these reconstructions can begin to be integrated to provide a long-term understanding of change in Valley technological choices by highlighting and explaining the differences and similarities in technological styles between them.

8.1 Identifying stylistic change and continuity in Valley copper smelting

Given the proximity of Non Pa Wai and Nil Kham Haeng (c. 3km), and the apparently continuous Iron Age production sequence (c. 6/500 BCE to c. 300 CE), it is likely that there is some continuity between the copper production technologies and the people who practiced them. Many of the shared technological characteristics are driven by the sites’ contiguous physical geographical affordances, i.e. the presence of metallogenic mineralisations, charcoal fuel, and presumably clay. However, the purpose of reconstructing the *chaînes opératoires* detailed in Chapters 5, 6, and 7, is to identify those features where technological choice and thus style can be expressed. The characteristics summarised in Table 8.1 are those thought by the author to be most useful for defining MeP2 and MeP3 technological styles in copper production, and their significance is explained below.

Characteristics	NPW2/MeP1	NPW3/MeP2	NKH3/MeP3
Founders' graves	YES	NO	YES
Pit features	-	YES	YES
Installation superstructure	-	PIT-RIM	?
Air supply	-	FORCED	FORCED
Reaction containment	-	CRUCIBLE	CLAY-LINED PIT
Distinct clay source	-	YES	YES
Slag homogeneity	-	LOW	HIGH
Copper content	-	HIGH	LOW
Sulphide content	-	LOW	HIGH
Tin presence	-	NO	YES
Ceramic/fuel contribution	-	LOW	HIGH
Slag liquidus	-	c. 1230°C	c. 1240°C
Deposit texture	-	ASHY	CRUSHED
Residual magnetite presence	-	YES	YES

Table 8.1 - Principal metallurgical style characteristics of NPW2/MeP1, NPW3/MeP2, and NKH3/MeP3.

Founders' graves:

Both extremes of the prehistoric Valley technological sequence, NPW2/MeP1 and NKH3/MeP3, share the presence of inhumations with metallurgical artefacts apparently interred as burial goods (Chapter 3). Founders' graves are considered a Valley technological style characteristic as this metal-related funerary behaviour suggests some degree of association between the deceased's identity and their presumed involvement in industrial activities and may also reflect the embeddedness of copper production in local peoples' lives. These 'founders' graves are the only readily discernable link between the consumption and founding-only evidence of MeP1 Bronze Age contexts and the Iron Age extraction period MeP3, and may be indicative of continuity in some aspects of Valley metal technologies from c. 1450 BCE to c. 300 CE. The location of NPW3/MeP2 human remains is at present unknown.

Pit features:

Shifting from matters of metallurgical burials to metallurgical production, both MeP2 and MeP3 contexts have evidence for metallurgy-associated pits. The use of pits in copper smelting activities is rather ephemeral at Non Pa Wai and only slightly better documented at Nil Kham Haeng due to the two sites' highly disturbed stratigraphies (see Chapter 2). However, the *in situ* pits and associated smelting debris at seemingly MeP3 Khao Sai On (Ciarla 2007b) provide a reasonable analogy for probably contemporaneous Nil Kham Haeng at least. The containment of high temperature reactions within depressions in the ground is by no means unusual, but it is a choice and represents a shared stylistic trait in the copper production *chaînes opératoires* of the Iron Age Khao Wong Prachan Valley.

Installation superstructure:

An important Valley style characteristic is installation superstructure or furnace evidence. Whilst the early Iron Age Non Pa Wai furnace evidence has always been tentative, the interpretation of thick coarse-fabric fragments as low pit-rims is relatively conservative (Figure 5.3 & 5.4), especially in light of Roberto Ciarla's 1986 field sketch (Figure 5.5), though it is acknowledged the same effect could have been achieved by MeP2 metalworkers by digging a slightly deeper pit. However, what was thought to be clear furnace evidence at later Iron Age Nil Kham Haeng, the presence of complete and fragmentary perforated ceramic cylinders in funerary and industrial contexts (Pigott *et al.* 1997: 130), should perhaps now be treated with caution as laboratory analyses and field experimentation have highlighted the relative lack of heat damage to these artefacts, especially when compared to the heavily vitrified and bloated 'slag-skins' (Chapters 6 and 7). There is no doubting the association of these cylinders with copper production activities at Nil Kham Haeng and Khao Sai On (Ciarla 2007b), but the author regards a wind-powered smelting furnace interpretation as implausible (Chapter 7). Even if a forced air blast were directed via an inclined tuyère through the lowermost perforation of the cylinder, and into the clay-lined pit below, it would surely result in greater degree of localised heat damage than that seen (Figure 6.7). The loss of vitrified layers through post-depositional degradation is unlikely as the internal surface appears intact. The eroded appearance of the cylinder exterior could be due to their being fired wet or incompletely fired, and subsequently spalled via steam expansion or eroded post-depositionally, respectively. Though a smelting attribution for the cylinders cannot yet be ruled out, the author cannot currently conceive of a physical configuration which could explain the differential heat damage between the 'slag-skins' and perforated fragments, artefact classes with near identical refractory qualities.

It is possible the perforated cylinders were used for the low temperature roasting of sulphidic ores, a process known to have been conducted in similar structures ethnographically (Craddock 1995), but this is not supported by mean normalised sulphate levels of c. 0.015wt% in the Valley perforated fragment bulk chemistry (Appendix B.3). The use of perforated cylinders in founding activities (alloying and/or casting) would still involve temperatures in excess of 1000°C, but crucially, the containment of metal within a crucible (one would assume) would mean the only fluxing agent in contact with the inner wall of the cylinder would be charcoal ash, instead of the huge quantity of iron oxide present in a smelting charge. This could explain the lower level of thermal degradation to the cylinder fabric, but we have yet to identify, study, and test the MeP3 crucible evidence for a founding interpretation. It is always possible the cylinders were used for cooking the metalworkers' food, but, in any case, the perforations seen in the MeP3 ceramic cylinders

are a distinctive technological choice (cf. Bassiakos *et al.* 2008), and their presence at both Nil Kham Haeng and neighbouring Khao Sai On is an interesting link between the two sites as they have not been recorded anywhere else in Southeast Asia. Where and when the ceramic perforation tradition begins remains unknown, as only one possible perforation, and very vague at that, was seen on the MeP2 ceramics (Figure 5.4). In the light of Rispoli *et al.*'s (forthcoming) chronological revision, the perforated ceramic cylinder from Niuheiliang (Liaoning Province, northeast China), speculatively cited as analogical by Pigott & Ciarla (2007: Figure 12b), would now date to at least 1400 years before the earliest MeP3 production at Nil Kham Haeng as well as being over 3500km distant, and is thus an unlikely progenitor. However, if 'founders' graves' were to be studied at a regional level, it would be important to note the particular metallurgical behaviours attested by grave goods. Most examples (including those from MeP1) seem to relate to casting activities, but if the author's rejection of the MeP3 perforated cylinders as smelting furnaces is correct, then there exist no inhumations corresponding to extractive metallurgy. Additionally, if the author's tentative reinterpretation of the cylinders as casting furnaces is true, then the MeP3 graves might be consistent with a tentative regional founder's grave tradition (e.g. Higham in press b), albeit with a distinct 'no moulds' assemblage.

Air supply:

If the perforated cylinders are dismissed as smelting furnaces for the time being, the resultant technological reconstructions for MeP2 and MeP3 copper smelting become superficially comparable (Figure 7.31), and share a requirement for forced draught provision, despite the absence of any archaeological evidence. Although the Valley has seasonal strong winds, neither of the copper production techniques appear to be wind driven, due to the inability of natural draughts to drive enclosed or subterranean smelting reactions. This interpretation lifts any seasonal restriction on copper smelting based on the absence of wind, and also means that, in theory at least, Valley production might have been a year round activity¹, an outcome which would marginally undermine White & Pigott's (1996: 159) "part-time" criteria for 'community specialisation'.

Due to our having only negative evidence for forced draught, one cannot do more than speculate as to their original form. However, the technical improvements detectable

1 Even the monsoons following the windy season need not prevent high temperature activity so long as the installation is protected from direct heavy rainfall. Whilst casting quality may be affected by atmospheric moisture, the heat generation capacity of small prehistoric furnace should be sufficient to overcome this climatic limitation (cf. Bronson & Charoenwongsa 1994).

between MeP2 and MeP3 techniques, could be partially explained by developments in air delivery, perhaps a change from blowpipes to hand-operated bag or piston bellows, the lack of archaeological evidence for which can be explained by the use of organic materials like bamboo or leather. The lack of any suggestion of a shift to capital-intensive or labour-intensive air delivery is thus still consistent with White & Pigott's (1996) 'community specialisation' interpretation for Valley copper production.

Reaction containment:

Unless one is prepared to lose much of the copper metal product in an open fire, it is preferable to contain the smelting reaction in some way. A major difference between the MeP2 and MeP3 styles concerns the method with which this containment was accomplished. The thick organic-tempered crucibles recovered in abundance at early Iron Age Non Pa Wai are far rarer at later Iron Age Nil Kham Haeng, where they appear to have been superseded by lining the smelting pit with organic-tempered clay. Although the crucibles and 'slag-skins' would have performed similarly during the copper smelt, there is a fundamental difference at the end of the operation. The MeP2 slag cakes are thought to have been poured, perhaps to collect the copper metal by density separation (although much remained in the slag). Pouring the molten slag could of course be accomplished by lifting and tipping the MeP2 crucible, but this is not possible with a MeP3 fixed clay pit lining, where the micro-structural evidence suggests the slag was not quenched prior to crushing (Chapter 6). On the current evidence, the employment of technical ceramics undergoes a substantial change over the course of the Valley Iron Age, representing an even more significant shift in technological choice with regards to the means of separating metal from waste product and the labour cost of production. Given the predominance of intact MeP2 slag cakes it is likely that after pouring the contents of the crucible into a pit in the ground, early Iron Age Valley metalworkers simply snapped off the freshly smelted copper which probably formed as nodules on the surface and discarded the rest of the slag. Conversely, the largely crushed MeP3 slag suggests that the copper was extracted by hand down to prill level from the pulverised contents of the clay-lined pit.

Distinct clay source:

Not only are the technical ceramics from NPW3/MeP2 and NKH3/MeP3 different in form and use, there is also chemical evidence for their being made from separate sources of clay². The major element bulk chemistries for ceramics from the two sites are highly comparable

2 Due to the very close association of slag and ceramic in the NKH3/MeP3 'slag-skins', these samples were not analysed by [P]ED-XRF and thus bulk trace element data are not available.

with c. 65wt% SiO₂, c. 20wt% Al₂O₃, c. 10wt% Fe₂O₃, and c. 5wt% CaO, representing an entirely typical composition for a prehistoric fabric (technical or otherwise), and commensurate with the local geology (Figure 8.1). However, a normalised ternary plot for the prominent trace elements, strontium, zinc, and zirconium, reveals a clear separation between the technical ceramics from the two sites (Figure 8.1). The author previously identified this patterning using principal components analysis of the compositional data (Pryce & Pigott 2008: 144, Figure 7), but in fact the relationship is so strong that such a manipulation is unnecessary. This trace element patterning is clear whether the ceramic was heavily slagged or not (as the MeP2 crucibles were), suggesting clay chemistry, and not slag contamination, is the cause of ceramic segregation. The implication of this result is that Valley metal workers were using different, but probably local, sources of clay in preparing their technical ceramics. Given the consecutive chronologies of the sites, it is possible the clay source used at early Iron Age Non Pa Wai was exhausted and a fresh deposit exploited at later Iron Age Nil Kham Haeng. However, though we have no knowledge of present day clay sources (no one having looked for them), it seems more likely that those making technical ceramics simply used the nearest available material given the almost identical major element chemistry, and thus refractory behaviour, of fabrics from the two sites (e.g. Freestone 1989).

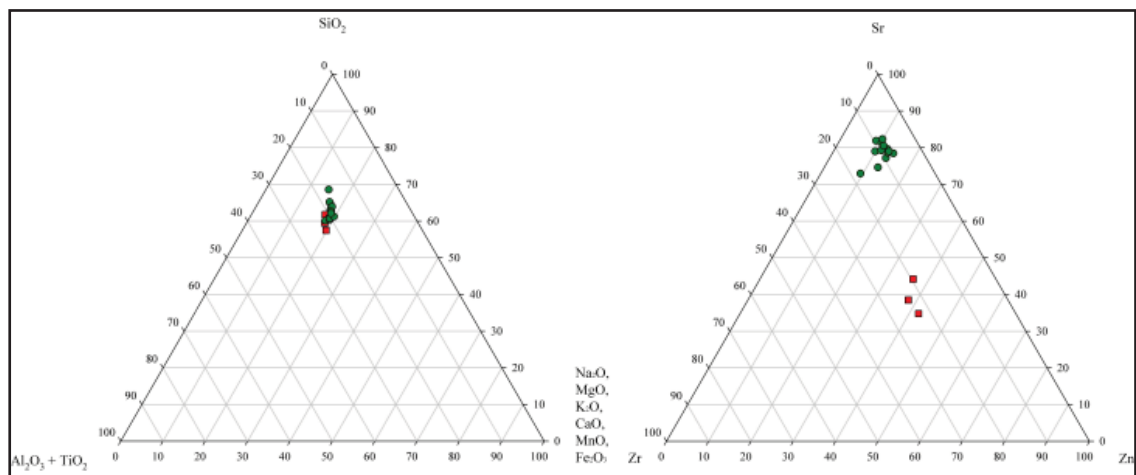


Figure 8.1 - Ternary plot of major oxide comparability in NPW3/MeP2 and NKH3/MeP3 technical ceramics (left) versus trace element separation. Image: author.

Slag homogeneity:

As would be hoped of our predominant evidence source, comparing the slag from the two production sites has been particularly rewarding for the identification of technological change in the Iron Age Khao Wong Prachan Valley. The macroscopically obvious increase in the homogeneity of MeP3 slags when compared with MeP2 samples is corroborated by respectively lower coefficients of variation in the bulk compositional data from the trace elements and minor oxides through to the three predominant major oxides: FeO, SiO₂, and CaO (Figure 8.2, Table 8.2).

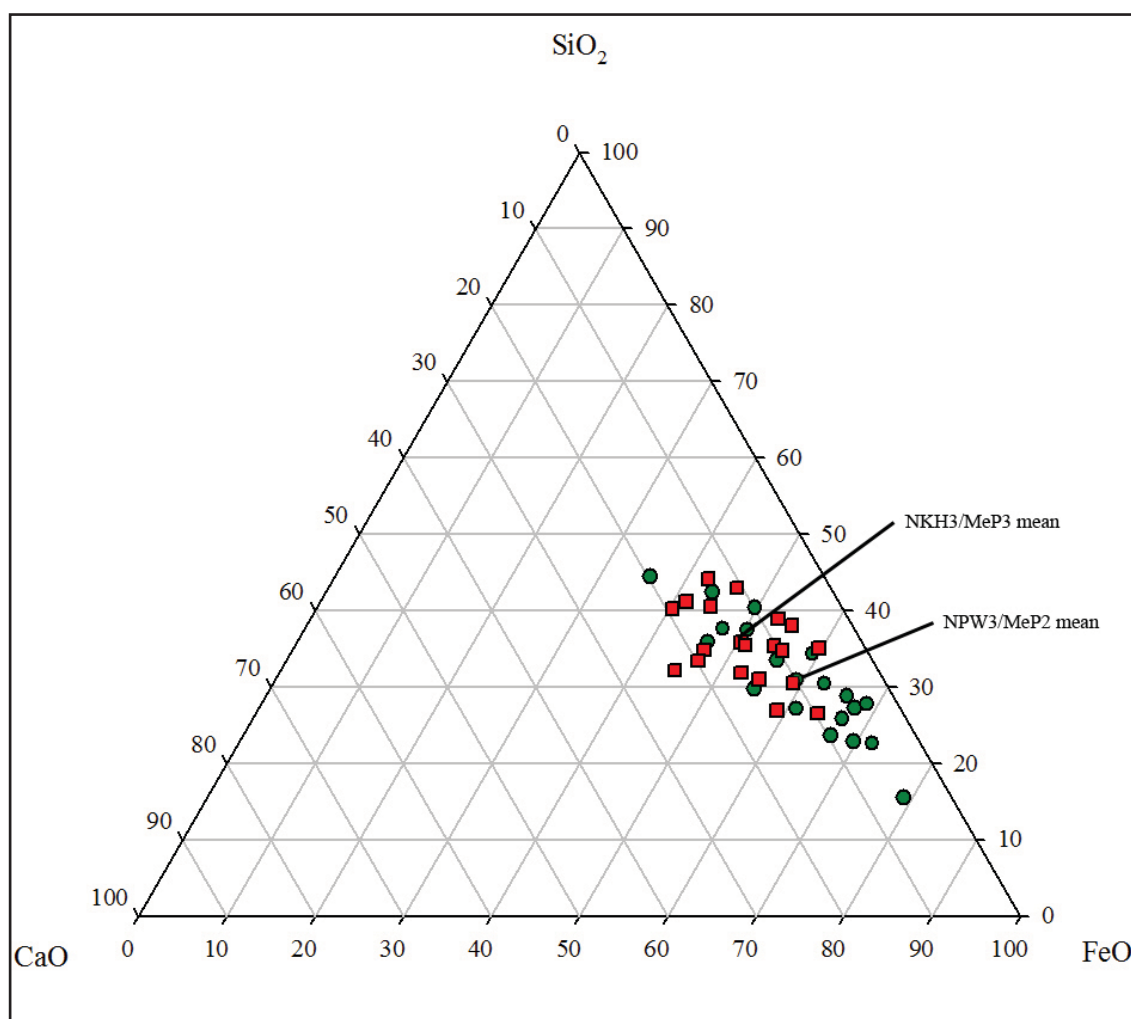


Figure 8.2 - Ternary plot of the three principal slag-forming oxides in Valley slag. Image: author.

	Na ₂ O	MgO	Al ₂ O ₃	SiO ₂	P ₂ O ₅	SO ₃	K ₂ O	CaO	TiO ₂	MnO	FeO	Cu	Zn	As	Sr	Sn	Ba
	wt%	wt%	wt%	wt%	wt%	wt%	wt%	wt%	wt%	wt%	wt%	wt%	ppm	ppm	ppm	ppm	ppm
Non Pa Wai																	
mean	0.54	0.48	3.21	27.13	0.16	2.48	0.12	8.74	0.08	0.30	52.09	4.23	3849	15	165	2	56
std dev	0.18	0.42	1.44	6.71	0.19	2.88	0.08	4.21	0.04	0.18	10.62	3.95	13107	13	112	1	66
CV	33%	88%	45%	25%	121%	116%	65%	48%	51%	58%	20%	93%	341%	87%	68%	47%	118%
Nil Kham Haeng																	
mean	0.45	0.99	5.16	29.55	0.19	1.72	0.32	11.13	0.15	0.33	42.61	1.64	909	11	322	28	98
std dev	0.11	0.41	1.40	4.35	0.12	1.26	0.14	3.95	0.06	0.11	6.14	0.68	786	6	341	27	83
CV	25%	41%	27%	15%	63%	73%	43%	35%	39%	32%	14%	42%	86%	53%	106%	97%	85%

Table 8.2 - Means, standard deviations, and coefficients of variation for [P]ED-XRF bulk chemical analyses of slag from MeP2 and MeP2 contexts. Selected oxides and elements after normalisation.

In light of the reasonably uniform geological environment, and the consequently inconclusive mineral analyses (Chapters 5 and 6), it is argued that the chemical patterning can be regarded as a near direct proxy for technological behaviour (e.g. Rehren *et al.* 2007), and thus increasing compositional conformity can be interpreted as increasing technological standardisation (e.g. Humphris *et al.* 2009). However, standardisation of product (or by-product) does not necessarily equate to a change in the context of

production. As slag composition is a result of the choices, practices, and techniques of ancient metalworkers, we must ask where in the *chaînes opératoires* do the discrepancies between slag samples from the two sites occur, and what can this tell us about the development and transfer of metallurgical knowledge and know-how in the Valley, an aspect discussed later in section 8.3.

Copper content:

A number of interesting technological patterns can be discerned within the slag bulk chemistry using only linear scatter plots. Firstly, plotting copper oxide against iron oxide for the MeP2 and MeP3 data indicates that although the R^2 value for MeP3 slag is higher than that for MeP2 samples, they both show there is no significant correlation between the two compounds in either phase (Figure 8.3). This suggests that the primary cause of copper loss at both sites is unreacted ore minerals, with poor phase separation due to viscosity a long second (Davenport *et al.* 2002: 273, Gilchrist 1989). Although the early Iron Age Non Pa Wai production technique could produce occasional low copper losses, these were inconsistent and frequently offset by incompletely reacted charges. Whereas the later Iron Age Nil Kham Haeng smelters were still losing some metal product, the quantities were systematically low and probably related to slight variation in charge composition, process temperature, or the intensity of mechanical metal recovery post smelt.

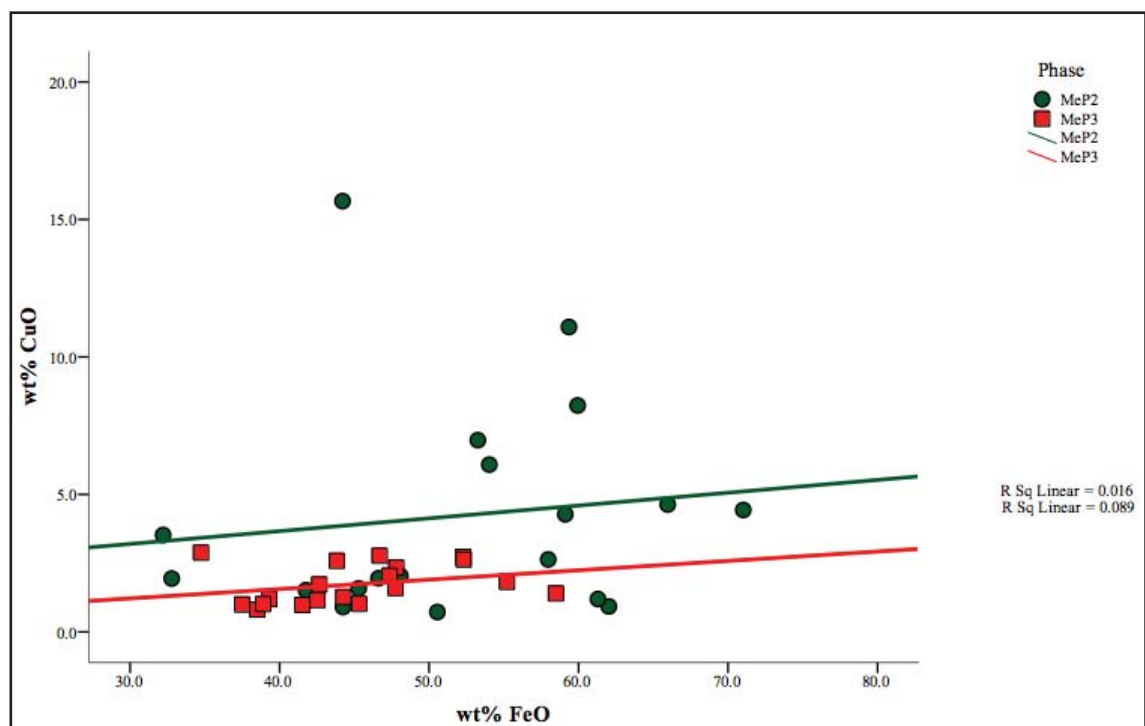


Figure 8.3 - Scatter plot showing the lack of correlation between copper oxide and iron oxide levels in [P] ED-XRF bulk chemical analyses of Valley slag. Image: author.

Sulphide content:

Likewise, the relationship between copper and sulphur compounds seems to follow a similar pattern at the two sites (Figure 8.4). The occasionally elevated quantities of sulphur, but lack of correlation with copper (R^2 0.025), in MeP2 samples suggests that whilst sulphidic minerals were sometimes incorporated within the smelting charge, it was sporadic and probably not intentional. That this irregular relationship was potentially caused by the misidentification by ancient metalworkers of mineral species is perhaps confirmed by the highest level of sulphur being due to large fragments of sphalerite in NPWMS7 (Chapter 5). In the MeP3 samples, the copper/sulphur correlation is still weak (R^2 0.359), but the much increased uniformity of both compounds could be explained by the systematic inclusion of sulphidic minerals intermixed amongst oxidic minerals within the smelting charge, resulting in the regular presence of matte prills within the slags (Chapter 6). It seems an apparent paradox that MeP3 metalworkers probably used more sulphidic minerals but had less sulphur in their slags. Possible explanations for this could plausibly be a roasting stage in the later Iron Age *chaîne opératoire*, despite the absence of direct evidence, and/or a better control of charge reactants and their proportions.

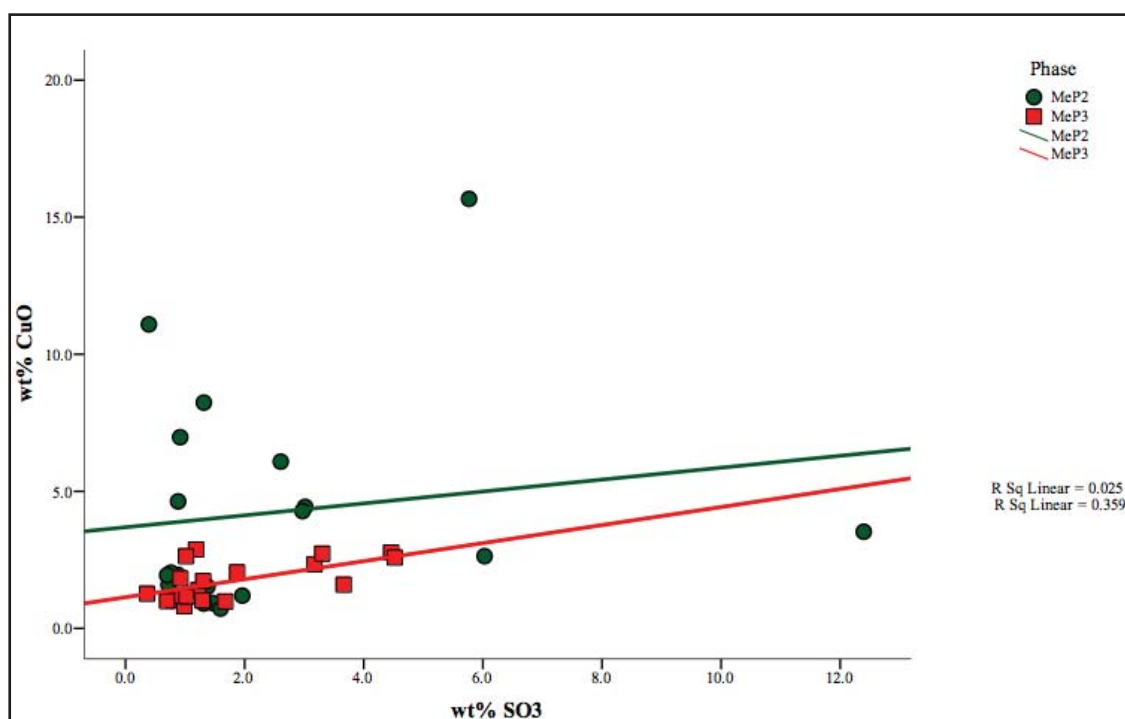


Figure 8.4 - Scatter plot showing the lack of correlation in [P]ED-XRF bulk chemical data between copper and sulphur compounds in MeP2 slags, compared with a weak relationship in MeP3 samples. Image: author.

Tin presence:

An intriguing relationship is to be seen between copper and tin compounds in the Valley slag samples (Figure 8.5). The early Iron Age Non Pa Wai slag contains almost no trace of the element, but samples from later Iron Age Nil Kham Haeng, irregularly contain tin in

small quantities (<100ppm). Although the local geological system is reportedly deficient in tin-bearing minerals (William Vernon pers. comm. and Table B.2), this chemical patterning suggests there is some slight difference between the mineral component of the smelting charges in MeP2 and MeP3 production. It is also possible, though unlikely considering the low levels, that the presence of tin in MeP3 slags is indicative of minerals or metals from other areas entering the local smelting system. On a practical basis there would be no need to import copper minerals to the Khao Wong Prachan Valley considering their relative abundance. Thus, if foreign material were wholly or partially the source of

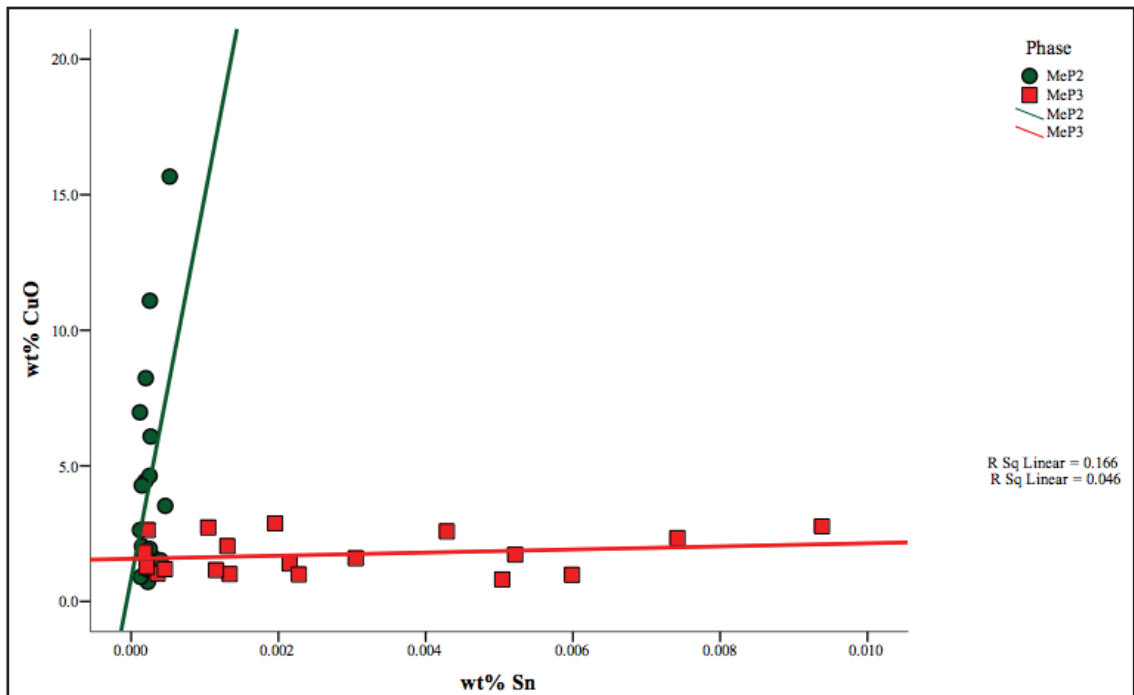


Figure 8.5 - Scatter plot showing the consistent absence of tin in [P]ED-XRF bulk chemical analyses of MeP2 slags, versus sporadic trace level presence in MeP3 samples. Image: author.

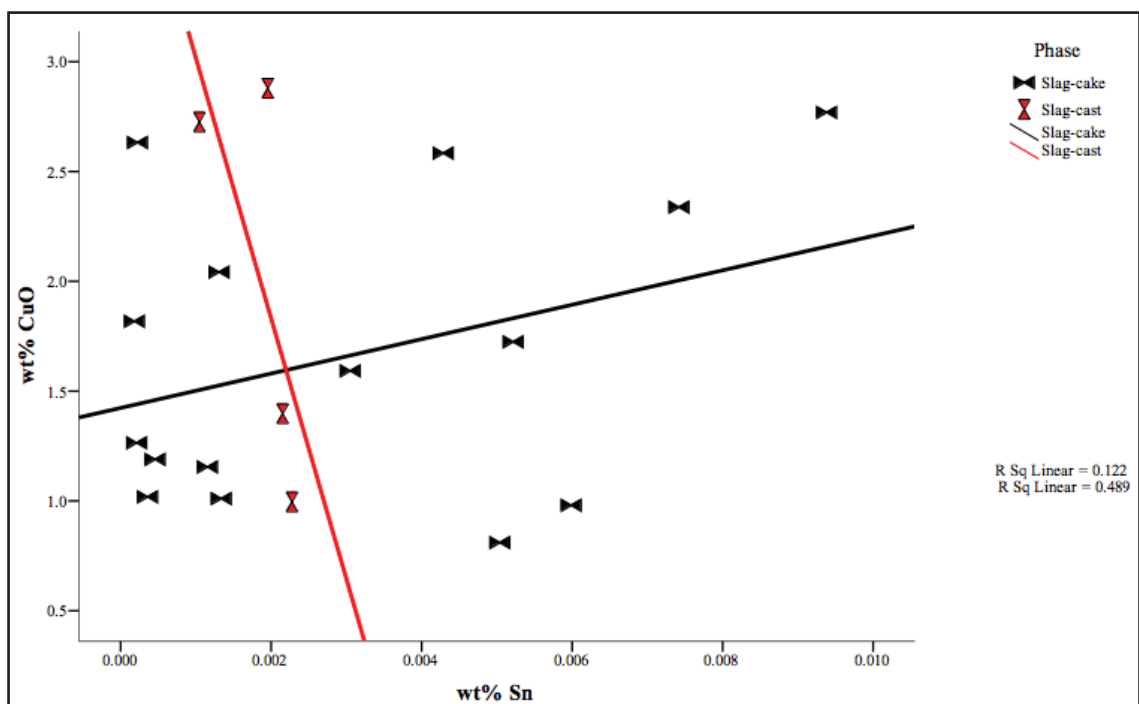


Figure 8.6 - Scatter plot showing the lack of correlation in [P]ED-XRF bulk chemical data between tin compound content and MeP3 slag morphology. Image: author.

the tin, it is more probable that some extraneous metal was being refined or recycled at Nil Kham Haeng, with the secondary production and consumption sites of northeast Thailand being a potential source (Chapter 1). This eventuality would indicate some conflation of archaeometallurgical evidence at the site, but there is no correspondence between tin content and the two categories of MeP3 slag morphology, slag-casts and slag-cakes (Figure 8.6). Therefore, whilst the later Iron Age reconstruction may need modification, this must await future evidence.

Ceramic/fuel contribution:

A further significant difference between the MeP2 and MeP3 slag bulk chemistries concerns the relative abundance of those elements and oxides associated with ceramic and fuel ash contributions to the smelting system. A substantial chemical contribution from ceramics and/or fuel ash to slag formation could dilute the copper content, therefore artificially conveying the image of a more efficient smelting technique. This possibility was semi-quantitatively assessed with data from Table 8.2.

	MgO	Al ₂ O ₃	SiO ₂	K ₂ O	CaO	TiO ₂	Total
	wt%	wt%	wt%	wt%	wt%	wt%	wt%
NPW3/MeP2	0.5	3.2	27.1	0.1	8.7	0.1	39.8
	<i>1.2</i>	<i>8.1</i>	<i>68.2</i>	<i>0.3</i>	<i>22.0</i>	<i>0.2</i>	
NKH3/MeP3	1.0	5.2	29.5	0.3	11.1	0.2	47.3
	<i>2.5</i>	<i>13.0</i>	<i>74.3</i>	<i>0.8</i>	<i>28.0</i>	<i>0.4</i>	

Table 8.3: Mean [P]ED-XRF bulk chemical analyses of slag from NPW3/MeP2 and NKH3/MeP2 contexts. Major oxide data (except iron oxide) associated with ash, ceramic, and gangue are re-normalised (in *italics*) according to the MeP2 total to simulate high copper loss in MeP3 samples.

The major oxides associated with ash, ceramic, and gangue contributions (but excluding iron oxide) were retained, and the mean figures for MeP2 and MeP3 samples were both re-normalised using the MeP2 total (Table 8.3). This data manipulation approximately simulated the effect of MeP3 samples having a copper loss equal to the MeP2 slag. The simulation oxide data in italics continue to be higher in MeP3 samples, indicating a greater contribution to slag chemistry from ash, ceramic, and/or gangue. The reasonable positive correlation (R^2 s 0.527 and 0.613 for MeP2 and MeP3 respectively) between potash and titania in Valley slags also suggest a trend towards increasing levels of ceramic degradation and/or fuel ash accumulation over time (Figure 8.7). This relatively consistent patterning could suggest that the MeP3 smelting operation was hotter and/or longer than its MeP2 predecessor, both options could imply greater effort in the provision of forced blast, as well as deleteriously impacting local reserves of fuel.

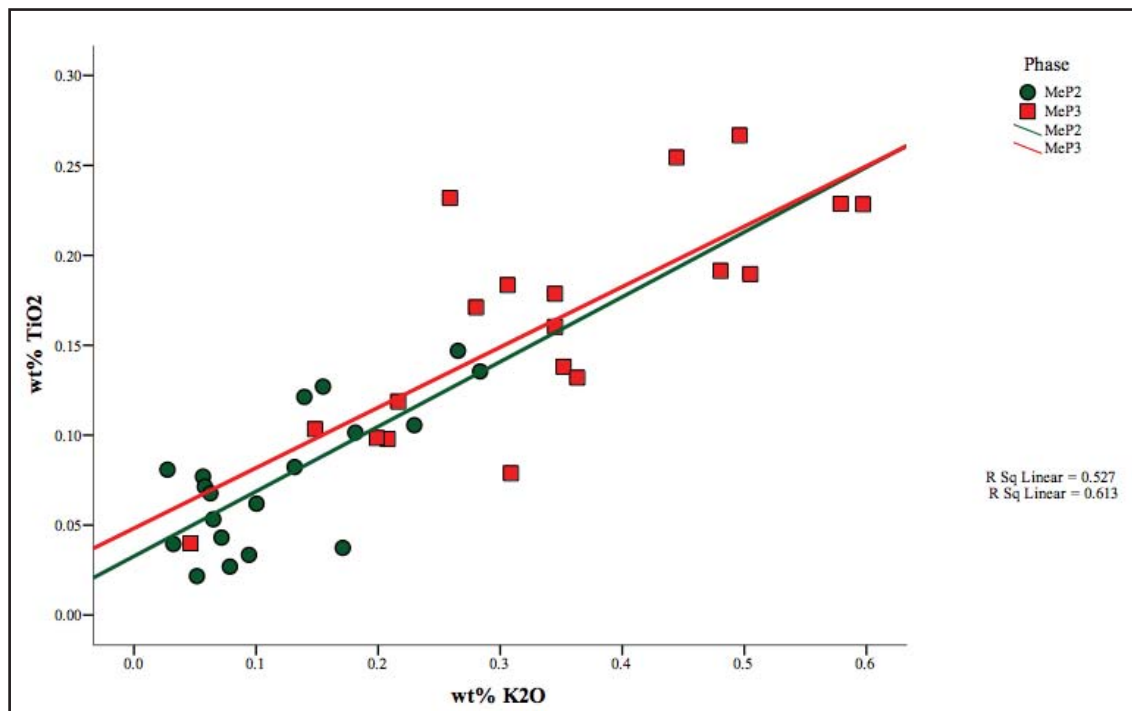


Figure 8.7 - Scatter plot showing the positive correlation of titania and potash in [P]ED-XRF bulk chemical analyses of MeP2 and MeP3 slag samples, with increased concentrations in the latter. Image: author.

In order to further differentiate between the two technological styles, the bulk chemical data were also processed using Principal Components Analysis (PCA - see Chapter 4) to discern the factors chiefly contributing to compositional variation in the MeP2 and MeP3 slag samples³. The author appreciates statistical manipulation is very much part of the interpretive process, and thus focused on those elements and oxides most likely to relate to the choices and techniques practiced by the Iron Age Valley metalworkers⁴. Nevertheless, numerous combinations of chemical data were calculated to produce a significant concentration of variation within the first three principal components. The analysis presented (Figure 8.8) reduced the data for twelve predominant major, minor, and trace elements and oxides (MgO, Al₂O₃, SiO₂, SO₃, K₂O, CaO, TiO₂, FeO, CuO, Zn, Sr, and Zr) into three factors comprising 48.0%, 16.5%, and 12.5% of the variation respectively, thus accounting for a cumulative 77.0%. The three chemical groupings obtained can be separated into those dominated by 1) FeO and CuO, 2) SO₃ and Zn, and 3) the remaining elements and oxides.

Removing the data for NPWMS7, which contained a large inclusion of sphalerite, did not substantially modify the intermediary SO₃ and Zn group, which remained closely associated with the FeO and CuO group. The significant differentiation is between the

³ The author is especially grateful to Michael Charlton for instruction in the use of Principal Component Analysis.

⁴ i.e. remaining way of trace element patterning in the absence of clear mineralogical data.

factor dominated by FeO and CuO, and that containing the remainder. When PC1 and PC2 or PC1 and PC3 are displayed as bivariate plots and marked by metallurgical phase (Figure 8.9), while overlap remains, there is a degree of separation between Non Pa Wai and Nil Kham Haeng smelting processes on the basis of factorised bulk slag chemistry.

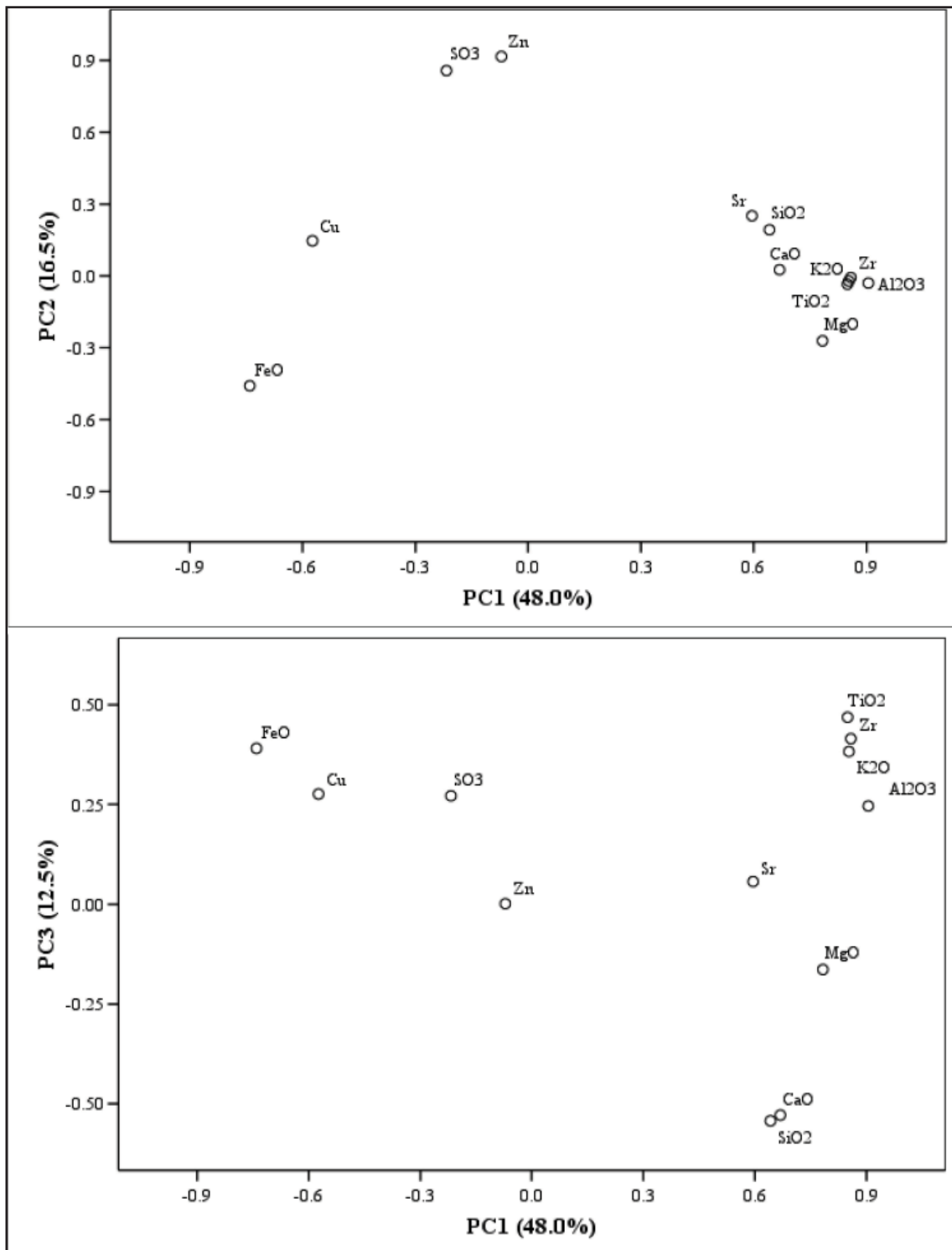


Figure 8.8 - Plots showing those elements and compounds dominating variation in three principal components generated from [P]ED-XRF bulk chemical analyses of Valley slag samples. Image: author.

Therefore, the PCA corroborates the patterning already noted (Figures 8.3 and 8.7), the MeP2 slag bulk chemistry is dominated by iron oxide and copper oxide, and the MeP3 slag bulk chemistry is characterised by alkali oxides and trace elements derived from gangue mineral liquefaction, technical ceramic degradation, and fuel ash contribution. The interpretation of these differentiating factors follows several paths:

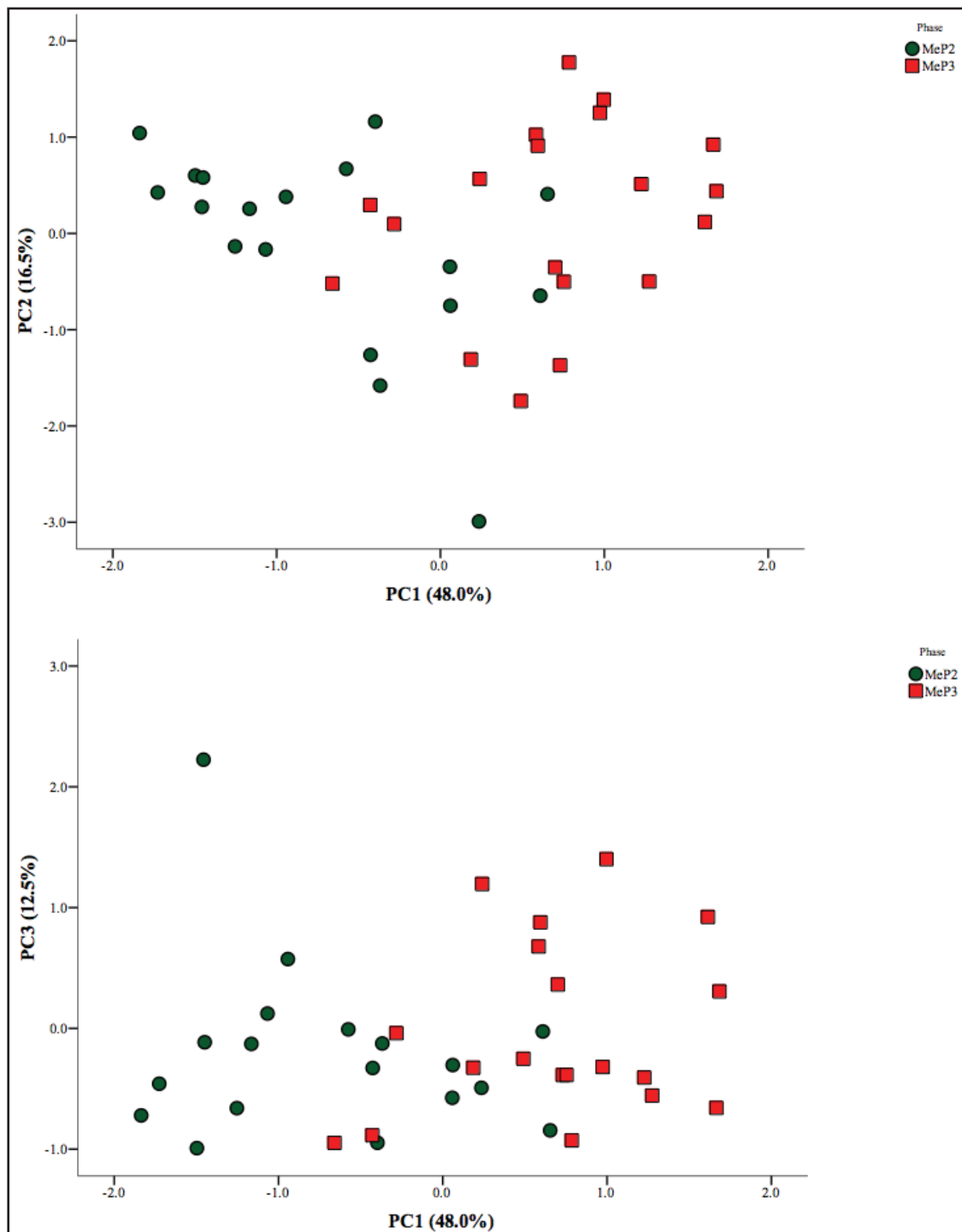


Figure 8.9 - Scatter plots showing the metallurgical phase attribution of those elements and compounds dominating variation in three principal components generated from [P]ED-XRF bulk chemical analyses of Valley slag samples. Image: author.

- The inconsistent but frequently high level of copper loss at early Iron Age Non Pa Wai distinguishes the copper production process practiced there as an inefficient⁵ one, whereas the metalworkers at later Iron Age Nil Kham Haeng were systematically better in recovering metal product.

- The high variation in major slag-forming components (SiO_2 , CaO , Al_2O_3), but especially FeO (also see Table 8.2), for the MeP2 smelting technology is indicative of a non-uniform smelting charge and process parameters, whereas the greater compositional convergence of the MeP3 smelting technology is suggestive of increased standardisation in the smelting charge. This could represent either some consensus amongst metalworkers on the type and proportion of minerals selected, or decreased variation in the mineral suite available. Given that we know almost nothing about Valley mining techniques due to recent industrial activity (as opposed to Phu Lon, see e.g. Pigott & Weisgerber 1998), it is difficult to differentiate whether skill or geology is the more likely factor and thus both must remain options.

- The clustering of alkali and earth elements and oxides in the PCA factor associated with MeP3 production (Figure 8.9) is best explained as the chemical contribution of technical ceramics and fuel ash dissolving into the melt (e.g. calcia, magnesia, potash, and titania, see Jackson *et al.* 2005, Merkel 1990: 110). This suite of components would typically be regarded as fluxes, producing a more fluid melt with less impedance to the agglomeration of copper prills - i.e. a more efficient MeP3 smelting technique. (e.g. Davenport *et al.* 2002, Gilchrist 1989, Eisenhüttenleute 1995).

Slag liquidus:

However, as introduced in Chapter 4, and discussed in Chapters 5 and 6, the behaviour of some components (e.g. MgO , Al_2O_3 , CaO) can vary considerably depending on the prevailing partial pressure of oxygen and their abundance at the time of slag formation (e.g. Kongoli & Yazawa 2001). The liquidus temperatures for the MeP2 and MeP3 slag matrices and constituent phases were calculated using, arguably, the most appropriate thermodynamic models available for copper smelting systems, and the figures derived from these Flogen diagrams are summarised in Table 8.4.

5 As mentioned earlier in this thesis, an assessment of efficiency assumes technical optimisation not necessarily related to the aims of ancient Valley smelters.

Slag component	MeP2	MeP3
Olivine (Flogen)	c. 1240°C	c. 1235°C
Magnetite (Flogen)	>1300°C	>1300°C
Glass (Flogen)	c. 1180°C	c. 1175°C
Matrix (Flogen)	c. 1240°C	c. 1240°C
<i>Matrix (traditional)</i>	<i>c. 1170°C</i>	<i>c. 1130°C</i>

Table 8.4 - Summary of liquidus estimates derived from SEM-EDS matrix analyses of Valley slag samples.

The author suggests these numbers should not be read too literally considering the many assumptions, error margins, and interpretations required to produce them. However, on a comparative basis they are of use, and we can see the Flogen-generated liquidus temperatures for the MeP2 and MeP3 matrices are the same. The estimates produced by the traditional ternary diagrams are lower overall, but the difference between the Valley traditions is increased to c. 40°C. The latter discrepancy equates to 3 to 4% of the MeP2 and MeP3 liquidus estimates as opposed to c. 0.8% using the Flogen method. However, both temperature differences are probably insignificant technologically given the variable conditions in ancient smelting processes (Bourgarit 2007)⁶. Therefore, the *minimum* operating temperatures of the early and later Iron Age copper smelting processes can be considered approximately equal at c. 1200°C to c. 1250°C.

This is where one must recall the fundamental difference between a liquidus (minimum) temperature and the actual reaction temperature. Experimental archaeometallurgical research (e.g. Catapotis *et al.* 2008, Merkel 1990) has demonstrated ancient furnace designs can generate heat several hundred degrees in excess of liquidus. Indeed, actual temperature must exceed liquidus (the point at which the melt is *just* molten) if any significant density separation of metal and slag is to occur. Considering the comparable degree of slag/ceramic contact in both MeP2 and MeP3 reconstructions (slag-to-crucible for the former and slag-to-‘slag-skin’ for the latter, the MeP2 pit rims not appearing to be heat damaged and the MeP3 perforated ceramics now excluded from the smelting reconstruction), it is conceivable that the concentration of alkali and earth metal components in the later Iron Age slag was indeed caused by actual process temperatures substantially in excess of the liquidus estimate, or the MeP3 smelt running for a longer time. Although accurate

⁶ As the purpose of the present section is comparative, the analytical benefit of using the Flogen diagrams is relatively minor, but in terms of the individual technological reconstructions, the effect can be striking. Table 8.3 indicates the difference in using the Flogen calculation produces a c. 70°C increase in liquidus estimate for the MeP2 slag matrix, which is large but perhaps within error margins. However, the huge c. 110°C increase for the MeP3 slag matrix equates to a near 10% difference in liquidus estimate, a figure which is arguably technologically significant and could have a major impact on the overall reconstruction.

quantitative smelt duration estimates cannot be derived from the experiments carried out (Chapter 7), the lower mass of the whole archaeological MeP3 slag cakes (c. 500g) as compared with their MeP2 equivalents (c. 2000g) suggests a reduced charge size for the later Iron Age smelt might counteract the potential for a shorter early Iron Age smelt⁷. Thus, on a qualitative basis, MeP2 and MeP3 processes probably had a similar duration.

Whilst extensive further experimental testing would be necessary to establish whether the MeP3 process was much hotter than that of MeP2, we do know that where fully liquid slag did form (as analysed by SEM-EDS area scans, see Chapters 5 and 6), the temperature required was similar in both technologies, as evidenced by their convergent liquidus estimates. Therefore, the limiting factor preventing the complete reaction of the MeP2 charge into a homogenous slag was probably not a lack of heat energy, but rather the compositionally and granulometrically unbalanced nature of that charge as indicated by the highly variable bulk analyses (Table 8.2) and the presence of large unreacted inclusions (see images in Chapters 5 and 6). Although a more effective generation and distribution of heat (perhaps through refinements in forced draught delivery) may have been an important factor in the improving trend of copper production in the late prehistoric Valley, it was not the critical one. The author would contest that the pivotal technological development was the standardisation of a relatively well-balanced charge at later Iron Age Nil Kham Haeng.

Although we cannot completely discount the geological availability factor, this fundamental shift in metallurgical behaviour might imply:

- The improved identification and differentiation of copper-bearing minerals by metalworkers, as evidenced by the absence of unrelated unreacted metal-bearing minerals (e.g. sphalerite but excluding magnetite) in MeP3 slags, as well as the more consistently cupriferous excavated mineral assemblage.
- The improved removal of unwanted gangue and presumably grading in desired minerals by metalworkers carrying out beneficiation activities, as evidenced by the near absence of gangue minerals in the MeP3 slags, and the finer size of any extant inclusions.
- The improved combination of these selected, processed, and sorted minerals into an effective charge by metalworkers preparing the smelt, as evidenced by the well-reacted and relatively homogenous texture of the MeP3 slags.

⁷ Duration of heat exposure testing (e.g. Hein *et al.* 2007) on the crucibles and slag-skins was not carried out during the present study, but given the almost certain multiple use of the former it is unlikely to be an informative approach.

Deposit texture:

Further evidence for improved charge formulation being the primary driver of technological change in Valley copper production can be deduced from the nature of the MeP2 and MeP3 archaeological deposits themselves. The 3 to 4m of loose ashy NPW3/MeP2 deposit certainly manifest a period of industrial metallurgical activity, but the lack of conscientiousness and efficiency is encapsulated by the frequent presence of whole slag cakes, whose remnant copper content is sufficient for them to potentially be considered an 'ore'. The texture and composition of the MeP2 matrix stands in monumental contrast to that seen at NKH3/MeP3. In excess of 3 hectares and up to 6m of pulverised material is a poignant attestation of the excruciatingly intense production of copper in the later Iron Age Valley. The author cannot emphasise enough the interpretive impact of such a deposit of crushed mineral and slag, testimony to the massive expenditure of labour and the sheer determination of metalworkers in the pursuit of copper (Pigott *et al.* 1997, White & Pigott 1996). The textural similarity of the contemporaneous smelting deposit at Khao Sai On perhaps indicates this extractive metallurgical fervour was a phenomenon not exclusive to Nil Kham Haeng, and that the later Iron Age marks a shift in local metallurgical ethos, perhaps in response to rising regional demand.

Residual magnetite presence:

Thus the author makes the case for an increased thoroughness and expertise in smelting charge preparation being the pre-eminent behavioural development in Iron Age Valley copper production. It is then deeply intriguing that a contradictory vein can be adduced by the presence of residual magnetite fragments in MeP2 and MeP3 slags. These almost ubiquitous mineral inclusions cannot realistically be regarded as a flux considering their vast excess and frequently sharp unreacted boundaries (cf. Bennett 1989: 332). Neither can the magnetite be regarded a source of solid oxygen to drive sulphur out of the smelting system, as could have been argued for the addition of mineral haematite (Kaiura & Tohuri 1979), and has been argued for mineral malachite (Burger *et al.* 2007). Nor does the author subscribe to Rostoker *et al.*'s (1989) theoretically sound idea of the magnetite (or slag as was originally suggested) functioning as a gas-trapping mineral blanket as there is no archaeological basis for it in the prehistoric Valley slag evidence. Therefore, the author is lead to conclude the magnetite fragments conferred no particular technical benefit, and were presumably charged throughout the smelt, as would explain the lack of interaction of the mineral inclusions with the surrounding slag. This technological style element remains unexplained behaviourally.

Considering the proximity of magnetite and sulphidic copper minerals at Khao Tab Kwai, and their shared characteristics of high density and lustre, residual inclusions in early Iron Age Non Pa Wai slags could be interpreted as mineralogical misidentification, which would be entirely coherent with the generally poor charge composition in MeP2 production. How then does this correlate with residual magnetite presence in later Iron Age Nil Kham Haeng slag, when all the other evidence points towards a substantial improvement in smelting charge formulation? Though its purpose remains unexplained, and is perhaps inexplicable, it would appear the addition of crushed mineral magnetite during the smelt is a unifying characteristic of local prehistoric metal production. Therefore, the author regards this behaviour as complementary rather than contradictory evidence for the general trend of technological continuity in the Iron Age Khao Wong Prachan Valley.

Archaeological evidence like that encountered in the Iron Age Khao Wong Prachan Valley is a gift, and it is only by considering, as far as practicable, the entirety of the metallurgical assemblage that the author was able to identify the technological changes above. Whilst the author fully accepts the important role of technical ceramics in defining technological styles and, potentially, identifying technological transmissions, a predominant emphasis as advised by White & Hamilton (in press), “refractory technology is the real key to determining the source of Southeast Asian metallurgy”, would have resulted in critical slag evidence for metallurgical behavioural change being overlooked.

8.2 Explaining stylistic change and continuity in Valley copper smelting

The author is happy to concede that the explanation of behavioural change is infinitely more difficult and tentative than its identification. However, the overwhelming majority of the evidence substantiates the general premise for a substantial shift in the intensification, standardisation, and efficiency of Khao Wong Prachan Valley extractive copper metallurgy at c. 300BCE, the apparent MeP2/MeP3 boundary. It is further proposed that the improved formulation of the smelting charge, and all the associated metallurgical behaviours this involves in mining, beneficiation, and the mechanical processing of slag, is *the* critical technological change over the MeP2/MeP3 transition, and best represents the technological stylistic shift in Valley metallurgy. Although it is possible the MeP3 metalworkers were exogenous to the Khao Wong Prachan Valley and brought their own metallurgical tradition with them, this scenario is unlikely given the absence of any such population discontinuity in the general archaeological evidence. In that case, it is probably safe to regard the later Iron Age smelting technique as a solely autochthonous development of early Iron Age practice, as indicated by continuous magnetite addition to the smelting charge. However, the Valley metalworkers were producing a commodity from a relatively sparse distribution of metallogenic deposits, and thus the shift in production behaviour

may have been in response to stimuli from the wider regional arena.

It is improbable that local needs alone could be responsible for the unquantifiable but certainly enormous output of MeP2 and MeP3 metalworkers, and thus we must consider that increasing local copper supply may have been a response to greater regional demand. This is not a new idea (e.g. Mudar & Pigott 2003), but the revised Valley chronology means the attested intensive copper production is now wholly contemporaneous with the apparently increased incidence of bronze grave goods across Thailand and mainland Southeast Asia, predominantly evidenced in the interment of individuals with bronze arm bangles (e.g. Higham 2004, White 1988: 177, see Chapter 1). If we assume metal deposition in regional burial contexts is even partly correlated to general consumption behaviour then this might well constitute the motivation for the industrial scale production evidenced in the Khao Wong Prachan Valley. Though there is no reason to challenge White and Pigott's (1996) community-based interpretation of the social context of production, the acceleration in the intensity and ethos of local metal supply over MeP2 and MeP3 would be commensurate with the notion of accelerating regional bronze demand, largely for competitive consumption between increasingly ranked societies in other areas. This could be seen as especially well evidenced at sites in the Mun River catchment just a few hundred kilometres to the east over the Loei-Petchabun range, some of which (e.g. Ban Non Wat and Ban Lum Kaeo) appear to have evidence for the alloying and casting of bronze artefacts (e.g. Higham 2006, in press b, Higham & Higham 2009, Higham *et al.* 2007, Higham & Thosarat 2004, O'Reilly 2000, 2003, 2008).

If Khao Wong Prachan Valley copper was largely destined to fulfil regional demand, but there is no evidence of exogenous control over those metalworkers, what goods or services were supplied in return for metal remains a frustrating unknown, as is our current inability to discuss prehistoric Thai copper-base metal exchange given the dearth of lead isotope and trace element data. Mudar and Pigott (2003) suggest foodstuffs could have been imported to counteract the Valley's claimed agricultural marginalism. Whilst this is an interesting hypothesis, ongoing archaeobotanical studies may substantiate it by identifying potential gaps in the local subsistence base⁸. Although the social standing of local metalworkers relative to their non-metal producing neighbours cannot at present currently be reliably estimated, Shennan's (1999) economic model for Bronze Age copper smelting in the Austrian Alps has possibly interesting analogies for the prehistoric Valley. The Mitterberg example described an exchange system whereby small autonomous communities living in areas unsuited for farming, mined and smelted copper to gain access to agricultural products and exotic goods (*ibid.*: 360-362). The *low efficiency* of Mitterberg copper

8 A point for whom the credit goes to Bérénice Bellina.

production meant that metalworkers were consistently at an economic disadvantage when participating in regional exchange networks, a factor partially responsible for generating and proliferating social stratification in the area. Although there are obvious similarities between Mudar & Pigott's (2003) and Shennan's (1999) economic models, the latter can be taken a little further in the context of the prehistoric Khao Wong Prachan Valley. Throughout this chapter, the author has made the case for low efficiency NPW3/MeP2 and higher efficiency NKH3/MeP3 copper production, which would superficially suggest that the later Iron Age Valley metalworkers may have been able to exchange copper on improved terms relative to their early Iron Age antecedents. However, the definition of 'efficiency' employed has related to the loss of copper product, and not necessarily to labour 'efficiency' as per Shennan's hypothesis (1999). Whilst NKH3/MeP3 copper production was certainly more effective in reducing metal loss, this 'efficiency' came at the price of a much increased labour input in the crushing of minerals and slag, resulting in reduced labour efficiency. Therefore, on present knowledge, we cannot estimate whether the MeP2/MeP3 shift in Valley metallurgical ethos coincided with a modification of metalworkers' participation in regional exchange systems, nor whether this had an effect on their relative social status.

Though most likely an incomplete account, the consumption of bronze in the Valley area (see Chapter 2) suggests that one of the mediums of regional exchange could have been the provision of tin, whether in the form of tin/bronze ingots and/or bronze artefacts. For the direction of this interaction we would automatically turn eastwards towards the Mun River sites, a reasonable likelihood considering the recent excavation from an Iron Age 1 burial at Ban Non Wat (c. 420-200 BCE, Charles Higham pers. comm.) of two copper-base artefacts typologically comparable to those recovered from, chronologically overlapping, NKH3/MeP3 contexts (Figure 8.10), as well as the copper-base artefacts recorded from Nong Nor (Higham *et al.* 1997: 177, Figure 5). However, we should not ignore the possibility of an about-face to the extensive tin deposits of west-central Thailand, also a couple of hundred kilometres distant (Coote 1990, 1991, Kanjanajuntorn 2006). With even wider repercussions, we must remember the revised Valley chronology also nudges the industrial production of copper into greater contemporaneity with the increasingly evidenced networks of trans-Asiatic interaction (e.g. Ambrose *et al.* 2009, Bellina 2001, 2003, 2007, Bellina & Glover 2004, Bellina & Silapanth 2008, Hung *et al.* 2007). This exchange has already linked metallurgical technologies from South Asia to East Asia via the entrepôt and production site of Khao Sam Kaeo (Bellina 2008, Murillo-Barroso *et al.* forthcoming), coeval with MeP2 production at Non Pa Wai, as well as MeP3 output from Nil Kham Haeng and Khao Sai On, and we should not disregard the possibility of Valley metal having been exchanged over very long ranges - typologically 'Valley-like' ingots have been reported from Bali c. 3000km away (Soejono 1972). On a similar vein, Pigott *et*

al. (1997) noted that in late prehistory higher sea levels would have meant the coastline was much closer to the Khao Wong Prachan Valley than today, potentially facilitating greater access to or participation in contemporary maritime exchange networks. Unfortunately, the compositional and/or isotopic data for Thai copper-base artefacts currently available are too sparse or inconsistent (in terms of analytical methodology) to facilitate the analytical demonstration of Valley copper exchange (see Chapter 9).



Figure 8.10 - Two copper-base artefacts from an Iron Age 1 burial at Ban Non Wat. Image: courtesy of Charles Higham.

8.3 The origins of Khao Wong Prachan Valley metallurgy

Questions on archaeological origins, technological or otherwise, frequently linger on the boundaries of speculation due to the unlikelihood of the material record preserving ‘firsts’ (Killick 2008: 3045). Nevertheless, logic can be applied to distinguish between the available options for Valley metallurgy, namely the independent local invention of technology, the introduction of an established technology by foreigners, the local adoption of foreign technology (not necessarily a complete adoption), or the local innovation (inspired invention) of technology. In light of the revised chronology, the author’s discussion of the origins of Khao Wong Prachan Valley metallurgy takes a different turn to those that have gone before (e.g. Ciarla 2007a, Pigott & Ciarla 2007, Pigott *et al.* 1997, White & Hamilton in press), in that we must now make a sharp differentiation between the earliest currently known evidence for local copper-base consumption and founding (MeP1 burials, c. 1450BCE - c. 800BCE), and the first definite evidence for local copper smelting (MeP2 industry, c. 6/500BCE - c. 300BCE). A lead isotope-based characterisation of the Valley production system during MeP2 and MeP3 could be the backdrop for compositional and isotopic analysis of MeP1 metal artefacts. Were the Bronze Age artefact compositions consistent with the attested Iron Age Valley production, these analyses would suggest Bronze Age Valley smelting did indeed take place (as per the old chronology), but the archaeological evidence has not yet been discerned. If however, the signatures of MeP1 artefacts were external to the Valley system, this would support the current interpretation of the first Southeast Asian copper smelting evidence belonging to the Iron Age. Whilst this essential work is forthcoming, the discussion concentrates on what we currently know

about Southeast Asian copper smelting: that it may not begin before c. 6/500 BCE.

By c. 6/500BCE, copper-base metal may have been used in the Khao Wong Prachan Valley for up to 900 years, and in northeastern Thailand and northern Vietnam for up to 1500 years (J. White 2008, White & Hamilton in press). We do not know how evenly distributed this metal was, but surely the degree of late 2nd millennium/early 1st millennium bronze exposure amongst the Valley populace rules out any suggestion the MeP2 technology might be an independent invention of copper-base extractive metallurgy. As for the introduction of smelting technology by foreigners, there is no evidence to suggest the Valley was even partially re-peopled during the early 1st millennium BCE, and though there remains a gap between the end of NPW2/MeP1 (c. 800BCE) and the beginning of NPW3/MeP2 (c. 6/500BCE), the identification of the caliche interface as a post-depositional formation within the deposit rather than an on ancient land surface (Chapter 2, Figure 2.7) undermines any substantial ‘total abandonment’ theory. This leaves the processes of adoption of foreign technology and local innovation of technology as the most plausible explanations for the appearance of the MeP2 smelting process. However, the author would suggest any adoption process was far from a complete transmission of extractive metallurgical knowledge and know-how (cf. White & Hamilton in press for their argument on the degree of transmission in the earliest Southeast Asian metal technologies). In the absence of any comparable prehistoric Southeast Asian smelting sites it is currently impossible to know what other regional extractive metallurgical processes were like. Mining and smelting (copper extraction) require different skills than alloying and casting (copper-base founding), and there is likewise a distinct dissimilarity between the rudimentary MeP2 copper production of the early Iron Age Valley, and the relatively sophisticated Bronze Age founding techniques attested in the local MeP1, and also those of northeastern Thailand (Higham in press a, J. White 2008, White & Hamilton in press). Laying oneself at the mercy of future research, the author is inclined to regard the inefficient and non-standardised nature of MeP2 smelting in the Valley as representing at the most a very imperfect and/or selective adoption of an as yet unknown technology, or possibly a local innovation. Considering Valley metalworkers were familiar with high temperature founding processes and technical ceramics from MeP1, the exploitation of local minerals into the simple MeP2 crucible-based reaction is not an unreasonable step in a environment of growing regional metal demand. Indeed, the early Iron Age technique is so crude it is tempting to label it an ‘experimental’ mode of production (cf. White & Hamilton in press), an argument supported by the consistently high CVs in bulk chemical data (Bettinger & Eerkens 1999, Eerkens 2000, Eerkens & Bettinger 2001, Eerkens & Lipo 2005, Eerkens & Lipo 2007). Were this the case, then local metalworkers achieved an admirable feat in developing their knowledge of bronze founding principles into a wasteful but effective means of primary copper production. This MeP2 Valley

initiative could have then followed a trajectory of increasing proficiency and intensity into the relative efficiency and uniformity of the MeP3 smelting process. At this juncture the interpretive capacity of the current Valley data is probably exhausted, and awaits further investigation. Though the future may prove the author wrong, the metallurgical significance of the Khao Wong Prachan Valley is not likely to ever be undermined, just reinterpreted.

Summary

This chapter has provided a synthesis of the two copper smelting *chaînes opératoires* for Non Pa Wai and Nil Kham Haeng developed in Chapters 5 and 6, and revised in light of the field experimentation reported in Chapter 7. The integration of these data have furnished a narrative of increasing technical skill and knowledge on the part of Iron Age Valley metalworkers. The rudimentary nature of MeP2 copper smelting at Non Pa Wai could be interpreted as experimental phase in extractive Valley metallurgy, which developed into the simple but effective techniques employed by MeP3 metalworkers at Nil Kham Haeng. Given the Iron Age context of these technological changes it is conceivable that Valley metalworkers were responding to an apparently growing regional demand for copper-base metal by increasing the intensity of their production, particularly in terms of labour input. These interpretations, offered in view of the just-discussed data, demonstrate how a technological approach of reconstructing high-resolution *chaînes opératoires* from both laboratory and field studies can permit the identification of ancient technological choices and the subsequent definition of technological styles based on the configuration of those choices. As such, the technological choice and style concepts are compatible and useful to structure both data generation and interpretation.

Chapter 9

Conclusion

The original research aim was to produce a diachronic account of change and continuity in technological choices and styles in prehistoric copper smelting activities in the Iron Age Khao Wong Prachan Valley. Guided by the theoretical and methodological framework of the social constructionist *chaîne opératoire technique*, improved reconstructions of prehistoric copper smelting activities at Non Pa Wai and Nil Kham Haeng have been developed, necessitating significant revisions to previous efforts (e.g. Bennett 1989, Pigott *et al.* 1997). Nevertheless, it has been repeatedly acknowledged that considerable gaps and conflations probably continue to exist in the Valley *chaînes opératoires* offered in this thesis. These deficiencies are due partly to relatively low sample numbers and the absence of clear mineralogical information to calculate the smelting charge. However, the major issue is the lack of precise provenancing due to the stratigraphically unique, complicated, and often disturbed industrial deposits at Non Pa Wai and Nil Kham Haeng (Chapter 2). Had the stratigraphic contexts been less problematic, they might well have provided an improved intra-site order to the enormous archaeometallurgical assemblages that characterise both of these sites.

The early Iron Age Non Pa Wai process may be summarised as the inefficient and non-standardised crucible-based reduction of oxidic and some sulphidic copper ores with an archaeologically invisible air delivery system, whilst the Nil Kham Haeng process was the more efficient and standardised bowl furnace-based reduction of sulphidic and some oxidic copper ores. Due to the presence of perforated ceramic cylinders in NKH3/MeP3 copper smelting contexts, it was thought that the later Iron Age smelt may have been wind-driven. However, an informative field testing programme suggested that the process was probably not wind-powered and that these enigmatic cylinders should be decoupled from the smelting *chaînes opératoires* at Nil Kham Haeng and Khao Sai On, implying once again that organic-based air delivery mechanisms must be missing from the archaeological record.

Whilst a degree of technological fuzziness is regrettably inevitable, the reconstructed *chaînes opératoires* for prehistoric Valley copper smelting were used to identify those characteristic technological choices, or artefactual representations of them, that the author believes were most definitive of the two technological styles currently discernable. In this thesis it is argued that decreasing variability and copper loss in the Nil Kham

Haeng slag samples when compared to those from Non Pa Wai represents the increasing standardisation and intensification of the Valley copper smelting process during the course of Iron Age. It is also proposed that this shift in metallurgical ethos may be interpreted as the result of copper producing communities responding to rising demand for copper/bronze in increasing ranked late prehistoric Thai communities, as especially well evidenced in the Upper Mun River Valley only c. 200km to the east. Furthermore, due to the relatively rudimentary early Iron Age copper smelting process attested at Non Pa Wai, it was speculated that prehistoric extractive metallurgy in the Valley may have been a local innovation derived from experimentation and long-term familiarity with copper-base founding techniques.

The implications of this new interpretation of copper-base extractive metallurgy in the Iron Age Khao Wong Prachan Valley can be discussed on the regional stage. White & Hamilton's (in press) term, "common Southeast Asian crucible production", was introduced in Chapter 1 and refers to the relatively small (c. 10cm diameter) spouted crucibles known for some time from Phu Lon (Vernon 1996-1997), Non Nok Tha (Bayard & Solheim 1991 in White & Hamilton in press), Ban Chiang (Vernon 1997), Ban Na Di (Higham 1988a), and more recently from Ban Non Wat (Higham 2008b). These crucibles appear in contexts from the early 2nd millennium BCE onwards, and for White & Hamilton (in press) are characteristic of a small scale, simple, mobile, low capital investment, though not unsophisticated (refractory quartz slurry lagging) technology that was practiced by multiple widely distributed craft production communities supplying relatively local demand in a decentralised prehistoric economy (White & Pigott 1996). These combined characteristics are taken to constitute the "southern metallurgical tradition" (White 1988, White & Hamilton in press), and in this their interpretation seems perfectly reasonable. White & Hamilton (in press) go on to compare the "common Southeast Asian crucible production" with a geographically distinct variant known as "Khao Wong Prachan Valley crucible production", which refers of course to the copper production that has been the focus of the present study (and for the sake of Nil Kham Haeng can be assumed to include bowl furnaces too).

Whilst recognising that prehistoric Valley metallurgy is also relatively simple, small scale, mobile, and commensurate with a 'community craft specialisation' organisation of production, White & Hamilton (in press) crucially do not distinguish between the stage of production represented by the archaeometallurgical remains. The significant morphological and volumetric differences between the 'common' versus 'Valley' crucibles could well be indicative of their variant primary functions. The 'common Southeast Asian crucible production', absent from Valley assemblages, seems to represent only secondary copper-

base production (founding) activities, and even at Phu Lon where the smelting of local minerals is very likely, the crucible evidence has not yet demonstrated it (Vernon 1996-1997) - though it would be far from a technical impossibility to reduce copper minerals in such a vessel (e.g. Tylecote 1974). In contrast, though Valley crucibles are likely to have been used for melting and casting metals too, it seems that their principal purpose was primary extractive metallurgical production, or smelting. Therefore White and Hamilton (in press) are not comparing like with like.

However, the relative proliferation of the ‘common Southeast Asian crucible production’ to some extent must be commensurate with the relative intensity of archaeological site prospection in northeast Thailand. The smaller ‘common’ crucibles represent secondary production sites, widely distributed amongst potential consumers and where metalworkers perhaps had better access to alloying materials like tin and lead via riverine communication and exchange. The larger ‘Valley’ crucibles represent primary production sites, which though still quite reasonably perceived as specialist craft communities acting on their own behalf, are to some extent constrained in their location by the availability of copper minerals and subsequently fewer in number. Thus whilst ‘Valley’ crucibles appear and may well be geographically distinct, it is also possible that this variant may one day be reported from as yet undiscovered production sites located in the comparatively under-explored uplands of the Loei-Petchabun Volcanic Belt (Figure 2.2 and 2.3). Given the current level of evidence it may be equally valid to state that at a ‘prehistoric Thai metallurgy’ scale, the “common” and “Valley” types of crucible production should perhaps be considered as necessarily complementary rather than awkwardly opposing characteristics of the ‘southern metallurgical tradition’.

The author believes the Valley data may also be examined for their relevance to the longstanding ‘origins of metallurgy’ debate. Made available to the author in mid 2008 and still in press at the time of writing, Joyce White and Elizabeth Hamilton (in press) have proposed the “Rapid Eurasian Technological Expansion Model” (or RETEM) to explain the presence of early 2nd millennium BCE copper-base metallurgy in northeast Thailand (see summary in Chapter 1). Developed from earlier thinking (e.g. White 1986, 1997, 2000), RETEM is part of a growing body of scholarship on trans-Eurasian social interactions and transmissions of metallurgical technologies, a discussion that has for some time extended as far as China and Southeast Asia (e.g. Chiou-Peng 1998, Ciarla 2007a, Higham 2002: 113-117, 2006: 18, Linduff *et al.* 2000, Mei 2000, 2003, 2004, Pigott & Ciarla 2007: 76, White 1997, 2008). White and Hamilton (in press, citing mainly Kohl 2007), describe that towards the end of the 3rd millennium BCE, the Eurasian metallurgical evidence indicates a significant intensification in production behaviour, and the long-distance movements

of nomadic metal-using pastoralists with horses and wheeled transport. Based on similar material culture and tight dating within a few centuries (e.g. Hanks *et al.* 2007), it is argued that the “Seima-Turbino transcultural phenomenon” (Chernykh 1992: 215-234 cited in White & Hamilton in press) expanded very rapidly from a supposed ‘homeland’ in the Altaï and Sayan mountains of western Mongolia/southern Siberia, to the Baltic in the west and to the Gansu Corridor in the east (e.g. Fitzgerald-Huber 1995; 2003 cited in White & Hamilton in press; Mei 2003). Building upon the observations of others (e.g. Sherratt 2006), White and Hamilton (in press) claim close typological and technological similarities between early Southeast Asian metallurgical traditions and late 3rd/early 2nd millennium BCE ‘Seima-Turbino’ metallurgy, and would thus preliminarily extend the ‘phenomenon’ into Southeast Asia (Figure 9.1).

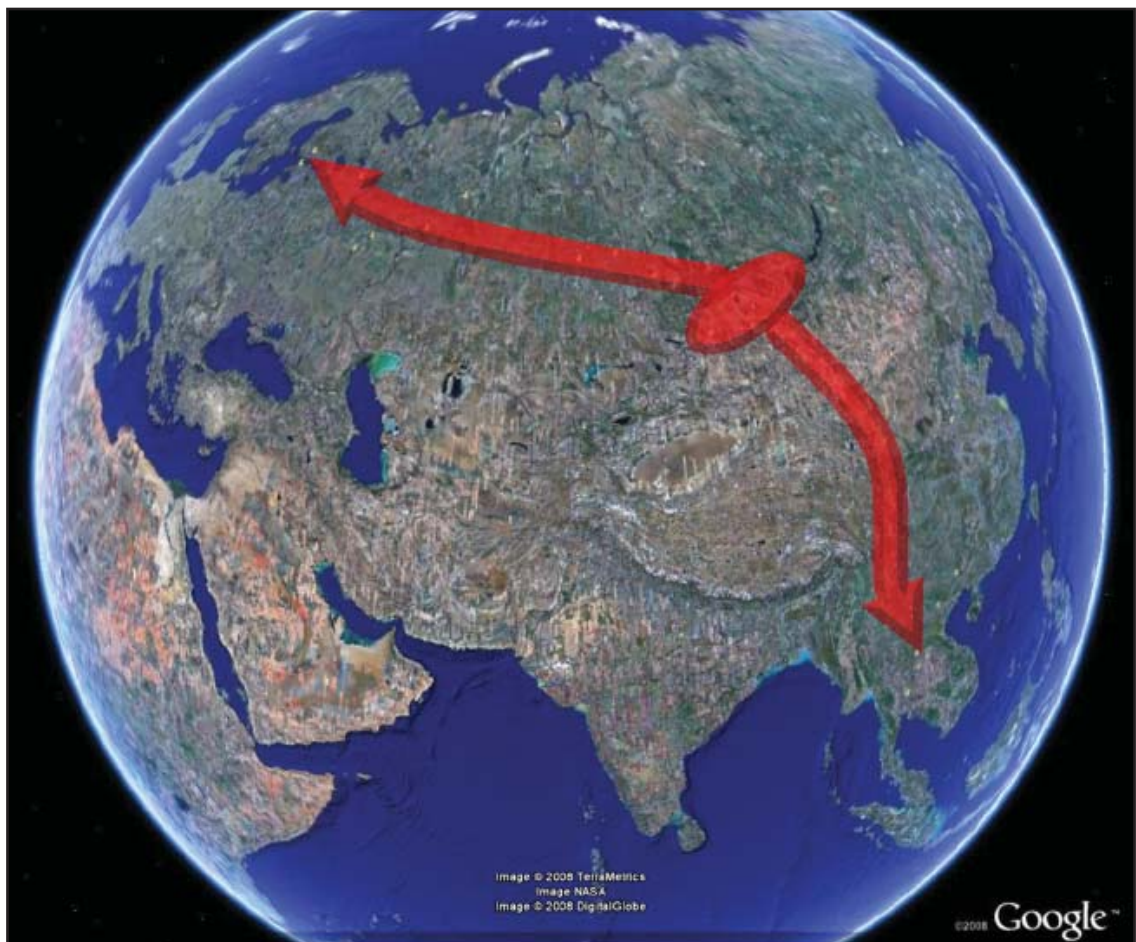


Figure 9.1 - From its supposed centre in the Altaï mountains, the proposed “Seima-Turbino transcultural phenomenon” (Chernykh 1992: 215-234 cited in White & Hamilton in press); extends c. 4000km to the northwest and the Gulf of Finland, and another c. 4000km southeast to the Mekong River. Image: courtesy of Google Earth™ mapping service, modified by the author.

The radical nature of the ‘Rapid Eurasian Technological Expansion Model’ comes not from the enormous *range* over which cultural interactions and transmissions are proposed, but rather the means for explaining the *rate* at which it seems to have taken place.

“The consistency of the artifact kit across different cultures suggests that Seima-Turbino metal workers trained locals in the technology, and/or took up residence in

foreign groups, and/or foreigners came to live with the Seima-Turbino migrants” (White & Hamilton in press).

On the basis of well-documented technological transmission theory (e.g. Bettinger & Eerkens 1999, Eerkens 2000, Eerkens & Bettinger 2001, Eerkens & Lipo 2005, Eerkens & Lipo 2007), White and Hamilton (in press) argue that the low degree of variation they perceive in the ‘Seima-Turbino’ metallurgical assemblage is due to direct social learning environments and a high degree of co-operative interaction between social groups; over a territory spanning in excess of 8000km. Complex technologies like metallurgy tend to require extended apprenticeship to be successfully transmitted; a situation not normally thought to exist outside of kin groups or those without a close cultural affinity (e.g. Charlton 2007: 209, Epstein 1998, Keller & Keller 1996, Roberts 2008). However, even if taught directly, one would expect more variation in techniques and products to be introduced with each sequential transmission of metallurgical knowledge and know-how. Therefore, White & Hamilton (in press) contest that the uniformity of the ‘Seima-Turbino’ metallurgical tradition, within a relatively small chronological window, is due to the movement of experienced metalworkers far and fast across Eurasia¹, but critically, “without a complete migration of the source culture and population”² (White & Hamilton in press).

RETEM is not for the faint of heart and as David Killick (2008: 3045) emphasises, “[t]his proposal [aimed at Pigott & Ciarla 2007 but equally applicable to White & Hamilton in press] will be hotly debated, as there is as yet almost no relevant data from the geographically intermediate zone comprising south-western China, Vietnam and Laos.” Likewise, the summary dismissal of potential technological transmissions from the Indian subcontinent incurs a certain disquietude; the absence of evidence needed to produce alternative South/Southeast Asian transmission models could well be due to the lack of focused research in the intermediary area. This type of reception was of course anticipated by White & Hamilton (in press), who concede that their model desperately needs more primary data and detailed analysis. They go on to offer a manifesto of the steps needed to substantiate the ‘Seima-Turbino’ theory by a variety of measures (e.g. biological, botanical, linguistic, zoological), but concentrate their recommendation on the comprehensive technological

1 The potential motivation for ‘Seima-Turbino’ metal workers to behave like this is yet to be substantially expanded upon.

2 This low intensity introduction of genotypes and phenotypes would presumably be difficult to detect by bioarchaeologists, who have currently found no evidence to substantiate suggestions for large-scale prehistoric population movement (Oxenham & Tayles 2006: 347); though acknowledging the discipline is young and critical data are incomplete.

analysis of metallurgical ceramics (e.g. crucibles, furnaces, moulds) from contemporary contexts across Eurasia. Although a solid theoretical framework need not imply a watertight archaeological case, it does offer substantial support and render the ‘Rapid Eurasian Technological Expansion Model’ worthy of further consideration.

Needless to say, the new Khao Wong Prachan Valley interpretation could be used to support both White’s ‘early’ and Higham’s ‘late’ hypotheses for the origins of Southeast Asian metallurgy (see Chapter 1). However, though we must proceed with caution, at present it is possible to make one significant modification to RETEM (White & Hamilton in press) using the revised understanding of Valley metallurgy developed in this thesis. White and Hamilton (as per Pigott and Ciarla 2007) are absolutely correct in differentiating between copper-base consumption and production contexts, but they do not distinguish sufficiently between different stages in the copper-base production sequence; namely extraction (mining, beneficiation, smelting, refining) and founding technologies (refining, alloying, casting, forging, finishing). In fairness, White and Hamilton (in press) produced their model prior to Rispoli *et al.*’s (forthcoming) revised Khao Wong Prachan Valley chronology, and its immediate effect is to remove the region’s most important strut for 2nd millennium BCE *extractive* metallurgy (e.g. Pigott *et al.* 1997). With the definite evidence for Valley smelting confined at present to the 1st millennium BCE, White and Hamilton’s (in press) claim for a ‘near complete transmission’ of Seima-Turbino metallurgical technologies to Thailand hangs by a single ¹⁴C thread at Phu Lon³ - a site that to date evidences only prehistoric mining activity, as smelting remains to be proven. Critically, the present study’s MeP2 data (see Chapter 5) could be interpreted as representing an experimental phase of copper smelting in the mid 1st millennium BCE Khao Wong Prachan Valley (see Chapter 8), which might be considered counter-intuitive c. 1500 years (Rispoli *et al.* forthcoming) after White & Hamilton’s (in press) preferred inception of Thai copper-base metallurgy. Thus, in light of the present study, RETEM holds, though not necessarily as a complete transmission as it appears that 2nd millennium BCE Thai metallurgy, and the cultural transmissions that introduced it, concerned only copper-base consumption and founding behaviour. Three possible explanations for this are: either the evidence for early 2nd millennium BCE extractive metallurgy has not been found or recognised yet; the postulated Seima-Turbino migrants transmitted mining and/or smelting techniques to northeast Thailand that were for some reason not relayed to, or accepted in, central Thailand; or those immigrant metalworkers never brought this aspect of copper-base metallurgical technology to Thailand.

3 Though White and Hamilton (in press) cite the excavator’s current opinion on the context of the charcoal sample (Pigott & Ciarla 2007: 82), they prefer to stick by an earlier paper by Pigott and Weisgerber (1998: 151) with a more amenable assignation.

We presumably still have as much to learn about ancient Siberian cultures as we do for those in Southeast Asia, but perhaps there was a separation in Siberian societies between those who mined and smelted metals, and those who alloyed and cast them. Thus, it is possible the putative migrants arriving in Southeast Asia had never practiced extractive metallurgy and thus could not transmit it. An alternative might be the supply of copper-base metal down the major (i.e. Mekong) rivers in the 2nd millennium BCE was sufficient to make primary production in Southeast Asia unnecessary. The evidence we then discern for intensive regional mining and smelting in the 1st millennium BCE could then be attributed to the interruption of copper-base metal supply from the northwest, or a local response to the steep rise in demand from Southeast Asian societies engaged in increasing competitive social display (e.g. Higham & Higham 2009).

In view of the findings of this thesis, and the near complete⁴ absence of metal provenancing data, one useful strategy for regional archaeometallurgical research could be a lead isotope analysis-based (LIA) investigation of the circulation of copper/bronze in prehistoric Southeast Asia. All sourcing techniques are based around the Provenance Postulate, ‘that variation between sources is greater than that within a source’ (Wilson & Pollard 2001). The pertinent issue in LIA is, what does variability in lead isotope ratios represent in metallurgical samples? A sample’s lead isotope (LI) ratios are a reflection of the geological age of the materials from which the sample was retrieved. These ratios are not modified by high temperatures or extreme redox conditions, but are highly susceptible to a metal artefact’s life history (e.g. the alloying and recycling). These issues have been heavily debated by archaeometallurgists (e.g. Budd *et al.* 1993, Budd *et al.* 1996, Budd *et al.* 1995, Gale & Stos-Gale 1995, Hall 1995, Muhly 1995, Pernicka 1995, Tite 1996) and it is now widely accepted that lead isotope ratios combined with trace element analysis can provide meaningful analytical results, but only when integrated with a solid understanding of a region’s multiple strands of archaeological evidence. Once armed with a secure appreciation of methodological limitations, and a corresponding lowering of spatial resolution expectations, archaeometallurgical provenancing approaches hold great potential for synthetic discussions of diachronic trends in regional and inter-regional metal exchange (e.g. Begemann *et al.* 1999, Gale & Stos-Gale 1982, Gale *et al.* 1985, Giussani *et al.* 2007, Hosler & Macfarlane 1996, Müller *et al.* 2007, Stos-Gale 1989, 1993, Stos-Gale *et al.* 1997, Weeks 2007).

The wide geographical distribution of copper-base ‘ingots’, comparable to those from the later Iron Age Khao Wong Prachan Valley (Chapters 2 and 8), suggests metal may

4 The author is aware of two small lead-isotope studies from Vietnam (Le Canh Lam pers. comm.) and Thailand (Surapol Natapintu pers. comm.).

have been exchanged over long distances in prehistoric Southeast Asia. However, typological evidence must be reinforced with technological, compositional, and isotopic analyses to provide a more robust classificatory triangulation. The analytical section of the proposed Southeast Asian copper-base metal provenance project could commence with compositionally and isotopically characterising the Khao Wong Prachan Valley and Phu Lon smelting systems, providing two primary production signatures against which to test comparable analyses of ingots and secondary production centres; which would include the consideration of processing techniques and apparatus (e.g. crucibles, furnaces, and adhering copper scoria). Any copper signature not falling on the mixing line between the Valley and Phu Lon can be assumed to correspond to as yet undiscovered primary production systems; a likely eventuality considering the mineral wealth of Southeast Asia and the huge areas yet to be investigated archaeologically in Laos and southwestern China. As the project moves on to study typologically-defined classes of copper alloy artefacts in consumption contexts, one would expect the primary production signatures to be increasingly obscured. However, a methodical analytical progression via secondary production evidence, accounting for the compositional/isotopic contribution of alloying materials, should permit some degree of linkage to be made from either end of the production and consumption sequence, especially as evidence of manufacturing technique would also be considered. This sequence can be seen as a proxy for social interaction, with the potential to tentatively identify exchange networks between copper producing and consuming societies in prehistoric Southeast Asia, and should constitute the metallurgical response to Bellina's (2001) siliceous stone, Hung *et al.*'s (2007) nephrite, and Ambrose *et al.*'s (2009) obsidian studies, as well as being complementary to Laure Dussubieux's (The Field Museum, Chicago, US) planned isotopic provenance study on Southeast Asian glass. The data generated would also be of immediate use for colleagues conducting archaeometallurgical research in South and East Asia.

In addition to LIA-based provenance research, a complementary avenue for Southeast Asian archaeometallurgists will be to continue studying metallurgical assemblages within a coherent theoretical and methodological framework, as offered by the *chaîne opératoire technique*, which may allow better grounded comparisons and discussions of cultural/technological transmission within prehistoric Southeast Asia and potentially further afield into East and South Asia. Informed by the concepts of technological choice and technological style, this thesis ultimately hoped to provide a primary production reference point as scholars continue to develop a fuller picture of the role of metal in Southeast Asian history.

Appendix A: Sample Catalogue

KWPV mineral samples

Sample	Site	Op	Area	Level	Tag	Period	Date Tagged	Siliceous	Ferruginous	Pyritic	Copper Carbonates	Copper Sulphides
NPWM1	NPW	A	C	6	32995	MeP2 (7/600-300 BC)	27-Feb-1986	X			X	
NPWM2	NPW	B	D	9	36001	MeP2 (7/600-300 BC)	13-Mar-1986	X				
NPWM3	NPW	B	PI	2	36894	MeP2 (7/600-300 BC)	12-Feb-1986	X				
NPWM4	NPW	B	B	7	36006	MeP2 (7/600-300 BC)	5-Mar-1986	X			X	
NPWM5	NPW	B	C	11	36007	MeP2 (7/600-300 BC)	12-Mar-1986	X			X	
NPWM6	NPW	B	C	11	36890	MeP2 (7/600-300 BC)	13-Mar-1986		X		X	
NPWM7	NPW	B	A	6	36878	MeP2 (7/600-300 BC)	26-Feb-1986	X				
NPWM8	NPW	C	A	?	36002	MeP2 (7/600-300 BC)	13-Feb-1986	X			X	
NPWM9	NPW	C	E	11	36009	MeP2 (7/600-300 BC)	11-Mar-1986	X	X		X	
NPWM10	NPW	C	O	19	32996	MeP2 (7/600-300 BC)	25-Mar-1986		X			
NPWM11	NPW	M	A	15	36005	MeP2 (7/600-300 BC)	23-Mar-1986	X	X			
NPWM12	NPW	N	PI	2	32946	MeP2 (7/600-300 BC)	20-Feb-1986		X		X	
NPWM13	NPW	X	-	2	32994	MeP2 (7/600-300 BC)	12-Mar-1986	X	X	X	X	
NKHM1	NKH	1	SWQ	9	3492	MeP3 (300 BC-300 AD)	7-Mar-1990	X	X		X	
NKHM2	NKH	1	-	-	23	MeP3 (300 BC-300 AD)	6-Feb-1990	X	X		X	
NKHM3	NKH	1	NEQ	7	3454	MeP3 (300 BC-300 AD)	5-Mar-1990	X	X			
NKHM4	NKH	2	E	3	1076	MeP3 (300 BC-300 AD)	13-Feb-1990	X	X			
NKHM5	NKH	3	SW	3	158	MeP3 (300 BC-300 AD)	8-Feb-1990	X	X		X	
NKHM6	NKH	4	SEQ	4	1146	MeP3 (300 BC-300 AD)	8-Mar-1990	X	X	X		X

Table A.1: Contexts and macro-characteristics for KWPV mineral samples.



NPWM1



NPWM4



NPWM5



NPWM6



NPWM8



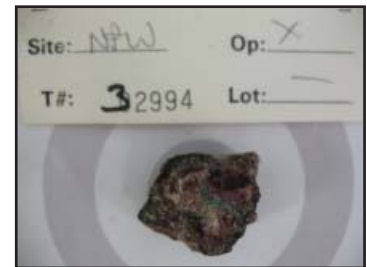
NPWM9



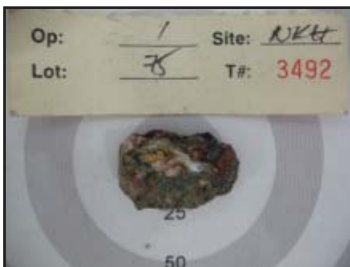
NPWM10



NPWM12



NPWM13



NKHM1



NKHM2



NKHM5



NKHM6

KWPV technical ceramic samples

Sample	Site	Op	Area	Level	Tag	Period	Date Tagged	Mass (g)	Com- ment	Hi- fired	Lo-fired	Bloated/ Vitrified	Slagged	Copper sign	Perforated
NPWTC1	NPW	2	NWQ	3	12026	MeP2 (7/600-300 BC)	2-Mar-1992	500	Crucible	X		X	X		X
NPWTC2	NPW	2	SWQ	5	14706	MeP2 (7/600-300 BC)	22-Mar-1992	100	Crucible	X		X	X		
NPWTC3	NPW	2	SE	1	7385	MeP2 (7/600-300 BC)	23-Jan-1992	920	Crucible	X		X	X		X
NPWTC4	NPW	2	SWQ	2	7683	MeP2 (7/600-300 BC)	12-Feb-1992	205	Crucible	X		X	X		X
NPWTC5	NPW	2	SEQ	2	7940	MeP2 (7/600-300 BC)	5-Feb-1992	200	Crucible	X		X	X		X
NPWTC6	NPW	2	NEQ	3	13359	MeP2 (7/600-300 BC)	14-Mar-1992	485	Crucible	X		X	X		X
NPWTC7	NPW	2	SE/SW	2	7391	MeP2 (7/600-300 BC)	2-Feb-1992	80	Crucible	X		X	X		X
NPWTC8	NPW	2	NWQ	5	14620	MeP2 (7/600-300 BC)	19-Mar-1992	135	Crucible	X		X	X		X
NPWTC9	NPW	2	NE	2	8277	MeP2 (7/600-300 BC)	3-Feb-1992	220	Crucible	X		X	X		X
NPWTC10	NPW	2	NWQ	3	10884	MeP2 (7/600-300 BC)	26-Feb-1992	85	Crucible	X		X	X		X
NPWTC11	NPW	C			36696	MeP2 (7/600-300 BC)	15-Apr-1986	450	Furnace		X				
NPWTC12	NPW	C			36692	MeP2 (7/600-300 BC)	15-Apr-1986	655	Furnace		X				
NPWTC13	NPW	C			36694	MeP2 (7/600-300 BC)	15-Apr-1986	450	Furnace		X				X
NKHTC1	NKH	1	NEQ	14	4643	MeP3 (600 BC - 300 AD)	27-Mar-1990	500	Furnace		X				
NKHTC2	NKH	2	-	5	3570	MeP3 (600 BC - 300 AD)	16-Mar-1990	300	Furnace		X				
NKHTC3	NKH	3	SEQ	18	3808	MeP3 (600 BC - 300 AD)	20-Mar-1990	700	Furnace		X				X
NKHTC4	NKH	4	NWQ	1	386	MeP3 (600 BC - 300 AD)	14-Feb-1990		Slag skins	X		X	X		X
NKHTC5	NKH	4	NEQ	3	1841	MeP3 (600 BC - 300 AD)	20-Feb-1990		Slag skins	X		X	X		X
NKHTC6	NKH	3	NEQ	6	4012	MeP3 (600 BC - 300 AD)	14-Feb-1990		Slag skins	X		X	X		X

Table A.2: Contexts and macro-characteristics for KWPV technical ceramic samples.



NPWTC1



NPWTC2



NPWTC3



NPWTC4



NPWTC5



NPWTC6



NPWTC7



NPWTC8



NPWTC9



NPWTC10



NPWTC11



NPWTC12



NPWTC13



NKHTC1



NKHTC2



NKHTC3



NKHTC4



NKHTC5



NKHTC6

KWPV slag samples

Sample	Site	Op	Area	Level	Tag	Date tagged	Mass (g)	Size (mm)	Colour	Streak	Homogeneity	Porosity	Density	Magnetism
NPWMS1	NPW	7	-	1	9055	15-Feb-1992	1640	<100	Black	Brown	Medium	Medium	Low-Medium	Weak
NPWMS2	NPW	7	-	1	9967	26-Feb-1992	240	<80	Brown	Brown	Low-Medium	Medium	Medium	Strong
NPWMS3	NPW	1	-	-	14223	16-Mar-1992	140	<80	Green	Grey	Medium-High	Low-Medium	Medium-High	Strong
NPWMS4	NPW	7	A	1	13975	18-Mar-1992	160	<60	Grey	Grey	Low-Medium	Low-Medium	Medium	Strong
NPWMS5	NPW	B	A	13	36807.1	31-Mar-1986	150	<30	Grey	Brown	Low-Medium	Medium	Medium	Strong
NPWMS6	NPW	M	A	6	36714	8-Mar-1986	1325	<140	Black	Brown	Medium-High	Medium	Medium-High	Strong
NPWMS7	NPW	M	A	7	36719	20-Mar-1986	NA	NA	NA	NA	NA	NA	NA	NA
NPWMS8	NPW	B	A	15	36807.2	31-Mar-1986	300	<50	Grey	Brown	Low-Medium	Medium	Medium	Strong
NPWMS9	NPW	3	A	1	6807	27-Jan-1992	90	<70	Green	Green	Medium	Medium-High	Low-Medium	Weak
NPWMS11	NPW	A	B	4	36787	3-Jan-1986	160	<70	Black	Brown	Medium	Medium	Medium	Strong
NPWMS12	NPW	B	B	15	36809.1	31-Mar-1986	170	<40	Grey	Brown	Medium	Low-Medium	Medium-High	Strong
NPWMS13	NPW	B	C	14	36809.2	1-Jan-1986	110	<40	Grey	Brown	Medium	Low-Medium	Medium-High	Strong
NPWMS14	NPW	B	C	13	36809.3	27-Mar-1986	670	<40	Grey	Grey	Medium-High	Low-Medium	Medium	Strong
NPWMS16	NPW	7	SEQ	1	15104	25-Mar-1992	45	<50	Brown	Brown	Medium-High	Low-Medium	Medium-High	Strong
NPWMS17	NPW	8	UNIT 1	2	11485	2-Mar-1992	110	<70	Green	Grey	Medium-High	Low-Medium	Medium-High	Strong
NPWMS18	NPW	8	UNIT 1	2	11605	3-Mar-1992	25	<50	Grey	Grey	Medium-High	Medium	Medium	Weak
NPWMS19	NPW	8	UNIT 1	2	13443	16-Mar-1992	780	<140	Black	Green	Medium	Low-Medium	Medium-High	Weak
NPWMS20	NPW	8	UNIT 1	3	14371	22-Mar-1992	110	<80	Grey	Brown	Low-Medium	Medium	Medium	Strong
NPWMS21	NPW	7	-	1	8486	12-Feb-1992	930	<100	Grey	Green	Low-Medium	Medium	Medium	Strong

Table A.3i: Contexts and macro-characteristics for KWPV slag samples - NPW

Fe stain	Cu stain	Smell	Ceramic	Fuel	HCl(aq)	SiO ₂	CaCO ₃	Crystal Size	Viscosity	Flowmarks	Layering	Pulverisation	Orientation	Product M
Strong	Weak	None	?	No	?	?	?	Medium	Medium	No	?	?	Yes	?
None	None	None	?	Yes	?	Yes	Yes	Medium	Medium	No	No	No	No	?
None	None	None	No	No	?	No	No	Medium-High	Low-Medium	No	No	No	?	?
Weak	Strong	None	No	No	?	No	No	Medium-High	Medium-High	No	?	No	No	Cu
None	Strong	None	Yes	No	?	No	No	Medium-High	Medium	?	?	?	No	Cu
None	Weak	None	?	No	?	No	No	Low-Medium	Medium	No	Yes	No	Yes	Cu
NA	NA	NA	NA	NA	NA	NA	NA	NA	NA	NA	NA	NA	NA	NA
Weak	Strong	None	Yes	No	?	No	Yes	Medium-High	Medium-High	No	No	?	No	Cu
None	Weak	None	?	No	?	No	No	Medium	Medium-High	No	No	No	No	?
Weak	Weak	None	No	No	?	No	No	Medium	Medium	No	No	No	No	Cu
Weak	Strong	None	No	No	?	No	No	Medium	Medium	?	?	?	No	Cu
Weak	Strong	None	No	No	?	No	No	Medium	Medium	?	?	?	No	Cu
Weak	Strong	None	?	No	?	?	?	Medium-High	Medium	?	No	?	No	Cu
None	Strong	None	No	No	?	?	No	Medium	Low-Medium	No	?	No	Yes	Cu
None	None	None	?	No	?	No	No	Medium	Low-Medium	No	No	No	No	?
None	Weak	None	No	No	?	No	No	Medium	Low-Medium	Yes	No	No	Yes	Cu
Weak	Weak	None	?	Yes	?	?	?	Medium	Low-Medium	No	No	No	Yes	Cu
Weak	Strong	None	No	Yes	?	No	Yes	Medium-High	Medium-High	No	No	No	?	Cu
Weak	Weak	None	?	Yes	?	No	Yes	Medium	Medium-High	No	No	No	?	Cu

Table A.3ii: Contexts and macro-characteristics for KWPV slag samples - NPW

Sample	Site	Op	Area	Level	Tag	Date tagged	Mass (g)	Size (mm)	Colour	Streak	Homogeneity	Porosity	Density	Magnetism
NKHMS2	NKH	1	-	-	4835	28-Mar-1990	265	<140	Black	Brown	Low-Medium	Medium	Medium	Strong
NKHMS3	NKH	1	-	-	1105	6-Feb-1990	45	<40	Black	Black	Medium-High	Low-Medium	Medium-High	Strong
NKHMS4	NKH	2	A	3-4	630	11-Feb-1990	45	<50	Black	Brown	Medium-High	Low-Medium	Medium	Weak
NKHMS5	NKH	2	C	6	5432	29-Mar-1990	30	<30	Grey	Black	Low-Medium	Medium	Medium	Strong
NKHMS6	NKH	2	D	5	4797	27-Mar-1990	30	<40	Grey	Grey	Low	High	Low-Medium	Strong
NKHMS7	NKH	2	E	3	3427	13-Feb-1990	30	<50	Grey	Brown	Medium-High	Low-Medium	Medium	Weak
NKHMS8	NKH	4	H	4	2040	21-Feb-1990	65	<60	Black	Brown	Medium-High	Low-Medium	Medium	Strong
NKHMS9	NKH	4	J	4	2042	22-Feb-1990	150	<70	Black	Black	Medium	Medium	Medium	Strong
NKHMS10	NKH	3	NEQ	18	3659	16-Mar-1990	95	<70	Grey	Grey	Medium	Low-Medium	Medium	Strong
NKHMS11	NKH	1	NEQ	8	2359	5-Mar-1990	100		Black	Brown	Medium-High	Low-Medium	Medium	Strong
NKHMS12	NKH	3	NEQ	6	515	15-Feb-1990	70	<80	Green	Grey	Medium-High	Low-Medium	Medium	Strong
NKHMS13	NKH	1	NEQ	11	3790	-	175	<100	Silver	Brown	Medium	Medium	Medium	Weak
NKHMS14	NKH	3	NEQ	18	4706	16-Mar-1990	125	<60	Grey	Grey	Medium	Medium	Medium	Strong
NKHMS15	NKH	1	NWQ	9	3179	15-Mar-1990	200	<120	Silver	Grey	Medium	Medium	Medium	Strong
NKHMS17	NKH	2	NWQ	4A	2793	11-Mar-1990	110	<80	Black	Grey	Medium	Low-Medium	Medium	Weak
NKHMS18	NKH	2	NWQ	4A	3390	11-Mar-1990	100	<70	Silver	Grey	Medium	Low-Medium	Medium	Strong
NKHMS19	NKH	3	SEQ	195	4294	22-Mar-1990	195	<60	Black	Green	Medium	Medium	Medium	Strong
NKHMS20	NKH	3	SEQ	24	5923	30-Mar-1990	150	<70	Grey	Grey	Medium	Low-Medium	Medium-High	Strong
NKHMS21	NKH	3	SWQ	18	3843	21-Mar-1990	140	<90	Grey	Grey	Medium	Medium	Medium	Strong

Table A.3iii: Contexts and macro-characteristics for KWPV slag samples - NKH

Fe stain	Cu stain	Smell	Ceramic	Fuel	HCl(aq)	SiO2	CaCO3	Crystal Size	Viscosity	Flowmarks	Layering	Pulverisation	Orientation	Product M
Strong	Strong	None	?	Yes	?	No	No	Medium	Medium	?	No	No	Yes	Cu
None	Weak	None	No	No	?	No	No	Low-Medium	Low-Medium	No	No	No	Yes	Cu
None	Weak	None	?	No	?	No	No	Medium	Low-Medium	?	No	No	Yes	Cu
Weak	Strong	None	No	No	?	No	No	Medium	Medium	No	No	No	Yes	Cu
None	Strong	None	Yes	No	?	No	?	Medium	Medium-High	No	Yes	No	Yes	Cu
Weak	None	None	No	No	?	No	No	Medium	Medium	No	No	No	No	?
Weak	Weak	None	No	No	?	No	No	Medium-High	Low-Medium	?	No	No	?	Cu
None	Strong	None	No	No	?	No	No	Medium	Medium-High	No	?	No	No	Cu
Strong	Strong	None	No	No	?		No	Medium	Medium	?	Yes	No	No	Cu
Weak	Strong	None	No	No	?	No	No	Medium	Low-Medium	No	No	No	Yes	Cu
None	None	None	?	No	?	No	No	Medium	Medium	No	No	No	No	?
Weak	Weak	None	?	Yes	?	No	No	Medium-High	Low-Medium	No	No	No	?	Cu
Weak	Strong	None	No	No	?	No	No	Medium-High	Medium	No	No	?	?	Cu
Weak	Weak	None	?	Yes	?			Medium	Medium	No	No	No	Yes	Cu
Weak	Strong	None	No	No	?	No	No	Medium	Low-Medium	?	?	No	Yes	Cu
None	Weak	None	No	No	?	No	?	Medium	Medium	No	No	No	?	Cu
Strong	Strong	None	No	Yes	?	Yes	No	Medium	Low-Medium	No	No	No	Yes	Cu
None	Strong	None	No	No	?	No	No	Medium-High	Medium	No	No	No	Yes	Cu
Weak	Strong	None	No	No	?	No	No	Medium-High	Medium	No	No	No	Yes	Cu
Weak	Strong	None	No	Yes	?	No	No	Medium-High	Medium	No	No	No	No	Cu
Weak	Strong	None	No	Yes	?	No	No	Medium	Medium	?	No	No	Yes	Cu

Table A.3.iv: Contexts and macro-characteristics for KWPV slag samples - NKH



NPWMS1



NPWMS2



NPWMS3



NPWMS4



NPWMS5



NPWMS6



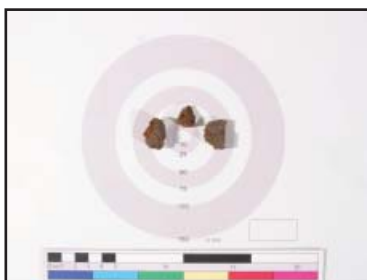
NPWMS7 - width c.15cm



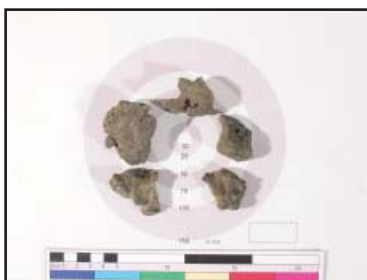
NPWMS8



NPWMS9



NPWMS10



NPWMS11



NPWMS12



NPWMS13



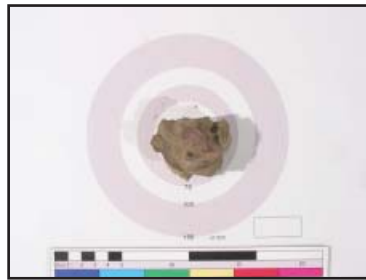
NPWMS14



NPWMS15



NPWMS16



NPWMS17



NPWMS18



NPWMS19



NPWMS20



NPWMS21



NKHMS1



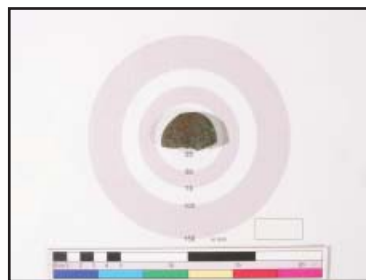
NKHMS2



NKHMS3



NKHMS4



NKHMS5



NKHMS6



NKHMS7



NKHMS8



NKHMS9



NKHMS10



NKHMS11



NKHMS12



NKHMS13



NKHMS14



NKHMS15



NKHMS16



NKHMS17



NKHMS18



NKHMS19



NKHMS20



NKHMS21

Appendix B

Compositional data

	Na ₂ O	MgO	Al ₂ O ₃	SiO ₂	P ₂ O ₅	SO ₃	Cl	K ₂ O	CaO	TiO ₂	V ₂ O ₅	Cr ₂ O ₃	MnO	Fe ₂ O ₃	Co	Ni	Cu	Zn	Ga	Sr	Y	Zr	Nb	Ba	La	Ce	Nd	Totals				
	wt%	wt%	wt%	wt%	wt%	wt%	wt%	wt%	wt%	wt%	wt%	wt%	wt%	wt%	wt%	ppm	ppm	ppm	ppm	ppm	ppm	ppm	ppm	ppm	ppm	ppm	ppm	ppm	ppm	wt%		
certified	0.00	1.03	0.67	8.78	15.70	0.48		49.00	0.35	0.94	0.33	3.16	19.02																	99.45		
[PJED-XRF 23/01/07	0.62	0.03	0.01	7.71	14.19	0.61	0.00	0.04	47.51	0.23	0.81	0.32	2.73	18.97	77	<10	<10	13	12	317	<10	17	19	403	23	21	48	93.90				
[PJED-XRF 24/01/07	0.71	0.03	0.01	7.74	14.23	0.63	0.00	0.05	47.54	0.24	0.82	0.31	2.73	18.96	111	<10	<10	13	12	317	<10	14	20	402	22	22	48	94.10				
[PJED-XRF 26/01/07	0.65	0.04	0.05	7.82	14.20	0.61	0.00	0.05	47.58	0.24	0.82	0.32	2.74	18.97	64	<10	<10	13	12	316	<10	17	20	398	23	21	48	94.19				
OP mean	0.66	0.03	0.02	7.76	14.21	0.62	0.00	0.05	47.54	0.24	0.82	0.32	2.73	18.97	84	n.a.	n.a.	13	12	316	n.a.	16	20	401	23	21	48	94.07				
OP std dev	0.05	0.00	0.02	0.06	0.02	0.01	0.00	0.00	0.04	0.00	0.00	0.00	0.00	0.01	24	n.a.	n.a.	0	0	0	n.a.	2	1	2	0	0	0	0	0	0		
OP CV	7%	1%	88%	1%	0%	1%	0%	5%	0%	2%	0%	1%	0%	0%	29%	n.a.	n.a.	1%	3%	0%	n.a.	10%	3%	1%	1%	2%	2%	0%	0%	0%		
cert. δ relative 23/01/07	0.62	-0.99	-0.66	-1.08	-1.50	0.14		-1.49	-0.12	-0.13	-0.01	-0.43	-0.05																			
cert. δ relative 24/01/08	0.71	-0.99	-0.66	-1.04	-1.46	0.15		-1.46	-0.11	-0.12	-0.02	-0.43	-0.06																			
cert. δ relative 26/01/09	0.65	-0.99	-0.62	-0.96	-1.50	0.14		-1.42	-0.11	-0.12	-0.01	-0.42	-0.04																			
certified	2.22	7.23	13.50	49.90	0.27	0.00		0.52	11.40	2.73	0.00	0.00	0.13	12.30																	100.20	
[PJED-XRF 07/12/06	2.26	4.47	15.32	45.36	0.19	0.01	0.00	0.42	9.38	1.93	0.05	0.04	0.17	12.59	138	94	140	101	22	389	<10	26	99	11	127	11	15	<10	92.29			
[PJED-XRF 08/12/06	2.20	4.51	15.48	45.47	0.18	0.01	0.00	0.42	9.38	1.94	0.05	0.03	0.17	12.58	147	99	137	101	23	391	<10	26	95	10	125	11	15	<10	92.54			
[PJED-XRF 09/12/06	2.30	4.60	15.56	46.18	0.18	0.01	0.00	0.44	9.54	1.96	0.04	0.04	0.18	12.68	138	101	136	104	21	391	<10	26	97	12	128	11	16	<10	93.82			
[PJED-XRF 23/01/07	1.65	5.39	15.09	41.73	0.08	0.13	0.00	0.48	10.86	2.32	0.02	0.04	0.15	12.14	190	93	139	86	22	394	<10	25	158	28	118	20	41	<10	90.21			
[PJED-XRF 24/01/07	1.56	5.41	15.06	41.73	0.08	0.14	0.00	0.48	10.85	2.33	0.02	0.03	0.15	12.13	195	94	139	85	21	392	<10	25	162	27	120	21	36	<10	90.10			
[PJED-XRF 26/01/07	1.71	5.45	15.12	41.69	0.08	0.13	0.00	0.48	10.84	2.32	0.02	0.03	0.15	12.12	175	94	134	84	20	391	<10	25	163	27	121	19	39	<10	90.28			
OP mean	1.95	4.97	15.27	43.69	0.13	0.07	0.00	0.45	10.14	2.13	0.03	0.04	0.16	12.37	164	96	138	93	21	391	<10	25	129	19	123	15	27	n.a.	91.54			
OP std dev	0.34	0.49	0.22	2.18	0.05	0.07	0.00	0.03	0.78	0.21	0.02	0.00	0.01	0.27	26	<10	<10	<10	<10	<10	<10	<10	<10	<10	<10	<10	<10	13	n.a.			
OP CV	18%	10%	1%	5%	41%	98%	86%	7%	8%	10%	52%	3%	9%	2%	16%	3%	2%	10%	5%	0%	2%	27%	47%	3%	31%	47%	n.a.					
cert. δ relative 07/12/06	0.04	-2.76	1.82	-4.54	-0.08	0.01		-0.10	-2.02	-0.80	0.05	0.04	0.04	0.29																		
cert. δ relative 08/12/06	-0.02	-2.72	1.98	-4.43	-0.09	0.01		-0.10	-2.02	-0.79	0.05	0.03	0.04	0.28																		
cert. δ relative 09/12/06	0.08	-2.63	2.06	-3.72	-0.09	0.01		-0.08	-1.87	-0.77	0.04	0.04	0.05	0.38																		
cert. δ relative 23/01/07	-0.57	-1.84	1.59	-8.17	-0.19	0.13		-0.04	-0.54	-0.41	0.02	0.04	0.02	-0.16																		
cert. δ relative 24/01/07	-0.66	-1.82	1.56	-8.17	-0.19	0.14		-0.04	-0.55	-0.40	0.02	0.03	0.02	-0.17																		
cert. δ relative 26/01/07	-0.51	-1.78	1.62	-8.21	-0.19	0.13		-0.04	-0.56	-0.41	0.02	0.03	0.02	-0.18																		

Table B.1: KWPV Certified Reference Materials [PJED-XRF bulk chemical analyses; all detected elements reported. 'OP' refers to the author's analyses. Data not normalised.

	Na ₂ O	MgO	Al ₂ O ₃	SiO ₂	P ₂ O ₅	SO ₃	Cl	K ₂ O	CaO	TiO ₂	V ₂ O ₅	Cr ₂ O ₃	MnO	Fe ₂ O ₃	Co	Ni	Cu	Zn	Ga	As	Br	Rb	Sr	Y	Zr	Nb	Ba	La	Ce	Nd	Hf	Pb	Th	Totals		
wt% wt%	wt%	wt%	wt%	wt%	wt%	wt%	wt%	wt%	wt%	wt%	wt%	wt%	wt%	wt%	wt%	wt%	wt%	wt%	wt%	wt%	wt%	wt%	wt%	wt%	wt%	wt%	wt%	wt%	wt%	wt%	wt%	wt%	wt%	wt%	wt%	wt%
certified	0.09	1.48	10.62	17.80	2.02	0.64	0.59	3.92	0.48	0.14	0.06	0.28	0.28	47.48																						85.60
[P]ED-XRF 23/01/07	0.27	1.19	12.09	15.96	1.98	0.34	0.00	0.54	3.69	0.40	0.13	0.07	0.27	47.66	409	49	<10	319	11	220	13	<10	1008	106	219	<10	137	157	372	116	<10	<10	<10	<10	84.91	
[P]ED-XRF 24/01/07	0.29	1.17	12.10	15.94	1.97	0.35	0.00	0.55	3.71	0.40	0.13	0.07	0.28	47.71	367	62	<10	322	11	219	14	<10	1008	105	230	<10	132	148	368	114	<10	<10	<10	<10	84.98	
[P]ED-XRF 26/01/07	0.26	1.13	12.29	16.20	2.00	0.34	0.00	0.55	3.75	0.41	0.13	0.07	0.28	48.16	404	56	10	322	12	234	14	<10	1013	108	216	14	135	153	367	110	<10	<10	<10	<10	85.89	
OP mean	0.27	1.16	12.16	16.03	1.98	0.34	0.00	0.55	3.72	0.40	0.13	0.07	0.28	47.84	393	56	n.a.	321	11	224	14	n.a.	1010	106	222	n.a.	135	153	369	113	n.a.	n.a.	n.a.	n.a.	85.26	
OP std dev	0.02	0.03	0.12	0.15	0.01	0.01	0.00	0.00	0.03	0.00	0.00	0.00	0.00	0.00	0.28	23	7	n.a.	2	1	9	1	n.a.	3	1	7	n.a.	3	5	3	3	n.a.	n.a.	n.a.	n.a.	
OPCV	6%	3%	1%	1%	1%	2%	0%	1%	1%	1%	1%	0%	1%	1%	6%	12%	n.a.	1%	8%	4%	4%	n.a.	0%	1%	3%	n.a.	2%	3%	1%	3%	n.a.	n.a.	n.a.	n.a.		
cert. δ relative	23/01/07	0.18	-0.28	1.47	-1.84	-0.04	-0.30	-0.05	-0.22	-0.08	-0.01	0.01	-0.01	-0.01	0.18																					
cert. δ relative	24/01/07	0.20	-0.31	1.48	-1.86	-0.04	-0.29	-0.04	-0.21	-0.08	-0.01	0.01	-0.01	-0.01	0.23																					
cert. δ relative	26/01/07	0.17	-0.34	1.68	-1.60	-0.02	-0.30	-0.04	-0.16	-0.08	-0.00	0.01	-0.01	-0.01	0.68																					
certified	0.07	0.52	38.70	54.90	0.12	0.00	1.33	0.22	2.03	0.00	0.00	0.00	0.00	1.60																						99.49
[P]ED-XRF 07/12/06	0.50	0.59	36.77	44.89	0.10	0.01	0.00	1.08	0.17	1.48	0.04	0.04	0.00	1.68	21	66	28	34	50	<10	<10	41	311	52	385	22	130	40	67	<10	21	45	33	87.50		
[P]ED-XRF 08/12/06	0.50	0.57	36.69	44.63	0.10	0.02	0.00	1.08	0.17	1.47	0.04	0.04	0.01	1.67	21	68	28	35	51	<10	<10	41	310	52	381	23	135	43	65	<10	21	44	32	87.11		
[P]ED-XRF 09/12/06	0.50	0.58	36.66	44.81	0.10	0.02	0.00	1.08	0.17	1.48	0.04	0.04	0.00	1.68	21	68	29	35	52	<10	<10	41	311	53	388	22	132	39	64	<10	21	44	32	87.31		
[P]ED-XRF 26/01/07	0.42	0.58	36.34	44.70	0.11	0.05	0.00	1.06	0.19	1.47	0.04	0.04	0.01	1.69	27	69	28	35	51	<10	<10	41	312	51	384	23	139	47	73	<10	21	46	33	86.82		
OP mean	0.48	0.58	36.62	44.76	0.10	0.02	0.00	1.07	0.17	1.47	0.04	0.04	0.01	1.68	23	68	28	35	51	n.a.	n.a.	41	311	52	385	22	134	42	67	n.a.	21	45	32	87.19		
OP std dev	0.04	0.01	0.19	0.12	0.00	0.01	0.00	0.01	0.01	0.01	0.00	0.00	0.00	0.01	3	1	0	1	1	n.a.	n.a.	0	1	1	3	1	4	3	4	n.a.	0	1	1	1		
OPCV	8%	1%	1%	0%	4%	61%	0%	1%	5%	0%	1%	1%	29%	0%	13%	2%	2%	2%	2%	1%	n.a.	0%	0%	1%	1%	3%	3%	8%	6%	n.a.	1%	2%	2%	2%		
cert. δ relative	07/12/06	0.43	0.07	-1.93	-10.01	-0.02	0.01	-0.25	-0.05	-0.55	0.04	0.04	0.00	0.08																						
cert. δ relative	08/12/06	0.43	0.05	-2.01	-10.27	-0.02	0.02	-0.25	-0.05	-0.56	0.04	0.04	0.01	0.07																						
cert. δ relative	09/12/06	0.43	0.06	-2.04	-10.09	-0.02	0.02	-0.25	-0.05	-0.55	0.04	0.04	0.00	0.08																						
cert. δ relative	26/01/07	0.35	0.06	-2.36	-10.20	-0.01	0.05	-0.27	-0.03	-0.56	0.04	0.04	0.01	0.09																						

Table B.1ii: KWPV Certified Reference Materials [P]ED-XRF bulk chemical analyses; all detected elements reported. 'OP' refers to the author's analyses. Data not normalised.

	Na ₂ O	MgO	Al ₂ O ₃	SiO ₂	P ₂ O ₅	SO ₃	Cl	K ₂ O	CaO	TiO ₂	V ₂ O ₅	Cr ₂ O ₃	MnO	Fe ₂ O ₃	Co	Ni	Cu	Zn	Ga	As	Rb	Sr	Y	Zr	Ba	La	Ce	Nd	Hf	Pb	Th	Totals			
	wt%	wt%	wt%	wt%	wt%	wt%	wt%	wt%	wt%	wt%	wt%	wt%	wt%	wt%	wt%	wt%	wt%	wt%	wt%	wt%	wt%	wt%	wt%	wt%	wt%	wt%	wt%	wt%	wt%	wt%	wt%	wt%	wt%		
certified	0.79	1.85	14.40	66.60	0.28	0.00	1.96	2.37	0.78	0.00	0.00	0.13	7.18																				96.34		
[PJED-XRF 07/12/06]	0.41	1.52	16.43	57.94	0.27	0.01	0.01	1.66	1.87	0.56	0.03	0.13	7.45	82	42	55	69	18	<10	66	111	30	181	463	14	32	<10	<10	14	<10	88.44				
[PJED-XRF 08/12/06]	0.35	1.50	16.50	58.31	0.27	0.01	0.01	1.65	1.89	0.56	0.03	0.13	7.51	94	46	55	71	19	<10	66	111	30	179	467	13	33	<10	<10	14	<10	88.87				
[PJED-XRF 09/12/06]	0.35	1.48	16.52	58.53	0.27	0.01	0.01	1.68	1.92	0.57	0.02	0.13	7.53	99	40	53	67	18	<10	65	112	31	177	471	12	31	<10	<10	14	<10	89.16				
[PJED-XRF 26/01/07]	0.47	1.47	16.38	57.90	0.27	0.04	0.01	1.66	1.92	0.56	0.03	0.13	7.51	85	45	52	69	18	<10	66	111	30	171	471	13	38	<10	<10	16	<10	88.50				
OP mean	0.39	1.49	16.46	58.17	0.27	0.02	0.01	1.66	1.90	0.56	0.03	0.13	7.50	90	43	54	69	18	n.a.	66	111	30	177	468	13	34	n.a.	n.a.	15	n.a.	88.74				
OP std dev	0.06	0.02	0.06	0.30	0.00	0.01	0.00	0.01	0.02	0.00	0.00	0.00	0.00	0.03	8	3	2	1	1	n.a.	0	1	0	4	4	1	3	n.a.	n.a.	1	n.a.				
OP CV	15%	2%	0%	1%	1%	69%	9%	1%	1%	4%	3%	0%	0%	9%	6%	3%	2%	3%	n.a.	1%	1%	2%	2%	1%	5%	9%	n.a.	n.a.	7%	n.a.					
cert. δ relative 07/12/06	-0.38	-0.33	2.03	-8.66	-0.01	0.01		-0.30	-0.51	-0.22	0.03	0.03	0.00	0.27																					
cert. δ relative 08/12/06	-0.44	-0.35	2.10	-8.29	-0.01	0.01		-0.31	-0.48	-0.22	0.03	0.03	0.00	0.33																					
cert. δ relative 09/12/06	-0.44	-0.37	2.12	-8.07	-0.01	0.01		-0.29	-0.46	-0.21	0.02	0.03	0.00	0.35																					
cert. δ relative 26/01/07	-0.32	-0.38	1.98	-8.70	-0.01	0.04		-0.30	-0.45	-0.22	0.03	0.03	0.00	0.33																					
'agreed'	0.59	0.39	7.20	23.97	0.25	0.04	0.96	1.42	0.30	0.03	0.01	3.03	61.68																					99.87	
[PJED-XRF 23/01/07]	0.83	0.29	7.26	21.73	0.10	0.43	0.00	1.07	1.40	0.22	0.00	0.02	2.67	68.01	241	<10	<10	20	12	26	<10	78	131	100	998	107	345	86	10	14	12	104.23			
[PJED-XRF 24/01/07]	0.82	0.31	7.32	21.91	0.10	0.42	0.00	1.07	1.42	0.23	0.01	0.02	2.72	68.15	266	<10	11	19	11	25	<10	77	131	103	1005	109	338	73	10	14	12	104.74			
[PJED-XRF 26/01/07]	0.86	0.35	7.36	21.87	0.11	0.35	0.00	1.06	1.43	0.23	0.01	0.02	2.70	67.80	234	<10	<10	18	<10	18	<10	77	132	105	999	108	361	90	10	14	11	104.37			
OP mean	0.84	0.32	7.31	21.84	0.10	0.40	0.00	1.07	1.42	0.22	0.01	0.02	2.70	67.99	247	n.a.	n.a.	19	8	23	n.a.	77	131	103	1001	108	348	83	10	14	12	104.44			
OP std dev	0.02	0.03	0.05	0.10	0.01	0.05	0.00	0.01	0.02	0.01	0.00	0.00	0.03	0.18	17	n.a.	n.a.	1	7	4	n.a.	0	0	2	4	1	11	9	0	0	0	0			
OP CV	2%	9%	1%	0%	7%	11%	0%	1%	1%	3%	25%	2%	1%	0%	7%	n.a.	n.a.	5%	87%	18%	n.a.	0%	0%	2%	0%	1%	3%	11%	2%	0%	0%	2%			
cert. δ relative 23/01/07	0.24	-0.10	0.06	-2.24	-0.15	0.39		0.11	-0.02	-0.09	-0.03	0.01	-0.36	6.33																					
cert. δ relative 24/01/07	0.23	-0.08	0.12	-2.06	-0.15	0.38		0.11	-0.00	-0.07	-0.02	0.01	-0.31	6.47																					
cert. δ relative 26/01/07	0.27	-0.04	0.16	-2.10	-0.14	0.31		0.10	0.01	-0.07	-0.02	0.01	-0.33	6.12																					

Table B.1 iii: KWPV Certified Reference Materials [PJED-XRF bulk chemical analyses; all detected elements reported. 'OP' refers to the author's analyses. Data not normalised.

	Na ₂ O	MgO	Al ₂ O ₃	SiO ₂	P ₂ O ₅	SO ₃	K ₂ O	CaO	MnO	Fe ₂ O ₃	CuO	Ni	Zn	As	Se	Rb	Sr	Y	Zr	Mo	Ag	Sn	Ba	La	Ce	Hf	Ta	Pb	Total		
	wt%	wt%	wt%	wt%	wt%	wt%	wt%	wt%	wt%	wt%	wt%	ppm	ppm	ppm	ppm	ppm	ppm	ppm	ppm	ppm	ppm	ppm	ppm	ppm	ppm	ppm	ppm	ppm	ppm	ppm	wt%
NKHM1	0.39	3.55	9.66	32.03	0.07	4.48	0.05	18.99	0.63	16.04	3.15	91	235	<10	11	<10	1163	22	74	<10	21	<10	584	15	28	120	133	110	89.3		
NKHM2	1.18	0.57	7.98	59.53	0.06	0.01	0.10	7.44	0.13	9.85	5.62	64	247	61	<10	<10	955	17	94	<10	<10	<10	31	11	13	147	160	30	92.7		
NKHM3	0.40	0.67	2.09	78.32	0.06	4.82	0.05	3.13	0.12	6.81	3.44	82	3766	17	16	<10	288	<10	<10	<10	21	<10	23	21	13	100	110	52	100.4		
NKHM4	0.17	0.41	5.89	72.46	0.12	1.50	0.10	6.26	0.14	8.47	5.20	74	113	<10	10	<10	633	<10	57	<10	11	<10	63	11	17	137	150	15	100.8		
NKHM5	0.75	0.37	4.63	43.87	0.10	8.48	0.19	6.35	0.13	20.60	15.70	170	419	13	83	<10	363	<10	<10	<10	38	<10	127	10	17	<10	<10	<10	101.3		
NKHM6	0.79	0.35	0.92	39.99	0.13	31.72	0.02	3.72	0.17	24.30	16.11	13	1502	1226	67	<10	131	<10	<10	<10	163	<10	190	<10	13	<10	<10	<10	118.5		
<i>or taking into account the pyritic component:</i>																															
NKHM6	0.79	0.35	0.92	39.99	0.13	12.69	0.02	3.72	0.17	16.98	16.11	13	1502	1226	67	<10	131	<10	<10	<10	163	<10	190	<10	13	<10	<10	<10	92.2		
<i>S</i>																															
<i>Fe</i>																															
NPWM1	0.59	0.07	8.11	66.43	0.05	0.00	0.07	9.81	0.17	8.25	1.56	<10	58	<10	<10	<10	1065	12	57	<10	<10	<10	17	12	16	70	78	<10	95.3		
NPWM2	0.51	0.08	5.84	68.26	0.01	0.01	0.07	5.47	0.20	7.00	7.55	116	811	<10	<10	<10	675	<10	<10	<10	<10	<10	25	14	13	167	187	61	95.2		
NPWM3	0.99	0.08	2.29	76.41	0.07	0.03	0.07	0.24	0.01	7.45	2.68	17	111	<10	<10	<10	20	<10	<10	<10	<10	<10	16	<10	12	92	137	16	90.4		
NPWM4	0.72	0.31	3.94	67.09	0.08	0.01	0.07	6.99	0.18	12.43	2.02	50	266	14	<10	<10	367	<10	<10	<10	<10	<10	36	14	11	82	92	26	93.9		
NPWM5	5.09	1.25	14.52	62.24	0.17	0.01	1.20	1.66	0.09	3.97	2.12	166	951	<10	<10	23	701	<10	72	<10	<10	<10	350	<10	13	73	81	<10	92.6		
NPWM6	0.54	2.62	3.41	7.55	0.13	0.01	0.20	2.75	0.10	74.90	4.15	30	1115	<10	<10	<10	45	<10	<10	<10	<10	<10	13	<10	13	<10	<10	16	96.5		
NPWM7	0.53	0.10	7.50	55.01	0.09	0.01	0.08	7.57	0.08	12.37	7.33	57	245	10	<10	<10	746	<10	<10	<10	<10	<10	39	10	13	193	200	<10	90.8		
NPWM8	0.66	0.07	0.76	77.04	0.04	0.05	0.05	0.67	0.89	3.45	6.53	93	207	<10	<10	<10	26	<10	<10	<10	86	<10	22	<10	12	140	157	18	90.3		
NPWM9	0.77	1.47	12.89	32.33	0.18	0.01	0.50	18.36	0.22	18.31	2.16	11	135	27	<10	<10	328	18	41	264	<10	<10	48	85	96	110	286	87.3			
NPWM10	0.10	0.16	0.67	1.23	0.00	0.30	0.27	0.09	0.17	96.29	0.15	19	217	<10	<10	<10	12	<10	<10	<10	<10	<10	41	10	14	70	78	23	99.5		
NPWM11	0.17	7.62	9.09	15.92	0.07	0.04	0.27	0.19	0.41	22.58	21.48	350	3251	15	<10	<10	<10	<10	13	<10	<10	16	10	17	<10	<10	<10	78.2			
NPWM12	0.10	0.36	1.02	3.89	0.19	0.14	0.19	0.10	0.07	84.49	1.23	30	948	16	11	<10	<10	<10	<10	<10	<10	10	10	13	177	200	20	91.9			
NPWM13	2.02	0.07	0.03	18.29	0.01	48.38	0.12	3.87	0.12	54.36	1.10	1296	68	167	118	<10	35	<10	<10	<10	24	<10	342	10	14	110	248	<10	128.6		
<i>or taking into account the pyritic component:</i>																															
NPWM13	2.02	0.07	0.03	18.29	0.01	19.35	0.12	3.87	0.12	37.98	1.10	1296	68	167	118	<10	35	<10	<10	<10	24	<10	342	10	14	110	248	<10	83.2		
<i>S</i>																															
<i>Fe</i>																															

Table B.2: KWPV mineral sample [P]ED-XRF bulk chemical analyses; all detected elements reported. Data not normalised.

	Na ₂ O wt%	MgO wt%	Al ₂ O ₃ wt%	SiO ₂ wt%	P ₂ O ₅ wt%	SO ₃ wt%	K ₂ O wt%	CaO wt%	TiO ₂ wt%	MnO wt%	Fe ₂ O ₃ wt%	CuO wt%	Ni ppm	Zn ppm	As ppm	Se ppm	Rb ppm	Sr ppm	Y ppm	Zr ppm	Ag ppm	Ba ppm	La ppm	Ce ppm	Hf ppm	Ta ppm	Pb ppm	Total wt%
NKHTC1	0.65	0.31	18.73	51.81	0.18	0.02	1.32	3.93	0.54	0.19	9.72	0.19	32	188	17	<10	61	155	20	102	<10	246	<10	21	24	26	21	87.68
NKHTC2	0.81	0.31	18.08	55.06	0.32	0.01	1.20	4.13	0.51	0.13	8.95	0.26	18	189	21	<10	69	231	20	102	<10	479	<10	14	27	29	16	89.88
NKHTC3	0.44	0.33	20.06	52.07	0.23	0.01	0.91	5.38	0.62	0.20	10.67	0.22	24	171	17	<10	46	173	26	106	<10	199	14	17	26	27	14	91.21
NPWTC1	1.41	0.97	14.86	63.12	0.13	0.01	0.36	4.19	0.43	0.19	6.53	0.18	31	55	11	<10	14	424	13	103	<10	203	<10	16	21	23	<10	92.48
NPWTC2	1.21	1.26	17.18	53.61	0.31	0.01	0.49	4.93	0.50	0.19	8.46	0.06	44	98	20	<10	17	624	15	62	<10	223	10	13	13	15	<10	88.32
NPWTC3	1.51	1.38	17.94	53.58	0.09	0.01	0.49	4.62	0.51	0.20	8.57	0.13	55	66	11	<10	16	526	15	74	<10	180	<10	16	19	27	<10	89.10
NPWTC4	1.23	1.52	15.92	54.81	0.48	0.01	0.62	4.58	0.49	0.12	7.57	0.44	64	115	16	<10	33	625	12	57	<10	469	<10	12	34	38	<10	87.94
NPWTC5	1.48	1.80	19.19	54.91	0.22	0.01	0.52	4.19	0.56	0.17	8.53	0.19	59	87	12	<10	16	500	15	62	<10	164	<10	14	23	26	<10	91.86
NPWTC6	1.56	1.42	16.42	60.44	0.20	0.01	0.47	4.86	0.51	0.16	7.52	0.40	42	58	11	<10	17	545	15	63	<10	183	11	12	33	41	<10	94.06
NPWTC7	1.27	1.15	16.10	59.78	0.14	0.01	0.43	4.94	0.49	0.17	7.41	0.10	36	90	12	<10	16	527	15	89	<10	151	10	17	16	19	<10	92.07
NPWTC8	1.40	1.47	18.37	55.65	0.24	0.01	0.45	5.07	0.52	0.19	9.09	1.10	51	82	17	<10	16	654	15	68	<10	198	10	20	57	63	<10	93.68
NPWTC9	1.71	1.42	17.86	54.75	0.20	0.01	0.52	4.63	0.51	0.18	8.65	3.10	69	88	14	16	16	528	14	56	13	172	10	15	99	110	<10	93.65
NPWTC10	1.89	1.50	16.38	59.44	0.14	0.01	0.43	4.92	0.49	0.20	7.79	0.14	38	78	11	<10	15	552	14	67	<10	233	<10	20	20	22	<10	93.45
NPWTC11	1.31	1.27	16.46	54.46	0.31	0.01	1.11	5.78	0.48	0.17	7.90	0.18	52	74	17	<10	41	617	13	58	<10	299	<10	15	22	24	<10	89.57
NPWTC12	1.40	1.29	16.19	54.68	0.15	0.01	0.76	4.82	0.45	0.16	7.62	0.31	58	94	11	<10	37	567	13	57	<10	342	<10	13	29	35	<10	87.96
NPWTC13	1.26	1.48	16.65	55.16	0.19	0.01	0.55	4.95	0.48	0.16	8.12	0.23	63	85	14	<10	26	615	13	64	<10	305	<10	17	25	30	<10	89.37

Table B.3: KWPV technical ceramic sample [PJED-XRF bulk chemical analyses; all detected elements reported. Data not normalised.

	MgO	Al ₂ O ₃	SiO ₂	SO ₃	K ₂ O	CaO	TiO ₂	MnO	FeO	CuO	Total
	wt%	wt%	wt%	wt%	wt%	wt%	wt%	wt%	wt%	wt%	wt%
NPWTC1	0.4	1.8	16.2	0.0	0.1	2.3	0.9	0.0	66.2	0.5	88.5
NPWTC3	0.8	1.3	28.7	0.0	0.8	8.9	0.0	1.6	43.5	0.2	85.8
NPWTC8	0.6	1.0	26.3	0.0	0.1	3.6	0.0	0.8	53.2	0.6	86.1
NKHTC4	0.3	5.4	28.5	1.0	1.6	8.5	0.3	0.7	37.0	0.1	83.4
NKHTC5	2.2	2.4	24.0	0.0	0.6	16.3	0.2	0.4	36.8	0.3	83.2
NKHTC6	0.4	6.3	28.5	0.0	0.5	15.8	0.1	0.4	30.1	1.0	83.1

Table B.4: KWPV crucible slag and slag-skin olivine crystal SEM-EDS phase analyses. Data not normalised.

	MgO	Al ₂ O ₃	SiO ₂	SO ₃	K ₂ O	CaO	TiO ₂	MnO	FeO	CuO	Total
	wt%	wt%	wt%	wt%	wt%	wt%	wt%	wt%	wt%	wt%	wt%
NPWTC3 primary	0.3	0.5	0.8	0.0	0.0	0.4	0.0	0.5	88.5	0.5	91.6
NPWTC8 primary	0.1	0.7	0.1	0.0	0.0	0.1	0.0	0.2	87.9	1.7	90.9
NKHTC5 residual	1.1	1.3	0.3	1.0	1.6	0.2	0.4	0.3	90.4	0.1	96.9
NKHTC6 residual	0.2	0.3	0.4	0.0	0.1	0.3	0.1	0.1	93.4	0.1	95.0
NKHTC6 primary	0.4	5.4	2.0	0.0	0.0	1.1	0.6	0.2	76.6	0.3	86.6

Table B.5: KWPV crucible slag and slag-skin magnetite spinel SEM-EDS phase analyses. Data not normalised.

	MgO	Al ₂ O ₃	SiO ₂	P ₂ O ₅	K ₂ O	CaO	TiO ₂	MnO	FeO	CuO	Total
	wt%	wt%	wt%	wt%	wt%	wt%	wt%	wt%	wt%	wt%	wt%
NPWTC1	1.4	4.3	38.6	0.0	0.2	13.1	1.0	0.0	21.9	0.7	81.1
NPWTC3	1.7	2.1	34.2	0.0	0.1	15.7	0.0	1.1	27.8	0.1	82.8
NPWTC8	0.2	2.6	35.1	0.5	0.3	11.9	0.0	0.5	32.3	0.2	83.4
NKHTC4	2.3	4.6	31.9	0.0	-0.0	17.1	0.5	0.4	23.3	0.0	80.1
NKHTC5	1.5	8.0	21.6	0.0	0.9	13.5	0.2	0.4	34.1	0.1	80.3
NKHTC6	1.1	4.5	30.4	0.0	0.1	18.3	0.2	0.2	25.8	0.1	80.7

Table B.6: KWPV crucible slag and slag-skin glass SEM-EDS phase analyses. Data not normalised.

	S	Fe	Cu	Sn	Total
	wt%	wt%	wt%	wt%	wt%
NPWTC1	0.0	3.4	99.3	0.0	102.7
NKHTC4	17.4	57.5	3.4	0.0	78.3
NKHTC5	0.0	1.4	99.8	0.0	101.2

Table B.7: KWPV crucible slag and slag-skin prills SEM-EDS phase analyses. Data not normalised.

	MgO wt%	Al ₂ O ₃ wt%	SiO ₂ wt%	P ₂ O ₅ wt%	SO ₃ wt%	K ₂ O wt%	CaO wt%	TiO ₂ wt%	MnO wt%	FeO wt%	CuO wt%	Total wt%
NPWTC1 spectrum 1	1.1	4.1	37.1	0.0	0.0	0.3	8.8	1.0	0.0	29.8	4.1	86.2
NPWTC1 spectrum 2	0.8	3.6	35.4	0.0	0.0	0.2	8.1	0.8	0.0	31.8	5.9	86.8
NPWTC1 spectrum 3	1.2	4.3	37.4	0.0	0.0	0.2	8.9	1.3	0.0	28.2	4.1	85.5
NPWTC3 spectrum 1	1.1	1.9	32.9	0.0	0.0	0.3	14.1	0.0	1.2	30.6	0.8	82.9
NPWTC3 spectrum 2	0.9	2.2	31.4	0.0	0.0	0.4	12.9	0.0	1.3	33.5	1.5	84.0
NPWTC3 spectrum 3	1.1	1.4	33.3	0.0	0.0	0.3	14.2	0.0	1.2	30.7	0.6	82.7
NPWTC8 spectrum 1	0.0	1.6	19.3	0.1	0.0	0.1	3.5	0.0	0.5	62.0	1.1	88.2
NPWTC8 spectrum 2	0.0	1.9	22.9	0.5	0.0	0.2	4.9	0.0	0.4	55.7	1.3	87.7
NPWTC8 spectrum 3	0.0	1.8	25.1	0.2	0.0	0.1	5.1	0.0	0.4	50.3	2.7	85.8
NKHTC4 spectrum 1	1.5	6.1	27.8	0.0	0.6	0.6	11.3	0.3	0.5	26.7	0.5	75.9
NKHTC4 spectrum 2	1.1	6.1	28.1	0.0	0.8	0.7	10.8	0.4	0.4	30.4	0.8	79.8
NKHTC4 spectrum 3	0.9	6.0	24.2	0.0	0.6	0.6	9.5	0.2	0.5	26.3	0.3	69.1
NKHTC5 spectrum 1	1.8	6.2	20.0	0.0	0.0	0.6	11.9	0.4	0.3	41.5	1.0	83.7
NKHTC5 spectrum 2	1.9	5.6	17.9	0.0	0.0	0.4	10.1	0.3	0.4	47.0	1.5	85.1
NKHTC5 spectrum 3	1.7	6.4	19.7	0.0	0.0	0.6	11.3	0.3	0.5	41.8	1.0	83.0
NKHTC6 spectrum 1	0.6	4.8	23.9	0.5	0.0	0.6	9.4	0.0	0.4	34.1	2.8	77.1
NKHTC6 spectrum 2	0.7	5.5	21.7	0.5	0.0	0.3	9.8	0.0	0.4	39.5	2.1	80.4
NKHTC6 spectrum 3	0.6	5.5	24.2	0.2	0.0	0.4	9.0	0.0	0.4	27.3	3.9	71.6

Table B.8: KWPV crucible slag and slag-skin matrices SEM-EDS phase analyses. Data not normalised.

	Na ₂ O	MgO	Al ₂ O ₃	SiO ₂	P ₂ O ₅	SO ₃	K ₂ O	CaO	THO ₂	MnO	FeO	CuO	Ni	Zn	As	Se	Sr	Y	Zr	Mo	Ag	Sn	Ba	La	Ce	Nd	Hf	Ta	Pb	Total		
	wt%	wt%	wt%	wt%	wt%	wt%	wt%	wt%	wt%	wt%	wt%	wt%	ppm	ppm	ppm	ppm	ppm	ppm	ppm	ppm	ppm	ppm	ppm	ppm	ppm	ppm	ppm	ppm	ppm	ppm	ppm	wt%
NPWMS1	0.63	0.30	1.34	22.31	0.01	2.42	0.03	9.72	0.08	0.12	50.16	5.65	73	295	12	75	20	<10	27	<10	<10	<10	31	27	35	57	190	<10	<10	92.84		
NPWMS2	0.50	0.32	2.87	31.61	0.02	0.80	0.05	10.28	0.07	0.19	42.47	1.78	<10	866	14	11	178	<10	22	<10	<10	<10	116	25	23	52	94	<10	<10	91.10		
NPWMS3	0.50	0.44	3.62	23.52	0.35	1.38	0.15	4.52	0.12	0.24	58.56	0.87	10	965	12	<10	172	14	34	<10	<10	<10	<10	27	32	56	84	<10	11	94.41		
NPWMS4	0.50	0.66	2.73	20.53	0.04	6.02	0.06	8.42	0.07	0.21	57.86	2.63	72	448	13	18	45	<10	28	<10	19	<10	<10	28	26	58	140	<10	11	99.82		
NPWMS5	0.30	0.52	4.55	34.54	0.11	0.68	0.17	8.46	0.10	0.39	42.56	1.49	123	626	<10	13	276	10	26	<10	16	<10	<10	24	24	50	87	<10	<10	93.98		
NPWMS6	0.38	0.17	1.81	13.54	0.04	2.93	0.05	4.70	0.02	0.09	68.96	4.31	15	571	19	29	23	<10	11	<10	22	<10	<10	30	28	63	210	10	15	97.10		
NPWMS7	0.18	0.03	3.61	29.96	0.09	11.94	0.13	9.70	0.08	0.50	31.02	3.40	111	55817	12	103	324	<10	26	<10	24	<10	<10	26	31	55	130	<10	<10	96.30		
NPWMS8	0.49	0.11	1.51	18.21	0.01	0.77	0.03	4.42	0.03	0.11	57.92	4.07	12	822	13	11	27	<10	20	<10	55	<10	36	28	26	59	180	<10	12	87.81		
NPWMS9	0.41	1.07	4.27	28.50	0.16	1.50	0.22	9.21	0.10	0.21	47.48	0.68	<10	361	<10	<10	172	<10	25	294	<10	<10	117	25	22	53	63	<10	<10	93.92		
NPWMS11	0.51	1.20	6.19	25.15	0.55	0.74	0.26	12.94	0.14	0.61	46.65	1.97	18	630	<10	<10	194	17	40	<10	<10	<10	29	26	37	55	103	<10	<10	97.03		
NPWMS12	0.80	0.39	4.40	23.80	0.06	0.84	0.13	5.48	0.11	0.36	49.01	6.42	138	1100	10	84	168	<10	32	<10	58	<10	235	27	26	59	207	10	9	92.02		
NPWMS13	0.82	0.16	1.25	18.80	0.10	0.38	0.08	6.17	0.03	0.63	57.40	10.72	18	1404	16	27	133	<10	13	<10	67	<10	<10	30	28	63	<10	14	13	96.70		
NPWMS14	0.38	0.06	3.20	32.80	0.01	1.23	0.06	13.04	0.06	0.30	41.40	0.85	<10	1385	12	<10	203	<10	22	<10	<10	<10	84	24	24	51	64	<10	<10	93.58		
NPWMS16	0.61	0.38	2.67	22.01	0.05	2.87	0.10	6.18	0.06	0.26	57.03	4.13	15	793	13	46	120	<10	15	<10	19	<10	35	28	28	59	177	<10	11	96.48		
NPWMS17	0.36	0.16	2.12	25.50	0.63	1.87	0.06	4.67	0.05	0.16	58.51	1.14	11	1818	11	10	92	<10	<10	<10	<10	<10	27	25	57	96	<10	11	95.45			
NPWMS18	0.82	0.30	2.53	28.99	0.24	6.53	0.08	5.41	0.05	0.22	50.02	17.73	264	942	14	289	304	<10	22	<10	249	<10	76	33	31	70	<10	18	12	113.15		
NPWMS19	0.39	1.29	2.70	36.60	0.23	0.63	0.08	16.21	0.03	0.51	29.51	1.75	22	445	<10	31	88	<10	13	<10	11	<10	130	22	20	46	75	<10	<10	90.02		
NPWMS20	0.70	0.14	1.57	22.33	0.10	1.21	0.16	2.84	0.03	0.12	55.23	7.59	12	631	61	272	64	<10	20	23	76	<10	33	28	26	59	<10	12	13	92.15		
NPWMS21	0.49	0.86	5.01	30.36	0.04	1.30	0.27	14.78	0.13	0.24	39.47	1.43	161	332	<10	38	407	<10	42	<10	<10	<10	25	24	23	51	80	<10	<10	94.50		

Table B.9i: KWPV slag sample [P]ED-XRF bulk chemical analyses; all detected elements reported. Data not normalised.

	Na ₂ O	MgO	Al ₂ O ₃	SiO ₂	P ₂ O ₅	SO ₃	K ₂ O	CaO	TiO ₂	MnO	FeO	CuO	Ni	Zn	As	Se	Rb	Sr	Y	Zr	Mo	Ag	Sn	Ba	La	Ce	Nd	Hf	Pb	Total	
	wt%	wt%	wt%	wt%	wt%	wt%	wt%	wt%	wt%	wt%	wt%	wt%	ppm	ppm	ppm	ppm	ppm	ppm	ppm	ppm	ppm	ppm	ppm	ppm	ppm	ppm	ppm	ppm	ppm	ppm	wt%
NKHMS2	0.66	0.54	4.03	28.75	0.37	4.22	0.33	8.31	0.15	0.31	44.19	2.62	18	773	<10	83	<10	258	<10	50	13	34	89	84	25	24	53	120	<10	94.64	
NKHMS3	0.45	2.14	7.33	26.08	0.17	0.76	0.42	12.85	0.24	0.35	42.98	0.97	31	429	<10	27	<10	168	14	57	<10	<10	<10	51	32	46	52	70	<10	94.84	
NKHMS4	0.48	0.66	5.96	29.14	0.36	3.11	0.34	8.07	0.17	0.34	46.79	2.29	30	787	28	48	<10	257	12	58	27	25	73	126	25	24	53	113	<10	97.88	
NKHMS5	0.42	0.75	3.28	22.75	0.14	1.15	0.19	8.34	0.09	0.32	54.78	1.31	12	918	12	10	<10	160	<10	27	10	12	20	31	27	25	57	96	10	93.66	
NKHMS6	0.51	0.92	3.30	30.52	0.06	1.25	0.30	16.16	0.08	0.22	40.99	1.66	47	717	<10	10	<10	185	<10	24	<10	12	50	46	25	24	52	88	<10	96.10	
NKHMS7	0.34	0.83	2.87	30.63	0.02	0.87	0.04	4.62	0.04	0.21	52.17	1.72	10	853	<10	<10	<10	126	<10	21	17	18	<10	<10	26	24	56	110	10	94.49	
NKHMS8	0.18	1.52	4.43	38.33	0.27	0.95	0.21	11.57	0.11	0.54	36.98	0.78	<10	797	21	<10	<10	362	13	33	12	<10	48	196	23	25	49	58	51	96.04	
NKHMS9	0.44	0.76	5.13	37.49	0.34	1.63	0.34	9.27	0.13	0.30	40.46	0.95	<10	673	10	25	<10	406	11	50	48	13	58	177	24	24	50	66	<10	97.42	
NKHMS10	0.47	0.79	6.65	24.88	0.10	1.74	0.24	11.29	0.22	0.35	44.05	1.90	<10	2326	19	17	<10	350	24	46	13	17	12	<10	24	53	53	100	<10	92.98	
NKHMS11	0.44	1.03	5.11	34.66	0.01	0.65	0.14	14.60	0.10	0.55	35.01	0.93	<10	823	<10	<10	<10	425	<10	29	<10	11	21	<10	23	22	49	61	<10	93.37	
NKHMS12	0.43	1.25	6.71	29.60	0.30	0.34	0.47	11.33	0.18	0.49	41.63	1.19	10	397	<10	<10	<10	328	14	46	<10	<10	<10	85	24	25	51	75	<10	94.03	
NKHMS13	0.59	0.79	7.12	30.40	0.23	4.28	0.47	6.24	0.25	0.29	41.54	2.45	<10	620	<10	42	<10	153	13	43	<10	27	41	82	24	24	51	110	<10	94.77	
NKHMS14	0.42	1.60	6.30	26.52	0.13	0.89	0.26	19.03	0.16	0.41	36.86	1.12	<10	353	<10	<10	<10	197	14	49	<10	<10	<10	66	24	36	51	67	<10	93.79	
NKHMS15	0.49	0.77	5.26	31.78	0.23	3.53	0.46	5.72	0.18	0.27	46.01	1.53	<10	466	<10	18	<10	180	11	45	<10	25	29	104	24	26	52	92	<10	96.34	
NKHMS17	0.48	1.36	6.14	32.07	0.41	1.18	0.53	11.74	0.21	0.39	35.38	0.92	<10	527	<10	17	<10	358	13	61	<10	11	12	145	23	26	47	60	<10	90.94	
NKHMS18	0.62	1.04	5.92	31.83	0.10	1.09	0.55	15.28	0.21	0.23	31.99	2.65	128	3261	<10	80	12	1518	<10	71	<10	11	18	309	23	26	49	100	<10	92.06	
NKHMS19	0.51	0.72	3.21	23.10	0.08	3.20	0.19	12.13	0.10	0.17	50.56	2.64	112	600	10	47	<10	106	10	31	<10	11	10	13	26	25	56	130	<10	96.71	
NKHMS20	0.34	0.57	5.06	24.98	0.25	0.94	0.28	8.56	0.17	0.30	48.27	2.43	<10	568	<10	10	<10	80	33	49	83	<10	<10	153	25	33	54	120	<10	92.26	
NKHMS21	0.31	0.82	4.26	27.83	0.13	0.94	0.33	16.46	0.12	0.27	38.93	1.06	10	343	<10	<10	<10	125	14	40	<10	<10	11	74	24	24	51	68	<10	91.54	

Table B.9ii: KWPV slag sample [PJED-XRF bulk chemical analyses; all detected elements reported. Data not normalised.

	MgO	Al ₂ O ₃	SiO ₂	K ₂ O	CaO	TiO ₂	MnO	FeO	CuO	ZnO	Total
	wt%	wt%	wt%	wt%	wt%	wt%	wt%	wt%	wt%	wt%	wt%
NPWMS1	1.2	0.0	26.5	0.0	6.5	0.0	0.0	61.8	0.0	0.0	96.0
NPWMS2	0.6	0.7	28.7	0.0	5.1	0.0	0.0	57.0	0.0	0.0	92.0
NPWMS3	0.9	0.0	22.6	0.0	1.0	0.0	0.3	66.1	0.0	0.0	90.9
NPWMS5	0.8	0.0	16.4	0.0	3.8	0.0	0.5	58.5	0.0	0.0	80.0
NPWMS6	0.7	0.4	27.0	0.1	12.3	0.0	0.1	53.6	0.0	0.0	94.2
NPWMS7	4.2	0.0	23.6	0.0	1.6	0.0	1.1	52.3	0.0	5.2	88.1
NPWMS8	0.8	0.0	26.4	0.0	12.0	0.0	0.0	55.9	0.0	0.0	95.0
NPWMS12	0.6	0.0	16.7	0.0	5.2	0.0	1.2	56.0	0.0	0.0	79.7
NPWMS13	1.3	0.0	23.6	0.0	4.3	0.0	2.4	58.8	0.3	0.0	90.7
NPWMS14	3.7	0.0	31.7	0.0	1.2	0.0	0.4	66.5	0.0	0.0	103.5
NPWMS18	0.0	3.3	25.2	0.0	10.9	0.0	0.2	28.7	0.4	0.0	68.6
NPWMS19	0.3	0.0	16.8	0.0	10.6	0.0	1.2	47.7	0.0	0.0	76.6
NKHMS4	2.1	0.0	26.3	0.0	3.2	0.0	0.8	63.1	0.0	0.0	95.4
NKHMS5	1.8	0.0	26.0	0.0	5.4	0.0	0.6	60.6	0.0	0.0	94.5
NKHMS7	1.2	0.0	24.4	0.0	0.6	0.0	0.0	61.7	0.0	0.0	87.9
NKHMS13	1.9	0.5	23.1	0.0	1.7	0.0	0.5	62.2	0.0	0.0	89.9
NKHMS17	1.5	7.1	26.8	0.2	12.3	0.7	0.4	44.1	0.0	0.0	93.0

Table B.10: KWPV slag samples olivine crystal SEM-EDS phase analyses. Data not normalised.

	Al ₂ O ₃	SiO ₂	CaO	TiO ₂	FeO	Total
	wt%	wt%	wt%	wt%	wt%	wt%
NPWMS1	2.6	0.9	0.4	1.6	88.0	93.5
NPWMS2	1.7	0.7	0.2	0.4	90.1	93.0
NPWMS5	1.4	0.2	0.2	0.3	83.6	85.7
NPWMS6	2.5	0.0	0.0	0.0	90.7	93.2
NPWMS7	0.2	0.0	0.0	0.0	91.2	91.3
NPWMS8	0.2	0.0	0.1	0.0	86.5	86.8
NPWMS12	0.7	0.1	0.2	0.0	84.7	85.7
NPWMS13	0.2	0.0	0.2	0.0	89.9	90.2
NPWMS14	6.2	5.8	1.7	0.6	80.1	94.4
NPWMS18	1.4	7.3	1.5	0.2	74.3	84.8
mean	1.7	1.5	0.4	0.3	85.9	89.9
std dev	1.8	2.7	0.6	0.5	5.4	
CV	107%	179%	138%	162%	6%	

Table B.11: KWPV slag samples primary magnetite SEM-EDS phase analyses. Data not normalised.

	Al ₂ O ₃	SiO ₂	SO ₃	FeO	CuO	Total
	wt%	wt%	wt%	wt%	wt%	wt%
NPWMS1	0.0	0.0	0.0	95.2	0.0	95.2
NPWMS6	0.3	0.5	0.0	88.5	0.5	89.8
NPWMS7	0.4	0.3	0.0	91.2	0.1	91.9
NPWMS13	0.6	0.4	0.0	90.5	0.0	91.5
NKHMS4	1.4	0.8	0.0	91.1	0.5	93.8
NKHMS5	0.5	8.4	2.4	63.7	2.2	77.2
NKHMS13	3.3	0.5	0.0	86.9	0.2	90.8
NKHMS18	0.4	1.1	0.0	88.6	0.0	90.1

Table B.12: KWPV slag samples, residual magnetite SEM-EDS phase analyses. Data not normalised.

	MgO	Al ₂ O ₃	SiO ₂	P ₂ O ₅	SO ₃	K ₂ O	CaO	MnO	FeO	CuO	ZnO	Total
	wt%	wt%	wt%	wt%	wt%	wt%	wt%	wt%	wt%	wt%	wt%	wt%
NPWMS1	0.0	3.5	35.5	0.0	0.0	0.0	18.8	0.0	35.8	0.0	0.0	93.6
NPWMS2	0.0	3.5	37.4	0.0	0.0	0.0	18.7	0.0	31.7	0.0	0.0	91.4
NPWMS3	0.0	8.5	28.5	1.5	0.9	0.6	10.5	0.0	22.0	0.0	0.0	72.5
NPWMS5	0.0	5.0	21.9	0.9	0.0	0.0	14.1	0.0	24.2	0.0	0.0	66.1
NPWMS6	0.0	6.0	34.8	0.0	0.0	0.0	20.1	0.0	29.1	0.0	0.0	90.1
NPWMS7	2.7	2.5	34.8	0.0	0.0	0.0	18.1	0.0	21.2	0.0	2.3	81.7
NPWMS8	0.0	2.7	24.4	0.0	0.0	0.0	14.3	0.0	28.4	0.0	0.0	69.8
NPWMS12	0.0	2.5	23.4	0.0	0.0	0.0	14.5	0.0	29.1	0.0	0.0	69.5
NPWMS13	0.0	1.9	33.9	0.0	0.0	0.0	18.6	0.8	29.6	0.0	0.0	84.8
NPWMS14	0.0	11.1	43.3	0.7	0.0	0.0	17.2	0.0	29.7	0.0	0.0	101.9
NPWMS18	0.0	3.3	25.2	0.0	0.0	0.0	10.9	0.0	28.7	0.0	0.0	68.1
NPWMS19	1.6	1.7	25.3	0.0	0.0	0.0	15.2	0.0	22.9	0.0	0.0	66.8
NKHMS4	0.7	5.5	35.4	0.0	0.0	0.0	19.7	0.0	29.1	0.0	0.0	90.5
NKHMS5	0.0	6.1	33.7	0.0	0.9	0.7	18.2	0.0	31.3	0.0	0.0	90.9
NKHMS7	0.0	4.8	39.4	0.0	0.0	0.0	12.1	0.0	26.6	0.0	0.0	82.9
NKHMS13	0.0	7.7	30.4	0.6	1.8	0.9	13.0	0.0	27.5	0.0	0.0	81.9
NKHMS17	2.2	5.6	35.1	0.7	0.0	0.0	17.2	0.0	30.4	0.0	0.0	91.2

Table B.13: KWPV slag samples, glass phase SEM-EDS analyses. Data not normalised.

Elements	S	Fe	Ni	Cu	Zn	Total
Sample	wt%	wt%	wt%	wt%	wt%	wt%
NPWMS1	25.7	40.4	0.0	29.5	0.5	96.1
NPWMS3	26.1	24.2	0.0	41.8	0.0	92.1
NPWMS6	20.6	5.8	0.0	73.8	0.0	100.2
NPWMS7	27.5	9.9	0.0	30.6	27.2	95.2
NPWMS13i	0.0	24.2	0.0	51.3	0.0	75.5
NPWMS13ii	1.4	0.0	0.0	86.2	0.0	87.6
NKHMS4	23.1	10.8	0.0	65.9	0.0	99.8
NKHMS5	27.4	6.5	0.0	59.5	0.0	93.4
NKHMS7i	18.0	3.2	0.0	73.5	0.0	94.6
NKHMS7ii	18.4	4.0	0.0	75.1	0.0	97.6
NKHMS13i	13.5	31.3	0.0	38.7	0.0	83.5
NKHMS13ii	25.1	31.4	0.0	31.6	0.0	88.0
NKHMS18i	0.0	1.0	1.2	98.9	0.0	101.1
NKHMS18ii	16.5	2.0	0.0	77.6	0.0	96.1

Table B.14: KWPV slag samples, copper-base prills SEM-EDS phase analyses. Data not normalised.

	MgO wt%	Al ₂ O ₃ wt%	SiO ₂ wt%	P ₂ O ₅ wt%	SO ₃ wt%	K ₂ O wt%	CaO wt%	MnO wt%	FeO wt%	CuO wt%	ZnO wt%	Total wt%
NPWMS1 spectrum 1	0.5	2.3	28.5	0.0	1.9	0.0	11.6	0.0	50.5	0.0	0.0	95.2
NPWMS1 spectrum 2	0.0	2.0	26.6	0.0	1.7	0.0	10.3	0.0	50.8	0.6	0.0	92.0
NPWMS1 spectrum 3	0.6	2.2	27.3	0.0	1.6	0.0	10.5	0.0	52.6	0.6	0.0	95.3
NPWMS2 spectrum 1	0.0	2.8	33.5	0.0	0.0	0.0	12.6	0.0	41.3	0.8	0.0	91.0
NPWMS2 spectrum 2	0.5	2.9	32.6	0.0	0.0	0.0	13.2	0.0	42.3	0.0	0.0	91.6
NPWMS2 spectrum 3	0.4	2.9	32.6	0.0	0.0	0.0	13.1	0.0	41.4	1.0	0.0	91.4
NPWMS3 spectrum 1	0.4	2.5	19.5	0.3	0.9	0.1	14.1	0.3	51.5	1.0	0.0	90.5
NPWMS3 spectrum 2	0.4	3.2	22.9	0.4	1.1	0.2	12.9	0.0	57.7	1.4	0.0	100.1
NPWMS3 spectrum 3	0.4	3.0	20.5	0.5	0.8	0.2	14.2	0.0	53.5	0.7	0.0	93.7
NPWMS5 spectrum 1	0.3	1.7	13.4	0.4	0.0	0.0	6.4	0.3	49.5	1.2	0.0	73.2
NPWMS5 spectrum 2	0.3	2.0	15.6	0.4	0.2	0.0	6.2	0.0	47.4	1.8	0.0	73.9
NPWMS5 spectrum 3	0.3	1.9	14.8	0.3	0.0	0.0	6.0	0.3	48.9	1.8	0.0	74.3
NPWMS6 spectrum 1	0.0	3.1	25.9	0.0	1.5	0.0	12.2	0.0	48.6	1.5	0.0	92.9
NPWMS6 spectrum 2	0.0	2.9	24.2	0.0	1.1	0.0	9.9	0.0	49.4	3.0	0.0	90.5
NPWMS6 spectrum 3	0.4	3.0	26.2	0.0	1.5	0.0	12.9	0.0	49.1	1.9	0.0	95.1
NPWMS7 spectrum 1	0.9	4.6	29.1	0.0	0.9	0.0	11.4	0.5	31.5	0.0	6.3	85.3
NPWMS7 spectrum 2	0.9	4.1	27.5	0.0	1.5	0.2	10.7	0.6	31.6	0.0	6.6	83.7
NPWMS7 spectrum 3	0.9	4.4	29.6	0.0	1.1	0.2	11.3	0.6	31.6	0.0	7.3	87.0
NPWMS8 spectrum 1	0.2	1.2	15.1	0.0	0.0	0.0	4.7	0.3	46.7	0.7	0.0	68.9
NPWMS8 spectrum 2	0.2	1.4	17.3	0.0	0.0	0.0	5.3	0.0	48.0	0.5	0.0	72.9
NPWMS8 spectrum 3	0.3	1.3	16.4	0.0	0.0	0.0	5.6	0.0	49.9	0.6	0.0	74.1
NPWMS12 spectrum 1	0.3	1.3	16.3	0.0	0.0	0.1	7.2	0.6	44.3	0.9	0.0	70.9
NPWMS12 spectrum 2	0.2	1.4	16.9	0.0	0.0	0.1	6.8	0.5	44.5	2.6	0.0	73.0
NPWMS12 spectrum 3	0.2	1.4	18.0	0.0	0.0	0.0	6.7	0.6	45.0	2.4	0.0	74.4
NPWMS13 spectrum 1	0.0	1.7	21.5	0.0	0.0	0.0	7.8	1.1	49.8	6.7	0.0	88.6
NPWMS13 spectrum 2	0.0	1.4	23.1	0.0	0.0	0.0	5.7	0.7	53.8	6.1	0.0	90.8
NPWMS13 spectrum 3	0.5	1.6	21.9	0.0	0.0	0.0	8.3	0.9	51.3	3.6	0.0	88.2
NPWMS14 spectrum 1	1.0	4.5	32.4	0.4	0.0	0.0	3.6	0.0	49.3	3.1	0.0	94.4
NPWMS14 spectrum 2	1.1	4.7	33.6	0.0	0.0	0.0	4.4	0.3	53.0	2.5	0.0	99.5
NPWMS14 spectrum 3	1.2	4.6	33.6	0.0	0.0	0.0	4.2	0.0	52.9	2.3	0.0	98.8
NPWMS18 spectrum 1	0.2	1.8	20.6	0.0	0.1	0.0	4.7	0.0	38.9	0.8	0.0	67.2
NPWMS18 spectrum 2	0.3	2.0	21.4	0.0	0.1	0.0	5.3	0.0	41.8	1.0	0.0	72.0
NPWMS18 spectrum 3	0.3	2.1	21.9	0.0	0.2	0.0	5.7	0.0	42.6	1.6	0.0	74.4
NPWMS19 spectrum 1	0.8	1.6	20.8	0.0	0.0	0.0	12.6	0.5	29.2	0.3	0.0	65.9
NPWMS19 spectrum 2	0.8	1.8	21.8	0.0	0.0	0.0	13.1	0.7	30.4	0.3	0.0	68.9
NPWMS19 spectrum 3	1.0	1.8	23.2	0.2	0.0	0.0	13.9	0.6	30.6	0.4	0.0	71.7

NKHMS4 spectrum 1	0.9	4.6	30.3	0.7	1.0	0.4	10.3	0.0	43.5	0.6	0.0	92.2
NKHMS4 spectrum 2	0.6	4.8	30.6	0.6	0.8	0.4	9.7	0.4	42.3	0.0	0.0	90.2
NKHMS4 spectrum 3	0.5	4.9	31.5	0.0	0.9	0.5	11.2	0.5	42.0	0.6	0.0	92.7
NKHMS5 spectrum 1	0.7	3.1	27.7	0.0	0.7	0.2	10.2	0.0	47.3	0.9	0.0	91.0
NKHMS5 spectrum 2	0.9	3.5	28.1	0.0	0.6	0.4	10.8	0.5	48.9	0.9	0.0	94.6
NKHMS5 spectrum 3	0.9	3.4	28.2	0.0	0.7	0.0	9.8	0.0	47.0	1.2	0.0	91.3
NKHMS7 spectrum 1	0.6	2.2	30.0	0.0	0.0	0.0	5.2	0.0	47.0	1.2	0.0	86.2
NKHMS7 spectrum 2	0.7	2.5	30.7	0.0	0.0	0.0	5.6	0.0	47.2	1.0	0.0	87.7
NKHMS7 spectrum 3	0.5	2.4	30.0	0.0	0.5	0.0	5.2	0.0	45.9	0.8	0.0	85.1
NKHMS13 spectrum 1	0.5	4.9	26.6	0.0	1.1	0.4	7.0	0.0	44.1	0.6	0.0	85.3
NKHMS13 spectrum 2	0.6	5.0	26.6	0.0	1.5	0.5	7.4	0.0	44.0	0.0	0.0	85.6
NKHMS13 spectrum 3	0.5	4.8	25.9	0.0	1.3	0.3	6.6	0.4	43.6	0.7	0.0	84.0
NKHMS17 spectrum 1	1.3	5.5	30.5	0.0	0.0	0.7	13.2	0.0	38.9	0.0	0.0	90.1
NKHMS17 spectrum 2	1.1	5.7	31.3	0.0	0.5	0.5	13.4	0.0	39.8	0.0	0.0	92.4
NKHMS17 spectrum 3	1.1	5.7	31.0	0.7	0.6	0.7	13.2	0.5	39.4	0.0	0.0	93.0
NKHMS18 spectrum 1	1.3	4.4	26.5	0.0	0.0	0.5	16.0	0.0	33.3	0.0	0.0	82.1
NKHMS18 spectrum 2	1.2	4.6	26.9	0.0	0.0	0.6	16.1	0.0	32.8	0.8	0.9	83.9
NKHMS18 spectrum 3	1.2	4.7	26.6	0.0	0.0	0.5	16.3	0.0	33.8	0.6	0.0	83.9

Table B.15: KWPV slag matrices SEM-EDS phase analyses. Data not normalised.

Burn 1

Temperatures:

Time Minutes	Channel 1 °C	Channel 2 °C	Channel 3 °C	Channel 4 °C	Channel 5 °C	Channel 6 °C	Channel 7 °C	Channel 8 °C
0	15.2	15.1	13.1	14.7	15.1	13.6	14.5	13.8
1	15.2	15.1	13.0	14.8	15.0	13.5	14.4	13.8
2	15.1	15.1	12.9	14.5	15	13.4	14.3	13.7
3	15.2	15.2	12.8	14.8	14.9	13.4	14.3	13.9
4	15.3	15.2	13.2	15.3	15.0	14.0	14.4	14.2
5	15.3	15.2	13.4	15.4	15.1	14.5	14.4	14.9
6	18.3	16.3	15.1	17.2	18.1	17.3	15.8	17.6
7	18.6	16.3	15.8	18.8	18.6	19.5	15.9	18.3
8	20.7	16.6	21.8	22.7	19.3	26.8	17.6	27.6
9	62.6	35.6	33.4	126.5	73.2	75.8	34.0	72.7
10	63.4	56.7	55.0	113.8	45.7	74.0	38.7	73.1
11	60.1	45.3	43.1	90.8	54.0	97.9	43.0	72.3
12	51.0	37.1	38.0	77.7	39.7	57.9	36.8	52.1
13	38.1	31.3	36.1	64.4	34.7	50.3	34.1	45.0
14	34.6	31.1	51.7	57.7	39.8	64.1	37.1	53.8
15	40.6	33.6	50.1	58.3	49.6	59.1	36.9	50.3
16	112.9	34.4	40.0	54.6	76.1	90.6	33.1	44.4
17	120.9	33.6	33.3	51.6	99.4	101.1	33.5	40.5
18	82.1	47.9	28.9	51.1	82.7	155.4	33.4	46.8
19	104.0	53.5	30.1	52.2	117.1	238.0	39.1	77.8
20	105.5	57.4	62.6	65.4	153.8	282.5	76.4	149.4
21	74.0	272.7	524.9	355.9	171.2	349.0	335.7	731
22	136.0	407.3	738.7	708.8	259.9	346.3	399.0	726.6
23	228.0	521.3	754.5	845.9	322.6	622.8	617.0	894.3
24	381.6	647.2	864.9	741.9	369.4	822.0	709.7	891.7
25	437.5	705.1	889.2	720.5	338.2	751.3	711.7	783.3
26	500.0	807.6	937.8	744.9	334.4	841.5	750.5	832.0
27	609.9	813.0	929.4	725.2	425.1	911.6	776.4	890.3
28	678.8	826.0	970.3	740.4	591.6	943.2	837.1	974.1
29	643.0	850.6	950.1	748.7	612.8	945.6	864.9	943.1
30	614.1	778.6	916.5	750.0	569.6	983.3	801.3	932.3
31	634.7	741.2	1000.1	763.9	547.9	1028.4	814.6	915.2
32	687.3	825.6	1027.6	785.1	558.9	1018	872.1	923.4
33	691.7	861.5	1009.0	761.4	554.6	998.6	848.5	887.1
34	722.1	846.7	1051.7	742.7	565.4	960.1	796.6	882.8
35	818.1	863.1	1044.7	746.8	613.7	939.9	763.6	885.2
36	893.3	823.3	1027.2	732.7	625.7	931.0	756.4	870.7
37	912.2	833.8	1051.4	723.5	693.6	912.5	757.5	865.7
38	877.6	840.9	1139.2	737.1	758.6	985.4	816.3	900.1
39	1011.2	895.2	1165.4	753.8	895.8	989.5	841.1	919.0
40	1038.7	858	1156.5	763.5	916.6	997.7	843.0	981.7
41	1008.2	819.6	1021.3	758.1	885.1	965.4	817.7	975.2
42	948.7	803.5	953.1	740.4	837.6	936.1	762.7	913.2

43	924.0	790.4	921.8	728.3	812.9	939.9	734.4	914.1
44	929.4	817.6	979.0	717.3	834.5	968.4	723.7	893.1
45	949.0	827.9	997.6	713.1	843.5	980.3	720.5	896.5
46	931.8	792.0	1049.0	710.8	867.6	981.4	717.8	903.4
47	919.9	754.3	988.3	706.8	932.8	1020.8	712.2	909.4
48	923.9	772.0	917.7	707.8	902.4	981.1	718.7	923.0
49	915.8	758.3	894.2	713.3	958.1	910.9	717.6	905.9
50	920.5	762.9	865.3	714.7	1003.3	891.8	708.7	954.4
51	934.6	732.5	858.2	707.3	992.9	933.9	706.2	994.7
52	1008.5	743.8	840.8	708.3	945.4	977.4	705.9	933.7
53	1066.5	742.7	821.8	706.7	864.9	896.6	692.2	876.9
54	998.5	744.1	813.0	700.8	842.2	872.9	679.2	854.3
55	975.0	750.1	806.6	696.6	827.0	866.4	670.3	845.7
56	921.5	791.4	801.1	697.5	877.5	851.4	659.3	837.6
57	917.0	778.9	792.7	694.0	915.3	851.2	651.2	827.7
58	873.0	745.7	782.5	692.6	942.0	847.6	639.7	817.0
59	892.4	775.3	782.7	683.7	957.4	861.3	635.4	806.3
60	988.1	843.4	790.9	723.2	945.9	869.5	678.6	818.9
61	989.4	841.3	792.5	733.7	939.2	861.6	721.6	842.4
62	970.6	824.2	790.3	730.0	914.0	841.0	718.2	842.2
63	971.2	827.8	788.7	723.0	909.9	820.7	708.1	819.1
64	977.4	841.8	790.8	721.3	945.9	810.9	717.3	823.7
65	974.2	854.9	788.4	723.0	964.7	806.6	728.8	839.0
66	953.3	855.3	785.4	712.4	943	806.3	714.3	833.2
67	930.7	837.3	777.0	707.5	934.9	802.5	700.4	814.1
68	914.1	828.4	770.1	706.0	920.4	794.6	693.6	800.1
69	910.3	828.2	763.8	708.7	902.9	789.7	687.7	789.4
70	922.9	842.3	759.0	716.7	886.9	790.5	690.3	790.3
71	918.5	850.0	751.3	713.7	898.8	780.5	698.6	814.2
72	914.6	842.6	756.1	722.0	915.4	776.5	721.4	827.7
73	899.3	824.2	755.7	718.0	890.0	772.7	730.4	833.7
74	884.9	815.3	751.5	716.4	872.5	768.5	727.2	825.4
75	871	831.1	750.4	722.9	859.5	766.5	723.8	833.2
76	855.1	838.3	748.9	741.5	849.0	769.2	722.6	833.1
77	861.0	843.9	749.5	749.2	848.3	782.2	731.8	833.9
78	862.5	849.7	749.1	741.1	805.8	786.0	728.8	844.6
79	852.1	814.2	748.1	738.2	795.7	793.7	726.9	847.7
80	827.9	791.5	746	730.6	796.9	797.5	722.0	831.6
81	822.6	782.1	737.8	719.4	760.3	805.1	715.8	818.5
82	843.6	764.0	731.8	711.3	747.8	799.3	702.6	822.2
83	868.2	751.7	732.9	705.4	724.4	812.3	704.2	846.4
84	958.6	746.3	737.6	703.4	691.2	817.9	710.9	858.9
85	987.2	745.2	737.8	699.6	651.4	831.4	709.3	855.3
86	842.0	740	738.0	703.8	753.2	821.1	712.3	853.2
87	857.2	723.7	781.4	710.1	779.8	799.9	701.6	855.6
88	862.8	706.1	821.3	700.5	750.1	786.9	688.1	844.9
89	816.5	691.9	763.9	691.5	732.9	759.8	672.3	829.3
90	798.8	680.7	749.8	685.3	734.1	757.4	664.1	807.2

91	788.7	668.4	748.8	681.4	738.2	743.8	652.7	796.6
92	775.5	657.3	743.2	675.9	714.9	733.6	641.6	787.3
93	780.1	646.4	735.3	670.3	681.8	724.4	631.2	779.3
94	787.0	636.5	728.9	664.4	645.9	725.3	621.3	771.8
95	805.6	623.5	719.7	659.5	701.8	734.7	616.4	762.6
96	802.8	621.7	714.5	651.9	732.3	745.3	608.8	756.3
97	747.3	619.8	707.7	644.7	731.5	738.8	602.1	749.4
98	686.7	619.0	690.7	636.3	715.0	731.8	597.1	740.0
99	654.0	619.0	680.6	626.7	695.5	741.1	594.7	731.2
100	632.7	612.5	673.9	615	669.3	752.9	593.1	721.8
101	617.8	610.5	669.9	607.5	667.4	753.3	591.6	712.1
102	609.9	606.7	644.0	603.2	677.3	748.5	588.6	703.4
103	583.2	607.6	671.0	598.6	673.7	746.9	586.3	693.6
104	555.8	599.6	693.9	591.4	656.8	749.0	582.7	696.5
105	532.7	594.0	701.8	587.2	629.5	782.7	577.9	701.0
106	511.3	588.6	702.4	582.1	601.8	809.7	572.8	697.1
107	535.0	583.3	699.6	576.3	583.5	820.2	566.3	690.6
108	554.1	578.2	694.7	570.6	576.8	825.9	559.8	683.3
109	536.3	570.5	690	563.9	569.9	832.9	553.3	675.3
110	520.9	570.5	685.0	565.6	562.9	826.6	550.0	667.0
111	500.2	567.0	680.8	559.7	548.4	822.1	545.5	660.5
112	484.2	563	676.2	553.3	539.0	823.0	540.8	653.6
113	470.9	558.5	671.0	547.8	527.2	822.9	536.6	646.1
114	459.1	553.0	665.5	543.0	512.9	823.5	532.4	638.6
115	453.4	551.3	660	543.2	507.8	820.4	528.9	631.6
116	434.4	551.0	647.5	542.0	462.1	831.4	526.6	626.8
117	417.9	550.1	609.9	540.6	469.8	815.3	525.6	636.7
118	460.1	554.9	601.3	544.9	584.8	796.3	523.6	633.9
119	480.4	554.2	599.4	543.1	540.4	801.8	520.4	617.8
120	481.0	551.8	598.7	539.7	491.3	802.4	517.9	606.7
121	461.6	563.6	597.5	538.5	462.8	811.4	517.0	600.1
122	462.0	547.4	596.5	531	459.0	811.3	514.4	598.5
123	447.4	549.7	595.8	530.6	437.1	813.8	513.4	598.1
124	557.0	543.2	597.3	532.2	446.0	803.1	513.8	599.8
125	658.6	537.5	603.0	531.7	613.0	801.7	514.6	600.6
126	684.8	529.2	608.3	524.9	635.1	809.9	512.6	600.4
127	689.5	524.7	611.5	520.1	614.9	820.5	509.8	598.4
128	685.9	523.1	613.3	518.5	601.2	831.0	506.7	595.9
129	677.6	520.4	614.2	519.3	589.8	821.0	504.3	592.7
130	669.2	522.3	615.3	521.6	568.5	814.7	502.6	590.7
131	659.9	526.2	619.2	525.1	551.2	814.3	502.3	590.2
132	650.0	528.9	621.8	522.0	535.9	818.8	502.6	589.6
133	637.4	522.1	623.0	513.0	522.4	818.3	502.1	586.3
134	621.5	512	621.0	507.2	508.6	811.2	500.7	580.3
135	606.4	511.8	616.4	510.2	491.2	801.7	499.7	574.1
136	594.4	505.5	611.5	505.9	477.1	795.4	498.4	567.9
137	583.8	503.1	607.3	503.5	465.1	792.5	497.2	562.0
138	573.6	501.7	603.7	503.2	448.8	792.9	496.2	557.4

139	565.3	495.5	600.7	497.2	436.6	796.2	495.6	552.3
140	555.8	494.1	597.3	499.1	425.4	794.1	495.4	546.8
141	546.3	494.2	594.2	498.5	407.9	798.9	494.8	542.7
142	538.7	487.7	591.7	490.2	401.2	803.6	493.9	537.7
143	530.4	489.3	588.8	492.7	393.3	803.3	493.8	532.7
144	522.8	489.2	586.6	493.8	374.6	810.2	495.3	529.3
145	515.6	488.0	585.0	492.4	365.7	814.1	497.0	525.6
146	508.9	494.3	583.3	500.1	342.5	818.6	503.2	523.0
147	506.0	504.4	582.3	502.7	319.4	834.7	514.0	521.4
148	504.9	505.2	581.5	496.1	313.4	851.1	525.1	520.8
149	503.3	509.0	578.9	503.5	310.8	852.5	533.9	519.5
150	500.1	513.5	576.7	509.9	292.5	879.6	550.5	519.7
151	498.7	519.6	575.5	514.0	282.9	898.2	571.0	521.8
152	495.5	517.5	574.8	519.5	276.4	907.8	591.7	526.0
153	491.7	515.8	574.1	523.1	272.5	905.9	609.1	531.8
154	486.8	514.3	573.4	523.4	274.3	896.2	618.3	536.9
155	477.1	511.1	572.1	523.8	277.0	894.2	621.3	540.3
156	468.7	515.0	570.6	534.9	266.9	905.2	633.5	545.8
157	456.0	507.5	569.9	527.6	285.4	879.3	645.3	549.7
158	448.5	506.3	569.5	538.5	285.2	871.3	659.0	551.0
159	436.1	500.1	570	543.3	275.8	876.8	680.1	556.6
160	424.1	495.6	570.7	551.3	267.5	885.1	703.1	566.7
161	411.9	490.4	571.1	557.3	258.8	894.7	718.3	582.3
162	400.4	488.2	571.4	571.2	247.0	909.2	727.7	605.0
163	389.2	485.7	571.6	587.1	233.4	924.7	748.6	627.6
164	378.9	482.1	571.9	602.2	225.3	951.9	775.8	647.1
165	369.5	480.3	572.1	621.0	217.1	989.1	796.2	662.8
166	361.4	476.5	572.7	639.8	210.2	1060.1	806.6	678.0
167	354.0	473.4	573.5	654.5	207.1	1101.2	810.6	686.0
168	348.0	468.7	574.4	662.7	209.2	1080.0	804.4	686.2
169	341.1	468.1	575.2	674.0	201.7	1105.0	817.2	690.3
170	342.0	466.3	579.2	680.6	194.9	1135.7	809.3	697.6
171	359.1	460.3	584.1	666.4	218.8	1079.4	750.3	701.7
172	375.4	470.8	584.6	650.4	229.4	1097.6	709.6	685.9
173	384.3	473.8	583.9	634.7	223.7	1037.9	684.6	670.4
174	385.8	462.1	583.1	620.7	219.9	966.3	669.8	658.3
175	384.0	456.6	582.0	610.6	215.2	863.2	658.6	649.1
176	381.2	451.9	580.6	601.9	208.8	787.5	650.1	642.3
177	376.1	445.0	579.3	591.5	207.9	748.5	641.2	635.9
178	370.3	438.6	577.6	581.1	213.4	706.3	630.9	627.9
179	366.4	437.0	575.3	574.4	210.8	637.1	620.3	619.8
180	367.9	432.6	555.9	566.7	205.6	607.9	611	613.4
181	403.7	424.4	549.2	560.6	233.0	696.0	601.2	610.8
182	437.4	408.5	557.7	557	262.1	809.4	591.0	604.5
183	454.7	403.2	561.5	557.3	287.2	798.6	580.3	598.0
184	465.2	398.4	562.3	555.3	302.2	780.5	569.3	592.0
185	469.5	394.7	562.3	551.9	306.2	760.7	559.1	586.3
186	468.8	390.0	561.8	547.9	303.6	751.0	549.8	580.7

187	465.4	386.3	560.8	543.8	299.4	742.5	541.3	575.3
188	460.3	383.2	559.7	539.0	293.4	757.9	533.6	570.1
189	453.6	379.4	559.0	533.5	284.7	801.0	527.0	565.1
190	444.2	374.6	557.3	527.7	278.6	805.5	521.5	559.5
191	434.6	371.8	554.9	523.4	274.5	765.2	516.5	554.2
192	424.2	368.6	552.4	517.4	267.9	726.0	510.8	548.8
193	413.2	366.7	549.7	511.3	260.5	671.3	505.7	543.1
194	403.6	365.9	547.0	504.5	253.0	647.0	501.2	537.9
195	396.6	366.5	545.2	498.3	243.6	645.3	498.9	532.8
196	391.7	367	544.0	492.5	235.2	642.3	498.6	527.8
197	390.1	375.6	537.3	486.5	223.7	891.9	499.8	457.2
198	398.2	380.7	534.3	480.8	210.7	943.5	498.1	445
199	402.7	378.9	531.9	475.1	202.0	854.0	495.0	463.5
200	403.9	375.5	530.8	469.7	194.4	801.3	491.8	470.9
201	401.7	372.0	530.5	465.7	188.1	743.5	489.4	471.7
202	397.9	369.0	530.4	461.8	180.3	674.1	487.5	470.3
203	392.0	367.0	530.4	456.9	175.9	620.5	486.9	468.1
204	383.3	363.7	530.4	454.5	173.9	535.8	487.1	465.8
205	374.5	360.9	530.2	451.3	169.6	459.4	487.8	463.3
206	365.6	357.2	530.1	446.0	168.6	550.1	488.9	460.9
207	355.6	355	530.1	443.5	180.6	601.9	489.3	458.4
208	347.2	353.2	529.2	444.0	192.5	592.6	485.8	456.1
209	341.0	350.8	525.0	444.3	201.8	584.2	479.6	451.2

Burn 2

Record sheet:

KWPV EXPERIMENTS: FIAVE, TRENTO, ITALIA

OPERATOR: OP
BURN: 2

DATE: 05/09/2007
PAGE: 1

PARAMETRES

OXYGEN/SULPHUR RATIO: 2.5
FUEL/CHARGE RATIO: 1

REACTANTS	MASS (kg)	PRODUCTS	MASS (kg)
MAGNETITE	0.83	SLAG	1250
CHALCOPYRITE	0.99	COPPER	
MALACHITE	2.98	MATTE	
LIME	0.28	OTHER	unreached 77kg 0.276
SILICA	0.62		
	<u>5.70</u> / 3		

ASPIRATION (DELETE): NATURAL FAN BELLOWS
WINDSPEED (BACKGROUND) ~125
WINDSPEED (ARTIFICIAL) ~75
AIR VOLUME (PER TUYERE)

PERFORATED FURNACE N
CRUCIBLE N
FURNACE LINING N

TIMED RECORD

TIME	ACTION	DESCRIPTION
10:45	thermocouples on malachite on	
11:41	ignition fan on	
11:45	1st charge in	complete 1kg charcoal
11:57	2nd charge	complete 1kg charcoal
12:03	2nd charge	complete
12:07	3rd charge	complete 1kg charcoal
12:14	chimney failure	
12:20	chimney replaced & fan restarted	some fuel lost
12:24	3rd charge	complete
12:27	4th charge	complete 1kg charcoal
12:40	5th charge	complete 1kg charcoal / 1kg iron
12:54	5th charge	complete
13:03	6th charge	complete 1kg charcoal / 1kg iron
13:40	7th charge	complete
13:50	-	complete
14:25	-	allowing to burn down

Burn 2

Temperatures:

Time Minutes	Channel 1 °C	Channel 2 °C	Channel 3 °C	Channel 4 °C	Channel 5 °C	Channel 6 °C	Channel 7 °C	Channel 8 °C
0	28.1	40.9	41.0	15.4	13.0	13.1	13.4	13.3
1	28.3	41.1	40.9	15.6	13.0	13.2	13.5	13.4
2	29.2	42.0	41.5	15.8	13.1	13.2	13.7	13.4
3	30.2	42.6	42.3	15.8	13.0	13.2	13.6	13.4
4	31.3	42.9	42.4	15.7	13.0	13.1	13.6	13.3
5	32.2	43.2	42.8	15.6	12.9	13.1	13.5	13.3
6	33.2	43.0	42.9	15.4	12.9	13.2	13.6	13.3
7	344.1	265.6	146.2	15.3	13.0	13.2	13.6	13.3
8	765.7	773.5	572.9	14.9	12.8	13.2	13.5	13.3
9	770.3	785.5	618.5	15.0	13.0	13.3	13.7	13.4
10	762.2	771.5	622.1	15	13.0	13.3	13.6	13.4
11	752.4	759.1	623.9	14.9	13.1	13.4	13.8	13.5
12	741.4	750.5	619.3	14.8	13.2	13.4	13.8	13.4
13	731.4	742.9	613.9	38.8	13.1	13.3	13.6	13.2
14	723.7	734.9	609.6	228.7	13.1	13.3	13.6	13.1
15	716.3	729.5	605.4	297.6	13.1	13.4	13.6	13.1
16	710.2	725	600.9	276.9	13.1	13.4	13.6	13.1
17	704.8	721.1	596.9	626.7	13.3	13.5	13.8	13.2
18	700.1	718.4	592.8	760.4	13.4	13.5	13.9	13.3
19	696.1	715.7	588.8	769.3	13.2	13.4	13.7	13.2
20	690.8	713.1	585.0	771.3	13.3	13.5	13.8	13.3
21	687.2	709.8	581.6	776.3	13.4	13.6	13.9	13.4
22	682.7	707.4	577.9	781.1	13.4	13.6	13.9	13.4
23	678.8	705.0	574.7	785.4	13.5	13.6	13.9	13.4
24	677.6	701.4	572	788.4	13.6	13.7	14.0	13.4
25	678.8	696.7	580.7	754.2	13.7	13.8	14.1	13.4
26	709.3	701.7	608.2	297.1	13.7	13.8	14.2	13.5
27	714.1	691.5	613.6	130.5	13.7	13.8	14.2	13.5
28	716.8	677.8	615.0	66.1	13.6	13.7	14.1	13.4
29	717.9	665.5	615.4	42.3	13.6	13.8	14.1	13.5
30	720.2	654.7	615.6	33.8	13.9	13.9	14.4	13.5
31	723.0	644.4	615.1	28.9	14.1	14.1	14.6	13.7
32	726.1	634.8	614.9	26.2	14.1	14.2	14.5	13.7
33	728.4	626.3	614.2	24.4	14.0	14.1	14.5	13.7
34	730.1	639.8	616.2	23.6	13.7	14.0	14.2	13.6
35	733.2	655.3	625.7	23.1	13.9	14.1	14.3	13.7
36	745.6	670.0	637.7	77.8	13.9	14.1	14.3	13.7
37	738.1	664.3	639.8	644.8	14.0	14.1	14.4	13.7
38	729.7	658.6	639	694.2	14.1	14.2	14.4	13.8
39	722.5	653.7	636.8	696	13.9	14.1	14.2	13.8
40	716.7	649.6	633.5	702.6	13.9	14.1	14.2	13.7
41	711.6	646.7	630.2	711.2	13.8	14.1	14.1	13.7
42	707.0	644.7	627.1	721.9	13.9	14.2	14.3	13.8

43	702.7	647.5	624.1	731.4	14.0	14.2	14.4	13.8
44	700.1	689.6	627.9	735.1	14.1	14.3	14.5	13.9
45	697.3	690.6	637.3	730	14.0	14.3	14.4	13.9
46	694.6	690.2	639.5	736.5	14.1	14.4	14.5	14.0
47	692.4	691.4	639.4	747.0	14.1	14.4	14.5	14.0
48	690.2	693.3	638.4	758.3	13.9	14.3	14.3	13.9
49	687.9	695.8	637.2	769.1	13.8	14.3	14.2	13.9
50	685.7	698.8	635.5	779.8	13.7	14.2	14.1	13.8
51	683.6	702.0	634	788.8	13.6	14.1	14.0	13.7
52	681.6	704.0	632.8	797.3	13.5	14.1	13.8	13.6
53	680.7	705.6	631.8	805.7	15.0	16.4	15.1	17.1
54	692.8	706.6	631.6	814.1	19.9	23.2	20.2	35.7
55	701.2	741.9	631.6	827.0	26.3	38.6	30.8	54.2
56	708.0	798.6	631.6	849.2	23.0	31.4	23.6	47.7
57	710.6	809.4	631.2	876.3	22.4	21.1	17.3	28
58	712.6	818.2	630.7	898.7	29.9	58.8	25.3	124.3
59	714.6	823.6	630.2	914.3	19.7	286.6	92.3	595.1
60	715.7	825.2	630.0	930.3	39.9	518.5	194.6	1004.5
61	716.6	823.6	630.0	941.4	233.6	662.7	337.9	1157.3
62	718.1	822.1	629.9	951.6	447.8	769.5	453.3	1162.2
63	719.9	820.7	630	955.4	484.5	824.6	547.1	1208.8
64	722.1	820.4	630.2	953.7	465.4	819.0	593.3	1082.0
65	724.4	817.8	630.6	936.7	459.3	763.7	633.4	865.7
66	724.9	826.4	631.0	921.2	488.0	740.1	661.2	794.5
67	724.6	850	631.6	927.1	507.8	723.2	729.4	756.5
68	724.5	852.9	631.8	930.3	517.3	708.8	752.5	737.7
69	725.0	846.2	632.0	928.3	528.1	698.8	750.5	778.2
70	725.0	844.1	631.6	927.2	586.0	715.5	820.5	1099.9
71	725.7	841.9	631.0	924.3	643.5	741.9	699.0	1039.2
72	727.5	836.4	630.1	923.5	670.6	763	651.5	1057.4
73	730.6	828.8	629.1	933.2	697.4	775.5	631.5	1062.0
74	728.2	824.7	628.6	937.6	707.5	787.2	627.4	1056.3
75	729.4	820.5	629.7	934.6	712.8	795.2	613.1	1040.1
76	728.3	744.7	595.3	919.5	738.9	801.4	606.6	1035.9
77	778.3	743.2	634.6	736.8	764.8	808.3	612.6	1040.9
78	678.2	740.2	696.5	208.9	788.5	815.6	617.5	1055.2
79	648.3	737.1	641.7	95.5	805.8	822.2	631.3	1061.9
80	642.3	735.6	681.5	52.7	819.9	831.4	644.8	1082.3
81	637.3	739.0	692.3	34.5	837.3	836.7	651.0	1140
82	632.2	740.3	693.2	25.9	851.6	843.0	659.5	1195.5
83	628.6	743.8	690.5	21.0	863.7	849.2	668.9	1167.3
84	635.5	652.5	834.7	18.4	781.3	854.8	670.2	1120.9
85	649.0	628.1	602.1	17.2	250.1	846	379.3	906.4
86	708.2	635.2	586.0	16.5	121.6	785.5	308.4	748.6
87	712.2	634.3	596.7	16.3	102.1	599.9	460.5	682.6
88	717.4	632.1	600.0	16.5	141.2	504.0	339.3	574.4
89	737.8	630.0	601.1	16.6	244.1	552.1	291.1	601.6
90	741.8	627.9	598.7	16.5	257.8	586.9	302.2	606.1

91	732.4	625.1	596.5	16.4	238.9	583.3	270.1	608.1
92	727.1	621.9	594.8	16.6	236.4	680.1	325.0	653.2
93	724.4	617.7	592.8	16.8	461.4	660.5	649.2	703.2
94	720.9	613.7	590.3	16.9	916.3	672.9	967.4	770.0
95	665.9	609.4	587.3	17.3	1153.3	717.4	1127.4	851.2
96	430.0	512.4	587.4	55.5	1192.4	782.2	1106.4	911.2
97	599.8	249.8	583.4	109.5	1199.6	824.5	1151.5	940.8
98	611.2	112.4	580.8	100.9	1142.1	829.9	1185.8	963.2
99	613.0	70.6	578.3	82.5	1189.9	840.4	1204.4	986.3
100	606.6	464.9	523.0	67.4	985.3	841.1	1023.6	1025.9
101	607.8	600.1	161.3	55.4	1064.3	846.2	1058.2	1060.2
102	609.4	607.7	63.8	46.4	1102.8	856.2	1111.9	1081.0
103	618.1	626.4	48.7	40.1	1099.2	861.2	1125.3	1079.3
104	605.3	630.4	38.6	35.8	1120.5	862.7	1155.8	1062.0
105	258.6	635.5	33.4	35.8	1063.6	861.9	1163.3	1070.2
106	127.9	642.9	29.1	38.8	1203.5	859.5	1101.8	1082.0
107	70.1	312.8	25.3	28.8	1266.1	858.5	1092.8	1095.9
108	36.9	88.2	21.7	21.0	1268.0	852.2	1076.4	1096.6
109	24.8	40.7	20.1	18.5	1281.4	849.0	1055.9	1098.3
110	17.8	22.1	16.8	14.9	1251	849.6	1065.1	1109.9
111	14.6	16.0	14.5	12.9	1264.2	849.1	1086.5	1108.1
112	14.1	15.6	14.5	13.2	1242.4	849.1	1110.4	1111.5
113	13.5	14.9	13.4	12.3	1122.1	846.2	1077.4	1109.2
114	12.2	13.4	12.3	11.8	878.7	840.8	1003.5	1071.0
115	10.5	11.2	10.2	9.9	1044.2	840.2	993.5	1070.7
116	10.5	10.9	10.2	10.1	1045.7	838.7	989.7	1084.1
117	11.1	11.4	10.8	10.8	1011.1	833.2	977.1	1083.0
118	10.3	9.9	9.2	9.4	1062.7	829.7	976.1	1085.1
119	8.7	7.6	6.8	7.1	1088.6	827.0	977.8	1098.6
120	8.6	6.9	6.3	6.7	1071.4	825.0	988.2	1123.8
121	9.1	7.2	6.7	7.2	1039.9	821.9	985.0	1136.0
122	10.4	8.3	8.0	8.6	1033.1	819.3	976.3	1150.3
123	13.2	11.1	11.2	11.5	1049.9	818.8	964.4	1174.4
124	344.4	429.1	17.5	40.8	1106.8	820.6	953.4	1201.5
125	738.4	716.4	17.6	25.1	1121.4	818.9	955.5	1166.3
126	794.3	722.7	19.2	18.7	1138.0	817.3	958.6	1144.7
127	801.3	722.6	18.9	17.0	1100.5	817.2	963.0	1147.9
128	803.0	722.2	17.5	15.2	1124.1	817.9	969.5	1134.5
129	803.6	723.1	18.0	16.2	1200.9	818.8	970.3	1112.5
130	794.8	727.4	17.5	17.3	1146.9	819.5	969.4	1098.2
131	793.1	732.6	19.5	18.0	1119.8	820.2	970.5	1078.6
132	793.9	740.2	19.3	19.1	1084.1	820.4	976.9	1061.0
133	793.9	751.6	18.1	19.8	1045.0	819.6	982.5	1044.1
134	793.4	765.1	14.9	17.8	1008.6	817.9	979.1	1026.1
135	793.6	771.5	17.3	20.2	984.1	817.4	982.1	1012.5
136	799.7	776.9	20.4	23.0	965.8	817.3	1003.9	1004.1
137	806.5	785.4	18.5	21.4	940.2	816.1	995.1	993.2
138	809.1	789.8	18.6	20.6	925.3	814.3	966.6	982.0

139	829.3	791.6	18.2	19.5	913.1	813.4	979.7	974.3
140	851.8	793.5	18.2	20.4	902.0	812.7	988.5	966.8
141	848.2	794.9	19.0	22.0	891.8	810.5	975.3	960.5
142	843.2	795.6	18.2	20.6	882.3	808.9	992.5	956.9
143	839.7	797.5	20.2	22.6	879.2	807.2	993.9	953.4
144	837.3	798.3	21.4	24.8	888.9	804.5	982.8	947.8
145	835.0	799.3	20.2	23.8	920.5	801.9	968.4	942.9
146	832.8	798.8	19.4	23.3	947.9	798.7	989.6	937.8
147	832.4	799.7	18.5	22.2	976.1	795.6	1014.0	933.2
148	831.7	802.5	18.1	22.1	986.3	794.2	1041.7	929.3
149	831.9	805.3	18.3	22.4	984.2	792.2	1091.0	927.3
150	832.6	806.1	19.0	23.4	943.2	790.1	1136.9	924.6
151	834.8	804.7	19.7	24.1	923.4	788.1	1141.0	916.1
152	836.7	804.0	18.4	22.5	901.1	786.8	1118.8	902.8
153	837.1	802.9	23.1	325.3	884.7	785.8	1095.5	886.7
154	835.5	800.8	25.6	803.2	904.3	783.6	1145.2	872.2
155	840.1	796.6	24.8	728.6	894.5	782.2	1168.2	854.4
156	846.4	794.4	26.2	218.7	886.5	781.6	1196.4	836
157	843.3	793.5	24.5	67.5	888.2	782.0	1203.9	813.4
158	837.2	793.3	21.9	31.7	897.3	781.9	1144.8	790.8
159	832.2	794.3	22.1	23.5	895.2	782.3	1084.4	772.9
160	827.5	796.2	23.1	21.4	895.4	781.9	1077.7	767.4
161	824.0	796.4	25.4	22.2	878.7	779.5	1072.1	767.8
162	821.6	796.1	26.3	23.1	865.2	776.7	1061.8	765.7
163	820.3	795.8	26.6	23.7	853.2	774.6	1055.4	760.9
164	819.0	794.0	27.3	23.5	844.5	772.9	1040.9	751.0
165	815.7	793.5	26.2	22.3	837.8	772.0	1006.7	737.9
166	812.9	793.1	24.1	21.2	836.0	771.5	1005.9	725.7
167	812.9	791.0	22.1	19.7	835.4	770.9	1011.7	713.0
168	812.3	786.3	22.2	19.4	829.1	770.6	990.8	697.0
169	808.5	781.7	24	20.7	827.5	768.8	987.1	687.3
170	804.7	776.9	24.4	21.3	833.3	767.3	1008.4	679.1
171	802.8	772.1	24.0	20.6	858.1	765.9	1026.4	669.6
172	802.8	770.5	25.8	22.8	900.0	765	1041.6	662.1
173	801.9	772.6	27.4	24.1	921.3	767.0	1057.0	652.3
174	799.8	772.8	27.9	24	883.3	766.3	1063.8	639.3
175	795.0	778.3	27.5	23.2	938.0	765.3	1074.1	637.3
176	278.2	267.4	19.5	17.2	946.6	765.0	1075.5	631.6
177	56.9	53.6	13.0	12.3	949.9	764.6	1070.5	621.3
178	31.3	27.9	16.3	15.5	944.0	764.8	1069.5	613.7
179	19.5	16.4	14.5	14.3	929.5	763.9	1059.1	603.1
180	17.7	14.4	14.6	14.6	907.0	763.9	1049.9	592.4
181	18.2	14.7	15.2	15.0	857.9	762.4	1043.3	580.7
182	18.8	15.2	15.8	15.7	863.7	759.5	1031.8	571.0
183	16.4	13.1	13.4	13.7	861.5	758.3	1022.3	562.4
184	18.4	15.1	15.9	15.7	858.7	757.6	1015.5	553.7
185	18.9	15.9	16.8	16.5	860.8	756.9	1013.5	545.3
186	18.7	15.8	16.7	16.5	846.6	756.4	1011.6	540.2

187	17.3	14.6	15.1	14.8	809.6	756.1	983.2	532.5
188	17.4	14.7	15.0	14.7	803.0	754.2	975.2	526.7
189	16.7	14.0	14.3	14.1	829.5	753.6	967.6	520.8
190	16.4	13.9	14.2	13.9	835.6	753.2	965.1	515.2
191	15.7	13.4	13.6	13.3	834.7	752.1	961.1	508.2
192	16.4	14.3	14.7	14.2	844.4	751.4	961.7	502.0
193	18.0	15.9	16.6	15.8	849.6	751.9	966.2	496.1
194	17.0	15.3	15.7	15.1	838.5	752.0	963.8	491.9
195	17.3	15.5	16.1	15.4	835.4	752.1	950.9	487.0
196	20.1	17.7	18.9	17.9	824.3	752.6	941.5	482.1
197	22.2	19.6	21.0	20.1	815.4	753.3	941.0	477.9
198	19.5	17.3	17.8	17.5	774.2	750.5	995.4	474.1
199	16.9	15.1	15.3	15.0	791.2	749.3	995.1	469.3
200	19.4	17.0	17.8	17.1	788.3	750.1	987.5	464.7
201	19.7	16.8	17.8	17.3	770.4	749.1	968.0	460.7
202	17.1	14.7	15.4	15.2	751.1	745.1	990.9	457.6
203	16.8	14.4	15.2	15.0	736.0	742.8	1013.6	456.6
204	16.1	13.7	14.1	14.1	719.3	742.3	1002.5	456.9
205	17.0	14.5	15.0	14.7	699.6	742.1	1015.0	454.9
206	18.2	15.5	16.1	15.6	704.0	741.0	1037.2	450.7
207	19.2	16.4	17.1	16.6	701.5	740.3	1047.7	446.1
208	18.2	15.9	16.3	16.2	695.0	740.4	1051.1	442.0
209	17.6	15.7	16.0	15.8	677.8	740.8	1050.9	438.6
210	17.4	15.5	15.9	15.6	657.5	742.2	1035.6	435.5
211	16.6	15.0	15.3	15.0	656.7	743.1	1029.4	432.2
212	16.4	14.9	15.3	14.9	647.1	744.0	1058.6	428.3
213	17.2	15.6	17.8	15.6	639.3	744.6	1064.6	424.9
214	16.9	15.7	471.4	15.6	633.6	744.7	1040.6	421.8
215	18.9	17.5	136.5	17.2	630.8	745.7	1043.7	418.1
216	19.7	18.1	43.3	18.0	633.2	746.7	1064.6	414.8
217	18.8	17.4	23.8	17.4	635.9	748.1	1079.9	411.4
218	18.3	17.1	18.7	17.3	641.4	749.6	1055.1	409.0
219	18.1	16.9	17.4	17.1	653.7	750.2	1033.5	409.7
220	21.3	19.4	19.9	19.6	654.2	750.2	1032.8	408.3
221	21.7	19.5	20.1	19.8	655.7	749.7	1024.5	406.2
222	20.2	18.1	18.5	18.6	659.6	749.7	1014.7	404.2
223	20.1	17.8	18.4	18.3	658.2	749.3	1007.7	402.4
224	18.6	16.5	17.1	16.9	654.3	750.0	977.8	399.0
225	21.4	18.9	19.6	19.5	650.6	749.5	967.0	396.6
226	21.7	18.8	19.7	19.3	649.6	748.9	960.4	395.7
227	21.2	18.1	19.3	18.9	649.0	749.1	957.6	394.2

Burns 3 & 4

Record sheets:

KWPV EXPERIMENTS: FIAVE, TRENTO, ITALIA

OPERATOR: *OP* DATE: *06/09/07*
 BURN: *3* PAGE: *1*

PARAMETRES

OXYGEN/SULPHUR RATIO: *2.5*
 FUEL/CHARGE RATIO: *1.*

<u>REACTANTS</u>	<u>MASS (kg)</u>	<u>PRODUCTS</u>	<u>MASS (kg)</u>
MAGNETITE	<i>0.58</i>	SLAG	<i>1.320</i>
CHALCOPYRITE	<i>0.69</i>	COPPER	<i>0.9</i>
MALACHITE	<i>2.09</i>	MATTE	<i>unrendido 0.11</i>
LIME	<i>0.80</i>	OTHER	
SILICA	<i>0.45</i>		
	<i>4</i>		

ASPIRATION (DELETE): NATURAL FAN ~~BELLOWS~~
 WINDSPEED (BACKGROUND) *7m/s*
 WINDSPEED (ARTIFICIAL)
 AIR VOLUME (PER TUYERE)

PERFORATED FURNACE *Y/N*
 CRUCIBLE *Y/N*
 FURNACE LINING *Y/N*

TIMED RECORD

<u>TIME</u>	<u>ACTION</u>	<u>DESCRIPTION</u>
<i>10:23</i>	<i>temp e hand logging</i>	<i>commences</i>
<i>10:36</i>	<i>1st chrg charcoal</i>	<i>1 kg charcoal</i>
<i>10:57</i>	<i>2nd chrg</i>	<i>1 kg charcoal</i>
<i>11:50</i>	<i>add charcoal 3rd charge</i>	<i>1 kg charcoal</i>
<i>12:12</i>	<i>fan on</i>	
<i>12:18</i>	<i>4th charge</i>	<i>1 kg charcoal / 1 kg ruse</i>
<i>12:37</i>	<i>5th chrg</i>	
<i>12:55</i>	<i>6th chrg</i>	
<i>13:42</i>	<i>7th ch</i>	
<i>14:21</i>	<i>fan off</i>	<i>furnace checked</i>

KWPV EXPERIMENTS: FIAVE, TRENTO, ITALIA

OPERATOR: OP
 BURN: 4

DATE: 06/09/07
 PAGE: 1

PARAMETRES

OXYGEN/SULPHUR RATIO: 2.5
 FUEL/CHARGE RATIO: 2

REACTANTS	MASS (kg)	PRODUCTS	MASS (kg)
MAGNETITE	0.42	SLAG	0.84
CHALCOPYRITE	0.50	COPPER	-
MALACHITE	1.52	MATTE	-
LIME	0.14	OTHER	unreacted 0.07
SILICA	0.32		
	<u>2.9</u>		

ASPIRATION (DELETE): ~~NATURAL~~ FAN ~~BELLOWS~~
 WINDSPEED (BACKGROUND) 1.5 m/s
 WINDSPEED (ARTIFICIAL) 1.5 m/s
~~AIR VOLUME (PER TUYERE)~~

PERFORATED FURNACE N
 CRUCIBLE N
 FURNACE LINING Y

TIMED RECORD

TIME	ACTION	DESCRIPTION
14:55	ignition	1st charge
15:04	2nd charge	1st charge of
15:18	3rd charge	1st charcoal / 500g mineral.
15:53	4th charge	" "
16:11	5th charge	" "
16:40	6th charge	" "
17:00	7th charge	" "
17:43	8th charge	800g / 400g
18:15	fm off	

Burns 3 & 4

Temperatures: consecutive experiments (data from channels 2 and 4 reflect ongoing probe failure)

Time Minutes	Channel 1 °C	Channel 2 °C	Channel 3 °C	Channel 4 °C	Channel 5 °C	Channel 6 °C	Channel 7 °C	Channel 8 °C
0	10.5	11.6	10.6	10.4	12.6	13.4	13.1	12.9
1	10.4	10.9	10.5	10.3	12.5	13.4	13.1	12.9
2	10.1	10.0	10.2	10.0	12.0	13.2	12.8	12.6
3	10.1	10.1	10.2	10.0	11.8	13	12.7	12.3
4	10.1	10.3	10.1	10.0	11.9	13.1	12.9	12.5
5	10.4	10.5	10.4	10.2	12.1	13.2	13.0	12.5
6	10.5	10.6	10.5	10.3	12.4	13.2	13.1	12.7
7	10.5	10.6	10.5	10.4	12.3	13.2	13.0	12.7
8	10.5	10.6	10.5	10.3	12.0	13	12.8	12.6
9	10.9	10.9	10.8	10.7	12.2	13.2	12.9	12.6
10	11.1	11.0	11.0	10.8	12.3	13.2	13.0	12.6
11	11.4	11.4	11.3	11.1	12.5	13.4	13.4	12.9
12	11.6	11.7	11.6	11.3	12.6	13.6	13.6	13.2
13	11.8	11.8	11.7	11.5	12.8	13.9	13.9	13.4
14	12.1	12.0	12.0	11.7	12.9	13.9	13.9	13.5
15	12.2	12.3	12.2	11.9	12.9	13.9	14.1	13.6
16	13.0	13.1	12.9	12.7	13.0	14.0	14.1	13.9
17	13.0	13.1	12.8	13.1	12.9	13.4	13.3	36.2
18	12.9	13.0	12.6	13.3	12.9	12.8	13.3	174.6
19	13.0	13.0	12.7	13.2	13.0	13.0	45.7	351.4
20	13.1	13.0	12.8	13.2	13.5	13.3	59.1	426.8
21	13.3	13.2	12.8	13.4	13.9	22.3	59.2	442.5
22	13.6	13.4	13.0	13.7	38.9	51.6	63.4	409.4
23	13.8	13.6	13.2	13.8	40.2	68.3	53.8	244.5
24	12.4	12.7	11.9	12.8	56.2	83.8	76.2	189.1
25	11.0	11.6	8.4	12.2	32.1	87.1	244.6	234.8
26	11.3	11.5	7.8	11.6	15.9	131.5	674.4	790.3
27	10.9	11.1	7.8	10.9	28.3	170.4	448.8	648.7
28	11	11.1	9.3	10.6	39.9	184.3	343.0	574.7
29	11.2	11.3	10.8	10.6	42.6	209.1	339.8	555.5
30	11.2	11.3	11.1	10.6	45.6	234.4	341.6	545.4
31	11.2	11.2	11.1	10.6	53.1	291.0	377.7	542.8
32	11.3	11.3	11.3	10.8	56.6	370.4	388.2	532.1
33	11.4	11.4	11.4	10.9	58.4	457.7	428.1	542.4
34	11.7	11.7	11.7	11.3	72.8	546.8	487.5	587.2
35	11.7	11.7	11.6	11.3	153.3	644.4	545.9	614.1
36	11.6	11.6	11.5	11.2	310.1	716.5	581.9	632.0
37	11.3	11.3	11.2	11.0	466.8	734.7	610.7	638.8
38	11.3	11.4	11.3	11.2	543.8	797.3	625.8	645.1
39	11.6	11.7	11.6	11.4	577.5	807.3	645.9	712.8
40	11.3	11.4	11.2	11.1	589.9	804.1	649.5	715.3
41	11.2	11.4	11.2	11.1	632.1	800.6	662.6	730.5

42	11.4	11.5	11.3	11.2	664.5	812.0	681.5	732.5
43	12.0	12.2	12.0	11.8	678.1	838.3	688.3	752.8
44	12.6	12.8	12.6	12.3	669.4	839.9	689.9	767.2
45	13.0	13.3	13.1	12.9	693.4	850.1	687.9	767.4
46	13.2	13.5	13.3	13.2	709.5	871.6	767.8	772.6
47	13.0	13.0	12.8	12.5	709.3	891.2	776.0	740.4
48	455.8	75.7	143.3	13.4	704.1	893.0	772.9	736.4
49	817.4	737.3	722.7	14.4	723.9	907.2	795.7	734.1
50	854.4	791.7	913.7	15.0	727.5	893.8	794.7	726.4
51	863.6	810.1	903.7	15.8	723.9	863.1	806.6	728.4
52	885.2	775.1	918.3	14.9	726.3	869.9	832.3	735
53	899.9	761.4	916.2	13.9	739.3	835.3	838.5	750.1
54	859.0	781.6	918.9	16.1	755.1	860.7	824.7	762.4
55	834.7	894.6	971.7	16.9	737.6	864.8	821.6	769.3
56	929.1	1030.0	1027.5	16.4	717.6	864.5	826.7	756.5
57	977.9	1030.4	999.3	16.2	736.9	856.3	814.0	752.4
58	1042.7	1052.0	1031.8	15.9	753.7	872.9	814.7	750.6
59	1059.5	1061.4	1037.7	17.2	765.5	864.7	813.0	743.0
60	1030.1	982.8	1003.8	20.3	775.5	874.1	818.4	752.1
61	1019.9	976.4	988.5	22.6	788.3	890.9	823.3	767.7
62	992.8	990.7	997.5	23.1	792.4	938.5	832.9	775.2
63	942.9	1004.3	1014.3	21.9	792.5	941.4	838.1	792.4
64	927.0	1053.8	1008.4	21.2	810.7	948.4	836.3	790.7
65	975.5	970.2	950.7	20.3	835.9	954.0	834.6	794.0
66	972.4	968.2	948.5	20.7	837.8	947.6	836.3	793.8
67	981.9	1012.8	973.3	21.6	851.5	942.8	826.1	806.1
68	1002.3	1038.4	999.1	20.3	867.5	946.9	817.5	803.5
69	1023.1	1062.8	1003.3	19.8	884.7	945.3	822.7	804.0
70	1035.1	1081.2	1017.9	20.4	874.8	925.9	832.3	813.9
71	1008.3	1088.0	1036.4	21.8	884.7	945.6	840.6	819.9
72	988.1	1096.4	1043.1	23.2	869.8	947.8	851.8	834.5
73	982.8	1082.5	1055.7	24.0	896.3	962.5	842.5	849.1
74	986.6	1070.7	1059.2	22.5	934.9	963.8	844.5	858.5
75	987.8	1032.7	1043.0	184.1	915.9	966.1	853.9	853.2
76	979.5	985.5	875.6	480.1	900.0	942.3	862.2	871.7
77	992.4	881.9	752.2	559.1	899.6	923.3	865.6	875.5
78	1018.0	909.4	901.6	553.0	900.4	931.2	866.9	873.4
79	1025.9	927.6	908.2	558.3	907.1	956.4	864.4	882.4
80	1036.8	938.1	912.7	583.2	904.5	960.6	866.7	878.7
81	1053.5	950.5	918.3	595.0	898.8	964.8	857.4	869.1
82	1090.2	963.3	930.1	592.2	902.2	961.2	867.5	868.7
83	1108.9	966.4	932.7	571.8	899.9	959.6	884.5	849.1
84	1107.5	968.0	935.2	449.7	897.9	953.2	887.4	850.4
85	1115.8	970.0	938	426.6	897.3	958.3	889.5	846.9
86	1110.3	973.5	940.7	399.4	886.6	954.3	888.4	831.1
87	1105.3	977.2	940.4	406.5	879.3	941.6	883.4	826.2
88	1091.0	977.8	938.0	432.9	884.3	940.9	882.7	829.4
89	1073.0	967.6	932.5	408.3	875.9	938.6	877.7	837.6

90	1065.9	955.5	928.6	395.0	867.8	931.6	871.6	830.9
91	1059.6	947.3	925.8	379.3	896.5	950.2	877.5	862.0
92	1048.7	941	922.6	365.6	896.5	947.1	880.9	861.4
93	1043.0	936.0	919.4	356.9	887.3	938.7	874.7	845.0
94	1025.1	930.4	916.2	339.1	877.5	936.7	874.2	843.1
95	1009.3	919.7	912.7	333.9	883.3	936.7	865.4	839.2
96	994.7	910.1	909.8	225.3	869.6	943.3	867.1	839.4
97	986.0	905.7	907.4	112.1	873.6	944.6	856.4	838.2
98	981.9	903.5	907.0	64.3	869.8	948.9	815.7	844.7
99	978.8	900.2	907.9	42.4	867.6	949.8	803.6	849.9
100	972.5	894.6	906.7	32.6	869.9	955.2	786.3	860.8
101	958.3	878.3	906.9	27.3	889.8	957.6	784.2	868.3
102	924.5	854.6	895.3	24.5	933.9	969.3	787.6	872.9
103	901.5	845.8	881.2	22.7	954.9	977.6	793.5	867.4
104	889.2	845.2	868.3	21.9	954.5	982.1	749.8	859.7
105	887.1	844.6	858.8	21.6	947.8	977.2	707.4	856.1
106	892.0	841.2	852.5	21.2	951.4	972.9	701.7	859.3
107	901.2	839.3	848.9	21.1	949.1	976.6	721.8	867.0
108	911.8	841.2	848.4	20.8	957.3	983.3	810.5	884.5
109	925.2	844.5	849.4	20.7	957.9	1015.5	840.7	900.3
110	939.7	848.9	851.1	20.7	1099.3	976.5	997.6	1155.8
111	960.8	854.2	855.5	20.8	1169.8	987.1	1122.6	1205.8
112	976.0	858.3	858.5	20.8	1142.6	1067.0	1095.2	1148.2
113	989.4	860.7	863.4	20.8	1054.8	1066.8	1097.5	1011.7
114	1000.8	862.9	868.5	20.7	836.9	1101.7	1128.5	1090.6
115	1007.3	865.8	873.6	20.7	897.4	1117.7	1143.9	1075.2
116	994.4	869.1	877.9	21.1	1038.7	1023.8	1067.2	887.9
117	960.5	909.7	886.6	21.1	1152.8	1122.0	1071.7	1001.8
118	922.1	957.6	876.8	21.1	1123.0	1047.7	1109.6	1083.9
119	901.9	959.9	863.4	20.9	1032.1	1001.4	1164.9	1050.0
120	895.6	707.5	854.5	20.8	968.7	1016.7	1094.4	1030.9
121	901.4	953.3	849.8	20.7	912.1	1060.1	1068.7	1009.5
122	917.6	997.8	849.3	20.3	832.7	1031.0	1092.4	992.5
123	935.8	1028.2	852.2	20.1	854.2	1000.3	1082.1	975.3
124	952.5	1051.7	857.5	20.5	982.1	974.8	1068.9	988.1
125	967.6	1073.7	864.5	21	892.4	1008.4	1076.3	1029.6
126	979.8	1077.4	861.1	21.3	838.5	1006.6	1070.1	1027.4
127	980.8	1011.1	848.6	21.8	900.8	985.5	1076.3	1061.3
128	981.2	1046.3	852.2	22.1	940.6	1013.3	1071.7	1033.8
129	989.0	1050.2	856.3	22.4	855.4	1043.1	1100.2	993.9
130	998.6	1054.6	862.4	22.4	795.7	972.7	1038.3	1001.0
131	1005.8	1039.0	868.8	22.6	849.9	927.9	1017.8	935.4
132	1007.3	1011.5	873.5	22.8	783.2	924.2	1057.2	908.1
133	1009.7	1011.7	877.5	22.8	671.8	943.6	1082.9	898.9
134	1010.9	1024.7	880.6	22.8	583.3	944.0	1093.0	915.0
135	1004.9	1021.5	882.6	22.8	521.4	934.1	1088.3	928.2
136	996.5	1014.5	883.8	22.8	470.8	942.1	1088.0	914.8
137	991.3	1008.0	883.8	22.9	477.2	915.1	1037.5	876.8

138	987.9	1001.4	883.8	23.2	540.2	902.7	1010.2	846.1
139	985.3	1002.6	884.1	23.4	598.6	920.8	1030.5	831.5
140	981.7	993.0	885.4	22.1	618.3	933.8	1049.3	825.6
141	969.2	865.6	816.5	22.4	670.8	908.6	1018.4	815.5
142	891.5	877.9	1072.9	23.4	689.5	924.7	1016.7	829.0
143	1028.5	968.9	1061.7	23.5	662.1	952.3	1007.3	894.3
144	1041.8	973.6	1102.9	25.5	332.1	977.7	989.1	884.1
145	1054.1	994.3	1093.3	25.0	666.9	950.8	963.1	862.8
146	1053.9	978.4	1104.8	24.4	905.0	961.7	960.1	852.7
147	1068.4	1028.9	1103.7	24.0	827.7	955.9	971.9	850.6
148	1080.9	1006.8	1107.9	23.6	631.8	959.6	985.9	860.1
149	1089.6	1015.1	1126.6	23.3	515.0	964.9	981.2	870.4
150	1097.2	1059.5	1121.1	23.0	422.4	959.9	976.6	882.7
151	1065.1	1115.8	1087.6	22.9	608.5	952.4	973.8	884.6
152	1073.5	1105.6	1093.6	22.6	813.3	902.5	972.1	869.8
153	1061.2	1043.1	839.7	22.9	928.8	849.2	954.0	839.9
154	1048.8	828.0	904.3	24.8	909.6	847.3	961.9	853.2
155	628.9	1001.2	1084.5	27.9	838.5	857.2	966.2	873.5
156	976.5	1025.7	1114.1	27.9	674.4	874.6	975.3	926.1
157	989.5	1028.7	1134.1	27.2	630.1	884.8	978.3	947.1
158	983.2	1012.1	1148.9	26.6	579.5	878.9	972.1	924.0
159	986.6	994.8	1149.6	26.3	564.5	870.2	967.8	901.8
160	994.3	974.5	1135.3	26.5	531.6	878.6	960	890.2
161	1013.3	955.7	1087.9	26.5	484.8	892.4	961.5	870.7
162	1021.4	949.1	1090.4	26.2	425.4	897.6	959.6	847.2
163	1035.4	960.3	1102.0	26.0	350.8	895.9	954.7	822.5
164	1051.4	1037.1	1096.7	26.3	467.8	901.2	965.7	796.1
165	1078.2	1022.6	1103.0	25.1	445.4	904.1	974.2	767.4
166	1071.8	991.0	1111.5	24.4	298.6	884.7	944.6	741.0
167	1075.9	963.7	1087.7	24.2	386.3	860.1	919.2	730.8
168	1082.6	951.9	1086.4	24.3	403.3	881.8	935.6	744.8
169	1109.3	945.2	1075.3	24.2	450.0	878.6	950.7	694.8
170	1114.4	982.0	1072.0	24.6	389.6	880.9	952.0	648.6
171	1114.8	1004.6	1063.2	24.9	361.8	882.6	939.2	629.5
172	1092.8	927.1	1094.4	24.7	441.2	894.5	940.4	628.4
173	1084.8	868.0	1061.2	24.9	453.5	917.8	942.3	602.5
174	1089.2	859.3	1062.9	24.8	438.7	917.6	935.7	570.6
175	1083.3	869.2	1072.8	25.1	396.8	914.6	925.2	572.9
176	1077.8	863.0	1077.7	25.8	310.1	931.9	930.7	559.6
177	1071.5	841.6	1071	26.4	266.5	916.0	935.6	531.5
178	1070.2	826.5	1098.6	26.2	259.1	914.5	938.6	505.8
179	1074.8	809.5	1109.2	26.0	242.2	911.5	943.7	485.0
180	1073.4	795.7	1099.4	25.9	224.9	904.4	941.4	490.4
181	1075.3	784.4	1075.5	25.8	210.7	910.0	942.6	486.8
182	1068.6	777.5	1116.7	26.0	241.2	912.2	946	464.1
183	1056.4	784.5	1115.3	25.9	229.9	916.8	947.3	439.5
184	1067.1	781.1	1123.2	25	203.8	935.3	952.2	411.4
185	1072.5	783.8	1102.4	25.5	170.1	936.1	958.7	382.8

186	1067.5	785.1	1086.9	25.5	133.2	928.6	966.6	358.1
187	1066.9	797.4	1042.5	25.1	112.3	915.1	966.6	342.2
188	1063.9	808.4	1012.2	24.9	104.6	887.7	971.2	333.3
189	1044.3	818.2	1001.7	24.6	102.0	860.5	970.4	322.5
190	963.3	841.2	977.4	24.4	93.8	840.1	971.6	306.0
191	941.3	558.0	915.3	24.7	88.2	805.1	972	287.6
192	944.8	948.4	806.5	24.3	83.6	763.5	968.6	269.4
193	828.8	917.7	624.8	24.1	79.6	703.6	965.1	250.2
194	276.5	906.1	861.1	24.1	76.7	658.2	962.4	230.3
195	114.2	919.2	896.7	783.4	74.0	612.6	954.8	212.5
196	62.0	953.2	945.3	1020.1	70.7	571.1	947.8	195.9
197	36.2	969.1	983.1	1024.7	79.4	722.4	914.9	194.9
198	28	984.1	997.7	1028.6	81.9	783.3	900.8	199.1
199	23.0	1000.1	1009.1	1006.4	83.4	792.6	893.8	194.1
200	20.4	1019.6	1023.9	988.5	90.6	772.1	882.5	202.1
201	19.1	999.3	1043.9	1020.1	87.8	768.5	881.2	240.2
202	18.7	937.1	1020.3	1046.4	88.3	751.9	883.3	297.6
203	18.9	917.3	1038.6	1062.4	89.3	750.7	887.8	317.2
204	19.4	915.4	1040.3	1097.4	89.9	771.2	889.5	315.5
205	20.0	911	1026.8	1014.4	98.0	763.3	890.1	324.5
206	20.1	894.4	997.5	921.8	189.5	730.6	895.6	329.3
207	20.4	896.1	979.8	901.8	175.1	701.7	897.7	345.4
208	20.9	905.1	974.3	909.6	144.8	686.3	899.8	367.9
209	20.5	909.3	971.8	893.6	95.0	654.5	900.9	363.4
210	19.4	910.1	970.8	879.8	61.7	620.0	904.8	347.6
211	18.6	914.4	971.0	872.1	49.5	594.9	911.0	322.5
212	18.8	920.5	971.4	870.8	59.6	592.6	914.8	301.7
213	19.1	681.3	970.8	918.0	91.8	574.3	927.0	297.9
214	19.3	952.6	973.2	919.3	102.8	614.6	960.0	286.1
215	19.3	948.5	974.3	945.6	97.5	618.2	975.0	272.5
216	19.8	862.8	971.5	963.0	186.8	575.3	906.8	285.1
217	20.7	821.5	960.0	970.0	319.3	535.9	854.5	299.3
218	21.7	810.2	964.6	991.3	327.2	518.1	847.4	311.1
219	22.6	767.3	967.2	1000.8	155.5	515.2	903.2	318.7
220	23.4	770.3	970.3	1024.3	89.5	496.2	954.4	314.6
221	23.7	777	974.4	1043.0	66.2	483.3	980.5	300.8
222	23.7	745.4	968.8	1016.4	53.5	474.1	990.8	301.9
223	22.8	758.1	957.9	736.8	46.4	467.1	999.2	286.5
224	22.4	795.1	965.8	177.4	37.8	443.3	1001.2	262.8
225	314.0	758.4	983.9	72.9	39.4	426.4	1000.7	239.5
226	1015.7	334.6	991.6	45.8	40.2	411.7	1006.1	225.5
227	978.6	857.2	958.9	32.7	36.2	396.9	1010.6	214.5
228	1004.8	882.6	1017.1	26.4	33.5	375.7	1011.1	205.6
229	1023.3	886.8	1043.9	23.7	32.6	356.9	1008.0	196.3
230	1079.6	901.3	1057.4	22.5	29.1	354.1	1002.7	188.3
231	1053.4	897.4	1045.0	22.5	28.1	373.6	991.7	183.8
232	1016.2	906.2	1034.0	22.7	27.0	354.7	989.2	179.7
233	996.3	904.3	1031.8	22.6	26.2	329.1	990.3	172.4

234	1007.2	906.4	1017.9	21.8	26.4	319.8	989.5	165.5
235	1001.4	898.0	982.2	20.0	25.3	312.9	987.4	160.0
236	968.9	896.8	954.1	18.8	24	304.6	984.7	156.4
237	957.6	903.8	949.5	18.4	22.2	298.4	980.5	154.1
238	953.2	907.1	944.0	18.7	39.1	295.1	908.4	152
239	949.5	906.9	932.3	19.3	64.8	293.7	845.1	157.4
240	947.5	905.9	908.8	19.8	85.2	293.5	810.4	164.3
241	956.3	661.7	904.1	20.2	103.5	292.6	786.2	170.5
242	955.8	490.4	894.5	20.7	121.9	292.1	768.8	175.4
243	936.9	959.2	926.6	21.1	138.0	291.5	754.6	179.6
244	958.1	988.7	944.4	21.9	150.7	290.1	722.3	173.1
245	397.6	1008.4	982.2	22.1	90.4	177.1	316.2	91.5
246	563.9	953.8	953.8	22.1	47.6	84.4	139.1	51.2
247	1067.5	963.3	942.9	22.2	31.7	51.8	77.9	34.6
248	1062.9	977.2	944.8	22.4	24.9	36.6	50.5	27.3
249	1038.2	983.0	957.6	22.9	22.7	30.1	38.0	24.4
250	964.2	981.7	949.4	23.2	21.8	27.6	33.6	22.7
251	999.3	992.2	949.1	23.0	21.0	26.1	30.9	21.5
252	1061.2	1000.5	946.5	22.6	20.9	25.3	29.1	20.3
253	1069.4	1007.7	944.3	22.6	20.7	24.8	27.9	19.9
254	1078.4	1007.4	996.9	22.8	20.7	24.4	26.7	19.9
255	1064.5	1012.0	1055.3	22.7	20.4	23.9	26.2	20.0
256	1026.0	1019.3	1037.9	22.8	19.8	23.6	25.5	19.6
257	1033.5	1024.5	1039.5	22.9	19.9	23.3	25.5	19.7
258	1051.7	1027.6	1047.6	23.4	20.7	23.7	26.7	20.1
259	1065.1	1031.7	1049.9	23.7	20.9	23.9	27.5	20.4
260	1066.2	1036.6	1057.5	23.2	20.6	23.7	27.5	19.9
261	1069.0	1039.8	1064.1	22.6	20.0	23.4	26.6	19.3
262	1072.9	1058.6	1065.0	22.2	19.2	23.2	26.4	19.6
263	1062.0	1071.2	1054.1	21.9	18.1	23.4	25.8	19.3
264	1045.7	1075.3	1050.1	21.7	18.3	23.3	25.6	18.4
265	1045.0	1069.2	1057.4	21.7	32.5	38.8	40.2	20.8
266	1043.9	1067.3	1070.3	21.3	37	55.8	61.2	41.0
267	1068.2	1073.9	1082.7	21.0	44.4	62.8	68.4	53.7
268	1074.2	1036.7	1100.1	21.0	52.7	64.4	72.0	59.5
269	1075.5	1024.5	1117.1	21.1	55.4	65.3	71.8	63.8
270	1022.6	1033.2	1083.0	20.9	54.7	65.4	70.8	65.6
271	980.6	486.9	1087.7	20.9	56.2	67.5	71.5	68.0
272	950.4	1020.7	1068.5	21.2	65.4	75.6	78.0	78.0
273	931.7	1039.4	1090.8	21.5	54.8	66.4	70.6	64.0
274	920.9	1055.8	1092.9	21.3	87.0	73.1	72.8	74.7
275	915.9	1050.9	1084.0	19.6	199.4	163.1	62.9	144.9
276	909.6	1072.1	1083.1	18.9	536.7	460.8	64.9	395.6
277	901.3	1070.5	1084.9	20.1	906.1	690.3	127.2	677.9
278	894.9	1080.5	1110.9	22.9	1026.1	736.2	403.4	896.7
279	890.8	1089.6	1125.5	26.9	1080.5	775.4	609.8	1066.5
280	888.6	1089.3	1136.7	28.5	1081.1	790.8	742.0	1085.4
281	887.4	1088.8	1133.6	34.7	1118.2	774.5	713.7	1055.4

282	887.4	1086.4	1126.8	31.3	1119.1	782.6	717.2	1206.8
283	888.8	1086.5	1117.2	29.9	1125.5	812.4	781.8	1210.8
284	891.0	1089.2	1111.5	30.4	1149.4	813.2	813.7	962.4
285	895.1	1093.7	1108.4	29.2	1113.6	808.8	838.2	1017.9
286	898.9	1095.8	1105.0	27.4	1115.9	815.7	847.0	973.2
287	901.9	1095.1	1098.0	27.6	1168.3	853.1	867.7	951.5
288	904.7	1098.2	1089.9	27.5	1159.7	901.0	835.4	945.4
289	907.3	1091.8	1080.1	29.6	1206.7	942.3	844.6	974.2
290	909.1	1103.8	1064.2	29.5	1217.6	909.9	883.2	953.0
291	913.0	1103.3	1060.9	30.4	1138.2	883.9	868.7	968.5
292	916.8	1103.2	1053.0	34.1	1149.9	908.8	855.8	1015.5
293	919.0	1100.2	1076.9	32.6	1123.7	906.9	870.5	1091.7
294	924.3	1090.9	1071.6	30.8	943.1	894.3	884.2	1059.6
295	922.1	1061.5	1079.9	30.0	890.1	887.5	895.8	1062.5
296	914.5	1059.7	1089.7	29.5	1004.2	855.8	843.4	1051.1
297	908.2	1061.1	1060.6	30.0	1065.2	846.6	806.4	1100.9
298	904.1	1057.2	1053.4	30.9	1122.0	840.7	809.3	1136.4
299	901.8	1053.5	1041.8	31.4	1133.7	824.7	811.5	1120.6
300	900.5	1053.7	1029.0	31.3	1127.5	812.8	815.1	1150.3
301	898.9	1053.2	1026.7	30.4	1112.0	805.8	821.8	1132.6
302	897.2	998.3	1045.4	29.7	1082.2	826.3	827.9	1145.2
303	895.8	975.2	1065.9	27.4	1135.0	810.8	816.3	1192.5
304	894.9	992.8	1072.2	26.6	1077.2	799.0	818.1	1137.6
305	893.4	993.3	1063.3	25.6	1048.7	791.5	817.0	1149.6
306	891.2	979.0	1071.3	25.5	1059.9	789.4	810.9	1178.8
307	889	972.2	1075.6	25.6	1076.1	794.7	811.1	1254.6
308	886.7	986.5	1072.3	25.2	1070.4	801.0	811.3	1216.6
309	883.3	1004.8	1062.4	27.2	1065.0	800.8	809.8	1137.8
310	880.0	972.7	1065.2	30.3	1058.2	799.1	794.7	1153.3
311	878.4	965.4	1068.3	31.2	1003.2	787.1	798.2	1134.1
312	878.2	969.6	1064.8	31.2	959.2	768.1	811.2	1206.2
313	878.1	977.2	1057.2	29	948.4	758.3	807.7	1221.4
314	877.4	1014.5	1025.7	32.4	940.2	750.9	786.8	1219.8
315	876.7	1003.9	1006.2	35.5	921.3	741.1	781.9	1222.1
316	880.3	997.1	987.8	34.3	918.9	736.4	778.4	1233.3
317	879.6	989.0	975	32.1	888.3	732.4	766.2	1213.8
318	879.4	986.5	969.6	28.0	859.8	732.1	767.4	1184.7
319	880.9	987.8	967.8	25.6	868.2	730.4	763.0	1128.9
320	884.0	990.2	967.5	25.0	954.7	728.3	756.0	1070.6
321	888.4	993.8	968.5	25.2	930.8	724.3	752.1	1070.4
322	888.0	998.9	971.1	25.9	829.4	724.7	756.2	1144.2
323	884.7	1003.7	973.2	27.9	742.0	725.8	762.3	1109.8
324	882.3	1009.0	974.5	30.6	670.4	725.4	762.7	1173.9
325	880.6	1010.4	975.5	33.3	623.2	722.0	762.8	1176.3
326	880.7	1019.4	978.0	34.6	583.7	719.9	760.1	1139.7
327	884.0	1029.7	984.7	34.1	491.7	721.8	765.2	1118.4
328	888.2	1041.0	991.0	34	453.0	725.4	783.3	1089.8
329	892.3	1049.2	996.7	33.6	454.3	728.8	802.3	1114.3

330	896.3	1061.3	1002.4	32.8	533.2	727.2	788.5	979.9
331	899.8	1071.8	1009.6	30.5	565.3	735.8	793.4	1002.7
332	902.7	1076.2	1014.7	31.7	727.2	738.5	805.4	1048.0
333	905.6	1080.2	1018.9	30.3	1108.0	739.5	823.2	1060.8
334	907.1	1069.5	1018.8	28.0	1125.2	733.0	804.0	1157.2
335	905.4	1061.6	1004.8	26.3	1119.0	726.9	808.6	1239.7
336	900.1	1062.9	1018.6	25.2	1089.2	719.8	812.5	*****
337	893.3	1067.8	1043.4	24.2	1018.9	704.4	811.6	1241.9
338	885.3	1067.6	1051.3	25.1	970.0	694.2	812.6	1193.9
339	877.2	1071.6	1058.1	25.4	952.0	688.1	804.7	1160.8
340	870.3	1074.3	1060.9	25.6	941.0	684.7	796.7	1157.8
341	864.5	1075.1	1064.4	25.8	959.1	681.8	788.1	1181.2
342	859.8	1071.0	1059.7	25.8	979.9	678.8	781.9	1085.1
343	856.1	1072.5	1060.1	25.3	1071.1	676.3	777.0	1062.4
344	853.7	1076.3	1069.6	24.4	1094.3	676.1	773.5	1050.8
345	851.4	1078.1	1079.6	24.2	1075.4	677.7	780.8	1054.8
346	849.4	1076.9	1083.4	23.8	1028.6	682.6	806.0	1020.0
347	848.4	1085.9	1087.6	25.6	1007.2	680.5	831.1	1048.5
348	848.0	1095.5	1088.0	25.7	1001.6	679	829.2	1093.1
349	847.8	1097.5	1078.7	23.8	973.5	678.6	823.8	1156.3
350	847.4	1101.9	1049.8	23.3	952.4	678.0	807.5	1164.1
351	847.7	1101.4	1045.7	23.2	922.7	679.4	800.8	1173.2
352	848.4	1097.0	1039.9	22.4	937.5	685.2	799.0	1106.1
353	849.0	1099.8	1036.4	23.6	947.2	683.7	805.3	1080.0
354	849.5	1100.2	1021.7	23.3	930.9	679.6	799.1	1078.9
355	850.0	1096.1	1016.6	22.1	897.3	677.2	789.6	1048.4
356	851.2	1084.6	1021.0	20.7	895.9	679.1	780.6	1023.3
357	853.2	1077.6	1068.3	20.7	883.8	676.1	772.9	996.2
358	854.8	1081.6	1062.6	22.4	879.6	672.2	761.7	990.4
359	856.0	1077.3	1060.2	24.5	875.9	668.0	747.5	998.3
360	858.2	1079.1	1057.9	26.5	864.3	663.9	736.2	1045.9
361	860.7	1072.5	1027.9	26	849.7	660.1	727.3	1069.1
362	863.1	*****	980.0	26.9	845.9	656.2	717.4	1058.8
363	763.7	845.1	934.1	28.1	850.9	652.5	707.9	1037.3
364	235.1	757.4	928.2	29.2	831.5	649.5	702.7	1023.1
365	593.0	755.2	968.2	28.2	799.3	647.2	698.1	1021.3
366	1069.0	765.4	985.9	27.3	839.0	646.0	686.9	1001.0
367	1102.5	819.1	991.3	27.2	864.9	644.4	687.5	1058.9
368	1041.2	864.7	986.2	27.6	872.3	642.3	682.1	1108.7
369	971.6	883.2	961.8	29.4	885.7	639.7	674.8	1104.5
370	961.7	867.1	947.8	29.1	889.9	636.7	668.8	1128.3
371	958.0	858.8	938.2	26.6	856.5	634.0	660.8	1098.0
372	955.5	858.6	932.8	26.1	891.3	632.9	655.8	1074.1
373	953.1	871.7	928.9	26.6	927.8	629.9	659.1	1099.7
374	950.8	893.8	926.4	25.4	915.9	628.1	664.5	1086.4
375	956.1	902.8	922.4	24.9	875.9	627.9	658.7	1058.6
376	958.9	972.7	920.8	26.0	906.5	627.7	651.4	1054.1
377	949.5	456	913.4	26.7	897.7	626.9	638.6	1017.8

378	916.4	*****	902.9	27.7	909.4	626.0	628.0	1003.9
379	889.2	816.8	728.9	26.3	899.4	626.0	638.7	990.3
380	875.5	*****	214.8	25.2	925.9	627.5	636.9	960.9
381	842.0	799.4	755.5	26.3	953.7	626.8	641	956.4
382	825.9	722.0	813.8	26.7	962.0	625.5	637.0	948.9
383	812.4	1029.4	811.7	26.0	958.9	623.7	636.9	943.3
384	798.1	1077.8	801.0	25.1	949.7	622.0	632.1	939.3
385	788.2	1124.7	792.2	25.2	951.5	620.5	624.1	935.6
386	781.1	856.8	786.0	25.8	980.2	619.4	626.8	922.0
387	785.7	811.4	782.5	25.9	984.4	618.3	621.8	914.4
388	794.5	*****	782.0	26.0	970.2	617.2	611.2	917.1
389	438.5	300.2	466.1	24.4	951.3	616.6	607.7	914.1
390	102.7	24.3	105.7	19.7	935.7	616.3	601.0	890.9
391	35.4	13.9	35.3	16.7	973.7	617.2	594.4	883.9
392	21.7	-17.7	23.2	16.9	985.0	617.3	596.3	878.2
393	19.4	25.4	21.1	17.4	996.5	616.9	590.9	878.3
394	18.2	26.6	19.9	17.1	986.3	616.4	587.1	880.9
395	17.7	*****	19.4	17.3	958.0	616.0	589.7	893.1
396	17.8	4.8	19.3	17.6	925.3	615.8	584.5	909.1
397	17.8	-90.2	18.4	17.0	900.5	614.9	577.0	904.1
398	18.0	36.4	19.2	18.1	871.3	614.1	574.8	900.9
399	17.1	-175.2	19.1	18.2	814.9	612.9	571.9	897.8
400	16.2	-129.9	18.7	18.0	595.6	617.1	578.5	872.6
401	16.2	31.0	19.0	18.5	445.8	625.5	569.2	852.5
402	15.8	-29.2	18.7	18.3	390.5	635.9	564.7	838.8
403	16.1	-129.9	19.3	19.1	513.7	640.3	553.6	809.0
404	14.9	-110.4	18.9	18.7	587.4	637.0	543.8	787.2
405	13.9	-91.1	18.5	18.4	638.6	630.5	536.5	807.2
406	13.1	-119.8	17.9	18.0	657.0	625.3	533.6	822.4
407	12.8	-124.4	17.7	18.1	629.9	623.2	533.8	829.1
408	12.9	-104.1	18.0	18.6	600.6	622.1	532.2	832.5
409	11.7	35.9	16.0	17.1	533.0	621.6	528.8	838.8
410	11.3	29.2	14.4	15.5	490.4	621.5	530.5	846.8
411	10.7	29.0	12.9	13.8	544.2	622.5	528.9	846.4
412	12.3	29.2	13.7	14.5	592.8	623.7	519.5	860.1
413	12.9	31.1	13.8	14.4	605.3	625.9	518.2	862.5
414	12.8	32.5	13.5	13.9	613.7	627.7	515.5	867.2
415	13.9	34.1	14.2	14.4	543.9	629.3	515.8	869.2
416	13.7	36.6	13.8	13.9	497.6	631	512.0	867.9
417	13.3	41.5	13.4	13.3	453.2	631.9	512.1	867.1
418	13.2	48.8	13.3	13.1	510.1	632.7	524	875.7
419	13.6	48.0	13.4	13.2	489.5	642.1	687.6	891.2
420	13.4	50.5	13.1	12.9	486.7	641.7	689.1	891.4
421	77.9	*****	14.2	13.9	529.6	634.4	680.3	914.1
422	186.0	119.0	16.5	16.0	545.9	625.9	673.5	933.1
423	150.8	*****	17.1	16.8	548.6	617.7	667.7	946.7
424	71.1	*****	16.5	16.6	540.9	610.0	661.1	955.4
425	39.4	*****	15.8	16.1	529.0	602.9	654.1	954.5

426	26.1	*****	15.3	15.8	510.3	596.9	647.9	941.1
427	20.2	*****	15.2	15.8	485.1	592.0	647.1	921.8
428	17.7	*****	15.5	15.8	450.4	588.1	647.1	905.0
429	16.1	*****	15.7	15.4	454.0	586.0	651.1	921.2
430	15.1	*****	15.7	15.2	453.0	584.2	660.6	938.2
431	14.4	*****	15.5	15.2	430.1	582.2	665.5	933.2
432	14.3	*****	15.4	15.3	398.7	580.3	667.4	925.1
433	14.3	*****	15.6	15.4	366.4	578.5	668.9	909.2
434	14.2	*****	15.4	15.3	340.4	577.0	670.6	894.4
435	14.4	*****	15.5	15.4	310.3	575.9	675.5	882.7
436	14.6	*****	15.8	15.4	280.9	575.2	673.2	878.6
437	14.8	*****	15.9	15.3	256.2	574.7	668.1	882.6
438	14.7	*****	15.9	15.4	245.0	573.8	664.9	888.2
439	14.5	*****	15.8	15.2	229.0	572.9	660.3	894.3
440	14.5	*****	15.8	15.1	207.6	572.2	656.0	899.8
441	14.6	*****	15.7	15.0	232.1	572.6	668.5	876.7
442	14.7	31.2	15.6	14.9	273.3	573.8	668.9	836.9
443	14.5	868.6	15.6	14.7	284.1	568.0	639.6	795.5
444	14.4	*****	15.5	14.8	298.4	562.8	610.2	749.5
445	14.4	*****	15.6	14.9	306.7	566.5	619.9	745.3
446	14.2	*****	15.6	14.7	297.1	566.3	623.7	747.7
447	14.1	*****	15.5	14.8	278.9	565.8	625.2	753.0
448	14	*****	15.5	14.8	272.5	565.6	638.0	755.4
449	14.2	*****	15.6	14.8	265.6	566.0	638.1	753.3
450	15.2	*****	15.9	14.8	253.4	566.6	628.1	754.6
451	15.9	*****	16.1	14.8	243.8	569.8	635.4	756.1
452	16.3	*****	16.3	14.8	257.1	576.4	677.0	759.0
453	16.4	*****	16.4	14.6	260.2	583.9	682.2	760.8
454	16.5	*****	16.4	14.5	253.6	593.1	680.4	761.6
455	16.5	*****	16.5	14.4	243.7	603.1	681.6	762.9
456	16.6	*****	16.6	14.3	230.2	614	678.5	767.3
457	16.6	*****	16.6	14.3	217.8	624.5	679.0	775.2
458	16.6	*****	16.7	14.2	189.1	635.6	680.1	777.0
459	16.6	*****	16.8	14.2	178.2	641.9	674.7	775.2
460	16.6	*****	16.8	14.1	190.4	646.6	662.8	760.6
461	16.7	*****	16.8	14.0	199.7	659.8	653.5	749.5
462	16.8	*****	16.9	13.8	195.2	673.6	650.0	744.2
463	16.7	*****	16.9	13.6	206.1	678.8	642.3	741.4
464	16.7	*****	16.9	13.5	205.6	687.1	639.8	740.5
465	16.7	*****	17.0	13.7	197.0	694.5	640.3	740.6
466	16.7	*****	17	13.7	193.9	699.2	639.8	743.5
467	16.7	*****	17.0	13.7	186.5	707.1	643.4	747.1
468	16.3	*****	16.6	14	176.2	716.5	647.6	748.9
469	15.6	*****	15.5	13.8	169.0	722.8	650.2	750.1
470	15.1	*****	14.9	13.7	161.6	726.7	653.1	752.4
471	14.6	*****	14.4	13.4	149.4	736.1	661.3	753.4
472	14.3	*****	14.2	13.1	138.9	751.1	666.4	754.2
473	14.1	800.0	14.1	13.0	149.0	739.7	670.1	746.7
474	13.8	1229.3	13.9	13.0	183.0	689.9	628.1	705.4

KWPV EXPERIMENTS: FIAVE, TRENTO, ITALIA

OPERATOR: OP
 BURN: 6

DATE: 07/09/07
 PAGE: 1

PARAMETRES

OXYGEN/SULPHUR RATIO: |
 FUEL/CHARGE RATIO: |

REACTANTS	MASS (kg)	PRODUCTS	MASS (kg)
MAGNETITE		SLAG	3
CHALCOPYRITE		COPPER	
MALACHITE		MATTE	
LIME		OTHER	
SILICA			

ASPIRATION (DELETE): NATURAL FAN BELLOWS
 WINDSPEED (BACKGROUND) 7.2
 WINDSPEED (ARTIFICIAL)
 AIR VOLUME (PER TUYERE)

PERFORATED FURNACE Y/N
 CRUCIBLE Y/N
 FURNACE LINING Y/N

TIMED RECORD

TIME	ACTION	DESCRIPTION
15:28	1st chrg	1 kg chrgd
15:35	2nd chrg	"
15:36	3rd chrg	"
15:43	4th "	1 kg chrgd / 1 kg smelt
15:55	5th "	"
16:25	6th "	735/735
17:00	Shutdown	

Burns 5 & 6

Temperatures: consecutive experiments

Time Minutes	Channel 1 °C	Channel 4 °C	Channel 5 °C	Channel 6 °C	Channel 7 °C	Channel 8 °C
0	13.5	13.3	10.0	10.5	10.7	10.6
1	13.7	13.4	10.0	10.6	10.7	10.7
2	13.9	13.5	10.0	10.7	10.8	10.8
3	13.9	13.6	10.0	10.7	10.8	10.8
4	14.2	13.8	10.0	10.8	10.9	10.9
5	14.4	13.9	10.0	10.9	11.5	11.0
6	14.7	14.2	10.4	11.6	15.5	12.3
7	15.1	14.5	10.4	11.6	15.2	12.6
8	13.9	13.2	10.4	11.5	15.0	12.3
9	13.2	12.6	12.3	12.5	18.5	13.9
10	13.4	12.7	12.6	12.7	16.1	13.6
11	14.1	13.4	12.3	11.9	14.6	12.9
12	14.7	14.0	15.1	19.8	23.7	18.7
13	15.0	14.3	28.0	33.9	38.7	29.8
14	15.3	14.6	33.9	31.4	37.2	35.6
15	15.4	14.6	41.1	30.2	34.7	37.6
16	16	15.3	52.0	29.4	33.5	38.2
17	15.6	14.8	50.6	29.5	36.4	37.1
18	15	14.3	45.0	30.6	38.9	38.2
19	14.7	13.9	63.5	33.9	45.0	44.0
20	14.8	14	77.7	34.1	49.1	47.1
21	14.8	14	87.9	35.3	51.5	48.1
22	14.3	13.5	96.3	37.2	52.5	47.6
23	14.3	13.5	98.9	41.7	53.5	50.2
24	15	14.0	104.8	49.0	56.6	51.7
25	15.8	14.7	112.4	57.0	58.8	53.1
26	17.4	15.9	117.5	63.9	62.5	55
27	17.3	15.8	122.2	74.2	64.7	57.2
28	17.4	15.8	129.3	88.5	65.9	61.7
29	17.8	16.3	139.4	105.3	67.4	69.1
30	17.5	16	157.4	132.2	66.3	73.7
31	18.1	16.5	174	157.5	69.5	78.2
32	20.4	18.4	190.9	175.0	69.5	83.4
33	20.6	18.5	222.8	190.6	72.9	93.5
34	19.8	17.9	235.6	202.0	76.6	100.4
35	19.1	17.2	234.1	209.3	77.7	107.8
36	19.5	17.7	238.2	217.9	80.5	116.2
37	19.9	18.0	243.8	228.1	82.7	121.9
38	19.1	17.5	259.3	237.1	89.6	125.6
39	17.5	16.3	279.2	246.5	97.1	130.1
40	17.1	16.0	293.6	257.7	102.5	135.7
41	17.1	16.0	281.3	271.1	107.6	141.8
42	17.1	15.9	271.6	285.8	115.1	149.8

43	16.6	15.6	280.1	302.5	125.3	158.7
44	16.1	15.2	292.6	320.9	136.0	167.9
45	16.0	15.2	302	339.9	148.3	179.6
46	16.3	15.3	307.5	358.6	161.4	183.4
47	16.3	15.4	315.1	378.9	171.0	187.4
48	16.5	15.5	319.5	398.7	183.0	193.1
49	16.9	15.8	323.1	417.2	196.1	201.2
50	17.5	16.4	327.8	438.9	206.6	210.3
51	17.6	16.5	333.3	457.6	221.6	221.2
52	17.5	16.5	340.3	473.6	239.5	233.4
53	17.5	16.5	349.0	485.8	245.6	245.8
54	17.8	16.8	360.6	494.5	254.2	254.4
55	18.0	17.0	370.7	503.6	267.7	260.9
56	18.2	17.3	381.3	512.9	277.3	268.4
57	17.9	17.0	392.5	523.0	280.8	282.3
58	17.6	16.7	403.0	535.1	285.8	299.9
59	17.7	16.9	411.7	546.4	291.8	317.4
60	18.3	17.5	420.7	556.1	298.1	330.5
61	18	17.2	433.2	560.7	310.0	337.9
62	17.2	16.4	450.6	566.6	322.7	346.7
63	17.1	16.3	459.0	571.7	326.9	356.9
64	17.1	16.2	464	571.9	326.2	360.4
65	17.0	16.2	467.7	569.8	326.8	371.3
66	17.8	17.1	474.7	569.1	326.1	379.8
67	18.1	17.1	474.4	570.0	325.3	387.8
68	18.0	17.0	476.0	572.6	324.0	399.9
69	17.1	16.1	479.6	576.6	322.9	408.1
70	16.6	15.7	484	580.9	323.2	416.2
71	16.5	15.6	487.9	584.5	325.1	421.1
72	16.2	15.3	492.6	588.1	328.7	426.6
73	15.8	15.0	499.1	592.7	334.7	432.6
74	15.9	15.0	507.0	598.1	340.5	437.7
75	16.0	15.2	524.0	601.5	346.5	444.2
76	16.3	15.5	540.7	605.4	353.3	450.4
77	16.4	15.5	550.6	609.5	361.7	457.3
78	16.4	15.4	561.1	612.5	370.2	464.1
79	16.1	15.1	571.3	615.1	380.8	470.8
80	16.4	15.3	575.9	617.9	390.7	476.4
81	16.8	15.7	577.4	619.4	399.4	478.9
82	16.7	15.7	588.1	621.2	411.3	484.5
83	17.0	16.0	592.0	623.5	423.8	486.7
84	17.4	16.4	596.9	624.9	435.7	489.1
85	17.3	16.3	595.5	627.9	446.1	492.3
86	17.8	16.8	595.9	630.3	458.5	495.0
87	17.3	16.3	598.8	633.9	480.6	501.6
88	17.3	16.4	603.5	636	494.8	504.9
89	17.1	16.2	607.5	637.5	503.2	507.6
90	17.0	16.0	612.5	639.9	509.9	513.6

91	16.9	16.0	617.8	642.2	516.3	519.5
92	16.8	15.9	648.2	648.1	542.6	549.1
93	16.7	15.8	709.6	659.7	588.4	642.7
94	17.2	16.2	760.9	685.7	628.3	687.5
95	17.5	16.5	798.3	707.6	675.9	738.7
96	17.4	16.4	848.7	722.3	703	790.9
97	17.3	16.4	888.4	735.8	726.2	814.1
98	17.7	16.8	937.1	757.6	745.9	828.1
99	17.6	16.7	918.8	765.2	741.3	811.1
100	17.1	16.2	931.6	786.6	751.7	822.0
101	17.0	16.1	949.0	795.2	767.3	836.3
102	17.0	16.2	970.9	802.8	775.0	852.7
103	17.1	16.3	978.0	812.9	757.7	834.8
104	16.9	16.1	951.6	822.4	737.7	815.5
105	16.6	15.7	966.4	824.4	743.5	817.7
106	16.7	15.8	972.9	822.5	746.1	821.2
107	16.5	15.4	986.1	829.9	731.8	824.6
108	16.7	15.7	1016.3	833.9	726.0	821.4
109	16.7	15.7	1005.5	836.2	725.6	813.8
110	16.6	15.7	1007.9	834.8	727.8	814.8
111	16.6	15.9	1030.1	835.1	733.1	837.8
112	16.6	15.9	1007.7	838.7	739.8	837.9
113	16.6	15.8	982.1	835.7	737.1	811.1
114	16.8	15.9	960.4	834.8	740.4	837.0
115	16.9	16.1	949.4	830.6	738.6	844.1
116	17.1	16.3	946.2	825.9	739.1	863.5
117	17.7	16.9	943.2	821.7	739.7	870.0
118	18.2	17.1	941	815.2	738.5	878.1
119	17.8	16.7	946.5	812.1	739.5	883.7
120	17.6	16.4	959.9	806.1	743.0	886.2
121	17.7	16.5	971.7	802.1	752.2	892.2
122	17.7	16.5	976.3	799	761.9	902.5
123	17.9	16.6	982.2	795.1	772.8	912.6
124	17.3	15.9	993.3	795.0	794.2	917.6
125	17.0	15.6	1014.7	796.1	784.0	917.3
126	17.3	15.9	1047.4	796.7	764.7	908.3
127	17.6	16.3	1071.8	793.3	754.3	903.7
128	17.4	16.2	1074.3	793.9	750.5	888.6
129	17.6	16.3	1058.1	787.7	736.7	856.7
130	17.6	16.4	1050	784.5	730.0	829.0
131	17.4	16.3	1044.6	779.8	721.3	807.4
132	17.4	16.3	1043.0	775.1	715.0	799.2
133	17.9	16.8	1037.4	770.9	710.4	803.6
134	17.7	16.6	1023.3	768.1	707.3	806.3
135	17.1	16.0	1020.5	772.7	706.4	794.0
136	17.0	15.9	1020.8	777.5	703.5	777.9
137	17.6	16.5	1010.0	771.6	702.2	769.8
138	18.0	16.8	994.8	770.0	702.4	779.7

139	18.1	16.9	983.3	787.1	702.8	789.4
140	18.3	17.1	976.4	791.0	702.7	791.5
141	18.3	16.9	970.3	790.8	702.5	800.1
142	18.2	17.0	966.9	787.3	702.3	806.4
143	18.2	16.9	962.6	782.6	702.8	805.7
144	17.9	16.6	957.6	777.6	703.4	806.3
145	18.2	16.9	952.5	771.1	703.8	811.4
146	18.1	16.8	949.5	766.9	704.7	821.9
147	17.8	16.4	946.6	773.4	703.1	834.9
148	17.8	16.5	940.0	768.4	698.3	814.9
149	17.6	16.3	930.7	769.9	694.5	808.4
150	17.5	16.3	920.6	801.9	698.0	806.2
151	17.4	16.2	908.5	809.8	712.6	783.0
152	17.1	16	895.9	812.0	722.0	770.1
153	17.0	16.0	883.7	812.2	724.6	762.0
154	17.2	16.1	872.8	808.8	720.8	766.4
155	16.8	15.8	863.6	803.3	719.7	781.8
156	16.6	15.7	856.0	797.7	724.4	784.9
157	16.4	15.5	849.2	789.3	719.9	772.0
158	16.2	15.3	842.6	789.5	709.7	757.6
159	16.2	15.2	836.1	787.8	703.5	746.7
160	16.3	15.3	830.5	787.2	698.2	738.1
161	16.6	15.5	826.2	785.5	693.4	733.0
162	17.0	16.0	821.5	780.5	688.4	732.4
163	17.2	16.1	817.1	773.5	683.9	734.4
164	17.3	16.2	813.4	764.5	681.6	737.5
165	17.5	16.4	811.0	752.9	680.5	740.8
166	17.5	16.3	808.9	743.9	679.4	745.1
167	17.1	16.0	806.0	737.5	678.5	752.1
168	16.8	15.7	802.6	737.6	681.2	766.2
169	17.0	15.9	800.2	756.0	684.6	779.4
170	17.2	16.1	797.9	767.6	688.1	791.0
171	17.2	16.1	794.5	747.8	690.0	792.7
172	17.1	16.0	789.9	720.1	685.2	789.5
173	17.1	16.0	785.6	701.7	682.5	788.1
174	17.1	16.0	781.2	687.8	679.5	781.7
175	17.1	16	776.3	676.9	670.2	777.7
176	17.3	16.2	771.2	668.6	660.5	779.2
177	17.2	16.2	766.8	662.7	652.3	783.4
178	17.0	16.0	762.7	658.9	646.1	789.3
179	16.5	15.5	758.8	656.0	640.4	793.5
180	16.3	15.4	754.7	653.0	635.2	801.5
181	16.3	15.5	750.8	650.1	631.1	811.2
182	16.3	15.5	748.0	647.4	627.7	822.8
183	16.4	15.6	746.2	644.7	624.6	837.7
184	16.9	16.0	745.2	642.3	623.3	834.2
185	17.1	16.2	743.6	640.4	635.2	812.1
186	17.1	16.1	740.2	636.8	646.7	813.3

187	16.9	16	736.4	631.0	652.8	842.4
188	16.8	16.0	731.3	624.5	657.0	857.9
189	17.0	16.2	725.5	618.7	655.3	869.7
190	16.6	15.7	720.0	613.3	654.7	880.1
191	16.3	15.5	715.3	608.3	655.8	893.2
192	16.2	15.5	710.6	603.6	657.9	902.7
193	16.3	15.5	705.8	598.7	661.8	907.5
194	16.3	15.5	701.1	594.0	672.5	913.0
195	16.4	15.6	696.4	589.3	689.7	908.2
196	16.4	15.5	691.5	584.7	698.1	888.7
197	16.3	15.3	685	579.6	692.6	874.6
198	16.4	15.4	677.8	574.7	684.0	867.0
199	16.5	15.5	670.0	570.3	675.7	856.8
200	16.7	15.7	662.5	565.8	669.6	851.5
201	17.1	16.1	655.7	561.6	665.5	854.5
202	17.4	16.4	649.2	557.4	663.0	861.9
203	17.2	23.8	643.6	553.4	661.5	865.0
204	17	32.3	638.4	549.5	661.1	864.0
205	16.8	22.7	633.9	545.5	660.8	860.5
206	16.8	18.6	629.8	541.7	660.4	856.3
207	16.8	17.2	625.9	537.9	659.7	851.4
208	17.0	16.8	622.2	534.1	658.6	848.6
209	17.1	16.6	618.4	530.1	656.6	847.9
210	17.1	16.5	614.2	525.9	654.2	846.7
211	17.3	16.6	610.3	521.8	652.3	844.5
212	17.3	16.5	606.4	517.6	651.6	840.9
213	17.4	16.6	602.3	513.3	651.8	836.3
214	17.3	16.5	597.9	509.1	653.4	831.3
215	17.4	65.5	593.8	504.9	655.9	826.9
216	17.6	660.1	589.4	500.6	656.2	821.1
217	17.7	195.4	585.1	496.3	656.0	813.8
218	17.0	81.6	581.0	492.0	656.7	794.7
219	16.9	43.8	577.2	488.0	663.4	778.8
220	17	28.9	573.3	483.2	674.0	768.5
221	17.2	22.7	569.1	477.9	682.7	761.8
222	17.3	19.9	564.9	472.8	690.4	757.5
223	17.1	18.6	560.5	467.9	700.4	755.0
224	16.7	18.0	556.2	463.1	713.5	754.7
225	16.9	17.6	551.7	458.7	718.8	753.8
226	16.9	17.4	546.8	454.3	719.4	749.3
227	16.7	17.0	541.4	450.2	714.0	746.9
228	16.6	16.7	535.6	446.5	703.1	745.9
229	16.8	16.5	530.2	442.6	686.2	730.9
230	16.9	16.4	523.4	437.8	664.2	711.1
231	17.0	16.2	514.7	432.4	644.9	694.8
232	16.6	15.8	505.9	426.6	627.2	679.0
233	16.5	15.6	497.6	421.0	608.1	663.7
234	16.5	15.4	489.9	415.6	591.5	647.0

235	16.6	15.3	482.3	410.3	576.5	632.2
236	16.6	15.4	475.5	405.4	564.2	618
237	16.7	15.6	468.8	400.5	553.4	604.5
238	16.7	15.8	462.8	396	534.3	591.6
239	17.9	16.0	457.0	390.6	507.5	579.5
240	18.4	16.3	451.8	377.3	481.8	556.7
241	17.4	16.4	447.0	361.7	455.3	527.6
242	16.7	16.3	442.7	347.1	433.2	501.4
243	16.5	16.5	438.9	331.6	413.0	473.9
244	17.2	17.1	436.2	322.8	398.5	451.4
245	17.7	17.4	433.9	313.6	382.0	426.7
246	17.8	17.6	18.8	299.2	360.5	402.5
247	17.8	17.5	5.1	287.2	342.2	380.6
248	17.7	17.5	12.7	276.2	326.5	360.8
249	17.7	17.8	15.9	264.4	311.5	342.6
250	17.9	18.0	17.0	253.6	297.6	325.7
251	18.2	18.2	17.7	244.7	284.6	310.3
252	18.1	18.1	18.0	236.9	272.9	295.9
253	18.0	18.0	18.4	229.6	263.2	282.3
254	17.8	17.9	18.3	221.5	253.1	269.0
255	17.8	17.9	18.3	214.1	244.1	256.8
256	17.9	17.9	18.4	208.3	235.7	245.2
257	17.9	18.0	18.5	201.4	228.3	233.2
258	17.9	18.1	18.4	193.0	221.5	226.5
259	17.9	17.9	18.4	185.5	213.6	216.1
260	17.6	17.9	18.6	178.7	206.0	205.9
261	17.6	17.9	211.2	172.4	199.0	196.6
262	17.7	17.8	18	166.8	193.2	188.2
263	17.8	17.6	18.4	161.3	187.8	180.6
264	17.7	17.4	18.7	155.8	181.4	173.0
265	17.4	17.2	19.7	151.6	175.6	165.7
266	17.2	17.1	22.1	147.8	171.3	158.8
267	17.2	17.0	24.5	143.8	167.4	152.7
268	17.4	16.8	18.1	139.6	163.4	146.9
269	18.2	16.4	19.6	136.3	159.9	141.4
270	18.4	16.0	19.7	133.0	156.0	136.4
271	18.4	16.2	32.0	129.8	151.8	131.9
272	18.3	16.4	32.6	127.2	148.0	128.0
273	18.4	16.3	33.0	124.2	145.1	124.9
274	18.4	16.3	33.3	121.5	142.1	121.6
275	18.3	16.7	33.4	118.9	139.0	118.5
276	18.1	16.6	32.7	116.4	136.1	115.3
277	17.9	16.6	32.7	113.7	132.9	112.2
278	17.9	16.3	31.7	109.1	127.4	108.2
279	17.6	16.6	32.3	107.5	125.6	104.5
280	17.6	16.9	35.5	122.5	152.4	102.1
281	17.8	16.9	41.9	167.6	177.2	100.9
282	17.8	16.7	47.1	173.1	182.1	101.4

283	17.7	16.8	40.5	166.3	186.4	105.0
284	17.6	16.9	35.8	157.1	168.4	108.3
285	17.5	17.0	40.6	150.3	154.3	108.1
286	17.6	16.9	39.8	150.1	157.6	109.5
287	17.6	17.1	31.4	149.5	172.7	117.6
288	17.5	17.3	42.3	165.2	222.6	138.7
289	17.2	17.4	129.2	236.5	332.4	175.8
290	17.2	17.5	207.2	295.7	447.7	222.8
291	17.2	17.7	325.6	340.9	533.5	267.1
292	17.2	17.6	438.1	404.7	587.2	308.1
293	17.3	17.6	509.8	450.3	644.5	348.5
294	17.2	17.6	559.5	457.5	679.5	395.2
295	17.2	17.5	569.9	485.2	716.8	441.9
296	17.0	17.3	575.5	505.0	704.4	480.4
297	16.9	17.1	604.9	521.4	649.7	504.6
298	17.0	17.0	627.2	553.9	645.5	540.9
299	16.9	17.3	667.5	570.9	667.9	581.4
300	16.8	17.4	661.0	593.1	676.3	611.5
301	16.8	17.3	679.2	610.8	689.0	635.2
302	16.9	17.5	681.1	616.0	709.3	652
303	17.2	17.5	728.0	630.3	760.7	661.6
304	17.3	17.1	692.2	646.3	781.5	669.7
305	17.1	17.0	710.7	656.7	788.2	675.7
306	17.1	17.0	743.0	671.9	780.8	681.2
307	17.3	16.7	716.0	671.2	746.2	675.4
308	17.2	16.3	716.8	671.8	714.8	674.0
309	17.2	15.9	736.2	672.0	703.9	684.4
310	17.1	15.8	718.8	670.2	703.2	698.7
311	17.0	15.8	749.1	668.8	708.7	711.8
312	16.7	15.8	750.0	668.6	726.2	721.3
313	16.8	15.9	763.7	670.6	749.8	726.9
314	16.8	16.2	767.7	671.3	775.6	727.1
315	16.8	16.3	787.2	672.1	794.6	727.2
316	16.8	16.4	752.1	674.3	813.8	729.1
317	16.8	16.5	760.2	677.0	823.8	729.3
318	16.7	16.3	777.2	676.8	818.9	727.0
319	16.8	16.3	759.9	677.6	817.9	723.7
320	16.9	16.1	632.0	680.4	821.8	718.9
321	16.7	16.3	522.5	682.0	824.1	714.0
322	16.7	16.4	491.1	683.6	830.0	707.6
323	16.6	16.2	531.0	686.5	826.3	705.3
324	16.5	16.0	497.5	686.5	790.3	699.7
325	16.5	15.8	443.5	686.1	765.2	699.7
326	16.4	15.8	410.5	686.1	748.7	703.2
327	16.5	15.9	376.8	685.5	736.4	707.1
328	16.5	15.9	348.0	684.2	728.8	710.8
329	16.5	16.2	341.9	683.9	724.2	717.1
330	16.4	16.5	353.2	685.3	729.0	710.7

331	16.4	16.7	344.9	684.1	742.3	697.5
332	16.3	16.9	330.9	682.8	752.7	688.0
333	16.3	17.0	320.5	681.6	757.8	683.3
334	16.2	17.0	307.5	680.7	761.2	681.3
335	16.2	16.7	293.6	681.2	772.1	680.6
336	16.1	16.3	281.1	682.5	785.9	677.8
337	16.0	16.2	276.4	684.9	792.8	674.5
338	16.2	16.1	301.3	687.8	778.2	672.5
339	16	16.3	278.1	687.5	752.8	668.6
340	16.1	16.4	260.9	687.5	738.3	666.2
341	16.2	16.5	246.9	687.5	731.5	667.8
342	16.3	16.8	236.7	689.4	733.7	670.5
343	16.4	16.9	227.0	694.2	733.0	669.7
344	16.3	17.0	220.9	697.0	734.2	668.8
345	16.3	16.9	212.1	699.8	736.5	668.0
346	16.2	16.6	204.9	702.6	737.9	665.4
347	16.3	16.4	197.8	704.8	745.8	660.8
348	16.2	16.4	197.3	705.6	772.4	656.9
349	16.3	16.5	190.8	703.6	796.5	655.2
350	16.1	16.7	182.7	700.8	809.0	654.0
351	16.1	16.8	175.5	699.1	817.9	654.5
352	16.2	16.7	169.8	697.4	825.8	655.1
353	16.2	16.8	164.8	695	825.0	654.0
354	15.9	16.8	159.2	692.8	820.4	652.1
355	16.2	16.9	152.5	691.3	816.7	650.8
356	16.2	16.9	145.4	690.7	820.8	650.6
357	16.0	16.9	139.0	691.4	823.2	651.4
358	15.9	17.0	132.9	691.1	816.4	652.6
359	15.9	17.0	127.5	691.1	806.7	652.3
360	15.6	16.9	122.4	692.3	796.3	650.2
361	15.6	16.5	118.4	694.2	785.5	648.5
362	15.6	16.0	115.8	691.9	751.2	646.5
363	15.7	15.8	113.5	691.0	718.2	642.9
364	15.6	15.8	108.6	692.6	690.5	635.4
365	15.5	15.8	104.9	699.2	667.6	626.6
366	15.6	16.0	100.2	706.6	649.0	619.9
367	15.4	16.3	96.0	712.5	630.8	615.2
368	15.5	16.5	93.2	716.6	618.7	611.6
369	15.5	16.6	107.2	713.9	615.7	608.5
370	15.6	16.7	120.8	700.7	604.4	598.8

Burn 7

Record sheet:

KWPV EXPERIMENTS: FIAVE, TRENTO, ITALIA

OPERATOR: OP
 BURN: 7

DATE: 09/09/07
 PAGE: 1

PARAMETRES

OXYGEN/SULPHUR RATIO: 2.5
 FUEL/CHARGE RATIO: 1

REACTANTS	MASS (kg)	PRODUCTS	MASS (kg)
MAGNETITE	0.83	SLAG	2.55
CHALCOPYRITE	0.99	COPPER	
MALACHITE	2.98	MATTE	
LIME	0.28	OTHER	
SILICA	0.62		

ASPIRATION (DELETE): NATURAL FAN BELLOWS
 WINDSPEED (BACKGROUND) 1.5 m/s
 WINDSPEED (ARTIFICIAL) 2.5 m/s
 AIR VOLUME (PER TUYERE)

PERFORATED FURNACE
 CRUCIBLE
 FURNACE LINING

TIMED RECORD

TIME	ACTION	DESCRIPTION
18:20	ignite	1 kg charcoal
~	power/recording on	
18:35	2nd chrg	1 kg chrg
18:45	3rd chrg	1 kg chrg
18:50	light fan	bugger, fan stopped
18:57	4th chrg	1 kg chrg
19:21	5th chrg	
19:38	6th chrg	1 kg charcoal / 1 kg metal
20:00	7th chrg	"
20:25	8th chrg	"
20:45	9th chrg	"
21:07	10th chrg	"
21:22	11th chrg	700 / 700

Burn 7

Temperatures:

Time Minutes	Channel 1 °C	Channel 2 °C	Channel 3 °C
0	16.4	17.1	17.1
1	16.3	17.1	17.1
2	16.3	16.9	17.0
3	16.0	16.5	16.9
4	15.7	16.1	16.8
5	15.8	16	16.6
6	15.9	15.9	16.5
7	15.9	15.8	16.7
8	15.8	16.0	17.4
9	15.9	16.8	17.4
10	15.5	19.4	16.6
11	15.3	21.6	16.4
12	15.2	23.0	16.2
13	15.0	23.7	16.0
14	15.0	24.6	16.2
15	15.0	24.2	16.4
16	15.0	18.9	17.3
17	15.3	19.8	17.9
18	17.0	20.4	17.6
19	19.9	20.8	18.6
20	46.8	21.9	19.3
21	79.9	25.5	19.2
22	94.8	32.0	18.9
23	111.9	43.1	20.0
24	151.6	69.2	22.3
25	197.6	116.3	26.6
26	238.8	193.1	53.9
27	278.4	240.0	106.1
28	307.1	297.4	201.4
29	330.5	340.4	278.5
30	353.6	353.7	311.6
31	383.3	387.0	380.9
32	420.3	423.0	428.5
33	459.9	452.5	467.9
34	509.8	468.0	485.8
35	566.9	482.9	511.5
36	618.1	498.7	533.2
37	646.0	523.0	554.3
38	656.4	551.7	586.5
39	653.9	576.4	610.1
40	658.4	604.6	604.4
41	674.5	631.7	594.9
42	664.4	629	544.2

43	648.6	614.8	537.2
44	663.1	609.2	549.5
45	686.5	596.9	560.4
46	679.4	570.0	557.0
47	648.0	546.0	542.6
48	642.6	531.9	530.1
49	680.6	533.5	536.2
50	681.0	538.0	549.1
51	669.0	560.7	609.3
52	659.9	597.4	621.8
53	650.1	630.2	621.9
54	646.3	667.4	611.7
55	646.7	699.6	624.3
56	648.3	712.0	658.7
57	656.3	728.7	672.2
58	669.3	750.4	664.8
59	676.4	773.2	657.4
60	676	761.3	650.7
61	675.3	721.7	636.0
62	678.8	733.1	616.3
63	681.7	740.1	617.5
64	684.8	719.1	635.9
65	691.5	703.6	649.5
66	702.7	694.9	663.6
67	709.0	686.3	685.7
68	720.1	681.7	706.3
69	724.3	679.0	711.3
70	726.9	679.3	717.3
71	726.0	678.1	721.4
72	750.1	683.6	718.9
73	762.5	677.7	743.9
74	754.2	672.3	774.7
75	754.5	665.8	769.3
76	751.1	662.6	761.0
77	745.5	662.8	758.8
78	740.4	663.5	753.8
79	742.8	662.2	751.9
80	754.8	662.0	751.1
81	764.8	663.9	744.7
82	765.8	663.6	732.2
83	758.5	658.9	719.5
84	761.3	655.0	732.3
85	769.3	651.4	739.0
86	782.4	649.8	746.6
87	797.4	650.1	757.6
88	802.8	651.5	758.2
89	803.4	652.2	769.5
90	799.2	653.5	767.8

91	810.0	659.2	773.5
92	807.9	664.0	803.9
93	799.0	660.0	796.5
94	803.1	658.5	794.9
95	799.1	651.4	801.2
96	788.9	642.4	803.7
97	781.7	635.3	807.9
98	778.0	629.9	810.7
99	771.2	625.9	813.3
100	771.2	622.8	817.7
101	788.0	620.4	828.9
102	801.5	618.3	835.4
103	782.5	618.4	829.2
104	762.6	620.5	816.0
105	748.0	616.0	802.0
106	734.2	613.1	796.9
107	724.6	611.1	793.9
108	723.5	608.8	793.3
109	718.9	606.0	811.2
110	714.3	602.9	834.0
111	719.8	599.6	825.1
112	735.3	596.8	802.0
113	747.3	594.2	774.5
114	768.7	592.2	772.5
115	777.2	590.5	779.1
116	773.6	589.0	769.1
117	767.7	588.4	761.2
118	763.3	587.9	744.6
119	790.1	587.4	745.3
120	806.9	586.8	746.0
121	819.2	586.2	741.1
122	826.0	597.7	728.2
123	862.7	706.4	729.6
124	893.8	794.1	725.5
125	923.3	858.9	714.2
126	940.4	904.8	714.1
127	940.1	929.3	707.9
128	953.2	935.5	691.2
129	905.3	880.8	669.2
130	885.7	910.7	649.9
131	890.7	954.2	629.8
132	911.1	974.0	612.2
133	924.4	977.7	604.4
134	926.0	990.0	608.8
135	926.2	1019.6	619.1
136	966.2	1029.8	622.6
137	1002.2	1034.1	623.8
138	996.4	1034.9	638.5

139	992.1	1031.6	645.6
140	996.1	1026.9	642.6
141	1008.3	1017.1	642.2
142	1016.0	1033.3	644.2
143	1014.7	1038.3	682.9
144	1022.2	1033.2	732.8
145	1032.4	1025.6	728.2
146	1024.7	1034.7	732.9
147	1008.8	1034.6	719.1
148	983.8	1041.8	697.9
149	955.9	1056.9	678.1
150	928.3	1053.6	662.2
151	919.4	999.5	690.7
152	908.7	1006.6	719.3
153	905.2	1034.0	737.3
154	899.2	1072.8	733.1
155	893.3	1095.6	736.3
156	888.1	1125.0	744.5
157	888.4	1106.3	750.8
158	889.3	1111.5	753.4
159	881.5	1136.2	750.4
160	870.9	1105.5	754.4
161	861.1	1084.4	759.7
162	853.1	1061.8	761.6
163	841.8	1042.3	754.3
164	825.8	1046.3	733.6
165	808.0	1035.4	717.8
166	791.6	1049.4	693.6
167	777.4	1055.9	667.2
168	767.2	1047.7	634.2
169	763.8	1054.4	598.1
170	777.0	1064.8	601.2
171	791.9	1034.6	660.2
172	791.2	1062.8	655.5
173	786.0	1079.4	645.6
174	781.7	1077.4	639.0
175	775.5	1057.4	632.7
176	774.9	1044.9	628.1
177	780.3	1056.3	624.4
178	787.7	1053.6	624.9
179	792.8	1059.1	625.7
180	788.3	1069.3	628.8
181	779.2	1070.1	643.5
182	765.0	1037.1	687.4
183	753.9	1042.8	715.2
184	748.5	1024.7	718.9
185	747.0	999.4	715.8
186	749.0	988.0	727.5

187	749.5	997.9	736.7
188	741.7	1011.6	742.0
189	738.8	1008.1	742.7
190	734.1	1021.1	740.9
191	727.1	1041.5	739.9
192	719.4	1048.0	737.6
193	716.6	1047.4	728.3
194	712.4	1047.8	728.0
195	705.4	1049.7	718.3
196	697.0	1044.1	713.1
197	688.4	1023.9	728.0
198	685.5	1017.3	737.7
199	681.9	1027.9	736.7
200	676.8	1038.5	736.7
201	670.3	1032.5	751.1

Burn 8

Record sheet:

KWPV EXPERIMENTS: FIAVE, TRENTO, ITALIA

OPERATOR: OP DATE: 09/09/07
 BURN: 8 PAGE: 1

PARAMETRES

OXYGEN/SULPHUR RATIO: 1
 FUEL/CHARGE RATIO: 1

REACTANTS	MASS (kg)	PRODUCTS	MASS (kg)
MAGNETITE	<u>0.74</u>	SLAG	} 2.02
CHALCOPYRITE	<u>0.88</u>	COPPER	
MALACHITE	<u>1.06</u>	MATTE	
LIME	<u>0.29</u>	OTHER	
SILICA	<u>0.76</u>		
	<u>3.73</u>		

ASPIRATION (DELETE): NATURAL FAN BELLOWS
 WINDSPEED (BACKGROUND) 1.5
 WINDSPEED (ARTIFICIAL) 7.5
 AIR VOLUME (PER TUYERE)

PERFORATED FURNACE Y N
 CRUCIBLE Y N
 FURNACE LINING Y N

TIMED RECORD

TIME	ACTION	DESCRIPTION
<u>10:45</u>	<u>1st ch</u>	<u>2 kg charcoal</u>
<u>11:20</u>	<u>3rd ch</u>	<u>1 kg charcoal</u>
<u>11:44</u>	<u>4th ch</u>	<u>1 kg ch</u>
<u>11:51</u>	<u>5th ch</u>	<u>1 kg</u>
<u>12:08</u>	<u>6th ch</u>	<u>1 kg charcoal / 1 kg needs</u>
<u>12:30</u>	<u>7th ch</u>	<u>725/725</u>
<u>12:28</u>	<u>7th ch</u>	<u>~</u>
<u>13:04</u>	<u>8th ch</u>	<u>~</u>
<u>13:30</u>	<u>9th ch</u>	<u>725/725</u>
<u>13:58</u>	<u>End of</u>	

Burn 8

Temperatures:

Time Minutes	Channel 1 °C	Channel 2 °C	Channel 3 °C
0	18.9	18.1	20.5
1	19.0	18.3	20.6
2	19.5	18.6	20.8
3	20.2	19.1	21.2
4	21.0	19.3	21.4
5	21.1	19.3	21.3
6	19.0	17.0	19.5
7	17.8	15.3	17.6
8	17.1	14.6	16.8
9	17.0	14.6	16.6
10	17.1	14.6	16.5
11	17.2	14.2	16.2
12	18.1	14.2	15.8
13	20.4	14.2	15.6
14	26.0	14.6	15.7
15	32.5	15.2	16.7
16	48.7	16.2	18.5
17	72.8	17.7	27.9
18	94.2	19.5	51.1
19	101.7	21.4	79.0
20	133.7	24.5	110.1
21	174.7	28.9	139.7
22	173.3	32.2	204.7
23	189.3	36	256.2
24	212.9	40.6	284.2
25	236.2	46.5	305.6
26	255.0	53.1	323.9
27	271.1	62.1	334.0
28	283.0	76.2	343.5
29	296	92.6	350.3
30	317.6	109.9	358.3
31	331.6	170.7	368.4
32	335	243.1	380.5
33	334.9	293.2	388.7
34	334.9	314.3	383.1
35	331.7	321.3	369.7
36	329.5	325.8	356.5
37	329.8	329.7	345.0
38	262.2	293.1	333.4
39	237.2	292.5	330.3
40	271.2	338.9	369.1
41	317.2	425.9	403.3
42	373.2	469.3	447.2

43	421.0	468.3	507.2
44	453.4	473.4	536.2
45	479.6	487.7	524.3
46	496.1	503.5	511.9
47	507.2	500.3	508.9
48	509.2	498.7	507.4
49	514.8	504.7	500.9
50	517.0	512.0	490.9
51	512.4	504.1	478.9
52	505.7	505.5	469.2
53	500.7	501.4	460.2
54	486.9	503.6	451.5
55	476.4	501.4	443.8
56	468.9	495.3	436.5
57	461.4	509.0	434.3
58	452.3	505.1	428.4
59	442.1	497.6	417.7
60	409.2	489.5	372.2
61	404.8	525.2	302.0
62	456.8	575.2	263.4
63	503.9	609.8	278.7
64	536.3	636.8	331.0
65	563.7	649.9	375.2
66	584.4	643.2	453.6
67	597.3	643.0	507.1
68	606.3	646.7	535.9
69	589.7	661.8	557.1
70	602.3	676.9	642.9
71	628.3	694.9	689.5
72	662.3	719.3	724.2
73	685.9	728.1	734.3
74	707.1	741.2	742.3
75	730.6	758	743.8
76	746.9	760.3	727.6
77	773.7	766.5	687.7
78	787.4	777.4	663.3
79	796.9	825.0	652.3
80	815.9	847.7	638.9
81	826.9	843.5	620.4
82	828.8	844.6	602
83	828.5	839.5	582.8
84	786.2	803.8	555.2
85	752.0	795.7	465.6
86	746.2	812.1	427.8
87	747.1	817.3	449.1
88	750.6	814.0	525.8
89	746	812.6	597.6
90	740.8	808.8	622.7

91	739.8	813.0	651.9
92	743.4	823.0	670.9
93	754.0	830.8	687.0
94	757.3	829.8	702.8
95	749.9	796.3	722.5
96	749.3	775.0	719.9
97	768.6	768.6	715.2
98	783.9	768.1	664.6
99	789.5	764.0	611.4
100	790.5	762.7	563.7
101	793.8	764.5	522.7
102	766.0	763.5	502.7
103	705.5	755.9	461.3
104	647.2	737.2	436.7
105	641.7	714.0	430.0
106	661.5	703.3	407.5
107	686.4	699.2	389.1
108	709.6	697.8	377.3
109	726.4	698.6	371.2
110	737.8	698.7	369.0
111	748.9	699.8	378.1
112	757.5	701.1	384.4
113	765.5	704.0	380.8
114	768.4	707.3	379.6
115	759.6	707.4	399.8
116	760.4	706.6	416.7
117	765.8	706.1	427.5
118	769.8	705.4	431.9
119	769.6	704.4	438.8
120	771.3	705.7	455.0
121	773.7	707.3	488.9
122	761.8	708.6	551.7
123	748.5	707.9	612.7
124	740.1	704.8	661.2
125	733.8	701.5	688.3
126	727.7	699.1	706.3
127	721.5	697.1	717.6
128	717.7	695.7	724.9
129	713.5	694.5	728.3
130	709.5	693.5	726.7
131	708.1	693.7	718.6
132	706.8	692.3	699.4
133	704.9	691.0	672.9
134	702.6	690.4	651.7
135	700.7	688.2	630.4
136	710.0	685.2	623.8
137	719.9	681.1	622.5
138	707.9	676.1	626.7

139	684.5	673.4	586.6
140	672.7	666.3	569.8
141	668.1	657.9	559.1
142	666.6	649.0	556.9
143	664.9	640.7	547.5
144	663.8	633.2	536.6
145	664.1	624.6	527.0
146	664.4	616.8	527.7
147	665.9	609.7	526.4
148	669.4	603.1	521.5
149	673.3	596.8	513.7
150	677.5	591.2	499.1
151	681.6	586.4	492.7
152	684.9	581.6	482.6
153	686.9	576.3	464.4
154	688.9	571.5	454.2
155	691.1	567.6	454.6
156	691.2	564.1	458.4
157	690.7	561.1	465.7
158	686.4	557.6	476.4
159	680.7	555.1	489.8
160	678.0	551.4	509.9
161	684.2	549.6	523.7
162	689.3	551.6	512.4
163	693.1	554.2	501.4
164	691.6	555.9	526.4
165	681.3	557.2	500.7
166	670.7	558.0	481.4
167	661.7	558.4	466.3
168	653.3	559.0	455.2
169	645.8	558.7	447.0
170	639.1	558.2	441.1
171	628.7	557.9	436.0
172	619.7	556.6	430.6
173	613.8	555.6	426.0
174	610.5	554.1	422.6
175	609.7	552.7	417.5
176	611.8	551.2	411.0
177	618.7	549.3	404.5
178	625.8	546.9	398.2
179	634.3	544.5	389.7
180	634.7	543.1	394
181	630.4	541.1	416.1
182	630.2	538.3	435.4
183	632.5	535.2	444.6
184	634.1	532.2	435.5
185	635.2	529.2	423.9
186	636.3	526.5	409.5

187	636.0	523.9	394.2
188	634.6	521.6	380.7
189	632.8	519.1	367.3
190	631.0	517.2	355.0
191	630.1	515.3	342.8
192	629.9	513.6	329.6
193	629.0	511.8	321.2
194	623.3	509.3	339.0
195	613.4	507.5	352.0
196	603.2	505.5	359.9
196	596.4	504.0	363.4

Burns 9

Record sheet:

KWPV EXPERIMENTS: FIAVE, TRENTO, ITALIA

OPERATOR: *OP* DATE: *10/9/07*
 BURN: *9* PAGE: *1*

PARAMETRES

OXYGEN/SULPHUR RATIO: *2.5*
 FUEL/CHARGE RATIO: *2*

REACTANTS	MASS (kg)	PRODUCTS	MASS (kg)
MAGNETITE	<i>0.83</i>	SLAG	} <i>< 3</i>
CHALCOPYRITE	<i>0.98</i>	COPPER	
MALACHITE	<i>2.98</i>	MATTE	
LIME	<i>0.28</i>	OTHER	
SILICA	<i>0.62</i>		
	<i>5.69</i>		

ASPIRATION (DELETE): *NATURAL* FAN BELLOWS

WINDSPEED (BACKGROUND) *15*
 WINDSPEED (ARTIFICIAL) *7.5*
 AIR VOLUME (PER TUYERE)

PERFORATED FURNACE Y/N
 CRUCIBLE Y/N
 FURNACE LINING Y/N

TIMED RECORD

TIME	ACTION	DESCRIPTION
<i>10:00</i>	<i>logging on</i>	
<i>10:07</i>	<i>ignited</i>	<i>2 kg charcoal</i>
<i>10:10</i>	<i>3rd charge</i>	<i>1 kg charcoal</i>
<i>10:15</i>	<i>temp restored</i>	<i>problem with probe 8</i>
<i>10:20</i>	<i>4th charge</i>	<i>1 kg charcoal</i>
<i>10:30</i>	<i>5th charge</i>	<i>" "</i>
<i>10:38</i>	<i>6th charge</i>	<i>2 kg charcoal / 1 kg mineral</i>
<i>10:52</i>	<i>7th charge</i>	<i>" "</i>
<i>11:10</i>	<i>8th charge</i>	<i>" "</i>
<i>11:32</i>	<i>9th charge</i>	<i>" "</i>
<i>12:00</i>	<i>10th charge</i>	<i>" "</i>
<i>12:18</i>	<i>11th charge</i>	<i>970 / 1940</i>
<i>12:56</i>	<i>12th charge</i>	<i>1 kg charcoal only</i>
<i>13:20</i>	<i>all off</i>	

Burns 9

Temperatures:

Time Minutes	Channel 6 °C	Channel 7 °C	Channel 8 °C
0	609.6	151.7	22.9
1	622.7	163.5	22.8
2	583.6	193.7	22.8
3	552.5	229.5	22.9
4	528.6	256.9	22.6
5	519.4	272.0	21.8
6	520.5	275.5	21.0
7	518.2	273.7	20.3
8	523.3	287.9	20.0
9	534.8	326.3	20.1
10	549.1	357.7	20.1
11	566.8	389.9	19.8
12	577.6	412.4	19.5
13	563.4	438.3	19.3
14	533.8	466.8	19.1
15	506.6	487.6	18.9
16	504.5	499.7	18.8
17	473.2	507.3	18.6
18	377.5	512.1	18.5
19	389.9	532.4	18.5
20	478.6	551.9	18.6
21	559.2	569.1	18.8
22	615.8	587.1	19.1
23	608.7	603.5	19.5
24	578.1	614.5	20.1
25	576.8	614.3	20.5
26	632.7	608.4	20.5
27	682.6	601.2	20.8
28	780.5	605.4	20.7
29	814.5	621.4	20.4
30	876.7	637.1	19.9
31	936.9	647.7	19.7
32	931.1	659.7	19.9
33	914.9	683.5	20.1
34	895.0	696.4	20.0
35	902.1	695.0	20.0
36	918.7	696.5	20.2
37	912.0	703.7	19.8
38	929.1	716.7	19.4
39	954.0	721.0	19.2
40	1015.1	728.1	19.2
41	1026.5	738.5	19.1
42	1002.7	746.1	19.2

43	980.1	743.8	19.4
44	967.5	749.5	19.7
45	1015.5	759.8	20.8
46	1023.7	775.7	21.0
47	1038.7	779.2	21.7
48	1119.8	778.4	22.2
49	1163.4	798.0	21.6
50	1166.4	787.3	20.8
51	1158.1	778.4	20.3
52	1149.3	778.6	20.1
53	1157.2	786.6	20.0
54	1134.3	792.2	20.0
55	1071.7	802.1	20.1
56	1042.4	819.2	20.2
57	1015.2	814.8	20.3
58	945.8	792.1	20.6
59	999.8	794.1	20.2
60	1063.4	798.6	20.2
61	1095.4	800.5	20.5
62	1106.3	801.2	20.6
63	1092.6	803.7	20.6
64	1106.1	805.2	21.1
65	1091.3	801.3	21.6
66	1136.1	811.2	21.3
67	1187.2	824.1	22.3
68	1196.9	832.5	25.7
69	1189.5	845.1	23.9
70	1184.2	862.4	22.5
71	1172.4	881.2	22
72	1159.4	886.8	21.9
73	1158.5	892	21.8
74	1166.4	903.1	21.7
75	1214.1	908.5	22.0
76	1177.8	909.4	22.3
77	1099.5	924.0	22.6
78	1044.9	932.5	22.8
79	1039.0	941.0	22.9
80	1068.2	957.8	23.3
81	1086.4	942.3	23.9
82	1103.2	956.2	24.3
83	1091.0	980.3	24.2
84	1084.5	977.6	24.6
85	1079.7	985.2	25.4
86	1094.9	1011.1	26.2
87	1131.4	1036.1	26.8
88	1144.5	1046.8	26.7
89	1131.7	1038.7	26.5
90	1125.2	1008.4	26.1

91	1142.6	1015.3	26.5
92	1137.1	1032.4	26.8
93	1123.9	1053.0	27.0
94	1084.5	1064.3	27.4
95	1022.9	1073.6	27.7
96	985	1081.0	27.7
97	971.1	1086.2	28.4
98	986.1	1093.4	28.8
99	983.0	1097.7	29.2
100	990.9	1096.1	29.4
101	983.0	1100.7	30.1
102	935.7	1103.9	29.4
103	1002.1	1093.0	29.7
104	1085.3	1086.9	29.8
105	1127.3	1076.2	30.0
106	1143.9	1041.7	29.3
107	1212.1	1017.3	29.3
108	1227.4	1021.5	29.6
109	1222.1	1033.7	29.7
110	1194.2	1050.8	30.3
111	1188.0	1066.3	30.5
112	1184.1	1068.9	30.2
113	1186.7	1072.3	29.5
114	1227.9	1085.5	29.4
115	1180.1	1095.3	29.6
116	1178.3	1107.0	29.8
117	1226.5	1118.3	30.5
118	1249.9	1121.7	30.9
119	1231.1	1124.4	31.3
120	*****	1126.1	30.2
121	*****	1137.5	30.2
122	*****	1139.5	30.8
123	1279.2	1136.8	30.6
124	1277.4	1136.3	30.3
125	1247.9	1126.8	29.9
126	1234.6	1105.8	30.2
127	*****	1124.1	30.5
128	*****	1128.7	30.1
129	1277.8	1127.3	30.5
130	1221.0	1129.3	30.4
131	1139.8	1134.4	30.6
132	1173.0	1141.7	30.9
133	1127.7	1142.4	32.2
134	1049.2	1145.4	32.5
135	975.8	1147.4	32.2
136	981.7	1112.5	32.1
137	869.2	1112.9	31.8
138	856.1	1120.4	32.0

139	830.5	1118.8	31.2
140	792	1124.6	30.9
141	841.3	1124.8	31.4
142	899.3	1121.2	31.3
143	899.4	1115.7	31.2
144	864.7	1116.3	31.6
145	879.7	1107.7	31.3
146	933.2	1090.9	31.0
147	929.8	1071.8	30.8
148	918.2	1049.4	30.8
149	994.8	1025.4	30.8
150	1016.5	1008.2	30.7
151	965.7	996.4	31.2
152	904.6	987.7	31.3
153	835.0	980.0	31.0
154	796.9	973.7	30.6
155	755.8	968.7	31.2
156	720.6	964.7	31.4
157	760.0	961.8	30.2
158	814.3	960.4	30.3
159	887.2	960.3	30.5
160	907.6	960.4	30.1
161	837.9	962.6	30.1
162	915.3	970.4	29.9
163	944.9	993.5	30.1
164	1027.0	1024	30.5
165	1051.2	1045.2	30.3
166	1044.4	1053.3	30.2
167	973.7	1059.0	30.1
168	900.1	1060.7	29.3
169	849.3	1056.4	28.5
170	801.7	1050.7	28.4
171	802.9	1045.7	28.4
172	817.9	1041.3	28.3
173	920.5	1037.0	28.5
174	887.3	1032.0	28.8
175	786.1	1028.4	28.4
176	761.2	1027.3	28.2
177	803.0	1024.4	27.9
178	948.4	1005.0	28.0
179	967.6	996.3	27.9
180	968.5	994.7	27.2
181	963.2	990.0	26.8
182	917.1	986.6	26.5
183	886.5	984.1	26.6
184	862.4	983.4	26.9
185	800.3	969.8	26.6
186	745.2	943.7	26.1

Burns 10

Record sheet:

KWPV EXPERIMENTS: FIAVE, TRENTO, ITALIA

OPERATOR: *OP*
 BURN: *10*

DATE: *11/01/07*
 PAGE: *1*

PARAMETRES

OXYGEN/SULPHUR RATIO: *1*
 FUEL/CHARGE RATIO: *2*

REACTANTS	MASS (kg)	PRODUCTS	MASS (kg)
MAGNETITE	<i>0.78</i>	SLAG	
CHALCOPYRITE	<i>0.89</i>	COPPER	
MALACHITE	<i>1.06</i>	MATTE	
LIME	<i>0.79</i>	OTHER	
SILICA	<i>0.76</i>		

ASPIRATION (DELETE): NATURAL FAN BELLOWS
 WINDSPEED (BACKGROUND) *7.5*
 WINDSPEED (ARTIFICIAL)
 AIR VOLUME (PER TUYERE)

PERFORATED FURNACE Y/N
 CRUCIBLE Y/N
 FURNACE LINING Y/N

TIMED RECORD

TIME	ACTION	DESCRIPTION
<i>14:50</i>	<i>ignition</i>	<i>2 kg charcoal</i>
<i>-</i>	<i>fan on</i>	
<i>15:10</i>	<i>3rd charge</i>	<i>1 kg char</i>
<i>15:15</i>	<i>4th charge</i>	<i>1 kg char</i>
<i>15:22</i>	<i>5th charge</i>	<i>2 kg charcoal / 1 kg mineral</i>
<i>15:36</i>	<i>6th charge</i>	<i>2 kg charcoal / 1 kg mineral</i>
<i>15:57</i>	<i>7th charge</i>	<i>770 / #340</i>
<i>16:18</i>	<i>8th charge</i>	
<i>16:45</i>	<i>9th charge</i>	
<i>17:19</i>	<i>10th charge</i>	<i>1 kg charcoal only</i>
<i>17:42</i>	<i>fan off</i>	

Burns 10

Temperatures:

Time Minutes	Channel 6 °C	Channel 7 °C
0	22.5	29.1
1	22.8	29.5
2	23.3	30.2
3	23.6	30.2
4	23.7	30.3
5	27.9	30.3
6	36.3	28.9
7	34.0	27.8
8	61.9	27.4
9	218.6	28.0
10	307.1	29.7
11	325.0	31.4
12	258.2	31.6
13	242.0	31.5
14	238.1	32.4
15	242.5	33.1
16	248.3	33.0
17	246.5	32.7
18	235.9	33.1
19	232.6	34.0
20	240.8	34.4
21	245.1	34.4
22	239.3	35.1
23	248.3	35.6
24	247.1	36.2
25	303.6	40.1
26	453.2	56.6
27	509.7	77.7
28	593.6	89.0
29	682.7	99.5
30	587.3	104.1
31	583.7	111.9
32	702.2	123.1
33	789.1	139.2
34	832.9	161.4
35	862.7	192.1
36	766.8	242.3
37	763.2	276.4
38	870.3	299.0
39	932.7	324.3
40	923.3	344.4
41	858.9	369.8
42	805.3	389.7

43	828.8	403.3
44	850.9	419.3
45	836.7	440.0
46	821.5	458.7
47	788.8	481.6
48	884.9	503.6
49	925.8	519.3
50	940.9	535.1
51	859.7	529.6
52	806.5	506.1
53	774.6	518.5
54	800.7	543.6
55	856.0	568.9
56	935.7	583.2
57	886.3	577.2
58	949.1	578.0
59	1001.3	580.6
60	1032.8	587.9
61	1030.6	602.6
62	1047.5	620.0
63	1063.8	642.6
64	1052.9	679.9
65	1044.3	702.8
66	1023.4	720.5
67	987.1	739.3
68	931.3	751.9
69	922	765.5
70	910.9	776.4
71	852.0	793.1
72	902.2	775.4
73	789.1	756.0
74	894.5	745.4
75	1032.2	739.0
76	983.7	728.5
77	1019.1	725.7
78	1067.8	724.9
79	1038.5	727.7
80	983.7	732.0
81	993.0	730.1
82	1007.0	717.2
83	1011.5	705.3
84	1033.2	700.3
85	998.1	699.4
86	1012.8	701.9
87	1077.9	705.0
88	1105.5	709.7
89	1142.7	715.2
90	1106.4	719.6

91	1109.1	724
92	1093.7	726.8
93	1052.5	729.8
94	1100.0	729.3
95	1109.7	723.0
96	1141.4	719.1
97	1168.3	716.9
98	1169.3	716.5
99	1174.6	716.7
100	1165.0	716.9
101	1159.5	716.7
102	1152.6	716.3
103	1125	716.8
104	1105.6	716.7
105	1070.7	714.7
106	1100.5	708.4
107	1177.5	703.9
108	1210.0	700.9
109	1178.3	698.9
110	1158.4	697.2
111	1135.5	695.6
112	1122.1	693.9
113	1123.8	691.7
114	1118.1	689.4
115	1101.3	687.0
116	1085.5	684.9
117	1072.6	683.2
118	1055.9	681.7
119	1034.4	680.5
120	1016.1	679.4
121	997.6	678.6
122	977.7	677.8
123	970.5	677.2
124	957.8	676.6
125	935.4	676
126	904.3	675.3
127	868.5	674.8
128	836.6	674.7
129	802.7	674.9
130	775.2	675.2
131	751.1	675.7
132	723.3	676.5
133	697.2	677.2
134	676.5	678.4
135	679.8	680.4
136	693.0	682.1
137	709.9	684.2
138	720.3	686.5

139	714.3	688.8
140	699.3	690.9
141	688.5	691.4
142	674.3	692.1
143	655.3	692.4
144	636.8	693.2
145	648.9	693.2
146	672.3	685.6
147	675.8	679.7
148	681.4	677.9
149	682.7	678.3
150	679.3	679.9
151	679.1	681.8
152	673.7	683.8
153	654.1	686.1
154	648.8	686.6
155	645.9	685.2
156	641.8	684
157	632.5	682.9
158	619.3	682.0
159	606.6	681.7
160	593.2	681.7
161	579.4	681.2
162	562.4	680.6
163	544.0	679.7
164	524.5	678.8
165	504.6	677.9
166	486.5	677
167	469.8	676.1
168	453.3	675.1
169	441.4	674.5
170	434.9	674.3
171	428.6	673.8
172	422.1	672.8
173	415.1	671.5
174	405.7	669.8
175	393.7	668.0
176	380.2	665.8
177	364.7	663.4

Bibliography

- Adams, J. (2006) From the Water Margins to the Centre Ground? *Journal of Maritime Archaeology*, 1: 1-8.
- Adams, M. J. (1977) Style in Southeast Asian Materials Processing: Some Implications for Ritual and Art. In Merrill, R. S. (Ed.) *Material Culture: Styles, Organization and Dynamics of Technology*. St. Paul, Minnesota, West Publishing Co.: 21-52.
- Adetuji, J., Doonan, R. C., & Williams, J. (1995) Mössbauer Spectroscopy of Ancient Copper Smelting Slag. *The Journal of Mossbauer studies*, 34: 488-492.
- Ambrose, W., Allen, C., O'connor, S., Matthew Spriggs, Oliveira, N. V., & Reepmeyer, C. (2009) Possible Obsidian Sources for Artefacts from Timor: Narrowing the Options Using Chemical Data. *Journal of Archaeological Science*, 36: 607-615.
- Andrews, K. & Doonan, R. (2003) *Test Tubes and Trowels: Using Science in Archaeology*, London, Tempus.
- Anon. (1988) *The Archaeological Sites of Thailand: Central Thailand*. Bangkok, Fine Arts Department.
- Appadurai, A. (Ed.) (1986) *The Social Life of Things*, Cambridge, Cambridge University Press.
- Appadurai, A. (1998) Habitus, Techniques, Style: An Integrated Approach to the Social Understanding of Material Culture. In Stark, M. T. (Ed.) *The Archaeology of Social Boundaries*. Washington, Smithsonian Institution Press.: 232-269.
- Armstrong, L. A. (1994) Interacting Technologies: The Analysis of Ingot Moulds and Associated Industrial Ceramics from Non Pa Wai, a Prehistoric Smelting Site in Central Thailand. Unpublished Masters thesis, Department of Anthropology, University of Pennsylvania, Philadelphia.
- Arnold, D. E. (1985) *Ceramic Theory and Cultural Process*, Cambridge, Cambridge University Press.
- Artioli, G. (2007) Crystallographic Texture Analysis of Archaeological Metals: Interpretation of Manufacturing Techniques. *Applied Physics A*, 89: 899-908.
- Artioli, G., Angelini, I., Burger, E., Bourgarit, D., & Colpani, F. (2007) *Petrographic and Chemical Investigations of the Earliest Copper Smelting Slags in Italy: Towards a Reconstruction of the Beginning of Copper Metallurgy*. Paper presented at the 'Archaeometallurgy in Europe II' conference in Aquileia (Italy), 17th-21st June 2007.
- Ascher, R. (1961) Experimental Archeology. *American Anthropologist*, 63: 793-816.
- Ashmore, P. J. (1999) Radiocarbon Dating: Avoiding Errors by Avoiding Mixed Samples. *Antiquity*, 73: 124-130.
- Atkins, P. & Paula, J. D. (2002) *Atkins' Physical Chemistry*, Oxford, Oxford University Press.

- Audouze, F. (2002) Leroi-Gourhan, a Philosopher of Technique and Evolution. *Journal of Archaeological Research*, 10: 277-306.
- Bachmann, H.-G. (1982) *The Identification of Slags from Archaeological Sites*, London, Institute of Archaeology; Occasional Publication 6.
- Bacus, E. A. (2004) A Consideration of Processes Underlying Philippine Pottery Complexes. In Paz, V. (Ed.) *Southeast Asian Archaeology - Wilhelm G. Solheim II Festschrift*. Diliman, Quezon City, Manila, University of the Philippines Press: 128-157.
- Bacus, E. A. (2006) Social Identities in Bronze Age Northeast Thailand: Intersections of Gender, Status, and Ranking at Non Nok Tha. In Bacus, E. A., Glover, I. C., & Pigott, V. C. (Eds.) *Uncovering Southeast Asia's Past: Selected Papers from the 10th International Conference of the European Association of Southeast Asian Archaeologists*. Singapore, National University of Singapore.: 105-115.
- Bamberger, M. & Wincierz, P. (1990) Ancient Smelting of Oxide Copper Ore. In Rothenberg, B. (Ed.) *The Ancient Metallurgy of Copper, Researches in the Arabah, 1959-1984*. London, Institute for Archaeo-Metallurgical Studies, Institute of Archaeology, University College London.: 123-157.
- Bamforth, D. B. (2002) Evidence and Metaphor in Evolutionary Archaeology. *American Antiquity*, 67: 435-452.
- Ban Chiang Project n.d. *The Ban Chiang Project Metals Database: Homepage*. University of Pennsylvania Museum of Archaeology and Anthropology. Retrieved 28th June 2009 from <http://seasia.museum.upenn.edu/metals/Web/index.html>.
- Bayard, D. T. (1972) Early Thai Bronze: Analysis and New Dates. *Science*, 176: 1411-1412.
- Bayard, D. T. (1979) The Chronology of Prehistoric Metallurgy in Northeast Thailand. In Smith, R. B. & Watson, W. (Eds.) *Early South-East Asia: Essays in Archaeology, History and Historical Geography*. Oxford, Oxford University Press: 156-132.
- Bayard, D. T. (1980) An Early Indigenous Bronze Technology in Northeastern Thailand: Its Implications for the Prehistory of East Asia. In Loofs-Wissowa, H. H. E. (Ed.) *The Diffusion of Material Culture: 28th International Congress of Orientalists, Proceedings of Seminar E, Canberra, January 1971*. Honolulu, Hawaii, Asian and Pacific Archaeology Series No. 9, Social Science Research Institute: 191-214.
- Bayard, D. T. (1981) Temporal Distribution and Alloy Variation in Early Bronzes from Non Nok Tha. *Current Anthropology*, 22: 697-699.
- Bayard, D. T. (1984) A Tentative Regional Phase Chronology for Northeast Thailand. In Bayard, D. T. (Ed.) *Southeast Asian Archaeology at the XVth Pacific Science Congress*. Dunedin, Otago University Studies in Prehistoric Anthropology: 161-168.
- Bayard, D. T. (1996-1997) Bones of Contention: The Non Nok Tha Burials and the Chronology and Context of Early Southeast Asian Bronze. In Bulbeck, F. D. & Barnard, N. (Eds.) *Ancient Chinese and Southeast Asian Bronze Age Cultures, Volume II. The Proceedings of a Conference Held at the Edith and Joy London Foundation Property, Kioloa, NSW, Australia, 8-12 February, 1988*. Taipei, SMC

Publishing: 889-940.

- Bayley, J., Dungworth, D., & Paynter, S. (2001) *Centre for Archaeology Guidelines: Archaeometallurgy*, Swindon, English Heritage Publications.
- Bayley, J. & Rehren, T. (2007) Towards a Functional and Typological Classification of Crucibles. In Niece, S. L., Hook, D., & Craddock, P. (Eds.) *Metals and Mines: Studies in Archaeometallurgy*. London, Archetype Publications Ltd: 46-55
- Bayliss, A., Ramsey, C. B., Plicht, J. V. D., & Whittle, A. (2007) Bradshaw and Bayes: Towards a Timetable for the Neolithic. *Cambridge Archaeological Journal*, 17: 1-28.
- Bellina, B. (2001) *Témoignages Archéologiques d'échanges entre l'inde et l'asie du Sud-Est: Morphologie, Morphométrie et Techniques de Fabrication des Perles en Agate et en Cornaline*. Unpublished doctoral thesis. Université Paris III, Paris.
- Bellina, B. (2003) Beads, Social Change and Interaction between India and Southeast Asia. *Antiquity*, 77: 285-297.
- Bellina, B. (2007) *Cultural Exchange between India and Southeast Asia: Production and Distribution of Hard Stone Ornaments, VIc. BC-VIc. AD*, Paris, Editions de la Maison des sciences de l'homme.
- Bellina, B. & Glover, I. C. (2004) The Archaeology of Early Contacts with India and the Mediterranean World from the Fourth Century BC to the Fourth Century AD. In Glover, I. C. & Bellwood, P. (Eds.) *Southeast Asia, from the Prehistory to History*. London, Routledge/Curzon Press: 68-88.
- Bellina, B. (2008) Dossier - the Archaeology of Trans-Asiatic Exchange: Technological and Settlement Evidence from Khao Sam Kaeo, Peninsula Thailand. *Bulletin de l'École française d'Extrême-Orient* 2006, 93: 249-390.
- Bellina, B. & Silapanth, P. (2008) Weaving Cultural Identities on Trans-Asiatic Networks: Upper Thai-Malay Peninsula - an Early Socio-Political Landscape. *Bulletin de l'École Française d'Extrême-Orient*, 93: 257-293.
- Bellwood, P. (2005) *First Farmers: The Origins of Agricultural Societies*, Oxford, Blackwell.
- Bellwood, P. (2007) *Prehistory of the Indo-Malaysian Archipelago*, Honolulu, University of Hawaii Press.
- Bellwood, P. & Glover, I. C. (2004) Southeast Asia: Foundations for an Archaeological History. In Glover, I. C. & Bellwood, P. (Eds.) *Southeast Asia – from Prehistory to History*. London, Routledge/Curzon: 4-20.
- Bennett, A. (1988a) Prehistoric Copper Smelting in Central Thailand. In Charoenwongsa, P. & Bronson, B. (Eds.) *Prehistoric Studies the Stone and Metal Ages in Thailand*. Bangkok: 125-135
- Bennett, A. (1988b) *Copper Metallurgy in Central Thailand*. Unpublished doctoral thesis. Institute of Archaeology, University College London, London.
- Bennett, A. (1989) The Contribution of Metallurgical Studies to South-East Asian Archaeology. *World Archaeology*, 20: 329-351.

- Bennett, A. (1990) Prehistoric Copper Smelting in Central Thailand. In Glover, I. E. (Ed.) *Southeast Asian Archaeology 1986*. Oxford, BAR: 109-120.
- Bennett, A. & Glover, I. C. (1992) Decorated High-Tin Bronzes from Thailand's Prehistory. In Glover, I. (Ed.) *Southeast Asian Archaeology 1990*. Hull University, Centre for Southeast Asian Studies: 187-208.
- Bennett, A. (2008) Bronze Casting Technology in Protohistoric Southeast Asia, the Technology and Its Origins. In Pautreau, J.-P., Coupey, A., Zeitoun, V., & Rambault, E. (Eds.) *Archaeology in Southeast Asia: From Homo Erectus to the Living Traditions, Choice of Papers from the 11th Euraseaa Conference, Bougon 2006*. Chiang-Mai, European Association of Southeast Asian Archaeologists: 151-164.
- Bentley, R. A. (2008) Complexity Theory. In Bentley, R. A., Maschner, H. D. G., & Chippindale, C. (Eds.) *Handbook of Archaeological Theories*. New York, Altamira Press: 245-270
- Bentley, R. A., Hahn, M. W., & Shennan, S. J. (2004) Random Drift and Culture Change. *Proceedings of the Royal Society B*, 271: 1443-1450.
- Bentley, R. A., Lipo, C., Maschner, H. D. G., & Marler, B. (2008a) Darwinian Archaeologies. In Bentley, R. A., Maschner, H. D. G., & Chippindale, C. (Eds.) *Handbook of Archaeological Theories*. New York, Altamira Press: 109-132
- Bentley, R. A. & Maschner, H. D. G. (2008) Introduction: On Archaeological Theories. In Bentley, R. A., Maschner, H. D. G., & Chippindale, C. (Eds.) *Handbook of Archaeological Theories*. New York, Altamira Press: 1-8
- Bentley, R. A., Maschner, H. D. G., & Chippindale, C. (Eds.) (2008b) *Handbook of Archaeological Theories*, New York, Altamira Press.
- Bentley, R. A. & Shennan, S. J. (2003) Cultural Transmission and Stochastic Network Growth. *American Antiquity*, 68: 459-485.
- Berstan, R., Stott, A. W., Minnitt, S., Ramsey, C. B., Hedges, R. E. M., & Evershed, R. P. (2008) Direct Dating of Pottery from Its Organic Residues: New Precision Using Compound-Specific Carbon Isotopes. *Antiquity*, 82: 702-713.
- Bertin, E. P. (1975) *Principles and Practice of X-Ray Spectrometric Analysis*, London, Kluwer Academic Publishers.
- Bettinger, R. L. & Eerkens, J. C. (1999) Point Typologies, Cultural Transmission, and the Spread of Bow-and-Arrow Technology in the Prehistoric Great Basin. *American Antiquity*, 64: 231-242.
- Bevan, A. & Conolly, J. (2004) GIS, Archaeological Survey, and Landscape Archaeology on the Island of Kythera, Greece *Journal of Field Archaeology*, 29: 123-138.
- Bevan, A., Conolly, J., & Tsaravopoulos, A. (2008) The Fragile Communities of Antikythera. *Archaeology International*, 10: 32-36.
- Binford, L. R. (1962) Archaeology as Anthropology. *American Antiquity*, 28: 217-225.
- van Binsbergen, W. M. J. (2005) Commodification: Things, Agency, and Identities: Introduction. In Geschiere, P. L. (Ed.) *Commodification: Things, Agency, and Identities: The Social Life of Things Revisited*. London, Global Book Marketing.:

- Bintliff, J. (2008) History and Continental Approaches. In Bentley, R. A., Maschner, H. D. G., & Chippindale, C. (Eds.) *Handbook of Archaeological Theories*. New York, Altamira Press: 147-164
- Blackman, M. J., Stein, G. J., & Vandiver, P. B. (1993) The Standardization Hypothesis and Ceramic Mass-Production - Technological, Compositional, and Metric Indexes of Craft Specialization at Tell Leilan, Syria. *American Antiquity*, 58: 60-80.
- Bleed, P. (2008) Skill Matters. *Journal of Archaeological Method and Theory*, 15: 154-166.
- Boone, J. L. & Smith, E. A. (1998) Is It Evolution Yet? A Critique of Evolutionary Archaeology. *Current Anthropology*, 39: S141-173.
- Bourgarit, D. (2007) Chalcolithic Copper Smelting. In Niece, S. L., Hook, D., & Craddock, P. (Eds.) *Metals and Mines: Studies in Archaeometallurgy*. London, Archetype Publications Ltd: 3-14
- Bouvet, P. (2008) Étude Préliminaire de Céramique «Indiennes» et Indianisantes du Site de Khao Sam Kaeo. *Bulletin de l'Ecole Française d'Extrême-Orient 2006*, 93: 353-390.
- Brandon, D. & Kaplan, W. D. (1999) *Microstructural Characterization of Materials*, Chichester and New York, John Willey & Sons.
- Brantingham, P. J. (2007) A Unified Evolutionary Model of Archaeological Style and Function Based on the Price Equation. *American Antiquity*, 72: 395-416.
- Bronson, B. (1992) Patterns in the Early Southeast Asian Metals Trade. In Glover, I., Suchitta, P., & Villiers, J. (Eds.) *Metallurgy, Trade and Urbanism in Early Thailand and Southeast Asia*. Bangkok, White Lotus.: 63-114.
- Bronson, B. & Charoenwongsa, P. (1986) *Eyewitness Accounts of the Early Mining and Smelting of Metals in Mainland Southeast Asia*, Bangkok, Thailand Academic Publishing Co.
- Bronson, B. & Charoenwongsa, P. (1994) Eyewitness Accounts of Early Mining and Smelting in Southeast Asia. *SPAFA Journal*, 4: 4-17.
- Broodbank, C. (1989) The Longboat and Society in the Cyclades During the Keros-Syros Culture. *American Journal of Archaeology*, 93: 319-337.
- Broodbank, C. (1993) Ulysses without Sails: Trade, Distance, Knowledge and Power in the Early Cyclades. *World Archaeology*, 24: 315-331.
- Broodbank, C. (2006) The Origins and Early Development of Mediterranean Maritime Activity. *Journal of Mediterranean Archaeology*, 19: 199-230.
- Brück, J. (2005) Experiencing the Past? The Development of a Phenomenological Archaeology in British Prehistory. *Archaeological Dialogues*, 12: 45-72.
- Buchwald, V. F. & Wivel, H. (1998) Slag Analysis as a Method for the Characterization and Provenancing of Ancient Iron Objects. *Materials Characterization*, 40: 73-96.

- Bunk, W. G. J., Hauptmann, A., Kölschbach, S., & Woelk, G. (2004) Wind-Powered Copper Smelting Technology from the 3rd Millennium Bc at Feinan/Jordan. In Kim, G.-H., Yi, K.-W., & Kang, H.-T. (Eds.) *Messages from the History of Metals to the Future Metal Age: Proceedings of the 5th International Conference on the Beginnings of the Use of Metals and Alloys (BUMA V), 21–24 April 2002*. Gyeongju, Korea: 331–338
- van Buren, M. & Mills, B. (2005) Huayrachinas and Tocoimbos: Traditional Smelting Technology of the Southern Andes. *Latin American Antiquity*, 16: 3-25.
- Burger, E., Bourgarit, D., Rostan, P., Carozza, L., & Artioli, G. (2007) *The Mystery of Plattenschlacke in Protohistoric Copper Smelting: Early Evidence at the Early Bronze Age Site of Saint-Veran, French Alps*. Paper presented at the 'Archaeometallurgy in Europe II' conference in Aquileia (Italy), 17th-21st June 2007.
- Carr, T. L. & Turner, M. D. (1996) Investigating Regional Lithic Procurement Using Multi-Spectral Imagery and Geophysical Exploration. *Archaeological Prospection*, 3: 109-127.
- Carver, M. O. H. (2005) *A Seventh-Century Princely Burial Ground and Its Context*, London, British Museum Press.
- Catapotis, M. & Bassiakos, Y. (2007) Copper Smelting at the Early Minoan Site of Chrysokamino on Crete. In Day, P. & Doonan, R. (Eds.) *Metallurgy in the Bronze Age Aegean*. Oxford, Oxbow Books Limited: 68-83.
- Catapotis, M., Pryce, T. O., & Bassiakos, Y. (2008) Preliminary Results from an Experimental Study of Perforated Copper-Smelting Shaft Furnaces from Chrysokamino (Eastern Crete). In Tzachili, I. (Ed.) *Aegean Metallurgy in the Bronze Age, Proceedings of an International Symposium Held at the University of Crete, Rethymnon, Greece, on November 19-21, 2004*. Athens, Ta Pragmata Publications: 113-121.
- Chapman, H. P. & Gearey, B. R. (2004) The Social Context of Seafaring in the Bronze Age Revisited. *World Archaeology*, 36: 452-458.
- Charlton, M. (2007) Iron Working in Northwest Wales: An Evolutionary Analysis. Unpublished doctoral thesis, UCL Institute of Archaeology, University College London, London.
- Chen, T.-C. & Yoon, J.-H. (2000) Interannual Variation in Indochina Summer Monsoon Rainfall: Possible Mechanism. *Journal of Climate*, 13: 1979-1986.
- Chescoe, D. & Goodhew, P. J. (1990) *The Operation of Transmission and Scanning Electron Microscopes*, Oxford, Oxford University Press.
- Childe, V. G. (1936) *Man Makes Himself*, London, Watts & Co.
- Childe, V. G. (1942) *What Happened in History*, London, Max Parrish.
- Childe, V. G. (1951) *Social Evolution*, London, Watts & Co.
- Childe, V. G. (1958) *The Prehistory of European Society*, London, Penguin Books.
- Childs, S. T. (1990) Refractory Ceramics and Iron Smelting in East-Africa. *Journal of the Minerals Metals & Materials Society*, 42: 36-38.

- Childs, S. T. (1991) Style, Technology and Iron-Smelting Furnaces in Bantu-Speaking Africa. *Journal of Anthropological Archaeology*, 10: 332-359.
- Childs, S. T. & Herbert, E. W. (2005) Metallurgy and Its Consequences. In Stahl, A. B. (Ed.) *African Archaeology: A Critical Introduction*. Oxford, Blackwell: 276-301.
- Chiou-Peng, T. (1998) Western Yunnan and Its Steppe Affinities. In Mair, V. H. (Ed.) *The Bronze Age and Early Iron Age Peoples of Eastern Central Asia*. Washington, D.C., Institute for the Study of Man: 280-304
- Chirikure, S. (2007) Metals in Society: Iron Production and Its Position in Iron Age Communities of Southern Africa. *Journal of Social Archaeology*, 7: 72-100.
- Chirikure, S. & Rehren, T. (2004) Ores, Furnaces, Slags, and Prehistoric Societies: Aspects of Iron Working in the Nyanga Agricultural Complex, AD 1300–1900. *African Archaeological Review*, 21: 135-152.
- Ciarla, R. (1986) *Excavation Notebook for Operation B, Non Pa Wai, TAP '86*. Unpublished report, University of Pennsylvania Museum.
- Ciarla, R. (1992) The Thai-Italian Lopburi Archaeological Project (Lorap): Preliminary Results. In Glover, I. C. (Ed.) *Southeast Asian Archaeology 1990*. Hull University, Centre for South-East Asian Studies: 111-128
- Ciarla, R. (1993) *TAP 1992-1993. Non Pa Wai - Operation 2 Preliminary Excavation Report*. Unpublished report, ISMEO.
- Ciarla, R. (2005) The Thai-Italian «Lopburi Regional Archaeological Project»: A Survey of Fifteen Years of Activities. In Piovano, I. (Ed.) *La Cultura Thailandese E Le Relazioni Italo-Thai*. Torino, CESMEO: 77-104.
- Ciarla, R. (2007a) Rethinking Yuanlongpo: The Case for Technological Links between the Lingnan (PRC) and Central Thailand in the Bronze Age. *East and West*, 57: 305-328.
- Ciarla, R. (2007b) A Preliminary Report on Lo.R.A.P. Archaeological Excavations at Prehistoric Khao Sai on, Lopburi Province, Central Thailand *East and West*, 57: 395-401.
- Ciarla, R. & Natapintu, S. (1992) Towards a Definition of Site Formation Processes in Monsoonal Environments: Preliminary Observations (in Italian). In Leonardi, G. (Ed.) *Proceedings of the International Seminar "Formation Processes and Excavation Methods in Archaeology: Perspectives", July 15-21*. University of Padua: 173-198.
- Clark, J. E. (1995) Craft Specialization as an Archaeological Category. *Research in Economic Anthropology*, 16: 267–294.
- Cœdès, G. (1969) *The Making of Southeast Asia*, Berkeley, University of California Press.
- Coles, J. M. (1979) *Experimental Archaeology*, London, Academic Press.
- Collard, M., Shennan, S., Buchanan, B., & Bentley, R. A. (2008) Evolutionary Biological Methods and Cultural Data. In Bentley, R. A., Maschner, H. D. G., & Chippindale, C. (Eds.) *Handbook of Archaeological Theories*. New York, Altamira Press: 203-223

- Coote, V. (1990) Ancient Base Metal Mines and Mining in Southwest Thailand. In Glover, I. C. & Glover, E. (Eds.) *Southeast Asian Archaeology 1986*. Oxford, BAR: 131-137.
- Coote, V. (1991) *The Ultratrace Element Geochemistry of Tin Ores and Bronze Using ICP-MS, and the Mining and Metals Trade in Prehistoric Thailand*. Unpublished doctoral thesis, Institute of Archaeology, University College London.
- Costin, C. L. (1991) Craft Specialisation: Issues in Defining, Documenting and Explaining the Organisation of Production. *Journal of Archaeological Method and Theory*, 3: 1-56.
- Costin, C. L. (2001) Crafts, Capitalism, and Women: The Potters of La Chamba, Colombia. *Latin American Antiquity*, 12: 113-114.
- Costopoulos, A. (2008) Simulating Society. In Bentley, R. A., Maschner, H. D. G., & Chippindale, C. (Eds.) *Handbook of Archaeological Theories*. New York, Altamira Press: 273-281.
- Courty, M.-A. & Roux, V. (1995) Identification of Wheel Throwing on the Basis of Ceramic Surface Features and Microfabrics. *Journal of Archaeological Science*, 22: 17-50.
- Courty, M.-A. & Roux, V. (1998) Identification of Wheel-Fashioning Methods: Technological Analysis of 4th- 3rd Millennium BC Oriental Ceramics. *Journal of Archaeological Science*, 25: 747-764.
- Coustures, M. P., Béziat, D., Tollon, F., Domergue, C., Long, L., & Rebiscoul, A. (2003) The Use of Trace Element Analysis of Entrapped Slag Inclusions to Establish Ore - Bar Iron Links: Examples from Two Gallo-Roman Iron-Making Sites in France (Les Martyrs, Montagne Noire, and Les Ferrys, Loiret) *Archaeometry*, 45: 599-613.
- Craddock, P. (1995) *Early Metal Mining and Production*, Edinburgh, Edinburgh University Press.
- Craddock, P. T. (1999) Paradigms of Metallurgical Innovation in Prehistoric Europe. In Hauptmann, A., Pernicka, E., Rehren, T., & Yalcin, U. (Eds.) *The Beginnings of Metallurgy*. Bochum, Bergbau Museum: 175-192.
- Crawford, J. (1830) *Journal of an Embassy from the Governor-General of India to the Courts of Siam and Cochin-China*, London, Henry Colburn & Richard Bentley.
- Cremschi, M., Ciarla, R., & Pigott, V. C. (1992) Palaeoenvironment and Late Prehistoric Sites in the Lopburi Region of Central Thailand. In Glover, I. (Ed.) *Southeast Asian Archaeology 1990. Proceedings of the Third Conference of the European Association of Southeast Asian Archaeologists*. Hull, Centre for Southeast Asian Studies: 167-177.
- Crew, P. & Crew, S. (Eds.) (1997) *Early Ironworking in Europe: Archaeology and Experiment*, Maentwrog, Plas Tan y Bwlch Occasional Paper 3.
- Cushing, F. H. (1894) Primitive Copper Working: An Experimental Study. *American Anthropologist*, 7: 93.
- DeMarrais, E., Castillo, L. J., & Earle, T. (1996) Ideology, Materialisation, and Power Strategies. *Current Anthropology*, 37: 15-31.

- Davenport, W. G. L., King, M., Schlesinger, M., & Biswas, A. K. (2002) *Extractive Metallurgy of Copper*, Oxford, Pergamon.
- David, N. & Kramer, C. (2001) *Ethnoarchaeology in Action*, Cambridge, Cambridge University Press.
- Davisona, K., Dolukhanovb, P., Sarsona, G. R., & Shukurova, A. (2006) The Role of Waterways in the Spread of the Neolithic. *Journal of Archaeological Science*, 33: 641-652.
- Dentz, F. (2008) *On the Use of Spaceborne Remote Sensing for Archaeology: A Case Study on Early Iron Reduction Sites at the Jordan Valley*. Unpublished Masters thesis, Department of Earth Observation and Space Systems, Delft University of Technology, Delft.
- Dillmann, P. & L'Héritier, M. (2007) Slag Inclusion Analyses for Studying Ferrous Alloys Employed in French Medieval Buildings: Supply of Materials and Diffusion of Smelting Processes. *Journal of Archaeological Science*, 34: 1810-1823.
- Dobres, M.-A. & Hoffman, C. R. (1994) Social Agency and the Dynamics of Prehistoric Technology. *Journal of Archaeological Method and Theory*, 1: 211-258.
- Dods, R. R. (2004) Knowing Ways/Ways of Knowing: Reconciling Science and Tradition. *World Archaeology*, 36: 547-557.
- Donaldson, C. H. (1976) An Experimental Investigation of Olivine Morphology. *Contributions to Mineralogy and Petrology*, 57: 187-213.
- Doonan, R. C. P. (1996) Sweat, Fire and Brimstone: Pre-Treatment of Copper Ore and the Effects on Smelting Techniques. *The Journal of the Historical Metallurgical Society*, 28: 85-98.
- Doonan, R. C. P., Hanks, B., Zdanovich, D., & Sotiropoulos, A. (2008) *The Organisation of Taskscapes in the Southern Ural Steppe During the Middle Bronze Age: Evidence from Field Survey and Laboratory Analysis*. Paper presented at the 'Archaeometallurgy in Europe II' conference in Aquileia (Italy), 17th-21st June 2007.
- Doonan, R. C. & Andrews, K. (in press) Space and Engagement with Technological Architecture: Lessons from Experimental Archaeology. In Gheorghiu, D. (Ed.) *Ceramics in the new Millennium*. Oxford, BAR Int series.
- Dunnell, R. C. (1978) Style and Function: A Fundamental Dichotomy. *American Antiquity*, 43: 192-202.
- Dunnell, R. C. (1982) Science, Social Science, and Common Sense: The Agonizing Dilemma of Modern Archaeology. *Journal of Anthropological Research*, 38: 1-25.
- Eerkens, J. C. (2000) Practice Makes within 5% of Perfect: Visual Perception, Motor Skills, and Memory in Artifact Variation. *Current Anthropology*, 41: 663-668.
- Eerkens, J. C. & Bettinger, R. L. (2001) Techniques for Assessing Standardization in Artifact Assemblages: Can We Scale Material Variability? *American Antiquity*, 66: 493-504.
- Eerkens, J. C. & Lipo, C. P. (2005) Cultural Transmission, Copying Errors, and the

- Generation of Variation in Material Culture and the Archaeological Record. *Journal of Anthropological Archaeology*, 24: 316-334.
- Eerkens, J. C. & Lipo, C. P. (2007) Cultural Transmission Theory and the Archaeological Record: Providing Context to Understanding Variation and Temporal Changes in Material Culture *Journal of Archaeological Research*, 15: 239-274.
- Ehlers, O. E. (2002) *On Horseback through Indochina. (Volume 3. Vietnam, Singapore, and Central Thailand)*, Bangkok, White Lotus.
- Eisenhüttenleute, V. D. (1995) *Slag Atlas*, Dusseldorf, Verlag Stahleisen GmbH.
- Ellingham, H. J. T. (1944) Reducibility of Oxides and Sulphides in Metallurgical Processes. *Journal of the Society of Chemical Industry*, 5: 125-133.
- Epstein, S. R. (1998) Craft Guilds, Apprenticeship, and Technological Change in Pre-Industrial Europe. *The Journal of Economic History*, 58: 684-717.
- Etienne, A. (2000) *Isan Travels: North East Thailand Economy in 1883-1884*, Bangkok, White Lotus.
- Eyre, C. O. (2003) Metal Age Complexity in Thailand; Socio-Political Development and Landscape Use in the Upper Chao Phraya Basin. *Bulletin of the Indo-Pacific Prehistory Association*, 23.
- Farr, H. (2006) Seafaring as Social Action. *Journal of Maritime Archaeology*, 1: 85-99.
- Flannery, K. V. (1968) Archaeological Systems Theory and Early Mesoamerica. In Meggers, B. J. (Ed.) *Anthropological Archaeology in the Americas*. Washington D.C., Anthropological Society of Washington: 67-87
- Fletcher, M. & Lock, G. (2005) *Digging Numbers: Elementary Statistics for Archaeologists*, Oxford, Oxford University School of Archaeology.
- Freestone, I. C. (1989) Refractory Materials and Their Procurement. In Hauptmann, A., Pernicka, E., & Wagner, G. A. (Eds.) *Old World Archaeometallurgy. Proceedings of the International Symposium, Heidelberg 1987*. Bochum, Selbstverlag des Deutschen Bergbau-Museums: 155-162.
- Fuller, D. Q. & Qin, L. (2009) Water Management and Labour in the Origins and Dispersal of Asian Rice. *World Archaeology*, 41: 88-111.
- Gabora, L. (2006) The Fate of Evolutionary Archaeology: Survival or Extinction? *World Archaeology*, 38: 690-696.
- Gabora, L. (2008) Mind. In Bentley, R. A., Maschner, H. D. G., & Chippindale, C. (Eds.) *Handbook of Archaeological Theories*. New York, Altamira Press: 283-296.
- Gardner, A. (2008) Agency. In Bentley, R. A., Maschner, H. D. G., & Chippindale, C. (Eds.) *Handbook of Archaeological Theories*. New York, Altamira Press: 95-108.
- Gardner, S. L. (1972) *Thailand's Mineral Resources and Economic Development*. Unpublished doctoral thesis, Department of Economics, University of Colorado, University Microfilms International, Michigan.
- Geschière, P. L. (Ed.) (2005) *Commodification: Things, Agency, and Identities: The Social*

Life of Things Revisited, London, Global Book Marketing.

- Gilchrist, J. D. (1989) *Extraction Metallurgy*, London, Pergamon.
- Glover, I. C. (1990) Ban Don Ta Phet: The 1984-85 Excavation. In Glover, I. C. & Glover, E. (Eds.) *Southeast Asian Archaeology 1986*. Oxford, BAR: 139-183.
- Glover, I. C. (2003) European Archaeology in Southeast Asia - the Past, the Present and a Future? In Källén, A. & Karlström, A. (Eds.) *Fishbones and Glittering Emblems. Southeast Asian Archaeology 2002*. Stockholm, Östasiatiska Museet: 23-31.
- Goldstein, J. I., Newbury, D. E., Joy, D. C., & Lyman, C. E. (2003) *Scanning Electron Microscopy and X-Ray Microanalysis*, New York and London, Kluwer Academic/Plenum Publishers.
- Gorman, C. F. (1969) Hoabinhian: A Pebble-Tool Complex with Early Plant Associations in Southeast Asia. *Science*, 163: 671-673.
- Gorman, C. F. (1970) Excavations at Spirit Cave, North Thailand: Some Interim Interpretations. *Asian Perspectives*, 13: 79-107.
- Gorman, C. & Charoenwongsa, P. (1976) Ban Chiang: A Mosaic of Impressions from the First Two Years. *Expedition*, 18: 14-26.
- Gosden, C. & Head, L. (1994) Landscape: A Usefully Ambiguous Concept. *Archaeology in Oceania*, 29: 113-116.
- Gosden, C. & Marshall, Y. (1999) The Cultural Biography of Objects. *World Archaeology*, 31: 169-178.
- Gosselain, O. P. (1992) Technology and Style: Potters and Pottery among Bafia of Cameroon. *Man*, 27: 559-586.
- Grave, P. & Kealhofer, L. (1999) Assessing Bioturbation in Archaeological Sediments Using Soil Morphology and Phytolith Analysis. *Journal of Archaeological Science*, 26: 1239-1248.
- Greene, K. (2004) Archaeology and Technology. In Bintliff, J. L., Earle, T., & Peebles, C. S. (Eds.) *A Companion to Archaeology*. Oxford, Blackwell: 155-173.
- van Grieken, R. & Markowicz, A. (2002) *Handbook of X-Ray Spectrometry*, New York, Marcel Dekker.
- Haaland, R. (2004) Iron Smelting- a Vanishing Tradition: Ethnographic Study of This Craft in South-West Ethiopia. *Journal of African Archaeology*, 2: 65-80.
- Hamilton, E. (2001) Bronze from Ban Chiang, Thailand: A View from the Laboratory. *Expedition*, 43: 7-8.
- Hanks, B. K., Epimakhov, A. V., & Renfrew, A. C. (2007) Towards a Refined Chronology for the Bronze Age of the Southern Urals, Russia. *Antiquity*, 81: 353-367.
- Haworth, H. F., Chiangmai, P. N., & Piancharoen, C. (1966) *Ground Water Resources Development of Northeastern Thailand*, Bangkok, Ground Water Division, Department of Mineral Resources, Ministry of National Development, Thailand.
- Hays-Gilpin, K. A. (2008) Gender. In Bentley, R. A., Maschner, H. D. G., & Chippindale, C. (Eds.) *Handbook of Archaeological Theories*. New York, Altamira Press: 335-

- Hegmon, M. (1992) Archaeological Research on Style. *Annual Review of Anthropology*, 21: 517-536.
- Hegmon, M. (1998) Technology, Style, and Social Practices: Archaeological Approaches. In Stark, M. T. (Ed.) *The Archaeology of Social Boundaries*. Washington, London, Smithsonian Institution Press: 264-279.
- Hegmon, M. (2003) Setting Theoretical Egos Aside: Issues and Theory in North American Archaeology. *American Antiquity*, 68: 213-243.
- Hein, A., Kilikolou, V., & Kassianidou, V. (2007) Chemical and Mineralogical Examination of Metallurgical Ceramics from a Late Bronze Age Copper Smelting Site in Cyprus. *Journal of Archaeological Science*, 34: 141-154.
- Henrich, J. (2001) Cultural Transmission and the Diffusion of Innovations: Adoption Dynamic Indicate That Biased Cultural Transmission Is the Predominate Force in Behavioral Change. *American Anthropologist*, 103: 992-1013.
- Henrich, J. & Boyd, R. (2001) Why People Punish Defectors: Conformist Transmission Stabilizes Costly Enforcement of Norms in Cooperative Dilemmas. *Journal of Theoretical Biology*, 208: 79-89.
- Henrich, J. & Gil-White, F. J. (2001) The Evolution of Prestige: Freely Conferred Deference as a Mechanism for Enhancing the Benefits of Cultural Transmission. *Evolution and Human Behavior*, 22: 165-196.
- Henry, J. (2002) *The Scientific Revolution and the Origins of Modern Science*, New York, Palgrave.
- Higham, C. F. W. (1975) Aspects of Economy and Ritual in Prehistoric Northeast Thailand. *Journal of Archaeological Science*, 2: 245-288.
- Higham, C. F. W. (1988a) Prehistoric Metallurgy in Southeast Asia: Some New Information from the Excavation of Ban Na Di. In Maddin, R. (Ed.) *The Beginning of the Use of Metals and Alloys: Papers from the Second International Conference on the Beginning of the Use of Metals and Alloys, Zhengzhou, China, 21-26 October, 1986*. Cambridge, Mass., MIT Press: 130-155.
- Higham, C. F. W. (1988b) Ban Chiang and Charcoal in Hypothetical Hindsight; a Comment. *Bulletin of the Indo-Pacific Prehistory Association*, 8: 75-78.
- Higham, C. F. W. (1989) *The Archaeology of Mainland Southeast Asia - from 10,000 BC to the Fall of Angkor*, Cambridge, Cambridge University Press.
- Higham, C. F. W. (1996) *The Bronze Age of Southeast Asia*, Cambridge, Cambridge University Press.
- Higham, C. F. W. (1996-1997) The Social and Chronological Contexts of Early Bronze Working in Southeast Asia. In Bulbeck, F. D. & Barnard, N. (Eds.) *Ancient Chinese and Southeast Asian Bronze Age Cultures, Volume II. The Proceedings of a Conference Held at the Edith and Joy London Foundation Property, Kioloa, NSW, Australia, 8-12 February, 1988*. Taipei, SMC Publishing: 821-888.
- Higham, C. F. W. (2002) *Early Cultures of Mainland Southeast Asia*, Bangkok, River Books Ltd.

- Higham, C. F. W. (2004) Mainland Southeast Asia from the Neolithic to the Iron Age. In Glover, I. C. & Bellwood, P. (Eds.) *Southeast Asia: From Prehistory to History*. New York, Routledge: 41-67
- Higham, C. F. W. (2006) Crossing National Boundaries: Southern China and Southeast Asia in Prehistory. In Bacus, E. A., Glover, I. C., & Pigott, V. C. (Eds.) *Uncovering Southeast Asia's Past: Selected Papers from the 10th International Conference of the European Association of Southeast Asian Archaeologists*. Singapore, National University of Singapore: 13-21.
- Higham, C. F. W. (2008a) Ban Non Wat: The First Five Seasons. In Pautreau, J.-P., Coupey, A., Zeitoun, V., & Rambault, E. (Eds.) *Archaeology in Southeast Asia: From Homo Erectus to the Living Traditions, Choice of Papers from the 11th Euraseaa Conference, Bougon 2006*. Chiang-Mai, European Association of Southeast Asian Archaeologists: 83-90.
- Higham, C. F. W. (2008b) Recasting Thailand: New Discoveries at Ban Non Wat. *Current World Archaeology*: 38-41.
- Higham, C. F. W. (2009) Thailand's Bronze Age Superburials: The Aristocrats of Ban Non Wat. *Current World Archaeology*, 35: 18-23.
- Higham, C. F. W. (in press a) Dating the Bronze Age of Southeast Asia: The Cultural Implications. *Journal of Southern Ethnology and Archaeology*.
- Higham, C. F. W. & Higham, T. F. G. (2009) Dating Southeast Asian Prehistory: New Radiometric Evidence from Ban Non Wat. *Antiquity* 82: 1-20.
- Higham, C. F. W. & Kijngam, A. (1984) *Prehistoric Investigations in Northeast Thailand: Excavations at Ban Na Di, Ban Chiang Hian, Ban Muang Phruk, Non Noi and Ban Kho Noi*, Oxford, BAR.
- Higham, C. F. W. & Thosarat, R. (1998) *Prehistoric Thailand. From Early Settlement to Sukhothai*, Bangkok, River Books.
- Higham, C. F. W. & Thosarat, R. (2004a) The Excavation of Khok Phanom Di. Volume VII: Summary and Conclusions, London, Society of Antiquaries of London.
- Higham, C. F. W. & Thosarat, R. (Eds.) (2004b) *The Excavation of Ban Lum Khao*, Bangkok, Thai Fine Arts Department.
- Higham, C. F. W. & Thosarat, R. (2006) Ban Non Wat: The First Three Seasons. In Bacus, E. A., Glover, I. C., & Pigott, V. C. (Eds.) *Uncovering Southeast Asia's Past: Selected Papers from the 10th International Conference of the European Association of Southeast Asian Archaeologists*. Singapore, National University of Singapore: 98-104.
- Higham, C. F. W., Higham, T. F. G., Hogg, A., & Thosarat, R. (1997) The Excavation of Nong nor, Central Thailand, 1991-93. In Ciarla, R. & Rispoli, F. (Eds.) *South-East Asian Archaeology 1992. Proceedings of the Fourth International Conference of the European Association of South-East Asian Archaeologists. Rome, 28th September - 4th October 1992*. Rome, Istituto Italiano per l'Africa e l'Oriente.:175-189
- Higham, C. F. W., Kijngam, A., & Talbot, S. (Eds.) (2007) *The Excavation of Noen U-Loke and Non Muang Kao*, Bangkok, Thai Fine Arts Department.
- Hofman, H. O. (1914) *Metallurgy of Copper*, New York and London, McGraw-Hill Book

Company.

- Hosler, D. (1995) Sound, Color and Meaning in the Metallurgy of Ancient West Mexico. *World Archaeology*, 27: 100-115.
- Hudson, B. (2008) Restoration and Reconstruction of Monuments at Bagan (Pagan), Myanmar (Burma), 1995–2008. *World Archaeology*, 40: 553-571.
- Huler, S. (2004) *Defining the Wind: The Beaufort Scale, and How a 19th Century Admiral Turned Science into Poetry*, New York, Crown Publishers.
- Humphris, J., Martínón-Torres, M., Rehren, T., & Reid, A. (2009) Variability in Single Smelting Episodes - a Pilot Study Using Iron Slag from Uganda. *Journal of Archaeological Science* 36: 359–369.
- Hung, H.-C., Iizuka, Y., Bellwood, P., Nguyene, K. D., Bellina, B., Silapanth, P., Dizon, E., Santiago, R., Datani, I., & Manton, J. H. (2007) Ancient Jades Map 3,000 Years of Prehistoric Exchange in Southeast Asia. *Proceedings of the National Academy of Sciences*, 104: 19745–19750.
- Ineson, P. R. (1989) *Introduction to Practical Ore Microscopy*, Harlow, Longman Scientific and Technical.
- Ingold, T. (1999) ‘Tools for the Hand, Language for the Face’: An Appreciation of Leroi-Gourhan’s Gesture and Speech. *Studies in History and Philosophy of Science Part C: Studies in History and Philosophy of Biological and Biomedical Sciences*, 30: 411-453.
- Ineson, P. R. (1989) *Introduction to Practical Ore Microscopy*, Harlow, Longman Scientific and Technical.
- Irwin, G. (2008) Pacific Seascapes, Canoe Performance, and a Review of Lapita Voyaging with Regard to Theories of Migration. *Asian Perspectives*, 47: 12-27.
- Jackson, C. M., Booth, C. A., & Smedley, J. W. (2005) Glass by Design? Raw Materials, Recipes and Compositional Data. *Archaeometry*, 47: 781-795.
- Jenkins, R. (1974) *Introduction to X-Ray Spectrometry*, London, John Wiley and Sons, Ltd.
- Jenkins, R. (1999) *X-Ray Fluorescence Spectrometry*, London, John Wiley and Sons, Ltd.
- Jolliffe, I. T. (2002) *Principal Component Analysis*, New York and London, Springer.
- Jones, A. (2002) *Archaeological Theory and Scientific Practice*, Cambridge, Cambridge University Press.
- Jones, A. (2004) Archaeometry and Materiality: Materials-Based Analysis in Theory and Practice. *Archaeometry*, 46: 327-338.
- Jordan, P. & Shennan, S. (2003) Cultural Transmission, Language, and Basketry Traditions Amongst the California Indians. *Journal of Anthropological Archaeology*, 22: 42-74.
- Juleff, G. & Bray, L. (2007) Minerals, Metal, Colours and Landscape: Exmoor’s Roman

- Lode in the Early Bronze Age. *Cambridge Archaeological Journal*, 17: 285-296.
- Kaiura, G. H. & Tohuri, J. M. (1979) Natural Convective Mass Transfer Rates between Solid Magnetite and Molten Mattes. *Metallurgical Transactions B*, 10: 595 - 606.
- Keller, C. M. (2001) Thoughts and Production: Insights of a Practitioner. In Schiffer, M. B. (Ed.) *Anthropological Perspectives on Technology*. Albuquerque, University of New Mexico Press: 33-45.
- Keller, C. M. & Keller, J. D. (1996) *Cognition and Tool Use: The Blacksmith at Work*, Cambridge, Cambridge University Press.
- Killick, D. (2001) Science, Speculation and the Origins of Extractive Metallurgy. In Brothwell, D. R. & Pollard, A. M. (Eds.) *Handbook of Archaeological Sciences*. Chichester, UK, John Wiley & Sons, Ltd.: 483-492.
- Killick, D. J. (2004a) Social Constructionist Approaches to the Study of Technology. *World Archaeology*, 36: 571-578.
- Killick, D. J. (2004b) What Do We Know About African Iron Working? *Journal of African Archaeology*, 2: 97-112.
- Killick, D. J. (2005) Comments IV: Is There Really a Chasm between Archaeological Theory and Archaeological Science? *Archaeometry*, 47: 185-189.
- Killick, D. (2008) Book Review - Metals and Mines: Studies in Archeometallurgy, Susan La Niece, Duncan Hook, Paul Craddock (Eds.). Archetype Publications, in Association with the British Museum, London (2007), Pp. XII D 250, 76 Illustrations, UK£45/ US\$90, ISBN: 978-1-904982-19-7. *Journal of Archaeological Science*, 35: 3044–3046.
- Knapp, A. B., Pigott, V. C., & Herbert, E. W. (Eds.) (1998) *Social Approaches to an Industrial Past: The Archaeology and Anthropology of Mining*, New York, Routledge.
- Knappett, C. (2005) *Thinking through Material Culture. An Interdisciplinary Perspective*, Philadelphia, University of Pennsylvania Press.
- Kongoli, F., Felton, A. D., & Dessureault, Y. (1998) Thermodynamic Modeling of Liquid Fe-Ni-Cu-Co-S Mattes. *Metallurgical and Materials Transactions B*, 29: 591-601.
- Kongoli, F. & Felton, A. D. (1999) Model Prediction of Thermodynamic Properties of Co-Fe-Ni-S Mattes. *Metallurgical and Materials Transactions B*, 30: 443-450.
- Kongoli, F. & Yazawa, A. (2001) Liquidus Surface of FeO-Fe₂O₃-SiO₂-CaO Slag Containing Al₂O₃, MgO, and Cu₂O at Intermediate Oxygen Partial Pressures. *Metallurgical and Materials Transactions B*, 32: 583-592.
- Kongoli, F. & Yazawa, A. (2003) Liquidus Surface of FeO-Fe₂O₃-SiO₂-CaO Slags at Constant CO₂/CO Ratios. *Materials Transactions*, 44: 2130-2135.
- Kongoli, F., McBow, I., & Yazawa, A. (2003) Liquidus Surface of “Lime Ferrite” Slags at Intermediate Oxygen Potentials. *Materials Transactions*, 44: 2136-2140.
- Kopytoff, I. (1986) The Cultural Biography of Things: Commoditisation as Process. In

- Appadurai, A. (Ed.) *The Social Life of Things*. Cambridge, Cambridge University Press: 64-94.
- Kuhn, S. L. (2004) Evolutionary Perspectives on Technology and Technological Change. *World Archaeology*, 36: 561-570.
- Kanjanajuntorn, P. (2006) Excavation at Nong Kwang, an Iron Age Site in Ratchaburi Province, West-Central Thailand. In Bacus, E. A., Glover, I. C., & Pigott, V. C. (Eds.) *Uncovering Southeast Asia's Past: Selected Papers from the 10th International Conference of the European Association of Southeast Asian Archaeologists*. Singapore, National University of Singapore: 116-127.
- Lahiri, N. (1995) Indian Metal and Metal-Related Artefacts as Cultural Signifiers: An Ethnographic Perspective. *World Archaeology*, 27: 116-132.
- Lai, K.-Y., Chen, Y.-G., Chung, L.-H., & Lâm, D. Đ. (2006) Active Tectonics and Quaternary Basin Formation Along the Điện Biên Phủ Fault Zone, Northwestern Việt Nam. *Journal of Geology*. Hanoi, IDM.
- Lasaponara, R. & Masini, N. (2007) Detection of Archaeological Crop Marks by Using Satellite Quickbird Multispectral Imagery *Journal of Archaeological Science*, 34: 214-221.
- Lechtman, H. (1976) A Metallurgical Site Survey in the Peruvian Andes. *Journal of Field Archaeology*, 3: 1-42.
- Lechtman, H. (1977) Style in Technology: Some Early Thoughts. In Lechtman, H. & Merrill, R. S. (Eds.) *Material Culture: Styles, Organization, and Dynamics of Technology*. St. Paul, West Publishing Co.: 3-20.
- Lechtman, H. (1984) Andean Value Systems and the Development of Prehistoric Metallurgy. *Technology and Culture*, 25: 1-36.
- Lechtman, H. (1988) Traditions and Style in Central Andean Metalworking. In Maddin, R. (Ed.) *The Beginning of the Use of Metals and Alloys: Papers from the Second International Conference on the Beginning of the Use of Metals and Alloys, Zhengzhou, China, 21-26 October, 1986*. Cambridge, MA, MIT Press: 344-378.
- Lechtman, H. (1991) The Production of Copper-Arsenic Alloys in the Central Andes: Highland Ores and Coastal Smelters? *Journal of Field Archaeology*, 18: 43-76.
- Lechtman, H. (1993) Technologies of Power: The Andean Case. In Henderson, J. & Netherly, P. (Eds.) *Configurations of Power in Complex Societies*. Ithaca, NY, Cornell University Press: 244-280.
- Lechtman, H. (1996) Arsenic Bronze: Dirty Copper or Chosen Alloy? A View from the Americas. *Journal of Field Archaeology*, 23: 477-514.
- Lechtman, H. (1999) Afterword. In Dobres, M.-A. & Hoffman, C. R. (Eds.) *The Social Dynamics of Technology: Practice, Politics, and World Views*. Washington D.C., Smithsonian Institution Press: 223-232.
- Lechtman, H. & Klein, S. (1999) The Production of Copper-Arsenic Alloys (Arsenic Bronze) by Cosmelting: Modern Experiment, Ancient Practice. *Journal of Archaeological Science*, 26: 497-526.
- Lemonnier, P. (1989) Towards an Anthropology of Technology. *Man*, 24: 526-527.

- Lemonnier, P. (1992) *Elements for an Anthropology of Technology*, Ann Arbor, Michigan, University of Michigan; Anthropological Paper 88.
- Lemonnier, P. (Ed.) (1993) *Technological Choices: Transformation in Material Cultures since the Neolithic*, London, Routledge.
- Levy, P. (1943) *Recherches Préhistoriques dans la Région de Mlu Prei*, Hanoi, Ecole Française d'Extrême-Orient.
- van Liere, W. (1980) Traditional Water Management in the Lower Mekong Basin. *World Archaeology*, 11: 265-280.
- Linduff, K. M., Rubin, H., & Shuyun, S. (Eds.) (2000) *The Beginnings of Metallurgy in China*, New York, Edwin Mellen Press.
- Loofs-Wissowa, H. H. E. (1983) The Development and Spread of Metallurgy in Southeast Asia: A Review of the Present Evidence. *Journal of Southeast Asian Studies*, XIV: 1-11.
- Lyman, R. L. & O'Brien, M. J. (1998) The Goals of Evolutionary Archaeology: History and Explanation. *Current Anthropology*, 39: 615-652.
- Lyman, R. L. & O'Brien, M. J. (2001) On Misconceptions of Evolutionary Archaeology: Confusing Macroevolution and Microevolution. *Current Anthropology*, 42: 408-409.
- Lyman, R. L. & O'Brien, M. J. (2003) Cultural Traits: Units of Analysis in Early Twentieth-Century Anthropology. *Journal of Anthropological Research*, 59: 225-250.
- Lyman, R. L. & O'Brien, M. J. (2006) Evolutionary Archaeology Is Unlikely to Go Extinct: Response to Gabora. *World Archaeology*, 38: 697-703.
- Majumdar, R. C. (1941) *Greater India*, Lahore.
- Martineau, R., Walter-Simonnet, A. V., Grobéty, B., & Buatier, M. (2007) Clay Resources and Technical Choices for Neolithic Pottery (Chalain, Jura, France): Chemical, Mineralogical and Grain-Size Analyses. *Archaeometry*, 49: 23-52.
- Martinón-Torres, M., Rojas, R. V., Cooper, J., & Rehren, T. (2007) Metals, Microanalysis and Meaning: A Study of Metal Objects Excavated from the Indigenous Cemetery of El Chorro De Maíta, Cuba. *Journal of Archaeological Science*, 34: 194-204.
- Martinón-Torres, M. and T. Rehren (2009). Post-medieval crucible production and distribution: a study of materials and materialities. *Archaeometry* 51: 49-74.
- Marwick, B. (2008) What Attributes Are Important for the Measurement of Assemblage Reduction Intensity? Results from an Experimental Stone Artefact Assemblage with Relevance to the Hoabinhian of Mainland Southeast Asia. *Journal of Archaeological Science*, 35: 1189-1200.
- McQuail, B. (1986) *Excavation Notebook for Square A, Non Pa Wai, TAP '86*. Unpublished report, University of Pennsylvania Museum.
- Mei, J. (2000) *Copper and Bronze Metallurgy in Late Prehistoric Xinjiang*, Oxford, Archaeopress.
- Mei, J. & Li, Y. (2003) Early Copper Technology in Xinjiang, China: The Evidence So

- Far. In Craddock, P. T. & Lang, J. R. S. (Eds.) *Mining and Metal Production through the Ages*. London, The British Museum Press: 111-121
- Mei, J. (2004) Early Copper-Based Metallurgy in China: Old Question, New Perspective. *Bulletin of Archaeology, University of Kanazawa*, 27: 109-118.
- Merkel, J. F. (1990) Experimental Reconstruction of Bronze Age Copper Smelting Based on Archaeological Evidence from Timna. In Rothenberg, B. (Ed.) *The Ancient Metallurgy of Copper, Researches in the Arabah, 1959-1984*. London, Institute for Archaeo-Metallurgical Studies, Institute of Archaeology, University College London: 78-122.
- Meyer, C., Ullrich, B, & C. D. M. Barlieb (2007). Archaeological Questions and Geophysical Solutions: Ground-Penetrating Radar and Induced Polarization Investigations in Munigua, Spain. *Archaeological Prospection* 14: 202–212.
- Miller, D. (Ed.) (2005) *Materiality*, London, Duke University Press.
- Miller, D. (2002) Smelter and Smith: Iron Age Metal Fabrication Technology in Southern Africa. *Journal of Archaeological Science*, 29: 1083-1131.
- Miller, D., Killick, D., & Van Der Merwe, N. J. (2001) Metal Working in the Northern Lowveld, South Africa, A.D. 1000-1890. *Journal of Field Archaeology*, 28: 401-417.
- Miller, H. (2007) *Archaeological Approaches to Technology*, New York, Elsevier.
- Morton, G. R. & Wingrove, J. (1969) Constitution of Bloomery Slags: Part I-Roman. *Journal of the Iron and Steel Institute*, 207: 1556-1564.
- Morton, G. R. & Wingrove, J. (1972) Constitution of Bloomery Slags: Part II-Medieval. *Journal of the Iron and Steel Institute*, 210: 478-488.
- Mouhot, H. (2000) *Travels in Siam, Cambodia, Laos, and Annam*, Bangkok, White Lotus Press.
- Mudar, K. (1992) *Prehistoric and Early Historic Settlements on the Central Plain: Analysis of an Archaeological Survey in Lopburi Province, Thailand*. Unpublished doctoral thesis, Department of Anthropology, University of Michigan, Ann Arbor,
- Mudar, K. (1995) Evidence for Prehistoric Dryland Farming in Mainland Southeast Asia: Results of Regional Survey in Lopburi Province, Thailand. *Asian Perspectives*, 34: 157-194.
- Mudar, K. & Pigott, V. C. (2003) Subsistence Changes and Community-Based Craft Production in Prehistoric Thailand. In Källén, A. & Karlström, A. (Eds.) *Fishbones and Glittering Emblems*. Stockholm, Östasiatiska Museet: 149-160.
- Muhly, J. D. (1981) The Origin of Agriculture and Technology - Aarhus, Denmark, November 21-25, 1978 .2. Summary - the Origin of Agriculture and Technology - West or East-Asia. *Technology and Culture*, 22: 125-148.
- Muhly, J. D. (1988) The Beginnings of Metallurgy in the Old World. In Maddin, R. (Ed.) *The Beginning of the Use of Metals and Alloys*. Cambridge, MA, MIT Press: 2-20
- Murillo, M., Pryce, T. O., Bellina, B., & Martínón-Torres, M. (forthcoming) Khao Sam

Kaero - an Archaeometallurgical Crossroads for Trans-Asiatic Technological Styles.

- Murowchick, R. E. (2001) The Political and Ritual Significance of Bronze Production and Use in Ancient Yunnan. *Journal of East Asian Archaeology*, 3: 133-192.
- Nakornsri, N. (1981) Geology and Mineral Resources of the Map Sheet Amphoe Ban Mi (ND47-4). Bangkok, Thai Department of Mineral Resources.
- Nakou, P. (1995) The Cutting Edge: A New Look at Early Aegean Metallurgy. *Journal of Mediterranean Archaeology*, 8: 1-32.
- Natapintu, S. (1979) *A Report of the Survey on Ban Ta Kae, Muang District, Lopburi Province* (in Thai). Bangkok, Fine Arts Department.
- Natapintu, S. (1980) *Preliminary Report on Ta Kae Excavation in 1980* (in Thai). Bangkok, Fine Arts Department.
- Natapintu, S. (1984) Ancient Settlement at Ban Tha Khae in Lopburi. *Muang Boran*, 10: 26-40.
- Natapintu, S. (1985) *Central Thailand Archaeological Project: Report on Preliminary Survey at Ban Phu Noi* (in Thai), Bangkok, Fine Arts Department.
- Natapintu, S. (1988) Current Research on Ancient Copper-Base Metallurgy in Thailand. In Charoenwongsa, P. & Bronson, B. (Eds.) *Prehistoric Studies: The Stone and Metal Ages in Thailand*. Bangkok, The Thai Antiquity Working Group: 107-124.
- Natapintu, S. (1991) Archaeometallurgical Studies in the Khao Wong Prachan Valley, Central Thailand. In Bellwood, P. (Ed.) *Indo-Pacific Prehistory 1990. Proceedings of the 14th Congress of the Indo-Pacific Prehistory Association*. Bangkok, Indo-Pacific Prehistory Association: 153-159.
- Natapintu, S. (2005) The Contribution of Archaeology to the Improvement of Life Quality at Ban Pong Manao Village, Lopburi Province, Central Thailand. In Piovano, I. (Ed.) *La Cultura Thailandese E Le Relazioni Italo-Thai*. Torino, CESMEO: 105-118.
- Natapintu, S. (2007) *Ancient Thai: Evolution of Prehistoric Thai* (in Thai), Bangkok, Matichon Publishing House.
- Neiman, F. D. (1995) Stylistic Variation in Evolutionary Perspective: Inferences from the Decorative Diversity and Interassemblage Distance in Illinois Woodland Ceramic Assemblages. *American Antiquity*, 60: 7-36.
- Nesse, W. (2003) *Introduction to Optical Mineralogy*, Oxford, Oxford University Press.
- Nocete, F., Queipo, G., Sáez, R., Nieto, J. M., Inácio, N., Bayona, M. R., Peramo, A., Vargas, J. M., Cruz-Aunon, R., Gil-Ibarguchi, J. I., & Santos, J. F. (2008) The Smelting Quarter of Valencina De La Concepción (Seville, Spain): The Specialised Copper Industry in a Political Centre of the Guadalquivir Valley During the Third Millennium BC (2750-2500 BC) *Journal of Archaeological Science*, 35: 717-732.
- Nürnberg, K. (1981) *Schlackenatlas*, Düsseldorf, Verlag Stahleisen M.B.H.
- O'Reilly, D. J. W. (2000) From the Bronze Age to the Iron Age in Thailand: Applying the

- Heterarchical Approach. *Asian Perspectives*, 39: 1-19.
- O'Reilly, D. J. W. (2003) Further Evidence of Heterarchy in Bronze Age Thailand. *Current Anthropology*, 44: 300-306.
- O'Reilly, D. J. W. (2008) Multivallate Sites and Socio-Economic Change: Thailand and Britain in Their Iron Ages. *Antiquity*, 82: 377-389.
- Olivier, L. (1999) The Hochdorf 'Princely' Grave and the Question of the Nature of Funerary Assemblages. In Murray, T. (Ed.) *Time and Archaeology*. London, Routledge: 109-138.
- Olsen, S. L. (1988) Introduction: Applications of Scanning Electron Microscopy to Archaeology. In Olsen, S. L. (Ed.) *Scanning Electron Microscopy in Archaeology*. New York, Academic Press: 3-7.
- Onsuwan-Eyre, C. (2006) *Prehistoric and Proto-Historic Communities in the Eastern Upper Chao Phraya River Valley*. Unpublished doctoral thesis, Department of Anthropology, University of Pennsylvania, Philadelphia.
- Orton, C. (2000) *Sampling in Archaeology*, Cambridge, Cambridge University Press.
- Ottaway, B. S. (2001) Innovation, Production and Specialization in Early Prehistoric Copper Metallurgy. *European Journal of Archaeology*, 4: 87-112.
- Oxenham, M. & Tayles, N. (2006) Synthesising Southeast Asian Population History and Palaeohealth. In Oxenham, M. & Tayles, N. (Eds.) *Bioarchaeology of Southeast Asia*. Cambridge, Cambridge University Press: 335-349.
- Pallegoix, J.-B. (1999) *Description of the Thai Kingdom or Siam: Thailand under King Mongkut*, Bangkok, White Lotus Press.
- Parker-Pearson, M. (1999) *The Archaeology of Death and Burial*, Sutton, Stroud.
- Paynter, S. (2006) Regional Variations in Bloomery Smelting Slag of the Iron Age and Romano-British Periods. *Archaeometry*, 48: 271-292.
- Petrequin, P. (1993) North Wind, South Wind. Neolithic Technical Choices in the Jura Mountains, 3700-2400 BC. In Lemonnier, P. (Ed.) *Technological Choices, Transformations in Material Cultures since the Neolithic*. London, Routledge.: 36-76.
- Pfaffenberger, B. (1988) Fetishised Objects and Humanised Nature: Towards an Anthropology of Technology. *Man*, 23: 236-252.
- Pfaffenberger, B. (1992) Social Anthropology of Technology. *Annual Review of Anthropology*, 21: 491-516.
- Pigott, V. C. (1984) The Thailand Archaeometallurgy Project 1984: Survey of Base Metal Resource Exploitation in Loei Province, Northeastern Thailand. *South-East Asian Studies Newsletter*, 17: 1-5.
- Pigott, V. C. (1992) The Archaeology of Copper Production at Prehistoric Non Pa Wai and Nil Kham Haeng in Central Thailand. *4th International Conference of the European Association of Southeast Asian Archaeologists*. Rome.
- Pigott, V. C. (1998) Prehistoric Copper Mining in the Context of Emerging Community

- Craft Specialisation in Northeast Thailand. In Knapp, A. B., Pigott, V. C., & Herbert, E. W. (Eds.) *Social Approaches to an Industrial Past*. London & New York, Routledge: 205-225
- Pigott, V. C. (1999a) Reconstructing the Copper Production Process as Practised among Prehistoric Mining/Metallurgical Communities in the Khao Wong Prachan Valley of Central Thailand. In Young, S. M. M., Pollard, M. A., Budd, P., & Ixer, R. A. (Eds.) *Metals in Antiquity*. Oxford, Archaeopress: 10-21.
- Pigott, V. C. (Ed.) (1999b) *The Archaeometallurgy of the Asian Old World*, Philadelphia, MASCA Research Papers in Science and Archaeology 16, University of Pennsylvania Museum.
- Pigott, V. C. & Ciarla, R. (2007) On the Origins of Metallurgy in Prehistoric Southeast Asia: The View from Thailand. In Niece, S. L., Hook, D., & Craddock, P. (Eds.) *Metals and Mines: Studies in Archaeometallurgy*. London, Archetype Publications Ltd.: 76-88
- Pigott, V. C., Mudar, K., Agelarakis, A., Kealhofer, L., Weber, S. A., & Voelker, J. C. (2006) A Program of Analysis of Organic Remains from Prehistoric Copper-Producing Settlements in the Khao Wong Prachan Valley, Central Thailand : A Progress Report. In Bacus, E. A., Glover, I. C., & Pigott, V. C. (Eds.) *Uncovering Southeast Asia's Past. Selected Papers from the 10th International Conference of the European Association of Southeast Asian Archaeologists*. Singapore, National University of Singapore:154-167.
- Pigott, V. C. & Natapintu, S. (1988) Archaeological Investigations into Prehistoric Copper Production: The Thailand Archaeometallurgy Project, 1984-86. In Maddin, R. (Ed.) *The Beginning of the Use of Metals and Alloys*. Cambridge, MA, M.I.T. Press: 156-162.
- Pigott, V. C. & Natapintu, S. (1996-1997) Investigating the Origins of Metal Use in Prehistoric Thailand. In Barnard, N. (Ed.) *Ancient Chinese and Southeast Asian Bronze Age Cultures*, Volume II. Taipei, SMC Publishing Inc.: 787-808.
- Pigott, V. C. & Weisgerber, G. (1998) Mining Archaeology in Geological Context. The Prehistoric Copper Mining Complex at Phu Lon, Nong Khai Province, Northeast Thailand. In Muhly, J. D. (Ed.) *Metallurgica Antiqua: In Honour of Hans-Gert Bachmann and Robert Maddin*. Bochum, Deutsches Bergbau-Museum Bochum: 135-161
- Pigott, V. C., Weiss, A., & Natapintu, S. (1997) Archaeology of Copper Production: Excavations in the Khao Wong Prachan Valley, Central Thailand. In Ciarla, R. & Rispoli, F. (Eds.) *South-East Asian Archaeology 1992. Proceedings of the Fourth International Conference of the European Association of South-East Asian Archaeologists. Rome, 28th September - 4th October 1992*. Rome, Istituto Italiano per l'Africa e l'Oriente: 119-157.
- Pryce, T. O. & Pigott, V. C. (2008) Towards a Definition of Technological Styles in Prehistoric Copper Smelting in the Khao Wong Prachan Valley of Central Thailand. In Pautreau, J.-P., Coupey, A., Zeitoun, V., & Rambault, E. (Eds.) *Archaeology in Southeast Asia: From Homo Erectus to the Living Traditions, Choice of Papers from the 11th Euraseaa Conference, Bougon 2006*. Chiang-Mai, European Association of Southeast Asian Archaeologists:139-150.

- Read, T. T. (1934) Metallurgical Fallacies in Archaeological Literature. *American Journal of Archaeology*, 38: 382-389.
- Reed, S. J. B. (1996) *Electron Microprobe Analysis and Scanning Electron Microscopy*, Cambridge, Cambridge University Press.
- Rehder, J. E. (1994) Blowpipes Versus Bellows in Ancient Metallurgy. *Journal of Field Archaeology*, 21: 345-350.
- Rehren, T. (2000) New Aspects of Ancient Egyptian Glassmaking. *Journal of Glass Studies*, 42: 13-24.
- Rehren, T., Charlton, M., Chirikure, S., Humphris, J., Ige, A., & Veldhuijzen, H. A. (2007) Decisions Set in Slag: The Human Factor in African Iron Smelting. In Niece, S. L., Hook, D., & Craddock, P. (Eds.) *Metals and Mines: Studies in Archaeometallurgy*. London, Archetype Publications Ltd.: 211-218.
- Rehren, T. & Pusch, E. B. (1997) New Kingdom Glass-Melting Crucibles from Qantir-Piramesses. *Journal of Egyptian Archaeology*, 83: 127-141.
- Reinecke, A. (1998) *Einführung in Die Archäologie Vietnams*, Köln, KAVA (Kommission f. Allgemeine und Vergleichende Archäologie des Deutsches Archäologisches Instituts).
- Reinecke, A. & Luyen, N. T. T. (in press) Recent Discoveries in Vietnam: Gold Masks and Other Precious Items. *Arts of Asia*, 39.
- Renfrew, C. (1972) *The Emergence of Civilisation: The Cyclades and the Aegean in the Third Millennium B.C.*, London, Methuen.
- Renfrew, C. (1975) Trade as Action at a Distance: Questions of Integration and Communication. In Sabloff, J. A. & Lamberg-Karlovsky, C. C. (Eds.) *Ancient Civilization and Trade*. Albuquerque, University of New Mexico Press: 3-60
- Richards, C. (2008) The Substance of Polynesian Voyaging. *World Archaeology*, 40: 206-223.
- Rice, P. M. (1987) *Pottery Analysis: A Sourcebook*, Chicago; London, University of Chicago Press.
- Rice, P. M. (1999) On the Origins of Pottery. *Journal of Archaeological Method and Theory*, 6: 1-54.
- Rispoli, F. (1990) *La Ceramica Di Non Pa Wai (Lopburi, Tailandia Centrale)*. Unpublished doctoral thesis, Dipartimento di Studi Orientali, Università' La Sapienza Roma, Roma.
- Rispoli, F. (1997) Late Third/Early Second Millennium Bce Pottery Traditions in Central Thailand: Some Preliminary Observations in a Wider Prospective. In Ciarla, R. & Rispoli, F. (Eds.) *South-East Asian Archaeology 1992. Proceedings of the Fourth International Conference of the European Association of South-East Asian Archaeologists. Rome, 28th September - 4th October 1992*. Rome, Istituto Italiano per l'Africa e l'Oriente: 59-67.
- Rispoli, F. (2007) The Incised & Impressed Pottery Style of Mainland Southeast Asia Following the Paths of Neolithization. *East and West*, 57: 235-304.

- Rispoli, F., Ciarla, R., & Pigott, V. C. (forthcoming) Khao Wong Prachan Valley Chronology.
- Roberts, B. (2008) Creating Traditions and Shaping Technologies: Understanding the Earliest Metal Objects and Metal Production in Western Europe. *World Archaeology*, 40: 354-372.
- Rostoker, W. & Dvorak, J. R. (1991) Some Experiments with Co-Smelting to Copper Alloys. *Archaeomaterials*, 5: 5-20.
- Rostoker, W., Pigott, V. C., & Dvorak, J. R. (1989) Direct Reduction to Metal by Oxide/Sulphide Mineral Interaction. *Archaeomaterials*, 3: 69-87.
- Rothenberg, B., Tylecote, R. F., & Boydell, P. J. (1978) *Chalcolithic Copper Smelting: Excavations and Experiments*, London, Thames & Hudson.
- Roux, V. (2003) A Dynamic Systems Framework for Studying Technological Change: Application to the Emergence of the Potter's Wheel in the Southern Levant. *Journal of Archaeological Method and Theory*, 10: 1-30.
- Roux, V. (2007) Ethnoarchaeology: A Non Historical Science of Reference Necessary for Interpreting the Past. *Journal of Archaeological Method and Theory*, 14: 153-178.
- Roux, V., Bril, B., & Dietrich, G. (1995) Skills and Learning Difficulties Involved in Stone Knapping: The Case of Stone-Bead Knapping in Khambhat, India. *World Archaeology*, 27: 63-87.
- Ruiz, I. M. (1993) Bronze Age Metallurgy in Southeast Spain. *Antiquity*, 67: 46-57.
- Rye, O. (1981) *Pottery Technology: Principles and Reconstruction*, Washington D.C., Taraxacum Press.
- Sackett, J. R. (1977) The Meaning of Style in Archaeology: A General Model. *American Antiquity*, 42: 369-380.
- Sackett, J. R. (1982) Approaches to Style in Lithic Archaeology. *Journal of Anthropological Archaeology*, 1: 59-112.
- Sackett, J. R. (1985) Style and Ethnicity in the Kalahari: A Reply to Wiessner. *American Antiquity*, 50: 154-159.
- Sackett, J. R. (1990) Style and Ethnicity in Archaeology: The Case for Isochrestism. In Conkey, M. W. & Hastorf, C. A. (Eds.) *The Uses of Style in Archaeology*. Cambridge, Cambridge University Press: 32-43.
- Salter, C. J. (1976) *A Study of the Trace and Minor Element Composition of Slag Inclusions in Ancient Iron Artefacts*. Unpublished doctoral thesis, Faculty of Physical Sciences, University of Oxford, Oxford.
- Schiffer, M. B. (1972) Archaeological Context and Systemic Context. *American Antiquity*, 37: 156-165.
- Schiffer, M. B. (2004) Studying Technological Change: A Behavioral Perspective. *World Archaeology*, 36: 579-585.
- Schmidt, P. (1997) *Iron Technology in East Africa*, Oxford, James Currey.

- Schwab, R., Heger, D., Höppner, B., & Pernicka, E. (2006) The Provenance of Iron Artefacts from Manching: A Multi-Technique Approach. *Archaeometry*, 48: 433-452.
- Scott, D. A. (1991) *Metallography and Microstructure of Ancient and Historic Metals*, Marina del Rey, California, The Getty Conservation Institute.
- Shanks, M. (2008) Post-Processual Archaeology and After. In Bentley, R. A., Maschner, H. D. G., & Chippindale, C. (Eds.) *Handbook of Archaeological Theories*. New York, Altamira Press:133-144
- Shennan, S. J. (1997) *Quantifying Archaeology*, Iowa City, University of Iowa Press.
- Shennan, S. J. (1999) Cost, Benefit, and Value in the Organization of Early European Copper Production. *Antiquity*, 73: 352-363.
- Shennan, S. J. (2000) Population, Culture History, and the Dynamics of Culture Change. *Current Anthropology*, 41: 811-835.
- Shennan, S. J. (2002) *Genes, Memes and Human History: Darwinian Archaeology and Cultural Evolution*, London, Thames and Hudson.
- Shennan, S. J. (2008) Evolution in Archaeology. *Annual Review of Anthropology*, 37: 75-91.
- Shennan, S. J. & Wilkinson, J. R. (2001) Ceramic Style Change and Neutral Evolution: A Case Study from Neolithic Europe. *American Antiquity*, 66: 577-593.
- Sherratt, A. (2006) The Trans-Eurasian Exchange: The Prehistory of Chinese Relations with the West. In Mair, V. H. (Ed.) *Contact and Exchange in the Ancient World*. Honolulu, University of Hawai'i Press: 30-61.
- Shoocondej, R. (2006) Late Pleistocene Activities at the Tham Lod Rockshelter in Highland Pang Mapha, Mae Hong Son Province, Northwestern Thailand. In Bacus, E. A., Glover, I. C., & Pigott, V. C. (Eds.) *Uncovering Southeast Asia's Past – Selected Papers from the Tenth Biennial Conference of the European Association of Southeast Asian Archaeologists 14th-17th September 2004*. Singapore, National University Press: 22-37.
- Sillar, B. & Tite, M. S. (2000) The Challenge of 'Technological Choices' for Materials Science Approaches in Archaeology. *Archaeometry*, 42: 2-20.
- Sinclair, A. (2000) Constellations of Knowledge: Human Agency and Material Affordance in Lithic Technology. In Robb, J. (Ed.) *Agency in archaeology*. New York and London, Routledge.
- Sitthithaworn, E. (1990) Metallogenic Map of Thailand. Bangkok, Department of Mineral Resources.
- Slingo, J. M. & Annamalai, H. (2000) 1997: The El Niño of the Century and the Response of the Indian Summer Monsoon. *The Monthly Weather Review*, 128: 1778-1797.
- Smith, C. S. (1977) *Metallurgy as a Human Experience: An Essay on Man's Relationship to His Materials in Science and Practice Throughout History*. Metals Park, OH, American Society for Metals.
- Soejono, R. P. (1972) The Distribution of Types of Bronze Axes in Indonesia. *Bulletin of*

the Archaeological Institute of the Republic of Indonesia, 9: 1-29.

- Solheim, W. G. (1968) Early Bronze in Northeastern Thailand. *Current Anthropology*, 9: 59-62.
- Spriggs, M. (1996-1997) The Dating of Non Nok Tha and the 'Gakashuin Factor'. In Bulbeck, F. D. & Barnard, N. (Eds.) *Ancient Chinese and Southeast Asian Bronze Age Cultures, Volume II. The Proceedings of a Conference Held at the Edith and Joy London Foundation Property, Kioloa, NSW, Australia, 8-12 February, 1988*. Taipei, SMC Publishing: 941-948.
- Stark, M. (2006) Early Mainland Southeast Asian Landscapes in the First Millennium A.D. *Annual Review of Anthropology*: 407-432.
- Stech, T. & Maddin, R. (1988) Reflections on Early Metallurgy in Southeast Asia. In Maddin, R. (Ed.) *The Beginning of the Use of Metals and Alloys: Papers from the Second International Conference on the Beginning of the Use of Metals and Alloys, Zhengzhou, China, 21-26 October, 1986*. Cambridge, Mass., MIT Press: 163-174.
- Steinberg, A. (1977) Technology and Culture: Technological Styles in the Bronzes of Shang China, Phrygia and Urnfield Central Europe. In Merrill, R. S. (Ed.) *Material Culture: Styles, Organization Material Culture: Styles, Organization and Dynamics of Technology*. St. Paul, Minnesota, West Publishing Co.: 62-70.
- Stone, P. G. & Planel, P. G. (1999) Introduction. In Stone, P. G. & Planel, P. G. (Eds.) *The Constructed Past: Experimental Archaeology, Education and the Public*. London, Routledge: 1-14.
- Stos-Gale, Z. A. (1989) Cycladic Copper Metallurgy. In Hauptmann, A., Pernicka, E., & Wagner, G. (Eds.) *Der Anschnitt, Beiheft 7: Old World Archaeometallurgy*. Bochum, Selbstverlag des Deutschen Bergbau-Museums: 279-291.
- Tabor, G. R., Molinari, D., & Juleff, G. (2005) Computational Simulation of Air Flows through a Sri Lankan Wind-Driven Furnace. *Journal of Archaeological Science*, 32: 753-766.
- Takaya, Y. (1968) Quaternary Outcrops in the Central Plain of Thailand. In Takimoto, K. (Ed.) *Geology and Mineral Resources in Thailand and Malaya*. Kyoto, The Centre for Southeast Asian Studies, Kyoto University: 8-68
- Takimoto, K. & Suzuka, T. (1968) General Statement on Geology and Ore Deposits in Thailand and Malaya. In Takimoto, K. (Ed.) *Geology and Mineral Resources in Thailand and Malaya*. Kyoto, The Centre for Southeast Asian Studies, Kyoto University: 1-6.
- Tan, H. V. (Ed.) (1994) *Van Hoa Dong Son O Vietnam*, Hanoi, Nha Xuat Ban Khoa Hoc Xa Hoi.
- Taylor, T. (2008a) Prehistory Vs. Archaeology: Terms of Engagement. *Journal of World Prehistory*, 21: 1-18.
- Taylor, T. (2008b) Materiality. In Bentley, R. A., Maschner, H. D. G., & Chippindale, C. (Eds.) *Handbook of Archaeological Theories*. New York, Altamira Press: 297-320.
- Thomas, G. R. & Young, T. P. (1999) The Determination of Bloomery Furnace Mass

- Balance and Efficiency. In Pollard, A. M. (Ed.) *Geoarchaeology: Exploration, Environments, Resources*. London, Geological Society: 155-164.
- Timberlake, S. (2007) The Use of Experimental Archaeology/Archaeometallurgy. In Niece, S. L., Hook, D., & Craddock, P. (Eds.) *Metals and Mines: Studies in Archaeometallurgy*. London, Archetype Publications Ltd.: 27-36.
- Tite, M. S., Freestone, I. C., Meeks, N. D., & Craddock, P. T. (1985) The Examination of Refractory Ceramics from Metal-Production and Metalworking Sites. In Phillips, P. (Ed.) *The Archaeologist and the Laboratory*. London, Council for British Archaeology: 50-55.
- Tite, M. S., Hughes, M. J., Freestone, I. C., Meeks, N. D., & Bimson, M. (1990) Technological Characterisation of Refractory Ceramics from Timna. In Rothenberg, B. (Ed.) *The Ancient Metallurgy of Copper, Vol. 2*. London, Institute for Archaeo-Metallurgical Studies, Institute of Archaeology, University College London: 158-175.
- Torrence, R. (1986) *Production and Exchange of Stone Tools: Prehistoric Obsidian in the Aegean*, Cambridge Cambridge University Press.
- Townend, S. (2002) Interpreting People Interpreting Things: A Heideggerian Approach to Experimental Reconstruction. *Papers from the Institute of Archaeology*, 13: 73-94.
- Trigger, B. G. (2006) *A History of Archaeological Thought*, Cambridge, Cambridge University Press.
- Tylecote, R. F. (1962) *Metallurgy in Archaeology*, London, Edward Arnold.
- Tylecote, R. F. (1974) Can Copper Be Smelted in a Crucible? *Journal of Historical Metallurgy*, 8: 54.
- Tylecote, R. F. (1987) *The Early History of Metallurgy in Europe*, London, Longman.
- Tylecote, R. F. (1992) *A History of Metallurgy*, London, Institute of Materials.
- Tylecote, R. F. & Merkel, J. F. (1985) Experimental Smelting Techniques: Achievements and Future. In Hughes, M. J. (Ed.) *Furnaces and Smelting Technology in Antiquity*. London, The British Museum Press: 3-20.
- Ucko, P. J. (1969) Ethnography and Archaeological Interpretation of Funerary Remains. *World Archaeology*, 1: 262-280.
- Veldhuijzen, H. A. (2003) 'Slag_Fun' - a New Tool for Archaeometallurgy: Development of an Analytical (P)Ed-Xrf Method for Iron-Rich Materials. *Papers from the Institute of Archaeology*, 14: 102-118.
- Veldhuijzen, H. A. (2005) Technical Ceramics in Early Iron Smelting. The Role of Ceramics in the Early First Millennium BC Iron Production at Tell Hammeh (Az-Zarqa), Jordan. In Prudêncio, I., Dias, I., & Waerenborgh, J. C. (Eds.) *Understanding People through Their Pottery; Proceedings of the 7th European Meeting on Ancient Ceramics (EMAC '03)*. Lisboa, Instituto Português de Arqueologia (IPA): 295-302.
- Vernon, W. W. (1988) Field Notes from Geological Survey of the Khao Wong Prachan Valley, 18th-23rd February 1988. Unpublished report, University of Pennsylvania

Museum.

- Vernon, W. W. (1996-1997) The Crucible in Copper-Bronze Production at Prehistoric Phu Lon, Northeast Thailand: Analyses and Interpretation. In Bulbeck, D. F. & Barnard, N. (Eds.) *Ancient Chinese and Southeast Asian Bronze Age Cultures*. Taipei, SMC Publishing: 809-820.
- Vernon, W. W. (1997). Chronological variation in crucible technology at Ban Chiang: A preliminary assessment. *Bulletin of the Indo-Pacific Prehistory Association* 16: 107-110.
- Wake, C. S. (1882) Notes on the Origin of the Malagasy. *Journal of the Anthropological Institute of Great Britain and Ireland*, 11: 21-33.
- Wang, D. N., Pigott, V. C., & Notis, M. R. (1998) *The Archaeometallurgical Analysis of Copper-Base Artifacts from Prehistoric Nil Kham Haeng, Central Thailand: A Preliminary Report*. Unpublished report, Lehigh University.
- Watt, I. M. (1997) *The Principles and Practice of Electron Microscopy*, Cambridge and New York, Cambridge University Press.
- Webster, G. S. (2008) Culture History: A Culture-Historical Approach. In Bentley, R. A., Maschner, H. D. G., & Chippindale, C. (Eds.) *Handbook of Archaeological Theories*. New York, Altamira Press: 11-27
- Weiss, A. (1992) *TAP'92 Nil Kham Haeng Report*. Unpublished report, Center for Conservation Biology, Stanford University.
- Wenger, E. (1998) *Communities of Practice: Learning, Meaning, and Identity*, Cambridge, Cambridge University Press.
- Wengrow, D. (2008) Prehistories of Commodity Branding. *Current Anthropology*, 49: 7-34.
- Wertime, T. A. (1964) Man's First Encounters with Metallurgy. *Science*, 146: 1257-1267.
- Wertime, T. A. (1968) A Metallurgical Expedition through the Persian Desert. *Science*, 159: 927-935.
- Whitbread, I. K. (1989) A Proposal for the Systematic Description of Thin Sections Towards the Study of Ancient Ceramic Technology. In Maniatis, Y. (Ed.) *Archaeometry: Proceedings of the 25th International Symposium*. Amsterdam, Elsevier: 127-138
- Whitbread, I. K. (1996) Detection and Interpretation of Preferred Orientation in Ceramic Thin Sections. *Proceedings of the 2nd Symposium of the Hellenic Archaeometrical Society*. Thessaloniki: 413-425
- White, A. (2008) A Developmental Perspective on Technological Change. *Antiquity*, 40: 597-608.
- White, J. C. (1982) *Ban Chiang: Discovery of a Lost Bronze Age*, Philadelphia, University of Pennsylvania and the Smithsonian Institution Traveling Exhibition Service.
- White, J. (1986) *A Revision of the Chronology at Ban Chiang and Its Implications for the Prehistory of Northeast Thailand*. Unpublished doctoral thesis, Department of

Anthropology, University of Pennsylvania, Philadelphia.

- White, J. C. (1988) Early East Asian Metallurgy: The Southern Tradition. In Maddin, R. (Ed.) *The Beginning of the Use of Metals and Alloys: Papers from the Second International Conference on the Beginning of the Use of Metals and Alloys, Zhengzhou, China, 21-26 October, 1986*. Cambridge, Mass., MIT Press: 175-181.
- White, J. C. (1995) Incorporating Heterarchy into Theory on Socio-Political Development: The Case from Southeast Asia. In Ehrenreich, R. E. A. (Ed.) *Heterarchy and the Analysis of Complex Societies*. Washington, D.C., American Archaeological Association: 101-123
- White, J. C. (1997) A Brief Note on New Dates for the Ban Chiang Cultural Tradition. In Tillotson, D. (Ed.) *Indo-Pacific Prehistory: The Chiang Mai Papers*. Canberra, Australian National University: 103-106.
- White, J. C. (2000) Review of "Prehistoric Thailand: From Early Settlement to Sukhothai" by Charles Higham & Rachanie Thosarat. *Journal of Asian Studies*, 59: 1093-1094.
- White, J. C. (2002) Series Editor's Preface. In Pietrusewsky, M. & Douglas, M. T. (Eds.) *Ban Chiang, a Prehistoric Village Site in Northeast Thailand I: The Human Skeletal Remains*. Philadelphia, University Museum of Archaeology and Anthropology: xvi-xvii.
- White, J. C. (2008a) Archaeology of the Middle Mekong: Introduction to the Luang Prabang Province Exploratory Survey. In Goudineau, Y. & Lorrillard, M. (Eds.) *Recherches Nouvelles Sur Le Laos*. Vientiane and Paris, Études thématiques n° 18 : École française d'Extrême-Orient: 36-52.
- White, J. C. (2008b) Dating Early Bronze at Ban Chiang, Thailand. In Pautreau, J.-P., Coupey, A., Zeitoun, V., & Rambault, E. (Eds.) *Archaeology in Southeast Asia: From Homo Erectus to the Living Traditions, Choice of Papers from the 11th Eurasea Conference, Bougon 2006*. Chiang-Mai European Association of Southeast Asian Archaeologists: 91-104.
- White, J. C. & Hamilton, E. G. (in press) The Sources of Early Southeast Asian Bronze Metallurgy. *Journal of World Prehistory*.
- White, J. C. & Pigott, V. C. (1996) From Community Craft to Regional Specialisation: Intensification of Copper Production in Pre-State Thailand. In Wailes, B. (Ed.) *Craft Specialization and Social Evolution: In Memory of V. Gordon Childe*. Philadelphia, University Museum Publications: 151-175.
- Wiessner, P. (1983) Style and Social Information in Kalahari San Projectile Points. *American Antiquity*, 48: 253-276.
- Wiessner, P. (1984) Reconsidering the Behavioral Basis for Style: A Case Study among the Kalahari San. *Journal of Anthropological Archaeology*, 3: 190-234.
- Wiessner, P. (1985) American Antiquity Style or Isochrestic Variation? A Reply to Sackett. *American Antiquity*, 50: 160-166.
- Wilson, L. & Pollard, A. M. (2001) The Provenance Hypothesis. In Brothwell, D. R. & Pollard, A. M. (Eds.) *Handbook of Archaeological Sciences*. Chichester, UK,

John Wiley & Sons, Ltd: 507-517.

Wobst, H. M. (1977) Stylistic Behavior and Information Exchange. In Cleland, C. E. (Ed.) *For the Director: Research Essays in Honor of James B. Griffin*. Ann Arbor, Michigan Museum of Anthropology: 317-342.

Workman, D. R. (1977) *Geology of Laos, Cambodia, South Vietnam and the Eastern Part of Thailand*, Overseas Geological and Mineral Resources 50, Institute of Geological Sciences.

Yazawa, A. (1980) Distribution of Various Elements between Copper, Matte, and Slag. *Erzmetall*, 33: 377-382.